antioxidants

Special Issue Reprint

Novel Therapies of Oxidative Stress-Induced Age-Related Neurodegenerative Diseases

Edited by
Ana-Maria Buga and Carmen Nicoleta Oancea

mdpi.com/journal/antioxidants

MDPI

Novel Therapies of Oxidative Stress-Induced Age-Related Neurodegenerative Diseases

Novel Therapies of Oxidative Stress-Induced Age-Related Neurodegenerative Diseases

Editors

Ana-Maria Buga
Carmen Nicoleta Oancea

MDPI

Basel • Beijing • Wuhan • Barcelona • Belgrade • Novi Sad • Cluj • Manchester

Editors

Ana-Maria Buga
Biochemistry Department
University of Medicine and Pharmacy of Craiova
Craiova
Romania

Carmen Nicoleta Oancea
Department of Biochemistry
University of Medicine and Pharmacy of Craiova
Craiova
Romania

Editorial Office
MDPI AG
Grosspeteranlage 5
4052 Basel, Switzerland

This is a reprint of articles from the Special Issue published online in the open access journal *Antioxidants* (ISSN 2076-3921) (available at: https://www.mdpi.com/journal/antioxidants/special_issues/oxidative_stress_age_related_neurodegenerative_diseases).

For citation purposes, cite each article independently as indicated on the article page online and as indicated below:

Lastname, A.A.; Lastname, B.B. Article Title. *Journal Name* **Year**, *Volume Number*, Page Range.

ISBN 978-3-7258-2225-6 (Hbk)
ISBN 978-3-7258-2226-3 (PDF)
doi.org/10.3390/books978-3-7258-2226-3

Contents

antioxidants

MDPI

Editorial

Oxidative Stress-Induced Neurodegeneration and Antioxidative Strategies: Current Stage and Future Perspectives

Ana-Maria Buga and Carmen-Nicoleta Oancea *

Department of Biochemistry, University of Medicine and Pharmacy of Craiova, 200349 Craiova, Romania; ana.buga@umfcv.ro

* Correspondence: carmen.oancea@umfcv.ro

Citation: Buga, A.-M.; Oancea, C.-N. Oxidative Stress-Induced Neurodegeneration and Antioxidative Strategies: Current Stage and Future Perspectives. *Antioxidants* **2023**, *12*, 1762. https://doi.org/10.3390/antiox12091762

Received: 7 September 2023
Revised: 9 September 2023
Accepted: 13 September 2023
Published: 14 September 2023

Neurodegenerative diseases (NDs) are the leading cause of neurological disorders, constituting a public health problem with an exponentially growing incidence rate [1]. By 2024, NDs are estimated to become the second-leading cause of mortality in the world [2]. The ageing population are at increased risk of NDs and stroke. Among the tissues, the brain is more susceptible to neurodegeneration. This process increases with age, and many researchers have asked whether the neurodegeneration process is a hallmark of ageing. However, major NDs affect people over 65 years old. Alzheimer's disease (AD) and Parkinson's disease (PD) are the leading NDs. According to the World Health Organization (WHO), Alzheimer's disease (AD) is the most common form of dementia worldwide and affects more than 50 million people over the age of 65. AD is misdiagnosed due to the fact that many people with mild cognitive impairments (MCIs) progress to AD [3]. In addition, ischemic stroke is not currently recognized as a neurodegenerative disorder, but a chronic neurodegenerative process appears after the initial phase of ischemic stroke in brain areas far away from the lesion [4,5]. Preclinical and clinical data show that post-stroke brains undergo long-term structural changes that lead to brain atrophy [5,6]. These structural changes represent the hallmark of neurodegenerative diseases, but it remains to be established whether there is a direct link between ischemic stroke survivors and an increased risk of AD. Neurodegeneration is not only an old-age health problem; it also affects young adults. Diseases such as multiple sclerosis (MS) and amyotrophic lateral sclerosis (ALS) are accompanied by neurodegeneration. MS and ALS affect the young, active population with a cumulative incidence of 3 million people worldwide (2.8 million for MS and 200.000 for ALS) [7]. However, brain tissue is not the only part of the human body that can be damaged; age-related macular degeneration (AMD) and glaucoma are characterized by neurodegeneration and permanent damage to the eyes [8]. There are currently no therapeutic interventions available to cure these disorders. Despite research efforts to cure NDs, the majority of promising interventions have failed in clinical trials. A common feature of many NDs is the enhancement of oxidative stress and inflammation that trigger mitochondrial disfunction and cellular death. In NDs, OS promotes the propagation of pathophysiological processes that determine the progression of most neurodegenerative states.

At the end of 2022, PubMed found that over 400,000 articles had been published regarding neurodegenerative diseases, and about 18,000 of these included references to oxidative stress along with mechanisms interconnected with NDs [9]. In this Special Issue (SI) of *Antioxidants*, entitled "Novel Therapies of Oxidative-Stress-Induced Age-Related Neurodegenerative Diseases", we highlighted the latest findings regarding neurodegeneration, antioxidants, nutrigenetics, nutraceuticals, or mitochondrial dysfunction. Since there is wide diversity in the ways neuroprotection can be obtained and in the ways neurodegenerative conditions can be treated, achieving neuroprotection and treating NDs, according to statistics, will become increasingly easy. This SI is well balanced and comprises five critical reviews and four original articles. These articles aim to review the recent findings in the ND field and highlight the gaps in knowledge and future research directions. The reviews

cover important directions such as (i) the identification of new potential biomarkers for age-related ND disease progression that can be modulated for therapeutic purposes [10]; (ii) the development of a new preclinical model for PD to test new potential drugs, with an increased potential to limit disease progression or cure it [11]; (iii) the role of nutraceuticals and physical exercise in controlling oxidative balance and improving functional outcomes in NDs [12,13]; (iv) mitochondrial function and oxidative stress in relation to successful cellular therapy for stroke [14].

Juan Segura-Aguilar and his colleagues studied a KEAP1/NRF2 transcriptional activation preclinical model for PD, because no current treatments for PD are guaranteed to work, and no one has studied the effect of antioxidants on idiopathic PD [11]. This model will be useful for the development of new potential antioxidant therapies [11]. This is an interesting study that led to the discovery of several phytochemical activators of KEAP1 (Kelch-like ECH-associated protein (1)/NRF2 (nuclear factor erythroid-derived 2-like (2), which can inhibit or decrease aminochrome-induced neurotoxicity [11]. In addition, Llido and colleagues provided evidence in relation to serum bilirubin levels as a predictor for the evolution of neurodegenerative diseases [10]. Bilirubin is a potent antioxidant molecule, and decreasing its concentration can predict disease progression.

The therapeutic potential of nutraceuticals, such as catechins, to limit the neurodegenerative process in glaucoma was reviewed by Tsz Kin Ng and colleagues, and the potential clinical benefits were emphasized [12]. They studied the pharmacokinetic aspects and therapeutic properties of catechins that underlie the possibility of using catechins, phenolic compounds particularly found in green tea, as adjuvants in clinical treatments of neurodegenerative diseases due to their antioxidant and anti-inflammatory properties [12]. New approaches to oxidative-stress-related to physical activity and nutraceuticals in normal ageing and neurodegenerative ageing were highlighted by Manuela Violeta Bacanoiu and colleagues. Physical exercise and nutraceuticals display a protective antioxidant effect by decreasing free radicals and proinflammatory markers [13].

Also, four original articles were published, with the aim of better understanding the role of oxidative stress in NDs and identifying new potential therapeutic interventions in order to restore redox balance. One study published in this SI by [15] and colleagues evaluated the neuroprotective mechanisms exerted by black pepper extract. Black pepper, native to South Africa and also called "Black Gold", is commonly used to treat colds, neuropathic pain, and respiratory diseases [15]. It has been shown to have anti-AChE and anti-amyloid activity and can restore antioxidant enzyme levels. It has also been shown to reduce ROS production and maintain mitochondrial membrane integrity in neuroblastoma cell cultures. ROS production is considered an important mediator of oxidative stress, neuroinflammation, and cell death [15]. Piperine, the main alkaloid of black pepper, has demonstrated anti-AChE and anti-amyloid activity. The study also showed competitive acetylcholine esterase (AchE) inhibition with promising cytotoxicity (IC50) values, the significant inhibition of Aβ fibrilization, and strong anti-glycation activity with the prevention of advanced glycation end-product (AGE) formation. Black pepper, through its multitarget neuroprotective mechanism, may represent a first step in the development of neurodegenerative disease therapies [15].

Another nutraceutical compound with antioxidant activity that was demonstrated in an article published in this Special Issue by Lee and colleagues is *Dipterocarpus tuberculatus Roxb*. Through its seven bioactive components, the methanolic extract of Dipterocarpus (MED) was able to strongly capture free radicals of 2,2-diphenyl-1-picrylhydrazyl (DPPH) and 2,2′-azono-bis-3-ethylbenzthiazoline-6-sulphonate (ABTS) [16]. MED treatment suppresses the increases in nitric oxide (NO) concentrations and reactive intracellular oxygen species (ROS), with a significant increase in superoxide dismutase (SOD) enzyme activity and recovery of antioxidant capacity. Protective effects have been demonstrated in retinal degeneration such as improving retinal thickness, the inner nuclear layer (INL), the photoreceptor layer (PL), and the outer nuclear layer (ONL) in Balb/c mice [16]. The well-known vitamin, vitamin C, with proven antioxidant properties, was studied by Nery Jara and

colleagues in terms of the worldwide deficiency [17]. The study highlighted significantly higher prevalences of deficiency in developing countries with negative consequences in human neurogenesis.

The complexity of the theme of this SI also brought to light the study conducted by Franziska T. Wunsch and colleagues, who studied defects in the glutathione system in an animal model of ALS [18]. The study, with an impressive bibliography, revealed that the reduced amount of glutathione obtained in the cervical spinal cord of wobbler mice is due to a decrease in glutathione synthesis due to a decrease in the expression of the speed-limiting enzyme glutamyl-cysteinyl-ligase. For the first time, evidence has been provided for impaired glutathione metabolism in ALS in wobbler mice, not limited to motor areas of the CNS, with the need to study whether reduced glutathione is a causative factor or consequence of neurodegeneration into ALS, but with the opening of a possible targeted therapy for ALS by specifically improving glutathione synthesis [18].

The significant importance of functional mitochondria in reducing oxidative damage by restoring mitochondrial integrity suggests a revolutionary effect in treating stroke with reduced neuroinflammation and reperfusion injury, which has been studied and published by Molly Monsour and colleagues [14]. With a better understanding of how important functional mitochondria are in recovering from a stroke, big improvements can be made in promoting mitochondrial transfer and making stem cells more useful for therapy.

This Special Issue, "Novel Therapies of Oxidative-Stress-Induced Age-Related Neurodegenerative Diseases," published nine papers, including four original research papers and five review articles, all of which addressed different aspects of neurodegenerative diseases, innovative therapies in NDs, and correlations of oxidative stress in their induction.

We would like to express our full appreciation to the authors who contributed papers to this Special Issue. The remarkable quality of these studies will certainly add new content and generate new openings in multidisciplinary research into the role of oxidative stress and the complex mechanisms underlying potential therapeutic benefits in neurodegenerative diseases.

Author Contributions: Conceptualization, A.-M.B. and C.-N.O.; writing—original draft preparation, C.-N.O.; writing—review and editing, A.-M.B. All authors have read and agreed to the published version of the manuscript.

Funding: This research was funded by the University of Medicine and Pharmacy of Craiova, grant number 26/531/4/31.05.2022.

Acknowledgments: We would like to express our gratitude to all the authors who contributed to this Special Issue, and to the *Antioxidants* team for their assistance during the review and editorial process.

Conflicts of Interest: The authors declare no conflict of interest.

References

1. Olufunmilayo, E.O.; Gerke-Duncan, M.B.; Holsinger, R.M.D. Oxidative Stress and Antioxidants in Neurodegenerative Disorders. *Antioxidants* **2023**, *12*, 517. [CrossRef] [PubMed]
2. Korovesis, D.; Rubio-Tomás, T.; Tavernarakis, N. Oxidative Stress in Age-Related Neurodegenerative Diseases: An Overview of Recent Tools and Findings. *Antioxidants* **2023**, *12*, 131. [CrossRef] [PubMed]
3. Rye, I.; Vik, A.; Kocinski, M.; Lundervold, A.S.; Lundervold, A.J. Predicting conversion to Alzheimer's disease in individuals with Mild Cognitive Impairment using clinically transferable features. *Sci. Rep.* **2022**, *12*, 15566. [CrossRef] [PubMed]
4. Stuckey, S.M.; Ong, L.K.; Collins-Praino, L.E.; Turner, R.J. Neuroinflammation as a Key Driver of Secondary Neurodegeneration Following Stroke? *Int. J. Mol. Sci.* **2021**, *22*, 13101. [CrossRef] [PubMed]
5. Syeda, T.; Sanchez-Tapia, M.; Pinedo-Vargas, L.; Granados, O.; Cuervo-Zanatta, D.; Rojas-Santiago, E.; Díaz-Cintra, S.; Torres, N.; Perez-Cruz, C. Bioactive Food Abates Metabolic and Synaptic Alterations by Modulation of Gut Microbiota in a Mouse Model of Alzheimer's Disease. *J. Alzheimer's Dis.* **2018**, *66*, 1657–1682. [CrossRef] [PubMed]
6. Brodtmann, A.; Werden, E.; Khlif, M.S.; Bird, L.J.; Egorova, N.; Veldsman, M.; Pardoe, H.; Jackson, G.; Bradshaw, J.; Darby, D.; et al. Neurodegeneration over 3 Years following Ischaemic Stroke: Findings from the Cognition and Neocortical Volume after Stroke Study. *Front. Neurol.* **2021**, *12*, 754204. [CrossRef] [PubMed]

7. Walton, C.; King, R.; Rechtman, L.; Kaye, W.; Leray, E.; Marrie, R.A.; Robertson, N.; La Rocca, N.; Uitdehaag, B.; van der Mei, I.; et al. Rising prevalence of multiple sclerosis worldwide: Insights from the Atlas of MS, third edition. *Mult. Scler.* **2020**, *26*, 1816–1821. [CrossRef] [PubMed]
8. Vyawahare, H.; Shinde, P. Age-Related Macular Degeneration: Epidemiology, Pathophysiology, Diagnosis, and Treatment. *Cureus* **2022**, *14*, e29583. [CrossRef] [PubMed]
9. Yoo, Y.-M.; Joo, S.S. Melatonin Can Modulate Neurodegenerative Diseases by Regulating Endoplasmic Reticulum Stress. *Int. J. Mol. Sci.* **2023**, *24*, 2381. [CrossRef] [PubMed]
10. Llido, J.P.; Jayanti, S.; Tiribelli, C.; Gazzin, S. Bilirubin and Redox Stress in Age-Related Brain Diseases. *Antioxidants* **2023**, *12*, 1525. [CrossRef] [PubMed]
11. Segura-Aguilar, J.; Mannervik, B. A Preclinical Model for Parkinson's Disease Based on Transcriptional Gene Activation via KEAP1/NRF2 to Develop New Antioxidant Therapies. *Antioxidants* **2023**, *12*, 673. [CrossRef] [PubMed]
12. Ng, T.K.; Chu, K.O.; Wang, C.C.; Pang, C.P. Green Tea Catechins as Therapeutic Antioxidants for Glaucoma Treatment. *Antioxidants* **2023**, *12*, 1320. [CrossRef] [PubMed]
13. Bacanoiu, M.V.; Danoiu, M.; Rusu, L.; Marin, M.I. New Directions to Approach Oxidative Stress Related to Physical Activity and Nutraceuticals in Normal Aging and Neurodegenerative Aging. *Antioxidants* **2023**, *12*, 1008. [CrossRef] [PubMed]
14. Monsour, M.; Gordon, J.; Lockard, G.; Alayli, A.; Borlongan, C.V. Mitochondria in Cell-Based Therapy for Stroke. *Antioxidants* **2023**, *12*, 178. [CrossRef]
15. Sharma, H.; Sharma, N.; An, S.S.A. Black Pepper (Piper nigrum) Alleviates Oxidative Stress, Exerts Potential Anti-Glycation and Anti-AChE Activity: A Multitargeting Neuroprotective Agent against Neurodegenerative Diseases. *Antioxidants* **2023**, *12*, 1089. [CrossRef] [PubMed]
16. Lee, S.J.; Roh, Y.J.; Kim, J.E.; Jin, Y.J.; Song, H.J.; Seol, A.; Park, S.H.; Douangdeuane, B.; Souliya, O.; Choi, S.I.; et al. Protective Effects of Dipterocarpus tuberculatus in Blue Light-Induced Macular Degeneration in A2E-Laden ARPE19 Cells and Retina of Balb/c Mice. *Antioxidants* **2023**, *12*, 329. [CrossRef] [PubMed]
17. Jara, N.; Cifuentes, M.; Martínez, F.; González-Chavarría, I.; Salazar, K.; Ferrada, L.; Nualart, F. Vitamin C Deficiency Reduces Neurogenesis and Proliferation in the SVZ and Lateral Ventricle Extensions of the Young Guinea Pig Brain. *Antioxidants* **2022**, *11*, 2030. [CrossRef] [PubMed]
18. Wunsch, F.T.; Metzler-Nolte, N.; Theiss, C.; Matschke, V. Defects in Glutathione System in an Animal Model of Amyotrophic Lateral Sclerosis. *Antioxidants* **2023**, *12*, 1014. [CrossRef] [PubMed]

antioxidants

MDPI

Article

Effects of Acetyl-L-Carnitine on Oxidative Stress in Amyotrophic Lateral Sclerosis Patients: Evaluation on Plasma Markers and Members of the Neurovascular Unit

Elena Grossini [1], Fabiola De Marchi [2], Sakthipriyan Venkatesan [1], Angelica Mele [2], Daniela Ferrante [3] and Letizia Mazzini [2,*]

[1] Laboratory of Physiology, Department of Translational Medicine, Università del Piemonte Orientale, 28100 Novara, Italy; elena.grossini@med.uniupo.it (E.G.); sakthipriyan.venkatesan@uniupo.it (S.V.)
[2] ALS Center, Neurology Unit, Department of Translational Medicine, Università del Piemonte Orientale, 28100 Novara, Italy; fabiola.demarchi@uniupo.it (F.D.M.); 20011892@studenti.uniupo.it (A.M.)
[3] Statistic Unit, Department of Translational Medicine, Università del Piemonte Orientale, 28100 Novara, Italy; daniela.ferrante@uniupo.it
* Correspondence: letizia.mazzini@uniupo.it; Tel.: +39-03213733962

Abstract: Oxidative stress, the alteration of mitochondrial function, and the neurovascular unit (NVU), play a role in Amyotrophic Lateral Sclerosis (ALS) pathogenesis. We aimed to demonstrate the changes in the plasma redox system and nitric oxide (NO) in 32 new ALS-diagnosed patients in treatment with Acetyl-L-Carnitine (ALCAR) compared to healthy controls. We also evaluated the effects of plasma on human umbilical cord-derived endothelial vascular cells (HUVEC) and astrocytes. The analyses were performed at the baseline (T0), after three months (T1), and after six months (T2). In ALS patients at T0/T1, the plasma markers of lipid peroxidation, thiobarbituric acid reactive substances (TBARS) and 4-hydroxy nonenal (4-HNE) were higher, whereas the antioxidants, glutathione (GSH) and the glutathione peroxidase (GPx) activity were lower than in healthy controls. At T2, plasma TBARS and 4-HNE decreased, whereas plasma GSH and the GPx activity increased in ALS patients. As regards NO, the plasma levels were firmly lower at T0–T2 than those of healthy controls. Cell viability, and mitochondrial membrane potential in HUVEC/astrocytes treated with the plasma of ALS patients at T0–T2 were reduced, while the oxidant release increased. Those results, which confirmed the fundamental role of oxidative stress, mitochondrial function, and of the NVU in ALS pathogenesis, can have a double meaning, acting as disease markers at baseline and potential markers of drug effects in clinical practice and during clinical trials.

Keywords: astrocytes; vascular endothelial cells; glutathione; mitochondria; nitric oxide; oxidants; disease progression

Citation: Grossini, E.; De Marchi, F.; Venkatesan, S.; Mele, A.; Ferrante, D.; Mazzini, L. Effects of Acetyl-L-Carnitine on Oxidative Stress in Amyotrophic Lateral Sclerosis Patients: Evaluation on Plasma Markers and Members of the Neurovascular Unit. *Antioxidants* **2023**, *12*, 1887. https://doi.org/10.3390/antiox12101887

Academic Editors: Ana-Maria Buga and Carmen Nicoleta Oancea

Received: 9 October 2023
Accepted: 19 October 2023
Published: 20 October 2023

1. Introduction

Amyotrophic lateral sclerosis (ALS) is a neurodegenerative disease characterized by a progressive deterioration of upper and lower motorneurons (MNs), whose underlying mechanism has not yet been clarified [1,2]. Indeed, various targets, such as neurotoxic microglia, astrocytic excitotoxicity, impaired DNA repair, protein misfolding/aggregation, impaired proteolysis, mitochondrial dysfunction, and axonal transport defects, appear to be involved in the ALS pathogenesis [3–5]. Regarding the widely known existence of a genetic basis in about 10–20% of ALS cases [6], environmental factors could also account for its onset. In addition to age and male sex, smoking, exposure to β-N-methylamino-L-alanine, physical activity, trauma, and agricultural chemicals could play a role as directly causative or as risk factors for developing ALS [7,8].

The uncertainties relating to the pathogenetic mechanisms may account for the lack of a truly effective treatment. To date, only riluzole [2,9,10] and edaravone have been

approved by the Food and Drug Administration (FDA) as therapeutic agents for ALS patients [11,12]; however, they have shown only limited benefits in slowing the disease progression. Given the lack of effective drugs and the ALS severity, the use of complementary and alternative therapies, such as special diets, nutritional integrators, and energy healing, is quite widespread [13]. Among these, the use of acetyl-L-carnitine (ALCAR) is undoubtedly relevant. ALCAR, one of the most common metabolites of carnitine in plasma and tissues [14,15], has anti-inflammatory and antioxidant properties [16]. The actions of ALCAR as an enhancer of the ATP synthesis from beta-oxidation of long-chain fatty acids and neurotransmitters like acetylcholine can explain its protective effects on the central nervous system (CNS) [17].

In addition, many experimental findings showed that ALCAR could protect mitochondria against oxidative stress [18]. With regard to this issue, ALCAR administration was able to induce mitochondrial biogenesis in hypoxic rats [19] and to increase mitochondrial mass after spinal cord injury [20]. In neurons and ALS animal models, ALCAR was found to exert protective effects through the modulation of mitochondrial function and neurotrophic activity [21]. Anti-apoptotic effect of acetyl-l-carnitine and I-carnitine in primary cultured neurons was reported, as well [22]. In relation to the clinical effects, however, only one study agrees on ALCAR supplementation in functional improvement [23].

A lack of detailed information about the ALCAR mechanisms of action can limit the clinical application. Indeed, a better understanding of the actions of ALCAR could be useful in clarifying its role in the management of patients affected by ALS. A possible target could be represented by the neurovascular unit (NVU), which is a network of vascular cells, glial cells, and neurons, whose alteration could hamper the blood–brain barrier (BBB) or blood–spinal cord barrier (BSCB), and lead to MNs damage due to harmful factors entering the CNS [24–26]. The existence of an altered balance between oxidants and antioxidants in the plasma of ALS patients has recently been demonstrated; moreover, plasma from ALS patients was found to exert deleterious effects on vascular endothelial cells and astrocytes in terms of cell survival, mitochondrial function, and oxidative stress [27]. It could, therefore, be hypothesized that the administration of ALCAR could modulate the plasma redox state and the response of the NVU to the unknown circulating mediating factors of the damage mentioned above.

In this study, we have therefore focused on the analysis of the plasma redox state in ALS patients treated with ALCAR, and on the effects of plasma on cell viability, mitochondrial membrane potential, nitric oxide (NO), and mitochondrial ROS (mitoROS) release by members of the NVU unit, such as vascular endothelial cells and astrocytes.

2. Materials and Methods

2.1. Patients

The study was performed on 32 consecutive patients diagnosed with ALS, according to the El Escorial criteria [28,29] at the Tertiary ALS Center at the "Maggiore della Carità University Hospital", Novara, Italy, in the period September 2020–September 2022. The comparison was performed with an age (65.5 (54–71)) and sex-matched (3 males and 2 females) control group (n = 5) collected from unrelated healthy patients' caregivers. The study was conducted following the Good Clinical Practice guidelines and the Declaration of Helsinki principles. The study was approved by the Hospital Ethical Committee (CE 54/17); each participant signed written informed consent for the handling of their clinical data and use of plasma samples for experimental purposes.

We adhered to the following inclusion criteria for the patients' recruitment: (1) aged 18–75 years; (2) defined, clinically probable, and probable laboratory-supported ALS (El Escorial Criteria); (3) within 24 months of symptoms onset; (4) patients on riluzole treatment from at least one month before starting the ALCAR treatment; that is, T0; (5) patients without relevant comorbidities (e.g., other neurological, oncological, autoimmune diseases); (6) patients were able to provide informed consent or had a legally authorized representative willing to do so.

For each participant, we collected demographic and clinical features, including age at onset, sex, phenotype (spinal vs. bulbar) and diagnostic delay. We also collected the ALS Functional Rating Scale–Revised (ALSFRS-R) score, the Forced Vital Capacity percentage (FVC%), Body Mass Index (BMI), and the mutational status (including *C9orf72*, *SOD1*, *TARDBP*, and *FUS*). Data were collected from clinical records using an anonymous data form. An alpha-numeric code was randomly assigned to each patient to keep data collection and analysis anonymous. Patients received acetyl-L-carnitine as per clinical practice 3 g/day per os. The clinical and laboratory investigations were conducted at the time of recruitment before starting the ALCAR treatment (T0) and after six months of treatment (T2). For the plasmatic dosage of the oxidants/antioxidants and NO, we also collected blood after three months (T1). In particular, at each timing point, clinical data and plasma samples were collected. For healthy controls, plasma sample collection was executed at T0, only.

2.2. Collection of Blood Samples

We collected blood samples at 9 am in ALS patients and healthy controls who were fasting, using specific tubes (BD Vacutainer, containing sodium heparin to prevent clotting). The centrifugation of the plasma samples was performed by means of a centrifuge (Eppendorf, mod. 5702, rotor A-4-38), at 3100 rpm, 4 °C, for 10 min. Thereafter, we aliquoted plasma into 5 tubes, which were kept at −80 °C at the Physiology Laboratory, Università del Piemonte Orientale. We used the samples to quantify the redox state markers and to stimulate the human vascular endothelial cells (HUVEC) and the astrocytes. A pseudonymized condition was followed when handling plasma samples.

2.3. Measurements of the Plasma Oxidants/Antioxidants and NO

2.3.1. Quantification of Thiobarbituric Acid Reactive Substances (TBARS) in Plasma Samples

Plasma lipid peroxidation was quantified by means of the TBARS assay Kit (Cayman Chemical, Ann Arbor, MI, USA), that examines the production of malondialdehyde (MDA) [27,30]. In order to perform this quantification, we added sodium dodecyl sulfate solution (100 µL) and Color Reagent (2 mL) to plasma samples (100 µL), which were boiled (1 h) and put on ice (10 min) to block the reaction. After centrifugation (10 min at 1600× *g*; 4 °C), 150 µL of each sample was transferred to a 96-well plate to quantify MDA, by means of a spectrophotometer (VICTOR™ X Multilabel Plate Reader; PerkinElmer; Waltham, MA, USA), at 530–540 nm excitation/emission wavelengths. A reference standard curve with the TBARS Standard was prepared to perform an accurate analysis of TBARS in the samples. The levels of TBARS were expressed as MDA (µM). We executed each measurement in triplicate.

2.3.2. Quantification of the 4-Hydroxy Nonenal (4-HNE) in Plasma Samples

Plasma lipid peroxidation was also examined through the 4-HNE ELISA Kit (FINE TEST; Wuhan Fine Biotech Co., Ltd., Wuhan, China), in which the sample or standard competes with a fixed amount of 4-HNE on the solid phase supporter for sites on the Biotinylated Detection Antibody specific to 4-HNE [31]. Briefly, 50 µL standard or sample was added to each well, together with 50 µL Biotin-labeled Antibody, and left to incubate for 45 min at 37 °C. After washing the plate, 100 µL of SABC working solution was added and left to incubate for 30 min at 37 °C. After washing again, 90 µL of TMB substrate solution was added and left in incubation for 10–20 min at 37 °C. Thereafter, 50 µL stop solution was added and the reading was performed at 450 nm through a spectrophotometer (VICTOR™ X Multilabel Plate Reader). A reference standard curve with the 4-HNE Standard was prepared to perform an accurate analysis of 4-HNE in the samples. The concentration of 4-HNE was expressed as pg/mL. We executed each measurement in triplicate.

2.3.3. Quantification of Glutathione (GSH) in Plasma Samples

The plasma GSH levels were measured by means of the Glutathione Assay Kit (Cayman Chemical) [27,31], which utilizes a carefully optimized enzymatic recycling method using glutathione reductase for the quantification of GSH. In this assay, the sulfhydryl group of GSH reacts with 5,5′-dithio-bis-2-nitrobenzoic acid (DTNB; Ellman's reagent) and produces a yellow-colored 5-thio-2-nitrobenzoic acid (TNB). The mixed disulfide, GSTNB (between GSH and TNB) that is produced is reduced by the glutathione reductase to recycle the GSH and produce more TNB. The rate of TNB production is directly proportional to this recycling reaction, which, in turn, is directly proportional to the concentration of GSH in the sample. Because of the use of glutathione reductase in the Cayman GSH assay kit, both the reduced (GSH) and the oxidized glutathione (GSSG) are measured and the assay reflects the total GSH. In order to perform the GSH quantification, we deproteinated plasma samples through the addition of a meta-phosphoric acid solution in an equal volume. Thereafter, we centrifuged the samples at 2000× *g* for 2 min, then we collected the supernatants and added 50 µL /mL of TEAM reagent to increase the pH. Then, we transferred 50 µL of each sample to a 96-well plate for the quantification of GSH by means of a spectrophotometer (VICTOR™ X Multilabel Plate Reader), at 405–414 nm excitation/emission wavelengths. In order to execute an accurate analysis of GSH plasma levels (as µM), we prepared a standard curve, as suggested by the Glutathione Assay Kit, and executed each measurement in triplicate.

2.3.4. Quantification of the Glutathione Peroxidase Activity (GPx) in Plasma Samples

The plasma glutathione peroxidase activity was measured by means of the Glutathione Peroxidase Assay Kit (Cayman Chemical), which measures the GPx activity via a coupled reaction with glutathione reductase [32]. Briefly, samples (20 µL) were incubated in an assay buffer (100 µL Tris-EDTA) and in a co-substrate mixture, which contained NADPH, glutathione, and glutathione reductase (50 µL). The reaction was initiated by adding 20 µL cumene hydroperoxide. After mixing for a few seconds, the reaction was read at 340 nm using a spectrophotometer (VICTOR™ X Multilabel Plate Reader) every min for five time-points. A standard curve was built to compare the GPx activity, which was expressed as nmol/min/mg protein after normalization to the total protein amount. We executed each measurement in triplicate.

2.3.5. Evaluation of Plasma NO

We analyzed the plasma NO as both nitrites and nitrites/nitrates (NOx) through the Nitrate/Nitrite Fluorometric Assay Kit (Cayman Chemicals). Briefly, the plasma samples were ultrafiltered through the Amicon® Ultra filter (30kDa MWCO Merck KGaA, Darmstadt, Germany) in order to remove proteins. For the NOx measurement, 10 µL of each sample was mixed with 70 µL assay buffer in a 96-well plate, followed by addition of the enzyme cofactor and of the nitrate reductase mixture. After incubation for 2 h, 2,3–diaminonaphthalene (DAN) and NaOH were added in each well and the absorbance was read through a spectrophotometer, as specified below. In order to measure the nitrites, after the addition of 10 µL of sample and 70 µL assay buffer, the DAN Reagent was immediately added in the 96-well plate and left in incubation for 10 min. After the addition of NaOH, the plate was immediately read at the excitation wavelength of 365 nm and emission wavelength of 430 nm through a spectrophotometer (VICTOR™ X Multilabel Plate Reader). Standard curves were built to compare the nitrites and NOx, which were expressed as µM. We executed each measurement in triplicate.

2.4. In Vitro Experiments

2.4.1. Effects of Plasma Samples on HUVEC and Astrocytes

For the in vitro experiments, the plasma of 10 patients at T0 and T2 and of 5 healthy controls at T0 was used. Non-treated cells were also included in the analyses. In particular, we used specific Transwell inserts in order to analyze cell viability (MTT assay), mitochondrial membrane potential, mitochondrial ROS (mitoROS), and NO release in HUVEC and

astrocytes treated with plasma samples (Figure 1). As in previous experiments [27], plasma samples (10% of the total volume of each insert), were placed in the apical surface of the insert for 3 h, while HUVEC cells or astrocytes were plated in the basal one. After 3 h stimulation with plasma, we removed the inserts and executed various assays, as described below. Different pools of HUVEC and astrocytes were used to perform the experiments, which were executed in triplicate and repeated three times.

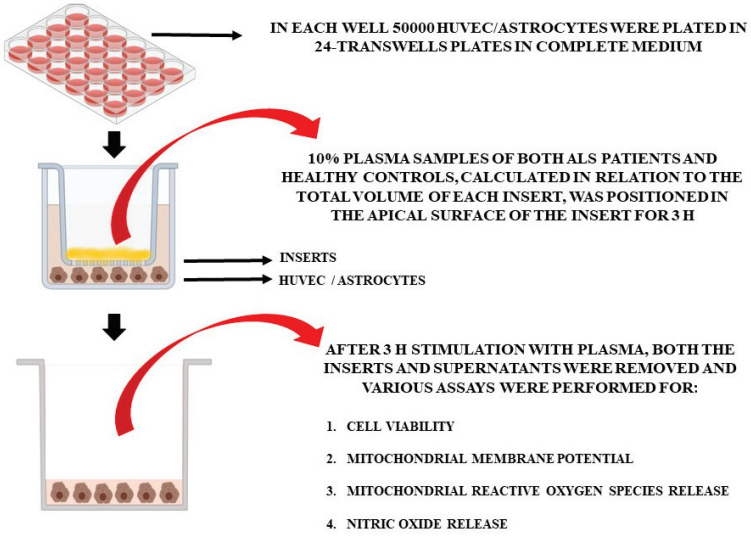

Figure 1. In vitro experimental protocol.

2.4.2. Cell Cultures

HUVEC (ATCC, catalog. no. CRL-1730TM), and mice immortalized astrocytes (kindly provided by prof. Dmitry Lim) [33], were cultured in Dulbecco's Modified Eagle's Medium (DMEM, Sigma-Aldrich, Milan, Italy) with 10% fetal bovine serum (FBS; Euroclone, S.p.A.; Pero, Milan, Italy), 2 mM L-glutamine (Euroclone) and 1% penicillin/streptomycin (Sigma-Aldrich).

2.4.3. Cell Viability

In HUVEC and astrocytes, the viability was examined using the 1% 3-[4,5-dimethylthiazol -2-yl]-2,5-diphenyl tetrazolium bromide (MTT; Life Technologies Italia, Monza, Italy) dye [27,34,35]. To perform this analysis, 50,000 HUVEC/astrocytes/well were plated in 24-Transwells plates in complete medium (DMEM supplemented with 10% FBS). After stimulation with plasma as described above, the medium was replaced with fresh culture medium (0% red phenol and 0% FBS). Then, the MTT dye was added to the well plates and left to incubate for 2 h at 37 °C. Thereafter, the medium was replaced with an MTT solubilization solution (dimethyl sulfoxide; Sigma) and mixed in order to dissolve the formazan crystals. In each sample, the absorbance was read at 570 nm through a spectrophotometer (VICTOR™ X Multilabel Plate Reader). The viability of HUVEC/astrocytes was compared with that of control cells (non-treated cells), which was set as 100%.

2.4.4. Mitochondrial Membrane Potential Measurement

We used the JC-1 assay in order to examine the mitochondrial membrane potential of HUVEC/astrocytes, as was the case in previous experiments [27,34,35]. Briefly, HUVEC and astrocytes (50,000 cells/well) positioned in 24-Transwells plates in complete medium were stimulated with plasma for 3 h, as described for the MTT assay. After stimulation, the medium was removed and cells were incubated for 15 min at 37 °C with the 5,51,6,61-

tetrachloro-1,11,3,31 tetraethylbenzimidazolyl carbocyanine iodide (JC-1) 1X diluted in Assay Buffer 1X (Cayman Chemical). After washing twice using the Assay Buffer 1X, the red (excitation 550 nm/emission 600 nm) and green (excitation 485 nm/emission 535 nm) fluorescence was read through a spectrophotometer (VICTOR™ X Multilabel Plate Reader; PerkinElmer). Data were normalized in relation to non-treated cells, taken as control.

2.4.5. MitoROS Release

The MitoROS release was examined using the Cayman's Mitochondrial ROS Detection Assay Kit (Cayman Chemical) [27,35,36]. In particular, 50,000 HUVEC/astrocytes/well were positioned in 24-Transwells plates in complete medium and they were stimulated with plasma, as was the case for cell viability and mitochondrial membrane potential quantification. After stimulation, we blocked the reactions by replacing the culture media with 120 μL of Cell-Based Assay Buffer. Then, we aspirated the Buffer and added 100 μL of Mitochondrial ROS Detection Reagent Staining Solution to each well. After incubation at 37 °C, with protection from light for 20 min, we removed the Staining Solution and washed each well three times with 120 μL of PBS. In each sample, the absorbance was read at excitation/emission wavelengths of 480 nm and 560 nm, respectively, through a spectrophotometer (VICTOR™ X Multilabel Plate Reader). Data were normalized in relation to non-treated cells taken as control.

2.4.6. NO Release

We used the Griess assay (Promega), to quantify the NO release in HUVEC and astrocytes [27,34]. To examine the NO release through the Griess assay, HUVEC and astrocytes (50,000 cells/well) were plated in 24-Transwells plates in complete medium and stimulated with plasma, as performed for MTT, JC-1 and mitoROS assays. At the end, we added an equal volume of Griess reagent in the sample's supernatants and the reading of each sample was performed at 570 nm, through a spectrophotometer (VICTOR™ X Multilabel Plate Reader). The NO release was quantified in relation to a standard curve, and the production of NO was expressed as nitrites (μM).

2.5. Statistical Analysis

The Research Electronic Data Capture software (REDCap 13.7.18, Vanderbilt University, Nashville, TN, USA) was used to collect data. For each patient, the mean of the multiple measurements was considered for the analysis. The median and interquartile range (IQR) were used to summarize quantitative variables. The Mann–Whitney test was used to test the differences between two groups and the difference between two time points was evaluated using the Wilcoxon signed-rank test. The correlation between quantitative variables was evaluated using the Spearman's correlation coefficient. A p-value < 0.05 was considered statistically significant. STATA software (StataCorp. 2021. Stata Statistical Software: Release 17. College Station, TX: StataCorp LLC) and Graph PAD (GraphPad 6.0 Software, San Diego, CA, USA) were used for statistical analysis.

3. Results

3.1. Clinical Data

Thirty-two patients (19 males and 13 females), with a median age of 67.00 (IQR: 58–70), were recruited for this study. The demographic and phenotypic features of enrolled patients are shown in Table 1. We did not observe any difference in sex and age between ALS patients and healthy controls (p-value > 0.05). At T1 (after three months), five patients left the study (due to death or loss at follow-up) and at T2, 11 patients left the study. In total, we analyzed 32 patients at T0, 27 patients at T1, and 21 patients at T2.

Table 1. ALS patients' demographic and phenotypic features. ALSFRS-R: Amyotrophic Lateral Sclerosis Functional Rating Scale—Revised; FVC: forced vital capacity; BMI: body mass index. The rate of disease progression was calculated as (ALSFRS-R at baseline—last available ALSFRS-R/months) and considered fast progressors if the rate was >0.8.

Patients' Features (n = 32)	
Sex (male/female)	19 (59%)/13 (41%)
Age at onset (median, IQR)	67 (58–70)
Phenotype (spinal/bulbar, %)	22 (69%)/10 (31%)
ALSFRS-R baseline (median, IQR)	39 (35–43)
FVC% baseline (median, IQR)	72 (49–94)
BMI baseline (median, IQR)	23.2 (20.0–26.0)
Rate of progression (fast/slow, %)	19 (59%)/13 (41%)

At T1, the median ALSFRS-R was 37 (IQR: 30.50–41.00), with an FVC% of 72 (IQR: 55–95) and BMI of 22.25 (IQR: 19.98–25.88). At T2, the median ALSFRS-R was 33 (IQR: 31.00–38.00), with an FVC% of 69 (IQR: 51–90) and BMI of 23.45 (IQR: 19.93–26.88).

3.2. Plasmatic Quantifications

In ALS patients at T0 and T1, the plasma TBARS and 4-HNE were higher (Figure 2A,B), whereas the plasma GSH levels and the GPx activity were lower than those found in healthy controls (Figure 2C,D). After six months of treatment with ALCAR (T2), plasma TBARS and 4-HNE decreased (Figure 2A,B) and plasma GSH and GPx activity increased in ALS patients (Figure 2C,D). Notably, regarding the lipid peroxidation markers, the TBARS levels measured at T2 were similar to those found in healthy controls at T0, whereas the 4-HNE levels were still higher.

Regarding NO evaluated as nitrites and NOx, the plasma levels were significantly lower at T0 and T1 than those measured in healthy controls. Despite the improvement observed at T2, however, they continued to be very low even 6 months after the start of ALCAR treatment (T2; Figure 2E,F).

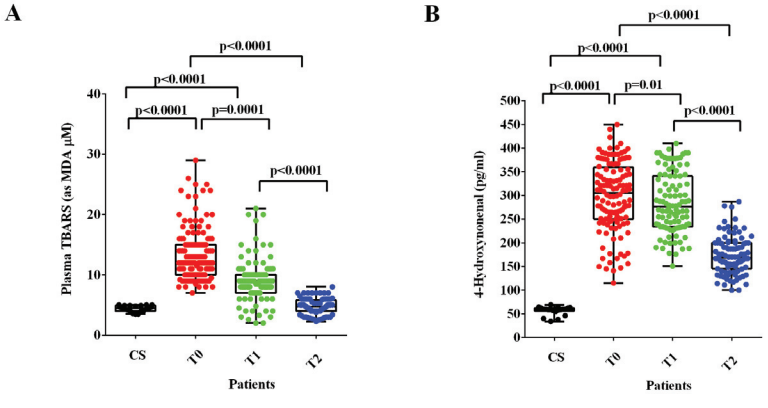

Figure 2. *Cont.*

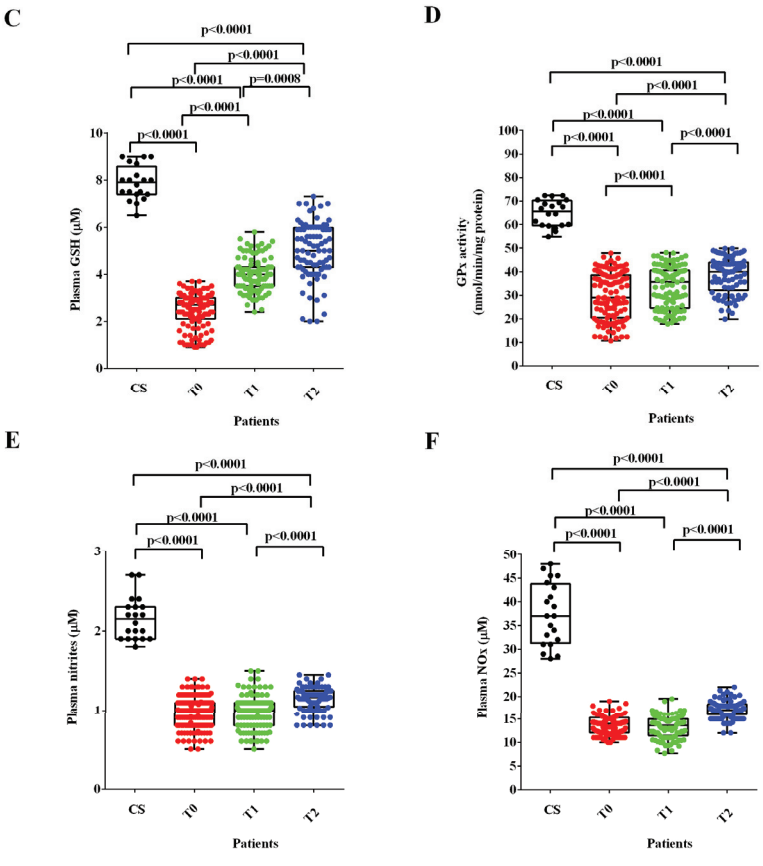

Figure 2. Plasma thiobarbituric acid reactive substances (TBARS), expressed as malonyldialdeide (MDA), (**A**), 4-hydroxy nonenal (4-HNE), (**B**), glutathione (GSH), (**C**), glutathione peroxidase activity (GPx), (**D**) and nitric oxide (NO) as nitrites (**E**) and nitrites/nitrates levels (NOx), (**F**) in ALS patients and healthy controls (CS) at recruitment (T0), after three months (T1) and six months (T2) Acetyl-L-Carnitine (ALCAR) treatment. Square brackets indicate significance between groups as p-value < 0.05.

3.3. In Vitro Experiments

We used the plasma of 10 ALS patients taken at T0 and T2 to stimulate HUVEC. We examined the effects on cell viability, mitochondrial membrane potential, mitoROS, and NO release compared with those elicited by plasma of five healthy controls at T0. As shown in Figure 3, plasma of ALS patients taken at T0 reduced cell viability, mitochondrial membrane potential, and NO release by HUVEC, while it increased mitoROS release. Meanwhile, the plasma of healthy controls did not have any effects on viability and mitochondria function, whereas it was able to increase NO release (Figure 3).

After 6 months of ALCAR treatment (T2), the plasma of ALS patients was still able to reduce viability and mitochondrial membrane and to increase the release of mitoROS in HUVEC compared with what was observed for the plasma of healthy controls. However, the effects were lower than those found with the plasma of the same patients at T0 (Figure 3A–C). It should be noted that the release of NO caused by ALS patients' plasma taken at T2 in HUVEC was even lower than that observed at T0 (Figure 3D).

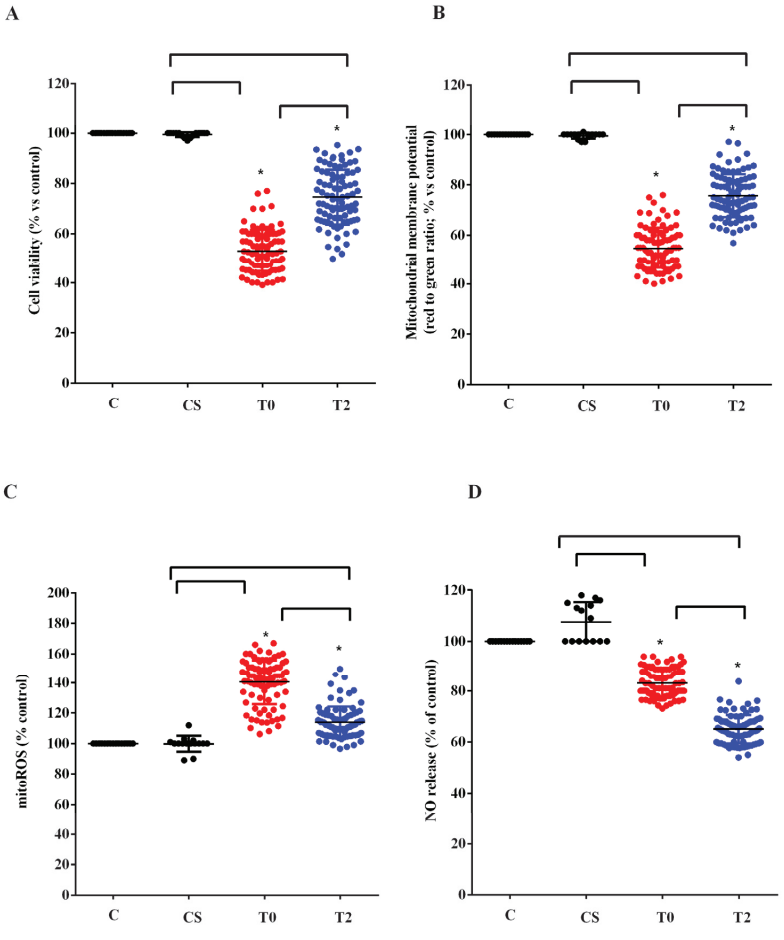

Figure 3. Effects of plasma of ALS patients and healthy controls (CS) on cell viability (**A**), mitochondrial membrane potential (**B**), mitochondrial reactive oxygen species (mitoROS) release (**C**), nitric oxide release (NO), (**D**) in human umbilical cord-derived endothelial vascular cells (HUVEC). T0: recruitment; T2: after six months of Acetyl-L-Carnitine (ALCAR) treatment. Square brackets indicate significance between groups as p-value < 0.05. * indicates p-value < 0.05 vs. C.

Similar results to those found in HUVEC were observed in astrocytes (Figure 4). In fact, also in this case the plasma of ALS patients at T0 reduced the viability and the mitochondrial membrane potential and increased the release of mitoROS. As observed in HUVEC, those effects were reduced when plasma of ALS patients at T2 was used to treat astrocytes. In the case of NO, it should be noted that while with the plasma of ALS patients at T0, we did not observe any particular effect, with plasma taken 6 months after starting ALCAR (T2), it was possible to observe an increase in the release of NO from the astrocytes (Figure 4D).

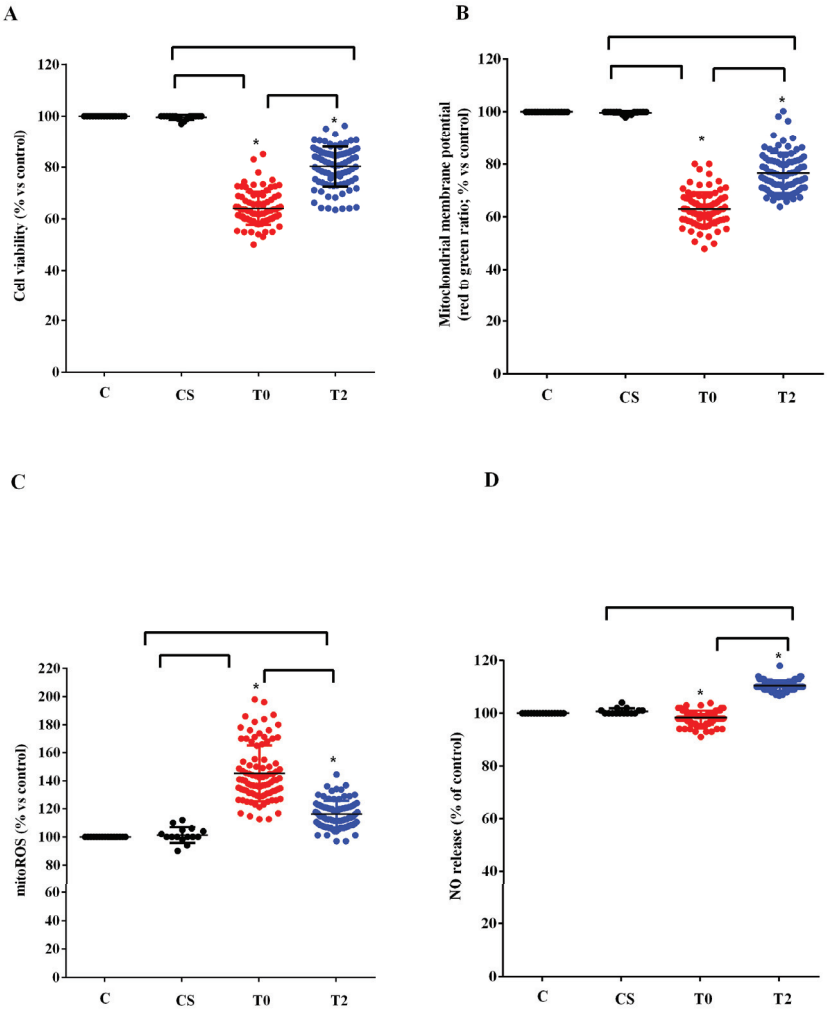

Figure 4. Effects of plasma of ALS patients and healthy controls (CS) on cell viability (**A**), mitochondrial membrane potential (**B**), mitochondrial reactive oxygen species (mitoROS) release (**C**), nitric oxide release (NO), (**D**) in astrocytes. T0: recruitment; T2: after six months of Acetyl-L-Carnitine (ALCAR) treatment. Square brackets indicate significance between groups as p-value < 0.05. * indicates p-value < 0.05 vs. C.

3.4. Clinical Correlations

No statistically significant correlation was found between clinical and demographic features (e.g., age, sex, site of onset, ALSFRS-R, FVC%, and BMI at baseline) and plasmatic values of TBARS, 4-HNE, GSH, GPx activity and NO at baseline and over time. Similarly, comparing the sporadic patients vs. a group of patients' carriers of the *C9Orf72* mutation, we did not observe any difference between the two groups at baseline and over the course of the disease in terms of oxidative stress markers. Interestingly, at T1, we observed higher levels of TBARS and 4-HNE in fast-progressing patients compared to slow progressors (p-value: 0.02). No other variables were associated with functional progressions.

4. Discussion

This study confirms that the balance between oxidants and antioxidants is affected in ALS and demonstrates that the treatment with ALCAR can improve the altered redox state condition in ALS patients. As has already been highlighted, the levels of MDA, expressed as TBARS, and the amount of 4-HNE in the plasma of patients affected by ALS at the time of recruitment were higher than those found in the group of healthy controls. A reduction in the plasma GSH rate and of the GPx activity accompanied this observation.

It is noted that the assays we used to quantify the plasma lipid peroxidation and the amount of the antioxidants in ALS patients and healthy controls are those widely used to conduct this type of investigation [27,30,31,37–42].

Regarding MDA, its levels have been shown to predict worse clinical outcomes in patients with cardiovascular diseases, Alzheimer's, and multiple sclerosis, and they are taken as a marker of ferroptosis [36]. Also, the TBARS assay is considered as a consistent and reproducible method for measuring MDA in biological fluids and cell lysates [43]. Notably, the procedure we followed in our study is the same used in recent papers to evaluate lipid peroxidation in plasma [37–39,44,45]. Moreover, we followed the same procedure to examine the plasma MDA levels in a previous study about ALS [27].

In addition, the 4-HNE levels, which we found to be increased in plasma, although with a decreasing trend in all time-points in ALS patients, have been associated with a greater clinical decline over an 18-month follow-up period [40].

Also, in this study, we used the DTNB-based spectrophotometric method for the quantification of the GSH levels, which was found to provide similar results to those of the chromatography-based method [46] and has been widely adopted to analyze the amount of plasma GSH [27,44,45,47,48].

Overall, therefore, our data confirm the previous conclusions relating to the presence of an alteration in the balance between oxidants and antioxidants in patients affected by neurodegenerative diseases, such as ALS. Hence, an increased level of protein carbonyl in the spinal cord and motor cortex of patients with sporadic ALS was shown [49,50]. Also, the activity/expression of SOD, catalase, glutathione reductase and glutathione transferase were found to be reduced in the cerebrospinal fluid or peripheral blood mononuclear cells of patients with familial or sporadic ALS [51–53].

Regarding GSH, which is well known to non-enzymatically react with ROS, a reduction in the GSH/oxidized glutathione (GSSG) ratio and of GSH levels has been observed in the cerebrospinal fluid of ALS patients [54]. In particular, the dysregulation of GSH homeostasis is believed to contribute to the development and progression of ALS [46,55].

In order to better investigate the level of antioxidants, in this study, we examined the activity of the GPx, as well. The results obtained confirm those relating to GSH, since the GPx activity was much lower than that found in plasma of controls at all time-points. Our data are also in agreement with previous observations found in plasma of ALS patients and in postmortem brain homogenates [42,52,56].

That alteration in the redox state could be associated with cellular dysfunction with particular regard to mitochondria. This was confirmed by the in vitro studies we performed by stimulating HUVEC and astrocytes with plasma of ALS patients. As previously found [27], the results obtained showed a reduction in viability of both cell types, which was accompanied by a decrease in mitochondrial membrane potential and an increased mitoROS release. We used the Mitochondrial ROS Detection Assay to investigate this, since we were focused on the analysis of the mitochondrial function of HUVEC and astrocytes. Those findings evidenced not only the role of unknown circulating factors capable of causing cellular damage through mitochondria dysfunction, but also of the members of the NVU in the onset of ALS.

Our data would support the knowledge that compromised mitochondria and oxidative stress could act as contributing factors for ALS pathology. Changes in mitochondria morphology have been shown in neurons and glial cells from ALS patients and animal models [57,58]. These alterations were also observed in both SOD1 and TDP43 ALS mice, indicating that

they are common denominators of different genetic forms of ALS [59,60]. Those changes could lead to a cascade of events capable of altering mitochondrial respiration and ATP production, thus causing an increase in oxidative stress [61]. The fact that in our study, the reduction in the mitochondrial membrane potential of HUVEC and astrocytes was accompanied by an increase in mitoROS release corroborates the above issues.

The treatment of ALS patients with ALCAR was able to improve the redox state of ALS patients. Hence, the levels of TBARS and 4-HNE were, in fact, reduced, whereas those of GSH and the GPx activity were already increased at 3 months after the initial ALCAR administration, compared to T0. The improvement in the oxidative stress condition was maintained even after 6 months after the onset of ALCAR treatment.

The beneficial effects found in plasma of patients were also observed in vitro, where we obtained a reduction in the harmful effects elicited by plasma of ALS patients. In fact, our results showed a decrease in mitochondrial damage and of mitoROS production in HUVEC and astrocytes. It could be underlined that the data we obtained can provide information on the protective effect of ALCAR. Currently, little knowledge is available regarding its actions on astrocytes and existing research mainly refers to the damage induced by ethanol or caused by spinal cord injury [62,63].

In addition, our findings corroborate the role of ALCAR as a protective agent in ALS through the modulation of the mitochondria function and oxidative stress [18–20]. Moreover, the data we obtained highlight the members of the NVU as a possible pharmacological target of ALCAR, which could be relevant knowledge with regard to ALS management. Indeed, the NVU may play a role in the pathophysiology of ALS by preventing unknown circulating factors from entering the CNS [64]. Indeed, studies in animal models and ALS patients have shown the degeneration of endothelial cells and astrocytes end-feet processes surrounding microvessels [65,66]. In addition, vascular dysfunction could represent an early pathogenic event in ALS as shown in SOD1 mutant mice and rats, in which brain–blood barrier alterations were reported before MNs degeneration [24–26,67].

Interestingly, at T1, throughout the disease course, we observed a difference in lipid peroxidation markers (TBARS and 4-HNE) between fast-progressing patients and slow progressors, which could indicate a stronger dysfunction in the oxidative stress in patients with a more severe disease and, likely, a minor beneficial effect of the available treatment. Our data on 4-HNE are, therefore, in agreement with the previous data, which showed a correlation between the aforementioned marker and a greater disease severity [40].

The results about plasma NO, which was evaluated based on nitrites and NOx levels, are worthy of discussion. They showed that plasma nitrites and NOx levels were lower not only in ALS patients than those of the healthy controls at T0, but even at T1, which was at 3 months from the start of ALCAR treatment. An increase in those plasma values was observed at T2, but it settled at levels much lower than those observed in healthy controls.

Our data, therefore, highlighted the presence of an endothelial dysfunction in ALS patients, which was not affected by the treatment with ALCAR.

This finding was confirmed by the in vitro experiments, since the plasma of ALS patients was able to reduce the NO release by HUVEC at both T0 and, in this case, more strongly, at T2.

Those results could add information about the role of endothelium in the ALS genesis, which has not yet been well investigated. Endothelial cell degeneration and vascular leakage was reported in SOD1 mutants prior to MNs damage and neurovascular inflammatory response, indicating that this damage plays a central role in ALS initiation. Also, reduced levels of tight junction proteins ZO-1, occludin, and claudin-5 were demonstrated before ALS onset, as was a reduction in blood flow through the cervical and lumbar spinal cord in pre-symptomatic G93A SOD1 mice [67]. Finally, circulating endothelial cells were found to be reduced in ALS patients [68].

In this way, therapeutic approaches aiming to protect the endothelium either as direct cytoprotection or through eliminating microenvironment influences should be improved [68,69].

In astrocytes treated with ALS plasma, we observed an increased NO release at T2, which is in agreement with previous data about this issue [70–73]. NO is well known to act both as a mediator of physiological and neuroprotective actions and as an effector of neural damage [70] depending on its concentration, its oxidative/reductive status, cellular specificity, and the nature of downstream target molecules [74–76].

Even if this aspect has not been analyzed, we could hypothesize a different activation–expression of various NO synthase (NOS) isoforms in HUVEC and astrocytes in response to plasma from ALS patients, which would be related to the condition of oxidative stress and/or inflammation. It is well known, in fact, that while the endothelial NOS isoform is involved in the physiologic and low amount of NO release, the inducible NOS isoform is responsible for the increased NO production which could be observed in conditions characterized by oxidative stress/inflammation [77]. It could therefore be hypothesized that the presence of unknown factors in the plasma of ALS patients is capable of having the opposite effect on the above NOS. The fact that the modulation of NO release we have observed in HUVEC and astrocytes was not counteracted by ALCAR could represent a crucial factor in drug-protective actions. Hence, our data would show that on the one hand, ALCAR would act as a protective factor on the redox state and on the mitochondrial function of the NVU members, while on the other hand it would not be so effective at maintaining the balance in NO release in the NVU. If the maintenance of endothelial function and the regulation of NO release are crucial to the pathophysiology of ALS and patients' management, the lack of ability of ALCAR to interfere with the aforementioned mechanisms could represent a bias.

Regarding the effects on oxidative stress and mitochondria, it was shown that ALCAR can be metabolized in neuronal mitochondria to free carnitine and acetyl-CoA [15]. The latter can be used as a substrate for lipids and neurotransmitters synthesis. Instead, free carnitine can be turned into products, such as carnitine derivatives of acyl-CoA conjugates, in the mitochondrial matrix, which could represent a valuable tool for reducing toxicity in oxidative stress conditions through the prevention of accumulation of long-chain fatty acids and long chain acyl-CoAs [78]. Furthermore, free carnitine has been reported to play a key role in the mitochondrial functions, fatty acid metabolism, and the production of ATP [79]. Moreover, many experimental findings demonstrated that ALCAR could protect mitochondria against oxidative stress. Also, ALCAR administration induced mitochondrial biogenesis in hypoxic rats and increased mitochondrial mass after spinal cord injury [15]. Considering what was reported above, our data corroborate the previous findings about the antioxidant effects of ALCAR, which are related to the modulation of mitochondrial function.

Our study has limitations: firstly, all patients were taking ALCAR and riluzole, although administration of these medications started one month before the baseline. As riluzole is the only drug approved to treat ALS in Europe, from an ethical point of view, it is not possible to hypothesize a control arm without riluzole and, similarly, in clinical practice, most of our patients routinely take ALCAR. Moreover, in this study, we used the same methods for assessing plasma oxidative stress as those adopted in the previous study, which focused on the evaluation of the same markers in ALS patients at T0 (before ALCAR treatment), in order to come to more meaningful conclusions about the effects of ALCAR treatment. However, it could be helpful to broaden the analysis of the oxidative stress markers by adding the quantification of hydrogen peroxide or superoxide. Also, the NO levels could be examined through a flow injection analysis. In addition, it could be useful to investigate the intracellular pathways implicated in plasma effects in HUVEC and astrocytes, particularly concerning NO release, and perform cross talk experiments between members of the NVU.

5. Conclusions

From the above analysis, we observed a fundamental role of oxidative stress, the alteration of mitochondrial function, and of the NVU in ALS pathogenesis at baseline

and over time. We also reported a significant improvement in these parameters over time during the concomitant ALCAR treatment. These results can have a double meaning, acting both as disease markers at baseline and as potential markers of drug effects in clinical practice and during clinical trials.

Author Contributions: Conceptualization, E.G., F.D.M. and L.M.; Software, S.V., D.F. and A.M.; Validation, E.G., S.V., D.F., A.M., F.D.M. and L.M.; Formal Analysis, D.F.; Investigation, S.V. and A.M.; Resources, E.G., F.D.M. and L.M.; Data Curation, E.G., S.V., D.F., A.M., F.D.M. and L.M.; Writing—Original Draft Preparation, E.G., S.V., D.F., A.M., F.D.M. and L.M.; Visualization, E.G., S.V., D.F., A.M., F.D.M. and L.M.; Supervision, E.G., S.V., D.F., A.M., F.D.M. and L.M.; Project Administration, E.G., F.D.M. and L.M.; Funding Acquisitions, E.G., F.D.M. and L.M. All authors have read and agreed to the published version of the manuscript.

Funding: The paper was realized with the support of the AGING Project for the Department of Excellence at the Department of Translational Medicine (DIMET), Università del Piemonte Orientale, Novara, Italy.

Institutional Review Board Statement: The Good Clinical Practice guidelines and the ethical principles of the Declaration of Helsinki were followed. The Hospital Ethical Committee of the "Maggiore della Carità" University Hospital also approved it (CE 54/17).

Informed Consent Statement: Informed consent was obtained from all subjects involved in the study.

Data Availability Statement: All relevant data are available within the manuscript.

Acknowledgments: The authors thank all study participants and their families and caregivers for their dedication and contribution to MND research.

Conflicts of Interest: The authors declare no conflict of interest.

References

1. Feldman, E.L.; Goutman, S.A.; Petri, S.; Mazzini, L.; Savelieff, M.G.; Shaw, P.J.; Sobue, G. Amyotrophic lateral sclerosis. *Lancet* **2022**, *400*, 1363–1380. [CrossRef] [PubMed]
2. Johnson, S.A.; Fang, T.; De Marchi, F.; Neel, D.; Van Weehaeghe, D.; Berry, J.D.; Paganoni, S. Pharmacotherapy for Amyotrophic Lateral Sclerosis: A Review of Approved and Upcoming Agents. *Drugs* **2022**, *82*, 1367–1388. [CrossRef]
3. Goutman, S.A.; Hardiman, O.; Al-Chalabi, A.; Chió, A.; Savelieff, M.G.; Kiernan, M.C.; Feldman, E.L. Recent advances in the diagnosis and prognosis of amyotrophic lateral sclerosis. *Lancet Neurol.* **2022**, *21*, 480–493. [CrossRef] [PubMed]
4. Vucic, S.; Rothstein, J.D.; Kiernan, M.C. Advances in treating amyotrophic lateral sclerosis: Insights from pathophysiological studies. *Trends Neurosci.* **2014**, *37*, 433–442. [CrossRef] [PubMed]
5. Mejzini, R.; Flynn, L.L.; Pitout, I.L.; Fletcher, S.; Wilton, S.D.; Akkari, P.A. ALS genetics, mechanisms, and therapeutics: Where are we now? *Front. Neurosci.* **2019**, *13*, 1310. [CrossRef]
6. Shatunov, A.; Al-Chalabi, A. The genetic architecture of ALS. *Neurobiol. Dis.* **2021**, *147*, 105156. [CrossRef]
7. Oskarsson, B.; Horton, D.K.; Mitsumoto, H. Potential Environmental Factors in Amyotrophic Lateral Sclerosis. *Neurol. Clin.* **2015**, *33*, 877–888. [CrossRef]
8. Alonso, A.; Logroscino, G.; Hernán, M.A. Smoking and the risk of amyotrophic lateral sclerosis: A systematic review and meta-analysis. *J. Neurol. Neurosurg. Psychiatry* **2010**, *81*, 1249–1252. [CrossRef]
9. Amyotrophic Lateral Sclerosis/Riluzole Study Group II; Lacomblez, L.; Bensimon, G.; Meininger, V.; Leigh, P.N.; Guillet, P. Dose-ranging study of riluzole in amyotrophic lateral sclerosis. *Lancet* **1996**, *347*, 1425–1431. [CrossRef]
10. Bensimon, G.; Lacomblez, L.; Meininger, V.; the ALS/Riluzole Study Group. A controlled trial of riluzole in amyotrophic lateral sclerosis. *N. Engl. J. Med.* **1994**, *330*, 585–591. [CrossRef]
11. Dash, R.P.; Babu, R.J.; Srinivas, N.R. Two Decades-Long Journey from Riluzole to Edaravone: Revisiting the Clinical Pharmacokinetics of the Only Two Amyotrophic Lateral Sclerosis Therapeutics. *Clin. Pharmacokinet.* **2018**, *57*, 1385–1398. [CrossRef] [PubMed]
12. Group WG on Behalf of the E (MCI-186) ALS 18 S. Exploratory double-blind, parallel-group, placebo-controlled study of edaravone (MCI-186) in amyotrophic lateral sclerosis (Japan ALS severity classification: Grade 3, requiring assistance for eating, excretion or ambulation). *Amyotroph. Lateral Scler. Front. Degener.* **2017**, *18* (Suppl. 1), 40–48. [CrossRef] [PubMed]
13. Bedlack, R.S.; Joyce, N.; Carter, G.T.; Paganoni, S.; Karam, C. Complementary and alternative therapies in amyotrophic lateral sclerosis. *Neurol. Clin.* **2015**, *33*, 909–936. [CrossRef] [PubMed]
14. Jones, L.L.; McDonald, D.A.; Borum, P.R. Acylcarnitines: Role in brain. *Prog. Lipid Res.* **2010**, *49*, 61–75. [CrossRef]
15. De Marchi, F.; Venkatesan, S.; Saraceno, M.; Mazzini, L.; Grossini, E. Acetyl-L-carnitine and Amyotrophic Lateral Sclerosis: Current evidence and potential use. *CNS Neurol. Disord. Drug Targets* **2023**. [CrossRef]

16. Zanelli, S.A.; Solenski, N.J.; Rosenthal, R.E.; Fiskum, G. Mechanisms of ischemic neuroprotection by acetyl-L-carnitine. *Ann. N. Y. Acad. Sci.* **2005**, *1053*, 153–161.
17. White, H.L.; Scates, P.W. Acetyl-L-carnitine as a precursor of acetylcholine. *Neurochem. Res.* **1990**, *15*, 597–601. [CrossRef]
18. Kidd, P.M. Neurodegeneration from mitochondrial insufficiency: Nutrients, stem cells, growth factors, and prospects for brain rebuilding using integrative management. *Altern. Med. Rev.* **2005**, *10*, 268.
19. Hota, K.B.; Hota, S.K.; Chaurasia, O.P.; Singh, S.B. Acetyl-L-carnitine-mediated neuroprotection during hypoxia is attributed to ERK1/2-Nrf2-regulated mitochondrial biosynthesis. *Hippocampus* **2012**, *22*, 723–736. [CrossRef]
20. Patel, S.P.; Sullivan, P.G.; Lyttle, T.S.; Magnuson, D.S.K.; Rabchevsky, A.G. Acetyl-L-carnitine treatment following spinal cord injury improves mitochondrial function correlated with remarkable tissue sparing and functional recovery. *Neuroscience* **2012**, *210*, 296–307. [CrossRef]
21. Bigini, P.; Larini, S.; Pasquali, C.; Muzio, V.; Mennini, T. Acetyl-L-carnitine shows neuroprotective and neurotrophic activity in primary culture of rat embryo motoneurons. *Neurosci. Lett.* **2002**, *329*, 334–338. [CrossRef] [PubMed]
22. Kira, Y.; Nishikawa, M.; Ochi, A.; Sato, E.; Inoue, M. L-carnitine suppresses the onset of neuromuscular degeneration and increases the life span of mice with familial amyotrophic lateral sclerosis. *Brain Res.* **2006**, *1070*, 206–214. [CrossRef] [PubMed]
23. Beghi, E.; Pupillo, E.; Bonito, V.; Buzzi, P.; Caponnetto, C.; Chiò, A.; Corbo, M.; Giannini, F.; Inghilleri, M.; Bella, V.L.; et al. Randomized double-blind placebo-controlled trial of acetyl-L-carnitine for ALS. *Amyotroph. Lateral Scler. Front. Degener.* **2013**, *14*, 397–405. [CrossRef] [PubMed]
24. Garbuzova-Davis, S.; Saporta, S.; Sanberg, P.R. Implications of blood-brain barrier disruption in ALS. *Amyotroph. Lateral Scler.* **2008**, *9*, 375–376. [CrossRef] [PubMed]
25. Garbuzova-Davis, S.; Ehrhart, J.; Mustafa, H.; Llauget, A.; Boccio, K.J.; Sanberg, P.R.; Appel, S.H.; Borlongan, C.V. Phenotypic characteristics of human bone marrow-derived endothelial progenitor cells in vitro support cell effectiveness for repair of the blood-spinal cord barrier in ALS. *Brain Res.* **2019**, *1724*, 146428. [CrossRef]
26. Yu, X.; Ji, C.; Shao, A. Neurovascular Unit Dysfunction and Neurodegenerative Disorders. *Front. Neurosci.* **2020**, *14*, 334. [CrossRef]
27. Grossini, E.; Garhwal, D.; Venkatesan, S.; Ferrante, D.; Mele, A.; Saraceno, M.; Scognamiglio, A.; Mandrioli, J.; Amedei, A.; De Marchi, F.; et al. The Potential Role of Peripheral Oxidative Stress on the Neurovascular Unit in Amyotrophic Lateral Sclerosis Pathogenesis: A Preliminary Report from Human and In Vitro Evaluations. *Biomedicines* **2022**, *10*, 691. [CrossRef]
28. Brooks, B.R.; Miller, R.G.; Swash, M.; Munsat, T.L. El Escorial revisited: Revised criteria for the diagnosis of amyotrophic lateral sclerosis. *Amyotroph. Lateral Scler. Other Mot. Neuron Disord.* **2000**, *1*, 293–299. [CrossRef]
29. Ludolph, A.; Drory, V.; Hardiman, O.; Nakano, I.; Ravits, J.; Robberecht, W.; Shefner, J. A revision of the El Escorial criteria-2015. *Amyotroph. Lateral Scler. Front. Degener.* **2015**, *16*, 291–292. [CrossRef]
30. Galiniak, S.; Mołoń, M.; Biesiadecki, M.; Bożek, A.; Rachel, M. The Role of Oxidative Stress in Atopic Dermatitis and Chronic Urticaria. *Antioxidants* **2022**, *11*, 1590. [CrossRef]
31. Grossini, E.; Farruggio, S.; Pierelli, D.; Bolzani, V.; Rossi, L.; Pollesello, P.; Monaco, C. Levosimendan Improves Oxidative Balance in Cardiogenic Shock/Low Cardiac Output Patients. *J. Clin. Med.* **2020**, *9*, 373. [CrossRef] [PubMed]
32. Bilgic, H.A.; Kilic, B.; Kockaya, B.D.; Sarac, B.E.; Suloglu, A.K.; Kalayci, O.; Karaaslan, C. Oxidative stress stimulation leads to cell-specific oxidant and antioxidant responses in airway resident and inflammatory cells. *Life Sci.* **2023**, *315*, 121358. [CrossRef] [PubMed]
33. Dematteis, G.; Vydmantaitė, G.; Ruffinatti, F.A.; Chahin, M.; Farruggio, S.; Barberis, E.; Ferrari, E.; Marengo, E.; Distasi, C.; Morkūnienė, R.; et al. Proteomic analysis links alterations of bioenergetics, mitochondria-ER interactions and proteostasis in hippocampal astrocytes from 3xTg-AD mice. *Cell Death Dis.* **2020**, *11*, 645. [CrossRef] [PubMed]
34. De Cillà, S.; Farruggio, S.; Cocomazzi, G.; Mary, D.; Alkabes, M.; Rossetti, L.; Vujosevic, S.; Grossini, E. Aflibercept and Ranibizumab Modulate Retinal Pigment Epithelial Cells Function by Acting on Their Cross Talk with Vascular Endothelial Cells. *Cell. Physiol. Biochem.* **2020**, *54*, 161–179. [PubMed]
35. Grossini, E.; Venkatesan, S.; Alkabes, M.; Toma, C.; de Cillà, S. Membrane Blue Dual Protects Retinal Pigment Epithelium Cells/Ganglion Cells-Like through Modulation of Mitochondria Function. *Biomedicines* **2022**, *10*, 2854. [CrossRef]
36. Roos, N.J.; Duthaler, U.; Bouitbir, J.; Krähenbühl, S. The uricosuric benzbromarone disturbs the mitochondrial redox homeostasis and activates the NRF2 signaling pathway in HepG2 cells. *Free Radic. Biol. Med.* **2020**, *152*, 216–226. [CrossRef]
37. Stufano, A.; Isgrò, C.; Palese, L.L.; Caretta, P.; De Maria, L.; Lovreglio, P.; Sardanelli, A.M. Oxidative Damage and Post-COVID Syndrome: A Cross-Sectional Study in a Cohort of Italian Workers. *Int. J. Mol. Sci.* **2023**, *24*, 7445. [CrossRef]
38. Bahrami, A.; Nikoomanesh, F.; Khorasanchi, Z.; Mohamadian, M.; Ferns, G.A. The relationship between food quality score with inflammatory biomarkers, and antioxidant capacity in young women. *Physiol. Rep.* **2023**, *11*, e15590. [CrossRef]
39. Dos Santos, J.M.; Taiar, R.; Ribeiro, V.G.C.; da Silva Lage, V.K.; Scheidt Figueiredo, P.H.; Costa, H.S.; Pereira Lima, V.; Sañudo, B.; Bernardo-Filho, M.; Sá-Caputo, D.D.C.D.; et al. Whole-Body Vibration Training on Oxidative Stress Markers, Irisin Levels, and Body Composition in Women with Fibromyalgia: A Randomized Controlled Trial. *Bioengineering* **2023**, *10*, 260. [CrossRef]
40. Devos, D.; Moreau, C.; Kyheng, M.; Garçon, G.; Rolland, A.S.; Blasco, H.; Gelé, P.; Timothée Lenglet, T.; Veyrat-Durebex, C.; Corcia, P.; et al. A ferroptosis-based panel of prognostic biomarkers for Amyotrophic Lateral Sclerosis. *Sci. Rep.* **2019**, *9*, 2918. [CrossRef]

41. Lan, J.; Zhou, Y.; Wang, H.; Tang, J.; Kang, Y.; Wang, P.; Liu, X.; Peng, Y. Protective effect of human umbilical cord mesenchymal stem cell derived conditioned medium in a mutant TDP-43 induced motoneuron-like cellular model of ALS. *Brain Res. Bull.* **2023**, *193*, 106–116. [CrossRef] [PubMed]
42. Dzik, K.P.; Flis, D.J.; Bytowska, Z.K.; Karnia, M.J.; Ziolkowski, W.; Kaczor, J.J. Swim Training Ameliorates Hyperlocomotion of ALS Mice and Increases Glutathione Peroxidase Activity in the Spinal Cord. *Int. J. Mol. Sci.* **2021**, *22*, 11614. [CrossRef] [PubMed]
43. Aguilar Diaz De Leon, J.; Borges, C.R. Evaluation of Oxidative Stress in Biological Samples Using the Thiobarbituric Acid Reactive Substances Assay. *J. Vis. Exp.* **2020**, *159*, e61122.
44. Grossini, E.; Concina, D.; Rinaldi, C.; Russotto, S.; Garhwal, D.; Zeppegno, P.; Gramaglia, C.; Kul, S.; Panella, M. Association Between Plasma Redox State/Mitochondria Function and a Flu-Like Syndrome/COVID-19 in the Elderly Admitted to a Long-Term Care Unit. *Front. Physiol.* **2021**, *12*, 707587. [CrossRef]
45. Zeppegno, P.; Krengli, M.; Ferrante, D.; Bagnati, M.; Burgio, V.; Farruggio, S.; Rolla, R.; Gramaglia, C.; Grossini, E. Psychotherapy with Music Intervention Improves Anxiety, Depression and the Redox Status in Breast Cancer Patients Undergoing Radiotherapy: A Randomized Controlled Clinical Trial. *Cancers* **2021**, *13*, 1752. [CrossRef] [PubMed]
46. Giustarini, D.; Fanti, P.; Matteucci, E.; Rossi, R. Micro-method for the determination of glutathione in human blood. *J. Chromatogr. B* **2014**, *964*, 191–194. [CrossRef]
47. Kalita, J.; Shukla, R.; Pandey, P.C.; Misra, U.K. Balancing between apoptosis and survival biomarkers in the patients with tuberculous meningitis. *Cytokine* **2022**, *157*, 155960. [CrossRef] [PubMed]
48. Safe, I.P.; Amaral, E.P.; Araújo-Pereira, M.; Lacerda, M.V.G.; Printes, V.S.; Souza, A.B.; Beraldi-Magalhães, F.; Monteiro, W.M.; Sampaio, V.S.; Barreto-Duarte, B.; et al. Adjunct N-Acetylcysteine Treatment in Hospitalized Patients With HIV-Associated Tuberculosis Dampens the Oxidative Stress in Peripheral Blood: Results from the RIPENACTB Study Trial. *Front. Immunol.* **2020**, *11*, 602589. [CrossRef]
49. Ferrante, R.J.; Browne, S.E.; Shinobu, L.A.; Bowling, A.C.; Baik, M.J.; MacGarvey, U.; Kowall, N.W.; Brown, R.H., Jr.; Beal, M.F. Evidence of increased oxidative damage in both sporadic and familial amyotrophic lateral sclerosis. *J. Neurochem.* **1997**, *69*, 2064–2074. [CrossRef]
50. Kim, K. Glutathione in the Nervous System as a Potential Therapeutic Target to Control the Development and Progression of Amyotrophic Lateral Sclerosis. *Antioxidants* **2021**, *10*, 1011. [CrossRef]
51. Babu, G.N.; Kumar, A.; Chandra, R.; Puri, S.; Singh, R.; Kalita, J.; Misra, U. Oxidant-antioxidant imbalance in the erythrocytes of sporadic amyotrophic lateral sclerosis patients correlates with the progression of disease. *Neurochem. Int.* **2008**, *52*, 1284–1289. [CrossRef] [PubMed]
52. Cova, E.; Bongioanni, P.; Cereda, C.; Metelli, M.R.; Salvaneschi, L.; Bernuzzi, S.; Guareschi, S.; Rossi, B.; Ceroni, M. Time course of oxidant markers and antioxidant defenses in subgroups of amyotrophic lateral sclerosis patients. *Neurochem. Int.* **2010**, *56*, 687–693. [CrossRef] [PubMed]
53. Kuźma, M.; Jamrozik, Z.; Barańczyk-Kuźma, A. Activity and expression of glutathione S-transferase pi in patients with amyotrophic lateral sclerosis. *Clin. Chim. Acta* **2006**, *364*, 217–221. [CrossRef] [PubMed]
54. Tohgi, H.; Abe, T.; Yamazaki, K.; Murata, T.; Ishizaki, E.; Isobe, C. Increase in oxidized NO products and reduction in oxidized glutathione in cerebrospinal fluid from patients with sporadic form of amyotrophic lateral sclerosis. *Neurosci. Lett.* **1999**, *260*, 204–206. [CrossRef] [PubMed]
55. Lee, M.; Hyun, D.; Jenner, P.; Halliwell, B. Effect of overexpression of wild-type and mutant Cu/Zn-superoxide dismutases on oxidative damage and antioxidant defences: Relevance to Down's syndrome and familial amyotrophic lateral sclerosis. *J. Neurochem.* **2001**, *76*, 957–965. [CrossRef]
56. Przedborski, S.; Donaldson, D.; Jakowec, M.; Kish, S.J.; Guttman, M.; Rosoklija, G.; Hays, A.P. Brain superoxide dismutase, catalase, and glutathione peroxidase activities in amyotrophic lateral sclerosis. *Ann. Neurol.* **1996**, *39*, 158–165. [CrossRef]
57. Boillée, S.; Velde CVande Cleveland, D.W. ALS: A disease of motor neurons and their nonneuronal neighbors. *Neuron* **2006**, *52*, 39–59. [CrossRef]
58. Van Es, M.A.; Hardiman, O.; Chio, A.; Al-Chalabi, A.; Pasterkamp, R.J.; Veldink, J.H.; Van den Berg, L.H. Amyotrophic lateral sclerosis. *Lancet* **2017**, *390*, 2084–2098. [CrossRef]
59. Dobrowolny, G.; Aucello, M.; Rizzuto, E.; Beccafico, S.; Mammucari, C.; Bonconpagni, S.; Belia, S.; Wannenes, F.; Nicoletti, C.; Del Prete, Z.; et al. Skeletal muscle is a primary target of SOD1G93A-mediated toxicity. *Cell Metab.* **2008**, *8*, 425–436. [CrossRef]
60. Magrané, J.; Cortez, C.; Gan, W.-B.; Manfredi, G. Abnormal mitochondrial transport and morphology are common pathological denominators in SOD1 and TDP43 ALS mouse models. *Hum. Mol. Genet.* **2014**, *23*, 1413–1424. [CrossRef]
61. Kausar, S.; Wang, F.; Cui, H. The Role of Mitochondria in Reactive Oxygen Species Generation and Its Implications for Neurodegenerative Diseases. *Cells* **2018**, *7*, 274. [CrossRef] [PubMed]
62. Abdul Muneer, P.M.; Alikunju, S.; Szlachetka, A.M.; Mercer, A.J.; Haorah, J. Ethanol impairs glucose uptake by human astrocytes and neurons: Protective effects of acetyl-L-carnitine. *Int. J. Physiol. Pathophysiol. Pharmacol.* **2011**, *3*, 48–56. [PubMed]
63. Karalija, A.; Novikova, L.N.; Kingham, P.J.; Wiberg, M.; Novikov, L.N. Neuroprotective effects of N-acetyl-cysteine and acetyl-L-carnitine after spinal cord injury in adult rats. *PLoS ONE* **2012**, *7*, e41086. [CrossRef]
64. Sorrentino, S.; Polini, A.; Arima, V.; Romano, A.; Quattrini, A.; Gigli, G.; Mozetic, P.; Moroni, L. Neurovascular signals in amyotrophic lateral sclerosis. *Curr. Opin. Biotechnol.* **2022**, *74*, 75–83. [CrossRef] [PubMed]

65. Garbuzova-Davis, S.; Haller, E.; Saporta, S.; Kolomey, I.; Nicosia, S.V.; Sanberg, P.R. Ultrastructure of blood–brain barrier and blood–spinal cord barrier in SOD1 mice modeling ALS. *Brain Res.* **2007**, *1157*, 126–137. [CrossRef]
66. Miyazaki, K.; Ohta, Y.; Nagai, M.; Morimoto, N.; Kurata, T.; Takehisa, Y.; Ikeda, Y.; Matsuura, T.; Abe, K. Disruption of neurovascular unit prior to motor neuron degeneration in amyotrophic lateral sclerosis. *J. Neurosci. Res.* **2011**, *89*, 718–728. [CrossRef]
67. Zhong, Z.; Deane, R.; Ali, Z.; Parisi, M.; Shapovalov, Y.; O'Banion, M.K.; Stojanovic, K.; Sagare, A.; Boillee, S.; Cleveland, D.W.; et al. ALS-causing SOD1 mutants generate vascular changes prior to motor neuron degeneration. *Nat. Neurosci.* **2008**, *11*, 420–422. [CrossRef]
68. Garbuzova-Davis, S.; Woods, R.L., III; Louis, M.K.; Zesiewicz, T.A.; Kuzmin-Nichols, N.; Sullivan, K.L.; Miller, A.M.; Hernandez-Ontiveros, D.G.; Sanberg, P.R. Reduction of circulating endothelial cells in peripheral blood of ALS patients. *PLoS ONE* **2010**, *5*, e10614. [CrossRef]
69. Zhong, Z.; Ilieva, H.; Hallagan, L.; Bell, R.; Singh, I.; Paquette, N.; Thiyagarajan, M.; Deane, R.; Fernandez, J.A.; Lane, S.; et al. Activated protein C therapy slows ALS-like disease in mice by transcriptionally inhibiting SOD1 in motor neurons and microglia cells. *J. Clin. Investig.* **2009**, *119*, 3437–3449. [CrossRef]
70. Levine, J.B.; Kong, J.; Nadler, M.; Xu, Z. Astrocytes interact intimately with degenerating motor neurons in mouse amyotrophic lateral sclerosis (ALS). *Glia* **1999**, *28*, 215–224. [CrossRef]
71. Alexianu, M.E.; Kozovska, M.; Appel, S.H. Immune reactivity in a mouse model of familial ALS correlates with disease progression. *Neurology* **2001**, *57*, 1282–1289. [CrossRef] [PubMed]
72. Engelhardt, J.I.; Tajti, J.; Appel, S.H. Lymphocytic infiltrates in the spinal cord in amyotrophic lateral sclerosis. *Arch. Neurol.* **1993**, *50*, 30–36. [CrossRef]
73. Nakamura, T.; Lipton, S.A. Protein S-Nitrosylation as a Therapeutic Target for Neurodegenerative Diseases. *Trends Pharmacol. Sci.* **2016**, *37*, 73–84. [CrossRef]
74. Calabrese, V.; Mancuso, C.; Calvani, M.; Rizzarelli, E.; Butterfield, D.A.; Stella, A.M.G. Nitric oxide in the central nervous system: Neuroprotection versus neurotoxicity. *Nat. Rev. Neurosci.* **2007**, *8*, 766–775. [CrossRef]
75. Contestabile, A.; Monti, B.; Polazzi, E. Neuronal-glial Interactions Define the Role of Nitric Oxide in Neural Functional Processes. *Curr. Neuropharmacol.* **2012**, *10*, 303–310. [CrossRef] [PubMed]
76. Ghasemi, M.; Fatemi, A. Pathologic role of glial nitric oxide in adult and pediatric neuroinflammatory diseases. *Neurosci. Biobehav. Rev.* **2014**, *45*, 168–182. [CrossRef] [PubMed]
77. Yuste, J.E.; Tarragon, E.; Campuzano, C.M.; Ros-Bernal, F. Implications of glial nitric oxide in neurodegenerative diseases. *Front. Cell. Neurosci.* **2015**, *9*, 322. [CrossRef]
78. Ferreira, G.C.; McKenna, M.C. L-Carnitine and acetyl-L-carnitine roles and neuroprotection in developing brain. *Neurochem. Res.* **2017**, *42*, 1661–1675. [CrossRef]
79. Virmani, M.A.; Cirulli, M. The Role of l-Carnitine in Mitochondria, Prevention of Metabolic Inflexibility and Disease Initiation. *Int. J. Mol. Sci.* **2022**, *23*, 2717. [CrossRef]

antioxidants

MDPI

Article

Defects in Glutathione System in an Animal Model of Amyotrophic Lateral Sclerosis

Franziska T. Wunsch [1,2], Nils Metzler-Nolte [3], Carsten Theiss [1,2] and Veronika Matschke [1,*]

[1] Department of Cytology, Institute of Anatomy, Ruhr-University Bochum, D-44801 Bochum, Germany; franziska.wunsch@rub.de (F.T.W.); carsten.theiss@rub.de (C.T.)
[2] International Graduate School of Neuroscience (IGSN), Ruhr-University Bochum, D-44801 Bochum, Germany
[3] Inorganic Chemistry I—Bioinorganic Chemistry, Faculty of Chemistry and Biochemistry, Ruhr-University Bochum, D-44801 Bochum, Germany; nils.metzler-nolte@rub.de
* Correspondence: veronika.matschke@rub.de; Tel.: +49-234-32-25018

Abstract: Amyotrophic lateral sclerosis (ALS) is a progredient neurodegenerative disease characterized by a degeneration of the first and second motor neurons. Elevated levels of reactive oxygen species (ROS) and decreased levels of glutathione, which are important defense mechanisms against ROS, have been reported in the central nervous system (CNS) of ALS patients and animal models. The aim of this study was to determine the cause of decreased glutathione levels in the CNS of the ALS model wobbler mouse. We analyzed changes in glutathione metabolism in the spinal cord, hippocampus, cerebellum, liver, and blood samples of the ALS model, wobbler mouse, using qPCR, Western Blot, HPLC, and fluorometric assays. Here, we show for the first time a decreased expression of enzymes involved in glutathione synthesis in the cervical spinal cord of wobbler mice. We provide evidence for a deficient glutathione metabolism, which is not restricted to the nervous system, but can be seen in various tissues of the wobbler mouse. This deficient system is most likely the reason for an inefficient antioxidative system and, thus, for elevated ROS levels.

Keywords: ALS; oxidative stress; wobbler mice; liver; hippocampus; cerebellum; glutamate cysteine ligase (GCL); glutathione synthetase (GSS); multidrug resistance protein (MRP); gamma-glutamyl transpeptidase (GGT)

Citation: Wunsch, F.T.; Metzler-Nolte, N.; Theiss, C.; Matschke, V. Defects in Glutathione System in an Animal Model of Amyotrophic Lateral Sclerosis. *Antioxidants* **2023**, *12*, 1014. https://doi.org/10.3390/antiox12051014

Academic Editors: Ana-Maria Buga and Carmen Nicoleta Oancea

Received: 20 March 2023
Revised: 24 April 2023
Accepted: 26 April 2023
Published: 27 April 2023

1. Introduction

Amyotrophic lateral sclerosis (ALS) is a progressive neurodegenerative disease characterized by the rapid degeneration of motor neurons in the motor cortex, brain stem, and spinal cord. To date, the pathogenesis and pathomechanisms of ALS have not been fully elucidated, with the majority of patients exhibiting signs of oxidative stress [1–5]. Similar to other neurodegenerative diseases, ALS is thought to be caused by a combination of genetic and environmental factors as well as age-related dysfunction [6]. The understanding of these genetic and pathophysiological mechanisms of ALS has led to the identification of promising therapeutic targets. However, over the past half-century, more than 50 randomized controlled trials (RCT) for proposed disease-modifying drugs have been negative [7]. Thus, no causative therapy exists so far [8].

Genetic studies of ALS have led to the development of numerous mouse models, which are highly relevant for understanding the pathophysiology of the disease and for the development of therapeutic targets. Among others, the wobbler mouse (WR) that spontaneously emerged in a C57BL/Fa strain is used as an ALS animal model [9]. These mice exhibit a spontaneous autosomal-recessive point mutation in the *vacuolar–vesicular protein sorting 54 (VPS54)* gene, which was soon linked to the degeneration of upper and lower motor neurons [10,11]. The point mutation results in a destabilization of the Golgi-associated retrograde protein (GARP) complex, which leads to an impairment of the retrograde vesicle

transport and a missorting of endosomal and Golgi-associated proteins [12]. Golgi dysfunctions in wobbler mice have been related to various pathological abnormalities in motor neurons [13]. Recently, mutations in the *VPS54* gene have been discovered in ALS patients within Project MinE (http://databrowser.projectmine.com/, accessed on 24 April 2023) [14]. However, the exact role of Golgi dysfunction in the development of ALS remains to be investigated [12]. In homozygous wobbler mice, motor neuron death develops over time, and these mice mimic ALS symptoms, as seen in ALS patients [13]. The course of disease in wobbler mice can be divided into three phases [15]. In the pre-symptomatic phase, starting postnatal (p0), no clinical symptoms are present. Clinical symptoms arise during the evolutionary phase from p20 until p40. Here, wobbler mice progressively develop an unsteady gait, muscle weakness, and characteristic head tremors. In addition to this, wobbler mice remain smaller than their healthy littermates [16]. In the following symptomatic phase or distinct clinical stage, starting from p40, all symptoms fully develop and stagnate. The mice ultimately die from insufficiency of the respiratory musculature [15].

Elevated levels of reactive oxygen species (ROS) have been reported in the spinal cord tissue of wobbler mice [17,18] as well as in different cells derived from ALS patients [3,4,19]. The consequences of oxidative stress, such as damage to DNA, proteins, and lipid membranes, can be found in ALS patients [1,5,20–23] as well as in different ALS mouse models [18,24–27].

For maintaining the cells' redox balance, an antioxidant detoxification system is vitally important [28]. This includes endogenous antioxidant enzymes and co-enzymes, such as glutathione and ubiquinone, as well as exogenous dietary antioxidant molecules, such as ascorbic acid and tocopherols. Glutathione is the most abundant antioxidant in the cell [28]. Reduced levels of glutathione are not only present in apoptosis but also precede neurodegeneration [29]. The bulk of plasma glutathione originates from the liver as hepatocytes export glutathione into plasma for inter-organ glutathione homeostasis [30]. Plasma glutathione has been reported to influence glutathione uptake at the blood–brain barrier [31–33]. Unlike astrocytes, neurons do not have an uptake mechanism for glutathione and, therefore, rely on their own synthesis to maintain adequate concentrations. Astrocytes play an essential role in providing neurons with substrates for glutathione synthesis [34]. In the central nervous system (CNS), glutathione is cleaved into its constituent amino acid in the extracellular space by enzymes located in the plasma membrane of different cell types of the CNS [35]. The generated cysteine and glycine can then be imported into other cells, such as neurons and oligodendrocytes, via different amino acid transporters [36]. Notably, cysteine has been reported to be the rate-limiting precursor for glutathione synthesis in neurons [37,38]. In the first step of glutathione synthesis, the enzyme γ-Glutamyl-cysteinyl-ligase (GCL), which consists of a catalytic (GCLC) and a modifier subunit (GCLM), creates γ-glutamyl-cysteine from the amino acids glutamate and cysteine under consumption of adenosine triphosphate (ATP). This first step of GSH synthesis is considered to be rate-limiting [39]. The next step is catalyzed by the glutathione synthetase (GSS). It adds glycine to the precursor γ-glutamyl-cysteine under the consumption of ATP, and glutathione is formed.

Accumulating evidence suggests that aberrant glutathione homeostasis is linked to the development and progression of ALS, as recently reviewed by Kim [40]. This includes low levels of glutathione in erythrocytes of ALS patients [41] and, importantly, the detection of reduced levels of glutathione by 31% in the precentral gyrus of ALS patients compared to healthy volunteers, using a magnet resonance (MR) spectroscopic technique [42]. Another MR spectroscopic imaging study revealed that glutathione levels in the motor cortex and corticospinal tract of ALS patients inversely correlate with time from diagnosis to imaging [43]. On the molecular level, reduced levels of glutathione and a decreased ratio of reduced glutathione (GSH)/oxidized glutathione (GSSG) in whole blood and the lumbar spinal cord have been reported in G93A-SOD1 transgenic mice [44,45] as well as in cervical spinal cord of wobbler mice [18].

In this study, we aim to determine the cause of glutathione depletion in the cervical spinal cord of wobbler mice. Therefore, we compared factors of glutathione synthesis and ROS levels in different organ systems (liver, blood) and different CNS areas (spinal cord, hippocampus, cerebellum) to clarify whether defects in glutathione homeostasis in wobbler mice are restricted to motor areas of the CNS.

2. Materials and Methods

2.1. Animals

All animal experiments were performed in accordance with EU guidelines 2010/63/EU concerning the protection of animals used for scientific purposes. Animal experiments were conducted according to German animal welfare regulations and approved by the local authorities (registration number Az. 84-02.04.2017.A085). Breeding, handling, and genotyping were carried out as described previously [16]. Mice always had free access to food and water and were kept at a 12-h night-and-day cycle. For each experiment, three to six homozygous wild-type (wt/wt) and wobbler (wr/wr) mice in the distinct clinical phase (p40) were used. Both genders were used.

2.2. Sample Collection

For qPCR, Western Blot, glutathione, and ROS analysis, mice were sacrificed by decapitation. The cervical part of the spinal cord, liver, hippocampus, and cerebellum were isolated, snap-frozen in liquid nitrogen, and stored at −80 °C. For the collection of whole blood, erythrocyte, and plasma samples, mice were deeply anesthetized with a combination of Ketamin (100 mg/kg) and Xylazin (10 mg/kg). After thoracic dissection, blood was collected from the left ventricle in a K3EDTA laminated vessel (#20.1341, Sarstedt, Nümbrecht, Germany). For erythrocyte and plasma collection, samples were centrifuged at 2000× *g* at 4 °C for 15 min. Afterward, the plasma and erythrocyte fraction were transferred to a clean tube. Blood samples were stored at −80 °C.

2.3. RNA-Isolation, Reverse Transcription, and Quantitative PCR

Total ribonucleic acid (RNA) was isolated from 15–20 mg of frozen tissue using the ReliaPrep™ RNA Tissue Miniprep System (#Z6111, Promega, Madison, WI, USA) following the manufacturer's protocol. Afterward, 500 ng of purified RNA was transcribed into complementary desoxyribonucleic acid (cDNA) using the GoScript™ Reverse Transcription Mix, Oligo(dT) (#A2791, Promega, Madison, WI, USA) according to the manufacturer's instructions. The quantitative real-time polymerase chain reaction (qPCR) was conducted with 400 ng of cDNA. qPCR was performed using the GoTaq® qPCR Master Mix (#A6001, Promega) on a CFX96 Real-Time PCR Detection System (Bio-Rad, Hercules, CA, USA). Specific primers used are shown in Table 1. Gene expression was investigated in triplicates and normalized to *Glyceraldehyde–phosphate dehydrogenase* (*GAPDH)*. The analysis was performed with tissue samples collected from at least four wild-type (WT) and four wobbler mice (WR). The obtained cycle threshold (Ct)-values were analyzed using the $2^{-\Delta\Delta Ct}$—method [46].

Table 1. Specific primers used for quantitative PCR.

Gene (Gene ID)	Sense Primer	Antisense Primer
Anpep (16790)	5′-TGGAGGATCTTTCTCCTTTGCC-3′	5′-GTGGCTGAGTTATCCGCTTT-3′
Eaat3 (20510)	5′-TTCCTACGGAATCACTGGCTG-3′	5′-TGTGTCCTCGAACCACGACT-3′
Gapdh (14433)	5′-GGAGAAACCTGCCAAGTATGA-3′	5′-TCCTCAGTGTAGCCCAAGA-3′
Gclc (14629)	5′-ACAAGGACGTGCTCAAGTGG-3′	5′-GTCTCAAGAACATCGCCTCCA-3′
Gclm (14630)	5′-CCCCGATTTAGTCAGGGAGTTT-3′	5′-TTTCATCGGGATTTATCTTCTCCAC-3′
Ggt1 (14598)	5′-GAAGCCCGACCACGTGTACT-3′	5′-CCACGGAACCACCTTCCTGT-3′
Ggt6 (71522)	5′-ACAAGCTACAACTCTGGGAGC-3′	5′-CTCCTTAGGGAGAGGACCAG-3′
Ggt7 (207182)	5′-TTCGTCGTCATCGGAGATGG-3′	5′-GCAGCTGAGAATGGGTCCTT-3′
Gls1 (14660)	5′-GGTCTTCCTGCAAAATCTGGA-3′	5′-CCTTAACACTGTTGCCCATCT-3′

Table 1. *Cont.*

Gene (Gene ID)	Sense Primer	Antisense Primer
Gls2 (216456)	5′-ACAAGACCGTGGTGAACCTG-3′	5′-GGCTGTGCGGGAATCATAGT-3′
Gss (14854)	5′-AGGACGACTATACTGCCCGT-3′	5′-AATCTGAGCGATTCAGGCCC-3′
Mrp1 (17250)	5′-GCTGGGCAGACCTCTTCTAC-3′	5′-CAGTGTTGGGCTGACCAGTA-3′
Mrp4 (239273)	5′-CGTTTGCTGACCTCATTGCC-3′	5′-ACGCCATGTTCATCCCTCTG-3′
Slc3a2 (17254)	5′-TGGTTATCATCGTTCGGGCG-3′	5′-GCCTACAAAGGCCTGAAGGT-3′
Slc7a11 (26570)	5′-CACTTTTTGGAGCCCTGTCC-3′	5′-CCAGCAAAGGACCAAAGACC-3′
Slc25a11 (67863)	5′-CTGGTGCATTTGTGGGAACG-3′	5′-ACATTTTTGTAGCCACGGCG-3′

2.4. SDS-PAGE and Western Blot

For protein isolation, 15–20 mg of frozen tissue was used. Tissue samples were subjected to Radioimmunoprecipitation Assay (RIPA) buffer (#9806, Cell Signaling Technology, Danvers, MA, USA), supplemented with protease inhibitor (#11873580001, Roche, Mannheim, Germany) and homogenized with a clearance pestle and a 27G syringe. Samples were kept on ice the whole time. Next, samples were centrifuged at 12,700× *g* for 15 min at 4 °C, and the supernatant was transferred to a clean tube. Protein concentration was determined by Pierce™ BCA Protein Assay Kit (#23225, Thermo Fisher Scientific, Waltham, MA, USA) following the manufacturer's protocol. A 4× Laemmli sample buffer (#161-0747, BioRad, Hercules, CA, USA) was added to the samples. For detection of GCLC, GSS, and gamma-glutamyl transferase 1 (GGT1), 50 µg and for multidrug resistance protein 4 (MRP4), 100 µg of total protein per lane were separated by sodium dodecyl–sulfate–polyacrylamide gel electrophoresis (SDS-PAGE). Next, proteins were transferred to membranes (Table 2) via Trans-Blot Turbo Transfer System (BioRad, Hercules, CA, USA). All membranes were blocked for 2 h at room temperature. Next, the primary antibodies (Table 2) were incubated at 4 °C overnight. For GCLC and MRP4, actin was chosen as a housekeeper. For protein detection of GSS and GGT1, Calnexin was chosen as a housekeeper. The next day, membranes were washed with Tris-Buffered Saline with 0.1%Triton™ X-100 (TBS-T) and incubated with the appropriate horseradish–peroxidase-conjugated secondary antibody (Table 2) for two hours at room temperature. After four washes with TBS-T and two washes with Tris-Buffered Saline (TBS), protein bands were visualized with Western Blotting Luminol Reagent (#sc-2048, Santa Cruz, Dallas, TX, USA) in an imaging system (ChemiDoc XRS+, Bio-Rad, Hercules, CA, USA). For semiquantitative analyses, the band intensities of the proteins of interest were normalized to the loading control. All values were then normalized to the mean value of the normalized WT signals and plotted as a percentage in a bar chart. Western Blot analysis was performed with tissue samples obtained from at least four wild-type (WT) and four wobbler mice (WR).

Table 2. Primary and secondary antibodies used for Western Blotting.

Antibody	Order Number	Dilution	Membrane
Anit-γGCSc mouse monoclonal IgG_{2a} antibody	#sc-390811, Santa Cruz, USA	1:200 in ROTI®-Block (#A151, Roth, Karlsruhe, Germany)	Nitrocellulose membrane (#1704270, biorad)
Anti-GSS mouse monoclonal IgG_1 antibody	#sc-166882, Santa Cruz, USA	1:200 in ROTI®-Block (#A151, Roth, Karlsruhe, Germany)	Nitrocellulose membrane (#1704270, biorad)
Anti-MRP4 rabbit monoclonal IgG antibody	#12705, Cell Signaling Technology, USA	1:1000 in 5% BSA (#8076.2, Roth) in TBS-T	PVDF membrane (#1704272, biorad)
Anti-GGT1 mouse monoclonal IgG_{2b} antibody	#sc-374495, Santa Cruz, USA	1:1000 in 5% BSA (#8076.2, Roth) in TBS-T	Nitrocellulose membrane (#1704270, biorad)
Anti-Actin rabbit polyclonal IgG antibody	#A5060, Sigma, St. Louis, MO, USA	1:250 in ROTI®-Block (#A151, Roth, Karlsruhe, Germany)	Nitrocellulose membrane (#1704270, biorad) or PVDF membrane (#1704272, biorad)

Table 2. *Cont.*

Antibody	Order Number	Dilution	Membrane
Anti-Calnexin rabbit polyclonal IgG antibody	#sc-11397, Santa Cruz, USA	1:200 in ROTI®-Block (#A151, Roth, Karlsruhe, Germany)	Nitrocellulose membrane (#1704270, biorad)
Horse anti-mouse IgG (H + L)-Horseradish Peroxidase antibody	#PI-2000, Vector Laboratories, Bulingame, CA, USA	1:10,000 in TBS-T	
Goat anti-rabbit IgG (H + L)-Horseradish Peroxidase conjugate	#1706515, BioRad, Hercules, CA, USA	1:10,000 in TBS-T	

2.5. HPLC

Total glutathione (tGSH) concentrations in whole blood were assessed by high-performance liquid chromatography (HPLC) separation and fluorescent detection using a glutathione HPLC kit (#KC 1800, Immundiagnostik, Bensheim, Germany), according to manufacturer's instructions. In brief, ethylenediaminetetraacetic acid (EDTA) whole blood samples were treated with an internal standard and a reducing agent. Samples were derivatized, precipitated, and treated with a reaction buffer. Then, 20 µL was injected into an HPLC system. The separation via HPLC followed an isocratic method at 30 °C and a flow rate of 1 mL/min using a reversed-phase column (NUCLEODUR 100-3 C18 ec, 3 µm, 125 × 4 mm, #760051.40, Macherey–Nagel, Düren, Germany). Chromatograms were recorded by a fluorescence detector using an excitation wavelength of 385 nm and an emission wavelength of 515 nm. Quantification was performed with an EDTA-blood calibrator included in the kit. Low-concentration and high-concentration control samples also included in the kit, were measured as reference material. Samples, controls, and calibrators were measured twice. Reference values: tGSH 763–1191 µmol/L. Intra-assay coefficient of variation (CV): tGSH 3.9%. Inter-assay CV: tGSH 4.2%. tGSH concentrations were calculated via the peak height by the internal standard method. HPLC analysis was performed with whole blood drawn from six wild-type and six wobbler mice.

2.6. Glutathione Assay

For measurement of glutathione in tissue, erythrocyte, and plasma samples, a GSH/GSSG Ratio Detection Assay Kit (#ab205811, Abcam, Cambridge, UK) was used, according to the manufacturer's instructions. In brief, 20 mg of tissue, 3 µL of erythrocytes, and 6 µL of plasma were diluted 1:20, 1:100, and 1:35, respectively, in ice-cold phosphate-buffered saline (PBS) containing 0.5% Nonidet P40 (PBS/0.5% NP40). Tissue samples were homogenized and centrifuged at 13,000× *g* at 4 °C for 15 min. Fifty µL of each sample were plated in duplicates in a 96-well plate suitable for fluorescence measurement. For measurement of reduced GSH only, 50 µL of GSH Assay mixture (GAM) was added to each well. For measurement of tGSH, 50 µL of total glutathione Assay mixture (tGAM) was added to each well. With the aid of tGAM, which contains nicotinamide adenine dinucleotide phosphate (NADPH) and Glutathione reductase, GSSG is converted to tGSH in an enzymatic reaction with a ratio of 1 mole GSSG to 2 moles of GSH. After an incubation of 25 min at room temperature, protected from light, fluorescence was read with a Cytation™ 5 imaging reader (BioTek Instruments, Winooski, VT, USA) at 490 nm excitation and 520 nm emission with a reading time of 100 ms. The concentration of reduced GSH can be calculated from a GSH standard curve. The concentration of oxidized GSSG is calculated as follows:

$$[\mathrm{GSSG}] = \frac{(\mathrm{tGSH} - \mathrm{GSH})}{2} \quad (1)$$

The glutathione assay was performed with tissue, erythrocyte, and plasma samples obtained from at least four wild-type and four wobbler mice.

2.7. ROS Assay

For the detection of ROS in tissue samples, OxiSelect™ ROS/RNS In Vitro Assay Kit (#STA-347, Cell Biolabs, San Diego, CA, USA) was used. In brief, 10 mg/mL of tissue was homogenized in ice-cold 1xPBS and centrifuged at 10,000× *g* for 5 min at 4 °C right after extraction. Homogenates were stored at −80 °C until use. The assay was performed according to the manufacturer's instructions. In brief, 50 µL of each sample was plated in triplicates in a 96-well plate suitable for fluorescence measurement. Then, 50 µL of catalyst was added to each well and incubated for 5 min at room temperature. Afterward, 100 µL of 2′-7′dichlorofluorescin diacetate (DCFH) solution was added to each well. Fluorescence was measured after an incubation of 20 min at room temperature, protected from light, using a Cytation™ 5 imaging reader (BioTek Instruments, Winooski, VT, USA) at 480 nm excitation and 530 nm emission with a reading time of 100 ms. ROS assay was conducted with tissue samples collected from four wild-type and four wobbler mice.

2.8. Statistical Analysis

Prism 6 (GraphPad Inc., La Jolla, CA, USA) was used for statistical analysis. Data represent mean values of at least three independent experiments ± standard error of the mean (SEM). Data were tested for significance using Student's *t*-test, and results with *p*-values < 0.05 were considered statistically significant.

3. Results

There is accumulating evidence pointing toward the involvement of reactive oxygen species in the neurodegenerative processes of ALS [1,3–5,19–23]. As glutathione is an important defense system against ROS and previous studies have reported reduced glutathione levels in ALS [41–43], we aimed to analyze glutathione metabolism in symptomatic wobbler mice in detail.

3.1. Physiological Glutathione Synthesis in Liver of Wobbler Mice

First, we aimed to investigate whether deficits already exist in the global glutathione production of the main organ for GSH synthesis, the liver. Therefore, we investigated mRNA and protein expression of enzymes involved in glutathione synthesis in the liver during the distinct clinical stage (p40) via qPCR and Western blot.

Gene expression of the catalytic (*Gclc*) and the modifier (*Gclm*) subunit of GCL was significantly upregulated in wobbler mice, while mRNA expression of *Gss* was not altered (Figure 1a). However, on the protein level, GCLC showed no alteration in wobbler mice compared to wild-type mice (Figure 1b), presumably resulting in an unaltered production of GSH precursor γ-glutamyl-cysteine. Interestingly, protein expression of GSS was significantly increased (Figure 1b). Protein expression of the cleaving enzyme GGT1 was also unaltered in the liver tissue of p40 wobbler mice compared to wild-type littermates (Figure 1b). Measurements of total GSH (tGSH), reduced form of glutathione (GSH), and oxidized form of glutathione (GSSG) levels showed no significant differences in liver tissue of p40 wobbler mice compared to wild-type mice (Figure 1c,d). The observed unaltered levels of tGSH and the GSH/GSSG ratio indicate that the liver of wobbler mice is not exposed to oxidative stress. This was confirmed by the following measurement of the levels of reactive oxygen species within the two genotypes. ROS levels in liver tissue of p40 wobbler and wild-type mice showed no significant alteration (Figure 1e).

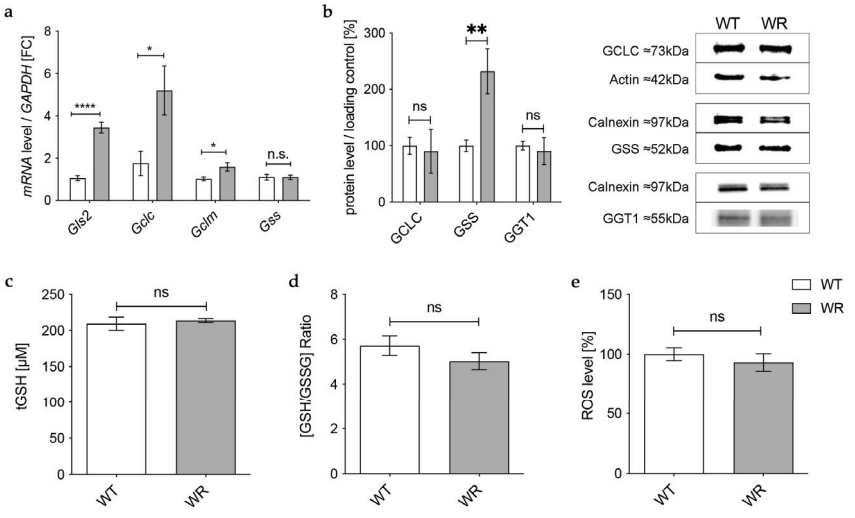

Figure 1. Physiological glutathione synthesis in liver of p40 wobbler mice. (**a**) mRNA expression levels of *Glutaminase 2* (*Gls2*), *Gclc*, *Gclm*, and *Gss* from the distinct clinical phase (p40) of wild-type (WT) and wobbler (WR) liver were investigated by qPCR. Significantly increased mRNA levels of *Gls2*, *Gclc*, and *Gclm* were observed in the liver of WR, while mRNA expression levels of *Gss* were not significantly altered. For relative quantification, the $2^{-\Delta\Delta Ct}$ method was performed using *GAPDH* for normalization. FC = Fold Change; N = 4. (**b**) Left: Semiquantitative analysis of protein expression levels in the liver of p40 WT and WR mice. GSS protein expression is increased in liver of WR, while protein expression of GCLC and GGT1 remains unchanged. Right: Representative Western Blots of GCLC (73 kDa), GSS (52 kDa), and GGT1 (55 kDa) in the liver of p40 WT and WR mice. Actin (42 kDa) and Calnexin (97 kDa) were used as loading controls, respectively. Bar charts represent the semiquantitative analysis of protein expression levels; N = 6. (**c**,**d**) Levels of tGSH (**c**) as well as the ratio of GSH/GSSG (**d**) in liver of p40 WR mice show no significant alterations compared to WT. tGSH, GSH, and GSSG levels of p40 WR mice compared to WT mice were analyzed via a fluorometric glutathione assay; N = 4. (**e**) ROS levels in liver tissue of p40 WR mice are unchanged compared to age-matched WT controls. ROS levels in liver tissue of p40 WR and WT mice were analyzed via a fluorometric assay; N = 4. All data are provided as mean ± SEM. Data were tested for significance using Student's *t*-test. Significant differences are indicated by ns. $p \geq 0.05$, * $p < 0.05$, ** $p < 0.01$, **** $p < 0.0001$.

3.2. Decreased Levels of Glutathione in Plasma and Erythrocytes of Wobbler Mice

Based on our findings in the liver tissue of wobbler mice, we hypothesized that physiological amounts of glutathione are released into the plasma by hepatocytes. For this reason, we analyzed glutathione amounts in whole blood, plasma, and erythrocytes of wobbler mice during the distinct clinical stage (p40). In whole blood, tGSH levels were analyzed with the aid of HPLC separation and fluorometric detection. tGSH levels in whole blood of p40 wobbler mice showed no significant alterations compared to age-matched wild-type controls (Figure 2a). A fluorometric glutathione assay was used for the measurement of tGSH, GSH, and GSSG levels in plasma and erythrocytes. In plasma, wobbler mice displayed significantly lower levels of tGSH as well as a significantly decreased ratio of GSH/GSSG compared to p40 wild-type mice (Figure 2b,c). tGSH levels were unaltered in the erythrocytes of wobbler mice compared to wild-type mice at the age of p40 (Figure 2d). In line with the findings in plasma, the ratio of GSH/GSSG in erythrocytes of p40 wobbler mice was significantly decreased compared to age-matched controls (Figure 2e).

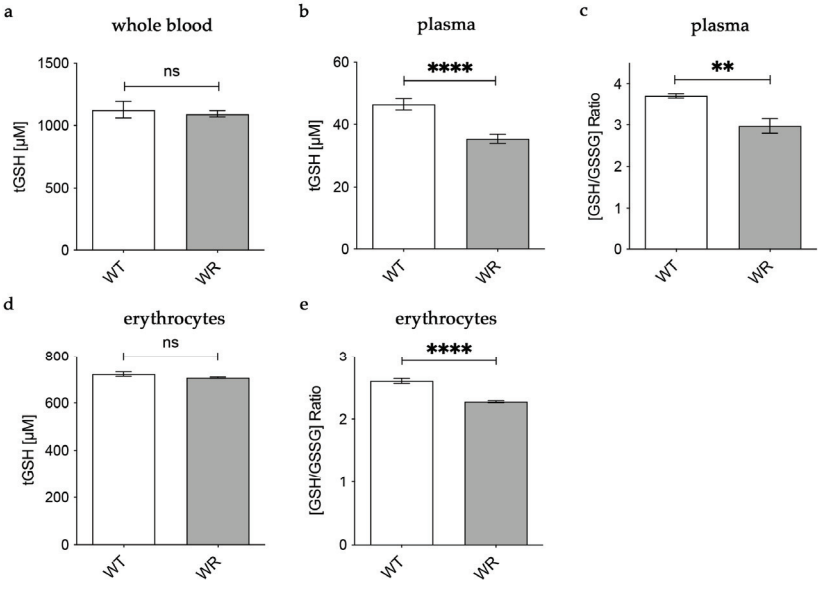

Figure 2. Decreased levels of glutathione in plasma of wobbler mice (p40). (**a**) HPLC measurement of tGSH displayed unaltered levels in whole blood of WR mice compared to WT mice; N = 6. (**b**) WR mice exhibit significantly lower levels of tGSH in plasma compared to WT mice; N = 7. (**c**) The ratio of GSH/GSSG is significantly decreased in plasma of WR mice compared to WT; N = 4. (**d**) Unaltered levels of tGSH in erythrocytes of p40 WR mice compared to WT mice; N = 4. (**e**) The ratio of GSH/GSSG is significantly decreased in erythrocytes of WR compared to WT; N = 4. All data are provided as mean ± SEM. Data were tested for significance using Student's *t*-test. Significant differences are indicated by ns. $p \geq 0.05$, ** $p < 0.01$, **** $p < 0.0001$.

3.3. Altered Expression of Enzymes Involved in Transport of Glutathione and Its Components in the Cervical Spinal Cord

In the next step we aimed to find out how the detected deficiency of plasma glutathione in wobbler mice is linked to the glutathione deficit in the cervical spinal cord reported by our group before [18]. First, we investigated gene expression of enzymes involved in transport of glutathione and its components in the cervical spinal cord of wobbler mice in the distinct clinical stage (p40) via qPCR (Figure 3a). mRNA expression of Mrp4, which has been assumed to transport glutathione across the blood–brain barrier [31,47], was not significantly altered (Figure 3a). However, multidrug resistance protein 1 (Mrp1), which is involved in glutathione export from astrocytes [48], showed a significantly elevated gene expression (Figure 3a). Unfortunately, we were unable to obtain a reliable Western Blot for MRP4 protein expression in spinal cord.

Besides the transport of glutathione itself, the import of amino acids is crucial for glutathione synthesis in order to achieve adequate glutathione concentrations in cells of the CNS. The cystine/glutamate exchanger system Xc- consists of a light chain xCT, encoded by *Solute carrier (Slc) 7a11 (Slc7a11)*, and a heavy chain 4F2hc, encoded by *Slc3a2* [49]. mRNA levels of *Slc7a11* were significantly elevated in wobbler mice, while mRNA levels of *Slc3a2* were not altered (Figure 3a). As glutathione synthesis takes place in the cytosol, GSH is imported into mitochondria via 2-oxoglutarate/malate carrier protein, which is encoded by *Slc25a11* [50]. mRNA levels of *Slc25a11* in the cervical spinal cord of wobbler mice showed no alterations compared to wild-type mice (Figure 3a). Unlike astrocytes, neurons do not contain an uptake mechanism for glutathione and, therefore, rely on their own synthesis [34]. We analyzed mRNA expression of excitatory amino acid transporter 3 *(Eaat3)*, the major transporter for the import of cysteine into neurons [36]. Remarkably, we

found a significant downregulation of *Eaat3* mRNA in the cervical spinal cord of wobbler mice (Figure 3a).

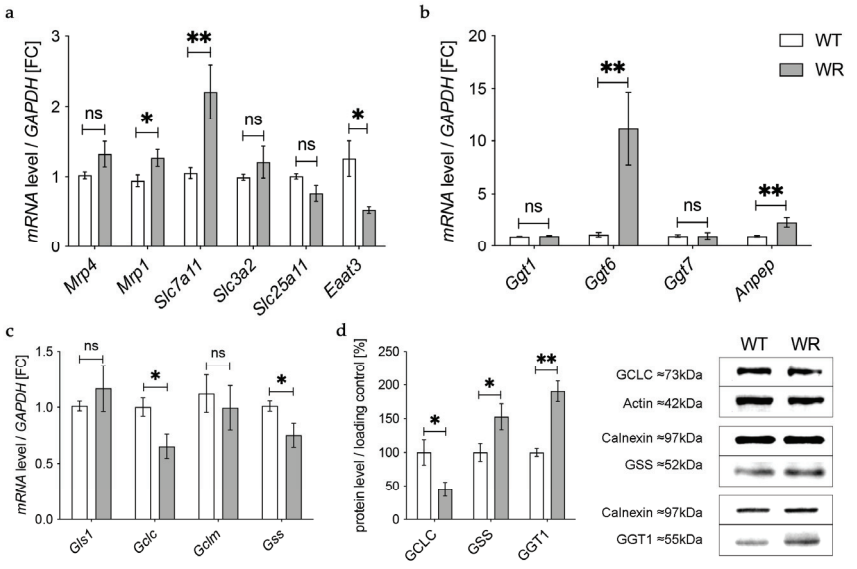

Figure 3. Altered glutathione metabolism and synthesis in the cervical spinal cord of wobbler mice. (**a**) mRNA expression levels of *Mrp4*, *Mrp1*, *Eaat3*, *Slc7a11*, *Slc3a2*, and *Slc25a11* in the cervical spinal cord of WT and WR mice from the distinct clinical stage (p40) were investigated by qPCR. mRNA levels of *Mrp1* and *Slc7a11* are significantly increased, while mRNA expression levels of *Eaat3* are significantly decreased. Unaltered mRNA levels of *Mrp4*, *Slc3a2*, and *Slc25a11*; N = 4–8. (**b**) Upregulation of genes involved in glutathione cleavage in the cervical spinal cord of wobbler mice (p40). Significantly increased mRNA levels of *Anpep* and *Ggt6* were measured, while mRNA expression levels of *Ggt1* and *Ggt7* are unaltered; N = 4. (**c**) Decreased mRNA expression levels of *Gclc* and *Gss*, alongside unaltered mRNA expression levels of *Gls1* and *Gclm* in the cervical spinal cord of WR mice compared to WT mice age p40. For relative quantification, the $2^{-\Delta\Delta Ct}$ method was performed using *GAPDH* for normalization. FC = Fold Change; N = 4. (**d**) Left: Semiquantitative analysis of protein expression levels in the spinal cord of p40 WT and WR mice. Right: Representative Western Blots of GCLC (73 kDa),GSS (52 kDa), and GGT1 (55 kDa) in the cervical spinal cord of p40 WT and WR mice. Actin (42 kDa) and Calnexin (97 kDa) were used as loading controls, respectively; N = 4–8. All data are provided as mean ± SEM. Data were tested for significance using Student's *t*-test. Significant differences are indicated by ns. $p \geq 0.05$, * $p < 0.05$, ** $p < 0.01$.

3.4. Upregulation of Enzymes Involved in Glutathione Cleavage in the Cervical Spinal Cord of Wobbler Mice

GSH released by astrocytes is cleaved to its constituent amino acids, which are later imported into neurons. For this reason, we next analyzed the gene expression of enzymes involved in glutathione cleavage in the cervical spinal cord of wobbler mice via qPCR (Figure 3b). First, GSH is hydrolyzed by the ectoenzyme γ-glutamyl-transferase (GGT) in the extracellular space [38]. Interestingly, the gene expression of *Ggt6* was significantly upregulated, while the gene expression of *Ggt1* and *Ggt7* was unaltered (Figure 3b). However, on the protein level, we found a significantly upregulated expression of GGT1 in the cervical spinal cord of p40 wobbler mice (Figure 3d). In the next step, the ectoenzyme aminopeptidase N (Anpep) further cleaves the resulting cysteinyl–glycine [35]. Remarkably, gene expression of *Anpep* was significantly upregulated (Figure 3b).

3.5. Decreased Levels of GCLC in the Cervical Spinal Cord of Wobbler Mice

The results described above demonstrate an upregulation of up to 40% of the investigated genes of enzymes involved in glutathione metabolism in the cervical spinal cord of p40 wobbler mice. Therefore, we next analyzed the gene expression of enzymes involved in glutathione synthesis in the cervical spinal cord of wobbler mice in the distinct clinical stage (p40) via qPCR. mRNA expression levels of *Glutaminase1 (Gls1)* and *Gclm* were unaltered, while mRNA expression levels of *Gclc* and *Gss* were significantly decreased in wobbler mice compared to wild-type (Figure 3c). To confirm whether this also applies to the protein level, a Western Blot analysis was performed. Here, protein expression of GCLC was significantly decreased in the cervical spinal cord of p40 wobbler mice (Figure 3d). However, Western Blot analysis of GSS displayed significantly increased protein expression in the cervical spinal cord of p40 wobbler mice compared to wild-type mice (Figure 3d).

3.6. Physiological Glutathione Metabolism in Hippocampus and Cerebellum of Wobbler Mice

To verify whether the observed changes in glutathione metabolism are specific to the spinal cord or if they also occur in other areas of the CNS of the wobbler mice, we performed the same analysis on hippocampal and cerebellar tissue from p40 wobbler and wild-type mice.

In the hippocampus, qPCR revealed an upregulation of all analyzed genes involved in the transport of glutathione and its components in wobbler mice compared to wild-type mice (Figure 4a), whereas Western Blot analysis of MRP4 indicated an unaltered protein expression (Figure 4b). mRNA expression levels of genes involved in glutathione cleavage in the hippocampus were not significantly altered or even decreased (Figure 4a). Protein expression of the cleaving enzyme GGT1 was unchanged in the hippocampus of p40 wobbler mice compared to wild-type mice (Figure 4b). For enzymes involved in glutathione synthesis in the hippocampus, qPCR showed significantly increased mRNA expression levels of *Gclc,* besides unaltered mRNA expression levels of *Gclm* and *Gss* (Figure 4a). However, on the protein level, Western Blot analysis revealed an unaltered expression of GCLC and a significantly upregulated expression of GSS (Figure 4b). Measurements of glutathione level in hippocampal tissue of p40 wobbler mice confirmed the assumption of unaltered glutathione synthesis in the hippocampus, as no significant alterations compared to wild-type mice were obtained (Figure 4c,d). Nevertheless, ROS assays of hippocampal tissue detected a modest but significant increase of reactive oxygen species in the hippocampus of wobbler mice compared to wild-type mice (Figure 4e).

In the cerebellum of p40 wobbler mice, qPCR showed a significant upregulation of all analyzed genes involved in the transport of glutathione and its components (Figure 5a). For enzymes involved in glutathione cleavage, only *Anpep* and *Ggt6* showed a significantly upregulated gene expression (Figure 5a). In contrast to mRNA expression, Western Blot analysis revealed a significantly decreased protein expression of MRP4 and a significantly increased protein expression of the cleaving enzyme GGT1 in the cerebellum of p40 WR mice compared to wild-type mice (Figure 5b). We also analyzed enzymes involved in glutathione synthesis in the cerebellum of p40 wobbler and wild-type mice. Here, mRNA levels of *Gclc* were significantly increased (Figure 5a). However, protein expression of GCLC was not significantly altered, while GSS was significantly increased (Figure 5b). The hypothesis of a sufficient metabolism and synthesis of glutathione in the cerebellum of p40 wobbler mice was confirmed by glutathione and ROS assays, which showed neither alterations in glutathione (Figure 5c,d) nor in ROS (Figure 5e) levels in cerebellum of p40 wobbler mice compared to wild-type mice.

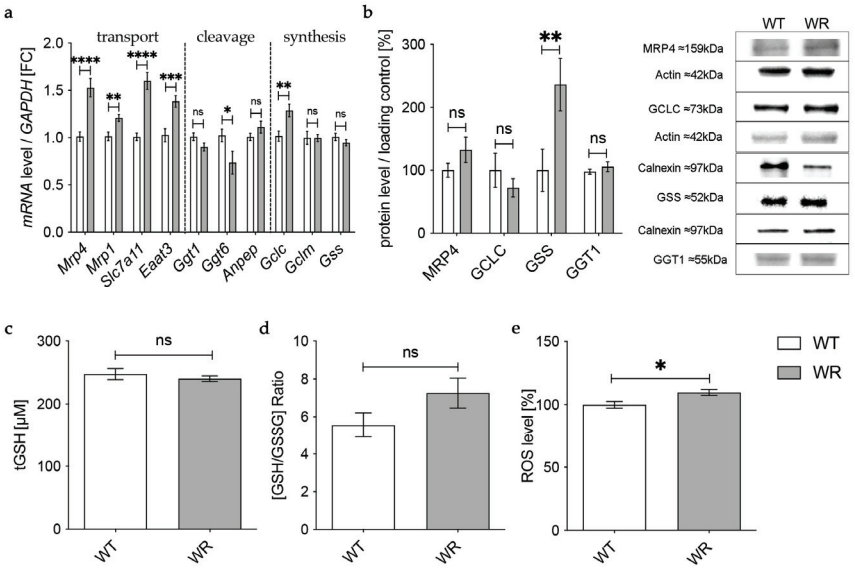

Figure 4. Physiological glutathione metabolism in hippocampus of wobbler mice. (**a**) mRNA expression levels of GSH transport relevant genes, *Mrp4*, *Mrp1*, *Slc7a11*, *Eaat3*, GSH cleavage relevant genes, *Ggt1*, *Ggt6*, *Anpep*, and GSH synthesis relevant genes, *Gclc*, *Gclm*, *Gss*, in the hippocampus of WT and WR mice from the distinct clinical stage (p40) were investigated by qPCR. Significantly increased mRNA levels of GSH transport-relevant genes were measured, while mRNA expression levels of *Ggt6* were significantly decreased. For relative quantification, the $2^{-\Delta\Delta Ct}$ method was performed using *GAPDH* for normalization; N = 4. (**b**) Left: Semiquantitative analysis of protein expression levels in the hippocampus of p40 WT and WR mice. Right: Representative Western Blots of MRP4 (159 kDa), GCLC (73 kDa), GSS (52 kDa), and GGT1 (55 kDa) in the hippocampus of p40 WT and WR mice. Actin (42 kDa) and Calnexin (97 kDa) were used as loading controls; N = 4. (**c**,**d**) tGSH (**c**) as well as [GSH/GSSG]-ratio (**d**) in hippocampus of p40 WR mice compared to WT mice was analyzed via a fluorometric glutathione assay. Neither tGSH nor the ratio of GSH/GSSG in hippocampus of WR mice is significantly altered compared to WT mice, age p40. N = 4. (**e**) ROS levels in hippocampus of WR and WT mice were detected via a fluorometric assay at the developmental stage p40. WR hippocampus shows significantly elevated levels of ROS compared to WT; N = 4. All data are provided as mean ± SEM. Data were tested for significance using Student's *t*-test. Significant differences are indicated by ns. $p \geq 0.05$, * $p < 0.05$, ** $p < 0.01$, *** $p < 0.001$, **** $p < 0.0001$.

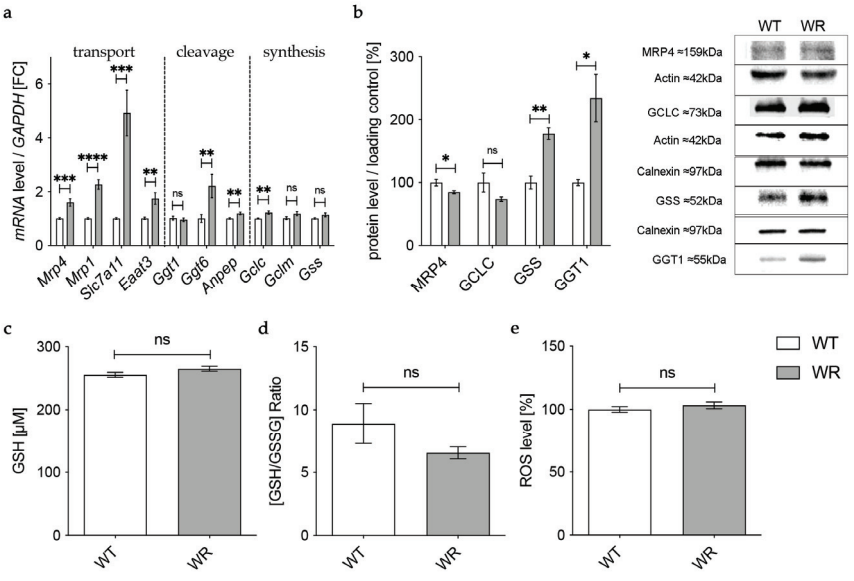

Figure 5. Physiological glutathione metabolism in cerebellum of WR mice. (**a**) mRNA expression levels of GSH transport relevant genes, *Mrp4*, *Mrp1*, *Slc7a11*, *Eaat3*, GSH cleavage relevant genes, *Ggt1*, *Ggt6*, *Anpep*, and GSH synthesis relevant genes, *Gclc*, *Gclm*, *Gss*, in the cerebellum of WT and WR mice from the distinct clinical stage (p40), were investigated by qPCR. Significantly increased mRNA levels of GSH transport, some cleavage relevant genes, as well as *Gclc* but no other GSH synthesis relevant genes. For relative quantification, the $2^{-\Delta\Delta Ct}$ method was performed using *GAPDH* for normalization; N = 4. (**b**) Left: Semiquantitative analysis of protein expression levels in the cerebellum of p40 WT and WR mice. Right: Representative Western Blots of MRP4 (159 kDa), GCLC (73 kDa), GSS (52 kDa), and GGT1 (55 kDa) in the cerebellum of p40 WT and WR mice. Actin (42 kDa) and Calnexin (97 kDa) were used as loading controls; N = 4. (**c**,**d**) tGSH (**c**) as well as [GSH/GSSG]-ratio (**d**) in cerebellum of p40 WR mice compared to WT mice was analyzed via a fluorometric glutathione assay. Neither tGSH nor the ratio of GSH/GSSG in cerebellum of WR mice is significantly altered compared to WT mice at the age of p40; N = 4. (**e**) Unaltered levels of reactive oxygen species in cerebellum of wobbler mice compared to wild-type were detected via a fluorometric assay at the developmental stage p40; N = 4. All data are provided as mean ± SEM. Data were tested for significance using Student's *t*-test. Significant differences are indicated by ns. $p \geq 0.05$, * $p < 0.05$, ** $p < 0.01$, *** $p < 0.001$, **** $p < 0.0001$.

4. Discussion

Increasing evidence points to a disturbed glutathione redox balance in regard to the development and progression of ALS [40]. As the glutathione system is an important antioxidant system within the cells, any change in homeostasis can have severe consequences for the well-being of the cells [51]. Since it is meanwhile known that signs of oxidative stress are present in both tissue and motor neurons of ALS animal models [17,18,24–27] as well as in postmortem tissue, plasma, urine, and cerebrospinal fluid of ALS patients [1,3–5,19,20,22,23,52], the intrinsic antioxidative systems seem to be functioning insufficiently. Furthermore, our previous study showed a reduced amount of total glutathione in the spinal cord of wobbler mice, lacking adequate protection against oxidative stress [18]. However, the precise mechanism leading to glutathione depletion remains to be determined. In our current study, we demonstrated that glutathione level is reduced in the spinal cord tissue of the ALS model wobbler mouse due to a decreased expression of the rate-limiting enzyme of the glutathione synthesis, GCLC, in addition to defective glutathione metabolism.

The liver has been reported to mainly determine the plasma glutathione concentration [30], which is positively correlated to the glutathione uptake across the blood–brain barrier [31–33]. Furthermore, ultrastructural changes in the liver of ALS patients have been reported before [53,54]. For this reason, the liver and plasma were examined for defects in glutathione content and synthesis. Our results show an unaltered or even increased protein expression of GGT1, GCLC, and GSS, respectively, leading to an unaltered glutathione cleavage and synthesis in the liver of symptomatic wobbler mice compared to wild-type mice. In accordance with the unaltered glutathione levels as well as unaltered ROS levels measured in the liver of symptomatic wobbler mice, we concluded that appropriate contents of glutathione are produced and hypothesize a physiological release of GSH by hepatocytes into the plasma. In whole blood and erythrocytes, we detected unchanged levels of total glutathione amount. Approximately 98% of glutathione in whole blood is localized inside erythrocytes as plasma glutathione is utilized for interorgan glutathione homeostasis [55,56]. Our results show a decreased ratio of GSH/GSSG in erythrocytes of symptomatic wobbler mice, indicating increased oxidation of GSH due to oxidative stress. As a result, GSH is decreased, which is in line with the finding of Babu et al., who reported decreased levels of GSH in erythrocytes of ALS patients [41]. Blasco et al. reported comparable results as they found an increased ratio of GSSG/GSH in the whole blood of ALS patients [52]. The unchanged total glutathione levels in erythrocytes of wobbler mice suggest a physiological glutathione synthesis in these cells. Interestingly, plasma glutathione levels were decreased in symptomatic wobbler mice compared to wild-type mice. Not only the total glutathione content in plasma was decreased, but also the ratio of GSH/GSSG, indicating a defective redox balance. Glutathione is sustainably exported from erythrocytes into plasma under physiological circumstances [56]. We assume a functioning export of glutathione from the liver into plasma as described above. This leaves us with two possible explanations for the decreased levels of total glutathione in the plasma of symptomatic wobbler mice: firstly, due to the disturbed redox balance in erythrocytes described above, their export of glutathione into plasma might be restricted [56]. Secondly, a considerable amount of plasma glutathione might be utilized to support glutathione homeostasis in neighboring cells and tissue [55]. It, thus, appears that changes in glutathione metabolism are not limited to the CNS in wobbler mice but also occur in other tissues. It is tempting to speculate that due to decreased levels of plasma glutathione, not enough glutathione is available for uptake across the blood–brain barrier [33]. Nevertheless, the impact of plasma glutathione on glutathione levels in the CNS remains controversial [57]. Interestingly, López-Blanch et al. reported that in isolated hepatocytes of two other ALS mouse models, SOD1G93A and FUS-R521C mice, GSH synthesis and efflux significantly increased while GSH concentration decreased in whole blood in both models at an advanced state of disease progression [58]. Considering the reported decreased levels of glutathione in the blood of ALS patients and different mouse models, including our results, alterations in blood glutathione appear to apply to more than one ALS genotype as a promising therapeutic approach in the future [41,52,58].

Glutathione transport across the blood–brain barrier is likely mediated by Multidrug Resistance Protein 4 (MRP4) [31,47]. Quantitative proteomics of MRP expression in brain capillary endothelial cells showed that only MRP4 is expressed at quantifiable levels at the blood–brain barrier [47,59]. In addition to glutathione, cysteine, and cystine uptake have been reported to influence glutathione contents in the central nervous system [34]. Cysteine, which is considered the rate-limiting amino acid for glutathione synthesis [60], can be imported into cells directly or in its oxidized form cystine via the cystine/glutamate exchanger system Xc- [61]. System Xc- is mainly expressed in glial cells [62] and is highly inducible by oxidative stress [63]. Astrocytes play an essential role in providing neurons with substrates for GSH synthesis [34]. GSH is released by astrocytes via MRP1 [48] and gap junction hemichannels [64]. In the extracellular space, glutathione is hydrolyzed by the ectoenzyme γ-glutamyl-transferase [38], located in the plasma membrane of non-neuronal cells [65]. In the next step, the ectoenzyme aminopeptidase N further cleaves the resulting

cysteinyl–glycine [35]. The generated cysteine and glycine can then be taken up by other cells, such as neurons and oligodendrocytes, via different amino acid transporters.

In the current study, we provide evidence that the reduced total glutathione contents in the cervical spinal cord of symptomatic wobbler mice reported earlier by our group [18] are caused by a reduced glutathione synthesis due to decreased protein expression of the rate-limiting enzyme in glutathione synthesis GCLC [39]. We assume this leads to reduced production of GSH precursor γ-glutamyl-cysteine, resulting in a decreased GSH production, although protein expression of GSS is upregulated. Similar to Junghans et al. [18], we studied tissue samples of the cervical spinal cord of wobbler mice and, thus, cannot differentiate between the different cell types, which should be addressed in the future. However, we can assume a possible mechanism based on the specific expression of the different proteins involved in glutathione metabolism in the cervical spinal cord (Figure 6). We hypothesize that less GSH is released by astrocytes due to reduced synthesis. Presumably compensatory, *Mrp1* mediating GSH export from astrocytes [48] is upregulated, resulting in less GSH available for cleavage in the extracellular space. We suspect that, as a compensatory mechanism, the cleaving enzymes *Anpep* and GGT1 are upregulated in the cervical spinal cord. GGT plays an essential role in the astrocytic supply of components for glutathione synthesis to neurons [38,66]. Inhibition of GGT decreased intracellular glutathione contents by about 25% in dissociated neuronal cultures [66]. Similarly, in transient neuron-astroglia co-cultures, glutathione content in the neuronal compartment increased by 165% after the application of astrocytes, while inhibition of GGT completely prevented this effect [38]. Moreover, several studies have demonstrated that GGT mRNA and protein expression, as well as its activity, increase after exposure to oxidative stress [67–69]. Aminopeptidase N is involved in the degradation and modulation of several peptides, including glutathione precursor cysteinyl–glycine [35,70]. As GGT is more specifically involved in GSH degradation, we focused on its protein expression. However, our results are limited to the fact that we cannot discuss protein activity. Finally, decreased GSH synthesis and release by astroglial cells lead to a decreased supply of amino acids essential for glutathione synthesis in neurons. In accordance with our result of reduced mRNA levels of *Eaat3*, decreased protein expression of EAAT3 has been reported in the cervical spinal cord of symptomatic wobbler mice [71]. As EAAT3 has been described to be the major transporter for cysteine import in neurons [36], its downregulation aggravates the deficient cysteine supply to neurons [37]. In cultured neurons, cysteine uptake and intracellular GSH contents were reduced by inhibition of EAAT3 but not by inhibition of other cysteine transporters [72]. EAAT3 null mice display reduced glutathione contents, increased oxidant levels, and suffer from age-dependent neurodegeneration along with cognitive impairments [36]. These changes could be reversed by treating the mice with N-Acetylcysteine, a membrane-permeable cysteine precursor [36]. We hypothesize that overall, the decreased glutathione synthesis due to a decreased expression of the rate-limiting enzyme GCLC and the release by astrocytes, as well as a decreased cysteine uptake in neurons, lead to an impaired glutathione synthesis in the cervical spinal cord. Due to the inadequate glutathione contents, neurons' and astrocytes' defense against ROS is severely impaired. Consecutively, this leads to elevated levels of ROS in the cervical spinal cord [17] and particularly in motor neurons of wobbler mice [18].

Interestingly, Riluzol, the only drug approved by the European Medical Agency for the treatment of ALS with a small significant effect on survival, has been reported to augment EAAT3 expression and decrease ROS in C6 astroglial cells [73]. In neurons, glutamate and cysteine transport capacities are regulated by EAAT3 recycling [74,75]. EAAT3 recycling from the plasma membrane is mediated by clathrin-dependent endocytosis, followed by recycling through Rab11-positive vesicles, from which transporter molecules can be dynamically mobilized to the cell surface to mediate cysteine uptake [76,77]. Defects in Rab11-dependent trafficking of EAAT3 to the cell surface have been reported in primary cortical neurons in a knock-in mouse model of Huntington's disease and result in impaired cysteine uptake and glutathione biosynthesis [78]. The wobbler mouse displays a point

mutation affecting VPS54, a component of the Golgi-associated retrograde protein (GARP) complex, tethering endosome-derived vesicles to the trans-Golgi network [12]. Recently, Wilkinson discovered that the specific disruption of both *scattered* (*scat*), the fly VPS54 ortholog, and *Rab11* gene expression result in muscle atrophy and reduced climbing ability in Drosophila [79]. Thus, there might be a connection between the VPS54 mutation and disturbed EAAT3 recycling at the plasma membrane, aggravating an impaired cysteine supply and glutathione synthesis in neurons. However, the exact mechanism of how the VPS54 mutation results in the ALS seen in wobbler mice remains to be explored.

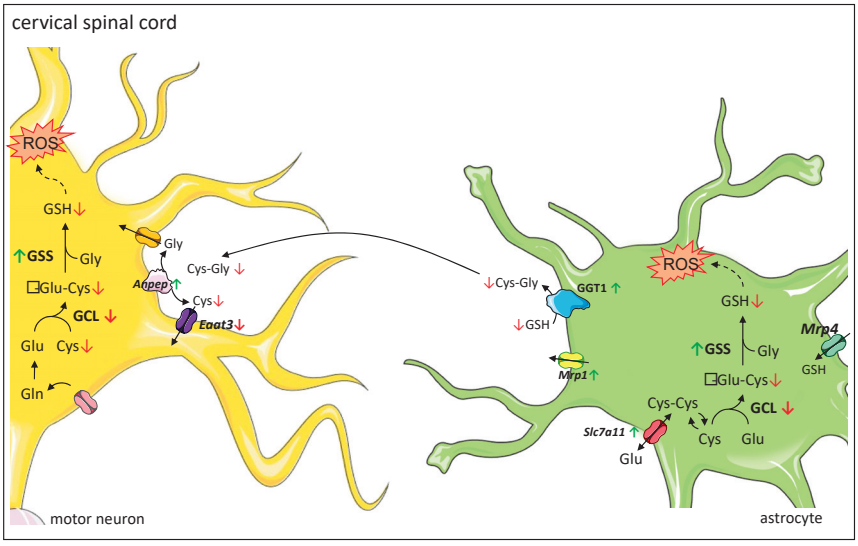

Figure 6. Proposed mechanism of dysregulated glutathione metabolism and synthesis in cervical spinal cord of wobbler mice. Glutathione metabolism between astrocytes and neurons: astrocytes import glutathione (GSH) via MRP4 (Multidrug Resistance Protein 4), while neurons do not contain an uptake mechanism for GSH and therefore rely on their own GSH synthesis. Both astrocytes and neurons can synthesize GSH from its constituent amino acids. Astrocytes can import cystine via the cystine/glutamate exchanger system Xc-. Astrocytes supply neurons with substrates for GSH synthesis. They export GSH via MRP1 (Multidrug Resistance Protein 1). In the next step, the ectoenzyme GGT (Gamma-Glutamyl Transferase) hydrolyzes GSH. The resulting Cysteinyl–Glycine (Cys-Gly) is cleaved by the ectoenzyme Aminopeptidase N (ANPEP). Next, the resulting amino acids are imported into neurons by different transporters, where they can be used for GSH synthesis. The main transporter for cysteine uptake in neurons is EAAT3 (Excitatory Amino Acid Transporter 3). Proposed mechanism of dysregulated glutathione metabolism and synthesis in the cervical spinal cord: a decreased protein expression of GCL (γ-Glutamyl-cysteinyl-ligase) leads to a decreased synthesis of γ-Glu-Cys (γ-Glutamyl-Cystein), resulting in a decreased GSH synthesis, even though protein expression of GSS (glutathione synthetase) is increased. Thus, less GSH is available for export from astrocytes via MRP1 and cleavage by GGT and ANPEP. As a compensatory mechanism, GGT1 is upregulated. However, EAAT3 is downregulated, which aggravates the deficient cysteine supply to neurons. Overall, this leads to an insufficient GSH synthesis in neurons. Due to the inadequate GSH levels, neurons' and astrocytes' defense against ROS (reactive oxygen species) is severely impaired. In astrocytes, increased levels of ROS lead to an increased expression of *Slc7a11* encoding for the light chain of system Xc-, enhancing cystine import in astrocytes. Legend: Green arrows indicate an upregulation; red arrows indicate a downregulation of corresponding enzyme on protein or mRNA levels. Cys-Cys: Cystine; Glu: Glutamate; Gln: Glutamine.

Based on the findings in the cervical spinal cord, we wondered whether deficits in glutathione homeostasis are limited to motoric areas of the CNS in wobbler mice. For this reason, we analyzed tissue samples of the cerebellum and hippocampus of p40 wobbler mice. Fifty percent of ALS patients suffer from additional extra motor manifestations, among them progressive cognitive abnormalities [6]. Fifteen percent of ALS patients meet the diagnostic criteria for frontotemporal dementia [80]. Repeat expansions in *chromosome 9 open reading frame 72* (*C9ORF72*) are currently the most important genetic cause of familial ALS and frontotemporal dementia, accounting for approximately 34.2% and 25.9% of the cases [81]. In accordance with this, hippocampal abnormalities have been identified in ALS patients [82] and wobbler mice [83]. Our results show unaltered glutathione levels besides an unaltered glutathione synthesis in the hippocampus of p40 wobbler mice compared to wild-type mice. Nevertheless, ROS levels were modestly elevated in the hippocampus of p40 WR mice. This gives rise to two possible interpretations: either the glutathione system is balanced in the hippocampus, and there is another cause for ROS production, or there is a glutathione deficit in some hippocampal cells, which is counterbalanced by other cells, leading to the measurement of unaltered levels of the bulk glutathione concentrations. As we measured the bulk of ROS and glutathione content in hippocampal tissue, we could not differentiate these levels in the different cell types and the extracellular space. For this reason, our measurements are likely to underestimate the degree of glutathione deficiency in neurons because a large share of brain glutathione is located in astrocytes [84]. Therefore, we cannot exclude a glutathione deficiency specifically in neurons nor in other cell types in the hippocampus of wobbler mice leading to oxidative stress. The upregulated gene expression of enzymes involved in glutathione transport in hippocampus might point towards this hypothesis. For this reason, future studies are needed to specifically differentiate glutathione and ROS levels in the different cell types.

Previous studies have revealed alterations in the cerebella of p40 wobbler mice [85,86]. Besides inflammatory processes, such as astrogliosis and microgliosis, no signs of neurodegeneration have been detected [86]. In addition to this, there is accumulating evidence of cerebellar involvement in ALS [87]. Focal cerebellar degeneration and cerebro–cerebellar connectivity alterations have been described in ALS patients in vivo via magnetic resonance imaging [88]. However, it remains unclear if cerebellar involvement is a primary or rather secondary compensatory mechanism as the motor cortex degenerates [89]. Our results demonstrate unaltered levels of ROS and glutathione in the cerebella of p40 wobbler mice compared to wild-type littermates. These results are in line with previous findings concerning the cerebellum of ALS mouse models. Aguirre et al. detected no oxidative DNA damage in the cerebellum of G93A SOD1 mice [27]. In symptomatic wobbler mice, Saberi et al. observed an inflammatory response but did not identify evidence of neuron cell death, while Klatt et al. identified a downregulation of proapoptotic factors linked to neuroprotection [85,86]. In addition to this, we report upregulated mRNA expression of enzymes involved in glutathione transport and cleavage, as well as upregulated protein levels for MRP4 and GGT1. We hypothesize this is an adaption due to the inflammatory processes described earlier [86]. This result is limited to the fact that for some genes, the verification remains to be determined on the protein level. Interestingly, these upregulated genes encode stress-inducible GSH metabolic enzymes whose induction is mediated by Nrf2 (nuclear factor erythroid 2-related factor 2) via ARE (antioxidant responsive element) [63,90,91]. The Nrf2 signaling pathway regulates the cellular response to stress and inflammation [92]. This might be the reason for the detected upregulation of genes and proteins encoding stress-inducible metabolic enzymes. Overall, we conclude that in the cerebellum of symptomatic wobbler mice, redox homeostasis is balanced.

Our data present decreased levels of GCLC in the cervical spinal cord but not in the cerebellum or hippocampus of wobbler mice. Key transcription factors involved in the regulation of Gclc gene expression are Nrf2 via ARE, NFκB (nuclear factor kappa B), and AP-1 (activator protein-1) [93]. Usually, oxidative stress leads to the induction of genes involved in antioxidative defense, including *Gclc* [93]. However, expression

of *Gclc* and *Gclm* can become dysregulated if oxidative conditions persist, as reported in liver injuries [94]. Therefore, we hypothesize that a decreased mRNA and protein expression of GCLC in the cervical spinal cord is due to prolonged oxidative stress. Feng et al. reported that selective deficiency of *Gclc* in mouse CNS leads to neurodegeneration, specifically progressive motor neuron loss marked by mitochondrial dysfunction [95]. Consistent with this finding, a previous study of our group presents abnormal morphology of mitochondria in motor neurons of p40 wobbler mice [96]. Interestingly, in G93A SOD1 mice, a reduced protein expression of Nrf2 and GCLC in the cervical spinal cord has been reported [97]. Target genes of the Nrf2-ARE signaling pathway include *Gclc*, *Gclm*, *Gss*, *Ggt*, *Mrp1*, *Eaat3,* and *Slc7a11* [90,91]. Importantly, our results show tissue-specific dysregulations in most Nrf2 target genes. Reduced mRNA and protein levels of the antioxidant regulator Nrf2 have been reported in the postmortem primary motor cortex and spinal cord tissue of ALS patients [98]. For this reason, the Nrf2-ARE pathway has been estimated as a promising therapeutic target [99]. Numerous Nrf2 activators are being tested in pre-clinical studies for the treatment of ALS [100]. Edaravone, approved for the treatment of ALS in the US and Japan, has also been reported to activate the Nrf2 signaling pathway [101]. Nevertheless, Edaravone has been shown to clinically benefit only a small subset of ALS patients [102,103]. In addition to this, different Nrf2 activators, Fingolimod and Dimethyl fumarate, showed no observable benefit on ALS functional rating scale (ALSFRS) in Phase II randomized controlled trials [104,105]. Moreover, clinical trials aiming to improve glutathione contents in ALS by supplementation of glutathione or Acetlycysteine have been negative so far [106,107]. Consistent with these previous approaches, our study suggests that glutathione homeostasis is disrupted in the ALS model of the wobbler mouse and, thus, may be a therapeutic target. However, our data cannot be explained by Nrf2 activation or inactivation alone; as for the cervical spinal cord, some Nrf2 target genes are upregulated, while others are downregulated or unaltered. Our data suggest that future studies are needed to differentiate defects in glutathione metabolism and synthesis in the different cell types, especially astrocytes and neurons, with the objective of finding cell-specific therapeutic targets.

Unexpectedly, in all analyzed tissues, protein levels of GSS were significantly upregulated, independent of mRNA levels of *Gss*. A proteome-wide quantitative survey of in vivo ubiquitylation sites mapped 11.054 putative endogenous ubiquitylation sites on more than 4000 human proteins [108]. Among them, they identified a ubiquitylation side on human GSS. Ubiquitinylated TDP-43 containing aggregates have been reported in the spinal cord of wobbler mice [109], and extensive oxidative stress impairs the proteasome leading to protein aggregation, as reviewed by Shang and Taylor [110]. Given these facts, we hypothesized that GSS protein levels might be elevated in the examined tissues due to ubiquitylation and impaired proteasomal degradation. However, our preliminary results from the investigation of free ubiquitin and polyubiquitinylated proteins via Western Blot in the liver, cervical spinal cord, hippocampal, and cerebellar tissue of p40 wild-type and wobbler mice do not support this hypothesis (Figure S1). Thus, there has to be a different cause of the significant upregulation of GSS protein expression in all four tissues examined. Nefedova et al. reported that all-*trans* retinoic acid (ATRA) selectively induced expression of GSS via extracellular signal-regulated kinase 1/2 (ERK1/2) in myeloid-derived suppressor cells (MDSC) [111]. As GSS promoter activity was not affected in this process, post-transcriptional regulation of GSS is most likely [93,111]. However, the exact mechanism of ERK 1/2 on GSS expression and if this applies to the observed elevated protein levels in the respective tissues in wobbler mice remains to be examined.

5. Conclusions

Our results are in line with findings of oxidative stress and dysregulated glutathione levels in other ALS animal models [24,44,45] and ALS patients [1,42,43]. Our study indicates that the reduced glutathione amount obtained in the cervical spinal cord of wobbler mice is due to a decreased glutathione synthesis due to a decreased expression of the rate-

limiting enzyme GCLC. For the first time, we provide evidence for a defective glutathione metabolism in the ALS in wobbler mice, which is not limited to motoric areas of the CNS. The detected decreased levels of glutathione in erythrocytes and plasma, besides alterations in glutathione metabolism and synthesis in all analyzed tissues of symptomatic wobbler mice, point toward the systemic character of ALS, as suggested before [112]. Although accumulating evidence suggests a direct or indirect involvement of aberrant glutathione homeostasis and metabolism in ALS [40], it remains unclear whether reduced glutathione is a causative factor or a result of neurodegeneration in ALS. So far, clinical trials aiming to improve glutathione contents in ALS by supplementation have been ineffective [106,107], as well as clinical trials targeting Nrf2 activating substances [102–105,113]. In consideration of our results, the dysregulations observed cannot be reversed by Nrf2 activation alone. Future studies are needed to differentiate defects in glutathione metabolism and synthesis in different cell types, especially astrocytes and neurons, in ALS. We conclude that the specific enhancement of glutathione synthesis might be a promising therapeutic target for ALS.

Supplementary Materials: The following supporting information can be downloaded at: https://www.mdpi.com/article/10.3390/antiox12051014/s1, Figure S1: No changes in the ubiquitinylation of proteins in different tissues of the p40 wobbler mouse.

Author Contributions: V.M. designed, conceptualized, and supervised the research; F.T.W. and V.M. performed all experiments with the support of C.T. and N.M.-N. (HPLC analysis); F.T.W. and V.M. analyzed, validated, and visualized the results; C.T. and N.M.-N. contributed expertise (HPLC) and intellectual feedback; F.T.W. and V.M. wrote the original manuscript draft; C.T. and N.M.-N. critically revised and edited this manuscript. All authors have read and agreed to the published version of the manuscript.

Funding: This research received no external funding.

Institutional Review Board Statement: All animal experiments were performed in accordance with EU guidelines 2010/63/EU concerning the protection of animals used for scientific purposes. Animal experiments were conducted according to German animal welfare regulations and approved by the local authorities (registration number Az. 84-02.04.2017.A085).

Informed Consent Statement: Not applicable.

Data Availability Statement: All data generated in this study are published in this article.

Acknowledgments: The authors gratefully acknowledge A. Lodwig, C. Grzelak, A. Harbecke, F. Opdenhoevel, and C. Lodwig for technical assistance, as well as T. Kolek-Vahstall for secretarial work. Graphical art in graphical abstract was prepared using (with modifications) Smart Servier Medical Art (https://smart.servier.com/, accessed on 19 March 2023) by Servier (Suresnes, France) licensed under a Creative Commons Attribution 3.0 Unported License (https://creativecommons.org/licenses/by/3.0/, accessed on 24 November 2022).

Conflicts of Interest: The authors declare no conflict of interest.

References

1. Ferrante, R.J.; Browne, S.E.; Shinobu, L.A.; Bowling, A.C.; Baik, M.J.; MacGarvey, U.; Kowall, N.W.; Brown, R.H., Jr.; Beal, M.F. Evidence of Increased Oxidative Damage in Both Sporadic and Familial Amyotrophic Lateral Sclerosis. *J. Neurochem.* **1997**, *69*, 2064–2074. [CrossRef]
2. Tam, O.H.; Rozhkov, N.V.; Shaw, R.; Kim, D.; Hubbard, I.; Fennessey, S.; Propp, N.; Fagegaltier, D.; Harris, B.T.; Ostrow, L.W.; et al. Postmortem Cortex Samples Identify Distinct Molecular Subtypes of ALS: Retrotransposon Activation, Oxidative Stress, and Activated Glia. *Cell Rep.* **2019**, *29*, 1164–1177.e5. [CrossRef]
3. Birger, A.; Ben-Dor, I.; Ottolenghi, M.; Turetsky, T.; Gil, Y.; Sweetat, S.; Perez, L.; Belzer, V.; Casden, N.; Steiner, D.; et al. Human iPSC-derived astrocytes from ALS patients with mutated C9ORF72 show increased oxidative stress and neurotoxicity. *Ebiomedicine* **2019**, *50*, 274–289. [CrossRef]
4. Lopez-Gonzalez, R.; Lu, Y.; Gendron, T.F.; Karydas, A.; Tran, H.; Yang, D.; Petrucelli, L.; Miller, B.L.; Almeida, S.; Gao, F.-B. Poly(GR) in C9ORF72 -Related ALS/FTD Compromises Mitochondrial Function and Increases Oxidative Stress and DNA Damage in iPSC-Derived Motor Neurons. *Neuron* **2016**, *92*, 383–391. [CrossRef]

5. Mitsumoto, H.; Garofalo, D.C.; Santella, R.M.; Sorenson, E.J.; Oskarsson, B.; Fernandes, J.A.M.; Andrews, H.; Hupf, J.; Gilmore, M.; Heitzman, D.; et al. Plasma creatinine and oxidative stress biomarkers in amyotrophic lateral sclerosis. *Amyotroph. Lateral Scler. Front. Degener.* **2020**, *21*, 263–272. [CrossRef]
6. Masrori, P.; van Damme, P. Amyotrophic Lateral Sclerosis: A Clinical Review. *Eur. J. Neurol.* **2020**, *27*, 1918–1929. [CrossRef]
7. Mitsumoto, H.; Brooks, B.R.; Silani, V. Clinical Trials in Amyotrophic Lateral Sclerosis: Why so Many Negative Trials and How Can Trials Be Improved? *Lancet Neurol.* **2014**, *13*, 1127–1138. [CrossRef]
8. Wong, C.; Stavrou, M.; Elliott, E.; Gregory, J.M.; Leigh, N.; Pinto, A.; Williams, T.L.; Chataway, J.; Swingler, R.; Parmar, M.K.B.; et al. Clinical trials in amyotrophic lateral sclerosis: A systematic review and perspective. *Brain Commun.* **2021**, *3*, fcab242. [CrossRef]
9. Falconer, D.S. Wobbler. Available online: https://scholar.google.com/scholar?hl=de&as_sdt=0%2C5&q=+DS+Falconer+-+Mouse+News+Lett%2C+1956&btnG= (accessed on 12 March 2022).
10. Duchen, L.W.; Strich, S.J. An hereditary motor neurone disease with progressive denervation of muscle in the mouse: The mutant 'wobbler'. *J. Neurol. Neurosurg. Psychiatry* **1968**, *31*, 535–542. [CrossRef]
11. Dahlke, C.; Saberi, D.; Ott, B.; Brand-Saberi, B.; Schmitt-John, T.; Theiss, C. Inflammation and neuronal death in the motor cortex of the wobbler mouse, an ALS animal model. *J. Neuroinflamm.* **2015**, *12*, 215. [CrossRef]
12. Schmitt-John, T. VPS54 and the wobbler mouse. *Front. Neurosci.* **2015**, *9*, 381. [CrossRef]
13. Moser, J.M.; Bigini, P.; Schmitt-John, T. The wobbler mouse, an ALS animal model. *Mol. Genet. Genom.* **2013**, *288*, 207–229. [CrossRef]
14. van Rheenen, W.; Pulit, S.L.; Dekker, A.M.; al Khleifat, A.; Brands, W.J.; Iacoangeli, A.; Kenna, K.P.; Kavak, E.; Kooyman, M.; McLaughlin, R.L.; et al. Project MinE: Study Design and Pilot Analyses of a Large-Scale Whole-Genome Sequencing Study in Amyotrophic Lateral Sclerosis. *Eur. J. Hum. Genet.* **2018**, *26*, 1537–1546. [CrossRef]
15. Boillée, S.; Peschanski, M.; Junier, M.-P. The Wobbler Mouse. *Mol. Neurobiol.* **2003**, *28*, 65–106. [CrossRef]
16. Ott, B.; Dahlke, C.; Meller, K.; Napirei, M.; Schmitt-John, T.; Brand-Saberi, B.; Theiss, C.; Saberi, D. Implementation of a Manual for Working with Wobbler Mice and Criteria for Discontinuation of the Experiment. *Ann. Anat.* **2015**, *200*, 118–124. [CrossRef]
17. Röderer, P.; Klatt, L.; John, F.; Theis, V.; Winklhofer, K.F.; Theiss, C.; Matschke, V. Increased ROS Level in Spinal Cord of Wobbler Mice due to Nmnat2 Downregulation. *Mol. Neurobiol.* **2018**, *55*, 8414–8424. [CrossRef]
18. Junghans, M.; John, F.; Cihankaya, H.; Schliebs, D.; Winklhofer, K.F.; Bader, V.; Matschke, J.; Theiss, C.; Matschke, V. ROS scavengers decrease γH2ax spots in motor neuronal nuclei of ALS model mice in vitro. *Front. Cell. Neurosci.* **2022**, *16*, 963169. [CrossRef]
19. Ahmed, M.S.; Hung, W.-Y.; Zu, J.S.; Hockberger, P.; Siddique, T. Increased Reactive Oxygen Species in Familial Amyotrophic Lateral Sclerosis with Mutations in SOD1. *J. Neurol. Sci.* **2000**, *176*, 88–94. [CrossRef]
20. Shaw, P.J.; Ince, P.G.; Falkous, G.; Mantle, D. Oxidative damage to protein in sporadic motor neuron disease spinal cord. *Ann. Neurol.* **1995**, *38*, 691–695. [CrossRef]
21. Simpson, E.P.; Henry, Y.K.; Henkel, J.S.; Smith, R.G.; Appel, S.H. Increased lipid peroxidation in sera of ALS patients: A potential biomarker of disease burden. *Neurology* **2004**, *62*, 1758–1765. [CrossRef]
22. Bonnefont-Rousselot, D.; Lacomblez, L.; Jaudon, M.-C.; Lepage, S.; Salachas, F.; Bensimon, G.; Bizard, C.; Doppler, V.; Delattre, J.; Meininger, V. Blood oxidative stress in amyotrophic lateral sclerosis. *J. Neurol. Sci.* **2000**, *178*, 57–62. [CrossRef]
23. Xiong, L.; McCoy, M.; Komuro, H.; West, X.Z.; Yakubenko, V.; Gao, D.; Dudiki, T.; Milo, A.; Chen, J.; Podrez, E.A.; et al. Inflammation-dependent oxidative stress metabolites as a hallmark of amyotrophic lateral sclerosis. *Free. Radic. Biol. Med.* **2021**, *178*, 125–133. [CrossRef]
24. Liu, D.; Wen, J.; Liu, J.; Li, L. The roles of free radicals in amyotrophic lateral sclerosis: Reactive oxygen species and elevated oxidation of protein, DNA, and membrane phospholipids. *FASEB J.* **1999**, *13*, 2318–2328. [CrossRef]
25. Towner, R.A.; Smith, N.; Saunders, D.; Lupu, F.; Silasi-Mansat, R.; West, M.; Ramirez, D.C.; Gomez-Mejiba, S.E.; Bonini, M.G.; Mason, R.P.; et al. In vivo detection of free radicals using molecular MRI and immuno-spin trapping in a mouse model for amyotrophic lateral sclerosis. *Free. Radic. Biol. Med.* **2013**, *63*, 351–360. [CrossRef]
26. Andrus, P.K.; Fleck, T.J.; Gurney, M.E.; Hall, E.D. Protein Oxidative Damage in a Transgenic Mouse Model of Familial Amyotrophic Lateral Sclerosis. *J. Neurochem.* **1998**, *71*, 2041–2048. [CrossRef]
27. Aguirre, N.; Beal, M.F.; Matson, W.R.; Bogdanov, M.B. Increased oxidative damage to DNA in an animal model of amyotrophic lateral sclerosis. *Free. Radic. Res.* **2005**, *39*, 383–388. [CrossRef]
28. Matschke, V.; Theiss, C.; Matschke, J. Oxidative stress: The lowest common denominator of multiple diseases. *Neural Regen. Res.* **2019**, *14*, 238–241. [CrossRef]
29. Aoyama, K.; Nakaki, T. Impaired Glutathione Synthesis in Neurodegeneration. *Int. J. Mol. Sci.* **2013**, *14*, 21021–21044. [CrossRef]
30. Ookhtens, M.; Kaplowitz, N. Role of the Liver in Lnterorgan Homeostasis of Glutathione and Cyst(e)ine. In *Seminars in Liver Disease*; Thieme Medical Publishers, Inc.: Stuttgart, Germany, 1998; Volume 18.
31. Nies, A.; Jedlitschky, G.; König, J.; Herold-Mende, C.; Steiner, H.; Schmitt, H.-P.; Keppler, D. Expression and immunolocalization of the multidrug resistance proteins, MRP1–MRP6 (ABCC1–ABCC6), in human brain. *Neuroscience* **2004**, *129*, 349–360. [CrossRef]
32. Kannan, R.; Chakrabarti, R.; Tang, D.; Kim, K.J.; Kaplowitz, N. GSH Transport in Human Cerebrovascular Endothelial Cells and Human Astrocytes: Evidence for Luminal Localization of Na q-Dependent GSH Transport in HCEC 1. *Brain Res.* **2000**, *852*, 374–382. [CrossRef]

33. Kannan, R.; Kuhlenkamp, J.F.; Jeandidler, E.; Trlnh, H.; Ookhtens, M.; Kaplowltz, N. Evidence for Carrier-Mediated Transport of Glutathione across the Blood-Brain Barrier in the Rat. *J. Clin. Investig.* **1990**, *85*, 2009–2013. [CrossRef]
34. Wang, X.F.; Cynader, M.S. Astrocytes Provide Cysteine to Neurons by Releasing Glutathione. *J. Neurochem.* **2000**, *74*, 1434–1442. [CrossRef]
35. Dringen, R.; Gutterer, J.M.; Gros, C.; Hirrlinger, J. Aminopeptidase N mediates the utilization of the GSH precursor CysGly by cultured neurons. *J. Neurosci. Res.* **2001**, *66*, 1003–1008. [CrossRef]
36. Aoyama, K.; Suh, S.W.; Hamby, A.M.; Liu, J.; Chan, W.Y.; Chen, Y.; Swanson, R.A. Neuronal glutathione deficiency and age-dependent neurodegeneration in the EAAC1 deficient mouse. *Nat. Neurosci.* **2006**, *9*, 119–126. [CrossRef]
37. Kranich, O.; Hamprecht, B.; Dringen, R. Different preferences in the utilization of amino acids for glutathione synthesis in cultured neurons and astroglial cells derived from rat brain. *Neurosci. Lett.* **1996**, *219*, 211–214. [CrossRef]
38. Dringen, R.; Pfeiffer, B.; Hamprecht, B. Synthesis of the Antioxidant Glutathione in Neurons: Supply by Astrocytes of CysGly as Precursor for Neuronal Glutathione. *J. Neurosci.* **1999**, *19*, 562–569. [CrossRef]
39. Dalton, T.P.; Chen, Y.; Schneider, S.N.; Nebert, D.W.; Shertzer, H.G. Genetically Altered Mice to Evaluate Glutathione Homeostasis in Health and Disease. *Free Radic. Biol. Med.* **2004**, *37*, 1511–1526. [CrossRef]
40. Kim, K. Glutathione in the Nervous System as a Potential Therapeutic Target to Control the Development and Progression of Amyotrophic Lateral Sclerosis. *Antioxidants* **2021**, *10*, 1011. [CrossRef]
41. Babu, G.N.; Kumar, A.; Chandra, R.; Puri, S.; Singh, R.; Kalita, J.; Misra, U. Oxidant–antioxidant imbalance in the erythrocytes of sporadic amyotrophic lateral sclerosis patients correlates with the progression of disease. *Neurochem. Int.* **2008**, *52*, 1284–1289. [CrossRef]
42. Weiduschat, N.; Mao, X.; Hupf, J.; Armstrong, N.; Kang, G.; Lange, D.; Mitsumoto, H.; Shungu, D. Motor cortex glutathione deficit in ALS measured in vivo with the J-editing technique. *Neurosci. Lett.* **2014**, *570*, 102–107. [CrossRef]
43. Andronesi, O.C.; Nicholson, K.; Jafari-Khouzani, K.; Bogner, W.; Wang, J.; Chan, J.; Macklin, E.A.; Levine-Weinberg, M.; Breen, C.; Schwarzschild, M.A.; et al. Imaging Neurochemistry and Brain Structure Tracks Clinical Decline and Mechanisms of ALS in Patients. *Front. Neurol.* **2020**, *11*, 590573. [CrossRef]
44. Chi, L.; Ke, Y.; Luo, C.; Gozal, D.; Liu, R. Depletion of reduced glutathione enhances motor neuron degeneration in vitro and in vivo. *Neuroscience* **2007**, *144*, 991–1003. [CrossRef]
45. Ross, E.K.; Winter, A.N.; Wilkins, H.M.; Sumner, W.A.; Duval, N.; Patterson, D.; Linseman, D.A. A Cystine-Rich Whey Supplement (Immunocal®) Delays Disease Onset and Prevents Spinal Cord Glutathione Depletion in the hSOD1^{G93A} Mouse Model of Amyotrophic Lateral Sclerosis. *Antioxidants* **2014**, *3*, 843–865. [CrossRef]
46. Livak, K.J.; Schmittgen, T.D. Analysis of relative gene expression data using real-time quantitative PCR and the $2^{-\Delta\Delta CT}$ Method. *Methods* **2001**, *25*, 402–408. [CrossRef]
47. Shawahna, R.; Uchida, Y.; Declèves, X.; Ohtsuki, S.; Yousif, S.; Dauchy, S.; Jacob, A.; Chassoux, F.; Daumas-Duport, C.; Couraud, P.-O.; et al. Transcriptomic and Quantitative Proteomic Analysis of Transporters and Drug Metabolizing Enzymes in Freshly Isolated Human Brain Microvessels. *Mol. Pharm.* **2011**, *8*, 1332–1341. [CrossRef]
48. Minich, T.; Riemer, J.; Schulz, J.B.; Wielinga, P.; Wijnholds, J.; Dringen, R. The multidrug resistance protein 1 (Mrp1), but not Mrp5, mediates export of glutathione and glutathione disulfide from brain astrocytes. *J. Neurochem.* **2006**, *97*, 373–384. [CrossRef]
49. Sato, H.; Tamba, M.; Ishii, T.; Bannai, S. Cloning and Expression of a Plasma Membrane Cystine/Glutamate Exchange Transporter Composed of Two Distinct Proteins. *J. Biol. Chem.* **1999**, *274*, 11455–11458. [CrossRef]
50. Wilkins, H.M.; Brock, S.; Gray, J.J.; Linseman, D.A. Stable over-expression of the 2-oxoglutarate carrier enhances neuronal cell resistance to oxidative stress via Bcl-2-dependent mitochondrial GSH transport. *J. Neurochem.* **2014**, *130*, 75–86. [CrossRef]
51. Aoyama, K. Glutathione in the Brain. *Int. J. Mol. Sci.* **2021**, *22*, 5010. [CrossRef]
52. Blasco, H.; Garcon, G.; Patin, F.; Veyrat-Durebex, C.; Boyer, J.; Devos, D.; Vourc'H, P.; Andres, C.R.; Corcia, P. Panel of Oxidative Stress and Inflammatory Biomarkers in ALS: A Pilot Study. *Can. J. Neurol. Sci.* **2017**, *44*, 90–95. [CrossRef]
53. Nakano, Y.; Hirayama, K.; Terao, K. Hepatic Ultrastructural Changes and Liver Dysfunction in Amyotrophic Lateral Sclerosis. *Arch. Neurol.* **1987**, *44*, 103–106. [CrossRef]
54. Nodera, H.; Takamatsu, N.; Muguruma, N.; Ukimoto, K.; Nishio, S.; Oda, M.; Izumi, Y.; Kaji, R. Frequent hepatic steatosis in amyotrophic lateral sclerosis: Implication for systemic involvement. *Neurol. Clin. Neurosci.* **2015**, *3*, 58–62. [CrossRef]
55. Griffith, O.W.; Meister, A. Glutathione: Interorgan Translocation, Turnover, and Metabolism. *Proc. Natl. Acad. Sci. USA* **1979**, *76*, 5606–5610. [CrossRef]
56. Giustarini, D.; Milzani, A.; Dalle-Donne, I.; Rossi, R. Red blood cells as a physiological source of glutathione for extracellular fluids. *Blood Cells, Mol. Dis.* **2008**, *40*, 174–179. [CrossRef]
57. Johnson, W.M.; Wilson-Delfosse, A.L.; Mieyal, J.J. Dysregulation of Glutathione Homeostasis in Neurodegenerative Diseases. *Nutrients* **2012**, *4*, 1399–1440. [CrossRef]
58. López-Blanch, R.; Salvador-Palmer, R.; Estrela, J.M.; Obrador, E. An Intercellular Flow of Glutathione Regulated by Interleukin 6 Links Astrocytes and the Liver in the Pathophysiology of Amyotrophic Lateral Sclerosis. *Antioxidants* **2021**, *10*, 2007. [CrossRef]
59. Agarwal, S.; Uchida, Y.; Mittapalli, R.K.; Sane, R.; Terasaki, T.; Elmquist, W.F. Quantitative Proteomics of Transporter Expression in Brain Capillary Endothelial Cells Isolated from P-Glycoprotein (P-gp), Breast Cancer Resistance Protein (Bcrp), and P-gp/Bcrp Knockout Mice. *Drug Metab. Dispos.* **2012**, *40*, 1164–1169. [CrossRef]
60. Lu, S.C. Regulation of glutathione synthesis. *Mol. Asp. Med.* **2009**, *30*, 42–59. [CrossRef]

61. Bannai, S. Exchange of cystine and glutamate across plasma membrane of human fibroblasts. *J. Biol. Chem.* **1986**, *261*, 2256–2263. [CrossRef]
62. Sato, H.; Tamba, M.; Okuno, S.; Sato, K.; Keino-Masu, K.; Masu, M.; Bannai, S. Distribution of Cystine/Glutamate Exchange Transporter, System x_c^-, in the Mouse Brain. *J. Neurosci.* **2002**, *22*, 8028–8033. [CrossRef]
63. Sasaki, H.; Sato, H.; Kuriyama-Matsumura, K.; Sato, K.; Maebara, K.; Wang, H.; Tamba, M.; Itoh, K.; Yamamoto, M.; Bannai, S. Electrophile Response Element-mediated Induction of the Cystine/Glutamate Exchange Transporter Gene Expression. *J. Biol. Chem.* **2002**, *277*, 44765–44771. [CrossRef] [PubMed]
64. Rana, S.; Dringen, R. Gap junction hemichannel-mediated release of glutathione from cultured rat astrocytes. *Neurosci. Lett.* **2007**, *415*, 45–48. [CrossRef] [PubMed]
65. Philbert, M.A.; Beiswanger, C.M.; Manson, M.M.; Green, J.A.; Novak, R.F.; Primiano, T.; Reuhl, K.R.; Lowndes, H.E. Glutathione S-transferases and gamma-glutamyl transpeptidase in the rat nervous systems: A basis for differential susceptibility to neurotoxicants. *Neurotoxicology* **1995**, *16*, 349–362.
66. Sedlak, T.W.; Paul, B.D.; Parker, G.M.; Hester, L.D.; Snowman, A.M.; Taniguchi, Y.; Kamiya, A.; Snyder, S.H.; Sawa, A. The Glutathione Cycle Shapes Synaptic Glutamate Activity. *Proc. Natl. Acad. Sci. USA* **2019**, *116*, 2701–2706. [CrossRef]
67. Pandur, S.; Pankiv, S.; Johannessen, M.; Moens, U.; Huseby, N.-E. γ-Glutamyltransferase is upregulated after oxidative stress through the Ras signal transduction pathway in rat colon carcinoma cells. *Free. Radic. Res.* **2007**, *41*, 1376–1384. [CrossRef]
68. DeNicola, G.M.; Karreth, F.A.; Humpton, T.J.; Gopinathan, A.; Wei, C.; Frese, K.; Mangal, D.; Yu, K.H.; Yeo, C.J.; Calhoun, E.S.; et al. Oncogene-induced Nrf2 transcription promotes ROS detoxification and tumorigenesis. *Nature* **2011**, *475*, 106–109. [CrossRef]
69. Liu, R.-M.; Shi, M.M.; Giulivi, C.; Forman, H.J. Quinones Increase γ-Glutamyl Transpeptidase Expression by Multiple Mechanisms in Rat Lung Epithelial Cells. *Am. J. Physiol. Lung Cell. Mol. Physiol.* **1998**, *14*, L330–L336. [CrossRef]
70. Mina-Osorio, P. The moonlighting enzyme CD13: Old and new functions to target. *Trends Mol. Med.* **2008**, *14*, 361–371. [CrossRef]
71. Bigini, P.; Bastone, A.; Mennini, T. Glutamate Transporters in the Spinal Cord of the Wobbler Mouse. *Neuroreport* **2001**, *12*, 1815–1820. [CrossRef]
72. Himi, T.; Ikeda, M.; Yasuhara, T.; Nishida, M.; Morita, I. Role of neuronal glutamate transporter in the cysteine uptake and intracellular glutathione levels in cultured cortical neurons. *J. Neural Transm.* **2003**, *110*, 1337–1348. [CrossRef]
73. Dall'Igna, O.P.; Bobermin, L.D.; Souza, D.O.; Quincozes-Santos, A. Riluzole increases glutamate uptake by cultured C6 astroglial cells. *Int. J. Dev. Neurosci.* **2012**, *31*, 482–486. [CrossRef] [PubMed]
74. Yang, W.; Kilberg, M.S. Biosynthesis, Intracellular Targeting, and Degradation of the EAAC1 Glutamate/Aspartate Transporter in C6 Glioma Cells. *J. Biol. Chem.* **2002**, *277*, 38350–38357. [CrossRef] [PubMed]
75. Fournier, K.M.; González, M.I.; Robinson, M.B. Rapid Trafficking of the Neuronal Glutamate Transporter, EAAC1: Evidence for Distinct Trafficking Pathways Differentially Regulated by Protein Kinase C and Platelet-Derived Growth Factor. *J. Biol. Chem.* **2004**, *279*, 34505–34513. [CrossRef] [PubMed]
76. González, M.I.; Susarla, B.T.S.; Fournier, K.M.; Sheldon, A.L.; Robinson, M.B. Constitutive endocytosis and recycling of the neuronal glutamate transporter, excitatory amino acid carrier 1. *J. Neurochem.* **2007**, *103*, 1917–1931. [CrossRef] [PubMed]
77. Malik, A.R.; Szydlowska, K.; Nizinska, K.; Asaro, A.; van Vliet, E.A.; Popp, O.; Dittmar, G.; Fritsche-Guenther, R.; Kirwan, J.A.; Nykjaer, A.; et al. SorCS2 Controls Functional Expression of Amino Acid Transporter EAAT3 and Protects Neurons from Oxidative Stress and Epilepsy-Induced Pathology. *Cell Rep.* **2019**, *26*, 2792–2804. [CrossRef]
78. Li, X.; Valencia, A.; Sapp, E.; Masso, N.; Alexander, J.; Reeves, P.; Kegel, K.B.; Aronin, N.; DiFiglia, M. Aberrant Rab11-Dependent Trafficking of the Neuronal Glutamate Transporter EAAC1 Causes Oxidative Stress and Cell Death in Huntington's Disease. *J. Neurosci.* **2010**, *30*, 4552–4561. [CrossRef]
79. Wilkinson, E.C.; Starke, E.L.; Barbee, S.A. Vps54 Regulates Lifespan and Locomotor Behavior in Adult Drosophila melanogaster. *Front. Genet.* **2021**, *12*, 762012. [CrossRef]
80. Lomen-Hoerth, C.; Murphy, J.; Langmore, S.; Kramer, J.H.; Olney, R.K.; Miller, B. Are Amyotrophic Lateral Sclerosis Patients Cognitively Normal? *Neurology* **2003**, *60*, 1094–1097. [CrossRef]
81. Van Blitterswijk, M.; Dejesus-Hernandez, M.; Rademakers, R. How Do C9ORF72 Repeat Expansions Cause Amyotrophic Lateral Sclerosis and Frontotemporal Dementia: Can We Learn from Other Noncoding Repeat Expansion Disorders? *Curr. Opin. Neurol.* **2012**, *25*, 689–700. [CrossRef]
82. Wightman, G.; Anderson, V.; Martin, J.; Swash, M.; Anderton, B.; Neary, D.; Mann, D.; Luthert, P.; Leigh, P. Hippocampal and Neocortical Ubiquitin-Immunoreactive Inclusions in Amyotrophic Lateral Sclerosis with Dementia. *Neurosci. Lett.* **1992**, *139*, 269–274. [CrossRef]
83. Thielsen, K.D.; Moser, J.M.; Schmitt-John, T.; Jensen, M.S.; Jensen, K.; Holm, M.M. The Wobbler Mouse Model of Amyotrophic Lateral Sclerosis (ALS) Displays Hippocampal Hyperexcitability, and Reduced Number of Interneurons, but No Presynaptic Vesicle Release Impairments. *PLoS ONE* **2013**, *8*, e82767. [CrossRef] [PubMed]
84. Raps, S.P.; Lai, J.C.; Hertz, L.; Cooper, A.J. Glutathione is present in high concentrations in cultured astrocytes but not in cultured neurons. *Brain Res.* **1989**, *493*, 398–401. [CrossRef] [PubMed]
85. Klatt, C.L.; Theis, V.; Hahn, S.; Theiss, C.; Matschke, V. Deregulated *miR-29b-3p* Correlates with Tissue-Specific Activation of Intrinsic Apoptosis in An Animal Model of Amyotrophic Lateral Sclerosis. *Cells* **2019**, *8*, 1077. [CrossRef]
86. Saberi, D.; Ott, B.; Dahlke, C.; Matschke, V.; Schmitt-John, T.; Theiss, C. The Spatiotemporal Pattern of Degeneration in the Cerebellum of the Wobbler Mouse. *J. Neuropathol. Exp. Neurol.* **2016**, *75*, 347–357. [CrossRef]

87. Prell, T.; Grosskreutz, J. The involvement of the cerebellum in amyotrophic lateral sclerosis. *Amyotroph. Lateral Scler. Front. Degener.* **2013**, *14*, 507–515. [CrossRef]
88. Bede, P.; Chipika, R.H.; Christidi, F.; Hengeveld, J.C.; Karavasilis, E.; Argyropoulos, G.D.; Lope, J.; Shing, S.L.H.; Velonakis, G.; Dupuis, L.; et al. Genotype-associated cerebellar profiles in ALS: Focal cerebellar pathology and cerebro-cerebellar connectivity alterations. *J. Neurol. Neurosurg. Psychiatry* **2021**, *92*, 1197–1205. [CrossRef]
89. Abidi, M.; de Marco, G.; Couillandre, A.; Feron, M.; Mseddi, E.; Termoz, N.; Querin, G.; Pradat, P.; Bede, P. Adaptive functional reorganization in amyotrophic lateral sclerosis: Coexisting degenerative and compensatory changes. *Eur. J. Neurol.* **2020**, *27*, 121–128. [CrossRef]
90. Baxter, P.S.; Hardingham, G.E. Adaptive regulation of the brain's antioxidant defences by neurons and astrocytes. *Free. Radic. Biol. Med.* **2016**, *100*, 147–152. [CrossRef]
91. Escartin, C.; Won, S.J.; Malgorn, C.; Auregan, G.; Berman, A.E.; Chen, P.-C.; Déglon, N.; Johnson, J.A.; Suh, S.W.; Swanson, R.A. Nuclear Factor Erythroid 2-Related Factor 2 Facilitates Neuronal Glutathione Synthesis by Upregulating Neuronal Excitatory Amino Acid Transporter 3 Expression. *J. Neurosci.* **2011**, *31*, 7392–7401. [CrossRef]
92. Saha, S.; Buttari, B.; Panieri, E.; Profumo, E.; Saso, L. An Overview of Nrf2 Signaling Pathway and Its Role in Inflammation. *Molecules* **2020**, *25*, 5474. [CrossRef]
93. Lu, S.C. Glutathione Synthesis. *Biochim. Biophys. Acta Gen. Subj.* **2013**, *1830*, 3143–3153. [CrossRef] [PubMed]
94. Yang, H.; Ko, K.; Xia, M.; Li, T.W.; Oh, P.; Li, J.; Lu, S.C. Induction of avian musculoaponeurotic fibrosarcoma proteins by toxic bile acid inhibits expression of glutathione synthetic enzymes and contributes to cholestatic liver injury in mice. *Hepatology* **2010**, *51*, 1291–1301. [CrossRef]
95. Feng, W.; Rosca, M.; Fan, Y.; Hu, Y.; Feng, P.; Lee, H.-G.; Monnier, V.M.; Fan, X. Gclc deficiency in mouse CNS causes mitochondrial damage and neurodegeneration. *Hum. Mol. Genet.* **2017**, *26*, 1376–1390. [CrossRef] [PubMed]
96. Stein, J.; Walkenfort, B.; Cihankaya, H.; Hasenberg, M.; Bader, V.; Winklhofer, K.F.; Röderer, P.; Matschke, J.; Theiss, C.; Matschke, V. Increased ROS-Dependent Fission of Mitochondria Causes Abnormal Morphology of the Cell Powerhouses in a Murine Model of Amyotrophic Lateral Sclerosis. *Oxidative Med. Cell. Longev.* **2021**, *2021*, 6924251. [CrossRef] [PubMed]
97. Wang, T.; Tomas, D.; Perera, N.D.; Cuic, B.; Luikinga, S.; Viden, A.; Barton, S.K.; McLean, C.A.; Samson, A.L.; Southon, A.; et al. Ferroptosis mediates selective motor neuron death in amyotrophic lateral sclerosis. *Cell Death Differ.* **2021**, *29*, 1187–1198. [CrossRef]
98. Sarlette, A.; Krampfl, K.; Grothe, C.; Von Neuhoff, N.; Dengler, R.; Petri, S. Nuclear Erythroid 2-Related Factor 2-Antioxidative Response Element Signaling Pathway in Motor Cortex and Spinal Cord in Amyotrophic Lateral Sclerosis. *J. Neuropathol. Exp. Neurol.* **2008**, *67*, 1055–1062. [CrossRef]
99. Johnson, D.A.; Johnson, J.A. Nrf2—A therapeutic target for the treatment of neurodegenerative diseases. *Free Radic. Biol. Med.* **2015**, *88*, 253–267. [CrossRef]
100. Jiménez-Villegas, J.; Ferraiuolo, L.; Mead, R.; Shaw, P.; Cuadrado, A.; Rojo, A. NRF2 as a therapeutic opportunity to impact in the molecular roadmap of ALS. *Free. Radic. Biol. Med.* **2021**, *173*, 125–141. [CrossRef]
101. Shou, L.; Bei, Y.; Song, Y.; Wang, L.; Ai, L.; Yan, Q.; He, W. Nrf2 mediates the protective effect of edaravone after chlorpyrifos-induced nervous system toxicity. *Environ. Toxicol.* **2019**, *34*, 626–633. [CrossRef]
102. Abe, K.; Aoki, M.; Tsuji, S.; Itoyama, Y.; Sobue, G.; Togo, M.; Hamada, C.; Tanaka, M.; Akimoto, M.; Nakamura, K.; et al. Safety and Efficacy of Edaravone in Well Defined Patients with Amyotrophic Lateral Sclerosis: A Randomised, Double-Blind, Placebo-Controlled Trial. *Lancet Neurol.* **2017**, *16*, 505–512. [CrossRef]
103. Witzel, S.; Maier, A.; Steinbach, R.; Grosskreutz, J.; Koch, J.C.; Sarikidi, A.; Petri, S.; Günther, R.; Wolf, J.; Hermann, A.; et al. Safety and Effectiveness of Long-Term Intravenous Administration of Edaravone for Treatment of Patients with Amyotrophic Lateral Sclerosis. *JAMA Neurol.* **2022**, *79*, 121–130. [CrossRef]
104. Vucic, S.; Henderson, R.D.; Mathers, S.; Needham, M.; Schultz, D.; Kiernan, M.C.; TEALS study group. Safety and Efficacy of Dimethyl Fumarate in ALS: Randomised Controlled Study. *Ann. Clin. Transl. Neurol.* **2021**, *8*, 1991–1999. [CrossRef]
105. Berry, J.D.; Paganoni, S.; Atassi, N.; Macklin, E.A.; Goyal, N.; Rivner, M.; Simpson, E.; Appel, S.; Grasso, D.L.; Mejia, N.I.; et al. Phase IIa trial of fingolimod for amyotrophic lateral sclerosis demonstrates acceptable acute safety and tolerability. *Muscle Nerve* **2017**, *56*, 1077–1084. [CrossRef]
106. Louwerse, E.S.; Weverling, G.J.; Bossuyt, P.M.M.; Meyjes, F.E.P.; De Jong, J.M.B.V. Randomized, Double-Blind, Controlled Trial of Acetylcysteine in Amyotrophic Lateral Sclerosis. *Arch. Neurol.* **1995**, *52*, 559–564. [CrossRef]
107. Chio, A.; Cucatto, A.; Terreni, A.A.; Schiffer, D. Reduced Glutathione in Amyotrophic Lateral Sclerosis: An Open, Crossover, Randomized Trial. *Ital. J. Neurol. Sci.* **1998**, *19*, 363–366.
108. Wagner, S.A.; Beli, P.; Weinert, B.T.; Nielsen, M.L.; Cox, J.; Mann, M.; Choudhary, C. A Proteome-wide, Quantitative Survey of In Vivo Ubiquitylation Sites Reveals Widespread Regulatory Roles. *Mol. Cell. Proteom.* **2011**, *10*, M111.013284. [CrossRef]
109. Dennis, J.; Citron, B. Wobbler mice modeling motor neuron disease display elevated transactive response DNA binding protein. *Neuroscience* **2009**, *158*, 745–750. [CrossRef]
110. Shang, F.; Taylor, A. Ubiquitin–proteasome pathway and cellular responses to oxidative stress. *Free. Radic. Biol. Med.* **2011**, *51*, 5–16. [CrossRef]
111. Nefedova, Y.; Fishman, M.; Sherman, S.; Wang, X.; Beg, A.A.; Gabrilovich, D.I. Mechanism of All-*Trans* Retinoic Acid Effect on Tumor-Associated Myeloid-Derived Suppressor Cells. *Cancer Res* **2007**, *67*, 11021–11028. [CrossRef]

112. Appel, S.H.; Beers, D.R.; Zhao, W. Amyotrophic Lateral Sclerosis Is a Systemic Disease: Peripheral Contributions to Inflammation-Mediated Neurodegeneration. *Curr. Opin. Neurol.* **2021**, *34*, 765–772. [CrossRef]
113. Abe, K.; Itoyama, Y.; Sobue, G.; Tsuji, S.; Aoki, M.; Doyu, M.; Hamada, C.; Kondo, K.; Yoneoka, T.; Akimoto, M.; et al. Confirmatory double-blind, parallel-group, placebo-controlled study of efficacy and safety of edaravone (MCI-186) in amyotrophic lateral sclerosis patients. *Amyotroph. Lateral Scler. Front. Degener.* **2014**, *15*, 610–617. [CrossRef]

antioxidants

MDPI

Article

Black Pepper (*Piper nigrum*) Alleviates Oxidative Stress, Exerts Potential Anti-Glycation and Anti-AChE Activity: A Multitargeting Neuroprotective Agent against Neurodegenerative Diseases

Himadri Sharma, Niti Sharma * and Seong Soo A. An *

Department of Bionano Technology, Gachon Bionano Research Institute, Gachon University, 1342 Seongnam-daero, Sujung-gu, Seongnam-si 461-701, Gyeonggi-do, Republic of Korea
* Correspondence: nitisharma@gachon.ac.kr (N.S.); seongaan@gachon.ac.kr (S.S.A.A.); Tel.: +82-31-750-8591 (N.S.); +82-31-750-8755 (S.S.A.A.)

Abstract: Neurodegenerative diseases (NDs) are a family of disorders that cause progressive structural and functional degeneration of neurons. Among all the organs in the body, the brain is the one that is the most affected by the production and accumulation of ROS. Various studies have shown that an increase in oxidative stress is a common pathophysiology for almost all NDs, which further affects various other pathways. The available drugs lack the wide spectrum necessary to confront these complexities altogether. Hence, a safe therapeutic approach to target multiple pathways is highly desirable. In the present study, the hexane and ethyl acetate extracts of *Piper nigrum* (black pepper), an important spice, were evaluated for their neuroprotective potential in hydrogen peroxide-induced oxidative stress in human neuroblastoma cells (SH-SY5Y). The extracts were also subjected to GC/MS to identify the important bioactives present. The extracts exhibited neuroprotection by significantly decreasing the oxidative stress and restoring the mitochondrial membrane potential in the cells. Additionally, the extracts displayed potent anti-glycation and significant anti-Aβ fibrilization activities. The extracts were competitive inhibitors of AChE. The multitarget neuroprotective mechanism displayed by *Piper nigrum* indicates it as a potential candidate in the treatment of NDs.

Keywords: neuroprotection; *Piper nigrum*; H_2O_2-induced stress; anti-acetylcholine esterase activity; anti-glycation; oxidative stress

Citation: Sharma, H.; Sharma, N.; An, S.S.A. Black Pepper (*Piper nigrum*) Alleviates Oxidative Stress, Exerts Potential Anti-Glycation and Anti-AChE Activity: A Multitargeting Neuroprotective Agent against Neurodegenerative Diseases. *Antioxidants* **2023**, *12*, 1089. https://doi.org/10.3390/antiox12051089

Academic Editors: Ana-Maria Buga and Carmen Nicoleta Oancea

Received: 31 March 2023
Revised: 8 May 2023
Accepted: 9 May 2023
Published: 12 May 2023

1. Introduction

Neurodegenerative diseases (NDs) are a family of disorders (Alzheimer's disease, Amyotrophic lateral sclerosis, Huntington's disease, Multiple sclerosis, Parkinson's disease, Prion disease, etc.) that lead to the progressive structural and/or functional degeneration of neurons. ND pathophysiology involves neuronal malfunction, synaptic dysfunction, and aggregation of specific proteins in the brain [1]. The progression, region affected, and extent of neurodegeneration in the brain are variable in different types of NDs. An increase in oxidative stress is a key point in defining the etiology of neurodegeneration. Oxygen is essential for the cells to meet their energetic demands, but the consumption of oxygen can also result in free radical production which can result in cellular damage [2]. Its accumulation may induce all the factors that are responsible for aging and the development of neurological disorders, such as cellular damage, mitochondrial cell death, and impairment of the DNA repair system. In addition, oxidative stress can be generated in the brain as a result of some environmental toxin or chemical which can produce ROS as a by-product [3]. This validates the need to screen new and safe medicinal agents from natural resources. Continuous efforts are being made to find agents that can lower oxidative stress in cells and provide protection from the risk of developing neurodegenerative disor-

ders [3]. In this perspective, numerous plants/bioactives have been reported to inhibit the production of free radicals [4] and provide neuroprotection.

Black pepper (*Piper nigrum* L.; Piperaceae family) is a flowering vine native to South Asia, crowned as the "King of Spices" due to its significant place culinarily for over 2000 years, and was the most valuable spice (called "Black Gold") traded from India to different parts of the world. The peppercorns were used as currency by ancient Greeks and European countries between 500 and 1500 AD [5]. It is traditionally used in the treatment of colds/coughs, neuropathic pain, gastric discomfort, respiratory diseases, etc. [6] and it has been reported to have numerous pharmacological actions, viz., antioxidant, anticancer, anti-asthmatic, antihypertensive, anti-inflammatory, anti-obesity, analgesic, CNS stimulant, hepatoprotective, immuno-modulatory, and antimicrobial properties [7]. The main bioactive component of black pepper is the alkaloid piperine which has been reported to have anti-AChE and anti-amyloid activity [8,9] and can restore the levels of antioxidant enzymes [10]. Additionally, due to its antioxidant properties, it has been shown to protect against cognitive decline and hippocampal nerve damage [11] and improve long-term potentiation (LTP) in the synaptic plasticity-impaired rat model [12].

Therefore, based on the above therapeutic importance of black pepper, we explored the role of the hexane and ethyl acetate extracts of black pepper (dried fruit) on H_2O_2-induced oxidative stress in SH-SY5Y neuronal cells. Moreover, the effect of black pepper extract on other important targets of neurodegeneration was also evaluated by studying its anti-fibrillation activity, acetylcholine esterase (AChE) inhibition, and advanced glycation end product (AGE) inhibition.

2. Materials and Methods

2.1. Chemicals

The chemicals 6,6′-dinitro-3,3′-dithiodibenzoic acid, bis(3-carboxy-4-nitrophenyl) disulfide (DTNB), acetyl thiocholine chloride, galantamine, gallic acid, ascorbic acid, 2,2′-azinobis-(3-ethylbenzothiazoline-6-sulfonic acid) (ABTS), 2,2-diphenyl-1-picrylhydrazyl (DPPH), 2,4,6-tripyridyl-s-triazine (TPTZ), Folin–Ciocalteu reagent (FCR), 2′,7′-dichlorofluorescin diacetate (DCFDA), tetramethylrhodamine, ethyl ester (TMRE), hydrogen peroxide, thioflavin T (ThT), bovine serum albumin (BSA), sodium azide, aminoguanidine, dextrose, and acetylcholinesterase (Electrophorus electricus, Type VI-S) were bought from Sigma-Aldrich (St. Louis, MO, USA). Aβ1-42 (Aggresure™) was acquired from AnaSpec (Fremont, CA, USA). The WST-8 kit was obtained from Roche Diagnostics GmbH (Mannheim, Germany). All organic solvents of HPLC grade were purchased from Sigma-Aldrich.

2.2. Plant Material and Extraction

The dried black pepper fruits were procured from the Expat Mart (Seoul, Republic of Korea). The samples were weighed and powdered using a pestle mortar. The powder was extracted sequentially in n-hexane and ethyl acetate. The extracted fractions were dried, weighed, and stored at 4 °C until further experiments.

2.3. Gas Chromatography–Mass Spectrometry (GC–MS) Method

The sample was analyzed on a fused-silica capillary column (DB-5ms UI, 30 m × 0.25 mm i.d., film thickness 0.25 μm, Agilent, Santa Clara, CA, USA) installed on a GCMS-QP2020 (Shimadzu, Kyoto, Japan). The oven temperature was programmed at 60 °C for 2 min, 100 °C at 4 °C/min, 290 °C at 10 °C/min, and finally to isothermic for 10 min. The split injection mode (1:10) was used and hexane and ethyl acetate fractions (1 μL, 1 mg/mL) were injected into the GC/MS via an auto-injector. The carrier gas was helium at a constant flow mode rate of 1 mL/min. The injection port, ion source, and interface temperatures were: 280, 280, and 150 °C, respectively. The energy of ionization was 70 eV. The mass spectra were obtained in full scan mode (40–700 AMU).

2.4. Determination of Total Phenolic Content

The Folin−Ciocalteu method [13], with modification for the 96-well format, was used to determine the total phenolic content of the extracts. Briefly, the extracts were incubated with 1N Folin−Ciocalteu reagent for 5 min at room temperature (RT) followed by the addition of a 10% sodium carbonate solution. The 96-well plate was incubated in the dark for 2 h at RT and the absorbance was measured at 765 nm (Multimode reader, Synergy-H1 BioTek, Agilent, Santa Clara, CA, USA). Gallic acid (10–200 mg/L) was used as a standard for calibration, and the results are expressed as mg gallic acid equivalent (GAE)/g of extract.

2.5. Determination of Total Flavonoids Content

The total flavonoids were estimated following the method of Ribarova et al. [14], with modifications for the 96-well plate format. To the extract, 10% aluminum chloride, 96% ethanol, and 1M sodium acetate were added and the 96-well plate was incubated in the dark at RT for 40 min. The absorbance was measured at 415 nm using a microplate reader (Synergy-H1 BioTek, Agilent, Santa Clara, CA, USA). The quercetin standard curve (10–100 μg/mL) was used to estimate the flavonoids in the extract and the results were expressed as mg quercetin equivalents per gram of sample (mg/g).

2.6. Determination of Antioxidant Capacity

2.6.1. Free Radical Scavenging by 2,2-Diphenyl-1-picrylhydrazylhydrate (DPPH) Radical

The method described previously [15], with minor modifications, was used to determine the DPPH radical scavenging capacity of the extracts. The diluted extract was mixed with 120 μM ethanolic DPPH. The 96-well plate was incubated in the dark for 30 min at RT and the absorbance was checked at 515 nm (Multimode reader, Synergy-H1 BioTek, Agilent, Santa Clara, CA, USA). Ascorbic acid (0.1–10 μg/mL) was used as a standard. Radical scavenging activity (RSA) was calculated using the following formula:

$$\% \text{ RSA} = (\text{Ab} - \text{Ae/Ab}) \times 100$$

where Ab = absorbance of the blank and Ae = absorbance of the extract.

2.6.2. Free Radical Scavenging by 2,2′-Azino-bis (3-Ethylbenzothiazoline-6-Sulfonic Acid) [ABTS] Radical

The free radical scavenging capacity of extracts was measured by the method described earlier [16]. ABTS radicals were generated by mixing equal volumes of ABTS (0.7 mM) and potassium persulfate (2.45 mM) kept in the dark at RT for 30 min. The extract was mixed with the ABTS radical solution and incubated in the dark for 30 min at RT. The absorbance was measured at 734 nm using the microplate reader (Synergy-H1 BioTek, Agilent, USA). Ascorbic acid (100 μg/mL) was used as a standard. The percentage of inhibition of ABTS+• was calculated as:

$$\% \text{ RSA} = (\text{Ab} - \text{Ae/Ab}) \times 100$$

where Ab = absorbance of the blank and Ae = absorbance of the extract.

2.6.3. Ferric Reducing Antioxidant Potential (FRAP) Assay

The FRAP assay was carried out to evaluate the metal-chelating ability of the extracts by modifying a previously described method [17]. The working FRAP reagent was prepared by mixing 10:1:1 volumes of 300 mM acetate buffer (pH 3.6), 10 mM TPTZ (2,4,6-tri(2-pyridyl)-s-triazine) in 40 mM hydrochloric acid, and 20 mM ferric chloride. A standard curve was prepared using $FeSO_4 \cdot 7H_2O$ at various concentrations (1 mM). For the assay, the extract was incubated with 300 μL of FRAP reagent, and the reduction of ferric tripyridyltriazine to a ferrous complex by the extract was monitored at 593 nm (Multimode

reader, Synergy-H1 BioTek, Agilent, USA) after 30 min of incubation at RT. FRAP values of the sample were expressed as μM Fe^{2+}/g.

2.7. Acetylcholinesterase Inhibitory Activity

The AChE activity was monitored by slight modifications to Ellman's method [18]. The extracts were incubated at 37 °C for 15 min with AChE and 10 mM ATCC in a phosphate buffer (100 mM, pH 7.6). The reaction was terminated by 15 mM DTNB, and the absorbance was measured at 412 nm using the plate reader (Synergy-H1 BioTek, Agilent, USA). Galantamine served as a positive control. The percent inhibition was calculated as:

$$\text{Percent Inhibitory activity (I\%)} = [(Ao - Ac) - (Bi - Bc)]/(Ao - Ac) \times 100$$

where Ao is the absorbance without inhibitor; Ac is the negative control without inhibitor; Bi is the absorbance with inhibitor; and Bc is the negative control with inhibitor. The IC_{50} values were determined by GraphPad Prism 9.5.

2.8. Thioflavin T (ThT) Assay

A previously reported method was followed with slight modification [19]. The assay was performed using 5 μM Aβ1-42 (Aggresure™ AnaSpec) in PBS (100 mM, pH 7.4) and was incubated with or without extract for 24 h at 37 °C. Next, 100 μM ThT was added, and the plate was incubated for 15 min more at 37 °C; after which the fluorescence (Ex 450 nm; Ems 490 nm) was measured (Synergy-H1 BioTek, Agilent, USA). Phenol red (100 μM) was used as the inhibitor control.

The aggregation inhibition was calculated as:

$$\text{Inhibition (\%)} = (Fc - Fi)/Fc \times 100\%$$

where Fi and Fc are the fluorescence intensity with and without the inhibitors, respectively.

2.9. Advanced Glycation End-Product (AGE) Inhibition Activity

The glycation reaction was carried out as described [20] by incubating the extracts in 100 mM phosphate buffer (pH 7.4) containing BSA, dextrose monohydrate, and sodium azide at 37 °C for 14 days. Aminoguanidine was used as a positive control. The fluorescence (Ex 370 nm; Ems 440 nm) was measured (Multimode reader, Synergy-H1 BioTek, Agilent, USA) and the percent glycation inhibition was calculated as:

$$\text{Inhibition (\%)} = [(C - T)/C \times 100]$$

where C and T are the fluorescence intensity in the absence and presence of the sample, respectively. The IC_{50} values were determined by GraphPad Prism 9.5.

2.10. Cell Culture

Human neuroblastoma SH-SY5Y cells (ATCC CRL-2266, Manassas, VA, USA) were maintained in Dulbecco's modified Eagle's medium (DMEM, Gibco) supplemented with 10% fetal bovine serum (FBS), 1% kanamycin, and 1% penicillin (Thermo Fisher Scientific, Waltham, MA, USA) at 37 °C with 5% CO_2, and a 95% humidified atmosphere in the incubator. The cells were passaged twice per week and the experiments were performed at 80–90% cell confluency.

2.10.1. Cell Viability Assay

For the cell viability assay, cells were seeded (1×10^4 cells/well) in sterile 96-well plates and subjected to various concentrations of extracts for 24 h. The extracts were removed and the cells were washed twice with 1X PBS and incubated in the fresh medium with 10% WST-8 reagent (Roche, Grenzach-Wyhlen, Germany) for 2 h. The absorbance

was measured at 450 nm in a multi-plate reader (Synergy-H1 BioTek, Agilent, USA). The percent cytotoxicity was calculated as:

$$\text{Cytotoxicity \%} = (\text{A control cells} - \text{A treated cells})/(\text{A control cells}) \times 100$$

where A control cells = absorbance of the control cells and A treated cells = absorbance of the treated cells.

The plot of percent cytotoxicity versus sample concentration was used to calculate the extract concentration that killed 50% of the cells (IC_{50}).

2.10.2. Neuroprotective Activity Assay

The neuroprotective effect of extracts on H_2O_2-induced oxidative stress in SH-SY5Y was performed as previously described [19]. The cells (1×10^4 cells/well) were seeded in a 96-well plate and incubated for 18–24 h. After stabilization, the cells were pre-treated with the extracts for 24 h. The extracts were then removed and treated with H_2O_2 (100 μM) for 6 h. A solvent control, H_2O_2 alone, and extract alone treatments were also included. After incubation, the % cell viability was determined using WST-8 reagent in triplicate experiments.

2.10.3. Measurement of Intracellular Reactive Oxygen Species (ROS)

The ROS was measured using 2′,7′-dichlorodihydrofluorescein diacetate (H2DCFDA) as previously described [19]. The cells (1×10^4 cells/well) were seeded in a 96-well plate and incubated for 18–24 h, after which they were pre-treated with the extract for 12 h. The extracts were then removed, followed by a 4 h treatment with H_2O_2 (100 μM). Then, 25 μM H2DCFDA was added and the cells were incubated for another 2 h in the dark at 37 °C. The fluorescence intensity (Ex 495 nm, Ems 520 nm) was measured by a microplate reader (Synergy-H1 BioTek, Agilent, USA). The ROS was calculated as a percentage of the untreated control cells (100%) in triplicate measurements.

2.10.4. Mitochondrial Membrane Potential (ΔΨm) Assay

The mitochondrial membrane potential was measured using the tetramethylrhodamine, methyl ester (TMRE) staining method [21]. The cells (1×10^4 cells/well) were seeded in a 96-well plate and incubated for 18–24 h; after which, they were pre-treated with the extract for 12 h. The extracts were then removed, followed by a 2 h treatment with H_2O_2 (200 μM). The cells were incubated for 1 h with 1 μM TMRE at 37 °C. The fluorescence (Ex 549 nm, Ems 575 nm) was read in a microplate reader (Synergy-H1 BioTek, Agilent, USA). The ΔΨm was calculated as a percentage of the untreated control cells (100%) in triplicate measurements.

2.10.5. Statistical Analysis

Statistical analysis was established by a one-way ANOVA followed by Dunnett's post-hoc test. Data are registered as the mean ± SD of at least three experiments. The symbols ###, *** represents $p < 0.001$, ##, ** represents $p < 0.01$, and #, * represents $p < 0.05$. The symbol # indicates significance compared to the H_2O_2 control while * indicates significance compared to the untreated control. The IC_{50} values were determined using non-linear regression. The Michaelis–Menten plot was drawn using a non-linear plot by GraphPad Prism 9.5, and the Vmax and Km were calculated from it. Lineweaver–Burk plots were drawn using linear regression analysis by GraphPad Prism 9.5.

3. Results and Discussion

3.1. GC–MS Analysis

The GC–MS chromatogram of *Piper nigrum* (Pep-H: Pepper Hexane, and Pep-EA: Pepper Ethylacetate) extracts were recorded to identify their bioactive compounds. The GC–MS chromatogram of Pep-EA was much clearer and a single major peak (52.4%) of piperi-

dine, 1-(5-(1,3-benzodioxol-5-yl)-1-oxo-2,4-pentadienyl)-, and (Z,Z)- {syn. chavicine} was recorded (Figure 1A). Chavicine is one of the four geometrical isomers of piperine [22] and has been reported to enhance memory in the mice model [23,24].

(**A**)

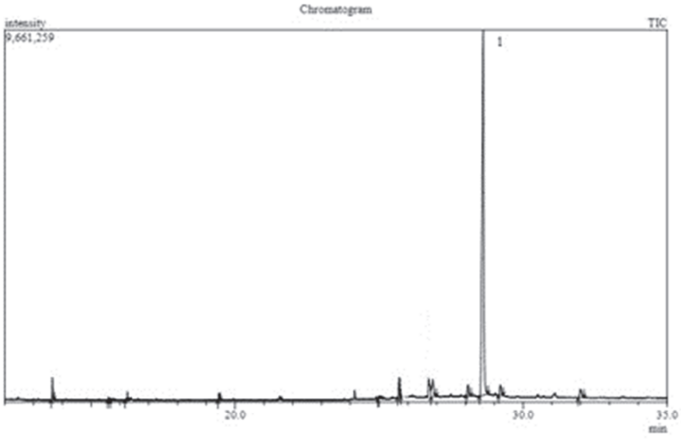

Major Peak No.	R. Time	Area	Area (%)	Height	Height (%)	Name
	3.064	102,832	0.18	89,379	0.49	Ethane, 1,1-diethoxy-
	3.204	176,877	0.31	106,801	0.59	Methyl 2-methoxypropenoate
	4.060	196,519	0.35	128,354	0.71	Acetic acid, butyl ester
	6.131	334,395	0.59	120,779	0.67	Benzenediazonium, 2-hydroxy-, hydroxide
	13.658	1,132,945	2.01	630,767	3.48	Caryophyllene
	15.621	123,055	0.22	56,483	0.31	Bicyclo[7.2.0]undec-4-ene, 4,11,11-trimethy l- 8-methylene-
	15.753	151,861	0.27	73,678	0.41	Caryophyllene oxide
	16.220	165,589	0.29	88,132	0.49	Isospathulenol
	19.439	416,247	0.74	233,383	1.29	2,4-Decadienamide, N-isobutyl-, (E, E)-
	25.022	255,259	0.45	114,968	0.64	(2,3-Diphenylcyclopropyl) methyl phenyl sulfoxide
	25.697	1,147,447	2.04	517,660	2.86	(E)-5-(Benzo[d][1,3] dioxol-5-yl)-1-(piperidine)
	25.791	303,106	0.54	129,526	0.72	Piperlonguminine
	26.867	1,968,676	3.50	442,736	2.45	Piperine
	28.086	1,043,906	1.85	336,384	1.86	Pyrrolidine, 1-[5-(1,3-benzodioxol-5-yl)-1-oxo-2,4-pentadienyl]-
1	**28.615**	**39,065,067**	**69.40**	**9,485,212**	**52.40**	**Piperidine, 1-(5-(1,3-benzodioxol-5-yl)-1-oxo-2,4-pentadienyl)-, (Z,Z)**
	29.217	962,392	1.71	267,971	1.48	(2E,4E,8E)-9-(Benzo[d][1,3]dioxol-5-yl)-1-(1-pyrrolidinyl)-
	31.997	1,183,204	2.10	270,058	1.49	(E)-9-(Benzo[d][1,3]dioxol-5-yl)-1-(piperidine)
		56,289,140	100.00	18,101,734	100.00	

Figure 1. *Cont.*

(**B**)

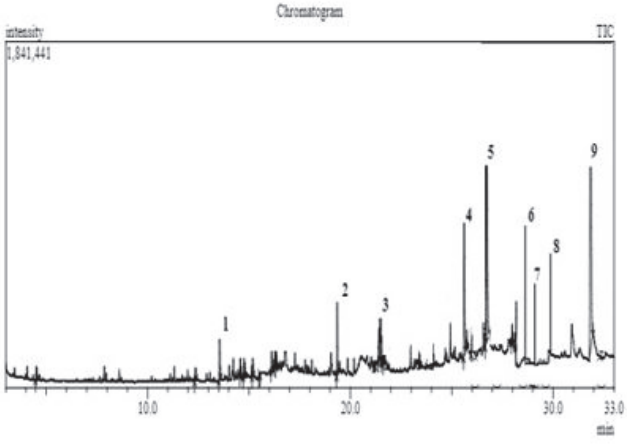

Major Peak No.	R.Time	Area	Area (%)	Height	Height (%)	Name
	4.511	236,194	0.66	138,736	0.98	Benzene, chloro-
	12.357	129,373	0.36	69,105	0.49	Piperonal
1	**13.554**	**1,391,565**	**3.87**	**816,740**	**5.79**	**Caryophyllene**
	14.572	269,151	0.75	156,944	1.11	.beta.-Bisabolene
	14.753	318,807	0.89	162,868	1.16	Tau-Cadinol acetate
	15.185	442,568	1.23	274,474	1.95	1,6,10-Dodecatrien-3-ol, 3,7,11-trimethyl-, (E)
	15.515	218,824	0.61	107,703	0.76	Butanoic acid, tridec-2-ynyl ester
	15.652	881,548	2.45	369,811	2.62	Caryophyllene oxide
	16.125	1,178,191	3.27	629,098	4.46	Isospathulenol
	16.287	158,466	0.44	84,858	0.60	Caryophylla-4(12),8(13)-dien-5.alpha.-ol
	16.341	145,254	0.40	84,528	0.60	.gamma.-Muurolene
2	**19.355**	**1,832,948**	**5.09**	**1,092,806**	**7.75**	**2,4-Decadienamide, N-isobutyl-, (E,E)-**
	21.190	179,566	0.50	88,016	0.62	(2E,4E)-1-(Pyrrolidin-1-yl)deca-2,4-dien-1-one
	21.235	130,266	0.36	83,701	0.59	Piperidine, 1-(1-oxo-3-phenyl-2-propenyl)-
	21.401	285,318	0.79	171,127	1.21	(2E,4E)-N-Isobutyldodeca-2,4-dienamide
3	**21.535**	**1,295,462**	**3.60**	**796,497**	**5.65**	**(E)-9-Octadecenoic acid ethyl ester**
	21.648	223,879	0.62	109,263	0.78	Vinyltriphenylphosphonium bromide
	23.390	130,225	0.36	77,036	0.55	(2E,4E)-1-(Piperidin-1-yl)dodeca-2,4-dien-1
	24.078	238,782	0.66	112,681	0.80	1,2-Propanediol, 3-benzyloxy-1,2-diacetyl-
4	**25.615**	**2,940,888**	**8.17**	**1,352,644**	**9.59**	**(E)-5-(Benzo[d][1,3]dioxol-5-yl)-1-(piperidine)**
	26.000	297,957	0.83	138,945	0.99	(E)-1-(Piperidin-1-yl)hexadec-2-en-1-one
5	**26.684**	**3,613,435**	**10.04**	**1,607,809**	**11.40**	**(2E,4E,10E)-N-Isobutylhexadeca-2,4,10-trienamide**
	27.978	248,667	0.69	96,541	0.68	(E)-9-(Benzo[d][1,3]dioxol-5-yl)-1-(piperidine)
	28.191	713,033	1.98	246,074	1.75	(E)-1-(Piperidin-1-yl)octadec-2-en-1-one
6	**28.451**	**3,662,410**	**10.18**	**1,228,280**	**8.71**	**Piperidine, 1-[5-(1,3-benzodioxol-5-yl)-1-oxo-2,4-pentadienyl]-, (Z,Z)-**
7	**28.527**	**3,128,629**	**8.70**	**978,393**	**6.94**	**(E)-7-(Benzo[d][1,3]dioxol-5-yl)-1-(piperidine)**
	28.937	1,723,340	4.79	524,223	3.72	(2E,4E,14E)-N-Isobutylicosa-2,4,14-trienamide
8	**29.092**	**3,940,332**	**10.95**	**1,084,074**	**7.69**	**(2E,4E,8E)-9-(Benzo[d][1,3]dioxol-5-yl)-1-(piperidin-1-yl)nona-2,4,8-trien-1-one**
9	**31.845**	**6,024,161**	**16.74**	**1,414,445**	**10.03**	**(E)-9-(Benzo[d][1,3]dioxol-5-yl)-1-(piperidine)**
		35,979,239	100.00	14,097,420	100.00	

Figure 1. Phytoconstituents identified in Pep-EA (**A**) and Pep-H (**B**) extracts from *Piper nigrum* using gas chromatography–mass spectrometry. Abbreviation: Pep-EA: Pepper-Ethyl acetate; Pep-H: Pepper-Hexane.

In the case of Pep-H, a total of 29 peaks were registered with only 9 peaks over 5%, namely, Caryophyllene (5.79%), 2,4-Decadienamide, N-isobutyl-, (E,E)- {syn. pellitorine} (7.75%), (E)-9-Octadecenoic acid ethyl ester (5.65%) {syn. ethyl elaidate}, (E)-5-(Benzo[d][1,3] dioxol-5-yl)-1-(piperidine) {syn. dihydropiperine} (9.59%), (2E,4E,10E)-N-Isobutylhexadeca-2,4,10-trienamide {syn. pipercide} (11.40%), Piperidine, 1-(5-(1,3-benzodioxol-5-yl)-1-oxo-2, 4-pentadienyl)-, (Z,Z)- {syn. chavicine} (8.71%), (E)-7-(Benzo[d][1,3]dioxol-5-yl)-1-(piperidine-1-yl) hept-6-en-1-one) {syn. piperolein A} (6.94%), (2E,4E,8E)-9-(Benzo[d][1,3]dioxol-5-yl)-1-(piperidin-1-yl)nona-2,4,8-trien-1-one) {syn. dehydropipernonaline} (7.69%), and (E)-9-(Benzo[d][1,3] dioxol-5-yl)-1-(piperidin-1-yl)hept-6-en-1-one) {syn. piperolein B} (10.03%) (Figure 1B).

The key bicyclic sesquiterpene contributing to the piquancy of Pep-H is β-Caryophyllene (BCP), which is also the first "dietary cannabinoid" with GRAS (generally recognized as safe) status and certified for food use by the FDA [25]. Apart from having a therapeutic role in several pathological conditions, it also has a positive impact on improving neurodegenerative diseases [26]. Pellitorine (PT), an amide alkaloid, has been reported for anti-septic, antibacterial, insecticidal, and anticancer activities [27,28] and also acts as a transient receptor potential cation channel, subfamily V, member 1 (TRPV1) antagonist, inhibiting exovanilloid-induced pain [29]. Dihydropiperine has a γ-aminobutyric acid (GABAA) receptor binding affinity. Piperolein A and B are known to activate thermosensitive receptors (TRP), TRPV1, and the transient receptor potential cation channel, subfamily A, member 1 (TRPA1), suggesting a role in thermoregulation [30]. In addition, pipercide exhibited antimalarial properties [24,31] whereas piperine and dehydropiperonaline from *P. retrofractum* acted as anti-obesity agents [32].

3.2. Phytochemical Estimation and Antioxidant Potential of Piper nigrum Extract

The total phenolic content (TPC) and flavonoid content (TFC) were estimated in the extracts using colorimetric assays. Phenols and flavonoids are secondary metabolites with an important role in the growth, communication, and defense of plants. Pep-EA had a higher phenol and flavonoid content compared to Pep-H. The phenolic content in the Pep-H and Pep-EA extracts was calculated to be 14.78 ± 1.99 mg GAE/g and 24.10 ± 0.67 mg GAE/g, respectively, while the flavonoid content was 20.15 ± 0.78 mg QE/g (Pep-H) and 41.86 ± 0.69 mg QE/g (Pep-EA).

Previously, the methanolic extract of black pepper had a TPC of 6.71 ± 0.34 mg GAE/g and TFC of 63.11 ± 3.16 mg QE/g [33]. However, the TPC (22.69 ± 0.58 µg GAE/g) and TFC (3.65 ± 0.62 µg GAE/g) were quite low in the ethyl acetate extract [34].

The antioxidant potential of the extracts was also evaluated by different assays. The percent of radical scavenging activity observed in the DPPH assay was lower in the case of Pep-H (34.39 ± 0.24%) compared to Pep-EA (54.8 ± 0.39%). However, the $ABTS^{+}$ radical scavenging activity and electron transfer (FRAP) were better in the case of Pep-EA (22.91 ± 1.19% and 41.65 ± 0.53 µM Fe^{2+}/g) compared to Pep-H (14.79 ± 0.58% and 6.41 ± 0.01 µM Fe^{2+}/g) at 50 µg/mL. In a previous study, the water extract of black pepper exhibited 26.67% (DPPH assay), 74.87% (ABTS assay), and 20.42% (FRAP assay) activity at 500 µg/mL [35]. The hydroalcoholic extract exhibited 43.1% (ABTS) and 43% (DPPH) activity [36]. The loss of phenols has been reported during the ripening and drying of black pepper, resulting in lower antioxidant activity compared to its green stage [37]. The higher TPC and TFC content in the case of Pep-EA can be correlated to the better antioxidant potential of Pep-EA; a positive correlation between the antioxidant potential and TPC has been reported earlier [38]. In GC–MS, chavicine (the most abundant isomer of piperine) was reported as the main phytocompound (52.4%) of Pep-EA. The antioxidant activity of piperine is well-established in vitro and in vivo studies [39,40]. However, substantial information on the antioxidant property of chavicine is lacking. From the antioxidant assay results obtained in our study, Pep-EA displayed better activity compared to Pep-H, suggesting the antioxidant potential of chavicine.

3.3. In Vitro Anti-Glycation Activity

Glycation is a non-enzymatic reaction that results in the formation of AGEs which are the cross-linked structures formed between proteins and reducing sugars, eventually leading to inflammation and oxidative stress in addition to affecting cell signaling. Chronic stress accelerates the formation and aggregation of AGEs in the body, which in turn fuels oxidative stress [41]. The AGEs are involved in the pathogenesis of age-related NDs, diabetic complications, chronic kidney disease, etc. [42]. Therefore, glycation is also an important therapeutic target for the treatment of NDs.

The BSA-AGE fluorescence assay was used to assess the in vitro anti-glycation potential of varying concentrations of Pep-H and Pep-EA. After two weeks of incubation with the BSA-glucose buffer, the extent of glycation inhibition was calculated. Pep-EA potentially inhibited the glycation with an IC_{50} value of 35.6 µg/mL, much lower than Aminoguanidine, the positive control (IC_{50} 91.42 µg/mL). In a previous report, a similar IC_{50} value of 91.2 µg/mL was reported for Aminoguanidine [43]. Pep-H also exhibited similar anti-glycation activity (IC_{50} 119.9 µg/mL) as the control (Figure 2). Previously, black pepper (hydro-alcoholic) extracts inhibited AGE formation by 67% in the BSA-glucose model [36].

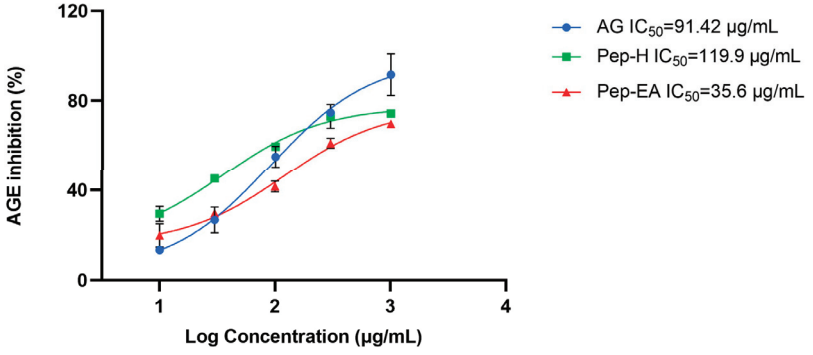

Figure 2. The anti-glycation activity exhibited by *Piper nigrum* extracts. Data are the mean ± SD of triplicates. Results were calculated using GraphPad Prism 9.5. Abbreviations: AG: Aminoguanidine; Pep-H: Pepper-Hexane; and Pep-EA: Pepper-Ethyl acetate.

It has been known that spices are a rich source of polyphenols and could inhibit AGE formation considerably [44] through their antioxidant nature, protein interaction, metal chelating action, and by blocking the AGE receptor (RAGE) [45]. The strong anti-glycation potential of flavonoids is due to their binding to proteins, which might prevent AGE formation [46,47]. Previously, the antioxidant properties of piperine were reported for its in vitro and in vivo dose-dependent anti-glycation action [48,49]. Therefore, the lower IC_{50} value shown by Pep-EA compared to Pep-H can be correlated to its higher flavonoid content, better antioxidant profile, and higher chavicine (an isomer of piperine) content. In addition, piperine forms a stable albumin-piperine complex by interacting with its subdomain IIA, which could be another possible mechanism for the anti-glycation action [50]. It is speculated that chavicine might form a complex with the albumin, such as piperine, and inhibit glycation. The potent anti-glycation activity shown by Pep-H could be the result of the synergistic action of phytocompounds. The superior anti-glycation activity of Pep-EA makes it a prospective compound in therapeutics for the future development of novel anti-AGE inhibitors.

3.4. Acetylcholinesterase Inhibitory Activity

To evaluate the neuroprotective effect of black pepper extracts, we also studied their anti-acetylcholine esterase (AChE; E.C.3.1.1.7) activity. The higher AChE induces apoptosis and affects synaptic integrity neurodevelopment [51] therefore AChE inhibition is desir-

able in the management of AD to maintain the level of the neurotransmitter acetylcholine (ACh) for cholinergic transmission. In this study, the pepper extracts displayed ~40% inhibition in preliminary screening at 100 µg/mL. Hence, the experiment to calculate IC_{50} values (half maximal inhibitory concentration) was conducted. The IC_{50} value of Pep-H was 41.72 µg/mL and that of Pep-EA was 28.59 µg/mL. In previous studies, the methanolic pepper extract had shown an IC_{50} value of 11.13 µg/mL [52] whereas the black pepper oil exhibited a strong AChE inhibition with a low IC_{50} value (5.9 µg/mL) [53]. The IC_{50} value of the positive control, Galantamine, was calculated as 0.94 µg/mL, like the previously reported value of 1.45 µg/mL [54]. The IC_{50} values of the extracts and the positive control have been shown in Figure 3.

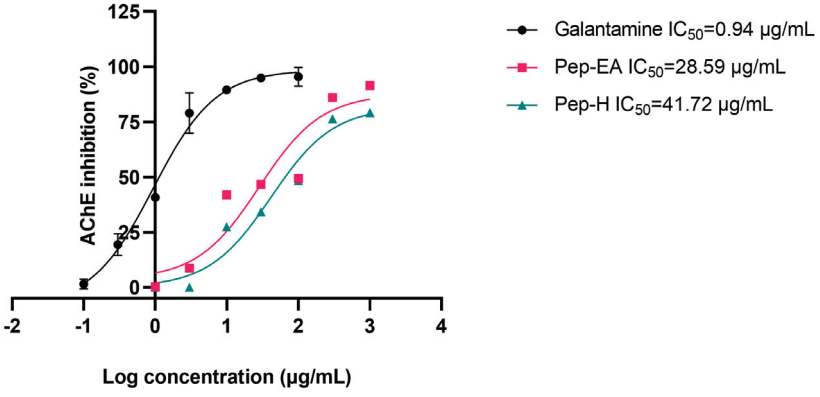

Figure 3. IC_{50} curve of *Piper nigrum* extracts with inhibitor control (Galantamine) against AChE. Data are the mean ± SD of triplicates. The IC_{50} values were calculated using GraphPad Prism 9.5. Abbreviations: Pep-H: Pepper-Hexane; Pep-EA: Pepper-Ethyl acetate.

The Lineweaver-Burk plot was used to elucidate the mechanism of AChE inhibition. Competitive inhibition was observed for both Pep-H and Pep-EA (Figure 4) and the kinetic parameter values (Table 1) were calculated from a non-linear fit (Michaelis-Menten equation).

Similar Vmax (the maximum rate at which an enzyme is catalyzed when the enzyme is saturated by the substrate) values were obtained for the no-inhibitor (1.375 µmole/min/mg) with Pep-H (1.364 µmole/min/mg at 50 µg/mL and 1.372 µmole/min/mg 100 µg/mL) and Pep-EA (1.333 µmole/min/mg at 50 µg/mL and 1.360 µmole/min/mg 100 µg/mL), while an increase in the Km (the concentration of substrate which permits the enzyme to achieve half Vmax) values was observed: 7.37 mM (no-inhibitor), Pep-H (8.35 mM; 8.75 mM), and Pep-EA (8.05 mM;10.08 mM) at 50 µg/mL and 100 µg/mL, respectively (Figure 4). The increased Km value in the presence of an inhibitor reduces the affinity of the enzyme for the substrate. These results indicate a competitive inhibition pattern where the inhibitor competes with the substrate for binding to the active site of the enzyme.

An in silico study proposed that the presence of several functional groups (C=O, R–O–R, and C–OH) in the benzodioxol moiety of *P. nigrum* components (such as piperine), facilitate hydrophobic connections (five in the case of piperine) with amino acids present in the proteins, resulting in enhanced enzyme inhibition [8,55]. The molecular docking studies of *P. longum* extract using *T. californica* AChE suggested a possible hydrogen bonding with Tyr_{70} [56]. In a previous docking study, β-caryophyllene (a bio-active component of Pep-H) exhibited a lower binding affinity (−8.3 kcal/mol) and interacted with Tyr_{114}, Trp_{126}, Trp_{351}, and Phe_{392} of the *T. castaneum* AChE enzyme [57]. In addition, β-caryophyllene interacted with Phe_{297} and Trp_{286} residues in AChE from *Electrophorus* [58]. The molecular docking of some alkaloids from the ethanolic extract of *P. nigrum* also formed a hydrogen bond with Ser_{200} and His_{440} at the catalytic site of *T. californica* AChE [59]. The reason for a superior IC_{50} value of Pep-EA compared to Pep-H could be due to the higher content of

chavicine compared to Pep-H. However, the Pep-H also displayed commendable AChE inhibition which could be the result of the synergistic action of bio-active components present in the extract as reported in the case of *P. longum* [56]. In the future, chavicine/piperine derivatives could be used as a pharmacophore for drug development in the treatment of NDs.

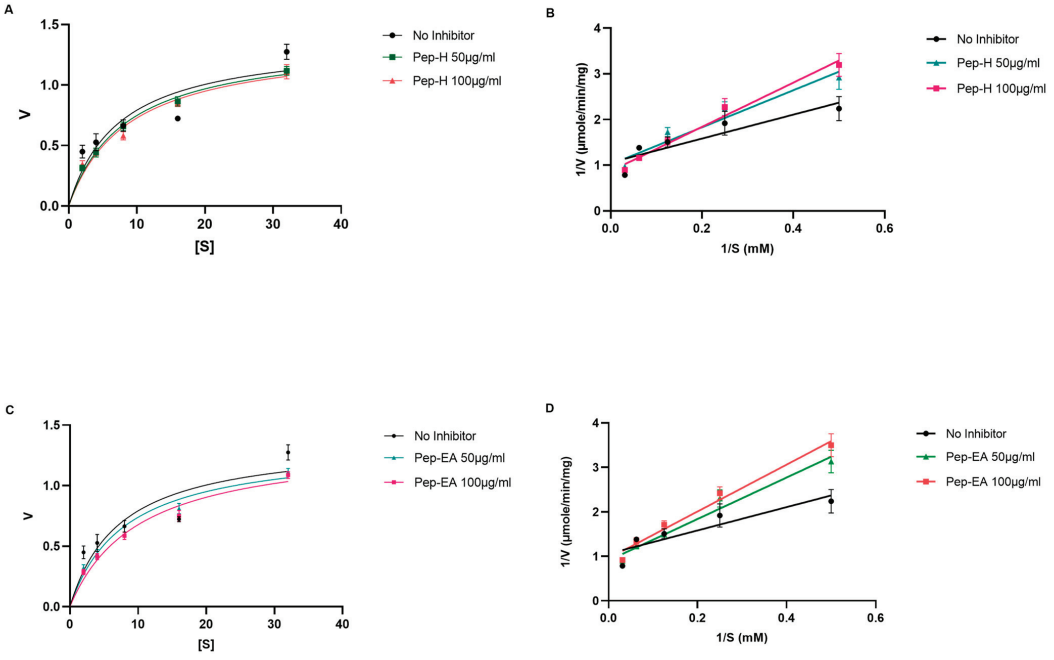

Figure 4. Michaelis-Menten (**A**,**C**) and Lineweaver-Burk (**B**,**D**) plot of AChE in the presence of 50 µg/mL and 100 µg/mL of *Piper nigrum* extracts (Pep-H and Pep-EA). The graphs were plotted using GraphPad Prism 9.5. Abbreviations: Pep-H: Pepper-Hexane; Pep-EA: Pepper-Ethyl acetate; V: Velocity of enzyme-catalyzed reaction; Vmax: Maximum velocity; and S: Substrate.

Table 1. Kinetic parameters.

	Vmax (µmole/min/mg)	Km (mM)	Type of Inhibition
No Inhibitor	1.375	7.371	
Pep-H (50 µg/mL)	1.396	8.379	Competitive
Pep-H (100 µg/mL)	1.364	8.755	Competitive
Pep-EA (50 µg/mL)	1.333	8.052	Competitive
Pep-EA (100 µg/mL)	1.360	10.080	Competitive

3.5. Piper nigrum Extract Reduced Aβ Fibrilization

Aβ fibrilization inhibition activity of the pepper extracts was assessed using a ThT assay. The fluorescence signal is increased upon binding of ThT to the amyloid β-sheet. The extracts were screened at 100 µg/mL for Aβ fibrilization inhibition with Phenol red as a positive control. A statistically significant reduction was seen in the extracts compared to the control (buffer + Aβ). Phenol red exhibited a 67.49 ± 3.73% inhibition (*** $p < 0.001$) at 50 µM, comparable to the previously described value [60]. Pep-H was statistically non-significant while Pep-EA exerted statistically significant (* $p < 0.05$) inhibition of 31.84 ± 7.76% compared to the control (Figure 5).

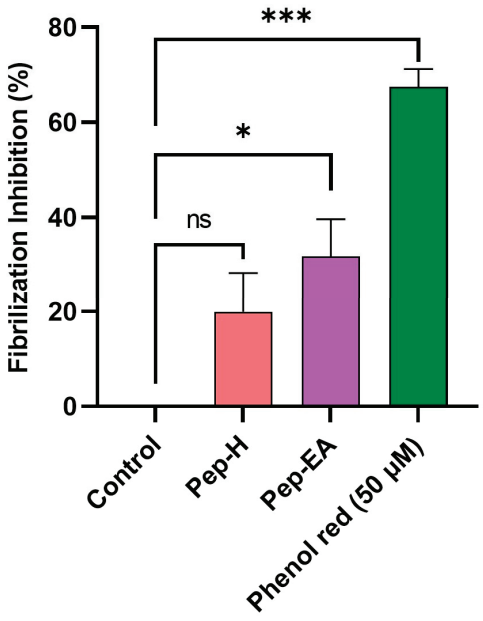

Figure 5. Aβ fibrilization inhibition in the presence of *Piper nigrum* extracts. The values are expressed as the mean ± SD (n = 3). Phenol Red (50 µM) was used as a positive control. A significant difference, * ($p < 0.05$) and *** ($p < 0.001$), using a one-way ANOVA followed by Dunnett's post-hoc was observed in the reduction in fibrilization vs. the negative control (buffer + Aβ). Abbreviations: Pep-H: Pepper-Hexane; Pep-EA: Pepper-Ethyl acetate.

Aβ fibrilization is the vital component of amyloid plaques in AD pathology which contribute to oxidative stress and neuroinflammation. It is speculated that the main component of Pep-EA, chavicine, might be interacting with the β sheet of the protein through π-stacking or hydrophobic interaction to exert anti-fibrilization activity [61]. Our results agree with a previous study, where *P. nigrum* (12.5 mg/kg/day) improved memory in an aluminum chloride-induced neurotoxicity mice model by significantly modulating the expression of amyloid-producing isoforms (APP770 and APP695) in the brain. The extract decreased the expression of the amyloidogenic APP770 isoform with a concomitant improvement in the expression of the APP695 (non-amyloidogenic) isoform in the hippocampus, amygdala, and cortex. Chavicine was identified as the main pharmacologically active component of the extract responsible for neuroprotection [23].

In a previous study, black pepper oil exhibited weak fibrilization inhibition (33.17 ± 6.67%) at 100 µg/mL [53]. However, no fibrilization inhibition was observed for black pepper water extract [62].

3.6. Cytotoxic Effect of Pepper Extracts on the SH-SY5Y Cell Line

The cellular viability in the neuroblastoma cell line (SH-SY5Y) was analyzed using WST-8 dye after 24 h of treatment with different concentrations of the extracts (1, 10, 25, and 50 µg/mL). No cytotoxicity was observed up to 50 µg/mL for Pep-H, however, for Pep-EA, the cell viability decreased to 76.57% (** $p < 0.01$) at 50 µg/mL (Figure 6). Hence, to minimize cell death due to the extract toxicity, concentrations lower than 50 µg/mL were used for the subsequent cell-based assays.

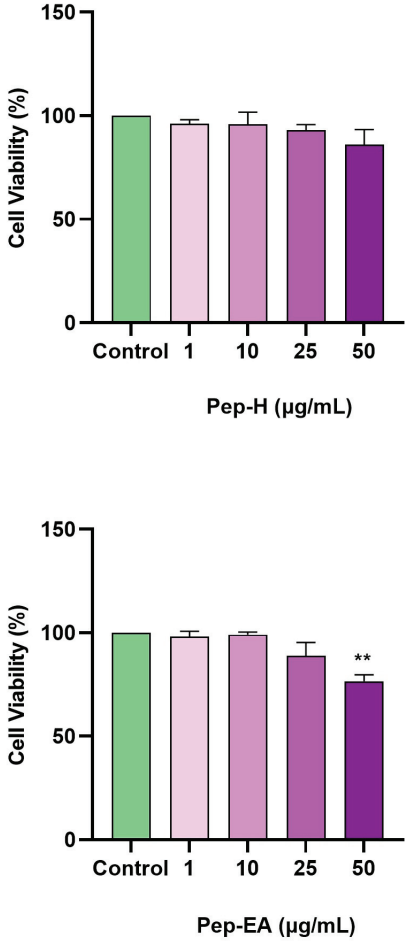

Figure 6. Cytotoxicity assay of *Piper nigrum* extracts on the SH-SY5Y cells. The cells were treated for 24 h with varying extract concentrations (1, 10, 25, and 50 µg/mL). The cell viability is reported as the percentage of the control group (100%). All data are presented as the mean ± SD (n = 3). A significant difference ** ($p < 0.01$) using a one-way ANOVA followed by Dunnett's post-hoc was observed in the % cell viability vs. the control group (no treatment). Abbreviations: Pep-H: Pepper-Hexane; P-EA: Pepper-Ethyl acetate.

3.7. Piper nigrum Provided Neuroprotection against H_2O_2-Induced Oxidative Stress in SH-SY5Y

The neuroprotective effects of the extracts were assessed by H_2O_2-induced oxidative stress in the SH-SY5Y cells. In the preliminary optimization experiment, H_2O_2 at 100 µM resulted in 50% cell survival after 6 h treatment. Therefore, 100 µM H_2O_2 was used to induce oxidative stress in SH-SY5Y cells pre-treated with different concentrations of the extracts (01, 0.3, 1, 3, 10, and 30 µg/mL) for 12 h.

Both the extracts displayed dose-dependent neuroprotection with a statistically significant effect at higher concentrations. Pep-EA performed better in protecting the cells against oxidative damage and significantly (# $p < 0.05$) increased the cell viability at 1 µg/mL and ## $p < 0.01$ at 3–30 µg/mL compared to H_2O_2 control. Pep-H significantly increased the cell viability at 3 µg/mL (# $p < 0.05$) and at 10 and 30 µg/mL (## $p < 0.01$) as compared to the H_2O_2 control. However, the lower concentrations (0.1–1 µg/mL) were ineffective for

Pep-H (Figure 7). From the results, it can be concluded that 10 µg/mL of both extracts is the best concentration to display maximum neuroprotection, after which the effect remains almost constant. The neuroprotective mechanism was further explored by measuring the ROS and the MMP.

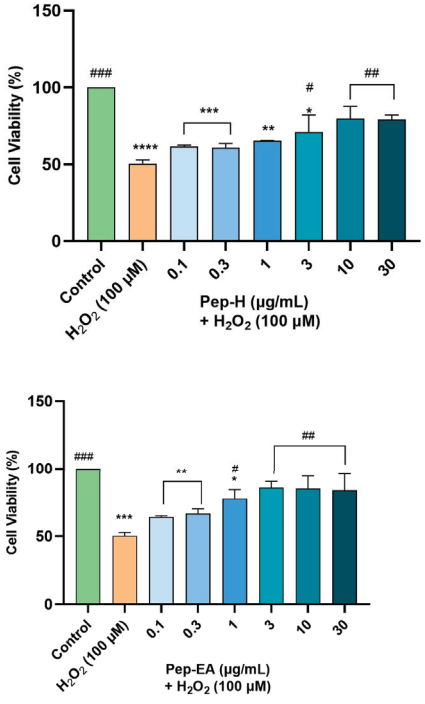

Figure 7. Neuroprotective effect of *Piper nigrum* extracts in H_2O_2-induced oxidative stress in neuroblastoma SH-SY5Y cells. The SH-SY5Y cells were preincubated with the extracts (0.1, 0.3, 1, 3, 10, and 30 µg/mL) for 12 h followed by 6 h of H_2O_2 (100 µM) treatment. The results indicate the % cell viability vs. the control cells, the mean ± SD (n = 3). A significant difference, */# ($p < 0.05$), **/## ($p < 0.01$), ***/### ($p < 0.001$), and **** ($p < 0.0001$) using a one-way ANOVA followed by Dunnett's post-hoc test was observed in the % cell viability vs. untreated cells (*) and H_2O_2 treated cells (#). Abbreviations: Pep-H: Pepper-Hexane; Pep-EA: Pepper-Ethyl acetate.

3.8. Piper nigrum Ameliorated H_2O_2-Induced ROS Generation

Oxidative stress and ROS generation are key characteristics of neurodegenerative diseases and have a damaging effect on cellular components including proteins, lipids, and DNA [63]. Hence, it is worth finding the compounds that can trim down intracellular ROS. As H_2O_2 is an important ROS generator, we used it to induce oxidative stress in the SH-SY5Y cell line. To evaluate the ROS scavenging activity of the pepper extracts, the cells were pre-treated with varying concentrations of the extracts for 12 h followed by H_2O_2 (100 µM) exposure for 4 h. The fluorescent dye (H2DCFDA) was used to monitor ROS production. H_2O_2 treatment generated 156.9 ± 5.0% ROS compared to the untreated cells (100%). Pre-treatment of the cells with extracts resulted in a dose-dependent decrease in ROS production in Pep-H. The Pep-EA was slightly more effective and significant at 1 µg/mL (121 ± 4.5%; $p < 0.05$) and 10 µg/mL (113.1 ± 2.4%; $p < 0.001$) compared to Pep-H (Figure 8). Thereby, 10 µg/mL of Pep-EA and 25 µg/mL of Pep-H are required for the maximum ROS reduction in the SH-SY5Y cell line. The dose-dependent reduction in ROS observed in our study indicates the antioxidant nature of the extracts which maintained a high level of cellular communication [64] and exerted a neuroprotective effect. Addi-

tionally, the effectiveness of Pep-EA in reducing ROS could be linked to better antioxidant activity and a higher chavicine content.

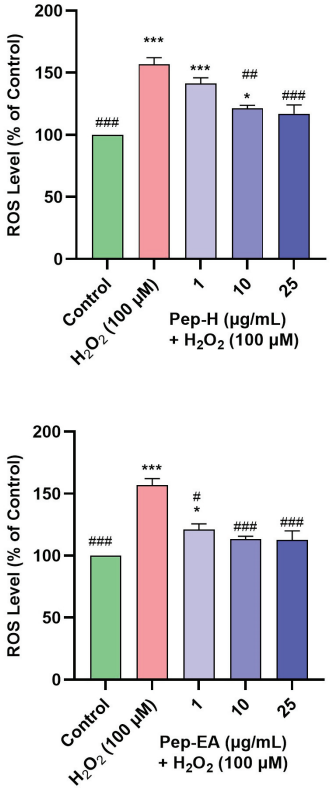

Figure 8. Effect of *Piper nigrum* extracts on H_2O_2-induced ROS production in SH-SY5Y cells. The SH-SY5Y cells were preincubated with the extracts (1, 10, and 25 µg/mL) for 12 h followed by 4 h of H_2O_2 (100 µM) treatment. The results indicate the % ROS level vs. the control cells (untreated cells). Values are the mean ± SD (n = 3). The data were analyzed by a one-way ANOVA followed by Dunnett's post-hoc test. A significant difference, */# (p <0.05), ## (p <0.01), and ***/### (p <0.001), was observed in the % ROS vs. untreated cells (*) and H_2O_2 treated cells (#). Abbreviations: Pep-H: Pepper-Hexane; Pep-EA: Pepper-Ethyl acetate.

3.9. Piper nigrum Improved Mitochondrial Membrane Potential

Mitochondria are the major site of ROS generation during electron transport and stimulate the production of proinflammatory cytokines. The mitochondrial membrane potential (ΔΨm) is disturbed due to oxidative damage to the cell which affects membrane permeability and the release of Cytochrome C and/or pro-apoptotic factors in the cytoplasm. Therefore, the loss of MMP is regarded as an early marker of apoptosis and a major contributor to NDs [65,66].

In the present study, H_2O_2 concentration and time of induction were optimized using a fluorescent dye (TMRE) which has an affinity for active mitochondria. In our experiment, H_2O_2 at 200 µM concentration reduced the MMP to ~50% of the untreated cells, hence, this condition was used for further examination. H_2O_2 treatment depolarized the mitochondria resulting in a decreased membrane potential. The cells pre-treated with Pep-H for 12 h followed by H_2O_2 (200 µM) treatment for 2 h (after removing the extracts) displayed a significant dose-dependent increase in MMP at 1 µg/mL (78.7 ± 2.0%; ## p < 0.01) and 10 µg/mL (88.0 ± 1.6%; ### p < 0.001), after which it declined significantly (60.5 ± 5.3%;

*** $p < 0.001$). The effect of Pep-EA was milder than Pep-H, showing improvement in MMP at 1 µg/mL (87.1 ± 2.9%; # $p < 0.05$) and 10 µg/mL (85.0 ± 9.6%; # $p < 0.05$) which decreased afterward (72.5 ± 9.8%; * $p < 0.01$) at 25 µg/mL (Figure 9). It appears that Pep-H displayed neuroprotection by improving MMP and inhibiting Cytochrome C release into the cytosol. However, the decrease in ΔΨm at higher concentrations (25 µg/mL) depicts the toxicity or ineffectiveness of both extracts in restoring MMP. In our experiment, Pep-EA effectively reduced ROS (Figure 8) but was not as effective in restoring MMP (Figure 9). No doubt mitochondria are the chief generators of intracellular ROS, however, they are not the only source. Other cellular sources include enzymes (xanthine oxidase, lipoxygenase, cyclooxygenase, and NADH/NADPH oxidase); the peroxisomal β-oxidation of fatty acids and microsomal metabolism of xenobiotics, etc. also contribute to ROS production [67,68]. Hence, it appears that Pep-EA is capable of scavenging ROS generated from other cellular sites as well.

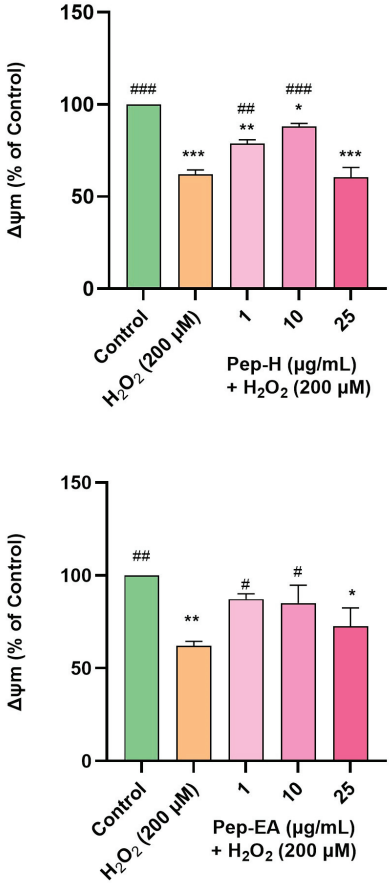

Figure 9. Mitochondrial membrane potential in SH-SY5Y cells exposed to 200 µM H_2O_2 for 2 h after 12 h pre-treatment with pepper extracts (1, 10, and 25 µg/mL). The results indicate % ΔΨm vs. the control cells (untreated cells). Values are the mean ± SD (n = 3). The data were analyzed by a one-way ANOVA followed by Dunnett's post-hoc test. A significant difference, */# ($p < 0.05$), **/## ($p < 0.01$), and ***/### ($p < 0.001$), was observed in the % cell viability vs. untreated cells (*) and H_2O_2 treated cells (#). Abbreviations: Pep-H: Pepper-Hexane; Pep-EA: Pepper-Ethyl acetate, and ΔΨm: Mitochondrial membrane potential.

Previously, the in vivo neuroprotective mechanism of piperine included protecting mitochondrial integrity via reducing oxidative stress and improving mitochondrial membrane potential and neuronal survival in a cerebral ischemia rat model [69,70] and streptozotocin-induced cognitively impaired rats [71].

4. Conclusions

The present study was conducted to explore the neuroprotective mechanism exerted by *Piper nigrum* extracts. H_2O_2, being the important mediator of oxidative stress, which eventually leads to Aβ aggregation, neuronal death, and neuroinflammation, was used to generate ROS in the human neuroblastoma SH-SY5Y. The *P. nigrum* extracts protected the cells from oxidative damage by reducing ROS production and maintaining mitochondrial membrane integrity, reflecting the antioxidant potential of the extracts. Pep-EA was able to scavenge ROS from other cellular sources as well. Additionally, the extracts displayed strong anti-glycation activity which might be possible due to the interaction of flavonoids with the proteins, preventing AGE formation. The extracts also competitively inhibited AChE and exhibited promising IC_{50} values, indicating that the bioactive components interacted with the amino acid residues at the active site of AChE. Moreover, black pepper-ethyl acetate extract significantly inhibited Aβ fibrilization. Better neuroprotection by Pep-EA is linked to a higher chavicine content. Hence, the multitarget neuroprotective mechanism presented by *Piper nigrum* makes it suitable for drug development in NDs. Previous studies have demonstrated that piperine (an isomer of chavicine) has a favorable pharmacokinetics profile with a high affinity towards brain tissue (98.4–98.5%), plasma protein (96.2–97.8%), and a brain distribution volume of 36.32 ± 1.40 mL/g [72]. Additionally, after dosing (100 and 200 mg), its C_{max} (the maximum drug concentration observed in the sampled blood or plasma) was reported as 3.77 μg/mL and 6.59 μg/mL, respectively, in healthy volunteers [73]. In contrast, the related literature on chavicine is limited; therefore, to fill this information gap, extensive investigations on the toxicity, bioavailability, and neuroprotective potential of chavicine in animal models and clinical trials are of utmost importance.

Author Contributions: Conceptualization, N.S. and S.S.A.A.; experimentation and data analysis, H.S. and N.S.; writing—original draft preparation, N.S.; writing—review and editing, N.S. and S.S.A.A.; funding acquisition, S.S.A.A. All authors have read and agreed to the published version of the manuscript.

Funding: This research was supported by the Gachon University research fund of 2022 (GCU- 202208910001) and by the National Research Foundation of Korea (NRF-2021R1A6A1A03038996).

Institutional Review Board Statement: Not applicable.

Informed Consent Statement: Not applicable.

Data Availability Statement: All data are provided in the article.

Conflicts of Interest: The authors declare no conflict of interest.

References

1. Taoufik, E.; Kouroupi, G.; Zygogianni, O.; Matsas, R. Synaptic dysfunction in neurodegenerative and neurodevelopmental diseases: An overview of induced plu-ripotent stem-cell-based disease models. *Open Biol.* **2018**, *8*, 180138. [CrossRef] [PubMed]
2. Gandhi, S.; Abramov, A.Y. Mechanism of oxidative stress in neurodegeneration. *Oxid. Med. Cell. Longev.* **2012**, *2012*, 428010. [CrossRef] [PubMed]
3. Kim, G.H.; Kim, J.E.; Rhie, S.J.; Yoon, S. The Role of Oxidative Stress in Neurodegenerative Diseases. *Exp. Neurobiol.* **2015**, *24*, 325–340. [CrossRef] [PubMed]
4. Cui, X.; Lin, Q.; Liang, Y. Plant-Derived Antioxidants Protect the Nervous System From Aging by Inhibiting Oxidative Stress. *Front. Aging Neurosci.* **2020**, *12*, 209. [CrossRef] [PubMed]
5. Aggarwal, B.B.; Kunnumakkara, A.B. *Molecular Targets and Therapeutic Uses of Spices: Modern Uses for Ancient Medicine*; World Scientific: Singapore, 2009.
6. Gülçin, I. The antioxidant and radical scavenging activities of black pepper (*Piper nigrum*) seeds. *Int. J. Food Sci. Nutr.* **2005**, *56*, 491–499. [CrossRef] [PubMed]

7. Saleem, A.; Naureen, I.; Naeem, M.; Tasleem, G.; Ahmed, H.; Farooq, U. Therapeutic Role of Piper nigrum L (Black Pepper) and Pharmacological Activities. *Sch. Int. J. Biochem.* **2022**, *5*, 15–21. [CrossRef]
8. Manap, A.S.A.; Tan, A.C.W.; Leong, W.H.; Chia, A.Y.Y.; Vijayabalan, S.; Arya, A.; Wong, E.H.; Rizwan, F.; Bindal, U.; Koshy, S.; et al. Synergistic Effects of Curcumin and Piperine as Potent Acetylcholine and Amyloidogenic Inhibitors With Significant Neuroprotective Activity in SH-SY5Y Cells via Computational Molecular Modeling and in vitro Assay. *Front. Aging Neurosci.* **2019**, *11*, 206. [CrossRef] [PubMed]
9. Aluko, R.E. Food-derived Acetylcholinesterase Inhibitors as Potential Agents against Alzheimer's Disease. *Efood* **2021**, *2*, 49–58. [CrossRef]
10. Hritcu, L.; Noumedem, J.A.; Cioanca, O.; Hancianu, M.; Postu, P.; Mihasan, M. Anxiolytic and antidepressant profile of the methanolic extract of Piper nigrum fruits in beta-amyloid (1–42) rat model of Alzheimer's disease. *Behav. Brain Funct.* **2015**, *11*, 13. [CrossRef] [PubMed]
11. Wang, C.; Cai, Z.; Wang, W.; Wei, M.; Kou, D.; Li, T.; Yang, Z.; Guo, H.; Le, W.; Li, S. Piperine attenuates cognitive impairment in an experimental mouse model of sporadic Alzheimer's disease. *J. Nutr. Biochem.* **2019**, *70*, 147–155. [CrossRef]
12. Nazifi, M.; Oryan, S.; Esfahani, D.E.; Ashrafpoor, M. The functional effects of piperine and piperine plus donepezil on hippocampal synaptic plasticity impairment in rat model of Alzheimer's disease. *Life Sci.* **2021**, *265*, 118802. [CrossRef]
13. Singleton, V.L.; Orthofer, R.; Lamuela-Raventós, R.M. Analysis of total phenols and other oxidation substrates and antioxidants by means of folin-ciocalteu reagent. In *Methods in Enzymology*; Elsevier: Amsterdam, The Netherlands, 1999; pp. 152–178.
14. Ribarova, F.; Ribarova, F.; Atanassova, M. Total phenolics and flavonoids in Bulgarian fruits and vegetables. *JU Chem. Met.* **2005**, *40*, 255–260.
15. Koleva, I.I.; Van Beek, T.A.; Linssen, J.P.H.; De Groot, A.; Evstatieva, L.N. Screening of Plant Extracts for Antioxidant Activity: A Comparative Study on Three Testing Methods. *Phytochem. Anal.* **2002**, *13*, 8–17. [CrossRef] [PubMed]
16. Re, R.; Pellegrini, N.; Proteggente, A.; Pannala, A.; Yang, M.; Rice-Evans, C. Antioxidant activity applying an improved ABTS radical cation decolorization assay. *Free Radic. Biol. Med.* **1999**, *26*, 1231–1237. [CrossRef]
17. Aktumsek, A.; Zengin, G.; Guler, G.O.; Cakmak, Y.S.; Duran, A. Antioxidant potentials and anticholinesterase activities of methanolic and aqueous extracts of three en-demic *Centaurea* L. species. *Food Chem. Toxicol.* **2013**, *55*, 290–296. [CrossRef]
18. Ellman, G.L.; Courtney, K.D.; Andres, V., Jr.; Featherstone, R.M. A new and rapid colorimetric determination of acetylcholinesterase activity. *Biochem. Pharmacol.* **1961**, *7*, 88–95. [CrossRef]
19. Tan, M.A.; Ishikawa, H.; An, S.S.A. *Pandanus amaryllifolius* Exhibits In Vitro Anti-Amyloidogenic Activity and Promotes Neuroprotective Effects in Amyloid-β-Induced SH-SY5Y Cells. *Nutrients* **2022**, *14*, 3962. [CrossRef]
20. Singh, P.; Jayaramaiah, R.H.; Agawane, S.B.; Vannuruswamy, G.; Korwar, A.M.; Anand, A.; Dhaygude, V.S.; Shaikh, M.L.; Joshi, R.S.; Boppana, R.; et al. Potential Dual Role of Eugenol in Inhibiting Advanced Glycation End Products in Diabetes: Proteomic and Mechanistic Insights. *Sci. Rep.* **2016**, *6*, 18798. [CrossRef]
21. Alvariño, R.; Alonso, E.; Lacret, R.; Oves-Costales, D.; Genilloud, O.; Reyes, F.; Alfonso, A.; Botana, L.M. Caniferolide A, a Macrolide from Streptomyces caniferus, Attenuates Neuroinflammation, Oxidative Stress, Amyloid-Beta, and Tau Pathology in Vitro. *Mol. Pharm.* **2019**, *16*, 1456–1466. [CrossRef]
22. Kozukue, N.; Park, M.-S.; Choi, S.-H.; Lee, S.-U.; Ohnishi-Kameyama, M.; Levin, C.E.; Friedman, M. Kinetics of Light-Induced Cis−TransIsomerization of Four Piperines and Their Levels in Ground Black Peppers as Determined by HPLC and LC/MS. *J. Agric. Food Chem.* **2007**, *55*, 7131–7139. [CrossRef]
23. Iqbal, G.; Iqbal, A.; Mahboob, A.; Farhat, S.M.; Ahmed, T. Memory Enhancing Effect of Black Pepper in the AlCl3 Induced Neurotoxicity Mouse Model is Mediated Through Its Active Component Chavicine. *Curr. Pharm. Biotechnol.* **2016**, *17*, 962–973. [CrossRef] [PubMed]
24. Li, X.; Shi, J.-R.; Yang, M.-S.; Lu, Y.; Chen, L.; Cao, H.-R. Study on the Extraction, Geometry Structure and Spectral Characterization of Piperine Alkaloid. *Guang pu xue yu guang pu fen xi = Guang pu* **2016**, *36*, 2082–2088. [PubMed]
25. Hartsel, J.A.; Eades, J.; Hickory, B.; Makriyannis, A. Chapter 53—Cannabis sativa and Hemp. In *Nutraceuticals*; Gupta, R.C., Ed.; Academic Press: Boston, MA, USA, 2016; pp. 735–754.
26. Francomano, F.; Caruso, A.; Barbarossa, A.; Fazio, A.; La Torre, C.; Ceramella, J.; Mallamaci, R.; Saturnino, C.; Iacopetta, D.; Sinicropi, M.S. β-Caryophyllene: A Sesquiterpene with Countless Biological Properties. *Appl. Sci.* **2019**, *9*, 5420. [CrossRef]
27. Lee, W.; Ku, S.-K.; Min, B.-W.; Lee, S.; Jee, J.-G.; Kim, J.A.; Bae, J.-S. Vascular barrier protective effects of pellitorine in LPS-induced inflammation in vitro and in vivo. *Fitoterapia* **2014**, *92*, 177–187. [CrossRef] [PubMed]
28. Ku, S.-K.; Lee, I.-C.; Kim, J.A.; Bae, J.-S. Anti-septic Effects of Pellitorine in HMGB1-Induced Inflammatory Responses In Vitro and In Vivo. *Inflammation* **2014**, *37*, 338–348. [CrossRef]
29. Lieder, B.; Zaunschirm, M.; Holik, A.-K.; Ley, J.P.; Krammer, G.E.; Somoza, V. The alkamide trans-pellitorine targets PPARγ via TRPV1 and TRPA1 to reduce lipid accumulation in devel-oping 3T3-L1 adipocytes. *Front. Pharmacol.* **2017**, *8*, 316. [CrossRef]
30. Okumura, Y.; Narukawa, M.; Iwasaki, Y.; Ishikawa, A.; Matsuda, H.; Yoshikawa, M.; Watanabe, T. Activation of TRPV1 and TRPA1 by Black Pepper Components. *Biosci. Biotechnol. Biochem.* **2010**, *74*, 1068–1072. [CrossRef]
31. Scott, I.M.; Puniani, E.; Jensen, H.; Livesey, J.F.; Poveda, L.; Sánchez-Vindas, P.; Durst, T.; Arnason, J.T. Analysis of Piperaceae Germplasm by HPLC and LCMS: A Method for Isolating and Identifying Unsaturated Amides from *Piper* spp Extracts. *J. Agric. Food Chem.* **2005**, *53*, 1907–1913. [CrossRef]

32. Kim, K.J.; Lee, M.-S.; Jo, K.; Hwang, J.-K. Piperidine alkaloids from Piperretrofractum Vahl. protect against high-fat diet-induced obesity by regulating lipid metabolism and activating AMP-activated protein kinase. *Biochem. Biophys. Res. Commun.* **2011**, *411*, 219–225. [CrossRef]
33. Al-Khayri, J.M.; Upadhya, V.; Pai, S.R.; Naik, P.M.; Al-Mssallem, M.Q.; Alessa, F.M. Comparative Quantification of the Phenolic Compounds, Piperine Content, and Total Polyphenols along with the Antioxidant Activities in the *Piper trichostachyon* and *P. nigrum*. *Molecules* **2022**, *27*, 5965. [CrossRef]
34. Zarai, Z.; Boujelbene, E.; Ben Salem, N.; Gargouri, Y.; Sayari, A. Antioxidant and antimicrobial activities of various solvent extracts, piperine and piperic acid from Piper nigrum. *LWT Food Sci. Technol.* **2013**, *50*, 634–641. [CrossRef]
35. Akbar, P.N.; Jahan, I.A.; Hossain, H.; Banik, R.; Nur, H.P.; Hossain, M.T. Antioxidant capacity of Piper longum and Piper nigrum fruits grown in Bangladesh. *World J. Pharm. Sci.* **2014**, *2*, 931–941.
36. Starowicz, M.; Zieliński, H. Inhibition of Advanced Glycation End-Product Formation by High Antioxidant-Leveled Spices Commonly Used in European Cuisine. *Antioxidants* **2019**, *8*, 100. [CrossRef] [PubMed]
37. Chatterjee, S.; Niaz, Z.; Gautam, S.; Adhikari, S.; Variyar, P.S.; Sharma, A. Antioxidant activity of some phenolic constituents from green pepper (Piper nigrum L.) and fresh nutmeg mace (Myristica fragrans). *Food Chem.* **2007**, *101*, 515–523. [CrossRef]
38. González-Palma, I.; Escalona-Buendía, H.B.; Ponce-Alquicira, E.; Téllez-Téllez, M.; Gupta, V.K.; Díaz-Godínez, G.; Soriano-Santos, J. Evaluation of the Antioxidant Activity of Aqueous and Methanol Extracts of Pleurotus ostreatus in Different Growth Stages. *Front. Microbiol.* **2016**, *7*, 1099. [CrossRef]
39. Abdel-Daim, M.M.; Sayed, A.A.; Abdeen, A.; Aleya, L.; Ali, D.; Alkahtane, A.A.; Alarifi, S.; Alkahtani, S. Piperine Enhances the Antioxidant and Anti-Inflammatory Activities of Thymoquinone against Microcystin-LR-Induced Hepatotoxicity and Neurotoxicity in Mice. *Oxidative Med. Cell. Longev.* **2019**, *2019*, 1309175. [CrossRef]
40. Mittal, R.; Gupta, R. In vitro antioxidant activity of piperine. *Methods Find. Exp. Clin. Pharmacol.* **2000**, *22*, 271–274. [CrossRef]
41. Giacco, F.; Brownlee, M. Oxidative Stress and Diabetic Complications. *Circ. Res.* **2010**, *107*, 1058–1070. [CrossRef]
42. Hipkiss, A.R. Glycotoxins: Dietary and Metabolic Origins; Possible Amelioration of Neurotoxicity by Carnosine, with Special Reference to Parkinson's Disease. *Neurotox. Res.* **2018**, *34*, 164–172. [CrossRef]
43. Kaewnarin, K.; Niamsup, H.; Shank, L.; Rakariyatham, N. Antioxidant and antiglycation activities of some edible and medicinal plants. *Chiang Mai J. Sci.* **2014**, *41*, 105–116.
44. Dearlove, R.P.; Greenspan, P.; Hartle, D.K.; Swanson, R.B.; Hargrove, J.L. Inhibition of Protein Glycation by Extracts of Culinary Herbs and Spices. *J. Med. Food* **2008**, *11*, 275–281. [CrossRef] [PubMed]
45. Tan, D.; Wang, Y.; Lo, C.-Y.; Ho, C.-T. Methylglyoxal: Its presence and potential scavengers. *Asia Pac. J. Clin. Nutr.* **2008**, *17*, 261–264. [CrossRef]
46. Bhattacherjee, A.; Datta, A. Mechanism of antiglycating properties of syringic and chlorogenic acids in in vitro glycation system. *Food Res. Int.* **2015**, *77*, 540–548. [CrossRef]
47. Sadowska-Bartosz, I.; Galiniak, S.; Bartosz, G. Kinetics of Glycoxidation of Bovine Serum Albumin by Methylglyoxal and Glyoxal and its Prevention by Various Compounds. *Molecules* **2014**, *19*, 4880–4896. [CrossRef] [PubMed]
48. Tupe, R.S.; Bangar, N.; Nisar, A.; Kulkarni, A.; Sankhe, N.; Chauhan, R.; Mistry, N.; Shaikh, S. Piperine exhibits preventive and curative effect on erythrocytes membrane modifications and oxidative stress against in vitro albumin glycation. *J. Food Biochem.* **2021**, *45*, e13846. [CrossRef] [PubMed]
49. Rauscher, F.M.; Sanders, R.A.; Watkins, J.B. Effects of piperine on antioxidant pathways in tissues from normal and streptozotocin-induced diabetic rats. *J. Biochem. Mol. Toxicol.* **2000**, *14*, 329–334. [CrossRef]
50. Yeggoni, D.P.; Rachamallu, A.; Kallubai, M.; Subramanyam, R. Cytotoxicity and comparative binding mechanism of piperine with human serum albumin and α-1-acid glycoprotein. *J. Biomol. Struct. Dyn.* **2015**, *33*, 1336–1351. [CrossRef]
51. Tsakiris, S.; Kalafatakis, K.; Gkanti, V.; Scott, C.A.M.-G.; Zarros, A.; Baillie, G.S. Acetylcholinesterase activity as a neurotoxicity marker within the context of experimentally-simulated hyperprolinaemia: An in vitro approach. *J. Nat. Sci. Biol. Med.* **2015**, *6*, 98–S101. [CrossRef]
52. Werawattanachai, N.; Kaewamatawong, R. Screening for Acetylcholinesterase Inhibitory Activity from the Piperaceae. *วารสารวิทยาศาสตร์ และ เทคโนโลยี มหาวิทยาลัย อุบลราชธานี* **2016**, *18*, 25.
53. Lomarat, P.; Sripha, K.; Phanthong, P.; Kitphati, W.; Thirapanmethee, K.; Bunyapraphatsara, N. In vitro biological activities of black pepper essential oil and its major components relevant to the prevention of Alzheimer's disease. *Thai J. Pharm. Sci. (TJPS)* **2015**, *39*, 94–101.
54. Balkrishna, A.; Pokhrel, S.; Tomer, M.; Verma, S.; Kumar, A.; Nain, P.; Gupta, A.; Varshney, A. Anti-acetylcholinesterase activities of mono-herbal extracts and exhibited synergistic effects of the phytoconstituents: A biochemical and computational study. *Molecules* **2019**, *24*, 4175. [CrossRef] [PubMed]
55. Magaña-Barajas, E.; Buitimea-Cantúa, G.V.; Hernández-Morales, A.; Torres-Pelayo, V.D.R.; Vázquez-Martínez, J.; Buitimea-Cantúa, N.E. In vitro α-amylase and α-glucosidase enzyme inhibition and antioxidant activity by capsaicin and piperine from *Capsicum chinense* and *Piper nigrum* fruits. *J. Environ. Sci. Health Part B* **2021**, *56*, 282–291. [CrossRef] [PubMed]
56. Khatami, Z.; Sarkheil, P.; Adhami, H. Isolation and characterization of acetylcholinesterase inhibitors from Piper longum Linn. *Planta Medica* **2016**, *81*, S1–S381. [CrossRef]
57. Ikawati, S.; Himawan, T.; Abadi, A.; Sarno, H.; Fajarudin, A. In Silico Study of Eugenol and trans-Caryophyllene also Clove Oil Fumigant Toxicity on Tribolium castaneum. *J. Trop. Life Sci.* **2022**, *12*, 339–349. [CrossRef]

58. Hung, N.H.; Quan, P.M.; Satyal, P.; Dai, D.N.; Van Hoa, V.; Huy, N.G.; Giang, L.D.; Ha, N.T.; Huong, L.T.; Hien, V.T.; et al. Acetylcholinesterase Inhibitory Activities of Essential Oils from Vietnamese Traditional Medicinal Plants. *Molecules* **2022**, *27*, 7092. [CrossRef]
59. Tu, Y.; Zhong, Y.; Du, H.; Luo, W.; Wen, Y.; Li, Q.; Zhu, C.; Li, Y. Anticholinesterases and antioxidant alkamides from *Piper nigrum* fruits. *Nat. Prod. Res.* **2016**, *30*, 1945–1949. [CrossRef] [PubMed]
60. Tan, M.A.; Zakharova, E.; An, S.S.A. Diaportheone A Analogues Instigate a Neuroprotective Effect by Protecting Neuro-blastoma SH-SY5Y Cells from Oxidative Stress. *Biology* **2021**, *10*, 199. [CrossRef] [PubMed]
61. Gazit, E. Mechanisms of amyloid fibril self-assembly and inhibition: Model short peptides as a key research tool. *FEBS J.* **2005**, *272*, 5971–5978. [CrossRef] [PubMed]
62. Kotormán, M.; Varga, A.; Kasi, P.B.; Nemcsók, J. Inhibition of the formation of amyloid-like fibrils with spices, especially cloves. *Acta Biol. Hung.* **2018**, *69*, 385–394. [CrossRef]
63. Manoharan, S.; Guillemin, G.J.; Abiramasundari, R.S.; Essa, M.M.; Akbar, M.; Akbar, M.D. The role of reactive oxygen species in the pathogenesis of Alzheimer's disease, Parkinson's disease, and Huntington's disease: A mini review. *Oxidative Med. Cell. Longev.* **2016**, *2016*, 8590578. [CrossRef]
64. Ghaffari, H.; Ghassam, B.J.; Nayaka, S.C.; Kini, K.R.; Prakash, H.S. Antioxidant and Neuroprotective Activities of *Hyptis suaveolens* (L.) Poit. Against Oxidative Stress-Induced Neurotoxicity. *Cell. Mol. Neurobiol.* **2014**, *34*, 323–331. [CrossRef] [PubMed]
65. Polster, B.M.; Fiskum, G. Mitochondrial mechanisms of neural cell apoptosis. *J. Neurochem.* **2004**, *90*, 1281–1289. [CrossRef]
66. Beal, M.F. Mitochondria take center stage in aging and neurodegeneration. *Ann. Neurol. Off. J. Am. Neurol. Assoc. Child Neurol. Soc.* **2005**, *58*, 495–505. [CrossRef] [PubMed]
67. Dröge, W. Free Radicals in the Physiological Control of Cell Function. *Physiol. Rev.* **2002**, *82*, 47–95. [CrossRef]
68. Starkov, A.A. The Role of Mitochondria in Reactive Oxygen Species Metabolism and Signaling. *Ann. N. Y. Acad. Sci.* **2008**, *1147*, 37–52. [CrossRef] [PubMed]
69. Kaushik, P.; Ali, M.; Salman, M.; Tabassum, H.; Parvez, S. Harnessing the mitochondrial integrity for neuroprotection: Therapeutic role of piperine against experimental ischemic stroke. *Neurochem. Int.* **2021**, *149*, 105138. [CrossRef] [PubMed]
70. Hua, S.; Liu, J.; Zhang, Y.; Li, J.; Zhang, X.; Dong, L.; Zhao, Y.; Fu, X. Piperine as a neuroprotective functional component in rats with cerebral ischemic injury. *Food Sci. Nutr.* **2019**, *7*, 3443–3451. [CrossRef]
71. Khalili-Fomeshi, M.; Azizi, M.G.; Esmaeili, M.R.; Gol, M.; Kazemi, S.; Ashrafpour, M.; Moghadamnia, A.A.; Hosseinzadeh, S. Piperine restores streptozotocin-induced cognitive impairments: Insights into oxidative balance in cerebrospinal fluid and hippocampus. *Behav. Brain Res.* **2017**, *337*, 131–138. [CrossRef]
72. Ren, T.; Wang, Q.; Li, C.; Yang, M.; Zuo, Z. Efficient brain uptake of piperine and its pharmacokinetics characterization after oral administration. *Xenobiotica* **2017**, *48*, 1249–1257. [CrossRef]
73. Itharat, A.; Kanokkangsadal, P.; Khemawoot, P.; Wanichsetakul, P.; Davies, N.M. Pharmacokinetics of piperine after oral administration of Sahastara remedy capsules in healthy volunteers. *Res. Pharm. Sci.* **2020**, *15*, 410–417. [CrossRef]

antioxidants

MDPI

Article

Protective Effects of *Dipterocarpus tuberculatus* in Blue Light-Induced Macular Degeneration in A2E-Laden ARPE19 Cells and Retina of Balb/c Mice

Su Jin Lee [1,†], Yu Jeong Roh [1,†], Ji Eun Kim [1], You Jeong Jin [1], Hee Jin Song [1], Ayun Seol [1], So Hae Park [1], Bounleuane Douangdeuane [2], Onevilay Souliya [2], Sun Il Choi [3,*] and Dae Youn Hwang [1,4,*]

[1] Department of Biomaterials Science (BK21 FOUR Program), Life and Industry Convergence Research Institute, College of Natural Resources and Life Science, Pusan National University, Miryang 50463, Republic of Korea
[2] Institute of Traditional Medicine, Ministry of Health, Vientiane 0103, Laos
[3] School of Pharmacy, Henan University, Kaifeng 475004, China
[4] Longevity & Wellbeing Research Center, Laboratory Animals Resources Center, College of Natural Resources and Life Science, Pusan National University, Miryang 50463, Republic of Korea
* Correspondence: sunil.choi@hotmail.com (S.I.C.); dyhwang@pusan.ac.kr (D.Y.H.); Tel.: +86-13271140312 (S.I.C.); +82-55-350-5388 (D.Y.H.)
† These authors contributed equally to this work.

Abstract: Natural products with significant antioxidant activity have been receiving attention as one of the treatment strategies to prevent age-related macular degeneration (AMD). Reactive oxygen intermediates (ROI) including oxo-N-retinylidene-N-retinylethanolamine (oxo-A2E) and singlet oxygen-induced damage, are believed to be one of the major causes of the development of AMD. To investigate the therapeutic effects of methanol extracts of *Dipterocarpus tuberculatus* Roxb. (MED) against blue light (BL)-caused macular degeneration, alterations in the antioxidant activity, apoptosis pathway, neovascularization, inflammatory response, and retinal degeneration were analyzed in A2E-laden ARPE19 cells and Balb/c mice after exposure of BL. Seven bioactive components, including 2α-hydroxyursolic acid, ε-viniferin, asiatic acid, bergenin, ellagic acid, gallic acid and oleanolic acid, were detected in MED. MED exhibited high DPPH and ABTS free radical scavenging activity. BL-induced increases in intracellular reactive oxygen species (ROS) production and nitric oxide (NO) concentration were suppressed by MED treatment. A significant recovery of antioxidant capacity by an increase in superoxide dismutase enzyme (SOD) activity, SOD expression levels, and nuclear factor erythroid 2–related factor 2 (NRF2) expression were detected as results of MED treatment effects. The activation of the apoptosis pathway, the expression of neovascular proteins, cyclooxygenase-2 (COX-2)-induced inducible nitric oxide synthase (iNOS) mediated pathway, inflammasome activation, and expression of inflammatory cytokines was remarkably inhibited in the MED treated group compared to the Vehicle-treated group in the AMD cell model. Furthermore, MED displayed protective effects in BL-induced retinal degeneration through improvement in the thickness of the whole retina, outer nuclear layer (ONL), inner nuclear layer (INL), and photoreceptor layer (PL) in Balb/c mice. Taken together, these results indicate that MED exhibits protective effects in BL-induced retinal degeneration and has the potential in the future to be developed as a treatment option for dry AMD with atrophy of retinal pigment epithelial (RPE) cells.

Keywords: age-related macular degeneration; *D. tuberculatus*; A2E; antioxidant; oxidative stress; inflammatory response

Citation: Lee, S.J.; Roh, Y.J.; Kim, J.E.; Jin, Y.J.; Song, H.J.; Seol, A.; Park, S.H.; Douangdeuane, B.; Souliya, O.; Choi, S.I.; et al. Protective Effects of *Dipterocarpus tuberculatus* in Blue Light-Induced Macular Degeneration in A2E-Laden ARPE19 Cells and Retina of Balb/c Mice. *Antioxidants* **2023**, *12*, 329. https://doi.org/10.3390/antiox12020329

Academic Editors: Ana-Maria Buga and Carmen Nicoleta Oancea

Received: 12 December 2022
Revised: 22 January 2023
Accepted: 27 January 2023
Published: 31 January 2023

1. Introduction

Age-related macular degeneration (AMD) is characterized by the deposition of lipofuscin and drusen and the development of abnormal blood vessels in the retina and macula, which eventually lead to the total loss of central vision [1,2]. Specifically, an important

component of lipofuscin, N-retinylidene-N-retinylethanolamine (A2E), which is produced from the reaction between phosphatidylethanolamine and vitamin A, plays an important role in the pathological progression of AMD. A2E accumulates in the retinal pigment epithelial (RPE) cells during the aging process [3]. Accumulated A2E can cause cellular injury due to its amphiphilic structure and photoreactivity and this is believed to be the pathophysiological process leading to atrophic AMD [4]. In the RPE cells, A2E contributes to the production of reactive oxygen species (ROS) and several by-products after exposure to blue light (BL) [5,6]. These products induce chronic inflammation through the activation of the complement system, cause lysosomal damage, increase cellular damage by destroying DNA and disrupt the intracellular autophagy process [7–9]. Several natural products with high antioxidant activities are being used for treatment and protection against A2E-induced damage in AMD. Significant protective effects against oxidative damage, apoptosis, and inflammatory response were detected in cells and animal models with retinal disorders and AMD phenotypes after treatment with *Aronia melanocarpa* [10], bilberry [11], Shihu Yeguang Pill [12], triphala [13], *Solanum melongena* L. [14], bilberry and lingonberry [15,16], *Vaccinium uliginosum* [17] and *Spirulina maxima* [18].

Dipterocarpus tuberculatus Roxb. is a species of flowering plant widely distributed in Southeast Asia including Bangladesh, Cambodia, Laos, Myanmar, Thailand, and Vietnam [19]. The therapeutic effects of this plant as an anti-inflammatory, anti-photoaging, and in promoting osseointegration have been reported recently. Ethanol (EtOH, 90%) extracts of this plant suppressed the lipopolysaccharide (LPS)-mediated inflammatory response in RAW264.7 cells and improved acute inflammatory symptoms in EtOH/HCl-induced gastric lesions of ICR mice through the regulation of 3′-phosphoinositide–dependent kinase 1/Nuclear factor kappa-light-chain-enhancer of activated B cells (PDK1/NF-κB), MyD88/TIR-domain-containing adaptor protein inducing IFN-β (TRIF-mediated) activated protein (AP)-1 and AP-1 signaling pathways [20,21]. Additionally, some significant anti-photoaging effects of the methanol extract of *Dipterocarpus tuberculatus* Roxb. (MED) in apoptosis, the cell cycle, extracellular matrix structure, and inflammation were detected in ultraviolet (UV)-irradiated primary normal human dermal fibroblasts (NHDF) cells and nude mice [22]. MED, coated on the surface of a titanium plate stimulated the proliferation and cell adhesion of MG63 cells as well as new bone formation and regeneration in tibia implantation models [23]. However, no study to date has elucidated the protective effects and the mechanism of action of *Dipterocarpus tuberculatus* Roxb. in retinal cells and animals with AMD phenotypes.

In this study, we investigated the protective effects of MED and the mechanisms involved in A2E-laden ARPE-19 cells and Balb/c mice after exposure to blue light (BL) to evaluate its potential as a treatment for AMD.

2. Materials and Methods

2.1. Preparation and Extraction of MED

The lyophilized sample of MED (FBM 213-075) was supplied from the International Biological Material Research Center of the Korea Research Institutes of Bioscience and Biotechnology (KRIBB, Daejeon, Korea). To collect the extract solution of MED, a ground dried powder was first prepared from dry stem samples of *Dipterocarpus tuberculatus* Roxb. using a blender. After mixing a 1:10 ratio of MED powder and methanol solution, they were subjected to two steps: (1) sonication for 15 min and (2) incubation for 2 h at room temperature, and these steps were repeated 10 times per day for 3 days. After that, the extracted solution was filtered through a filter with a 0.4 μm pore size and lyophilized using a Rotary Evaporator (EYELA, Bohemia, NY, USA). The lyophilized MED samples were deposited as voucher specimens of *Dipterocarpus tuberculatus* Roxb. (WP-20-001) at the functional materials bank of the Wellbeing RIS Center, Pusan National University (PNU). These lyophilized samples were prepared by dissolving them in dimethyl sulfoxide solution (DMSO; Duchefa Biochemie, Haarlem, The Netherlands) before treatment.

2.2. Determination of Bioactive Compounds in MED

The bioactive compounds in MED were determined in accordance with methods laid out in a previous study [22]. Seven bioactive compounds were identified in MED namely 2α-hydroxyursolic acid, ε-viniferin, asiatic acid, bergenin, ellagic acid, gallic acid, and oleanolic acid, using ultra-high-performance liquid chromatography (UHPLC)-electrospray ionization (ESI)-tandem mass spectrometry (MS/MS) (UHPLC-ESI-MS) analysis. Among these, three compounds with high content were quantified using the liquid chromatography-mass spectrometry (LC-MS) quantification method. The observed peak area ratios were calculated from the detected peak area in total running time (Supplementary Figure S1A).

2.3. Free radical Scavenging Activity of MED

The scavenging activity against 2,2-diphenyl-1-picrylhydrazyl (DPPH) radicals was determined using a previously described method [22,24]. Briefly, various solutions of MED (1 to 1000 μg/mL) were mixed with 0.1 mM DPPH (Sigma-Aldrich Co., St. Louis, MO, USA). After incubation at room temperature for 30 min, the absorbance of each mixture was determined at 517 nm using a VersaMax^{TM} microplate reader (Molecular Devices, Sunnyvale, CA, USA). Finally, the scavenging activity of MED against DPPH radicals was expressed as the reduction percent in absorbance. The IC_{50} value was defined as the MED concentration that gives a 50% decrease in the scavenging activity against DPPH radicals.

Additionally, the 2,2′-azono-bis-3-ethylbenzthiazoline-6-sulphonate (ABTS) radical scavenging activity was determined using an ABTS decolorization assay as described in a previous study [25]. A total of 25 μL of eleven different concentrations of MED (1 μg to 500 μg/mL) were mixed with 250 μL of ABTS working solution and incubated at room temperature for 4 min. Their absorbance was read at 734 nm in a UV-visible (UV–VIS) spectrophotometer (Thermo Fisher Scientific Inc., Wilmington, DE, USA). The data have been presented as ascorbic acid equivalent (Sigma-Aldrich Co., St. Louis, MO, USA), which was used as a standard.

2.4. Synthesis and Purification of A2E

To synthesize A2E, all-trans-retinal (100 mg, 352 μmol), ethanolamine (9.5 mg, 155 μmol) in ethanol (3 mL), and acetic acid (9.3 μL, 155 μmol) were mixed by vigorous vortexing for 2 min. The mixture was incubated for 48 h under dark conditions. Subsequently, the mixture was concentrated at 20 °C using a nitrogen evaporator (Biotage, TurboVap-LV, USA). An A2E sample was separated and purified using silica gel and HPLC. Separation on a Sep-Pak C18 cartridge (WAT023635, Waters, Milford, MA, USA) was performed using a step gradient elution with 5:95 MeOH/CH_2Cl_2, 5:95 MeOH/CH_2Cl_2, and 8:92:0.001 MeOH/CH_2Cl_2/TFA. Additionally, the fractions were further purified using a multiple preparative HPLC (LC-forte/R, YMC Co., Kyoto, Japan) with a YMC-Triart Prep C18 column (250 mm × 10.0 mm, 10 μm). The purity of the A2E was analyzed using the gradient HPLC method with a YMC-Triart C18 column (4.6 mm × 250 mm, 5 μm) (Supplementary Figure S1B).

2.5. Cell Culture and Cell Viabilities Assay

ARPE19 cells, derived from the human RPE, were sourced from the American Type Culture Collection (ATCC), (Manassas, VA, USA), and grown in an incubator maintained with a 5% CO_2, 95% atmosphere and 37 °C temperature using Dulbecco's Modified Eagle Medium (DMEM, Welgene, Gyeongsan, Korea) containing 10% fetal bovine serum (FBS).

To determine the optimal concentration of MED, ARPE19 cells (3×10^4 cells) were briefly seeded into each well of a 96-well plate. When the cells were up to 70–80% confluence, they were treated with various concentrations of MED (50, 100, 200, and 400 μM) for 24 h. Supernatants were discarded after incubation for 24 h, followed by the addition of fresh DMEM (200 μL) and 3-(4,5-dimethylthiazol-2-yl)-2,5-diphenyltetrazolium bromide (MTT) solution (20 mg/mL and 50 μL) to each well. After incubation for 4 h, the formazan precipitates in the cells were dissolved in DMSO (Duchefa Biochemie, Haarlem, The Nether-

lands), and their absorbance was determined at 570 nm using a VersaMax™ microplate reader (Molecular Devices, San Jose, CA, USA). Based on the above results, the optimal concentration of MED was determined at 50, 100, and 200 μg/m (Supplementary Figure S2).

Next, we determined an optimal dosage for A2E at specific BL irradiation levels to prepare the AMD cell model. To achieve this, ARPE19 cells cultured in the same manner as above were treated with various concentrations of A2E (5, 10, 20, 40, and 80 μM) for 24 h and irradiated with BL (430 nm, 6000 Lux) (SL-S2500, S tech LED, Gyeonggido, Republic of Korea) for 10 min. After further incubation for 24 h, the viability of cells was measured by an MTT assay as described in the section above. The non-irradiated group (Non treated group) did not receive any BL radiation, but the Vehicle + A2E treated group received only BL irradiation without A2E loading. Based on the above results, the optimal concentration of A2E was determined at 20 μM (Supplementary Figure S3).

To assess the protective effects of MED on the oxidative stress-induced cell death caused by BL in A2E-laden ARPE-19 cells, they were briefly divided into two groups; Not treatment group (Non treated group) and the A2E + BL treated group. The A2E + BL treated group was further classified into the following five groups; Vehicle (DMSO) treated group (Vehicle + A2E + BL treated group), Vitamin C (100 μM, positive control) treated group (Po + A2E + BL treated group), low concentration (50 μg/mL) MED treated group (LMED + A2E + BL treated group), medium concentration (100 μg/mL) MED treated group (MMED + A2E + BL treated group) and high concentration (200 μg/mL) MED treated group (HMED + A2E + BL treated group). Vitamin C was used as a positive control because it has been proven to have high antioxidant activity and a protective effect on macular degeneration [26]. When ARPE19 cells were up to 70–80% confluence, they were treated with three different concentrations of MED (50, 100, and 200 μg/mL), Vitamin C or DMSO of the same volume for 24 h, and then treated with 20 μM of A2E for 24 h. Subsequently, the cells were irradiated by BL (430 nm, 6000 Lux) for 10 min. After further incubation for 24 h, the viability of cells was measured by an MTT assay as described in the section above. Additionally, these cells were further subjected to a real-time-quantitative polymerase chain reaction (RT-qPCR), the Western blot test, and apoptotic cell analyses.

2.6. Analysis of Apoptotic Cells

The distribution of apoptotic and live cells was analyzed using a Muse™ Annexin V and Dead Cell Kit (Millipore Co., Billerica, MA, USA). After harvesting ARPE19 cells treated with MED, A2E, or BL, they (1×10^4 cells/mL) were mixed with the Muse™ Annexin V and Dead Cell Kit (Millipore Co., Billerica, MA, USA) reaction reagent and subsequently incubated for 20 min. These cells were analyzed using the Muse™ Cell Analyzer (Millipore Co., Billerica, MA, USA). Briefly, they were gated based on their size, their population was classified into four populations: live cells [Annexin V (−) and 7-AAD (−) population], early apoptotic cells [Annexin V (+) and 7-AAD (−) population], late apoptotic cells [Annexin V (+) and 7-AAD (+) population], mostly nuclear debris [Annexin V (+) and 7-AAD (+) population].

2.7. Determination of Intracellular ROS Levels

The intracellular ROS levels determined using 2′,7′-dichlorofluorescein diacetate staining analysis (DCFH-DA; Sigma-Aldrich Co., St. Louis, MO, USA) based on this probe can be deacetylated by intracellular esterase to nonfluorescent 2′,7′-dichlorodihydrofluorescein (DCFH). This chemical reacted with intracellular hydrogen peroxide or other oxidizing ROS and was consequently changed into fluorescent 2′,7′-dichlorofluorescein (DCF). ARPE19 cells were subsequently treated with MED, A2E, or BL as described previously. After the final incubation, the cells were treated with 10 μM DCF-DA for 30 min at 37 °C and subsequently washed with 1× PBS. The green fluorescence in ARPE19 cells was observed using a fluorescent microscope (Evos m5000, Thermo Fisher Scientific Inc., Waltham, MA, USA) at 400× magnification.

2.8. Analysis of Nitric Oxide (NO) Concentrations

The level of nitrite in the ARPE19 cells was determined as an indicator of NO production using the Griess reagent as in a previous study [22]. Briefly, the culture supernatants were collected from subset groups of ARPE19 cells after subsequent treatment with MED, A2E, or BL. These supernatants (100 μL) were mixed with 100 μL of modified Griess reagent (Invitrogen Co., Carlsbad, CA, USA) in 96-well plates. After incubation for 5 min, the absorbance at 540 nm was detected using a Versamax^{TM} microplate reader (Molecular Devices, San Jose, CA, USA).

2.9. Analysis of Superoxide Dismutase (SOD) Activity

The SOD activity in the ARPE19 cells was assessed using a SOD assay kit (Dojindo Molecular Technologies Inc., Rockville, MD, USA) according to the procedure suggested by the manufacturer. Briefly, ARPE19 cells were harvested from the subset groups after treatment with MED, A2E, or BL. They were lysed by repetitive freezing and thawing in 100 μL of 1× PBS, and then their lysates were collected by centrifugation at 5000× *g* for 5 min. After diluting with 1× PBS in seven ratios (1/1, 1/2, 1/22, 1/23, 1/24, 1/25, and 1/26), these samples (20 μL each) were divided into individual wells of a 96-well plate. The solution in each well was thoroughly mixed with water-soluble tetrazolium salt-1 (WST-1) working solution (200 μL) and enzyme working solution (20 μL). After incubation at 37 °C for 20 min, their absorbance was measured at 450 nm using a VersaMax^{TM} microplate reader (Molecular Devices, San Jose, CA, USA). Finally, the SOD activity of each group was determined using the following equation:

$$\text{SOD activity (inhibition rate \%)} = [(\text{A blank 1} - \text{A blank 3}) - (\text{A sample} - \text{A blank 2})]/(\text{A blank 1} - \text{A blank 3}) \times 100 \quad (1)$$

where, A blank 1, 2, and 3 represented the absorbance level of blanks 1, 2, and 3, and 'A sample' indicated the absorbance level of sample.

2.10. Western Blot Analysis

The total cellular proteins were prepared from ARPE19 cells, using the Pro-Prep Protein Extraction Solution (Intron Biotechnology Inc., Seongnam, Republic of Korea). After lysis of ARPE19 cells, total proteins were harvested, and their concentration was sequentially determined using a SMARTTM Bicinchoninic Acid Protein Assay Kit (Thermo Fisher Scientific Inc., Waltham, MA, USA). Then, proteins bound to the nitrocellulose membranes were incubated with the specific primary antibodies (Supplementary Table S1) overnight at 4 °C. The intensity for each protein was analyzed on the membrane, which developed with an Amersham ECL Select Western Blotting detection reagent (GE Healthcare, Little Chalfont, UK) using the Fusion Solo-2 (Vilber, San Leandro, Collégien, France). Finally, the density of each protein was quantified using the AlphaView Program (Cell Biosciences Inc., Santa Clara, CA, USA).

2.11. RT-qPCR Analysis

The relative quantities of inflammatory cytokines (TNF-α, IL-6, IL-1β and NF-κB) mRNA were determined by RT-qPCR analyses [27,28]. After isolating total RNA molecules using RNA Bee solution (Tet-Test Inc., Friendswood, TX, USA), complement DNA (cDNA) was synthesized with reverse transcriptase (Superscript II, Thermo Fisher Scientific Inc., Waltham, MA, USA). Four specific genes were amplified with 2× Power SYBR Green (Toyobo Co., Osaka, Japan) [29] using specific primers (Supplementary Table S2). Finally, the expression of each gene was quantified at a relative level to that of the actin (housekeeping gene) by comparing the Cts at a constant fluorescence intensity [30].

2.12. Experimental Design for Animal Study

The study protocol for the AMD animal model was carefully reviewed and approved by the Pusan National University-Institutional Animal Care and Use Committee (PNU-IACUC) (Approval Number PNU-2022-0103). Male Balb/c mice (5 weeks old) were pro-

vided from Samtako BioKorea Inc. (Osan, Korea), and bred in the barrier facility of the PNU-Laboratory Animal Resources Center (PNU-LARC), accredited by the AAALAC International (Unit Number; 001525) and the Korea Food and Drug Administration (KFDA) (Unit Number; 000231). They were supplied, ad libitum, with filtered tap water and a standard irradiated chow diet (Samtako BioKorea Co., Osanm, Korea). All mice were maintained in a specific pathogen-free (SPF) state, strict regulation of the light cycle, constant temperature (22 ± 2 °C) and relative humidity (50 ± 10%).

The therapeutic effects of MED in the AMD model were analyzed as described in a previous study [14]. Briefly, the 7-week-old Balb/c mice (Male, n = 24) were allocated to one of two groups; a non-irradiated group (Non treated group, n = 8) and a BL irradiated group (n = 16). The latter group was further assigned into four groups; the Vehicle-treated group (1× PBS, Vehicle + BL treated group, n = 8), the low-concentration MED-treated group (100 mg/kg, LMED + BL treated group, n = 8), or high-concentration MED-treated group (200 mg/kg, HMED + BL treated group, n = 8). However, only the Vehicle treated group was not assigned to the Non treated group based on the 3R principle of PNU-IACUC to reduce the number of animals because there was no significant difference between the Non treated group and the Vehicle treated group in the preliminary experiment. After adapting to the dark conditions for three days, they were orally administrated with the same volume of vehicle solution (1× PBS), or MED solution (100 mg/kg or 200 mg/kg) once a day for 4 days in dark cages. The dosages for MED treatment used in the AMD model were decided based on the results from previous research on the anti-AMD effects of natural products [11,31] and the therapeutic effects of *Dipterocarpus tuberculatus* Roxb. [21,22]. At 24 h after the final administration, they were exposed to BL for 2 h and subsequently bred for 24 h under dark conditions. Subsequently, all mice were sacrificed using CO_2 and their eye samples were collected for histopathological analyses.

2.13. Histopathological Analysis

After the collection of the eyeballs from the Blab/c mice, the entire eye was fixed in 10% formalin and then embedded in paraffin wax. After sectioning into 4 μm thick slices, they were stained using hematoxylin and eosin solution (H&E, Sigma-Aldrich Co., St. Louis, MO, USA). The histological features on these sections were observed by optical microscopy, after which the thickness of the whole retina, outer segment of the photoreceptors (OS), the outer nuclear layer (ONL), inner nuclear layer (INL), and inner plexiform layer (IPL) for photoreceptor degeneration in the retina was observed using the Leica Application Suite (Leica Microsystems, Glattbrugg, Switzerland)

2.14. Immunohistochemical (IHC) Staining Analysis

The tissue distribution of nuclear factor erythroid 2–related factor 2 (Nrf2), cyclooxygenase-2 (COX-2), and inducible nitric oxide synthase (iNOS) proteins were detected by IHC as described in a previous study [32]. After deparaffinization of tissue sections, anti-Nrf2 (Abcam, Cambridge, UK), anti-COX-2 (Cell Signaling Technology Inc., Danvers, MA, USA), anti-iNOS (Thermo Fisher Scientific Inc., Waltham, MA, USA) and goat alkaline phosphatase (AP) conjugated anti-rabbit IgG (1:200, Thermo Fisher Scientific Inc., Waltham, MA, USA), antibodies were sequentially treated onto these sections. Finally, the distribution of each protein in the retina was detected using stable diaminobenzidine (DAB) (Invitrogen Co., Waltham, MA, USA) and evaluated using the Leica Application Suite (Leica Microsystems).

2.15. Statistical Analysis

One-way ANOVA was used to determine the statistical significance between the Vehicle + A2E + BL (or Vehicle + BL) treated group and MED + A2E + BL (or MED + BL) treated group, and only a p value less than 0.05 was reported as statistically significant. All values in the results are represented as the means ± standard deviation (SD).

3. Results

3.1. Bioactive Compounds and Antioxidative Activity of MED

Firstly, we evaluated the antioxidative activity of MED based on its bioactive compound composition to predict its potential as a therapeutic drug for AMD. Seven bioactive compounds were detected in MED using HPLC analyses. Among these, asiatic acid was present in the highest amounts, followed by 2α-hydroxyursolic acid, oleanolic acid, bergenin, ε-viniferin, gallic acid, and ellagic acid (Figure 1a and Supplementary Figure S1A). Additionally, inhibitory activity against DPPH and ABTS radicals was significantly increased at 1–1000 μg/mL of MED, and the IC_{50} value for DPPH and ABTS radicals was determined to be 7.48 μg/mL and 505.12 μg/mL (Figure 1b,c). Specifically, the IC_{50} value for DPPH radicals was remarkably higher than that of the ABTS radicals (Figure 1b,c). These results suggest that MED shows strong antioxidative activity and has the potential for application as a protective drug for AMD.

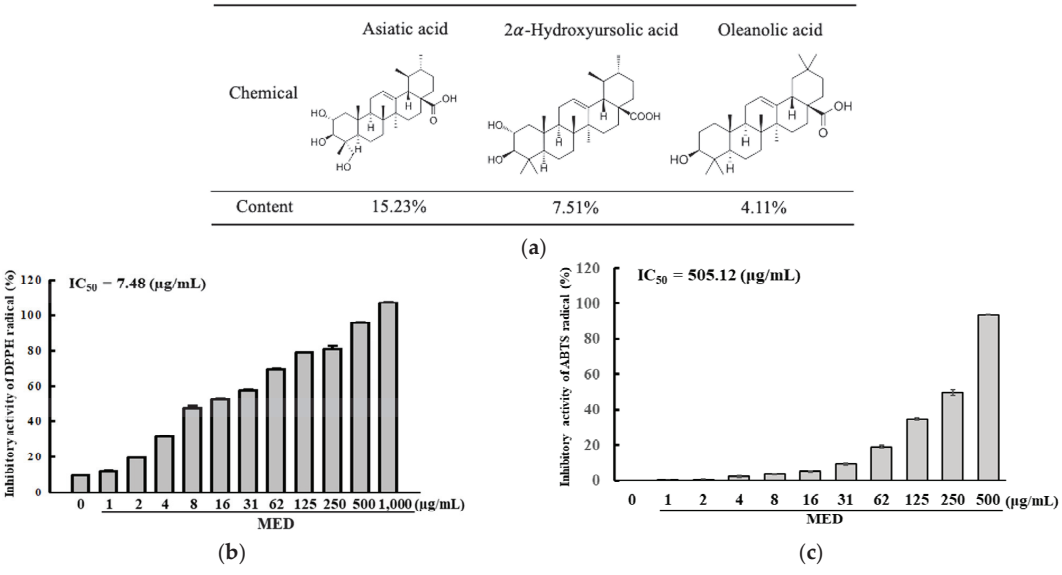

Figure 1. Main components and free radical scavenging activity of MED. (**a**) Concentration of asiatic acid, 2α-hydroxyursolic acid and oleanolic acid in MED. (**b**) DPPH radical scavenging activity of MED. This activity was measured in the concentration ranges from 1 to 1000 μg/mL of MED. Scavenging activity analysis for DPPH radicals was conducted with three MED samples. (**c**) ABTS radical scavenging activity of MED. This activity was measured in the concentration ranges from 1 to 500 μg/mL of MED. Scavenging activity analysis for ABTS radicals was conducted with three MED samples. All values in the results are represented as the means ± standard deviation (SD). Abbreviations: DPPH, 2,2-diphenyl-1-picrylhydrazyl; IC_{50}, half maximum inhibitory concentration; ABTS, 2,2′-azino-bis (3-ethylbenzothiazoline-6-sulfonic acid); MED, methanol extracts of *Dipterocarpus tuberculatus* Roxb.

3.2. Protective Effects of MED on the Oxidative Stress Caused by A2E + BL Treatment in ARP19 Cells

To investigate whether the treatment of MED can protect against the oxidative stress caused by AMD, changes in intracellular ROS production and NO concentration were measured in MED +A2E + BL treated ARPE19 cells. The number of DCF-stained cells representing intracellular ROS was remarkably higher in the Vehicle + A2E + BL treated group compared to the Non treated group. However, the above high values were significantly decreased by 18.2%, 50%, and 66.7% in the LMED + A2E + BL, MMED + A2E + BL, and HMED + A2E + BL treated groups, respectively, compared to the Vehicle + A2E + BL

treated group (Figure 2a,b). Additionally, a similar recovery pattern with a decrease rate of 8.6%, 20%, and 33.3%, respectively, was detected in the NO concentrations in the same groups although the rate of decrease was greater in the DCF stained cells (Figure 2c). Thus, these results indicate that MED may contribute to the decrease in oxidative stress in A2E + BL treated ARPE19 cells through the suppression of ROS and NO production.

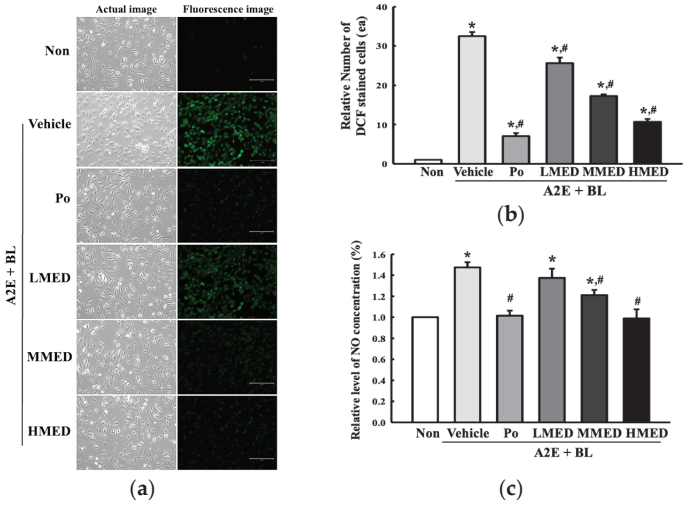

Figure 2. Detection of ROS and NO concentration in MED + A2E + BL treated ARPE19 cells. (**a**) Fluorescence image of DCF stained cells. The morphology of cells was detected using an optical and fluorescent microscope at 200× magnification. (**b**) Number of DCF stained cells. (**c**) NO concentration. NO concentration in the culture supernatants was determined using Griess reagent. DCFH-DA staining and NO assay were conducted using three wells per group, and these assays for each sample were analyzed in duplicates. All values in results are represented as the means ± standard deviation (SD). * indicated statically significance compared to the Non treated group, while # indicated statically significance compared to the Vehicle + A2E + BL treated group. Abbreviations: ROS, reactive oxygen species; NO, Nitric oxide; DCFH-DA, 20,70-Dichlorofluorescin diacetate; MED, methanol extracts of *Dipterocarpus tuberculatus* Roxb.; A2E, N-retinylidene-N-retinylethanolamine; BL, Blue light.

3.3. Protective Effects of MED against the Loss of Antioxidant Capacity Caused by A2E + BL Treatment in ARPE19 Cells

To examine whether the treatment of MED can protect against the reduction in antioxidative capacity in AMD, we measured the alterations in the SOD activity and expression, and the Nrf2 expression in MED + A2E + BL treated ARPE19 cells. Three parameters related to the antioxidative capacity exhibited a similar pattern in the three MED-treated groups. SOD activity was lower by 37% in the Vehicle + A2E + BL treated group compared to the Non treated group. However, this level was remarkably enhanced only in the HMED + A2E + BL treated group compared to the Vehicle + A2E + BL treated group (Figure 3a). However, a remarkable recovery in the expression level of antioxidative proteins was observed in all the MED-treated groups. The expression level of SOD and the Nrf2 proteins were decreased in the Vehicle + A2E + BL treated group compared to the Non treated group. However, the above decreased values were significantly increased in the three MED + A2E + BL treated groups. Especially, the levels of these proteins were higher than that of the Non treated group in the MMED + A2E + BL and HMED + A2E + BL treated groups (Figure 3b). Taken together, the data of the present study indicate that the protective effects of MED may be tightly associated with the recovery of antioxidative capacity loss caused by A2E + BL treatment in ARPE19 cells.

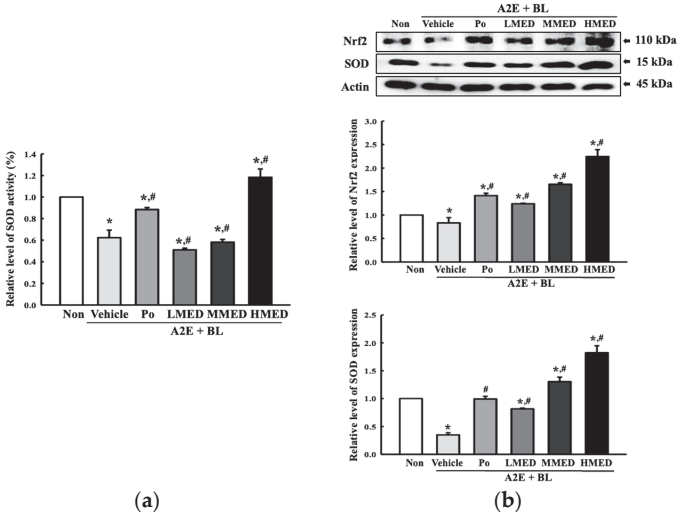

Figure 3. Determination of SOD and Nrf2 expression in MED + A2E + BL treated ARPE19 cells. (**a**) Measurement of SOD activity. SOD activity was measured in total cell lysate of ARPE19 cells using SOD assay kit. One SOD unit was defined as described in materials and methods. (**b**) Expression of SOD and NRF2 protein. After preparing total cell lysate from MED + A2E + BL treated ARPE19 cells, the expression level of SOD and Nrf2 protein was measured by Western blotting analysis. The total proteins homogenates were prepared from two to three samples per group, and Western blot analyses for each sample was analyzed in duplicate. All values in results are represented as the means ± standard deviation (SD). * indicated statically significance compared to the Non treated group, while # indicated statically significance compared to the Vehicle + A2E + BL treated group. Abbreviations: SOD, Superoxide dismutase; Nrf2, Nuclear factor erythroid 2–related factor 2; MED, methanol extracts of *Dipterocarpus tuberculatus* Roxb.; A2E: N-retinylidene-N-retinylethanolamine; BL, Blue light; WST-1, water-soluble tetrazolium salt-1.

3.4. Protective Effects of MED against Cell Death Caused by A2E + BL Treatment in ARPE19 Cells

To examine whether the treatment of MED can protect against cell death in AMD, the alterations of the cell viability were first analyzed in the MED + A2E + BL treated ARPE19 cells. A significant decrease in cell viability was successfully induced in the A2E + BL treated ARPE19 cells, and these levels were remarkably protected in a dose-dependent manner in the MED + A2E + BL treated group (Figure 4). Additionally, these cells were stained with Annexin V and PI to analyze the distribution of apoptotic cells. The total number of apoptotic cells remarkably increased 7.5-fold in the Vehicle + A2E + BL treated group compared to the Non treated group. However, these enhanced values gradually decreased in the three MED + A2E + BL treated groups, although the highest rate of decrease was detected in the HMED + A2E + BL treated group (Figure 5). Moreover, the alterations in the number of apoptotic cells were well reflected in the expression of proteins responsible for the regulation of apoptosis. The increased levels of the Bax/Bcl-2 ratio and the cleaved Cas-3/Cas-3 ratio in the A2E + BL treated cells, significantly decreased with MED pretreatment. Bax/Bcl-2 expressions decreased in a dose-dependent change in the MED-treated groups (Figure 6). Therefore, the above results suggest that the protective effect of MED on A2E + BL-induced cell death may be related to the suppression of apoptosis in ARPE19 cells.

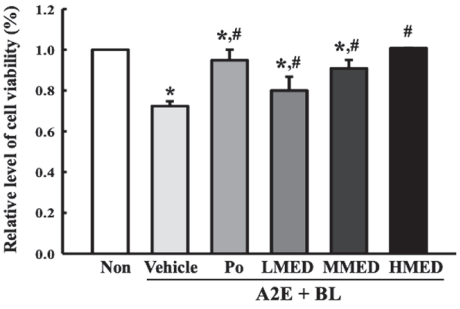

Figure 4. Determination of cell viability in MED + A2E + BL treated ARPE19 cells. After pretreatment of three different dosage MED for 24 h, their viability was determined using MTT assay. Two to three wells per group were used for the MTT assay, and optical density was measured in duplicates. All values in results are represented as the means ± standard deviation (SD). * indicated statically significance compared to the Non treated group, while # indicated statically significance compared to the Vehicle + A2E + BL treated group. Abbreviations: MTT, 3-(4,5-dimethylthiazol-2-yl)-2,5-diphenyltetrazolium bromide; MED, methanol extracts of *Dipterocarpus tuberculatus* Roxb.; A2E: N-retinylidene-N-retinylethanolamine; BL, Blue light.

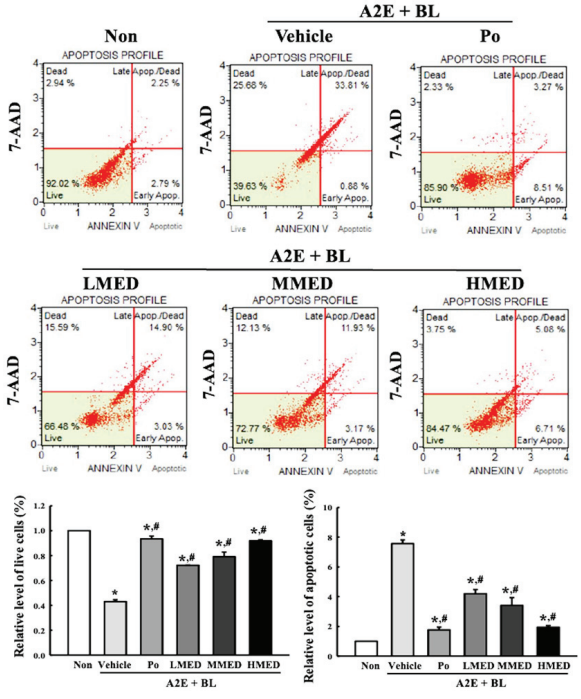

Figure 5. Apoptotic cell analysis in MED + A2E + BL treated ARPE19 cells. After staining with Annexin V and 7-AAD, the distribution of apoptotic cells was analyzed as described in materials and methods. All values in results are represented as the means ± standard deviation (SD). * indicated statically significance compared to the Non treated group, while # indicated statically significance compared to the Vehicle + A2E + BL treated group. Abbreviations: 7-AAD, 7-aminoactinomycin D; MED, methanol extracts of *Dipterocarpus tuberculatus* Roxb.; A2E: N-retinylidene-N-retinylethanolamine; BL, Blue light.

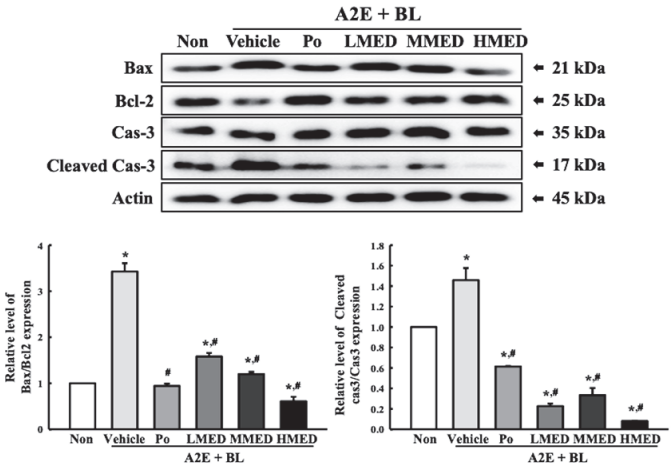

Figure 6. Expression of apoptotic proteins in MED + A2E + BL treated ARPE19 cells. After preparing total cell lysate from MED + A2E + BL treated ARPE19 cells, the expression level of Bax, Bcl-2, Cas-3 and Cleaved Cas-3 protein was measured by Western blotting analysis. The total proteins homogenates were prepared from two to three samples per group, and Western blot analyses for each sample was analyzed in duplicate. All values in results are represented as the means ± standard deviation (SD). * indicated statically significance compared to the Non treated group, while # indicated statically significance compared to the Vehicle + A2E + BL treated group. Abbreviations: Bax, Bcl-2-associated X protein; Bcl-2, B-cell lymphoma 2; Cas-3, Caspase-3; MED, methanol extracts of *Dipterocarpus tuberculatus* Roxb.; A2E: N-retinylidene-N-retinylethanolamine; BL, Blue light.

3.5. Protective Effects of MED on the Regulation of Angiogenesis Caused by A2E + BL Treatment in ARPE19 Cells

To investigate the therapeutic effect of MED on the regulation of angiogenesis caused by AMD, the alteration in the expression levels of matrix metalloproteinase (MMP) 2, 9 and vascular endothelial growth factor (VEGF) proteins in the MED + A2E + BL treated ARPE19 cells were analyzed. Treatment with MED led to a decrease in the expression levels of the three proteins, but there was a clear difference in the pattern of decrease. The expression level of MMP2 was significantly reduced equally in all MED-treated groups compared to the Vehicle + A2E + BL-treated group. However, the levels of MMP9 expression were significantly reduced in only the HMED + A2E + BL treated group. The decrease in expression was seen in both the LMED and MMED + A2E + BL treated groups; however, this decrease was not statistically significant. A significant dose-dependent decrease was seen in the expression of the VEGF proteins (Figure 7). These results suggest that MED may protect against the dysregulation of angiogenesis caused by A2E + BL treatment through the suppression of MMPs and VEGF expressions in ARPE19 cells.

3.6. Protective Effect of MED against the Inflammatory Response Caused by A2E + BL Treatment in ARPE19 Cells

To investigate the protective effects of MED against AMD-induced inflammatory response, alterations in the expression of the iNOS-induced COX-2 mediated pathway and inflammasome were measured in the MED + A2E + BL treated ARPE19 cells. The expression of iNOS and COX-2 were greater in the Vehicle + A2E + BL treated group than in the control group. The decrease in the expression of these proteins was dose-dependent in the MED-treated groups; however, their rate was different (Figure 8). Additionally, the protective effect of MED on the regulation of iNOS and COX-2 was well reflected in the inflammasome activation. The expression levels of three key members including NLR family pyrin domain containing 3 (NLRP3), apoptosis-associated speck-like protein containing a CARD (ASC),

and the cleaved of Cas-1 proteins, were higher in the Vehicle + A2E + BL treated group than the Non treated group. However, the above-increased values were significantly decreased in the LMED, MMED and HMED + A2E + BL treated groups compared to the Vehicle + A2E + BL treated group. Especially, the expression levels of NLRP3 and ASC in the MED + A2E + BL treated groups were lower than that of the Non treated group, while the cleaved Cas-1/Cas-1 ratio was completely recovered in the Non treated group (Figure 9). Furthermore, the protective effects of MED on the regulation of iNOS-induced COX-2 mediated pathway and inflammasome were well reflected in the regulation of inflammatory cytokine expressions. The MED + A2E + BL treated groups exhibited a significant decrease in the mRNA levels of TNF-α, IL-6, IL-1β and NF-κB compared to the Vehicle + A2E + BL treated group (Figure 10). Therefore, the above results for inflammatory responses suggest that MED can protect against the increased inflammatory response seen in A2E + BL treated cells through the regulation of the iNOS-induced COX-2 mediated pathway and NLRP3 inflammasome activation in ARPE19 cells.

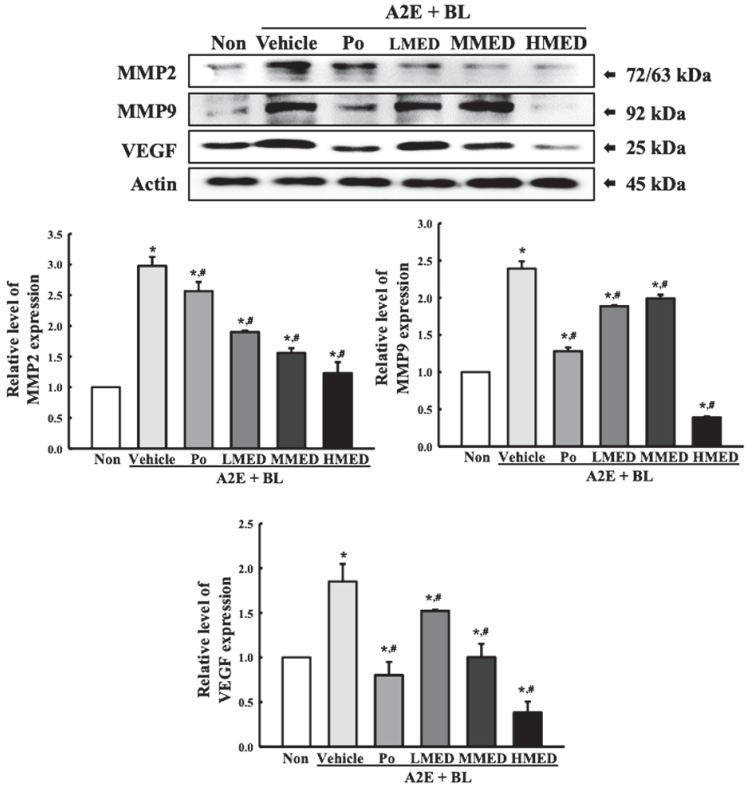

Figure 7. Expression of angiogenic proteins in MED + A2E + BL treated ARPE19 cells. After treatment with MED for 24 h, the expression levels of angiogenic proteins, including MMP2, MMP9, VEGF and actin were measured in total cell lysates using Western blot analysis. The total proteins homogenates were prepared from two to three samples per group, and Western blot analyses for each sample was analyzed in duplicate. All values in results are represented as the means ± standard deviation (SD). * indicated statically significance compared to the Non treated group, while # indicated statically significance compared to the Vehicle + A2E + BL treated group. Abbreviations: MMP, Matrix metalloproteinase; VEGF, Vascular endothelial growth factor; MED, methanol extracts of *Dipterocarpus tuberculatus* Roxb.; A2E: N-retinylidene-N-retinylethanolamine; BL, Blue light.

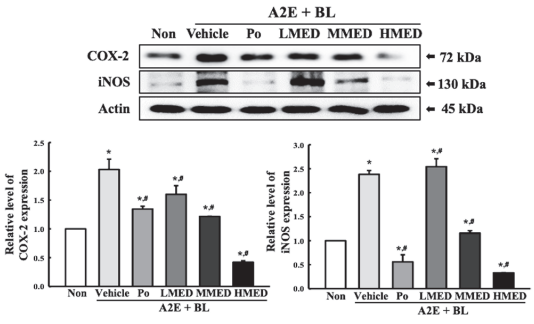

Figure 8. Expression of iNOS and COX-2 proteins in MED + A2E + BL treated ARPE19 cells. After treatment with MED for 24 h, the expression level of key regulators in iNOS-induced COX-2 mediated pathway, including iNOS, COX-2 and actin were measured in total cell lysates using Western blot analysis. The total proteins homogenates were prepared from two to three samples per group, and Western blot analyses for each sample was analyzed in duplicate. All values in results are represented as the means ± standard deviation (SD). * indicated statically significance compared to the Non treated group, while # indicated statically significance compared to the Vehicle + A2E + BL treated group. Abbreviations: COX-2, Cyclooxygenase-2; iNOS, Inducible nitric oxide synthase; MED, methanol extracts of *Dipterocarpus tuberculatus* Roxb.; A2E: N-retinylidene-N-retinylethanolamine; BL, Blue light.

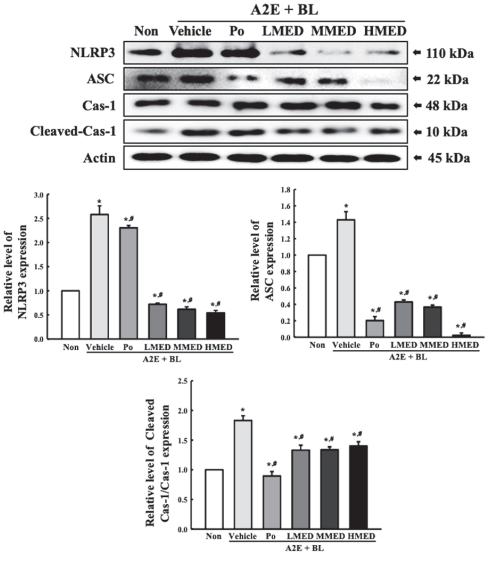

Figure 9. Expression of inflammasome in MED + A2E + BL treated ARPE19 cells. After treatment with MED for 24 h, the expression level of key regulators in inflammasome, including NLRP3, ASC, Cas-1, Cleaved Cas-1 and actin were measured in total cell lysates using Western blot analysis. The total proteins homogenates were prepared from two to three samples per group, and Western blot analyses for each sample was analyzed in duplicate. All values in results are represented as the means ± standard deviation (SD). * indicated statically significance compared to the Non treated group, while # indicated statically significance compared to the Vehicle + A2E + BL treated group. Abbreviations: NLRP3, NLR family pyrin domain containing 3; ASC, Apoptosis-associated speck-like protein; Cas-1, Caspase-1; MED, methanol extracts of *Dipterocarpus tuberculatus* Roxb.; A2E: N-retinylidene-N-retinylethanolamine; BL, Blue light.

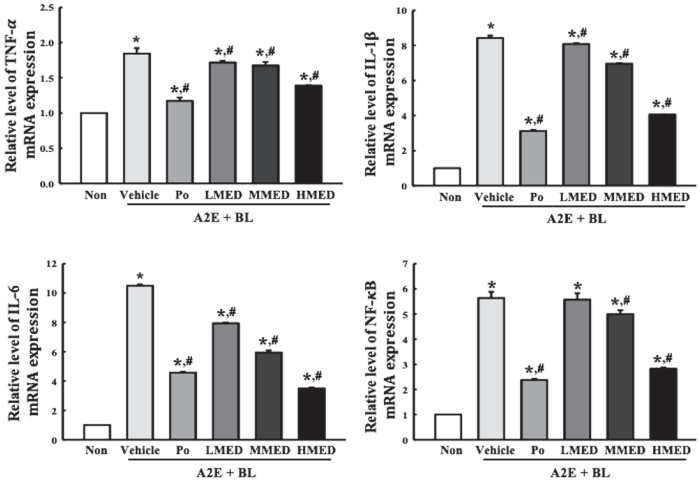

Figure 10. mRNA expression of inflammatory cytokines in MED + A2E + BL treated ARPE19 cells. The levels of TNF-α, IL-1β, IL-6, and NF-κB transcripts were measured in the total mRNA of ARPE19 cells by RT-qPCR using specific primers. The relative level of each transcript was determined based on the level of β-actin. The total RNAs were prepared from two to three samples per group, and RT-qPCR analyses for each sample were analyzed in duplicate. All values in results are represented as the means ± standard deviation (SD). * indicated statically significance compared to the Non treated group, while # indicated statically significance compared to the Vehicle + A2E + BL treated group. Abbreviations: TNF-α, tumor necrosis factor α; IL, Interleukin; NF-κB, Nuclear factor kappa light chain enhancer of activated B; MED, methanol extracts of *Dipterocarpus tuberculatus* Roxb.; A2E: N-retinylidene-N-retinylethanolamine; BL, Blue light.

3.7. Protective Effect of MED against the Photoreceptor Degranulation Caused by BL in the Retina of Balb/c Mice

Finally, we investigated the protective effects of MED against photoreceptor degeneration in the retina of the AMD mice model to confirm the protective effects of MED detected in the A2E + BL treated ARPE19 cells. To achieve this, the alterations of the thickness of the whole retina, OS, ONL, and INL were measured in the retinas of the Balb/c mice treated with MED + BL. As shown in Figure 11, the retinal thickness was lower in the Vehicle + BL treated group than in the Non treated group. However, the thickness was significantly increased in the LMED + BL and HMED + BL treated groups compared to the Vehicle + BL treated group. Additionally, a similar pattern of increase was detected in the thickness of the OS, ONL, and INL although the thickness of the IPL was maintained constant. Furthermore, the expression of antioxidative proteins and iNOS-induced COX-2 mediated pathway-related proteins were analyzed in the retinas of BL-exposed Balb/c mice to investigate whether the protective effect of MED against retinal degeneration has an association with the alteration of the antioxidative activity and inflammatory response. The tissue density of the Nrf2 proteins was lower in the retinas of Vehicle + BL treated mice than in the Non treated group. This level gradually recovered in the LMED + BL and HMED + BL treated groups although it did not recover to the level of the Non treated group (Figure 12a). A reverse pattern was detected in the COX-2 and iNOS-stained retinal tissues. The increase in their density in the Vehicle + BL treated group was remarkably decreased after the MED treatment (Figure 12b,c). Therefore, these results suggest that MED administration can protect against the retinal degeneration of BL-exposed Balb/c mice through the regulation of antioxidative activity and the inflammatory response.

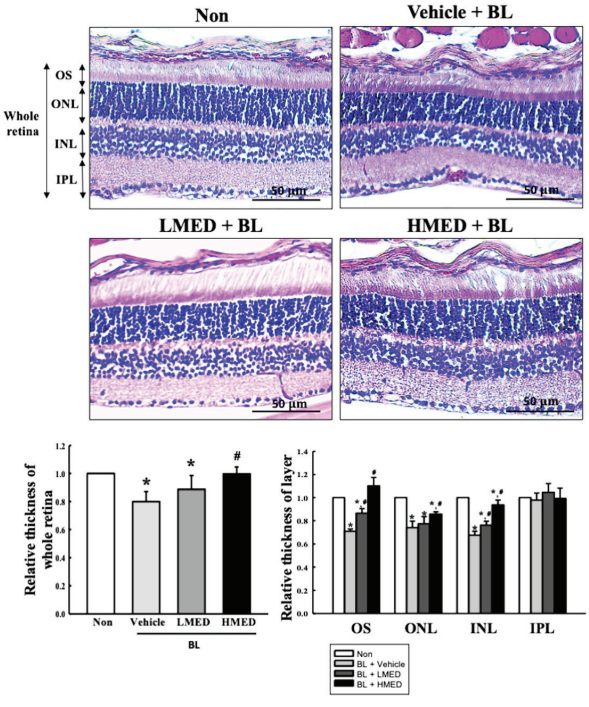

Figure 11. Histopathological structures in the retina of MED + BL treated Balb/c mice. H&E-stained sections of the retina were observed at 200× magnification using an optical microscope. The degree of histopathological changes in the retina tissue was measured by Image J program. The H&E-stained slides were prepared from three to five mice per group, the histopathological parameter analyses for each sample were measured in duplicate. All values in results are represented as the means ± standard deviation (SD). * indicated statically significance compared to the Non treated group, while # indicated statically significance compared to the Vehicle + A2E + BL treated group. Abbreviations: OS, Outer segment, ONL, Outer nuclear layer; INL, Inner nuclear layer; IPL, Inner plexiform layer; MED, methanol extracts of *Dipterocarpus tuberculatus* Roxb.; BL, Blue light.

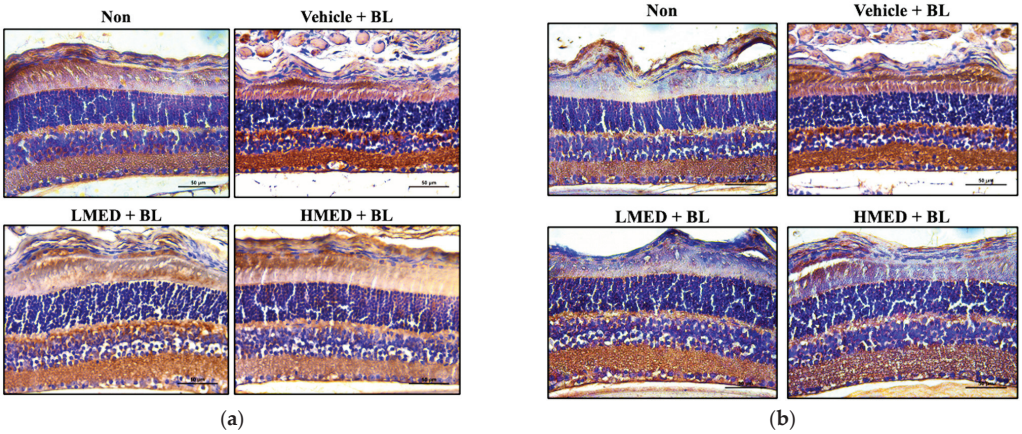

(**a**) (**b**)

Figure 12. *Cont.*

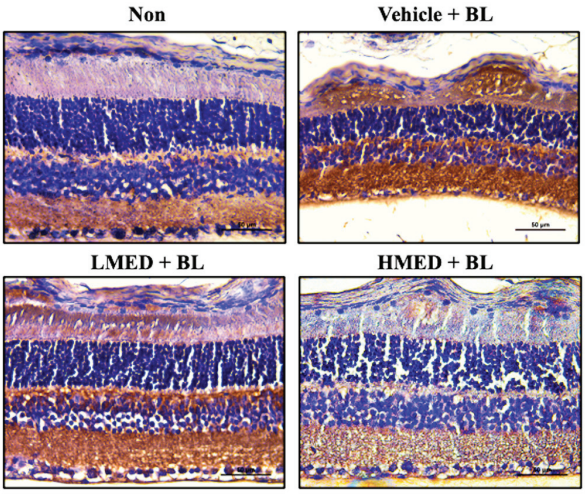

Figure 12. Tissue distribution of (**a**) Nrf2, (**b**) COX-2 and (**c**) iNOS protein in the retina of MED + BL treated Balb/c mice. After staining specific antibodies, the stained section of retina was observed at 200× magnification using light microscopy. Brown or dark brown indicates the expression of three proteins, and dark blue indicates the nucleus. The immunostained slides were prepared from three to five mice per group, the color density analyses for each sample were performed in duplicate. Abbreviations: Nrf2, Nuclear factor erythroid 2–related factor 2; COX-2, Cyclooxygenase-2; iNOS, Inducible nitric oxide synthase; MED, methanol extracts of *Dipterocarpus tuberculatus* Roxb.; BL, Blue light.

4. Discussion

Photochemical damage is induced by exposure of the retina to high-energy radiation [4]. During this process, the phagocytosis of the outer segment of photoreceptors and the production of superoxide anions are remarkably increased, leading to photo-oxidative stress in the retina [6,33]. Therefore, the administration of ROS scavengers can be considered one of the therapeutic strategies to protect or delay the progression of early AMD [34]. As part of a study aimed at identifying novel natural products with protective effects against AMD, we investigated the therapeutic effects and mechanism of action of MED in ARPE19 cells and Balb/c mice with AMD phenotypes. The results of our study provide novel scientific evidence that MED treatment may contribute to the protection against BL-induced retinal damage through the regulation of oxidative stress, apoptosis, neovascularization, and inflammatory response.

In the present study, the antioxidant properties of *Dipterocarpus tuberculatus* Roxb. are an important scientific and logical reason for its selection for evaluation as a potential therapeutic option for the treatment of AMD. As shown in Figures 1–3, MED showed high free radical scavenging activity, ROS suppressive activity and NO production, and stimulatory activity for SOD and Nrf2 expressions. Similar activities of other natural products have been reported in a few previous studies. The ethanol extract of *Dipterocarpus tuberculatus* Roxb. leaves and twigs suppressed the release of NO and prostaglandin E2 (PGE2) from LPS-stimulated RAW264.7 cells through the inhibition of COX-2 and iNOS transcriptions as well as the NF-κB signaling pathway [20]. NO concentrations, SOD activity, and Nrf2 expressions improved significantly in UV-irradiated NHDF cells after treatment with MED [22]. Studies also show that natural products with good antioxidative activity slow down the progression of AMD. A2E photo-oxidation-induced damages of ARPE19 cells significantly improved after treatment with procyanidins B2, *Arctium Lappa* L., *Prunella vulgaris* var. L., *Solanum melongena* L. through the suppression of oxidative stress and high

antioxidative activity [14,35–37]. Our study adds to the current body of evidence that suggests that natural products with high antioxidant activity can be considered potential treatments for a variety of diseases that occur due to oxidative damage.

Furthermore, in our study, asiatic acid, 2α-hydroxyursolic acid and ellagic acid are reported as the principal bioactive compounds as shown in Figure 1. They have high antioxidant activity and several biological functions even as a single compound. Asiatic acid is widely distributed in many fruits and vegetables and has various therapeutic effects on oxidative stress, inflammation and fulminant hepatic failure [38]. Similar to asiatic acid, 2α-hydroxyursolic acid has been discovered in a variety of medicinal herbs and fruits [39]. This compound shows also various pharmacological effects including antidiabetic activity, anti-inflammation, anti-obesity, anti-atherosclerosis, and anticancer [39–43]. Ellagic acid with high antioxidative activity is produced as a second metabolite through the hydrolysis of ellagitannins in various plants [44]. It has recently received a lot of attention because of its potential in the treatment of human diseases including diabetes, cancer, cardiovascular disease, and neurodegenerative diseases [45–48]. However, we believe that the protective effects of MED against AMD may be related to the synergistic effect of three compounds rather than the effect of a single component, although these effects include the effects of other unknown compounds.

Lipofuscin granules contain A2E and its oxidized forms (A2E-ox and A2E-2ox) accumulate in the retinal pigment epithelium with age, and this leads to macular degeneration [49,50]. During this process, the cumulative damage to the retina is accompanied by an increase in apoptosis, oxidative stress, and inflammation [51]. Based on the above scientific evidence, an in vitro model for AMD was established in ARPE19 cells laden with A2E and exposed to BL [49]. This model has been used to investigate the therapeutic effect of various natural products on AMD. Grape skin polyphenols, *Vaccinium uliginosum* L. extract, and procyanidins B2 significantly inhibited photo-oxidation-induced apoptosis in ARPE19 cells. Additionally, this inhibition involved the recoveries of the Bc1-2/Bax ratio, Cas-3, and Cas-9 cleavage, and recovery from endoplasmic reticulum (ER) stress [35,52,53]. Polyphenol-enriched *Vaccinium uliginosum* and norbixin reduced cell death, inhibited A2E accumulation, and resulted in improved photoprotection in ARPE19 cells and the primary culture of retinal cells, while the extract of *Curcuma longa* L. and curcuminoids protected against photo-oxidative damages and apoptosis in ARPE19 cells [17,54,55]. Similar effects of A2E accumulation, cell death, apoptosis, and cytokine expression were detected in ARPE-19 cells after treatment with *Arctium lappa* L., *Prunella vulgaris var* L., *Solanum melongena* L., and *Centella asiatica* [14,36,37,56]. In the present study, we investigated the therapeutic effects and the action mechanism of MED in A2E-laden ARPE19 cells after exposure to BL. MED treatment protected the cells by suppressing ROS and NO production, restoring antioxidant activity, suppressing the inflammatory response, and inhibiting apoptosis and angiogenesis. These results are consistent with previous research findings which investigated the therapeutic effects of various natural products in mammalian cells with AMD phenotypes. Therefore, our results provide the first evidence of the novel therapeutic function of MED against BL-induced macular degeneration in A2E-laden ARPE19 cells.

Meanwhile, the Nrf2 protein is well known as one of the important transcription factors that regulate the transcription of genes related to xenobiotics response and oxidative stress response to maintain cellular hemostasis [57]. Additionally, these responses involve many enzymes for detoxification including phase I, II and II drugs as well as the elimination of pro-antioxidants such as glutathione synthetase (GSS), SOD and catalase [58]. Recently, the regulatory mechanism of Nrf2 has been investigated in RPE cells by mimicking the onset of different eye diseases. Nrf2 overexpression improves the morphological structure of RPE cells and survival rate in mouse models of retinal degeneration through the regulation of multiple oxidative defense pathways and glutathione pathways [59]. Furthermore, the expression level of Nrf2 increased in the diabetic retinopathy conditions and is significantly recovered by treatment of polyunsaturated docosahexaenoic acid (DHA) in RPE cells [60]. A similar activation in the Nrf2 signaling pathway was induced in ARPE19 cells after

treatment with hydrogen peroxide. This activation was ameliorated with idebenone, a ubiquinone short-chain synthetic analog which has high antioxidant properties [61]. The activation of Nrf2 and transcriptional upregulation of its downstream genes were induced by tertbutyl hydroperoxide (t-BHP)-mediated oxidative stress in human RPE cells although these responses were attenuated by pretreatment of *Ginkgo biloba* extracts (GBE) [62]. In the present study, the expression level of Nrf2 was increased in A2E-laden ARPE19 cells after treatment with BL. Therefore, the results of the present study suggest that the action mechanism of Nrf2 may be considered a common mechanism involved in oxidative stress response triggered by various chemical and physical agents including hydrogen peroxide, t-BHP and BL as well as mimicking the condition of eye diseases such as diabetic retinopathy and retinitis pigmentosa. Furthermore, it is believed that this mechanism of Nrf2 has the potential to be useful for evaluating the efficacy of antioxidants.

Finally, the protective effects and action mechanism of natural products against AMD in retinal epithelial cells were verified in the experimental animal model with retinal damage although these cases are very rare. Among them, most of this damage in Balb/c mice was induced by exposure to BL at 10,000 Lux for 1 h/day for 2 weeks [14,17,36,54]. However, only one AMD model with an increase in the photoreceptor thickness and ONL was produced by intraperitoneal injection of N-methyl-N-nitrosourea (MNU) at a concentration of 50 mg/kg [56]. In the AMD models, the retinal cells recovered from the damage with the administration of several natural products. The polyphenol-enriched *Vaccinium uliginosum* L. fraction inhibited the decrease in ONL thickness and nuclei, while the administration of norbixin reduced the A2E accumulation in the retina of Abca4$^{-/-}$Rdh8$^{-/-}$ mice [17,54]. Similar improvement effects were observed in AMD model animals after treatment with *Arctium lappa* L., *Prunella vulgaris var.* L., and *Solanum melongena* L. [14,36,37]. Moreover, the thickness of the photoreceptors, ONL, and nuclei numbers in MNU-induced AMD model animals recovered when treated with *Centella asiatica* [56]. The results seen with MED administration on the retina of BL-exposed Balb/c mice were also similar. The thickness of the OS, ONL, and INL significantly improved after the administration of MED. The present study demonstrated the protective effects of MED against photo-oxidative damages in the retina of AMD animal models. These results suggest a new therapeutic role for MED that has not been investigated previously.

5. Conclusions

In the present study, we attempted to demonstrate the novel therapeutic effects of MED against AMD using a mammalian cell and an experimental animal model. To achieve this objective, the antioxidant activity of MED as well as changes in antioxidant capacity, anti-apoptosis, anti-angiogenesis, and anti-inflammatory response in A2E-laden ARPE19 cells after exposure to BL were investigated. Additionally, these effects were further assessed in the retinas of BL-exposed Balb/c mice. Our results provided the first scientific evidence that the high antioxidant activity of MED has the potential to prevent AMD and relieve symptoms related to the condition (Figure 13). However, our study had some limitations in that it did not directly compare all the results obtained in vitro to those at all layer levels of the retina due to restrictions on the collection of eye tissue samples. Moreover, the lack of any mechanism analyses in relation to lysosomal damage and disruption of the autophagy process in MED + A2E + BL treated ARPE19 cells and MED + BL treated mice should be considered as a drawback of our study. Therefore, further research involving animal models will be needed on some processes of cell damage to understand the mechanisms of action of MED and components.

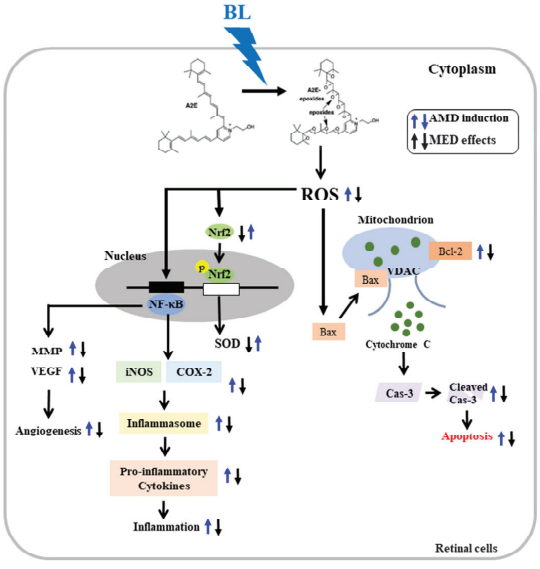

Figure 13. Suggested mechanism of prevention for AMD in the retinal cells. In this scheme, the treatment of MED is thought to inhibit apoptosis, angiogenesis and inflammatory response through enhancing antioxidant activity and suppressing oxidative stress retinal cells with photooxidative damages. Abbreviations: ROS, Reactive oxygen species; Nrf2, Nuclear factor erythroid 2–related factor 2; COX-2, Cyclooxygenase-2; iNOS, Inducible nitric oxide synthase; NLRP3, NLR family pyrin domain containing 3; ASC, Apoptosis-associated speck-like protein; Cas-1, Caspase-1; Bax, Bcl-2-associated X protein; Bcl-2, B-cell lymphoma 2; Cas-3, Caspase-3; BL, Blue light; MED, methanol extracts of *Dipterocarpus tuberculatus* Roxb.

Supplementary Materials: The following supporting information can be downloaded at: https://www.mdpi.com/article/10.3390/antiox12020329/s1, Figure S1: LC-MS analysis of A2E and MED.; Figure S2: Determination of optimal concentration of MED.; Figure S3: Determination of optimal concentration for A2E treatment under BL irradiation; Table S1: List of antibodies for Western blot analyses; Table S2: Primer sequences for RT-PCR analysis; Table S3: Antibodies list for Western blot analyses.

Author Contributions: Conceptualization, D.Y.H.; methodology, D.Y.H. and S.J.L.; software, S.J.L. and Y.J.R.; validation, S.J.L. and Y.J.R.; formal analysis, S.J.L. and Y.J.R.; investigation, S.J.L., Y.J.R., J.E.K., Y.J.J., H.J.S., A.S., S.H.P. and S.I.C.; resources, B.D. and O.S.; data curation, S.J.L. and Y.J.R.; writing—original draft preparation, D.Y.H. writing—review and editing, S.I.C.; visualization, D.Y.H. and S.I.C.; supervision, D.Y.H.; project administration, D.Y.H.; funding acquisition, D.Y.H. All authors have read and agreed to the published version of the manuscript.

Funding: This research was funded by BK21 FOUR Program through the National Research Foundation of Korea (NRF), grant number F21YY8109033 and F22YY8109033.

Institutional Review Board Statement: The animal study protocol was approved by the Pusan National University (PNU)–Institutional Animal Care and Use Committee (IACUC) (approval no. PNU-2022-0103).

Informed Consent Statement: Not applicable.

Data Availability Statement: Data is contained within the article and Supplementary Materials.

Acknowledgments: We thank Jin Hyang Hwang, the animal technician, for directing the Animal Facility and Care at the Laboratory Animal Resources Center.

Conflicts of Interest: The authors declare no conflict of interest.

References

1. Lim, L.S.; Mitchell, P.; Seddon, J.M.; Holz, F.G.; Wong, T.Y. Age-related macular degeneration. *Lancet* **2012**, *379*, 1728–1738. [CrossRef] [PubMed]
2. Al Gwairi, O.; Thach, L.; Zheng, W.; Osman, N.; Little, P.J. Cellular and molecular pathology of age-related macular degeneration: Potential role for proteoglycans. *J. Ophthalmol.* **2016**, *2016*, 2913612. [CrossRef]
3. Boyer, N.P.; Higbee, D.; Currin, M.B.; Blakeley, L.R.; Chen, C.; Ablonczy, Z.; Crouch, R.K.; Koutalos, Y. Lipofuscin and N-retinylidene-N-retinylethanolamine (A2E) accumulate in retinal pigment epithelium in absence of light exposure: Their origin is 11-cis-retinal. *J. Biol. Chem.* **2012**, *287*, 22276–22286. [CrossRef] [PubMed]
4. Sparrow, J.R.; Nakanishi, K.; Parish, C.A. The lipofuscin fluorophore A2E mediates blue light-induced damage to retinal pigmented epithelial cells. *Investig. Ophthalmol. Vis. Sci.* **2000**, *41*, 1981–1989.
5. Wu, Y.; Yanase, E.; Feng, X.; Siegel, M.M.; Sparrow, J.R. Structural characterization of bisretinoid A2E photocleavage products and implications for age-related macular degeneration. *Proc. Natl. Acad. Sci. USA* **2010**, *107*, 7275–7280. [CrossRef]
6. Jang, Y.P.; Zhou, J.L.; Nakanishi, K.; Sparrow, J.R. Anthocyanins protect against A2E photooxidation and membrane permeabilization in retinal pigment epithelial cells. *Photochem. Photobiol.* **2005**, *81*, 529–536. [CrossRef] [PubMed]
7. Zhou, J.; Jang, Y.P.; Kim, S.R.; Sparrow, J.R. Complement activation by photooxidation products of A2E, a lipofuscin constituent of the retinal pigment epithelium. *Proc. Natl. Acad. Sci. USA* **2006**, *103*, 16182–16187. [CrossRef]
8. Hammer, M.; Richter, S.; Guehrs, K.-H.; Schweitzer, D. Retinal pigment epithelium cell damage by A2E and its photo-derivatives. *Mol. Vis.* **2006**, *12*, 1348–1354.
9. Jeong, S.Y.; Gu, X.; Jeong, K.W. Photoactivation of N-retinylidene-N-retinylethanolamine compromises autophagy in retinal pigmented epithelial cells. *Food Chem. Toxicol.* **2019**, *131*, 110555. [CrossRef]
10. Xing, Y.; Liang, S.; Zhao, Y.; Yang, S.; Ni, H.; Li, H. Protection of *Aronia melanocarpa* fruit extract from sodium-iodate-induced damages in rat retina. *Nutrients* **2021**, *13*, 4411. [CrossRef]
11. Osada, H.; Okamoto, T.; Kawashima, H.; Toda, E.; Miyake, S.; Nagai, N.; Kobayashi, S.; Tsubota, K.; Ozawa, Y. Neuroprotective effect of bilberry extract in a murine model of photo-stressed retina. *PLoS ONE* **2017**, *12*, e0178627. [CrossRef] [PubMed]
12. Wu, H.; Xu, J.; Du, X.; Cui, J.; Zhang, T.; Chen, Y. Shihu Yeguang Pill protects against bright light-induced photoreceptor degeneration in part through suppressing photoreceptor apoptosis. *Biomed. Pharmacother.* **2020**, *126*, 110050. [CrossRef] [PubMed]
13. Shanmuganathan, S.; Angayarkanni, N. Chebulagic acid, chebulinic acid and gallic acid, the active principles of triphala, inhibit TNFα induced pro-angiogenic and pro-inflammatory activities in retinal capillary endothelial cells by inhibiting p38, ERK and NFκB phosphorylation. *Vascul. Pharmacol.* **2018**, *108*, 23–35. [CrossRef] [PubMed]
14. Pham, T.N.M.; Shin, C.Y.; Park, S.H.; Lee, T.H.; Ryu, H.Y.; Kim, S.-B.; Auh, K.; Jeong, K.W. *Solanum melongena* L. extract protects retinal pigment epithelial cells from blue light-induced phototoxicity in in vitro and in vivo models. *Nutrients* **2021**, *13*, 359. [CrossRef] [PubMed]
15. Wang, Y.; Zhao, L.; Lu, F.; Yang, X.; Deng, Q.; Ji, B.; Huang, F. Retinoprotective effects of bilberry anthocyanins via antioxidant, anti-inflammatory, and anti-apoptotic mechanisms in a visible light-induced retinal degeneration model in pigmented rabbits. *Molecules* **2015**, *20*, 22395–22410. [CrossRef]
16. Ogawa, K.; Kuse, Y.; Tsuruma, K.; Kobayashi, S.; Shimazawa, M.; Hara, H. Protective effects of bilberry and lingonberry extracts against blue light-emitting diode light-induced retinal photoreceptor cell damage in vitro. *BMC Complement. Altern. Med.* **2014**, *14*, 120. [CrossRef]
17. Lee, B.L.; Kang, J.H.; Kim, H.M.; Jeong, S.H.; Jang, D.S.; Jang, Y.P.; Choung, S.Y. Polyphenol-enriched *Vaccinium uliginosum* L. fractions reduce retinal damage induced by blue light in A2E-laden ARPE19 cell cultures and mice. *Nutr. Res.* **2016**, *36*, 1402–1414. [CrossRef]
18. Cho, H.M.; Jo, Y.D.; Choung, S.Y. Protective effects of spirulina maxima against blue light-induced retinal damages in A2E-laden ARPE-19 cells and Balb/c mice. *Nutrients* **2022**, *14*, 401. [CrossRef]
19. Surapinit, S.; Jong-aramruang, J.; Siripong, P.; Khumkratok, S.; Tip-pyang, S. Dipterostilbenosides A and B, oligostilbene glycosides from *Dipterocarpus tuberculatus*. *Nat. Prod. Commun.* **2014**, *9*, 1323–1326. [CrossRef]
20. Yang, W.S.; Lee, B.H.; Kim, S.H.; Kim, H.G.; Yi, Y.S.; Htwe, K.M.; Kim, Y.D.; Yoon, K.D.; Hong, S.; Lee, W.S.; et al. *Dipterocarpus tuberculatus* ethanol extract strongly suppresses in vitro macrophage-mediated inflammatory responses and in vivo acute gastritis. *J. Ethnopharmacol.* **2013**, *146*, 873–880. [CrossRef]
21. Kim, H.; Yang, W.S.; Htwe, K.M.; Lee, M.-N.; Kim, Y.-D.; Yoon, K.D.; Lee, B.-H.; Lee, S.; Cho, J.Y. *Dipterocarpus tuberculatus* Roxb. ethanol extract has anti-inflammatory and hepatoprotective effects in vitro and in vivo by targeting the IRAK1/AP-1 pathway. *Molecules* **2021**, *26*, 2529. [CrossRef] [PubMed]
22. Lee, S.J.; Kim, J.E.; Choi, Y.J.; Gong, J.E.; Park, S.H.; Douangdeuane, B.; Souliya, O.; Park, J.M.; Lee, H.S.; Kim, B.H.; et al. Therapeutic effects of *Dipterocarpus tuberculatus* with high antioxidative activity against UV-induced photoaging of NHDF cells and nude mice. *Antioxidants* **2021**, *10*, 791. [CrossRef]
23. Jung, J.; Choi, Y.J.; Lee, S.J.; Choi, Y.S.; Douangdeuane, B.; Souliya, O.; Jeong, S.; Park, S.; Hwang, D.Y.; Seo, S. Promoting effects of titanium implants coated with *Dipterocarpus tuberculatus* extract on osseointegration. *ACS Biomater. Sci. Eng.* **2022**, *8*, 847–858. [CrossRef] [PubMed]
24. Hassan, S.M.; Al Aqil, A.A.; Attimarad, M. Determination of crude saponin and total flavonoids content in guar meal. *Adv. Med. Plant Res.* **2013**, *1*, 24–28.

25. Lee, N.R.; Lee, S.M.; Cho, K.S.; Jeong, S.Y.; Hwang, D.Y.; Kim, D.S.; Hong, C.O.; Son, H.J. Improved production of poly-γ-glutamic acid by bacillus subtilis D7 isolated from doenjang, a Korean traditional fermented food, and it's antioxidant activity. *Appl. Biochem. Biotechnol.* **2014**, *173*, 918–932. [CrossRef]
26. Kagan, D.B.; Liu, H.; Hutnik, C.M. Efficacy of various antioxidants in the protection of the retinal pigment epithelium from oxidative stress. *Clin. Ophthalmol.* **2012**, *6*, 1471–1476. [CrossRef]
27. Song, B.R.; Lee, S.J.; Kim, J.E.; Choi, H.J.; Bae, S.J.; Choi, Y.J.; Gong, J.E.; Noh, J.K.; Kim, H.S.; Kang, H.G.; et al. Anti-inflammatory effects of *Capparis ecuadorica* extract in phthalic-anhydride-induced atopic dermatitis of IL-4/Luc/CNS-1 transgenic mice. *Pharm. Biol.* **2020**, *58*, 1263–1276. [CrossRef]
28. Kim, J.E.; Song, H.J.; Choi, Y.J.; Jin, Y.J.; Roh, Y.J.; Seol, A.; Park, S.H.; Park, J.M.; Kang, H.G.; Hwang, D.Y. Improvement of the intestinal epithelial barrier during laxative effects of phlorotannin in loperamide-induced constipation of SD rats. *Lab. Anim. Res.* **2023**, *39*, 1. [CrossRef]
29. Bae, S.J.; Kim, J.E.; Choi, H.J.; Choi, Y.J.; Lee, S.J.; Gong, J.E.; Seo, S.; Yang, S.Y.; An, B.S.; Lee, H.S.; et al. α-Linolenic acid-enriched cold-pressed perilla oil suppress high-fat diet-induced hepatic steatosis through amelioration of the ER stress-mediated autophagy. *Molecules* **2020**, *25*, 2662. [CrossRef]
30. Livak, K.J.; Schmittgen, T.D. Analysis of relative gene expression data using real-time quantitative PCR and the 2(−ΔΔC(T)) method. *Methods* **2001**, *25*, 402–408. [CrossRef]
31. Kim, J.; Lee, Y.M.; Jung, W.; Park, S.B.; Kim, C.S.; Kim, J.S. *Aster koraiensis* extract and chlorogenic acid inhibit retinal angiogenesis in a mouse model of oxygen-induced retinopathy. *Evid. Based Complement. Alternat. Med.* **2018**, *2018*, 6402650. [CrossRef] [PubMed]
32. Choi, Y.J.; Kim, J.E.; Lee, S.J.; Gong, J.E.; Jin, Y.J.; Lee, H.; Hwang, D.Y. Promotion of the inflammatory response in mid colon of complement component 3 knockout mice. *Sci. Rep.* **2022**, *12*, 1700. [CrossRef] [PubMed]
33. Fernández-Sánchez, L.; Lax, P.; Noailles, A.; Angulo, A.; Maneu, V.; Cuenca, N. Natural compounds from saffron and bear bile prevent vision loss and retinal degeneration. *Molecules* **2015**, *20*, 13875–13893. [CrossRef]
34. Ramkumar, H.L.; Tuo, J.; Shen, D.F.; Zhang, J.; Cao, X.; Chew, E.Y.; Chan, C.C. Nutrient supplementation with n3 polyunsaturated fatty acids, lutein, and zeaxanthin decrease A2E accumulation and VEGF expression in the retinas of Ccl2/Cx3cr1-deficient mice on Crb1(rd8) background. *J. Nutr.* **2013**, *143*, 1129–1135. [CrossRef] [PubMed]
35. Li, W.; Jiang, Y.N.; Sun, T.N.; Yao, X.; Sun, X. Supplementation of procyanidins B2 attenuates photooxidation-induced apoptosis in ARPE-19 cells. *Int. J. Food Sci. Nutr.* **2016**, *67*, 650–659. [CrossRef]
36. Kim, D.H.; Choi, Y.R.; Shim, J.; Choi, Y.-S.; Kim, Y.T.; Kim, M.K.; Kim, M.J. Suppressive effect of *Arctium lappa* L. leaves on retinal damage against A2E-induced ARPE-19 cells and mice. *Molecules* **2020**, *25*, 1737. [CrossRef]
37. Kim, J.; Cho, K.; Choung, S.Y. Protective effect of *Prunella vulgaris* var. L extract against blue light induced damages in ARPE-19 cells and mouse retina. *Free Radic. Biol. Med.* **2020**, *152*, 622–631. [CrossRef]
38. Lv, H.; Qi, Z.; Wang, S.; Feng, H.; Deng, X.; Ci, X. Asiatic acid exhibits anti-inflammatory and antioxidant activities against lipopolysaccharide and d-galactosamine-Induced fulminant hepatic failure. *Front. Immunol.* **2017**, *8*, 785. [CrossRef]
39. Jiang, X.; Li, T.; Liu, R.H. 2α-Hydroxyursolic acid inhibited cell proliferation and induced apoptosis in MDA-MB-231 human breast cancer cells through the p38/MAPK signal transduction pathway. *J. Agric. Food Chem.* **2016**, *64*, 1806–1816. [CrossRef]
40. Hou, W.; Li, Y.; Zhang, Q.; Wei, X.; Peng, A.; Chen, L.; Wei, Y. Triterpene acids isolated from *lagerstroemia speciosa* leaves as alpha-glucosidase inhibitors. *Phytother. Res.* **2009**, *23*, 614–618. [CrossRef]
41. Banno, N.; Akihisa, T.; Tokuda, H.; Yasukawa, K.; Higashihara, H.; Ukiya, M.; Watanabe, K.; Kimura, Y.; Hasegawa, J.; Nishino, H. Triterpene acids from the leaves of *Perilla frutescens* and their anti-inflammatory and antitumor-promoting effects. *Biosci. Biotechnol. Biochem.* **2004**, *68*, 85–90. [CrossRef] [PubMed]
42. Yamaguchi, Y.; Yamada, K.; Yoshikawa, N.; Nakamura, K.; Haginaka, J.; Kunitomo, M. Corosolic acid prevents oxidative stress, inflammation and hypertension in SHR/NDmcr-cp rats, a model of metabolic syndrome. *Life Sci.* **2006**, *79*, 2474–2479. [CrossRef] [PubMed]
43. Chen, H.; Yang, J.; Zhang, Q.; Chen, L.H.; Wang, Q. Corosolic acid ameliorates atherosclerosis in apolipoprotein E-deficient mice by regulating the nuclear factor-κB signaling pathway and inhibiting monocyte chemoattractant protein-1 expression. *Circ. J.* **2012**, *76*, 995–1003. [CrossRef]
44. Wink, M. Modes of action of herbal medicines and plant secondary metabolites. *Medicine* **2015**, *2*, 251–286. [CrossRef] [PubMed]
45. Lin, C.; Wei, D.; Xin, D.; Pan, J.; Huang, M. Ellagic acid inhibits proliferation and migration of cardiac fibroblasts by down-regulating expression of HDAC1. *J. Toxicol. Sci.* **2019**, *44*, 425–433. [CrossRef]
46. Javaid, N.; Shah, M.A.; Rasul, A.; Chauhdary, Z.; Saleem, U.; Khan, H.; Ahmed, N.; Uddin, M.S.; Mathew, B.; Behl, T.; et al. Neuroprotective effects of ellagic acid in alzheimer's disease: Focus on underlying molecular mechanisms of therapeutic potential. *Curr. Pharm. Des.* **2021**, *27*, 3591–3601. [CrossRef] [PubMed]
47. Amor, A.J.; Gómez-Guerrero, C.; Ortega, E.; Sala-Vila, A.; Lázaro, I. Ellagic acid as a tool to limit the diabetes burden: Updated evidence. *Antioxidants* **2020**, *9*, 1226. [CrossRef]
48. Harikrishnan, H.; Jantan, I.; Alagan, A.; Haque, M.A. Modulation of cell signaling pathways by *Phyllanthus amarus* and its major constituents: Potential role in the prevention and treatment of inflammation and cancer. *Inflammopharmacology* **2020**, *28*, 1–18. [CrossRef]

49. Arnault, E.; Barrau, C.; Nanteau, C.; Gondouin, P.; Bigot, K.; Viénot, F.; Gutman, E.; Fontaine, V.; Villette, T.; Cohen-Tannoudji, D.; et al. Phototoxic action spectrum on a retinal pigment epithelium model of age-related macular degeneration exposed to sunlight normalized conditions. *PLoS ONE* **2013**, *8*, e71398. [CrossRef]
50. Yakovleva, M.A.; Feldman, T.B.; Arbukhanova, P.M.; Borzenok, S.A.; Kuzmin, V.A.; Ostrovsky, M.A. Estimation of fluorescence lifetime of lipofuscin fluorophores contained in lipofuscin granules of retinal pigment epithelium of human cadaver eyes without signs of pathology. *Dokl. Biochem. Biophys.* **2017**, *472*, 19–22. [CrossRef]
51. Parmar, V.M.; Parmar, T.; Arai, E.; Perusek, L.; Maeda, A. A2E-associated cell death and inflammation in retinal pigmented epithelial cells from human induced pluripotent stem cells. *Stem Cell Res.* **2018**, *27*, 95–104. [CrossRef]
52. Zhao, Z.; Sun, T.; Jiang, Y.; Wu, L.; Cai, X.; Sun, X.; Sun, X. Photooxidative damage in retinal pigment epithelial cells via GRP78 and the protective role of grape skin polyphenols. *Food Chem. Toxicol.* **2014**, *74*, 216–224. [CrossRef] [PubMed]
53. Yoon, S.M.; Lee, B.L.; Guo, Y.R.; Choung, S.Y. Preventive effect of *Vaccinium uliginosum* L. extract and its fractions on age-related macular degeneration and its action mechanisms. *Arch. Pharm. Res.* **2016**, *39*, 21–32. [CrossRef] [PubMed]
54. Fontaine, V.; Monteiro, E.; Brazhnikova, E.; Lesage, L.; Balducci, C.; Guibout, L.; Feraille, L.; Elena, P.P.; Sahel, J.A.; Veillet, S.; et al. Norbixin protects retinal pigmented epithelium cells and photoreceptors against A2E-mediated phototoxicity in vitro and in vivo. *PLoS ONE* **2016**, *11*, e0167793. [CrossRef] [PubMed]
55. Park, S.I.; Lee, E.H.; Kim, S.R.; Jang, Y.P. Anti-apoptotic effects of *Curcuma longa* L. extract and its curcuminoids against blue light-induced cytotoxicity in A2E-laden human retinal pigment epithelial cells. *J. Pharm. Pharmacol.* **2017**, *69*, 334–340. [CrossRef] [PubMed]
56. Park, D.W.; Lee, Y.G.; Jeong, Y.J.; Jeon, H.; Kang, S.C. Preventive effects against retinal degeneration by *Centella asiatica* extract (CA-HE50) and asiaticoside through apoptosis suppression by the Nrf2/HO-1 signaling pathway. *Antioxidants* **2021**, *10*, 613. [CrossRef]
57. Jaramillo, M.C.; Zhang, D.D. The emerging role of the Nrf2-Keap1 signaling pathway in cancer. *Genes Dev.* **2013**, *27*, 2179–2191. [CrossRef]
58. He, F.; Antonucci, L.; Karin, M. NRF2 as a regulator of cell metabolism and inflammation in cancer. *Carcinogenesis* **2020**, *41*, 405–416. [CrossRef]
59. Wu, D.M.; Ji, X.; Ivanchenko, M.V.; Chung, M.; Piper, M.; Rana, P.; Wang, S.K.; Xue, Y.; West, E.; Zhao, S.R.; et al. Nrf2 overexpression rescues the RPE in mouse models of retinitis pigmentosa. *JCI Insight* **2021**, *6*, e145029. [CrossRef]
60. Bianchetti, G.; Clementi, M.E.; Sampaolese, B.; Serantoni, C.; Abeltino, A.; De Spirito, M.; Sasson, S.; Maulucci, G. Investigation of DHA-induced regulation of redox homeostasis in retinal pigment epithelium cells through the combination of metabolic imaging and molecular biology. *Antioxidants* **2022**, *11*, 1072. [CrossRef]
61. Clementi, M.E.; Pizzoferrato, M.; Bianchetti, G.; Brancato, A.; Sampaolese, B.; Maulucci, G.; Tringali, G. Cytoprotective effect of idebenone through modulation of the intrinsic mitochondrial pathway of apoptosis in human retinal pigment epithelial cells exposed to oxidative stress induced by hydrogen peroxide. *Biomedicines* **2022**, *10*, 503. [CrossRef] [PubMed]
62. Li, Y.; Zhu, X.; Wang, K.; Zhu, L.; Murray, M.; Zhou, F. *Ginkgo biloba* extracts (GBE) protect human RPE cells from t-BHP-induced oxidative stress and necrosis by activating the Nrf2-mediated antioxidant defense. *J Pharm. Pharmacol.* **2022**, rgac069. [CrossRef] [PubMed]

antioxidants

MDPI

Article

Vitamin C Deficiency Reduces Neurogenesis and Proliferation in the SVZ and Lateral Ventricle Extensions of the Young Guinea Pig Brain

Nery Jara [1], Manuel Cifuentes [2], Fernando Martínez [1,3], Iván González-Chavarría [4], Katterine Salazar [1,3], Lucas Ferrada [1] and Francisco Nualart [1,3,*]

[1] Laboratorio de Neurobiología y Células Madre, NeuroCellT, Departamento de Biología Celular, Facultad de Ciencias Biológicas, Universidad de Concepción, Concepción 4030000, Chile
[2] Department of Cell Biology, Genetics and Physiology, University of Malaga, 29010 Malaga, Spain
[3] Centro de Microscopía Avanzada CMA BIO BIO, Universidad de Concepción, Concepción 4030000, Chile
[4] Laboratorio de Lipoproteínas y Cáncer, Departamento de Fisiopatología, Facultad de Ciencias Biológicas, Universidad de Concepción, Concepción 4030000, Chile
* Correspondence: frnualart@udec.cl; Tel.: +56-041-220-3479; Fax: +56-041-225-5479

Abstract: Although scurvy, the severe form of vitamin C deficiency, has been almost eradicated, the prevalence of subclinical vitamin C deficiency is much higher than previously estimated and its impact on human health might not be fully understood. Vitamin C is an essential molecule, especially in the central nervous system where it performs numerous, varied and critical functions, including modulation of neurogenesis and neuronal differentiation. Although it was originally considered to occur only in the embryonic brain, it is now widely accepted that neurogenesis also takes place in the adult brain. The subventricular zone (SVZ) is the neurogenic niche where the largest number of new neurons are born; however, the effect of vitamin C deficiency on neurogenesis in this key region of the adult brain is unknown. Therefore, through BrdU labeling, immunohistochemistry, confocal microscopy and transmission electron microscopy, we analyzed the proliferation and cellular composition of the SVZ and the lateral ventricle (LVE) of adult guinea pigs exposed to a vitamin-C-deficient diet for 14 and 21 days. We found that neuroblasts in the SVZ and LVE were progressively and significantly decreased as the days under vitamin C deficiency elapsed. The neuroblasts in the SVZ and LVE decreased by about 50% in animals with 21 days of deficiency; this was correlated with a reduction in BrdU positive cells in the SVZ and LVE. In addition, the reduction in neuroblasts was not restricted to a particular rostro–caudal area, but was observed throughout the LVE. We also found that vitamin C deficiency altered cellular morphology at the ultrastructural level, especially the cellular and nuclear morphology of ependymal cells of the LVE. Therefore, vitamin C is essential for the maintenance of the SVZ cell populations required for normal activity of the SVZ neurogenic niche in the adult guinea pig brain. Based on our results from the guinea pig brain, we postulate that vitamin C deficiency could also affect neurogenesis in the human brain.

Keywords: vitamin C; ascorbic acid; subventricular zone; lateral ventricle extensions; adult neurogenesis

Citation: Jara, N.; Cifuentes, M.; Martínez, F.; González-Chavarría, I.; Salazar, K.; Ferrada, L.; Nualart, F. Vitamin C Deficiency Reduces Neurogenesis and Proliferation in the SVZ and Lateral Ventricle Extensions of the Young Guinea Pig Brain. *Antioxidants* **2022**, *11*, 2030. https://doi.org/10.3390/antiox11102030

Academic Editors: Ana-Maria Buga and Carmen Nicoleta Oancea

Received: 10 September 2022
Accepted: 3 October 2022
Published: 14 October 2022

1. Introduction

Scurvy is a disease caused by severe vitamin C deficiency produced in humans and animal models that cannot produce endogenous vitamin C and must obtain it from the diet [1]. Although the incidence of scurvy has been declining for decades, the prevalence of subclinical vitamin C deficiency is much higher than previously estimated [2,3] and the impact on human health might not be fully appreciated. Vitamin C is an essential antioxidant molecule, especially in the central nervous system, where it performs numerous and varied functions [4]. For example, vitamin C, which is taken up through specialized membrane transporters [5], modulates neurogenesis (i.e., the genesis of new neurons or

neuroblasts) [6] and neuronal differentiation (i.e., maturation of neuroblasts into fully functional neurons) [5,6].

The vitamin C transporter, SVCT2, is expressed in precursor cells of different embryonic and postnatal brain regions. During the beginning of the embryonic neurogenic period (E13), SVCT2 is expressed in the ventricular zone (VZ) and in the subventricular zone (SVZ), specifically in the radial glia cell body, and its high expression is maintained throughout the neurogenic period [7]. SVCT2 is also expressed in precursor cells during postnatal development of the cerebellum [8]. In postnatal cerebellum-derived neurospheres, the expression of nestin is correlated with SVCT2, demonstrating the transporter expression in cerebellar neural stem-like cells [8]. In addition, transient progenitors of adult mouse SVZ and RMS also express SVCT2, suggesting that vitamin C may be involved in a function along these neurogenic regions [9]. Treatment with vitamin C or its deficiency has also shown interesting findings. Initially, vitamin C treatment of embryonic stem cells and mesencephalic precursor cells was shown to increase the expression of genes involved in neurogenesis, differentiation and neurotransmission [10,11]. In vitro treatment of adult SVZ-derived neurospheres [9] and postnatal cerebellum-derived neurospheres [8] with vitamin C potentiates the neuronal phenotype by increasing expression of the neuronal markers. Moreover, the overexpression of SVCT2 in the mouse N2a cell line, through the incorporation of vitamin C and the subsequent phosphorylation of MAP-ERK1/2, induces the appearance of a differentiated phenotype, characterized by the development of filopodia and MAP-2-positive processes [12]. Furthermore, in the subgranular zone (SGZ), vitamin C deficiency reduces the number of neurons in the hippocampus of guinea pigs, altering spatial memory [13].

Although initially considered to occur only during infancy, it is now widely recognized that neurogenesis also takes place in the adult brain, mainly in two neurogenic niches: the SVZ in the lateral walls of the lateral ventricles (LV) [14,15] and the SGZ in the dentate gyrus of the hippocampus [16]. Of these regions, the SVZ stands out as the most extensive neurogenic area that harbors a greater number of neural stem cells (NSCs) [17]. The cellular architecture and composition of the SVZ has been described in several species. In mice, it consists mainly of four types of cells. The SVZ astrocytes or B cells correspond to NSCs, proliferating and originating transient progenitors or C cells. C cells, in turn, proliferate rapidly and differentiate into neuroblasts. Finally, ependymal cells correspond to a simple cuboidal epithelium that separates the ventricular cavity from the other cells of the SVZ [17,18].

Neuroblasts that originate from the SVZ are destined to form interneurons in the olfactory bulb (OB) [19]. To reach the OB, neuroblasts must migrate through a pathway known as the rostral migration stream (RMS) [19,20]. In humans, there is controversy regarding the existence of an RMS; however, neuroblasts migrating around a small ventricular cavity that connects the LV with the OB, named the lateral ventricle extension (EVL), have been described [21,22].

Numerous studies show that the SVCT2 transporter is expressed in progenitor cells and that vitamin C influences differentiation and neurogenesis [7–9,12]; however, the effect of this molecule or its deficiency on the adult neurogenesis that occurs in the SVZ as well as the effect on the cellular architecture and composition of this neurogenic region is unknown. Thus, in the present study, we describe the in vivo effect of vitamin C deficiency on adult neurogenesis in the SVZ, to later describe the in situ effects on the cellular architecture and composition of SVZ and EVL of the guinea pig brain. We use this model because the cellular architecture of SVZ and the presence of an EVL in the guinea pig brain is similar to that described in the human brain [23]. Additionally, guinea pigs do not synthesize vitamin C and must acquire it from their diet in a fashion similar to humans, which allows for modeling of vitamin C deficiency [1,24,25].

2. Materials and Methods

2.1. Animals

The animal care procedures were performed in accordance with the "Manual de Normas de Bioseguridad" (Comisión Nacional de Ciencia y Tecnología, CONICYT) and the Animal Care and Use Committee of the University of Concepcion (Concepción, Chile). Eighteen adolescent (1 month-old) male Pirbright guinea pigs (Instituto de Salud Pública, Santiago, Chile) were used in this study. The animals were housed under a 12-h light/dark cycle with food and water available ad libitum. No hierarchical fights were observed. Control animals (n = 7) were fed rabbit pellet and vegetables, whereas vitamin-C-deficient animals were not fed vegetables for 14 (n = 4) or 21 days (n = 7). All animals were kept under observation after scurvy induction according to the experimental animal care guidelines of the University of Concepcion to evaluate possible animal suffering before sacrifice. A loss of over 20% of the animal's weight was considered to be the human endpoint of the study. The experimental protocols were approved by the Concepción University Licensing Committee, grant numbers 1181243 and 1140477.

2.2. Tissue Processing

After they were anesthetized with a mixture of ketamine (60 mg/kg), xylazine (10 mg/kg) and acepromazine maleate (10 mg/kg), guinea pigs were perfused transcardially with 0.9% saline and then with 4% paraformaldehyde (PFA) in 0.1 M phosphate buffer (PB) (n = 2) or Bouin's fixative (n = 12) for light microscopy, or 2% PFA/2.5% glutaraldehyde in 0.1 M PB (n = 4) for electron microscopy. Brains were removed and post-fixed by immersing in the same fixative overnight at 4 °C. Bouin-fixed tissues were embedded in paraffin and cut into sequential 7 μm frontal sections. PFA-fixed tissues were cryo-protected by immersion in 30% sucrose for 24 h and then embedded in NEG50^{TM} (Thermo-Scientific, Waltham, MA, USA) to cut 50 μm frontal sections using a cryostat (MICROM HM520, Walldorf, Germany). PFA/glutaraldehyde-fixed tissues were cut into 150 μm frontal sections using a vibratome (Leica VT 1000S, Deer Park, IL, USA). For histological and immunohistochemical analysis, the tissues from 14 animals were analyzed, and tissues from four animals were analyzed for electron microscopy (Table S1).

2.3. Immunohistochemistry

After the 7 μm-thick sections were deparaffinized and rehydrated, endogenous peroxidase activity was inhibited by treatment with 3% H_2O_2 in methanol for 15 min. The sections were rinsed in Tris-HCl phosphate buffer (10 mM Tris, 120 mM NaCl, 8.4 mM Na_2HPO_4 and 3.5 mM KH_2PO_4; pH 7.8) and then incubated overnight at room temperature with the following primary antibodies diluted in 1% bovine serum albumin (BSA) in Tris-HCl phosphate buffer: anti-βIII-tubulin (1:1000, Promega, Madison, WI, USA), anti-PCNA (1:400, DAKO, Carpinteria, CA, USA) and anti-4-bromo-2′-deoxyuridine (BrdU; 1:200 Roche, Penzberg, Germany). The sections were rinsed and subsequently incubated for 2 h at room temperature with HRP-conjugated mouse anti-IgG (Jackson ImmunoResearch, West Grove, PA, USA). The peroxidase activity was developed using diaminobenzidine and H_2O_2. For immunohistochemical analysis of BrdU, the sections were treated with 2N HCl for 30 min at 37 °C and incubated with 5% BSA for 30 min before being incubated with the primary antibody. The images were obtained using an Axioplan 2 microscope (Carl Zeiss, Oberkochen, Germany) connected to a digital camera (Nikon, Digital Camera DXM1200, Melville, NY, USA). In all cases, omission of the primary antibody served as the negative control (Figure S1).

2.4. Multi-Labeling Immunofluorescence and Confocal Microscopy

Sections (50 μm-thick) were rinsed in Tris-HCl phosphate buffer and then co-incubated overnight at room temperature with lectin-diluted with 1% BSA in Tris-HCl phosphate buffer or with the following primary antibodies: anti-vimentin (1:200, Millipore, Darmstadt, Germany); anti-βIII-tubulin (1:1000, Promega) and FITC-conjugated isolectin B4 (1:10,

Sigma, St. Louis, MO, USA). After the sections were rinsed, they were co-incubated for 2 h at room temperature with the following fluorophore-conjugated secondary antibodies: Cy5-conjugated chicken anti-IgG (1:200, Jackson ImmunoResearch, Baltimore Pike, West Grove, PA, USA) and DyLight 547-conjugated mouse anti-IgG (1:200, Jackson ImmunoResearch). The sections were also incubated in Hoechst 33258 (Sigma, St. Louis, MO, USA) as a nuclear stain. Multi-labeled images were obtained by confocal spectral microscopy (LSM 780, Carl Zeiss). Z-sectioning was performed at 1 μm intervals, and optical stacks of at least 30 images were used for the analysis. Digital three-dimensional (3D) reconstructions were created using Zeiss LSM software (ZEN, Carl Zeiss Microscopy GmbH, Aalen, Germany).

2.5. Transmission Electron Microscopy

The 150 μm sections were washed in PB and immersed in 2% osmium tetroxide in PB for 1 h. After a washing step, samples were stained with 2% uranyl acetate in 70% ethanol for 3 h at 4 °C, dehydrated in ascending ethanol concentrations and incubated with propylene oxide for Araldite embedding. Then, sections were cured for 3 days at 60 °C. Serial semi-thin sections (1.5 μm) were cut on an ultramicrotome (Leica, Deer Park, IL, USA) and further stained with 1% toluidine blue. Finally, ultrathin (60 nm) sections were cut using a diamond knife on the ultramicrotome and examined under a Jeol Jem-1400 electron microscope (Jeol, Dearborn Road, Peabody, MA, USA).

2.6. In Vivo BrdU Labeling

Control and vitamin-C-deficient guinea pigs received an intraperitoneal (i.p.) injection of BrdU (Sigma) (100 mg/kg body weight per injection). Four hours after the injection, animals were sacrificed for the proliferation analysis.

2.7. Cell Quantification and Statistical Analysis

For each marker of interest (anti-βIII-tubulin and anti-BrdU), five sections (every 210 μm) from each region (LVE and SVZ) from each animal were immunolabeled. Sections were chosen from the same area within each region. After images around the entire ventricular cavity were obtained using a 20× objective, the ventricle was reconstructed using Canvas X software (ACD Systems International Inc, Victoria, BC, Canada) and the total number of positive cells around the ventricular cavity in one hemisphere was quantified using Image J software (ImageJ 1.53a, National Institute of Health, Bethesda, MD, USA). Data represent the mean ± SD of each region for three animals. Statistical comparisons between two or more groups of data were carried out using analysis of variance (ANOVA) followed by Bonferroni post-tests. A p-value < 0.05 was considered to be statistically significant. GraphPad software (Prism 9, GraphPad Software, Inc., La Jolla, CA, USA) was used for all data analyses.

3. Results

3.1. Decreased Number of Neuroblasts and Proliferative Cells in SVZ and LVE with Vitamin C Deficiency in Adult Guinea Pigs

To determine if vitamin C deficiency alters the production of neuroblasts in the SVZ and its presence in the LVE, coronal sections of the SVZ and LVE of vitamin-C-deficient and control animals were immunolabeled with anti-βIII tubulin to detect neuroblasts. In the SVZ, neuroblasts were found in the subependymal area (Figure 1A–C, arrows) with progressively reduced numbers coinciding with the days of deficiency (Figure 1A–C, arrows). In the LVE, neuroblasts maintained their subependymal location; however, their amount gradually decreased as the days of vitamin C deficiency elapsed (Figure 1D–F, arrows). To confirm these changes, neuroblasts in the SVZ (Figure 1G) and in the LVE (Figure 1H) were quantified. Both in the SVZ and LVE, the decrease in neuroblasts was significant and progressive with the days of vitamin C deficiency. Moreover, the decrease reached 41.67 ± 0.05 % in the SVZ (Figure 1G) and 49.92 ± 0.19% in the LVE (Figure 1H) in animals with 21 days of vitamin C deficiency.

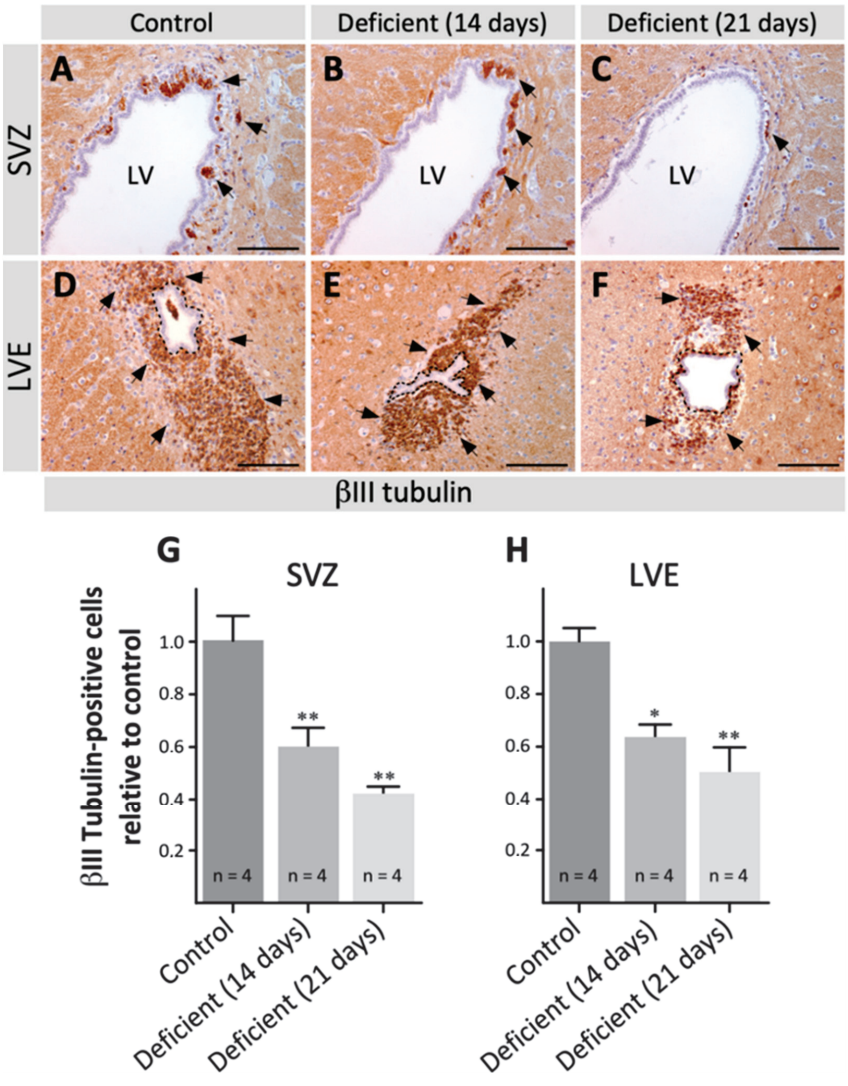

Figure 1. Analysis of neuroblasts in the brain of adult vitamin-C-deficient guinea pigs. Coronal sections of the brain of control guinea pigs (**A**,**D**) and the brain of guinea pigs with 14 (**B**,**E**) and 21 days (**C**,**F**) of vitamin C deficiency, labeled with anti-βIII tubulin (1:1000) to identify neuroblasts. In the SVZ (**A**–**C**) and LVE (**D**–**F**), neuroblasts progressively decreased with increasing days of vitamin C deficiency (arrows). (**G**,**H**) Neuroblasts were quantified in the SVZ (**G**) and LVE (**H**) of control and vitamin-C-deficient animals. The number of neuroblasts decreased progressively from the control animals to the 21-day deficient animals in both the SVZ and LVE. Data are presented as mean ± SD. Statistical analysis was performed using one-tailed ANOVA test and Bonferroni post-test; * $p < 0.05$, ** $p < 0.01$. $n = 4$. SVZ: subventricular zone. LV: lateral ventricle. LVE: lateral ventricle extension. Scale bar: 100 μm.

To determine whether the decrease in neuroblasts found in deficient animals was associated with a reduction in the number of proliferative cells in the neurogenic regions, coronal sections of the SVZ and LVE of vitamin-C-deficient and control animals were immunolabeled with anti-PCNA to identify proliferative cells. In the SVZ, PCNA-positive cells were found in the subependymal area (Figure 2A, arrows) and their number decreased

progressively (Figure 2A–C, arrows). Likewise, a decrease in PCNA-positive cells was also observed in the LVE of deficient animals (Figure 2D–F). To corroborate the results obtained through the anti-PCNA labeling, in vivo bromodeoxyuridine (BrdU) labeling was performed to specifically detect cells in the S-phase of the cell cycle. Then, coronal sections of the SVZ and LVE of vitamin-C-deficient and control animals were immunolabeled with an anti-BrdU antibody to detect proliferative cells and, subsequently, the number of BrdU-positive cells was quantified. In both the SVZ (Figure 3A–C) and LVE (Figure 3D–F), the number of BrdU-positive cells decreased in vitamin-C-deficient animals. In the SVZ, there was a significant decrease in BrdU-positive cells at 21 days of vitamin C deficiency (Figure 3G), while there was only a downward trend in the LVE (Figure 3H). Both PCNA and BrdU analysis demonstrated a decrease in the number of proliferative cells, suggesting a reduction in the proliferation of SVZ and LVE cells.

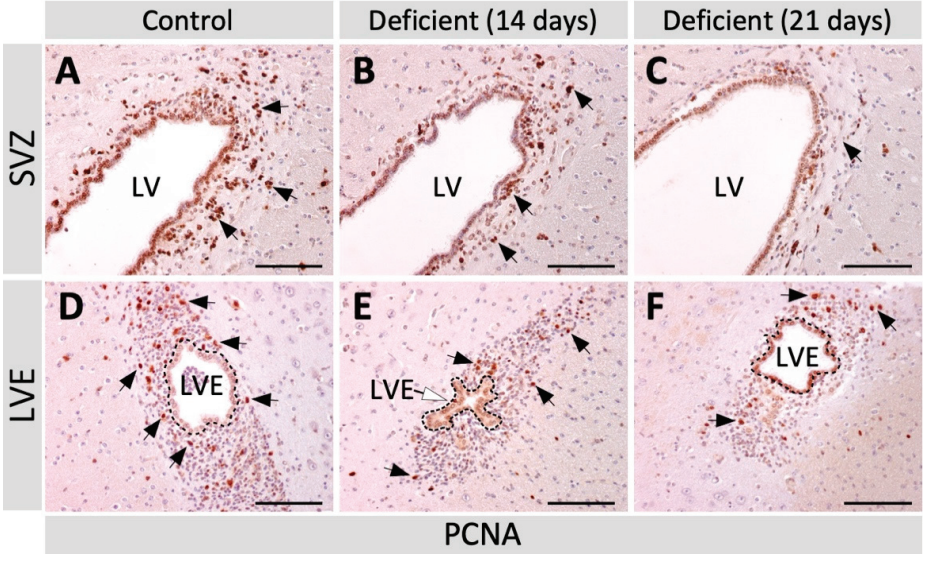

Figure 2. Analysis of PCNA-positive cells (B-type and C-type cells) in the brain of adult vitamin-C-deficient guinea pigs. Coronal sections of the brain of control guinea pigs (**A**,**D**) and the brain of guinea pigs with 14 (**B**,**E**) and 21 days (**C**,**F**) of vitamin C deficiency, labeled with anti-PCNA (1:100) as a proliferation marker. In the SVZ (**A**–**C**), PCNA-positive cells (arrows) progressively decreased with increasing days of vitamin C deficiency. In the LVE (**D**–**F**), PCNA-positive cells (arrows) decreased in vitamin-C-deficient animals (**E**,**F**). LVE: lateral ventricle extension. LV: lateral ventricle. SVZ: subventricular zone. $n = 4$. Scale bar: 100 μm.

To define whether vitamin C deficiency alters the cellular distribution of SVZ, coronal sections of the SVZ from control animals and from animals with 21 days of vitamin C deficiency were immunolabeled with anti-βIII tubulin to detect neuroblasts, anti-B4 isolectin to identify ependymal cells and anti-vimentin to identify ependymal cells and glial cells. Afterwards, 3D projections of Z-stacks of high-resolution confocal spectral images were generated (Figure 4). Although the neurogenic niche, and consequently, the clusters of neuroblasts, have always been associated with the most dorsal part of the LV, it is also possible to observe them in the medial and ventral areas of the LV (Figure 4A–D with higher magnification). In the vitamin-C-deficient animals, however, neuroblasts persisted in the dorsal part of the LV (Figure 4E,F) but practically disappeared in the medial (Figure 4E,G) and ventral (Figure 4E,H) parts of the LV, suggesting that the extent of neuroblast decrease could vary in different areas of the LV. This observation could apply not only in the dorso–ventral direction, but also in the rostro–caudal direction. For its part, the ependymal line

was observed without changes between both conditions, but this was not so in glial cells, which seemed to have been redistributed. In control animals, glial cells seemed to cover a larger space in the SVZ (Figure 4C,D); however, in deficient animals, they seemed to be mostly distributed in the area closer to the ventricle cavity (Figure 4G,H), an area where neuroblasts are usually found in control conditions.

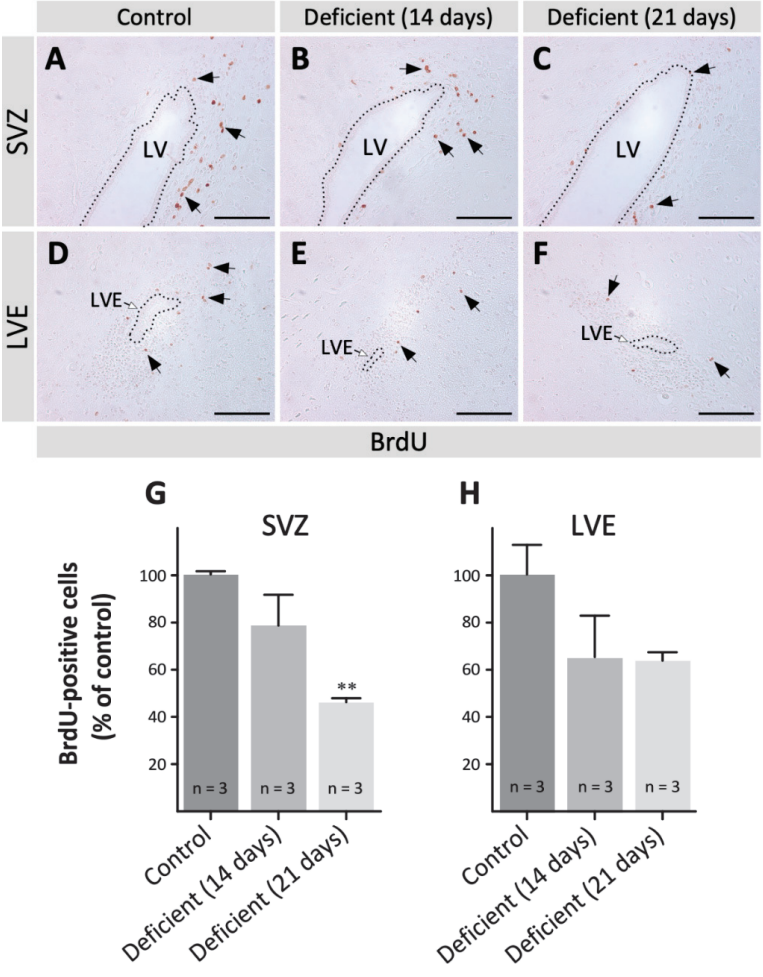

Figure 3. Analysis of BrdU-positive cells (B-type and C-type cells) in the brain of adult vitamin-C-deficient guinea pigs. Coronal sections of the brain of control guinea pigs (**A**,**D**) and the brain of guinea pigs with 14 (**B**,**E**) and 21 days (**C**,**F**) of vitamin C deficiency, labeled with anti-BrdU (1:200) as a proliferation marker. (**A**–**C**) In the SVZ, many BrdU-positive cells are observed in control animals (**A**) but they progressively decreased in guinea pigs with 14 (**B**) and 21 days (**C**) of vitamin C deficiency (arrows). (**D**–**F**) In the LVE, few BrdU-positive cells are observed in control animals (**D**) and even fewer in vitamin-C-deficient animals (**E**,**F**, arrows). (**G**,**H**) BrdU-positive cells were quantified in the SVZ (**G**) and LVE (**H**); their number decreased in the condition of vitamin C deficiency. Data are presented as mean ± SD. Statistical analysis was performed using one-tailed ANOVA test and Bonferroni post-test; ** $p < 0.01$. $n = 3$. LV: lateral ventricle. LVE: lateral ventricle extension. SVZ: subventricular zone. Scale bar: 100 μm.

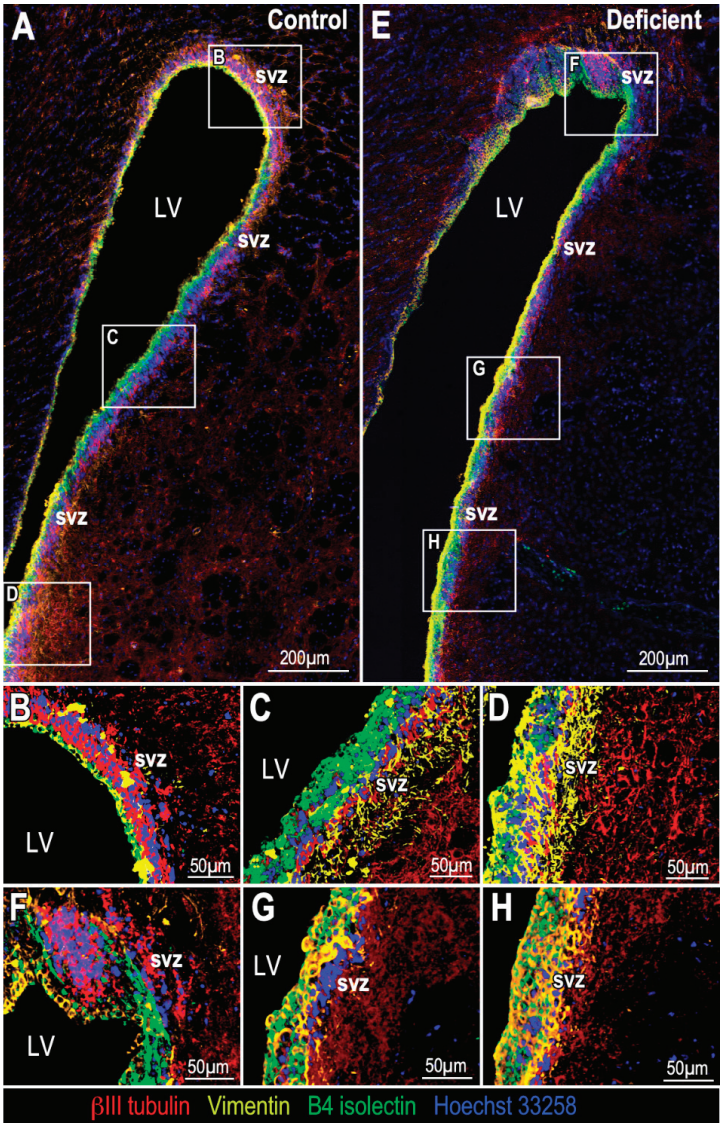

Figure 4. Multi-labeling analysis of neuronal and glial distribution in the SVZ of adult vitamin-C-deficient guinea pigs. Z-stacks projections, 3D reconstruction and tile scanning, using multiple markers: anti-βIII tubulin (1:1000, red), anti-vimentin (1:100, yellow), B4 isolectin (1:10, green) and Hoechst 33258 (1:1000, blue). (**A**) Glial and neuronal distribution in the SVZ of control guinea pigs. (**B**–**D**) Higher magnification of dorsal (**B**), medial (**C**) and ventral (**D**) areas of the LV in image A. (**E**) Glial and neuronal distribution in the SVZ of guinea pigs with 21 days of vitamin C deficiency. (**F**–**H**) Higher magnification of dorsal (**F**), medial (**G**) and ventral (**H**) area of the LV in image E; distribution of glial cells was different and the amount of neuroblasts (red) was lower along the LV of vitamin-C-deficient guinea pigs regarding control animals. LV: lateral ventricle. SVZ: subventricular zone.

Analysis of the LVE showed that apart from the evident decrease in the density of neuroblasts surrounding the LVE, an increase in the number of glial cells was observed in

deficient animals (Figure 5E,F). Regarding the size of the LVE (Figure 5A,D), it is important to note that its diameter can vary notoriously from one animal to another [23].

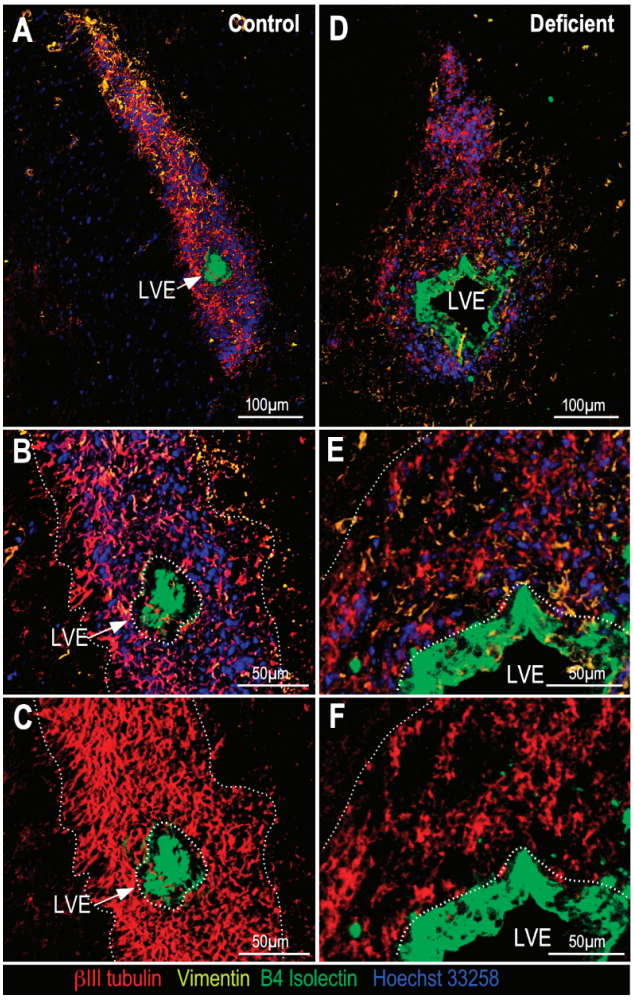

Figure 5. Multi-labeling analysis of neuronal and glial distribution in the LVE of adult vitamin-C-deficient guinea pigs. Z-stacks projections, 3D reconstruction and tile scanning, using multiple markers: anti-βIII tubulin (1:1000, red), anti-vimentin (1:100, yellow), B4 isolectin (1:10, green) and Hoechst 33258 (1:1000, blue). (**A**) Distribution of glial and neuronal cells in the LVE of control guinea pig brain. (**B**) Higher magnification of the LVE in image A. (**C**) Same image as in panel B, without blue (nuclei) and yellow (glial cells) channels. (**D**) Glial and neuronal distribution in the LVE of the brain of guinea pigs with 21 days of vitamin C deficiency. (**E**) Higher magnification of the LVE in image D. (**F**) Same image as in panel E, without blue (nuclei) and yellow (glial cells) channels. Here, the density of neuroblasts (red) was much lower than in the control (**C**, dotted lines); however, the number of glial cells (yellow) was similar. LVE: lateral ventricle extension.

To demonstrate that the decrease in neuroblasts is not restricted to a particular rostro–caudal area and can be observed throughout the entire LVE, a 3D reconstruction of 560 µm throughout the LVE was performed. One out of every five sections (serial sections) of the brain of vitamin-C-deficient and control animals were immunolabeled with anti-βIII-tubulin;

then, the images obtained were stacked using IMARIS® (Figure 6). The results confirmed that the decrease in neuroblasts occurred throughout the entire LVE of the vitamin-C-deficient guinea pig (Figure 6F–H) relative to the control guinea pig (Figure 6B–D).

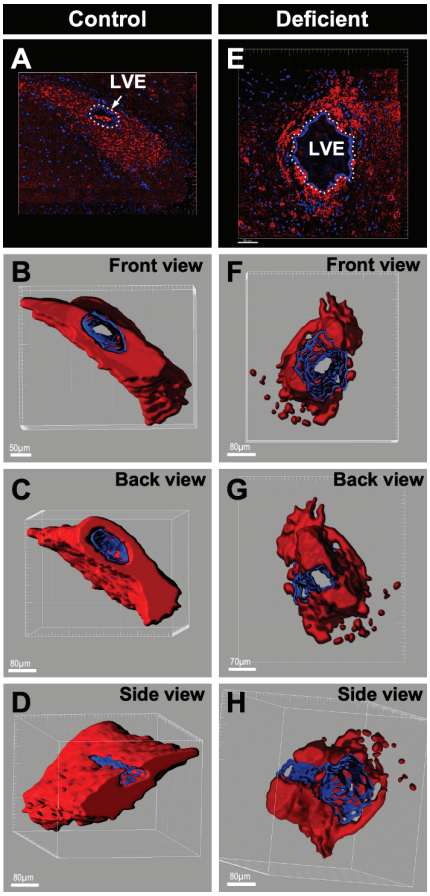

Figure 6. Three-dimensional reconstruction of the LVE and surrounding neuroblasts of control and vitamin-C-deficient guinea pigs. 3D reconstruction of Z-stacked coronal sections of the LVE of control guinea pigs and guinea pigs with 21 days of vitamin C deficiency labeled with anti-βIII tubulin (red, 1:1000) and hematoxylin (blue). (**A**) Z-stacked coronal sections of the LVE of control guinea pig. (**B**–**D**) Three different rotations of the 3D-reconstruction of the Z-stacked coronal sections in image A. (**E**) Z-stacked coronal sections of the LVE of guinea pigs with 21 days of vitamin C deficiency. (**F**–**H**) Three different rotations of the 3D-reconstruction of the Z-stacked coronal sections in image E. LVE: Lateral ventricle extension. Scale bar for images (**A**) and (**E**): 50 μm.

3.2. Vitamin C Deficiency Alters Cell Morphology and Cell Composition of the SVZ and LVE in Adult Guinea Pig Brain

To determine if vitamin C deficiency induces changes in the cytoarchitecture of the SVZ and LVE or in the morphology of their cells, their ultrastructure was explored through transmission electron microscopy, and SVZ and LVE cell types were identified according to their ultrastructural features [23]. In the SVZ, ependymal cells were identified by cilia and microvilli on their apical surface by their irregular nucleus and their electron-dense cytoplasm (Figure 7A–G, asterisks); neuroblasts were identified by their sparse electron-dense cytoplasm and their heterochromatic nucleus (Figure 7B–G, cells in red). Astrocytes

were identified by their electron-lucid cytoplasm and euchromatic nucleus (Figure 7B–G, cells in green), and type C cells by their electron-lucid cytoplasm and their irregular and large nucleus with numerous small clusters of condensed chromatins. However, it is worth mentioning that no type C cells were found in the images selected for the figure.

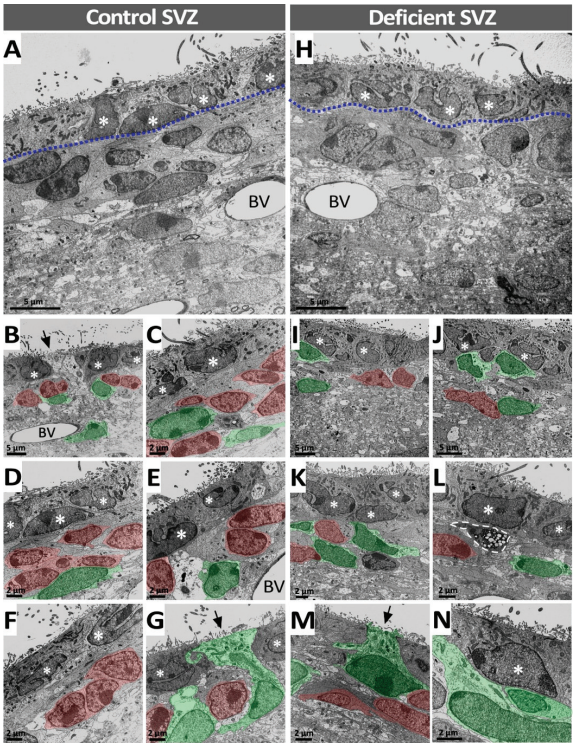

Figure 7. Ultrastructural analysis of the SVZ in vitamin-C-deficient guinea pigs. (**A**–**G**) Ultrathin sections of the SVZ in control guinea pigs; the ciliated ependymal cell line (dotted line) and different cell types in the subependymal area are observed (**A**). The ependymal cells (white asterisks) show cilia and apical microvilli, an irregular nucleus and an electron-dense cytoplasm (**B**–**G**). In the subependymal zone, neuroblasts (in red) have a heterochromatic nucleus and a scanty, electron-dense cytoplasm (**B**–**G**). Astrocytes (in green) have a euchromatic nucleus, an electron-lucent cytoplasm and often contact the ventricle (**G**, arrow). C-type cells are not detected in this set of images. (**H**–**N**) Ultrathin sections of the SVZ of vitamin-C-deficient guinea pigs showed that the cell distribution was similar to control SVZ; however, the number of cells was altered. A decline in the number of neuroblasts was observed and, consequently, cells in the subependymal area were mainly astrocytes (**I**–**N**). In addition, fewer astrocytes were observed contacting the ventricle (**M**, arrow). Apoptotic cell (dashed line) (**L**). LV: lateral ventricle. BV: blood vessel.

When the SVZ ultrastructure of control and vitamin-C-deficient animals were compared, no significant changes in cell morphology were observed. In the SVZ of deficient animals (Figure 7H–N), the ependymal cells maintained their apical cilia and microvilli, and their nuclei (asterisks) were observed as irregular as in the SVZ of control animals. Furthermore, neuroblasts (Figure 7H–N, cells in red) and astrocytes (Figure 7H–N, cells in green) also retained their distinctive ultrastructural features. Regarding the cellular composition of the SVZ in deficient animals, the number of cells forming part of the cellular architecture was notoriously lower when compared with the control (Figure 7H–N). Al-

though the number of astrocytes and ependymal cells seemed to remain unchanged, there was a marked decline in the number of neuroblasts.

Unlike that observed in the SVZ, differences between control and vitamin-C-deficient animals were found in the cell morphology of the LVE. In control animals, the ependymal cells had a flat shape and a regular nucleus (Figure 8A–G, asterisks), while the LVE of deficient animals had a cubic shape and an irregular nucleus (Figure 8H–N, asterisks). In the subependymal area of the LVE, the morphology of the cells was also different; nuclei with a more regular size and shape were observed in the control LVE (Figure 8A–G) compared with the LVE of a deficient animal (Figure 8H–N). The cytoarchitecture of the LVE of deficient animals also showed important differences compared with the control. Specifically, a large decrease in the number of neuroblasts was observed in the LVE of deficient animals (Figure 8H–N, cells in red), while astrocytes seemed to increase their number (Figure 8H–N, cells in green). Consequently, variation in the number of cells resulted in changes to their location. In the control LVE, neuroblasts were situated below the line of ependymal cell (Figure 8A–G, cells in red); however, in deficient animals, astrocytes were observed in that location (Figure 8H–N, cells in green).

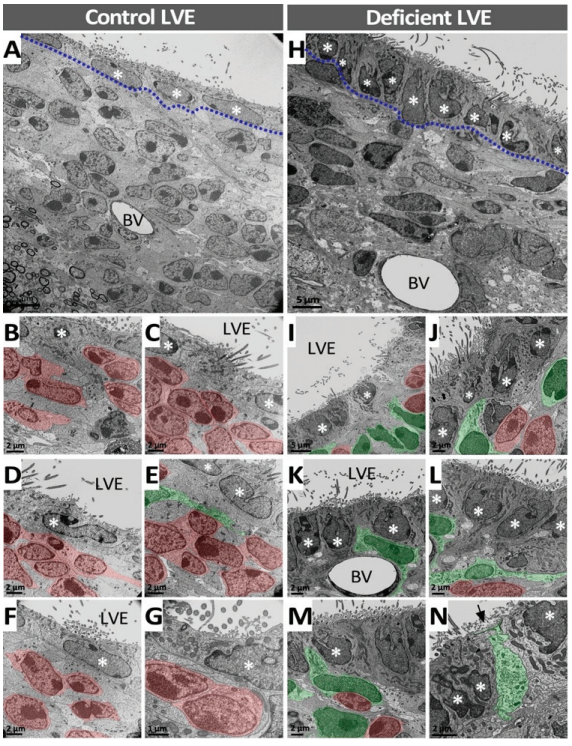

Figure 8. Ultrastructural analysis of the LVE of vitamin-C-deficient guinea pigs. (**A**–**G**) Ultrathin sections of the LVE of control guinea pigs; the ciliated ependymal cell line (dashed line) and a large number of cells in the subependymal area is identified (**A**). Neuroblasts (in red) and astrocytes (in green) exhibit a similar morphology to that described in the control SVZ; however, the ependymal cell nucleus (white asterisks) is more regular in the LVE (**B**–**G**) compared with the control SVZ. Most of the subependymal cells correspond to neuroblasts (**B**–**G**). (**H**–**N**) Ultrathin sections of the LVE of vitamin-C-deficient guinea pigs show that the cell distribution was similar to control LVE. However, the number of cells was dramatically decreased and the morphology of the ependymal cell nuclei (white asterisks) was significantly altered (**H**–**N**). Neuroblasts were reduced in number (cells in red), while the number of astrocytes (cells in green) increased (**I**–**N**). BV: blood vessel. LVE: lateral ventricle extension.

4. Discussion

In the present work, we described the effect of vitamin C deficiency on neurogenesis, and the cellular composition and morphology of the SVZ and LVE from adult guinea pig brain. We found that neuroblasts and proliferating cells in the SVZ and LVE are progressively and significantly reduced in proportion with the number of days under vitamin C deficiency. This reduction is not restricted to a particular area and is observed throughout the LVE. We also found that vitamin C deficiency alters the cellular morphology at the ultrastructural level, especially in cells from the LVE.

Vitamin C deficiency in adult guinea pig induced a progressive reduction in neuroblasts in the SVZ and LVE. This reduction was higher in 50% of the animals consuming a deficient diet for 21 days, which is consistent with a previous study from our group in which we showed that neurospheres isolated from the SVZ of adult rat brain treated with 200 μM vitamin C induced the production of new neurons through differentiation towards a neuronal lineage [9]. Thus, we hypothesized that reducing vitamin C produces the opposite effect (i.e., a decline in the production of neuroblasts). In addition, another study showed a significant reduction in the number of neurons in three different regions of the hippocampus from animals under vitamin C deficiency [13]. Overall, these findings show a vital role of vitamin C in adult brain neurogenesis.

We also showed that vitamin C deficiency progressively reduced the number of proliferating cells in SVZ and LVE, suggesting that the decrease in neuroblasts is directly associated with the lower proliferation. A previous study described that prenatal vitamin C deficiency induced a significant reduction in the volume of the postnatal hippocampus, attributed to reduced migration of neuroblasts towards the granular layer of the dentate gyrus [26], without considering a decrease in the proliferation of precursor cells nor reduced survival rate of new neurons [26]. The discrepancies between this [26] and the present study may be due to the inherent differences of the neurogenic niches. For instance, the proliferative capacity of the hippocampal dentate gyrus is lower at the SVZ [27,28], making this zone more likely to be affected. Furthermore, in the rat, BrdU-positive proliferative cells at the SVZ and RMS express the vitamin C transporter, SVCT2 [9], suggesting a role for vitamin C in the regulation of proliferative cells in the SVZ and LVE.

In the SVZ, NSCs proliferate to give rise to transient precursors, which in turn, and depending on the environment signals, can differentiate into cells of glial lineage, such as astrocytes and oligodendrocytes, or neuronal lineage, such as neuroblasts [27,28]. Based on this, the reduction in neuroblasts induced by vitamin C deficiency may be explained by (i) apoptosis of NSCs, transient precursors and/or neuroblasts; (ii) increased differentiation into the glial lineage in detriment of the neuronal lineage; and/or (iii) reduction in the proliferation of NSCs and/or transient precursors. First, we were unable to evaluate apoptosis because Bouin's fixative is not compatible with the TUNEL assay and immunostaining of cleaved caspase-3 did not work as expected. Nevertheless, we paid special attention to the presence of cells with apoptotic morphology during the ultrastructural analysis, finding no differences between control and deficient animals. Second, even when we observed a subtle increase in the number of glial cells in the EVL, it is unlikely that this increase could be due to an increase in glial cells generation, either by proliferation or differentiation from NSCs, since NSCs have not been detected in this area [23]. It is more likely that the increase was related to a redistribution of cells, triggered by the absence of neuroblasts that occupy the areas closest to the ventricular cavity. Thus, we propose that vitamin C deficiency reduces the number of neuroblasts via lower proliferation of NSCs and/or transient precursors, therefore impacting the genesis of neuroblasts. This hypothesis fits our findings of reduced proliferation and number of neuroblasts, without any significant variation in the number of glial cells, which is further supported by previous studies describing the positive effect of vitamin C on the proliferation and differentiation of NSCs, precursors and neuroblasts [29–31].

Many mechanisms could account for the effect of vitamin C deficiency on the reduced proliferation of NSCs and/or precursor cells: (i) a direct action over the expression of proteins

regulating proliferation and differentiation of NSCs, (ii) an indirect action due to increased oxidative stress and/or (iii) an indirect action due to reduced collagen synthesis. Regarding the first possibility, vitamin C is known to affect the epigenetic landscape of human embryonic stem cells through inducing specific histone demethylation events and the expression of certain genes [32]. This function could be related with the capacity of vitamin C to modulate the activity of Fe(II)/2-oxoglutarate-dependent oxygenases [33]—among them, histone demethylases Jhdm1a/1b [34] and DNA demethylase TET1 [35–37]. Regarding oxidative stress, it is widely documented that vitamin C deficiency increases reactive oxygen species (ROS) [38–41], which has a negative effect on NSC proliferation through inhibition of ERK1/2 [42]. Moreover, embryos from SOD2-null mice, which exhibit high levels of superoxide in the brain, are characterized by reduced neurogenesis in the SVZ, attributed to a reduced proliferative capacity of NSCs [42]. Lastly, in relation to collagen modulation, it is known that the basal lamina of blood vessels in the SVZ is mainly composed of collagen and laminin and is projected towards the subependymal zone [43], where collagen and laminin integrate diverse factors modulating neurogenesis through the astrocytic foot processes [44] (Mercier y col., 2002). Therefore, vitamin C deficiency could affect synthesis and deposition of collagen, reducing neurogenesis.

At the ultrastructural level, we observed that vitamin C deficiency is associated with a reduction in neuroblasts and a subtle increase in astrocytes in the SVZ and LVE, whereas ependymal cells remain unaffected. These changes also impact the distribution of these cells in a way that neuroblasts are localized immediately under the ependymal line in the LVE from control animals, while astrocytes occupy this place in LVE from deficient animals. Moreover, we observed relevant morphological differences in the LVE, but not in the SVZ, from deficient animals compared with the controls. The ependymal cells are flatter and show regular nuclei in control animals, whereas they show a cuboidal shape with irregular nuclei in deficient animals. Ependymal cells also show pleomorphic nuclei in the LVE from deficient animals. Evidence suggests that vitamin C deficiency induces nuclear and cellular morphological changes through increased oxidative stress and reorganization of the actin cytoskeleton [45]. In addition, oxidative stress promotes telomere shortening and chromosomic instability, in turn, altering the nuclear morphology [46]. Nevertheless, the fact that the morphological alterations in deficient animals were more evident in the LVE may be due to a lower availability of vitamin C from the CSF, contributing to higher oxidative damage.

5. Conclusions

Our data show the relevance of vitamin C in proliferation, differentiation and neurogenesis in the SVZ from adolescent guinea pig brain and how these processes impact on the maintenance of the normal cytoarchitecture of the SVZ and LVE. Vitamin C deficiency remains a serious health problem for a high percentage of the world population. For instance, in the United Kingdom, 46% of men and 35% of women within the low-income population had vitamin C deficiency [47]. In the U.S., the prevalence of vitamin C deficiency, adjusted by age, is ~7% of the population, which is reduced with a higher socioeconomic status [2]. In the Canadian youth between 20 and 29 years old, 14% have vitamin C deficiency [3]. Considering that these data come from developed countries, we infer that the prevalence of vitamin C deficiency could be significantly higher in developing countries. Based on our results observed in guinea pig brain and given the well-known similarities between guinea pig and human brains, we propose that vitamin C deficiency could have important negative consequences in human neurogenesis, especially for children and pregnant women.

Supplementary Materials: The following are available online at https://www.mdpi.com/article/10.3390/antiox11102030/s1, Figure S1: Negative controls without primary antibody in the SVZ of guinea pig brain, Table S1: Total number of animals used in the experiments.

Author Contributions: Conceptualization, N.J., M.C. and F.N.; methodology, N.J., M.C., F.M., L.F., K.S., I.G.-C. and F.N.; software, N.J. and M.C.; validation, N.J., M.C., F.M., I.G.-C., N.J. and F.N.; formal analysis, N.J., M.C. and F.N.; investigation, N.J., M.C., F.M., L.F., K.S., I.G.-C. and F.N.; resources, N.J., M.C. and F.N.; data curation, N.J. and F.N.; writing—original draft preparation, N.J. and F.N.; writing—review and editing, N.J. and F.N.; project administration, F.N.; funding acquisition, N.J. and F.N. All authors have read and agreed to the published version of the manuscript.

Funding: "This research was funded by FONDECYT, grant number 1221147 (to Francisco Nualart)", "FONDECYT grant number 11170959 (to Nery Jara)", "CONICYT-PIA, grant number ECM-12 (to Francisco Nualart)" and "FEDER-Andalucía, grant number UMA20-FEDERJA-112".

Institutional Review Board Statement: The study was conducted according to the guidelines of the Declaration of Helsinki, and approved by the Institutional Ethics Committee of Universidad de Concepción (protocol codes Fondecyt 1181243, approval date: 28 April 2018; and 1140477, approval date: 22 April 2014).

Informed Consent Statement: Not applicable.

Data Availability Statement: The data presented in this study are available in the article and Supplementary Materials.

Acknowledgments: We acknowledge the professionals at the Center of Advanced Microscopy CMA BIO BIO for their support in all kinds of microscopy issues.

Conflicts of Interest: The authors declare no conflict of interest.

References

1. Hirschmann, J.V.; Raugi, G.J. Adult scurvy. *J. Am. Acad. Derm.* **1999**, *41*, 895–906, quiz 907–810. [CrossRef]
2. Schleicher, R.L.; Carroll, M.D.; Ford, E.S.; Lacher, D.A. Serum vitamin C and the prevalence of vitamin C deficiency in the United States: 2003–2004 National Health and Nutrition Examination Survey (NHANES). *Am. J. Clin. Nutr.* **2009**, *90*, 1252–1263. [CrossRef] [PubMed]
3. Cahill, L.; Corey, P.N.; El-Sohemy, A. Vitamin C deficiency in a population of young Canadian adults. *Am. J. Epidemiol.* **2009**, *170*, 464–471. [CrossRef] [PubMed]
4. May, J.M. Vitamin C transport and its role in the central nervous system. *Subcell. Biochem.* **2012**, *56*, 85–103. [CrossRef] [PubMed]
5. Salazar, K.; Espinoza, F.; Cerda-Gallardo, G.; Ferrada, L.; Magdalena, R.; Ramirez, E.; Ulloa, V.; Saldivia, N.; Troncoso, N.; Oviedo, M.J.; et al. SVCT2 Overexpression and Ascorbic Acid Uptake Increase Cortical Neuron Differentiation, Which Is Dependent on Vitamin C Recycling between Neurons and Astrocytes. *Antioxidants* **2021**, *10*, 1413. [CrossRef] [PubMed]
6. Moretti, M.; Rodrigues, A.L.S. Functional role of ascorbic acid in the central nervous system: A focus on neurogenic and synaptogenic processes. *Nutr. Neurosci.* **2021**, 1–11. [CrossRef]
7. Silva-Alvarez, C.; Salazar, K.; Cisternas, P.; Martinez, F.; Liour, S.; Jara, N.; Bertinat, R.; Nualart, F. Apical Polarization of SVCT2 in Apical Radial Glial Cells and Progenitors During Brain Development. *Mol. Neurobiol.* **2017**, *54*, 5449–5467. [CrossRef]
8. Oyarce, K.; Silva-Alvarez, C.; Ferrada, L.; Martinez, F.; Salazar, K.; Nualart, F. SVCT2 Is Expressed by Cerebellar Precursor Cells, Which Differentiate into Neurons in Response to Ascorbic Acid. *Mol. Neurobiol.* **2018**, *55*, 1136–1149. [CrossRef]
9. Pastor, P.; Cisternas, P.; Salazar, K.; Silva-Alvarez, C.; Oyarce, K.; Jara, N.; Espinoza, F.; Martinez, A.D.; Nualart, F. SVCT2 vitamin C transporter expression in progenitor cells of the postnatal neurogenic niche. *Front. Cell. Neurosci.* **2013**, *7*, 119. [CrossRef]
10. Yu, D.H.; Lee, K.H.; Lee, J.Y.; Kim, S.; Shin, D.M.; Kim, J.H.; Lee, Y.S.; Oh, S.K.; Moon, S.Y.; Lee, S.H. Changes of gene expression profiles during neuronal differentiation of central nervous system precursors treated with ascorbic acid. *J. Neurosci. Res.* **2004**, *78*, 29–37. [CrossRef]
11. Shin, D.M.; Ahn, J.I.; Lee, K.H.; Lee, Y.S. Ascorbic acid responsive genes during neuronal differentiation of embryonic stem cells. *Neuroreport* **2004**, *15*, 1959–1963. [CrossRef]
12. Salazar, K.; Martinez, M.; Ulloa, V.; Bertinat, R.; Martinez, F.; Jara, N.; Espinoza, F.; Bongarzone, E.R.; Nualart, F. SVCT2 Overexpression in Neuroblastoma Cells Induces Cellular Branching that is Associated with ERK Signaling. *Mol. Neurobiol.* **2015**, *53*, 6668–6679. [CrossRef]
13. Tveden-Nyborg, P.; Johansen, L.K.; Raida, Z.; Villumsen, C.K.; Larsen, J.O.; Lykkesfeldt, J. Vitamin C deficiency in early postnatal life impairs spatial memory and reduces the number of hippocampal neurons in guinea pigs. *Am. J. Clin. Nutr.* **2009**, *90*, 540–546. [CrossRef]
14. Lois, C.; Alvarez-Buylla, A. Proliferating subventricular zone cells in the adult mammalian forebrain can differentiate into neurons and glia. *Proc. Natl. Acad. Sci. USA* **1993**, *90*, 2074–2077. [CrossRef]
15. Reynolds, B.A.; Weiss, S. Generation of neurons and astrocytes from isolated cells of the adult mammalian central nervous system. *Science* **1992**, *255*, 1707–1710. [CrossRef]

16. Kaplan, M.S.; Bell, D.H. Mitotic neuroblasts in the 9-day-old and 11-month-old rodent hippocampus. *J. Neurosci.* **1984**, *4*, 1429–1441. [CrossRef]
17. Doetsch, F.; Garcia-Verdugo, J.M.; Alvarez-Buylla, A. Cellular composition and three-dimensional organization of the subventricular germinal zone in the adult mammalian brain. *J. Neurosci.* **1997**, *17*, 5046–5061. [CrossRef]
18. Lim, D.A.; Alvarez-Buylla, A. The Adult Ventricular-Subventricular Zone (V-SVZ) and Olfactory Bulb (OB) Neurogenesis. *Cold Spring Harb. Perspect. Biol.* **2016**, *8*, a018820. [CrossRef]
19. Lois, C.; Alvarez-Buylla, A. Long-distance neuronal migration in the adult mammalian brain. *Science* **1994**, *264*, 1145–1148. [CrossRef]
20. Rousselot, P.; Lois, C.; Alvarez-Buylla, A. Embryonic (PSA) N-CAM reveals chains of migrating neuroblasts between the lateral ventricle and the olfactory bulb of adult mice. *J. Comp. Neurol.* **1995**, *351*, 51–61. [CrossRef]
21. Curtis, M.A.; Kam, M.; Nannmark, U.; Anderson, M.F.; Axell, M.Z.; Wikkelso, C.; Holtas, S.; van Roon-Mom, W.M.; Bjork-Eriksson, T.; Nordborg, C.; et al. Human neuroblasts migrate to the olfactory bulb via a lateral ventricular extension. *Science* **2007**, *315*, 1243–1249. [CrossRef] [PubMed]
22. Sanai, N.; Tramontin, A.D.; Quinones-Hinojosa, A.; Barbaro, N.M.; Gupta, N.; Kunwar, S.; Lawton, M.T.; McDermott, M.W.; Parsa, A.T.; Manuel-Garcia Verdugo, J.; et al. Unique astrocyte ribbon in adult human brain contains neural stem cells but lacks chain migration. *Nature* **2004**, *427*, 740–744. [CrossRef] [PubMed]
23. Jara, N.; Cifuentes, M.; Martinez, F.; Salazar, K.; Nualart, F. Cytoarchitecture, Proliferative Activity and Neuroblast Migration in the Subventricular Zone and Lateral Ventricle Extension of the Adult Guinea Pig Brain. *Stem Cells* **2016**, *34*, 2574–2586. [CrossRef] [PubMed]
24. Jara, N.; Ramirez, E.; Ferrada, L.; Salazar, K.; Espinoza, F.; Gonzalez-Chavarria, I.; Nualart, F. Vitamin C deficient reduces proliferation in a human periventricular tumor stem cell-derived glioblastoma model. *J. Cell. Physiol.* **2021**, *236*, 5801–5817. [CrossRef] [PubMed]
25. Ramirez, E.; Jara, N.; Ferrada, L.; Salazar, K.; Martinez, F.; Oviedo, M.J.; Tereszczuk, J.; Ramirez-Carbonell, S.; Vollmann, A.; Hau, P.; et al. Glioblastoma invasiveness and collagen secretion are enhanced by vitamin C. *Antioxid. Redox Signal.* **2022**, *37*, 538–559. [CrossRef] [PubMed]
26. Tveden-Nyborg, P.; Vogt, L.; Schjoldager, J.G.; Jeannet, N.; Hasselholt, S.; Paidi, M.D.; Christen, S.; Lykkesfeldt, J. Maternal vitamin C deficiency during pregnancy persistently impairs hippocampal neurogenesis in offspring of guinea pigs. *PLoS ONE* **2012**, *7*, e48488. [CrossRef] [PubMed]
27. Zhao, C.; Deng, W.; Gage, F.H. Mechanisms and functional implications of adult neurogenesis. *Cell* **2008**, *132*, 645–660. [CrossRef]
28. Alvarez-Buylla, A.; Kohwi, M.; Nguyen, T.M.; Merkle, F.T. The heterogeneity of adult neural stem cells and the emerging complexity of their niche. *Cold Spring Harb. Symp. Quant. Biol.* **2008**, *73*, 357–365. [CrossRef]
29. Cao, N.; Liu, Z.; Chen, Z.; Wang, J.; Chen, T.; Zhao, X.; Ma, Y.; Qin, L.; Kang, J.; Wei, B.; et al. Ascorbic acid enhances the cardiac differentiation of induced pluripotent stem cells through promoting the proliferation of cardiac progenitor cells. *Cell Res.* **2012**, *22*, 219–236. [CrossRef]
30. Choi, K.M.; Seo, Y.K.; Yoon, H.H.; Song, K.Y.; Kwon, S.Y.; Lee, H.S.; Park, J.K. Effect of ascorbic acid on bone marrow-derived mesenchymal stem cell proliferation and differentiation. *J. Biosci. Bioeng.* **2008**, *105*, 586–594. [CrossRef]
31. Mekala, N.K.; Baadhe, R.R.; Rao Parcha, S.; Prameela Devi, Y. Enhanced proliferation and osteogenic differentiation of human umbilical cord blood stem cells by L-ascorbic acid, in vitro. *Curr. Stem Cell Res. Ther.* **2013**, *8*, 156–162. [CrossRef]
32. Chung, T.L.; Brena, R.M.; Kolle, G.; Grimmond, S.M.; Berman, B.P.; Laird, P.W.; Pera, M.F.; Wolvetang, E.J. Vitamin C promotes widespread yet specific DNA demethylation of the epigenome in human embryonic stem cells. *Stem Cells* **2010**, *28*, 1848–1855. [CrossRef]
33. Monfort, A.; Wutz, A. Breathing-in epigenetic change with vitamin C. *EMBO Rep.* **2013**, *14*, 337–346. [CrossRef]
34. Wang, T.; Chen, K.; Zeng, X.; Yang, J.; Wu, Y.; Shi, X.; Qin, B.; Zeng, L.; Esteban, M.A.; Pan, G.; et al. The histone demethylases Jhdm1a/1b enhance somatic cell reprogramming in a vitamin-C-dependent manner. *Cell Stem Cell* **2011**, *9*, 575–587. [CrossRef]
35. Chen, J.; Guo, L.; Zhang, L.; Wu, H.; Yang, J.; Liu, H.; Wang, X.; Hu, X.; Gu, T.; Zhou, Z.; et al. Vitamin C modulates TET1 function during somatic cell reprogramming. *Nat. Genet.* **2013**, *45*, 1504–1509. [CrossRef]
36. Blaschke, K.; Ebata, K.T.; Karimi, M.M.; Zepeda-Martinez, J.A.; Goyal, P.; Mahapatra, S.; Tam, A.; Laird, D.J.; Hirst, M.; Rao, A.; et al. Vitamin C induces Tet-dependent DNA demethylation and a blastocyst-like state in ES cells. *Nature* **2013**, *500*, 222–226. [CrossRef]
37. He, X.B.; Kim, M.; Kim, S.Y.; Yi, S.H.; Rhee, Y.H.; Kim, T.; Lee, E.H.; Park, C.H.; Dixit, S.; Harrison, F.E.; et al. Vitamin C facilitates dopamine neuron differentiation in fetal midbrain through TET1- and JMJD3-dependent epigenetic control manner. *Stem Cells* **2015**, *33*, 1320–1332. [CrossRef]
38. Harrison, F.E.; Meredith, M.E.; Dawes, S.M.; Saskowski, J.L.; May, J.M. Low ascorbic acid and increased oxidative stress in gulo(−/−) mice during development. *Brain Res.* **2010**, *1349*, 143–152. [CrossRef]
39. Paidi, M.D.; Schjoldager, J.G.; Lykkesfeldt, J.; Tveden-Nyborg, P. Prenatal vitamin C deficiency results in differential levels of oxidative stress during late gestation in foetal guinea pig brains. *Redox Biol.* **2014**, *2*, 361–367. [CrossRef]
40. Harrison, F.E.; Dawes, S.M.; Meredith, M.E.; Babaev, V.R.; Li, L.; May, J.M. Low vitamin C and increased oxidative stress and cell death in mice that lack the sodium-dependent vitamin C transporter SVCT2. *Free Radic. Biol. Med.* **2010**, *49*, 821–829. [CrossRef]

41. Dixit, S.; Bernardo, A.; Walker, J.M.; Kennard, J.A.; Kim, G.Y.; Kessler, E.S.; Harrison, F.E. Vitamin C deficiency in the brain impairs cognition, increases amyloid accumulation and deposition, and oxidative stress in APP/PSEN1 and normally aging mice. *ACS Chem. Neurosci.* **2015**, *6*, 570–581. [CrossRef] [PubMed]
42. Hou, Y.; Ouyang, X.; Wan, R.; Cheng, H.; Mattson, M.P.; Cheng, A. Mitochondrial superoxide production negatively regulates neural progenitor proliferation and cerebral cortical development. *Stem Cells* **2012**, *30*, 2535–2547. [CrossRef] [PubMed]
43. Mercier, F.; Kitasako, J.T.; Hatton, G.I. Anatomy of the brain neurogenic zones revisited: Fractones and the fibroblast/macrophage network. *J. Comp. Neurol.* **2002**, *451*, 170–188. [CrossRef] [PubMed]
44. Guan, J.; Tong, W.; Ding, W.; Du, S.; Xiao, Z.; Han, Q.; Zhu, Z.; Bao, X.; Shi, X.; Wu, C.; et al. Neuronal regeneration and protection by collagen-binding BDNF in the rat middle cerebral artery occlusion model. *Biomaterials* **2012**, *33*, 1386–1395. [CrossRef]
45. Alexandrova, A.Y.; Kopnin, P.B.; Vasiliev, J.M.; Kopnin, B.P. ROS up-regulation mediates Ras-induced changes of cell morphology and motility. *Exp. Cell Res.* **2006**, *312*, 2066–2073. [CrossRef]
46. Coluzzi, E.; Colamartino, M.; Cozzi, R.; Leone, S.; Meneghini, C.; O'Callaghan, N.; Sgura, A. Oxidative stress induces persistent telomeric DNA damage responsible for nuclear morphology change in mammalian cells. *PLoS ONE* **2014**, *9*, e110963. [CrossRef]
47. Mosdol, A.; Erens, B.; Brunner, E.J. Estimated prevalence and predictors of vitamin C deficiency within UK's low-income population. *J. Public Health* **2008**, *30*, 456–460. [CrossRef]

antioxidants

MDPI

Review

Mitochondria in Cell-Based Therapy for Stroke

Molly Monsour [1], Jonah Gordon [1], Gavin Lockard [1], Adam Alayli [1] and Cesar V. Borlongan [2,*]

[1] University of South Florida Morsani College of Medicine, Tampa, FL 33602, USA
[2] Center of Excellence for Aging and Brain Repair, Department of Neurosurgery and Brain Repair, University of South Florida Morsani College of Medicine, Tampa, FL 33612, USA
* Correspondence: cborlong@usf.edu

Abstract: Despite a relatively developed understanding of the pathophysiology underlying primary and secondary mechanisms of cell death after ischemic injury, there are few established treatments to improve stroke prognoses. A major contributor to secondary cell death is mitochondrial dysfunction. Recent advancements in cell-based therapies suggest that stem cells may be revolutionary for treating stroke, and the reestablishment of mitochondrial integrity may underlie these therapeutic benefits. In fact, functioning mitochondria are imperative for reducing oxidative damage and neuroinflammation following stroke and reperfusion injury. In this review, we will discuss the role of mitochondria in establishing the anti-oxidative effects of stem cell therapies for stroke.

Keywords: stroke; stem cell; mitochondria; oxidation; neuroinflammation; reactive oxygen species

Citation: Monsour, M.; Gordon, J.; Lockard, G.; Alayli, A.; Borlongan, C.V. Mitochondria in Cell-Based Therapy for Stroke. *Antioxidants* **2023**, *12*, 178. https://doi.org/10.3390/antiox12010178

Academic Editors: Ana-Maria Buga and Carmen Nicoleta Oancea

Received: 2 January 2023
Revised: 9 January 2023
Accepted: 10 January 2023
Published: 12 January 2023

1. Introduction

The central nervous system is a highly active, energy intensive organ system that relies on careful homeostasis to maintain smooth function. The high energy demand places mitochondria in the forefront as the pivotal organelle maintaining and supplying neuronal energy demands [1]. Mitochondria are multi-functional organelles found in eukaryotic cells, with roles, such as energy production, regulation of apoptosis, buffering intracellular calcium, and the development of reactive oxygen species [2–4]. They are integral to functions within the central nervous system because they produce a majority of the energy needed for membrane ATPases, the influx and efflux of neurotransmitters, and the formation of new neural circuits [1,5].

Mitochondria exhibit an adaptive response to the fluctuating needs of their host cell in an effort to maintain bioenergetic and oxidative homeostasis [6,7]. In large, complex cells such as neurons, mitochondrial distribution plays a critical role in supplying the cell with needed energy [8,9]. The organelle may even move around the cell in response to metabolic demand. For example, certain mitochondria can move along axons using kinesin or dynein motors to reach areas with higher energy needs [10]. Other mitochondria are anchored into the membrane and remain stationary to supply a continuous source of energy to a local structure within the cell such as in dendrites [11]. Mitochondria may also fuse or undergo fission in order to respond to fluctuating energy demands. For example, mitochondrial fission allows the organelles to travel into growing spines and dendrites to promote neurogenesis and plasticity while blocking mitochondrial fission that results in neuronal degeneration and disruption of neuronal morphology [12,13].

Although neurons are typically lifelong cells and do not regenerate, mitochondria experience regular turnover to remove damaged organelles and minimize the unintentional release of proapoptotic signals and accumulation of reactive oxygen species [14]. This process is called mitophagy and occurs in cells all over the body. In the setting of neurodegenerative disease, mitophagy decreases and injured mitochondria accumulate. Normally, upon damage to mitochondria, there is a subsequent elevation of PTEN-induced kinase 1 (PINK1) in the mitochondrial outer membrane, which phosphorylates, and thus activates E3 ubiquitin ligase

Parkin [15,16]. In one mechanism, Parkin ubiquitinates and thus eliminates mitochondrial fusion proteins mitofusin1 and mitofusin2, resulting in mitochondrial fission, separating diseased mitochondrial components [17]. Additionally, Parkin ubiquitinates mitochondrial surface proteins; the ubiquitin moieties attract a battery of autophagy receptors, including optineurin and nuclear dot protein 52, among others. The autophagy receptors bind to LC3, a protein embedded in the autophagosome, thus connecting the two organelles, and allowing for mitophagy [18]. There is a careful balance of mitophagy that must be struck; too much can be detrimental to cell life and too little can be factorial in the etiology of neurodegenerative disease [19]. Defects in mitophagy are implicated in the development of neurodegenerative diseases, such as Alzheimer's and Parkinson's disease, and restoring this essential function may offer a therapeutic target for these diseases [20].

2. Mitochondrial Impairment in the Oxidative Stress following Stroke and Reperfusion Injury

Ischemic stroke is defined as a sustained lack of blood flow to an area of the brain resulting in local inflammation, oxidative stress, and cellular death. While the primary mechanisms of cell death relate to ischemic injury, mitochondrial damage is a primary component of secondary cell death, contributing to excitotoxicity, oxidative stress, free radical accumulation, impaired neurogenesis, angiogenesis, vasculogenesis, and inflammation [21,22]. Within the mitochondria, the Krebs cycle transfers energy from glycolytic molecules to electron carriers, propagating the oxidative phosphorylation pathway of maximal ATP production [23]. Mitochondria are vital to energy production via this oxidative phosphorylation; however, oxidative phosphorylation also notoriously results in free radical accumulation [24]. Thus, if malfunctioning, mitochondrial damage can result in reduced energy production and excessive accumulation of free radicals and oxidative stress following ischemic injury [25]. Furthermore, ischemic injury to mitochondria leads to their programmed death and release of cytochrome C. Cytochrome C then perpetuates neuronal death via apoptosis, furthering the release of ROS [26]. As oxidative phosphorylation requires oxygen, and ischemic stroke is defined by a lack of oxygen to neurons, it is incredibly logical to target underlying mitochondrial damage to ameliorate further cell death secondary to oxidative stress. Furthermore, reperfusion following ischemic stroke generates a large number of ROS, contributing to oxidative stress [27].

3. Repair of the Damaged Mitochondria in Stroke: Astrocytes-to Neurons Transfer of Mitochondria

As mitochondria are, by nature, functioning within eukaryotic cells, many groups have examined the role mitochondria play in the successful treatment of stroke with stem cells [28]. More mysterious, however, is whether the mitochondria mitigate ischemic damage via direct transfer or signaling molecules (Figure 1). Some research suggests stem cells physically transfer healthy mitochondria to deteriorating neuronal cells, similar to astrocytic aid in neuronal survival following stroke [29,30]. Others, however, perceptualize that direct mitochondrial energy metabolism within stem cells can modulate the stem cells' differentiation, ageing, immune regulation, apoptosis, proliferation, migration, and chemotaxis [31].

The immediate impacts of mitochondrial repair are extended via downstream antioxidant effects. ROS inhibit the Nuclear factor erythroid 2-related factor 2 (Nrf2) anti-oxidant pathway. Thus, by blocking the accumulation of ROS via mitochondrial transfer, the Nrf2 pathway can be restored following stroke and implement its anti-inflammatory and antioxidant pathways. Regarding cell-based therapies, the downstream reduction in ROS can also amplify stem cell viability and function. For instance, upregulation of Nrf2 and downstream antioxidant genes such as HO-1 augments neurogenesis and increases NSC viability via decreased apoptosis [32,33]. Thus, successive cell-based therapies may be synergistically effective due to the downstream antioxidant effects of restoring mitochondrial viability with the first cell dose. Alternatively, pre-emptive treatment with antioxidant agents may lower the workload of stem cells and their mitochondrial progenies [26]. Thus, there is a promising tie between enhancing mitochondrial efficacy and mitigating oxidative stress

following ischemic stroke. Ultimately, the profound impacts of restoring mitochondria functionality can contribute to neurological repair via its downstream anti-inflammatory and antioxidant impacts.

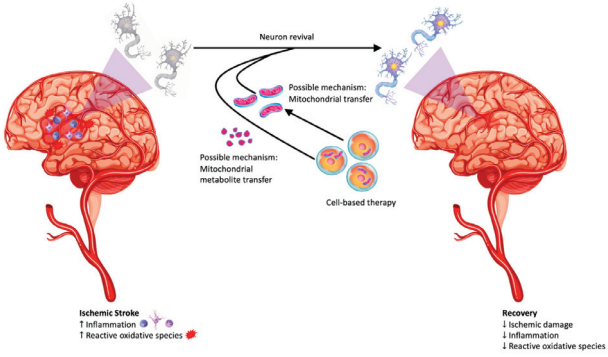

Figure 1. This figure exemplifies the neuroinflammatory and oxidative stress which occurs following an ischemic stroke. Using cell-based therapies, direct mitochondrial transfer theory and mitochondrial metabolite theories are demonstrated here. Mitochondrial restoration promotes recovery by decreasing ischemic damage, inflammation, and ROS.

4. Stem Cell-Neural Cell Crosstalk: Rescue of Mitochondria by Stem Cells

Mitochondria play a mitigating role in neuroinflammation, such as in the setting of ischemic cerebrovascular accident. This is of particular interest with the use of stem cell therapy. Stem cells exert their effects on endogenous cells in a variety of ways; they can release molecules to communicate in a paracrine fashion [34], release exosomes [35], and even alter energetic efficacy, inflammation, and oxidative stress via mitochondrial adaptations. After treatment with human bone marrow endothelial progenitor cells, rat models of ischemic stroke had restored endothelial cell, pericyte, and astrocyte morphology. Upon closer analysis, mitochondrial morphology was restored in these cells as well, suggesting changes to mitochondrial integrity may be responsible for this therapy's beneficial effect [36]. Regarding stem cell impacts on mitochondria, various theories have been proposed, such as direct mitochondrial transfer and mitochondrial metabolite transmission (Tables 1 and 2).

Table 1. In Vivo Stem Cell Studies Investigating the Role of Mitochondria in Ischemic Stroke. This table outlines cell-based preclinical trials finding improved functional outcomes attributed to the impact of mitochondrial activity in the background of ischemic insult.

Sample	Cell Type	Route	Dosage	Outcome
MCAO rats	Human Bone Marrow Endothelial Progenitor Cells	Intravenous	4×10^6 cells/mL	Endothelial cells, pericytes, and astrocytes demonstrate near normal morphology without perivascular edema. Mitochondrial morphology in endothelial cells and perivascular astrocytes shows near normal morphology and pinocytic vessels are observed in engrafted cells, which ameliorates post-stroke vasculature [36].
MCAO rats	Miro1-overexpressing Multipotent MSCs	Intravenous	3×10^6 cells/kg	Miro1, normally upregulated in the presence of ROS, promotes mitochondrial transfer to neural cells and reduces neurologic deficits after ischemic stroke [37].
MCAO rats	MSCs	Intra-arterial	5×10^5 cells	Mitochondrial transfer to injured cells of the cerebral microvasculature improves mitochondrial activity, upregulates angiogenesis, improves neurologic function, and decreases infarct volume [38].
MCAO rats	hUC-MSC-derived mitochondria	Intraventricular	Isolate from 3×10^7 cells	Transplanted mitochondria improve ischemic injury exemplified through inhibition of apoptosis, decreased astrogliosis, microglial downregulation, reduced infarct size, and enhanced preservation of motor function [39].
MCAO rats	Ischemic-hypoxic preconditioned olfactory mucosa MSCs	Intravenous	1×10^6 cells	Mitochondrial function is preserved through upregulation of downstream target genes (GRP78 and Bcl-2) by miR-181a and the presence of ROS is significantly reduced. Apoptosis and pyroptosis of neurons are inhibited [40].
Photothrombotic mPFC stroke mice	BM-MSC-derived mitochondria	Intranasal	12 µL	Mitochondrial transplant significantly reduced the presence of ROS in the mPFC following ischemia. Transplant also ameliorates memory impairment, upregulates ATP generation, improves mitochondrial membrane potential, and upregulates expression of synaptic markers (GAP-43 and PSD-95) [41].

Table 2. In Vitro Stem Cell Studies Investigating the Role of Mitochondria under Oxidative Stress. This table describes in vitro models of oxidative stress pertaining to various elements of mitochondrial function in stroke reperfusion.

Model of Injury	Cell Type	Outcome
Hypoxia-reperfusion	Rat Neural Stem Cells	Coenzyme Q10 achieves an antioxidant effect through interaction with the electron transport chain, increasing expression of survival proteins (pAkt, pGSK3-β, and Bcl-2) and reducing levels of cleaved caspase-3 [42].
OGD	Primary Rat Neural Cells	DJ-1, a protein involved in neuroprotection through regulation of oxidative stress, translocated to mitochondria and enhanced both cell viability mitochondrial activity while reducing ROS concentrations [43].
OGD	Primary Rat Neural Cells	Ischemic conditions promote the uptake of astrocyte-released mitochondrial particles by adjacent neurons, which increases survival signaling [29].
OGD	Human Endothelial Progenitor Cell-derived Extracellular Mitochondria	Incorporation of extracellular mitochondria promotes angiogenesis, decreases BBB permeability, and increases expression of TOM40, mtDNA copy number, and intracellular ATP [44].
Metabolic Switching Paradigm, OGD	Human MSCs, Primary Rat Neurons	Metabolic switching in MSCs yields greater energy generation, respiratory capacity, and ATP production. Co-culture with ODG neurons enhances cellular metabolism, decreases mitochondrial ROS mRNA, and overall improves cell viability [30].
Metabolic Switching Paradigm	Human MSCs	Metabolic switching in MSCs results in mitochondria with enhanced capability for oxidative phosphorylation [25].

Stem cells can form intercellular bridges named tunneling nanotubes [45], or directly fuse; these latter two mechanisms allow the exchange of cellular contents including organelles such as mitochondria [46]. The exchange of healthy mitochondria into an ischemic cell is very promising. Indeed, Babenko et al. found that mitochondrial transfer from multipotent mesenchymal stem cells (MMSC) to astrocytes is more robust in the setting of elevated reactive oxygen species (ROS) secondary to ischemic insult, compared to normal conditions. Mitochondrial Rho-GTPase 1 (Miro1) is a calcium-sensitive adaptor protein, assisting in the intracellular and intercellular transport of neuronal mitochondria [47], and when Miro1 is overexpressed in MMSCs, the mitochondrial donation to astrocytes is markedly increased [37]. Additionally, rats who underwent the middle cerebral artery occlusion (MCAO) stroke model and were then treated with MMSC-Miro1 had improved neurological function compared to MMSC therapy alone. Similarly, Liu et al. found that grafted MSCs in rats who underwent MCAO/reperfusion offered mitochondria to injured endothelial cells, rescuing mitochondrial activity and improving angiogenesis and neurologic function [38].

Direct implantation of mitochondria may surpass the cell-exudation step and provide equally beneficial results. In an OGD brain endothelial model, human endothelial progenitor cell-derived extracellular mitochondria promoted angiogenesis, blood brain barrier (BBB) impermeability, and increased ATP [44]. These results are incredibly pertinent to recent theories regarding BBB permeability as a major contributor to secondary cell death in stroke due to peripheral inflammatory and ROS influx [48,49]. In vivo, human umbilical cord-MSC-derived mitochondria also improved ischemic injury in rats, with treated rats showing decreased apoptosis, astrogliosis, neuroinflammation, and infarct size. Furthermore, some motor functional recovery was notable [39]. On a similar note, BM-MSC-derived mitochondria given to mice models of stroke reduced ROS, improves memory, enhanced energy efficacy, and increases synaptic marker expression. Interestingly, this study used an intranasal route for mitochondrial treatment, introducing a less invasive and possibly more direct mechanism of cell-based therapy administration [41]. A more direct route to the ischemic region would likely amplify cell survival and induce a more potent anti-inflammatory and antioxidant effect. Further studies should examine whether this administration method is superior to the more standard intravenous or intraarterial routes of administration. Whether exuded by stem cells themselves or extracted and implanted artificially, mitochondrial transfer demonstrates a clear benefit to reducing secondary mechanisms of cell death following stroke.

Of additional interest are the potential antioxidant roles of mitochondria. While direct mitochondrial transfer was not noted in the following studies, variations in mitochondrial function may lead to mitochondrial metabolite transmission and reduced ischemic damage. Coenzyme Q10 (CoQ10) is a component of the electron transport chain in mitochondria, and when applied to neural stem cells in the setting of hypoxia-reperfusion, defends them from injury. CoQ10 attenuates free radical formation and increases the expression of

antiapoptotic phosphorylated Akt (pAkt), phosphorylated glycogen synthase kinase 3-β (pGSK3-β), and B-cell lymphoma 2 (Bcl-2), while simultaneously decreasing proapoptotic cleaved caspase-3 [42]. DJ-1 is another molecule associated with antioxidant activity. DJ-1 promotes nuclear factor erythroid 2–related factor 2 (Nrf2) [50], which is a master switch for antioxidant genes, and decreases the expression of proapoptotic Bax [51]. In the oxygen-glucose deprivation (OGD) in vitro stroke model, it was observed that DJ-1 located to intact mitochondria, and when anti-DJ-1 antibody was administered, glutathione concentrations increased, and mitochondrial activity diminished [43].

Intriguingly, pre-conditioning stem cells may further exacerbate the beneficial impact of mitochondria in cell-based therapies for stroke. In one study, growing mesenchymal stem cells (MSC) under a metabolic switching paradigm (three days in a galactose medium and three days in a glucose medium) resulted in enhanced therapeutic effects of SCs in an in vitro OGD model of stroke. The MSCs grown under a metabolic switching paradigm generated more ATP, shifted their metabolism to favor oxidative phosphorylation, had a higher basal energy production, had a greater spare respiratory capacity, and leaked less hydrogen ions. Thus, these cells demonstrated greater efficiency during energy production and a superior ability to respond to stressful conditions (i.e., ischemic energy) compared to the MSCs cultured with a standard glucose medium. When applied to the in vitro stroke model, the switched MSCs showed greater cell viability, enhanced metabolism, reduced ROS from stem cell mitochondria, and elevated mitochondrial ATP production by the MSCs compared to the standardly cultured cells [25,30]. Since the only difference between the MSC groups involved metabolism, which is predominantly moderated by mitochondria, it is theorized that the superior efficacy of metabolically switched MSCs is due to the generation of "super mitochondria". It is plausible that the MSCs transferred these mitochondria to the damaged cells, allowing for greater recovery of ATP and metabolic recovery. Other groups have shown that, in vitro, co culture of PGD neurons with astrocyte conditioned media (including mitochondrial particles), restores neuronal viability and ATP production. Using fluorescent staining, the transfer of astrocytic mitochondria to ischemically stressed neurons was confirmed. In vivo, these results held true, showing that astrocytes use a CD38/cyclic ADP ribose signaling pathway to facilitate mitochondrial transfer to neurons following stroke in mice models [29]. Other studies have elucidated the amplification of stem cells' antioxidant properties following pre-conditioning as well. In rats treated with ischemic-hypoxic pre-conditioned olfactory mucosa MSCs, mitochondrial function was preserved, and ROS levels were significantly reduced [40].

Although the antioxidant and antiapoptotic properties of stem cells and mitochondria are exciting fields to investigate further, the deleterious effects of ROS on cells are indisputable. Prakash et al. investigated the effects of hydrogen peroxide on human dental pulp and MSC. Hydrogen peroxide triggered oxidative stress, prompting autophagy and mitophagy [19]. As discussed earlier, mitophagy is beneficial in clearing injured mitochondria, but there is a health balance that must be maintained. Ultimately, the ideal cell-based therapy would be able to withstand these toxic impacts of ROS, while simultaneously reducing ROS induced secondary cell death. Ongoing studies on mechanisms of mitochondrial repair following cell-based therapies show promise for uncovering this lucrative therapeutic goal.

5. Non-Cell-Based Approaches to Mitochondrial Repair in Stroke

Recent advancements in cell-based therapies encourage researchers to explore the processes of mitochondrial transfer from stem cells, however, other approaches to restoring mitochondrial integrity following stroke may involve pharmaceutical or life style changes [52]. Resveratrol, a SIRT1 activator, for instance, reduces ROS and ultimately improves mitochondrial glucose utilization and restoration [53,54]. Considering 54 studies of stroke rodent models, resveratrol decreased infarct volumes and improved neurobehavioral scores, likely via its enhancement of mitochondrial function [55]. Moreover, in an effort to reduce oxidative stress by restoring mitochondrial function, methylene blue can enhance the transfer of electrons along the oxidative phosphorylation pathway to reduce ROS and

increase ATP production efficiency [56]. In rats, methylene blue treatment normalized blood flow, decreased ischemic burden, and enhanced rodent functionality [57].

Oxidative burden may be effectively reduced by pharmaceuticals following stroke, but simple dietary additives such as ubiquinone, N-acetylcysteine, and/or anti-oxidant vitamins (i.e., C and E) may also reduce ROS following ischemic stroke [52]. Diet changes may also harbor potential to strengthen mitochondrial integrity following stroke. As previously discussed, stem cells cultured under metabolic switching conditions showed increased mitochondrial ATP production and decreased mitochondrial ROS mRNA when used to treat OGD neurons. These stem cells amplified oxidative phosphorylation over glycolytic metabolism to enhance the efficiency of energy metabolism. Metabolic switching in vitro may be mirrored by a ketogenic diet, which similarly minimizes glucose availability and could shift cells to generate more powerful mitochondria [25,30]. Yet another lifestyle adjustment includes exercise, as increased physical activity may improve mitochondrial function by enhancing oxidative phosphorylation and reducing oxidative stress [52]. Ultimately, while cell-based therapies are an exciting and rapidly developing field, alternative therapeutics may harbor benefits by similarly restoring mitochondrial integrity after stroke.

A number of clinical trials have been conducted with the goal of reducing oxidative stress following stroke [27]. Lipoic acid, involved in vitamin C and E recycling, is being tested in an ongoing clinical trial on reperfusion therapies for ischemic stroke in patients with diabetes (NCT 04041167). Salvianolic acid is also being studied as an antioxidant following stroke, as it is a potent oxidation, coagulation, and platelet aggregation inhibitor (NCT04931628). Edaravone, a ROS scavenger, has shown reduced mortality when administered with alteplase therapy or after endovascular revascularization [58,59]. Importantly, not all preclinical successes are translatable to clinical settings, however, and further investigation is needed [27,60–66].

6. Mitochondrial Repair in Other Disorders of the Central Nervous System

While the rescue of mitochondria has therapeutic promise in the treatment of stroke, mitochondrial damage plays a significant role in other degenerative CNS disorders, such as Alzheimer's disease (AD), Parkinson's disease (PD), and amyotrophic lateral sclerosis (ALS) [67]. As such, these conditions may also benefit from mitochondrial repair (Table 3).

Table 3. In Vitro and In Vivo Studies Targeting Mitochondrial Transfer in Neurodegenerative Diseases. This table delineates the utility of experimental agents to promote mitochondrial transfer in models of neurodegenerative disease.

Sample	Treatment	Route	Dosage	Outcome
Sigmar1(-/-) mice	BAPTA-AM, a selective intracellular calcium chelator or an endoplasmic reticulum stress inhibitor salubrinal	-	-	Restoration of calcium homeostasis and endoplasmic reticulum stability recovered mitochondrial movement and morphology, ultimately reducing motor neuron degeneration [68].
6-hydroxydopamine-induced selective parkinsonian rats	PC12 cell- and Human Osteosarcoma cybrid-derived mitochondria	Intracranial	1.05 μg	Peptide-mediated allogeneic mitochondrial delivery maintains mitochondrial function in the setting of oxidative stress and apoptotic death. Motor activity is improved up to three months following transplantation, and dopaminergic neuron loss is reduced [69].
G93A ALS mice neurons	ADSC-derived exosomes	-	200 μg/mL	Transplanted exosomes reduce aggregation of superoxide dismutase 1 and normalize mitochondrial phospho-CREB/CREB ratio and PGC-1α expression [70].
MPTP-HCL-induced parkinsonian mice	HepG2-derived mitochondria	Intravenous	0.5 mg/kg	Transplanted mitochondria distributed to the brain, liver, kidney, muscle, and heart. PD progression is halted through increased electron transport chain activity, reduced levels of reactive oxygen species, and prevention of apoptosis [71].
Aβ-ICV Alzheimer's Disease mice	HeLa cell-derived mitochondria	Intravenous	200 μg	Treated mice show enhanced cognitive performance, reduced loss of neurons, and reduced hippocampal gliosis. Mitochondrial function is further ameliorated peripherally in organs such as the liver [72].
Rotenone-induced Parkinson's neurons	iPSC- and hESC-derived DA neurons and astrocytes	-	-	iPSC-derived astrocytes and astrocytic conditioned media reduce degeneration of dopaminergic neurons and reverse axonal pruning through mitochondrial transfer [73].
5 x Familial Alzheimer's Disease mice	VBIT-4 (Voltage-Dependent anion channel-1 inhibitor)	PO (in drinking water)	20 mg/kg	VBIT-4 reduces neuronal cell death, downregulates neuroinflammation, and ameliorates metabolic dysfunction, leading to improved cognitive outcomes in behavioral assessments [74].

Alzheimer's disease is a neurodegenerative disorder often associated with the accumulation of amyloid-β plaques in the brain, although the true etiology of the disease is unclear and increasingly seems to be multifactorial in nature. The exact molecular cause of mitochondrial dysfunction in AD increasingly appears to be complex and not relegated to a single pathway. Early stages of the disease are characterized by degradation of mitochondrial function, such as a loss of calcium homeostasis, dysregulated neuronal apoptosis, and a significant increase in the abundance of reactive oxygen species [75,76]. The accumulation of (NH(2))-derived tau protein and amyloid-β plaques in mitochondria inhibits the function of the mitochondrial adenine nucleotide translocator-1, which suggests a potential mechanism for early mitochondrial dysfunction in AD [77]. Amyloid-β plaques also seem to inhibit mitochondrial transport, fission, and fusion, leading to neural degeneration and significantly decreased neuroplasticity [75]. Additionally, p9 mitochondrial tRNA hypermethylation seems to play a role in the pathogenesis of Alzheimer's disease by impairing RNA stability, translational processes and disrupting downstream pathways within the mitochondria [78]. For example, impaired protein translation as a result of hypermethylated p9 may cause a disruption in the folding of proteins involved in the electron transport chain, signaling dynamics, and homeostasis. On a macro scale, astrocytes seem to increase their rate of transmitophagy in AD mouse models, suggesting yet another mechanism for neurodegeneration. This disrupts the function of affected astrocytes by increasing reactive oxygen species and altering the supportive relationship between astrocytes and neurons [79]. More research must be performed to assess the role of transmitophagy in the initiation of neurodegenerative disease, although this finding suggests that the factors at play are not limited to intracellular and intra-mitochondrial processes. In fact, mitochondrial transfer in mice models of AD demonstrates improved cognition, decreased neuronal loss and gliosis in the hippocampus, and improved mitochondrial functionality [72]. Mitochondrial integrity in AD may also be restored by inhibiting the voltage-dependent anion channel-1 (VDAC-1), a mitochondrial protein overexpressed in AD. In vitro and in vivo inhibition of VDAC-1 resulted in reduced neuronal apoptosis, decreased inflammation, and repaired metabolic function. Cognitive decline was also ameliorated in treated mice. While metabolic homeostasis was restored, likely by restoring normal mitochondrial protein function, the Amyloid-β and hyperphosphorylated tau burdens were not decreased [74]. This is of interest as it suggests mitochondrial dysfunction may be equally pertinent to AD pathology as the well-recognized plaque and tangle pathologies. Stem cell therapy for AD is a focus of current research and early studies show that the transplantation of neural stem cells from mouse embryos may rescue the spatial learning and memory function and enhance the long-term potentiation of APP/PS1 transgenic mice [80]. Human neural stem cells also display a similar benefit by enhancing synaptogenesis and offer the benefit of a lower chance of rejection after implantation into humans [81]. Furthermore, human embryonic stem cells transplanted into the basal forebrain of AD mouse models differentiated into mature cholinergic neurons and subsequently rescued the mice's cognitive deficits and improved spatial learning [82].

The hallmark of Parkinson's disease is the degeneration of dopaminergic neurons in the substantia nigra. Its pathogenesis is multifactorial, but many associated genes, such as SNCA, LRRK2, VPS35, PINK1, DJ-1, and Parkin have been identified and linked to mitochondrial dysfunction [83]. For example, mutations in the SNCA gene cause overexpression of α-synuclein, which can disrupt mitochondrial membrane tethers and result in loss of ATP production and calcium homeostasis [84]. Gains of function in LRRK2, another commonly mutated gene, play a role in neurotransmitter release and arrest mitochondrial fission within the substantia nigra [85]. Loss-of-function mutations in Parkin, the most common genetic cause of autosomal recessive PD, allow for the accumulation of damaged mitochondria by removing the ability to degrade and ubiquitin-tag mitochondrial proteins [86]. Loss of Parkin also leads to the accumulation of parkin interacting substrate (PARIS), which causes a decrease in mitochondrial biogenesis and quantity [87]. Most therapeutics for PD focus on alleviating symptoms and there is currently no effective cure

for the disorder. Due to the major role of mitochondria in PD pathology, mitochondrial transfer may attenuate symptomology [88,89]. In 6-OHDA rat models of PD, mitochondria injected into the medial forebrain bundle improve mitochondrial function within substantia nigra neurons. These new mitochondria reduced dopaminergic cell death, improved cell functionality, and reduced oxidative DNA damage [69]. In mice, similar mitochondrial administration decreased ROS levels, cell apoptosis, and necrosis [71]. Stem cell therapy is a promising path because it may replace diseased cells and slow down or halt the progression of the disease. For example, human embryonic stem cells transplanted into PD rat models improve long-term survival and restore motor function [90]. Induced pluripotent stem cell (iPSC)-derived dopaminergic (DA) neurons have the most promising results in preclinical studies, where they successfully induced gradual improvement in motor function after implantation into primate models [91]. In an astrocytic conditioned media, iPSCs cultured with dopaminergic neurons demonstrate active mitochondrial transfer. Using a phopho-p38 pathway, the mitochondria from astrocytes were internalized by the neurons and dopaminergic degenerating neurons were salvaged. When the astrocyte media was ultrafiltered to remove mitochondria, these restorative effects were abolished, suggesting that the primary mechanism of dopaminergic neuronal recovery was due to mitochondrial transfer [73]. These are the preferred line of stem cells for transplantation because they reduce any risk for immunological response. Several clinical trials are ongoing in China, Australia, and Japan to evaluate the efficacy of this treatment.

Amyotrophic Lateral Sclerosis is another neurodegenerative disease heavily influenced by mitochondrial dysfunction. It is largely a sporadic disease without a clear hereditary genetic cause. However, many of the identified genes that do contribute to ALS have roles in impacting mitochondrial function and thus cause the dysfunction of mitochondria as a part of the progression of the disease. For example, mutations in SOD1 and TDP43 in mouse models significantly hinder of mitochondrial transportation and subsequently cause morphological defects and neuronal dysfunction during the early stages of ALS [92]. Sigmar1 mutations, a protein involved in endoplasmic reticulum and mitochondrial communication and calcium balance, also decreases mitochondrial ATP production and impairs neuronal function [68,93]. Using calcium scavenging and inhibiting the stress on the endoplasmic reticulum, mitochondrial dysfunction can be repaired in Sigmar1 mutant mice models of ALS. In addition to restored mitochondrial function, motor neuron degeneration was also diminished [68]. Stem cell therapy for ALS has shifted from attempts to replace lost motor neurons to a goal of providing a neuroprotective local environment for diseased cells [94]. A study examining exosomes from adipose derived stem cells effectively reduced pathological SOD1 levels in mice models of ALS. Furthermore, abnormally phosphorylated CREB and PGC-1α within mitochondria were normalized, proposing that stem cells may be capable of ameliorating ALS pathology via improved mitochondrial function [70]. Studies remain largely in the preclinical or early clinical phase, but results are increasingly promising. For example, the transplantation of human umbilical cord blood cells significantly increases the survival of and delay motor deterioration in SOD1 mouse models [95]. This may be due to the modulation of autoimmune processes to create a neuroprotective environment [96]. Recently, clinical trials aiming to assess the safety of stem cells in humans showed no significantly accelerated deterioration and overall safe clinical outcomes [94]. More studies need to be performed to assess potential benefits to human patients.

7. Conclusions

The paucity of effective therapies for stroke alongside our vast knowledge of the mechanisms of secondary cell death following ischemic injury is perplexing. The revolutionary strides in cell-based therapies have revamped treatment goals for stroke. However, the underlying mechanisms of success are frequently contemplated. With a better understanding of how stem cells modulate secondary cell death, these properties can be amplified to strengthen the efficacy of cell-based therapies. As the vitality of functioning mitochondria for

stroke recovery is better understood, greater strides in promoting mitochondrial transfer or metabolite exudation from stem cells may significantly magnify their therapeutic benefits.

Author Contributions: Conceptualization, M.M. and C.V.B.; investigation, M.M., J.G., G.L. and A.A.; writing—original draft preparation, M.M., J.G., G.L. and A.A.; writing—review and editing, M.M., J.G., G.L., A.A. and C.V.B.; visualization, M.M., J.G., G.L. and A.A.; supervision, C.V.B. All authors have read and agreed to the published version of the manuscript.

Funding: This research received no external funding.

Acknowledgments: We acknowledge the work of brgfx and macrovector who designed the vectors used in this figure. The vectors were downloaded from freepik.com.

Conflicts of Interest: C.V.B. declared leadership position with University of South Florida, patents holder and patent applications on stem cell biology and its therapeutic applications, consultant to a number of stem cell-based companies, and research funding from the NIH. All of the other authors declared no potential conflicts of interest.

References

1. Rangaraju, V.; Calloway, N.; Ryan, T.A. Activity-driven local ATP synthesis is required for synaptic function. *Cell* **2014**, *156*, 825–835. [CrossRef] [PubMed]
2. Dan Dunn, J.; Alvarez, L.A.; Zhang, X.; Soldati, T. Reactive oxygen species and mitochondria: A nexus of cellular homeostasis. *Redox. Biol.* **2015**, *6*, 472–485. [CrossRef] [PubMed]
3. Abate, M.; Festa, A.; Falco, M.; Lombardi, A.; Luce, A.; Grimaldi, A.; Zappavigna, S.; Sperlongano, P.; Irace, C.; Caraglia, M.; et al. Mitochondria as playmakers of apoptosis, autophagy and senescence. *Semin. Cell Dev. Biol.* **2020**, *98*, 139–153. [CrossRef] [PubMed]
4. Bravo-Sagua, R.; Parra, V.; López-Crisosto, C.; Díaz, P.; Quest, A.F.; Lavandero, S. Calcium Transport and Signaling in Mitochondria. *Compr. Physiol.* **2017**, *7*, 623–634. [CrossRef]
5. Cheng, A.; Hou, Y.; Mattson, M.P. Mitochondria and neuroplasticity. *ASN Neuro.* **2010**, *2*, e00045. [CrossRef]
6. Marques-Aleixo, I.; Oliveira, P.J.; Moreira, P.I.; Magalhães, J.; Ascensão, A. Physical exercise as a possible strategy for brain protection: Evidence from mitochondrial-mediated mechanisms. *Prog. Neurobiol.* **2012**, *99*, 149–162. [CrossRef]
7. Marques-Aleixo, I.; Santos-Alves, E.; Balça, M.M.; Rizo-Roca, D.; Moreira, P.I.; Oliveira, P.J.; Magalhães, J.; Ascensão, A. Physical exercise improves brain cortex and cerebellum mitochondrial bioenergetics and alters apoptotic, dynamic and auto(mito)phagy markers. *Neuroscience* **2015**, *301*, 480–495. [CrossRef]
8. Fabricius, C.; Berthold, C.H.; Rydmark, M. Axoplasmic organelles at nodes of Ranvier. II. Occurrence and distribution in large myelinated spinal cord axons of the adult cat. *J. Neurocytol.* **1993**, *22*, 941–954. [CrossRef]
9. Obashi, K.; Okabe, S. Regulation of mitochondrial dynamics and distribution by synapse position and neuronal activity in the axon. *Eur. J. Neurosci.* **2013**, *38*, 2350–2363. [CrossRef]
10. Pilling, A.D.; Horiuchi, D.; Lively, C.M.; Saxton, W.M. Kinesin-1 and Dynein are the primary motors for fast transport of mitochondria in Drosophila motor axons. *Mol. Biol. Cell* **2006**, *17*, 2057–2068. [CrossRef]
11. Faits, M.C.; Zhang, C.; Soto, F.; Kerschensteiner, D. Dendritic mitochondria reach stable positions during circuit development. *Elife* **2016**, *5*, e11583. [CrossRef] [PubMed]
12. Fukumitsu, K.; Hatsukano, T.; Yoshimura, A.; Heuser, J.; Fujishima, K.; Kengaku, M. Mitochondrial fission protein Drp1 regulates mitochondrial transport and dendritic arborization in cerebellar Purkinje cells. *Mol. Cell Neurosci.* **2016**, *71*, 56–65. [CrossRef] [PubMed]
13. Girard, M.; Larivière, R.; Parfitt, D.A.; Deane, E.C.; Gaudet, R.; Nossova, N.; Blondeau, F.; Prenosil, G.; Vermeulen, E.G.; Duchen, M.R.; et al. Mitochondrial dysfunction and Purkinje cell loss in autosomal recessive spastic ataxia of Charlevoix-Saguenay (ARSACS). *Proc. Natl. Acad. Sci. USA* **2012**, *109*, 1661–1666. [CrossRef] [PubMed]
14. Ashrafi, G.; Schwarz, T.L. The pathways of mitophagy for quality control and clearance of mitochondria. *Cell Death Differ.* **2013**, *20*, 31–42. [CrossRef]
15. Kondapalli, C.; Kazlauskaite, A.; Zhang, N.; Woodroof, H.I.; Campbell, D.G.; Gourlay, R.; Burchell, L.; Walden, H.; Macartney, T.J.; Deak, M.; et al. PINK1 is activated by mitochondrial membrane potential depolarization and stimulates Parkin E3 ligase activity by phosphorylating Serine 65. *Open Biol.* **2012**, *2*, 120080. [CrossRef]
16. Rüb, C.; Wilkening, A.; Voos, W. Mitochondrial quality control by the Pink1/Parkin system. *Cell Tissue Res.* **2017**, *367*, 111–123. [CrossRef] [PubMed]
17. Nardin, A.; Schrepfer, E.; Ziviani, E. Counteracting PINK/Parkin Deficiency in the Activation of Mitophagy: A Potential Therapeutic Intervention for Parkinson's Disease. *Curr. Neuropharmacol.* **2016**, *14*, 250–259. [CrossRef]
18. Heo, J.M.; Ordureau, A.; Paulo, J.A.; Rinehart, J.; Harper, J.W. The PINK1-PARKIN Mitochondrial Ubiquitylation Pathway Drives a Program of OPTN/NDP52 Recruitment and TBK1 Activation to Promote Mitophagy. *Mol. Cell.* **2015**, *60*, 7–20. [CrossRef]

19. Prakash, R.; Fauzia, E.; Siddiqui, A.J.; Yadav, S.K.; Kumari, N.; Singhai, A.; Khan, M.A.; Janowski, M.; Bhutia, S.K.; Raza, S.S. Oxidative Stress Enhances Autophagy-Mediated Death Of Stem Cells Through Erk1/2 Signaling Pathway-Implications For Neurotransplantations. *Stem. Cell Rev. Rep.* **2021**, *17*, 2347–2358. [CrossRef]
20. Batlevi, Y.; La Spada, A.R. Mitochondrial autophagy in neural function, neurodegenerative disease, neuron cell death, and aging. *Neurobiol. Dis.* **2011**, *43*, 46–51. [CrossRef]
21. Anthony, S.; Cabantan, D.; Monsour, M.; Borlongan, C.V. Neuroinflammation, Stem Cells, and Stroke. *Stroke* **2022**, *53*, 1460–1472. [CrossRef] [PubMed]
22. Wang, C.; Youle, R.J. The role of mitochondria in apoptosis*. *Annu. Rev. Genet.* **2009**, *43*, 95–118. [CrossRef] [PubMed]
23. Conte, F.; van Buuringen, N.; Voermans, N.C.; Lefeber, D.J. Galactose in human metabolism, glycosylation and congenital metabolic diseases: Time for a closer look. *Biochim. Biophys. Acta Gen. Subj.* **2021**, *1865*, 129898. [CrossRef]
24. Cadenas, E. Mitochondrial free radical production and cell signaling. *Mol. Aspects Med.* **2004**, *25*, 17–26. [CrossRef]
25. Monsour, M.; Gorsky, A.; Nguyen, H.; Castelli, V.; Lee, J.Y.; Borlongan, C.V. Enhancing oxidative phosphorylation over glycolysis for energy production in cultured mesenchymal stem cells. *Neuroreport* **2022**, *33*, 635–640. [CrossRef] [PubMed]
26. Gordon, J.; Lockard, G.; Monsour, M.; Alayli, A.; Borlongan, C.V. The Role of Concomitant Nrf2 Targeting and Stem Cell Therapy in Cerebrovascular Disease. *Antioxidants* **2022**, *11*, 1447. [CrossRef] [PubMed]
27. Jurcau, A.; Ardelean, A.I. Oxidative Stress in Ischemia/Reperfusion Injuries following Acute Ischemic Stroke. *Biomedicines* **2022**, *10*, 574. [CrossRef]
28. Lu, M.; Guo, J.; Wu, B.; Zhou, Y.; Wu, M.; Farzaneh, M.; Khoshnam, S.E. Mesenchymal Stem Cell-Mediated Mitochondrial Transfer: A Therapeutic Approach for Ischemic Stroke. *Transl. Stroke Res.* **2021**, *12*, 212–229. [CrossRef]
29. Hayakawa, K.; Esposito, E.; Wang, X.; Terasaki, Y.; Liu, Y.; Xing, C.; Ji, X.; Lo, E.H. Transfer of mitochondria from astrocytes to neurons after stroke. *Nature* **2016**, *535*, 551–555. [CrossRef]
30. Gorsky, A.; Monsour, M.; Nguyen, H.; Castelli, V.; Lee, J.-Y.; Borlongan, C.V. Metabolic Switching of Cultured Mesenchymal Stem Cells Creates Super Mitochondria in Rescuing Ischemic Neurons. *NeuroMolecular Med.* **2022**. [CrossRef]
31. Yan, W.; Diao, S.; Fan, Z. The role and mechanism of mitochondrial functions and energy metabolism in the function regulation of the mesenchymal stem cells. *Stem. Cell Res. Ther.* **2021**, *12*, 140. [CrossRef] [PubMed]
32. Bastianetto, S.; Menard, C.; Quirion, R. Neuroprotective action of resveratrol. *Biochim. Biophys. Acta* **2015**, *1852*, 1195–1201. [CrossRef]
33. Kahroba, H.; Ramezani, B.; Maadi, H.; Sadeghi, M.R.; Jaberie, H.; Ramezani, F. The role of Nrf2 in neural stem/progenitors cells: From maintaining stemness and self-renewal to promoting differentiation capability and facilitating therapeutic application in neurodegenerative disease. *Ageing Res. Rev.* **2021**, *65*, 101211. [CrossRef] [PubMed]
34. Liang, X.; Ding, Y.; Zhang, Y.; Tse, H.F.; Lian, Q. Paracrine mechanisms of mesenchymal stem cell-based therapy: Current status and perspectives. *Cell Transplant.* **2014**, *23*, 1045–1059. [CrossRef] [PubMed]
35. Lai, C.P.; Breakefield, X.O. Role of exosomes/microvesicles in the nervous system and use in emerging therapies. *Front. Physiol.* **2012**, *3*, 228. [CrossRef] [PubMed]
36. Garbuzova-Davis, S.; Haller, E.; Lin, R.; Borlongan, C.V. Intravenously Transplanted Human Bone Marrow Endothelial Progenitor Cells Engraft Within Brain Capillaries, Preserve Mitochondrial Morphology, and Display Pinocytotic Activity Toward Blood-Brain Barrier Repair in Ischemic Stroke Rats. *Stem. Cells* **2017**, *35*, 1246–1258. [CrossRef]
37. Babenko, V.A.; Silachev, D.N.; Popkov, V.A.; Zorova, L.D.; Pevzner, I.B.; Plotnikov, E.Y.; Sukhikh, G.T.; Zorov, D.B. Miro1 Enhances Mitochondria Transfer from Multipotent Mesenchymal Stem Cells (MMSC) to Neural Cells and Improves the Efficacy of Cell Recovery. *Molecules* **2018**, *23*, 687. [CrossRef]
38. Liu, K.; Guo, L.; Zhou, Z.; Pan, M.; Yan, C. Mesenchymal stem cells transfer mitochondria into cerebral microvasculature and promote recovery from ischemic stroke. *Microvasc. Res.* **2019**, *123*, 74–80. [CrossRef]
39. Pourmohammadi-Bejarpasi, Z.; Roushandeh, A.M.; Saberi, A.; Rostami, M.K.; Toosi, S.M.R.; Jahanian-Najafabadi, A.; Tomita, K.; Kuwahara, Y.; Sato, T.; Roudkenar, M.H. Mesenchymal stem cells-derived mitochondria transplantation mitigates I/R-induced injury, abolishes I/R-induced apoptosis, and restores motor function in acute ischemia stroke rat model. *Brain Res. Bull.* **2020**, *165*, 70–80. [CrossRef]
40. Zhuo, Y.; Chen, W.; Li, W.; Huang, Y.; Duan, D.; Ge, L.; He, J.; Liu, J.; Hu, Z.; Lu, M. Ischemic-hypoxic preconditioning enhances the mitochondrial function recovery of transplanted olfactory mucosa mesenchymal stem cells via miR-181a signaling in ischemic stroke. *Aging* **2021**, *13*, 11234–11256. [CrossRef]
41. Hosseini, L.; Karimipour, M.; Seyedaghamiri, F.; Abolhasanpour, N.; Sadigh-Eteghad, S.; Mahmoudi, J.; Farhoudi, M. Intranasal administration of mitochondria alleviated cognitive impairments and mitochondrial dysfunction in the photothrombotic model of mPFC stroke in mice. *J. Stroke Cerebrovasc. Dis.* **2022**, *31*, 106801. [CrossRef] [PubMed]
42. Park, J.; Park, H.-H.; Choi, H.; Seo Kim, Y.; Yu, H.-J.; Lee, K.-Y.; Joo Lee, Y.; Hyun Kim, S.; Koh, S.-H. Coenzyme Q10 protects neural stem cells against hypoxia by enhancing survival signals. *Brain Res.* **2012**, *1478*, 64–73. [CrossRef] [PubMed]
43. Kaneko, Y.; Tajiri, N.; Shojo, H.; Borlongan, C.V. Oxygen-glucose-deprived rat primary neural cells exhibit DJ-1 translocation into healthy mitochondria: A potent stroke therapeutic target. *CNS Neurosci. Ther.* **2014**, *20*, 275–281. [CrossRef]
44. Hayakawa, K.; Chan, S.J.; Mandeville, E.T.; Park, J.H.; Bruzzese, M.; Montaner, J.; Arai, K.; Rosell, A.; Lo, E.H. Protective Effects of Endothelial Progenitor Cell-Derived Extracellular Mitochondria in Brain Endothelium. *Stem. Cells* **2018**, *36*, 1404–1410. [CrossRef]

45. Gerdes, H.H.; Rustom, A.; Wang, X. Tunneling nanotubes, an emerging intercellular communication route in development. *Mech. Dev.* **2013**, *130*, 381–387. [CrossRef] [PubMed]
46. Torralba, D.; Baixauli, F.; Sanchez-Madrid, F. Mitochondria Know No Boundaries: Mechanisms and Functions of Intercellular Mitochondrial Transfer. *Front. Cell Dev. Biol.* **2016**, *4*, 107. [CrossRef]
47. Las, G.; Shirihai, O.S. Miro1: New wheels for transferring mitochondria. *Embo J.* **2014**, *33*, 939–941. [CrossRef]
48. Abdullahi, W.; Tripathi, D.; Ronaldson, P.T. Blood-brain barrier dysfunction in ischemic stroke: Targeting tight junctions and transporters for vascular protection. *Am. J. Physiol. Cell Physiol.* **2018**, *315*, C343–C356. [CrossRef]
49. Monsour, M.; Borlongan, C.V. The central role of peripheral inflammation in ischemic stroke. *J. Cereb. Blood Flow Metab.* **2023**, *0*, 271678X221149509. [CrossRef]
50. Clements, C.M.; McNally, R.S.; Conti, B.J.; Mak, T.W.; Ting, J.P. DJ-1, a cancer- and Parkinson's disease-associated protein, stabilizes the antioxidant transcriptional master regulator Nrf2. *Proc. Natl. Acad. Sci. USA* **2006**, *103*, 15091–15096. [CrossRef]
51. Fan, J.; Ren, H.; Jia, N.; Fei, E.; Zhou, T.; Jiang, P.; Wu, M.; Wang, G. DJ-1 decreases Bax expression through repressing p53 transcriptional activity. *J. Biol. Chem.* **2008**, *283*, 4022–4030. [CrossRef] [PubMed]
52. Russo, E.; Nguyen, H.; Lippert, T.; Tuazon, J.; Borlongan, C.V.; Napoli, E. Mitochondrial targeting as a novel therapy for stroke. *Brain Circ.* **2018**, *4*, 84–94. [CrossRef]
53. Borra, M.T.; Smith, B.C.; Denu, J.M. Mechanism of human SIRT1 activation by resveratrol. *J. Biol. Chem.* **2005**, *280*, 17187–17195. [CrossRef] [PubMed]
54. Chong, Z.Z.; Shang, Y.C.; Wang, S.; Maiese, K. SIRT1: New avenues of discovery for disorders of oxidative stress. *Expert. Opin. Ther. Targets* **2012**, *16*, 167–178. [CrossRef] [PubMed]
55. Liu, J.; He, J.; Huang, Y.; Hu, Z. Resveratrol has an Overall Neuroprotective Role in Ischemic Stroke: A Meta-Analysis in Rodents. *Front. Pharmacol.* **2021**, *12*, 795409. [CrossRef] [PubMed]
56. Wen, Y.; Li, W.; Poteet, E.C.; Xie, L.; Tan, C.; Yan, L.J.; Ju, X.; Liu, R.; Qian, H.; Marvin, M.A.; et al. Alternative mitochondrial electron transfer as a novel strategy for neuroprotection. *J. Biol. Chem.* **2011**, *286*, 16504–16515. [CrossRef]
57. Huang, S.; Du, F.; Shih, Y.Y.; Shen, Q.; Gonzalez-Lima, F.; Duong, T.Q. Methylene blue potentiates stimulus-evoked fMRI responses and cerebral oxygen consumption during normoxia and hypoxia. *Neuroimage* **2013**, *72*, 237–242. [CrossRef]
58. Enomoto, M.; Endo, A.; Yatsushige, H.; Fushimi, K.; Otomo, Y. Clinical Effects of Early Edaravone Use in Acute Ischemic Stroke Patients Treated by Endovascular Reperfusion Therapy. *Stroke* **2019**, *50*, 652–658. [CrossRef]
59. Kimura, K.; Aoki, J.; Sakamoto, Y.; Kobayashi, K.; Sakai, K.; Inoue, T.; Iguchi, Y.; Shibazaki, K. Administration of edaravone, a free radical scavenger, during t-PA infusion can enhance early recanalization in acute stroke patients-a preliminary study. *J. Neurol. Sci.* **2012**, *313*, 132–136. [CrossRef]
60. Tirilazad International Steering Committee. Tirilazad mesylate in acute ischemic stroke: A systematic review. *Stroke* **2000**, *31*, 2257–2265. [CrossRef]
61. Davalos, A.; Alvarez-Sabin, J.; Castillo, J.; Diez-Tejedor, E.; Ferro, J.; Martinez-Vila, E.; Serena, J.; Segura, T.; Cruz, V.T.; Masjuan, J.; et al. Citicoline in the treatment of acute ischaemic stroke: An international, randomised, multicentre, placebo-controlled study (ICTUS trial). *Lancet* **2012**, *380*, 349–357. [CrossRef] [PubMed]
62. Diener, H.C.; Cortens, M.; Ford, G.; Grotta, J.; Hacke, W.; Kaste, M.; Koudstaal, P.J.; Wessel, T. Lubeluzole in acute ischemic stroke treatment: A double-blind study with an 8-hour inclusion window comparing a 10-mg daily dose of lubeluzole with placebo. *Stroke* **2000**, *31*, 2543–2551. [CrossRef] [PubMed]
63. Gandolfo, C.; Sandercock, P.; Conti, M. Lubeluzole for acute ischaemic stroke. *Cochrane Database Syst. Rev.* **2002**, CD001924. [CrossRef]
64. Haley, E.C., Jr. High-dose tirilazad for acute stroke (RANTTAS II). RANTTAS II Investigators. *Stroke* **1998**, *29*, 1256–1257. [CrossRef]
65. Koziol, J.A.; Feng, A.C. On the analysis and interpretation of outcome measures in stroke clinical trials: Lessons from the SAINT I study of NXY-059 for acute ischemic stroke. *Stroke* **2006**, *37*, 2644–2647. [CrossRef]
66. Yamaguchi, T.; Sano, K.; Takakura, K.; Saito, I.; Shinohara, Y.; Asano, T.; Yasuhara, H. Ebselen in acute ischemic stroke: A placebo-controlled, double-blind clinical trial. Ebselen Study Group. *Stroke* **1998**, *29*, 12–17. [CrossRef] [PubMed]
67. Singh, A.; Kukreti, R.; Saso, L.; Kukreti, S. Oxidative Stress: A Key Modulator in Neurodegenerative Diseases. *Molecules* **2019**, *24*, 1583. [CrossRef]
68. Bernard-Marissal, N.; Medard, J.J.; Azzedine, H.; Chrast, R. Dysfunction in endoplasmic reticulum-mitochondria crosstalk underlies SIGMAR1 loss of function mediated motor neuron degeneration. *Brain* **2015**, *138*, 875–890. [CrossRef]
69. Chang, J.C.; Wu, S.L.; Liu, K.H.; Chen, Y.H.; Chuang, C.S.; Cheng, F.C.; Su, H.L.; Wei, Y.H.; Kuo, S.J.; Liu, C.S. Allogeneic/xenogeneic transplantation of peptide-labeled mitochondria in Parkinson's disease: Restoration of mitochondria functions and attenuation of 6-hydroxydopamine-induced neurotoxicity. *Transl. Res.* **2016**, *170*, 40–56 e43. [CrossRef]
70. Lee, M.; Ban, J.J.; Kim, K.Y.; Jeon, G.S.; Im, W.; Sung, J.J.; Kim, M. Adipose-derived stem cell exosomes alleviate pathology of amyotrophic lateral sclerosis in vitro. *Biochem. Biophys. Res. Commun.* **2016**, *479*, 434–439. [CrossRef]
71. Shi, X.; Zhao, M.; Fu, C.; Fu, A. Intravenous administration of mitochondria for treating experimental Parkinson's disease. *Mitochondrion* **2017**, *34*, 91–100. [CrossRef] [PubMed]

72. Nitzan, K.; Benhamron, S.; Valitsky, M.; Kesner, E.E.; Lichtenstein, M.; Ben-Zvi, A.; Ella, E.; Segalstein, Y.; Saada, A.; Lorberboum-Galski, H.; et al. Mitochondrial Transfer Ameliorates Cognitive Deficits, Neuronal Loss, and Gliosis in Alzheimer's Disease Mice. *J. Alzheimers Dis.* **2019**, *72*, 587–604. [CrossRef]
73. Cheng, X.Y.; Biswas, S.; Li, J.; Mao, C.J.; Chechneva, O.; Chen, J.; Li, K.; Li, J.; Zhang, J.R.; Liu, C.F.; et al. Human iPSCs derived astrocytes rescue rotenone-induced mitochondrial dysfunction and dopaminergic neurodegeneration in vitro by donating functional mitochondria. *Transl. Neurodegener.* **2020**, *9*, 13. [CrossRef]
74. Verma, A.; Shteinfer-Kuzmine, A.; Kamenetsky, N.; Pittala, S.; Paul, A.; Nahon Crystal, E.; Ouro, A.; Chalifa-Caspi, V.; Pandey, S.K.; Monsengo, A.; et al. Targeting the overexpressed mitochondrial protein VDAC1 in a mouse model of Alzheimer's disease protects against mitochondrial dysfunction and mitigates brain pathology. *Transl. Neurodegener.* **2022**, *11*, 58. [CrossRef] [PubMed]
75. Calkins, M.J.; Manczak, M.; Mao, P.; Shirendeb, U.; Reddy, P.H. Impaired mitochondrial biogenesis, defective axonal transport of mitochondria, abnormal mitochondrial dynamics and synaptic degeneration in a mouse model of Alzheimer's disease. *Hum. Mol. Genet.* **2011**, *20*, 4515–4529. [CrossRef] [PubMed]
76. Devi, L.; Ohno, M. Mitochondrial dysfunction and accumulation of the β-secretase-cleaved C-terminal fragment of APP in Alzheimer's disease transgenic mice. *Neurobiol. Dis.* **2012**, *45*, 417–424. [CrossRef] [PubMed]
77. Amadoro, G.; Corsetti, V.; Atlante, A.; Florenzano, F.; Capsoni, S.; Bussani, R.; Mercanti, D.; Calissano, P. Interaction between NH(2)-tau fragment and Aβ in Alzheimer's disease mitochondria contributes to the synaptic deterioration. *Neurobiol. Aging* **2012**, *33*, 833.e1–833.e25. [CrossRef] [PubMed]
78. Silzer, T.K.; Pathak, G.A.; Phillips, N.R. Mitochondrial tRNA methylation in Alzheimer's disease and progressive supranuclear palsy. *BMC Med. Genom.* **2020**, *13*, 71. [CrossRef] [PubMed]
79. Lampinen, R.; Belaya, I.; Saveleva, L.; Liddell, J.R.; Rait, D.; Huuskonen, M.T.; Giniatullina, R.; Sorvari, A.; Soppela, L.; Mikhailov, N.; et al. Neuron-astrocyte transmitophagy is altered in Alzheimer's disease. *Neurobiol. Dis.* **2022**, *170*, 105753. [CrossRef]
80. Zhang, W.; Wang, P.J.; Sha, H.Y.; Ni, J.; Li, M.H.; Gu, G.J. Neural stem cell transplants improve cognitive function without altering amyloid pathology in an APP/PS1 double transgenic model of Alzheimer's disease. *Mol. Neurobiol.* **2014**, *50*, 423–437. [CrossRef]
81. Ager, R.R.; Davis, J.L.; Agazaryan, A.; Benavente, F.; Poon, W.W.; LaFerla, F.M.; Blurton-Jones, M. Human neural stem cells improve cognition and promote synaptic growth in two complementary transgenic models of Alzheimer's disease and neuronal loss. *Hippocampus* **2015**, *25*, 813–826. [CrossRef]
82. Yue, W.; Li, Y.; Zhang, T.; Jiang, M.; Qian, Y.; Zhang, M.; Sheng, N.; Feng, S.; Tang, K.; Yu, X.; et al. ESC-Derived Basal Forebrain Cholinergic Neurons Ameliorate the Cognitive Symptoms Associated with Alzheimer's Disease in Mouse Models. *Stem. Cell Reports* **2015**, *5*, 776–790. [CrossRef] [PubMed]
83. Lill, C.M. Genetics of Parkinson's disease. *Mol. Cell Probes.* **2016**, *30*, 386–396. [CrossRef] [PubMed]
84. Paillusson, S.; Gomez-Suaga, P.; Stoica, R.; Little, D.; Gissen, P.; Devine, M.J.; Noble, W.; Hanger, D.P.; Miller, C.C.J. α-Synuclein binds to the ER-mitochondria tethering protein VAPB to disrupt Ca(2+) homeostasis and mitochondrial ATP production. *Acta Neuropathol.* **2017**, *134*, 129–149. [CrossRef] [PubMed]
85. Yue, M.; Hinkle, K.M.; Davies, P.; Trushina, E.; Fiesel, F.C.; Christenson, T.A.; Schroeder, A.S.; Zhang, L.; Bowles, E.; Behrouz, B.; et al. Progressive dopaminergic alterations and mitochondrial abnormalities in LRRK2 G2019S knock-in mice. *Neurobiol. Dis.* **2015**, *78*, 172–195. [CrossRef]
86. Ashrafi, G.; Schlehe, J.S.; LaVoie, M.J.; Schwarz, T.L. Mitophagy of damaged mitochondria occurs locally in distal neuronal axons and requires PINK1 and Parkin. *J. Cell. Biol.* **2014**, *206*, 655–670. [CrossRef]
87. Stevens, D.A.; Lee, Y.; Kang, H.C.; Lee, B.D.; Lee, Y.I.; Bower, A.; Jiang, H.; Kang, S.U.; Andrabi, S.A.; Dawson, V.L.; et al. Parkin loss leads to PARIS-dependent declines in mitochondrial mass and respiration. *Proc. Natl. Acad. Sci. USA* **2015**, *112*, 11696–11701. [CrossRef]
88. Prasuhn, J.; Davis, R.L.; Kumar, K.R. Targeting Mitochondrial Impairment in Parkinson's Disease: Challenges and Opportunities. *Front. Cell Dev. Biol.* **2020**, *8*, 615461. [CrossRef]
89. Fairley, L.H.; Grimm, A.; Eckert, A. Mitochondria Transfer in Brain Injury and Disease. *Cells* **2022**, *11*, 3603. [CrossRef]
90. Grealish, S.; Diguet, E.; Kirkeby, A.; Mattsson, B.; Heuer, A.; Bramoulle, Y.; Van Camp, N.; Perrier, A.L.; Hantraye, P.; Bjorklund, A.; et al. Human ESC-derived dopamine neurons show similar preclinical efficacy and potency to fetal neurons when grafted in a rat model of Parkinson's disease. *Cell Stem. Cell* **2014**, *15*, 653–665. [CrossRef]
91. Hallett, P.J.; Deleidi, M.; Astradsson, A.; Smith, G.A.; Cooper, O.; Osborn, T.M.; Sundberg, M.; Moore, M.A.; Perez-Torres, E.; Brownell, A.L.; et al. Successful function of autologous iPSC-derived dopamine neurons following transplantation in a non-human primate model of Parkinson's disease. *Cell Stem. Cell* **2015**, *16*, 269–274. [CrossRef] [PubMed]
92. Magrané, J.; Cortez, C.; Gan, W.B.; Manfredi, G. Abnormal mitochondrial transport and morphology are common pathological denominators in SOD1 and TDP43 ALS mouse models. *Hum. Mol. Genet.* **2014**, *23*, 1413–1424. [CrossRef] [PubMed]
93. Tagashira, H.; Shinoda, Y.; Shioda, N.; Fukunaga, K. Methyl pyruvate rescues mitochondrial damage caused by SIGMAR1 mutation related to amyotrophic lateral sclerosis. *Biochim. Biophys. Acta* **2014**, *1840*, 3320–3334. [CrossRef] [PubMed]
94. Goutman, S.A.; Savelieff, M.G.; Sakowski, S.A.; Feldman, E.L. Stem cell treatments for amyotrophic lateral sclerosis: A critical overview of early phase trials. *Expert Opin. Investig. Drugs* **2019**, *28*, 525–543. [CrossRef]

95. Chen, R.; Ende, N. The potential for the use of mononuclear cells from human umbilical cord blood in the treatment of amyotrophic lateral sclerosis in SOD1 mice. *J. Med.* **2000**, *31*, 21–30.
96. Garbuzova-Davis, S.; Willing, A.E.; Zigova, T.; Saporta, S.; Justen, E.B.; Lane, J.C.; Hudson, J.E.; Chen, N.; Davis, C.D.; Sanberg, P.R. Intravenous administration of human umbilical cord blood cells in a mouse model of amyotrophic lateral sclerosis: Distribution, migration, and differentiation. *J. Hematother. Stem. Cell. Res.* **2003**, *12*, 255–270. [CrossRef]

antioxidants

MDPI

Review

Bilirubin and Redox Stress in Age-Related Brain Diseases

John Paul Llido [1,2,3,†], Sri Jayanti [1,4,†], Claudio Tiribelli [1,*] and Silvia Gazzin [1]

[1] Liver Brain Unit "Rita Moretti", Italian Liver Foundation, Bldg. Q, AREA Science Park, Basovizza, 34149 Trieste, Italy; johnpaul.llido@fegato.it (J.P.L.); sri.jayanti@fegato.it or srij001@brin.go.id (S.J.); silvia.gazzin@fegato.it (S.G.)
[2] Department of Science and Technology, Philippine Council for Health Research and Development, Bicutan, Taguig City 1631, Philippines
[3] Department of Life Sciences, University of Trieste, 34139 Trieste, Italy
[4] Eijkman Research Centre for Molecular Biology, Research Organization for Health, National Research and Innovation Agency, Cibinong 16911, Indonesia
* Correspondence: ctliver@fegato.it; Tel.: +39-040-3757840
† These authors contributed equally to this work.

Abstract: Cellular redox status has a crucial role in brain physiology, as well as in pathologic conditions. Physiologic senescence, by dysregulating cellular redox homeostasis and decreasing antioxidant defenses, enhances the central nervous system's susceptibility to diseases. The reduction of free radical accumulation through lifestyle changes, and the supplementation of antioxidants as a prophylactic and therapeutic approach to increase brain health, are strongly suggested. Bilirubin is a powerful endogenous antioxidant, with more and more recognized roles as a biomarker of disease resistance, a predictor of all-cause mortality, and a molecule that may promote health in adults. The alteration of the expression and activity of the enzymes involved in bilirubin production, as well as an altered blood bilirubin level, are often reported in neurologic conditions and neurodegenerative diseases (together denoted NCDs) in aging. These changes may predict or contribute both positively and negatively to the diseases. Understanding the role of bilirubin in the onset and progression of NCDs will be functional to consider the benefits vs. the drawbacks and to hypothesize the best strategies for its manipulation for therapeutic purposes.

Keywords: Alzheimer's disease; dementia; sclerosis; schizophrenia; ataxia; therapy; brain cancers; NRF2; AHR; heme oxygenase

Citation: Llido, J.P.; Jayanti, S.; Tiribelli, C.; Gazzin, S. Bilirubin and Redox Stress in Age-Related Brain Diseases. *Antioxidants* **2023**, *12*, 1525. https://doi.org/10.3390/antiox12081525

Academic Editors: Ana-Maria Buga and Carmen Nicoleta Oancea

Received: 17 July 2023
Revised: 26 July 2023
Accepted: 27 July 2023
Published: 29 July 2023

1. Introduction

The redox status of the brain plays a relevant role in brain physiology and functioning, from regulating post-natal central nervous system (CNS) development to contributing to the diseases characterizing aging (e.g., Alzheimer's disease, Parkinson's disease, dementia, ataxia, tumors). Both direct oxidative damage and redox-induced alterations of cellular signaling (most of them shared with bilirubin and its metabolic enzymes) have been documented in the so-called physiologic senescence, when a reduction in the antioxidant capability and an increase in mitochondrial dysfunction, cytochrome C release, genome instability, and telomere attrition, are reported and contribute to the onset and progression of neurologic conditions and neurodegenerative diseases (NCDs) [1–5].

Bilirubin, a heme metabolite (Figure 1a), is not only a recognized powerful cellular antioxidant [6–8] but its level has been repeatedly correlated with the risk of developing chronic diseases typical of adult and eldered life (Figure 1c). Bilirubin is now considered as a biomarker of disease resistance, a predictor of all-cause mortality, and a molecule that may promote health in adults [9–12]. A large body of evidence comes from epidemiologic studies. A low total serum bilirubin (TSB) level (Figure 1b), with a possible cut-off of 0.4 mg/dL (0.7 uM), has emerged as a possible risk factor or as a biomarker for diseases characterized by oxidative impairment. Among them, the list of neurologic

and neurodegenerative diseases is long [11,12] (Figure 1c). The moderately elevated TSB present in Gilbert syndrome (GS) subjects, a population with genomic variants partly reducing the activity of the hepatic uridine diphosphate glucuronosyltransferase (UGT) 1A1 enzyme responsible for bilirubin conjugation (Figure 1a), has been correlated with a reduced prevalence of cardiovascular diseases (CVD), diabetes, metabolic syndrome, and certain cancers (Figure 1c) [9–11]. In agreement, GS subjects have increased antioxidant status (FRAP—ferric reducing ability potential), as well as reduced pro-oxidant and pro-inflammatory markers (apolipoprotein B—ApoB; C-reactive protein—CRP; interleukin—IL6; and IL1β) than normobilirubinemic subjects. In addition, a stronger protective effect in the fourth to the sixth decade of life was demonstrated [13]. Similarly, it has been suggested that a mild increase of TSB in neonates—the so-called physiologic hyperbilirubinemia leading to jaundice in 60–80% of newborns—may protect them from the oxidative challenge due to birth. In agreement, phototherapy, used to decrease the TSB level in severely hyperbilirubinemic neonates, has been reported to reduce the blood antioxidant capability [14–16]. On the contrary, a further increase in TSB may be toxic to the brain [17–20] (Figure 1c).

In addition to the "yin" and "yang" properties of serum bilirubin concentration, the presence of the enzymes involved in bilirubin metabolism (the yellow players—YPs, see Figure 2), has been reported in extra-hepatic cells, including the brain. At the cellular level, the YPs will not only produce but also recycle bilirubin. This recycling process accounts for the capability of nM amounts of bilirubin to counteract 10000 times higher amounts of reactive oxygen species (ROS) [6–8,21,22]. Additionally, YPs can act on multiple signaling pathways, enter the nucleus, activate the transcription of genes, and act as hormones, amplifying potential biologic functions. Moreover, the promoter of both HMOX1 and BLVRA possesses multiple binding sites for transcription factors (Figure 2a), making them ready to react on demand to stressors and inducers [3,9,11,12,23–44]. This finding definitively opened a new way of viewing the YPs as homeostatic factors and as part of the cellular defense system [12,23,45].

The YPs contribute to oxidative balance, antioxidant response, detoxification, the lowering of DNA damage and lipid peroxidation, and reducing mitochondrial dysfunction (Figure 2b). Due to bilirubin's lipophilic nature and its affinity for membrane lipids, a moderate level of bilirubin is known to act as an antioxidant complementary to the cytosolic GSH system in protecting transmembrane proteins and lipids from reactive oxygen species (ROS) and reactive nitrogen species (RNS) attack [7,21], and reducing the platelet prothrombotic phenotype [10] (see also Section 2.6). Moreover, bilirubin blunts inflammation by preserving the mitochondrial transmembrane potential, expressing cytochrome oxidase complex IV, blocking IL1β (interleukin 1 beta) release from macrophages, reducing the level of pro-caspase 1, and inhibiting the NLRP3 inflammasome [46] (see also Section 2.8).

The discussion on the advantages of modulating YPs or delivering exogenous bilirubin to tissues for therapeutic purposes is still ongoing. Of relevance to the discussion, bilirubin has already been used as a constituent on the shells of nanoparticles to exploit its anti-inflammatory and antioxidant properties [3,35,41–44,51,58,59]. On the other hand, excessive activation of YPs may worsen redox stress, mainly by increasing Fe^{2+} deposition at the site of the lesion and by disrupting the enzymatic activity of BLVRA (see later for details) [3,35,60]. Thus, the use of YPs for therapeutic purposes needs to be further explored and validated.

YPs are also involved in the level of neuronal calcium and glutamate balance by inhibiting excitotoxicity and acting on glucose and insulin homeostasis, lipid profile, cell energy, synaptic transmission and voltage control, circadian rhythms, immunity and inflammation, cell cycle, proliferation, differentiation, and apoptosis, and they are anti-microbial and can be used as a pain desensitizer (Figure 2b) [1,3,8,9,11,12,19,23–42,47–50]. The connections with the senescence of aging are strong. Moreover, in the context of NCDs, the YPs' antioxidant activity may be of particular importance due to the low intrinsic antioxidant defenses

of the CNS [4,51–53], combined with the lipid-rich environment requiring high levels of O2, making the brain prone to oxidative stress [2,4,54–57].

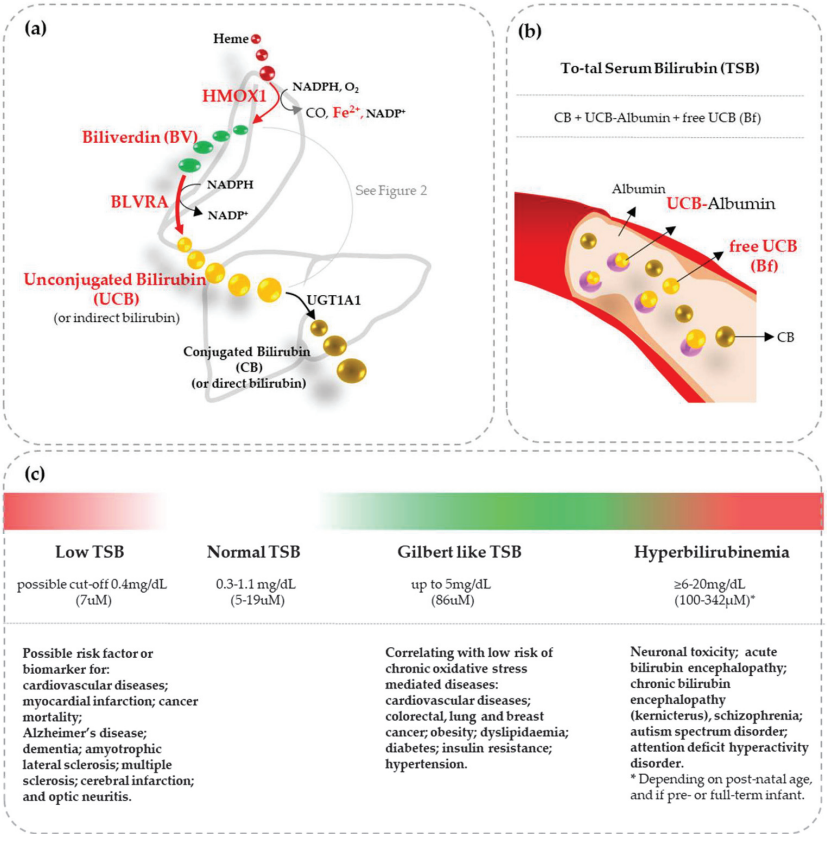

Figure 1. Bilirubin metabolism and clinical correlations among the blood bilirubin level and diseases. (**a**) Systemic bilirubin metabolism. Heme is oxidized to biliverdin (BV), a hydrophilic molecule, by the action of heme-oxygenase 1 (HMOX1), with the concomitant production of CO and Fe^{2+}. BV is then converted to bilirubin (at this point unconjugated bilirubin—UCB) by the action of biliverdin reductase A (BLVRA). UCB is highly hydrophobic and requires albumin to stay in solution in the blood and reach the liver. The liver is the deputy organ of body bilirubin clearance. In the liver, UCB is bound to glucuronic acid, becoming conjugated bilirubin (CB), by the action of the uridine diphosphate glucuronosyltransferase (UGT) 1A1 enzyme, making back CB hydrophilic, and easily excreted out the body in form of uro- and stercobilinogen. In red the most relevant to the review intermediated/enzymes. (**b**) The bilirubin species present in blood. Total serum bilirubin (TSB) accounts for UCB bound to albumin (or indirect bilirubin), CB (or direct bilirubin), and a minor part of UCB not bound to albumin (free bilirubin: Bf). Bf is the only circulating bilirubin that can diffuse across cellular bilayers and the blood-brain barrier entering the brain and the cells. When not differently stated, in this paper bilirubin means UCB, and we will focus only on the condition affecting it. (**c**) A resume of the correlation between TSB and chronic oxidative diseases (for references see text). Notably, the review focus on the changes in TSB due to UCB alterations. Reference on panel (**c**) "Low TSB": 9–12, 23, 48, 72, 176; "Gilbert like TSB": 9–13, 23, 48, 136, 145, 152, 153, 177, 220; and "Hyperbilirubinemia": 10, 17, 18, 20, 49, 50, 185–189, 193, 196, 197.

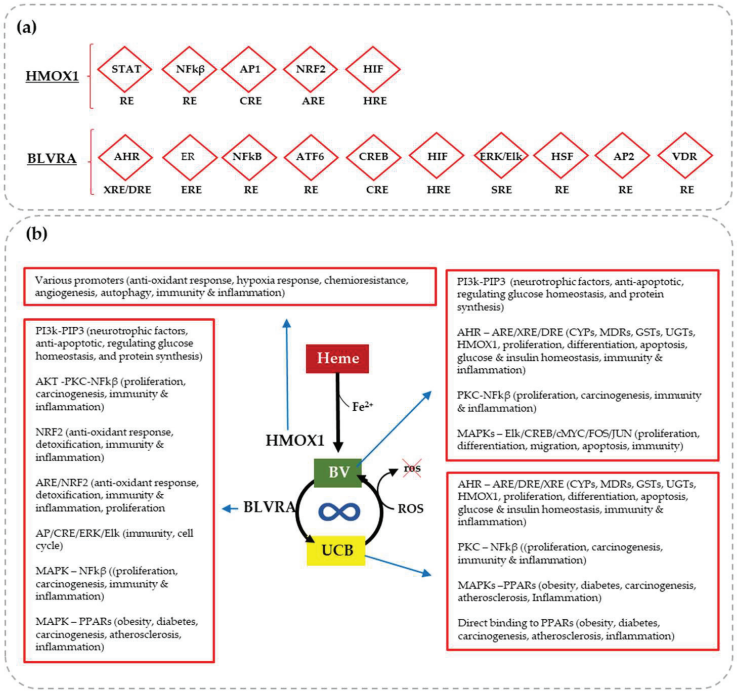

Figure 2. The yellow players (YPs) and their known biologic functions. (**a**) Both HMOX1 (heme oxygenase 1) and BLVRA (biliverdin reductase A) may react on demand under stressor thanks to the multiple binding sites for nuclear transcription factors on their promoter region. StRE: stress-responsive elements; STAT: signal transducer and activator of transcription; NFkβ: nuclear factor-kappa-B; RE: responsive element; AP1/2: AP2: activating enhancer binding protein; CRE: cAMP response elements; NRF2: NF-E2–related factor 2; ARE: antioxidant response elements; HIF: hypoxia-inducible factor; HRE: Hypoxia-responsive element; AHR: aryl hydrocarbon receptor; XRE/DRE: xenobiotic responsive element/DNA replication-related element; ER: estrogen receptor; ERE: estrogen responsive element; ATF6: activating transcription factor6; CREB: cyclic AMP response element binding protein; Elk/ERK: a member of ETS oncogene family/extracellular signal-regulated kinase; SRE: Serum Response Element; HSF: heat-shock factor; VDR: vitamin D receptor. (**b**) In turn, the YPs modulate numerous signaling pathways and transcription factors with potential effects on a plethora of biological functions relevant to the brain and to redox homeostasis. Heme: hemoglobin; BV: biliverdin; UCB: unconjugated bilirubin; ROS: reactive oxygen species (for references see text).

In this review, we will summarize the potential cross-play between redox imbalance in the age-dependent NCDs and the YPs, and discuss the pros and cons of their therapeutic modulation.

2. Oxidative Stress and the Role of Bilirubin in NCDs

2.1. Alzheimer's Disease (AD)

Alzheimer's disease (AD) is the most frequent neurodegenerative disease that causes gradual cognitive and memory deficits. Brain atrophy, amyloid-β (Aβ) plaques, and neurofibrillary tangles (NTF) in the brain are among the hallmarks of AD [61]. These features of AD are mainly induced by an imbalance between antioxidant defenses and the pro-oxidant status, either due to the increase of a free radical or the lack of antioxidants [62]. Protein carbonyls, lipid peroxidation, and RNA oxidation are increased in the human AD brain [63–65]. Oxidative stress is closely linked with pathological events in AD, including mitochondrial dysfunction,

impaired calcium homeostasis, metal dysregulation, protein misfolding, impaired autophagy, and inflammation. A single-cell transcriptomic study from an NFT-bearing neuron of the human AD brain revealed that oxidative phosphorylation and mitochondrial dysfunction are highly cell-type-dependent [66]. Oxidative stress leads to metabolic alterations in the AD brain, including glycolysis, calcium regulation, lipid metabolism, mitochondrial processes, and the activation of mTOR (mammalian target of rapamycin) complex 1, which results in reduced autophagy and the emergence of insulin resistance [67].

Both HMOX1 and BLVRA protein levels have been found to increase in the hippocampus of AD and mild-cognitive-impairment subjects. Belonging to the antioxidant cellular defense, their up-regulation has been interpreted as a reaction to the ongoing redox stress. Notably, the activity of BLVRA was decreased. The increased HMOX1 activity, combined with a decreased BLVRA activity, was suggested to lead to the accumulation of CO and iron, enhancing the nitrosative/oxidative stress and inducing changes in the BLVRA protein structure, leading to a non-functional enzyme and finally preventing the conversion of biliverdin into the cytoprotective bilirubin [60,68].

Low BLVRA activity has been demonstrated in an in vivo model of AD, where the reduction of BLVRA activity resulted in not only an increase in BACE1 phosphorylation (BACE1: beta-secretase 1, also known as beta-site amyloid precursor protein cleaving enzyme 1), which increased the Aβ deposits, but also in the induction of insulin resistance by down-regulating the insulin receptor (IR) and inhibiting insulin receptor substrate 1 (IRS1—illustrated in Figure 3), supporting the link between insulin resistance and AD pathology [69,70]. The modulation of BLVRA activity in insulin-mediated AD has been evaluated in a canine AD model in which subjects were treated with atorvastatin [69,70]. Atorvastatin increased BLVRA protein level and activity in the parietal cortex, followed by the increase of UCB, with a negative (protective) correlation with oxidative stress markers and cognition [70], confirming the intimate link between AD, redox stress, and the YPs. Also supportive of the molecular mechanisms of action of the YPs are the results obtained in the diet-induced obesity (DIO) mouse model. Bilirubin treatment induced a persistent improvement of insulin sensitivity and an increase in the expression of IR, SREBP1 (sterol regulatory element-binding protein), and PPARγ (peroxisome proliferator-activated receptor gamma) [71]. All of these are known targets of the bilirubin biological functions [11,12], implicating the possibility that UCB counteracts insulin resistance in AD.

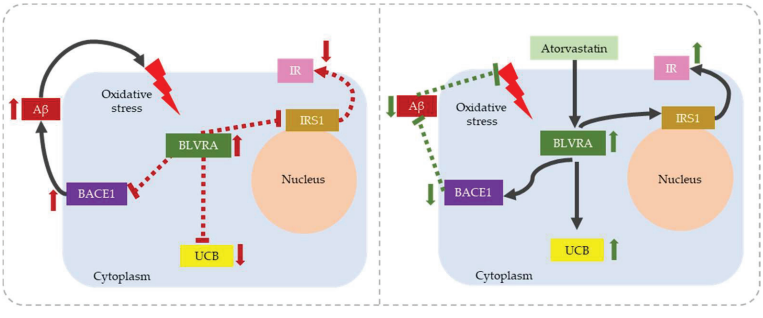

Figure 3. The role of BVRA in BACE-1 mediated insulin resistance in Alzheimer's disease. Left figure: Oxidative stress promotes BVRA protein modification leading to the increase of its protein level but decreasing its activity including BACE-1 phosphorylation which increases Aβ deposits and UCB production. BVRA impairment also limits IRS1 activation and down-regulates the insulin receptor. Right figures: Atorvastatin target BVRA by restoring its function and mediating the BACE-1 phosphorylation and increasing the production of UCB. Right figure: atorvastatin restores BLVRA function, prevents BACE phosphorylation, decreases Aβ deposits, and up-regulates the IR. Figures are adapted from Triani et al. [69] and Barone et al. [70]. BLVRA: biliverdin reductase A, the adult isoform of the enzyme, BACE1: β-site amyloid precursor protein cleaving enzyme 1, Aβ: amyloid beta, UCB: unconjugated bilirubin IR: insulin receptor, IRS: insulin receptor substrate 1.

In the clinic, TSB levels are reduced in AD patients, as they are in the majority of neurological diseases (Figure 1c) [72]. It is hypothesized that the transition from mild cognitive impairment to obvious AD is aided by reduced UCB concentration [73], pointing to the possible role of UCB in an early event of AD.

In the context of AD, increasing the level of bilirubin in the brain looks protective in three ways: (1) reducing redox stress; (2) reducing Aβ deposits; and (3) reverting insulin resistance.

2.2. Parkinson's Disease

Parkinson's disease (PD) is the fastest-growing neurological disorder and is characterized by tremors, rigidity, and bradykinesia due to dopaminergic neuron (DOPAn) loss in the substantia nigra. Nonmotor symptoms are also common [74,75]. Among the mechanisms involved in PD, oxidative stress has been recorded in both human samples and experimental models [76,77]. The deficiency and impairment of mitochondrial complex-I activity were found in postmortem studies, and the dopaminergic cell loss induced in animals by toxins and pesticides suggested acting by impairing mitochondrial function [78,79]. Moreover, neuro-inflammation, genetic involvement, and protein disruption that leads to α-synuclein aggregation are listed among the pathologic mechanisms of PD [80].

The hyperactivity of HMOX1 and BLVRA and their potential protection in PD have been reported in detail by Jayanti et al. [80]. In short, the overexpression of HMOX1 has been recorded both in human and PD models [3,81]. PD patients have significantly lower bilirubin/biliverdin ratios than controls, and the ratio is significantly linked with the disease severity [82,83], suggesting a disequilibrium among BV production/conversion to bilirubin and bilirubin production/consumption. TSB has been reported to be higher in the early stages, in patients with less-severe symptoms, and in patients with less need for levodopa (L-Dopa) [80], suggesting an early enhanced antioxidative potential [84]. Moreover, a decrease in TSB accompanies the progression to the late, more-severe stages of PD [80] (Figure 4). Even referring to the state-of-the-art, it is not known if the early increase and then the reduced level of TSB might be explained by the same mechanism of HMOX1/BLVRA activity described previously for AD [60].

Of relevance to the review, in a cellular model of PD, the use of BRUP1, an inducer of bilirubin production via the NRF2-HMOX1 axis (NRF2: nuclear factor erythroid 2-related), was found to counteract rotenone-induced neurotoxicity by suppressing ROS production and protein aggregation [85]. Supportive of this are the results of a recent study using a low-dose of bilirubin, which was able to prevent DOPAn loss in an organotypic brain culture model of the disease [86]. Even though the study found the involvement of oxidative stress in DOPAn demise, as well as the antioxidant activity of bilirubin by modulating the glutathione level, TNFα was demonstrated to be the determinant both in damage and bilirubin-conferred protection [86]. Of importance, redox stress and inflammation are intimately linked and the inhibition of one of them can repress the other [62,87]. Notably, the above-mentioned HMOX1 hyperactivation may enhance ROS production by iron accumulation, a well-known contributor in NCDs [88–90]. In this respect, supplying the brain with UCB may be an efficient and safe approach, as demonstrated by Jayanti et al. [86].

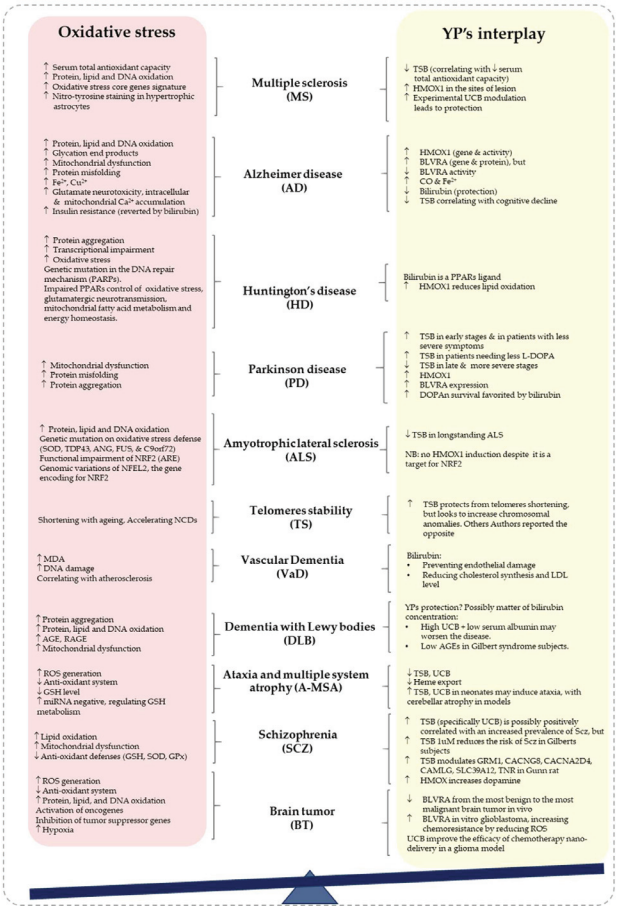

Figure 4. Cartoon summarizing the data on redox stress and YPs interplay in the context of the neurologic conditions. TSB: total serum bilirubin; UCB: unconjugated bilirubin; BVLRA: biliverdin reductase A; DOPAn: dopaminergic neurons; HMOX1: heme oxygenase 1; SOD: superoxide dismutase; TDP43: TAR DNA-binding protein 43; ANG: angiogenin; FUS: FUS RNA binding protein; C9orf72: chromosome 9 open reading frame 72 protein; NRF2: NFE2L2 NFE2 like bZIP transcription factor 2; ARE: antioxidant responsive elements; NFEL2: the gene encoding for the nuclear factor, erythroid 2; PPARs: peroxisome proliferator-activated receptor; AGE: advanced glycation end products; RAGE: receptor for advanced glycation end products; YPs: yellow players; ROS: reactive oxygen species; GSH: reduced glutathione; NCDs: neurologic and neurodegenerative diseases; NMDA: N-methyl-D-aspartate receptor; AHR: aryl hydrocarbon receptor; HMGCR: 3-hydroxy-3-methylglutaryl-CoA reductase; LDL: low density lipoprotein; Gpx: glutathione peroxidase; GRM1: metabotropic glutamate receptor 1; CACNG8: calcium voltage-gated channel auxiliary subunit gamma 8; CACNA2D4: alpha-2/delta voltage-dependent calcium channel; CAMLG: calcium modulating ligand; SLC39A12: solute carrier 39 member 12; TNR: tenascin receptor. References used: Oxidative stress/YP's interplay. MS, multiple sclerosis: 52, 93–96/97–101. AD, Alzheimer disease: 63–67/60, 68–70, 72, 73. HD, Huntington's disease: 126–128, 133, 134/12, 135–137, PD, Parkinson's disease: 76–80/3, 80–83, 85, 86. ALS, amyotrophic lateral sclerosis: 105–107, 110–115, 117–119/120–123. TS, telomere stability: 216, 217/218–220. VaD, vascular dementia: 149–151, 155/9, 136, 152, 153, 156–158. DLB, dementia with Lewy bodies: 139–143/144, 145. A-MSA, ataxia and multiple system atrophy: 201/32, 37, 202. SCZ: schizophrenia: 164–172/173–177, 185–190. BT, brain tumors: 207–209, 212, 213/210, 211, 214, 215.

2.3. Multiple Sclerosis (MS)

Multiple sclerosis (MS) is mainly referred to as a chronic inflammatory immune-mediated disease. MS patients can develop motor, sensory, and cognitive impairments depending on the location of demyelinating lesions [91]. Due to MS's inflammatory nature, targeting the immune response is the most widely used therapeutic approach but none of the drugs currently used prevents or counteracts progressive neurological deterioration [92].

Several pieces of evidence have linked oxidative damage with MS pathology [93]. Oxidized protein, lipids, and DNA are frequently present in MS plaques and are linked to oligodendrocyte apoptosis and neuronal death in the brains of MS patients [94,95]. In 2020, the relationship between oxidative stress and neuro-inflammation in MS was provided through a single-cell RNA-seq transcriptional profiling strategy in an experimental autoimmune encephalomyelitis (EAE) animal model of the disease. The study revealed that the resident immune cells, as well as the infiltrating monocyte/macrophage clusters, shared an oxidative stress core-gene signature (e.g., CYBB: cytochrome b-245 beta chain; NCF2: neutrophil cytosolic factor 2; NCF4: neutrophil cytosolic factor 4, all of them a sub-unit of the NADPH oxidase; and GPx1: glutathione peroxidase 1) [96] (Figure 4).

Studies on bilirubin protection in EAE started with the induction of HMOX1 and BLVRA, which led to a reduction in the symptoms as well as the inflammatory manifestation in the spinal cords of EAE animals [97,98]. Liu et al. then demonstrated that bilirubin prevents EAE by alleviating oxidative injury [99]. In the clinic, a reduction of TSB is often reported in MS subjects [72]. Notably, MS patients were found to have significantly lower serum total antioxidant capacity, and antioxidant capability is associated with disease severity [100], stressing the potential correlation between bilirubin, the antioxidant defense, and MS. Additionally, higher (more similar to control) TSB was found to be significantly correlated with lower disability status, lower MRI lesions, and shorter disease duration [101]. In the brain, hypertrophic astrocytes and foamy macrophages on the site of the lesion presented an increased nitrotyrosine staining, indicative of redox stress [52,94]. HMOX1 was up-regulated in the microglia—the resident macrophages [94].

Altogether these data show not only a tight link between inflammation and oxidative stress in MS but support the protective role of bilirubin in this condition. Therefore, next to the anti-inflammation and immune-modulator approach, targeting oxidative stress with UCB may provide more benefits. Final data on the pros and cons of the possible alternatives available deserve further, targeted evaluations, to achieve our goal.

2.4. Amyotrophic Lateral Sclerosis (ALS)

Amyotrophic lateral sclerosis (ALS) is a motor neuron disease (MND) characterized by progressive and painless muscle weakness due to the degeneration of both upper and lower motor neurons [102]. The disease is rare and is usually diagnosed late because of its clinical presentation heterogeneity and its similarity with other neurological diseases [103]. Death generally occurs 4 years after diagnosis due to respiratory failures [104]. Exposure to environmental factors, including electromagnetic fields, solvents, heavy metals, and pesticides has been linked with enhanced oxidative stress in ALS [105].

Since the life expectancy of ALS patients is relatively short, it is impossible to evaluate oxidative stress biomarkers over a long period. Nevertheless, an increasing number of studies have reported the elevation of protein and lipid oxidation levels, as well as DNA damage from various sample sources, including post-mortem neuronal tissues [106,107] and CSF [108,109], as well as plasma and urine from ALS patients [110]. Indeed, mutations in genes involved in oxidative stress defense have been reported in ALS cases, among them: superoxide dismutase 1 (SOD1), transactive response (TAR)-DNA binding protein (TARDBP, previously called TDP43—possibly by sequestrating miRNA and proteins relevant to mitochondrial functioning and leading to redox stress—[111]), angiogenin (ANG—involved in cell survival against oxidative stress [112,113]), fused-in sarcoma RNA binding protein (FUS—regulating the transcription of oxidative stress protein protection genes [114,115], and chromosome 9 open reading frame 72 (C9ORF72—associated with redox, mitochondrial, and NRF2 pathway

imbalance [105,116]). Most of them play their biological action by the transcription factor NRF2. NRF2 modulates redox homeostasis by activating the antioxidant response elements (ARE) system and up-regulating the gene expression of multiple antioxidants, including genes involved in glutathione homeostasis such as cysteine uptake transporter (xCT), glycine uptake transporter (GLY1), and γ-glutamyl-cysteine ligase catalytic and modulatory subunits (γ-GCL-c and γ-GCL-m, respectively) (Figure 4) [29]. For this reason, NRF2 has been considered a therapeutic target both in preclinical and clinical trials of ALS [116]. Nevertheless, the aim of modulating NRF2 as a therapy is hampered by its malfunctioning [117,118]. Genomic variations of NFEL2, the gene encoding for NRF2, have been associated with ALS risks and disease onset [119].

The progressive decrease of TSB level associated with the duration of ALS [120] and the absence of HMOX1 up-regulation despite the induction of NRF2/ARE [121,122] support gene malfunction. Notably, NRF2 is also a major inducer of HMOX1 [29], and the activation of the NRF2/HMOX1 pathway exerts neuroprotection in ALS in vivo models, where the pathway is fully functional [123], supporting the bilirubin-mediated protection in ALS.

The impossibility of modulating HMOX1 as a therapy in the clinic points to the need to deliver bilirubin in the brain in ALS patients. Alternatively, HMOX1 inducers via different signaling pathways (Figure 2) must be developed/used.

2.5. Huntington's Disease (HD)

Huntington's disease (HD) is an autosomal dominant neurological condition characterized by the expansion of CAG trinucleotide repeat in the gene encoding the huntingtin protein [124,125]. The mutant huntingtin protein disrupts cellular processes, inducing protein aggregation, transcriptional impairment, oxidative stress, and inflammation [126], leading to neurotoxicity (Figure 4). A GWAS study has identified the involvement of genes belonging to the DNA damage-repair system in HD triggered by the presence of ROS [127]. The production of PAR (poly APD-ribose) by PARPs is one of the first steps in the repair of DNA damage. The increase of PARP1 (PAR polymerase-1) and damaged DNA have been detected in the caudate nucleus of severely affected HD brains [128]. Therefore, targeting PARPs is probably one of the promising treatment strategies for HD [129–132]. PPARα has been identified as a substrate of PARP1 [133]. In addition to controlling energy homeostasis, mitochondrial fatty acid metabolism, excitatory glutamatergic neurotransmission, and also cholinergic/dopaminergic signaling in the brain, PPAR-α also regulates oxidative stress, energy balance, and fatty acid metabolism (Figure 4) [134].

Bilirubin is a direct ligand for PPAR-α, activating its pathway and increasing gene responsiveness [12,135,136]. The induction of HMOX1 has been demonstrated in an in vivo model of HD to be protective by reducing lipid oxidation, inducing antioxidants, and ameliorating inflammation [137], suggesting the protective role of UCB as the end product of HMOX1, through the PARP pathway. Moreover, the pharmacologic modulation of HMOX1 ameliorated the increased lipid peroxidation, nitrite concentration, and decreased endogenous antioxidants, with an improvement of the behavior, especially when combined with lithium chloride administration [137]. Data are still too few to draw a sound conclusion, but an enhancement of YP activity looks to be a promising therapeutic option.

2.6. Dementia with Lewy Bodies (DLB)

Dementia with Lewy bodies (DLB) is the second-most-frequent type of dementia after AD, and its typical symptoms include visuoperceptual dementia, which manifests as visual hallucinations, attention disturbances, and Parkinsonism [138]. Amyloid deposition, α-synuclein aggregates, and neuronal loss are among the pathological features of DLB [139,140]. Similar to AD, oxidative stress and mitochondrial dysfunction play a role in DLB pathogenesis. Protein and lipid oxidation as well as DNA damage are significantly increased in the parietal and temporal lobe cortex of DLB patients [141]. Moreover, lipo-oxidation, advanced glycation (AGE), and AGE receptor (RAGE) protein levels are up-regulated in the SN and frontal cortex in the early stages of DLB [142]. Meanwhile,

mitochondrial dysfunction is marked by low mitochondrial oxygen uptake and complex I activity in the brain cortex of DLB subjects (Figure 4) [143].

Zhong et al. reported an increased blood level of unconjugated bilirubin and low albumin concentration in DLB patients and suggested a worsening role of bilirubin in dementia as it enhances αβ deposition in the brain; this was supported by their in vitro experiments [144]. On the contrary, Kalousovà recorded low plasma levels of AGEs, particularly pentosidine and nepsilon carboxymethyl lysine, in GS subjects, in agreement with bilirubin-induced antioxidant protection [145]. To the best of our knowledge, data on the prevalence of DLB in the GS population, on HMOX1 and BLVRA expression, or on activity in DLB patients are not available, thus preventing conclusions from being made. Additional research is needed to understand whether the modulation of YPs might be beneficial or not in DLB.

2.7. Vascular Dementia (VaD)

Vascular dementia (VaD) is an umbrella term comprising dementia, caused by a large group of heterogeneous vascular brain lesions [146]. Cognitive alterations in VaD are different than in AD and are highly dependent on the neuronal region affected by vascular pathology [147]. VaD can be caused directly by having a stroke due to small vessel diseases such as cerebral micro-bleeds and cerebral micro-infarct, which is associated with atherosclerosis (fatty deposits accumulate to restrict vascular luminal diameter) formation [148]. The involvement of oxidative stress in VaD has been marked by the increase of malonaldehyde (MDA, a lipid peroxidase marker) and the oxidative DNA damage repair markers (e.g., SOD, CAT, GPx, GR, and/or oxo-guanine) in CSF and urine of VaD subjects (Figure 4) [149,150]. A 20-year prospective study revealed the association between atherosclerosis with the development of VaD [151].

Even if studies on the correlations between VaD and YPs are not available, bilirubin is known to be an anti-atherogenic molecule modifying cholesterol oxidation [152] and inhibiting cholesterol synthesis [153], thus reducing plaque formation [153]. Moreover, the antioxidant activity of bilirubin at the cellular membrane level has been reported to reduce the mean platelet volume and hyper-reactivity, as well as the prothrombotic phenotype, which is of possible relevance to VaD [10]. Bilirubin also affects AHR (aryl hydrocarbon receptor), a ligand-activator transcription factor. AHR is overexpressed in human atherosclerosis vessels [154] and is known to mediate oxidative stress and inflammation in atherosclerosis [155]. Interestingly, the activation of AHR by bilirubin is believed to have an athero-protective effect [9,136,156] via an anti-inflammatory action [157,158]. This confirms the complexity of the AHR pathway and supports the anti-atherogenic roles of bilirubin in VaD. Notably, due to the systemic nature of VaD, the increase of TSB might be a practicable approach.

2.8. Schizophrenia (Scz)

Schizophrenia (Scz) is a serious mental disorder characterized by the impaired perception of reality and corresponding changes in behavior [159,160]. Symptoms include psychosis (hallucinations, delusions, thought disorder, movement disorder) and negativity (loss of motivation, loss of interest or enjoyment in daily activities, withdrawal from social life), and are cognitive (attention, concentration, and memory) [161–163].

The role of oxidative stress in schizophrenia has been well-described, and several pathophysiological mechanisms including lipid peroxidation-induced neuronal damage, reduced antioxidant defenses, redox dysregulation of transcriptional factors, noncoding RNAs, epigenetic mechanisms, mitochondrial dysfunction, neurotransmitter alterations (e.g., glutamate, dopamine), metabolic abnormalities, and genetic variants associated with the previous mechanisms (e.g., on GSTs; glutathione cysteine ligase –GCL; Cacna1c—calcium voltage-gated channel subunit alpha1 C) have been documented (Figure 4) [164–172].

The correlation between TSB and Scz is debated [173]. Becklén et al. found a reduced TSB level in first-episode psychosis Scz patients (FEP, average 0.64 mg/dL) with respect to healthy subjects (average 0.88 mg/dL). The lower TSB was associated with a longer

duration of the untreated psychotic crisis. The author hypothesizes that the decreased bilirubin level resulted in reduced antioxidant protection [174]. Further supporting the role of bilirubin in Scz is the observation of a higher level of the pigment in patients in relapse (0.38 mg/dL) versus partial remission (0.34 mg/dL) [175]. Other studies reported a higher frequency of Scz in GS subjects where TSB is higher, suggesting either that a higher concentration of the pigment is a cofactor of the diseases or the existence of a genetic sub-type of Scz [176]. The last hypothesis might explain the opposite results obtained by Vitek et al., who reported in GS subjects a lower risk of Scz by up to 19% [177]. The causal connection between the pigment and Scz is not understood, and more studies are required. Of relevance, at high levels, bilirubin is known to bind to cellular membranes and modify their fluidity, interfering with mitochondrial cellular respiration and inducing a cellular energetic crisis and the production of ROS [178–180]. Moreover, highly elevated bilirubin activates microglia and the NLRP3 inflammasome and induces the release of pro-inflammatory molecules and glutamate, causing calcium imbalance, affecting neurotransmission, cellular division and differentiation, migration and myelination [10,49,181]. Furthermore, low physiologic concentrations of bilirubin have been reported to inhibit the inflammasome and related cytokine release in in vitro experiments on macrophages [182]. The relevance to microglia, the CNS resident macrophages, is not known. Notably, Scz is also considered a neurodevelopmental disease. In the neurodevelopmental hypothesis of Scz, perinatal challenges alter the synaptic formation and/or functioning, leading to manifestations at an adult age [183,184]. It is noteworthy to mention that the frequency of Scz is higher in subjects experiencing neonatal hyperbilirubinemia [185–189]. Alterations of schizophrenia-associated genes (GRM1—metabotropic glutamate receptor 1; CACNG8—calcium voltage-gated channel auxiliary subunit gamma 8; CACNA2D4—voltage-dependent calcium channel complex alpha-2/delta subunit; CAMLG—calcium modulating ligand; SLC39A12—solute carrier family 39 member 12; and TNR—tenascin R) were reported in the Gunn rat [190]. All of them are involved in the formation of the synaptic circuits, supporting the concept of Scz as neurodevelopmental disorder [191–193]. Moreover, most of these genes belong to the glutamate system, with glutamate perturbation being a shared characteristic of Scz and bilirubin-induced neurotoxicity [194–197]. This supports the interplay of excitotoxicity, calcium, and mitochondria in the triad in synaptic neurodegeneration [198].

In conclusion, the interplay of Scz and bilirubin is still confusing due to the lack of relevant information on the threshold of bilirubin differentiating protection from toxicity. Focused studies are needed to unravel the role of YPs in Scz and suggest their therapeutic application.

2.9. Ataxia and Multiple System Atrophy (A-MSA)

Ataxia (A-) is a group of symptoms of poor muscle control that usually results from cerebellar or brainstem damage, which can cause problems with walking, balance, coordination, speech, and eye movements [199,200]. Although the causes, onset, and progression of ataxia remain to be fully understood, oxidative stress via the excess generation of ROS and/or disruption of the antioxidant system results in cellular damage (Figure 4) [201]. It has to be mentioned that HMOX1 hyper-activation and Fe^{2+} accumulation have been reported to contribute to specific forms of ataxia, namely Friedreich and posterior column sensory ataxia [32,37]. TSB, namely UCB, was significantly lower, while homocysteine level, an oxidant biomarker, was higher in multiple system atrophy (MSA) patients than in healthy controls [202]. These data are essential because they simultaneously support the inverse correlation between TSB and a pro-oxidant status (homocysteine) and support bilirubin as a systemic antioxidant effector. In addition, the negative correlation between a low UCB and the presence of MSA indicates that bilirubin is a predictor, risk factor, or marker for developing the disease.

Solid clinic and research data are still needed, but the preliminary information suggests that the supplementation of bilirubin appears to be a safe and indiscriminate approach to treating A-MSA.

2.10. Brain Tumors in the Elderly

Brain tumorigenesis is favored in the elderly population by a progressive decrease of the antioxidant mechanisms, increasing the susceptibility to developing genetic mutations, oncogene activation, loss of tumor-suppressor gene function, angiogenesis, and a microtumor environment [203–206] (Figure 4).

The malignancy and response to treatments strongly depend on the delicate equilibrium between the oxidant and antioxidant environment of the tumor [207–209]. Meningiomas and low- and high-grade gliomas—the two most common brain cancers—present an increased protein and lipid peroxidation level and a decreased antioxidant capacity compared to control samples.

The BLVRA level was reduced, with a decreasing trend from the most-benign to the most-malignant brain tumors, in agreement with the increased pro-oxidant status of the cancer cells. The correlational studies among BLVRA expression and redox markers revealed a negative correlation with the advanced oxidation protein products; but a positive correlation with the ferric-reducing antioxidant power [210]. Due to the well-known antioxidant actions of the YPs, BLVRA down-regulation in brain tumors has been suggested as a biomarker [210]. Moreover, the induction of a hypoxia-mediated pro-oxidant environment in a human glioblastoma cell line was reported to enhance chemoresistance. BLVRA level was also up-regulated. Depletion of the BLVRA gene enhanced chemoresistance and intracellular ROS levels, supporting the protective role of the YP's induction as an antioxidant [211]. Chemotherapy efficacy is also limited by the low brain/tumor accessibility due to multidrug resistance transporters (MDRs), Pgp (P-glycoprotein), and BCRP (breast cancer resistance protein) expressed at the blood–brain barrier and in glioblastoma cells [212,213]. Both transporters are up-regulated by bilirubin [214,215].

Further information is needed before we are able to balance the two opposite effects. The successful delivery of UCB pegylated nanoparticles loaded with chemotherapeutic agents to glioma in mice offers preliminary data on a promising approach [51].

2.11. Telomere Stability in Neurodegeneration

Aging can also be considered as the accumulation of senescent cells contributing to body dysfunction. Telomeres—the genomic portions of TTAGGG repeats located at the ends of linear chromosomes—are bound and protected by a sheltering protein complex from being recognized as DNA damage that triggers a DNA damage response. Standard DNA polymerases replicate DNA templates without telomerase and nucleolytic processing generates chromosomes with progressively shortened telomeres after DNA replication. Beyond the critical length and stability, telomeres bind fewer capping proteins and are sensed as exposed DNA ends and misinterpreted as DNA damage, resulting in cell cycle inhibition and arrested proliferation. Telomere dysfunction, together with mitochondrial dysfunction (another hallmark of ageing) and oxidative stress, may accelerate the progression of neurodegenerative disorders like PD and AD [216,217] (Figure 4).

A significant positive association exists between mildly increased TSB and telomere length (TL) [218], similar to the longer telomeres observed in male individuals with mildly elevated bilirubin (GS), as well as in Gunn rats [219]. While a decrease of the nuclear anomalies reflecting DNA instability were reported in older individuals with GS, suggesting a protective effect of bilirubin against the consequence of variation in the genetic material [220], the opposite (increased chromosomal anomalies such as nucleoplasmatic bridges and nuclear buds) were observed in an animal model [219].

The discrepancy may be due to the bilirubin level, the duration of the challenge, or the model per se (human vs. rat).

3. Bilirubin as a Therapy

As we have discussed the potential of bilirubin's protective role in oxidative stress-mediated neurological diseases (Figure 4 and Table 1), the next question should be how we modulate bilirubin to reach a neuroprotective concentration.

Table 1. The main biomolecular effects of the YPs.

	Heme	HMOX	Fe^{2+}	BV	BLVR	UCB
Changes During Disease	Accumulating in the site of lesion	Usually induced (chemical induction, inhibition, and Ko models frequently used to assess its biologic and pathologic functions)	Increased as part of BBB breakdown, hemorrhage and HMXO1 induction.	Rarely quantified. Suddenly added to model of diseases to assess its functions.	Usually induced (with possible induction of defects in its enzymatic activity in high redox stress environment). Fewer chemical inducers/inhibitors are available to assess its functions. KO models are seldom used for this purpose.	TSB: both increased and decreased. Supposed to be increased if HMXO and BLVR induced Seldom added to models of diseases to assess its functions.
Target and Effect	Protective Reducing apoptosis and inducing SOD and HMOX1, mitochondrial functions and cytochrome C release, and ferritin production [30,31,137]. Enhancing redox stress and heme release, protein and lipid oxidation, metalloproteinases release and tissue damage, inhibiting the antioxidant response through NRF2, and impairing the proteasome and unfolded protein response, inducing mitochondrial dysfunctions and mitophagy and apoptosis (Frederic ataxia, posterior column ataxia, neurodegenerative diseases) [32,37].	Protective Reducing redox stress, increasing survival, inducing the transcription of the stress response genes, reducing lipid peroxidation [89] and inducing the synthesis and release of GSH [137]. Promoting proliferation and neuronal survival via PI3K/Akt/BDNF signaling, even migrating into the nuclei and acting as a transcription factor [9,11] (AD, PD, ischemia, HD [38]). Improving glutamate neurotoxicity, mitochondrial damage [137]. Antioxidant (by producing BV, UCB, and acting as a transcriptional factor [9,11]). Potentially dangerous if excessively induced (AD, PD, SCZ, Stroke, trauma [3,60]). Increasing cholesterol and products of cholesterol oxidation [99]. Increasing Fe^{2+} production in turn enhancing DNA damage, cell bioenergetic failure, mitophagy and autophagy, oxidizing catecholamine [3,60].	Damaging Worsening redox stress, enhancing protein and lipid oxidation, and DNA damage. Reducing SOD activity, inducing a cell bioenergetic failure, apoptosis, neuronal autophagy, damaging the BBB (via NFkβ, AP1) [32,89].	Protective Levering DNA damage (possibly by scavenging ROS directly or after conversion into UCB [27]), inducing BLVR translocation into nucleus [9,11], with multiple anti-inflammatory actions [9,11].	Protective Protective in meningioma and glioma [220], and EAE [98]. Modulating Tau deposition [43]; enhancing neuronal and synaptic plasticity (MAPK/PI3k) [60], Reducing apoptosis (MAPK/Akt [9,11]) Activating the stress responses gene (including HMOX) [29], ameliorating insulin brain resistance [70]. Inducing chemoresistance [211]. Missed Protection Missed protection in AD (gene up, activity down [60,68,73]).	Protective Protective (EAE, PD, stroke, ischemia, traumatic brain injury, cerebral atherosclerosis, glioma, etc. [11,51,86,99]). Activating the antioxidant response (NRF2 [29]); boosting survival and repair (AKT/CREB/BDNF [9,11]); increasing mitochondrial respiration, AMPA and Ca channels [11]; enhancing the transcription of the detoxification system (CYPs, UGT, by MAPK/NRF2) [11,156], inhibiting NMDA excitotoxicity and related neuronal death [28] Damaging Responsible for acute and chronic bilirubin encephalopathy (kernicterus), and suggested increasing the risk of ADHD, SCZ, autism [194], by inducing a plethora of mechanism (among them oxidative stress, apoptosis, glutamate neurotoxicity, inflammation, epigenetic alterations of brain development, reduced myelinating, cell death, ca imbalance, etc. [49,194]).

The first way is by inducing the systemic concentration of total serum bilirubin by HMOX1 inducers [41,107,221–223]. HMOX1 is easily induced by clinically used drugs with a recorded increase of TSB (e.g., some NSAIDs and hypolipidemic agents) [58]. This method will unfortunately provide no control regarding the amount of UCB that can enter the brain.

The second option is to enhance the UCB production in the brain by inducing HMOX1 locally. However, the activation of HMOX1 is followed by the increase of its side products, including iron, which will add more harm to already pre-existing HMOX1 hyper-activation in several neurological diseases [3,35,72].

The third option is to deliver the desired amount of UCB into the brain and, even better, into the targeted region. It is not an easy task, and the use of nanoparticles may be a solution [224–226]. The use of bilirubin nanoparticles has been studied in glioma in mice [51]. Interestingly, the future application of advanced technology such as the magnetic nanoparticle can be a sophisticated tool given the possibility to control the delivery in a paramagnetic field [227–229]. Further studies are needed to reach the use of UCB at this point.

4. Conclusions

A considerable amount of evidence suggests that bilirubin might be beneficial to the redox imbalance ongoing in aging. This supports the idea that increasing its level could be a prophylactic or therapeutic approach, although the modulation of YPs in the brain might also results in side effects. We still have a long way to go, but it is indubitable that bilirubin looks a very promising natural compound for use in the treatment of several NCDs.

Author Contributions: Conceptualization, S.J., J.P.L., C.T. and S.G.; writing—original draft preparation, S.J., J.P.L., C.T. and S.G.; writing—review and editing, S.J., J.P.L., C.T. and S.G.; visualization, S.J. and S.G.; All authors have read and agreed to the published version of the manuscript.

Funding: This research was funded in part by an internal grant of Fondazione Italiana Fegato (S.G.; C.T.; and in part J.P.L); in part by the Department of Science and Technology through the Philippine Council for Health Research and Development (DOST-PCHRD) (J.P.L); in part by a post-doctoral fellowship supported by National Research and Innovation Agency of Indonesia (S.J.).

Conflicts of Interest: The funders had no role in the design of the study; in the collection, analyses, or interpretation of data; in the writing of the manuscript; or in the decision to publish the results.

References

1. Kumar, A.; Yegla, B.; Foster, T.C. Redox Signaling in Neurotransmission and Cognition During Aging. *Antioxid. Redox Signal.* **2018**, *28*, 1724–1745. [CrossRef] [PubMed]
2. Gemma, C.; Vila, J. Oxidative Stress and the Aging Brain: From Theory to Prevention. In *Brain Aging: Models, Methods, and Mechanisms*; Riddle, D.R., Ed.; Frontiers in Neuroscience; CRC Press/Taylor & Francis: Boca Raton, FL, USA, 2007.
3. Schipper, H.M.; Song, W. The Sinister Face of Heme Oxygenase-1 in Brain Aging and Disease. *Prog. Neurobiol.* **2019**, *172*, 40–70. [CrossRef] [PubMed]
4. Finkel, T.; Holbrook, N.J. Oxidants, Oxidative Stress and the Biology of Ageing. *Nature* **2000**, *408*, 239–247. [CrossRef] [PubMed]
5. Terracina, S.; Petrella, C. Antioxidant Intervention to Improve Cognition in the Aging Brain: The Example of Hydroxytyrosol and Resveratrol. *Int. J. Mol. Sci.* **2022**, *23*, 15674. [CrossRef]
6. Sedlak, T.; Snyder, S. Bilirubin Benefits: Cellular Protection by a Biliverdin Reductase Antioxidant Cycle. *Pediatrics* **2004**, *113*, 1776–1782. [CrossRef]
7. Sedlak, T.W.; Saleh, M. Bilirubin and Glutathione Have Complementary Antioxidant and Cytoprotective Roles. *Proc. Natl. Acad. Sci. USA* **2009**, *106*, 5171–5176. [CrossRef]
8. Vasavda, C.; Kothari, R. Bilirubin Links Heme Metabolism to Neuroprotection by Scavenging Superoxide. *Cell Chem. Biol.* **2019**, *26*, 1450–1460.e7. [CrossRef]
9. Gazzin, S.; Vitek, L. A Novel Perspective on the Biology of Bilirubin in Health and Disease. *Trends Mol. Med.* **2016**, *22*, 758–768. [CrossRef]
10. Gazzin, S.; Masutti, F. The Molecular Basis of Jaundice: An Old Symptom Revisited. *Liver Int.* **2016**, *37*, 1094–1102. [CrossRef]
11. Wagner, K.-H.; Wallner, M. Looking to the Horizon: The Role of Bilirubin in the Development and Prevention of Age-Related Chronic Diseases. *Clin. Sci.* **2015**, *129*, 1–25. [CrossRef]

12. Creeden, J.F.; Gordon, D.M. Bilirubin as a Metabolic Hormone: The Physiological Relevance of Low Levels. *Am. J. Physiol.-Endocrinol. Metab.* **2020**, *320*, E191–E207. [CrossRef] [PubMed]
13. Wagner, K.-H.; Seyed Khoei, N. Oxidative Stress and Related Biomarkers in Gilbert's Syndrome: A Secondary Analysis of Two Case-Control Studies. *Antioxidants* **2021**, *10*, 1474. [CrossRef]
14. Chaudhari, H.; Goyal, S. Neonates with Sickle Cell Disease Are Vulnerable to Blue Light Phototherapy-Induced Oxidative Stress and Proinflammatory Cytokine Elevations. *Med. Hypotheses* **2016**, *96*, 78–82. [CrossRef]
15. Ayyappan, S.; Philip, S. Antioxidant Status in Neonatal Jaundice before and after Phototherapy. *J. Pharm. Bioallied. Sci.* **2015**, *7* (Suppl. 1), S16–S21. [CrossRef] [PubMed]
16. Sarici, D.; Gunes, T. Investigation on Malondialdehyde, S100B, and Advanced Oxidation Protein Product Levels in Significant Hyperbilirubinemia and the Effect of Intensive Phototherapy on These Parameters. *Pediatr. Neonatol.* **2015**, *56*, 95–100. [CrossRef]
17. Shapiro, S.M. Chronic Bilirubin Encephalopathy: Diagnosis and Outcome. *Semin. Fetal Neonatal Med.* **2010**, *15*, 157–163. [CrossRef] [PubMed]
18. Le Pichon, J.-B.; Riordan, S.M. The Neurological Sequelae of Neonatal Hyperbilirubinemia: Definitions, Diagnosis and Treatment of the Kernicterus Spectrum Disorders (KSDs). *Curr. Pediatr. Rev.* **2017**, *13*, 199–209. [CrossRef]
19. Jayanti, S.; Ghersi-Egea, J.-F. Severe Neonatal Hyperbilirubinemia and the Brain: The Old but Still Evolving Story. *Pediatr. Med.* **2021**, *4*, 37. [CrossRef]
20. Rose, J.; Vassar, R. Movement Disorders Due to Bilirubin Toxicity. *Semin. Fetal Neonatal Med.* **2015**, *20*, 20–25. [CrossRef]
21. Baranano, D.E.; Rao, M. Biliverdin Reductase: A Major Physiologic Cytoprotectant. *Proc. Natl. Acad. Sci. USA* **2002**, *99*, 16093–16098. [CrossRef]
22. Stocker, R.; Yamamoto, Y. Bilirubin Is an Antioxidant of Possible Physiological Importance. *Science* **1987**, *235*, 1043–1046. [CrossRef]
23. Vítek, L.; Tiribelli, C. Bilirubin: The Yellow Hormone? *J. Hepatol.* **2021**, *75*, 1485–1490. [CrossRef] [PubMed]
24. Kong, E.; Wang, H. Bilirubin Induces Pain Desensitization in Cholestasis by Activating 5-Hydroxytryptamine 3A Receptor in Spinal Cord. *Front. Cell Dev. Biol.* **2021**, *9*, 605855. [CrossRef]
25. Vitek, L.; Ostrow, J.D. Bilirubin Chemistry and Metabolism; Harmful and Protective Aspects. *Curr. Pharm. Des.* **2009**, *15*, 2869–2883. [CrossRef] [PubMed]
26. Kaur, H.; Hughes, M.N. Interaction of Bilirubin and Biliverdin with Reactive Nitrogen Species. *FEBS Lett.* **2003**, *543*, 113–119. [CrossRef] [PubMed]
27. Mancuso, C.; Barone, E. Inhibition of Lipid Peroxidation and Protein Oxidation by Endogenous and Exogenous Antioxidants in Rat Brain Microsomes in Vitro. *Neurosci. Lett.* **2012**, *518*, 101–105. [CrossRef] [PubMed]
28. Datla, S.R.; Dusting, G.J. Induction of Heme Oxygenase-1 In Vivo Suppresses NADPH Oxidase–Derived Oxidative Stress. *Hypertension* **2007**, *50*, 636–642. [CrossRef] [PubMed]
29. Qaisiya, M.; Coda Zabetta, C.D. Bilirubin Mediated Oxidative Stress Involves Antioxidant Response Activation via Nrf2 Pathway. *Cell. Signal.* **2014**, *26*, 512–520. [CrossRef]
30. Dang, T.N.; Robinson, S.R. Uptake, Metabolism and Toxicity of Hemin in Cultured Neurons. *Neurochem. Int.* **2011**, *58*, 804–811. [CrossRef]
31. Yang, F.; Zhang, Y. Hemin Treatment Protects Neonatal Rats from Sevoflurane-Induced Neurotoxicity via the Phosphoinositide 3-Kinase/Akt Pathway. *Life Sci.* **2020**, *242*, 117151. [CrossRef] [PubMed]
32. Gozzelino, R. The Pathophysiology of Heme in the Brain. *Curr. Alzheimer Res.* **2016**, *13*, 174–184. Available online: https://www.eurekaselect.com/135089/article (accessed on 27 July 2020). [CrossRef] [PubMed]
33. Gozzelino, R.; Jeney, V. Mechanisms of Cell Protection by Heme Oxygenase-1. *Annu. Rev. Pharmacol. Toxicol.* **2010**, *50*, 323–354. [CrossRef] [PubMed]
34. Maines, M.D. New Insights into Biliverdin Reductase Functions: Linking Heme Metabolism to Cell Signaling. *Physiology* **2005**, *20*, 382–389. [CrossRef] [PubMed]
35. Nitti, M.; Piras, S. Heme Oxygenase 1 in the Nervous System: Does It Favor Neuronal Cell Survival or Induce Neurodegeneration? *Int. J. Mol. Sci.* **2018**, *19*, 2260. [CrossRef]
36. Ryter, S.W.; Alam, J. Heme Oxygenase-1/Carbon Monoxide: From Basic Science to Therapeutic Applications. *Physiol. Rev.* **2006**, *86*, 583–650. [CrossRef]
37. Chiabrando, D.; Fiorito, V. Unraveling the Role of Heme in Neurodegeneration. *Front. Neurosci.* **2018**, *12*, 712. [CrossRef] [PubMed]
38. Chen, J. Heme Oxygenase in Neuroprotection: From Mechanisms to Therapeutic Implications. *Rev. Neurosci.* **2014**, *25*, 269–280. [CrossRef] [PubMed]
39. Kapitulnik, J.; Maines, M.D. Pleiotropic Functions of Biliverdin Reductase: Cellular Signaling and Generation of Cytoprotective and Cytotoxic Bilirubin. *Trends Pharmacol. Sci.* **2009**, *30*, 129–137. [CrossRef]
40. Lerner-Marmarosh, N.; Shen, J. Human Biliverdin Reductase: A Member of the Insulin Receptor Substrate Family with Serine/Threonine/Tyrosine Kinase Activity. *Proc. Natl. Acad. Sci. USA* **2005**, *102*, 7109–7114. [CrossRef]
41. Funes, S.C.; Rios, M. Naturally Derived Heme-Oxygenase 1 Inducers and Their Therapeutic Application to Immune-Mediated Diseases. *Front. Immunol.* **2020**, *11*, 1467. [CrossRef]

42. Luu Hoang, K.N.; Anstee, J.E. The Diverse Roles of Heme Oxygenase-1 in Tumor Progression. *Front. Immunol.* **2021**, *12*, 658315. [CrossRef]
43. Medina, M.; Garrido, J.J. Modulation of GSK-3 as a Therapeutic Strategy on Tau Pathologies. *Front. Mol. Neurosci.* **2011**, *4*, 24. [CrossRef]
44. Wang, H.; Cheng, Q. Cytoprotective Role of Heme Oxygenase-1 in Cancer Chemoresistance: Focus on Antioxidant, Antiapoptotic, and Pro-Autophagy Properties. *Antioxidants* **2023**, *12*, 1217. [CrossRef] [PubMed]
45. Funahashi, A.; Komatsu, M. Eel Green Fluorescent Protein Is Associated with Resistance to Oxidative Stress. *Comp. Biochem. Physiol. C Toxicol. Pharmacol.* **2016**, *181–182*, 35–39. [CrossRef] [PubMed]
46. Li, Y.; Sheng, H. Bilirubin Stabilizes the Mitochondrial Membranes during NLRP3 Inflammasome Activation. *Biochem. Pharmacol.* **2022**, *203*, 115204. [CrossRef]
47. Kumagai, A.; Ando, R. A Bilirubin-Inducible Fluorescent Protein from Eel Muscle. *Cell* **2013**, *153*, 1602–1611. [CrossRef] [PubMed]
48. Jayanti, S.; Vítek, L. The Role of Bilirubin and the Other "Yellow Players" in Neurodegenerative Diseases. *Antioxidants* **2020**, *9*, 900. [CrossRef]
49. Gazzin, S.; Jayanti, S. Models of Bilirubin Neurological Damage: Lessons Learned and New Challenges. *Pediatr. Res.* **2023**, *93*, 1838–1845. [CrossRef]
50. Watchko, J.F.; Tiribelli, C. Bilirubin-Induced Neurologic Damage—Mechanisms and Management Approaches. *N. Engl. J. Med.* **2013**, *369*, 2021–2030. [CrossRef] [PubMed]
51. Yu, M.; Su, D. D-T7 Peptide-Modified PEGylated Bilirubin Nanoparticles Loaded with Cediranib and Paclitaxel for Antiangiogenesis and Chemotherapy of Glioma. *ACS Appl. Mater. Interfaces* **2019**, *11*, 176–186. [CrossRef]
52. Halliwell, B.; Zhao, K. Nitric Oxide and Peroxynitrite. The Ugly, the Uglier and the Not so Good. *Free Radic. Res.* **1999**, *31*, 651–669. [CrossRef] [PubMed]
53. Franzoni, F.; Scarfò, G. Oxidative Stress and Cognitive Decline: The Neuroprotective Role of Natural Antioxidants. *Front. Neurosci.* **2021**, *15*, 729757. [PubMed]
54. Migliore, L.; Coppedè, F. Environmental-Induced Oxidative Stress in Neurodegenerative Disorders and Aging. *Mutat. Res. Genet. Toxicol. Environ. Mutagen.* **2009**, *674*, 73–84. [CrossRef]
55. Jové, M.; Pradas, I. Lipids and Lipoxidation in Human Brain Aging. Mitochondrial ATP-Synthase as a Key Lipoxidation Target. *Redox Biol.* **2019**, *23*, 101082. [CrossRef]
56. Bruce, K.D.; Zsombok, A. Lipid Processing in the Brain: A Key Regulator of Systemic Metabolism. *Front. Endocrinol.* **2017**, *8*, 60.
57. Butterfield, D.A. Brain Lipid Peroxidation and Alzheimer Disease: Synergy between the Butterfield and Mattson Laboratories. *Ageing Res. Rev.* **2020**, *64*, 101049. [CrossRef] [PubMed]
58. Vitek, L.; Bellarosa, C. Induction of Mild Hyperbilirubinemia: Hype or Real Therapeutic Opportunity? *Clin. Pharmacol. Ther.* **2019**, *106*, 568–575. [CrossRef]
59. Hinds, T.D.J.; Creeden, J.F. Bilirubin Nanoparticles Reduce Diet-Induced Hepatic Steatosis, Improve Fat Utilization, and Increase Plasma β-Hydroxybutyrate. *Front. Pharmacol.* **2020**, *11*, 594574. [CrossRef]
60. Barone, E.; Di Domenico, F. The Janus Face of the Heme Oxygenase/Biliverdin Reductase System in Alzheimer Disease: It's Time for Reconciliation. *Neurobiol. Dis.* **2014**, *62*, 144–159. [CrossRef]
61. Duyckaerts, C.; Delatour, B. Classification and Basic Pathology of Alzheimer Disease. *Acta Neuropathol.* **2009**, *118*, 5–36. [CrossRef]
62. Teleanu, D.M.; Niculescu, A.-G. An Overview of Oxidative Stress, Neuroinflammation, and Neurodegenerative Diseases. *Int. J. Mol. Sci.* **2022**, *23*, 5938. [CrossRef] [PubMed]
63. Hensley, K.; Hall, N. Brain Regional Correspondence Between Alzheimer's Disease Histopathology and Biomarkers of Protein Oxidation. *J. Neurochem.* **1995**, *65*, 2146–2156. [CrossRef] [PubMed]
64. Cioffi, F.; Adam, R.H.I. Molecular Mechanisms and Genetics of Oxidative Stress in Alzheimer's Disease. *J. Alzheimer's Dis.* **2019**, *72*, 981–1017. [CrossRef]
65. Nunomura, A.; Perry, G. RNA Oxidation Is a Prominent Feature of Vulnerable Neurons in Alzheimer's Disease. *J. Neurosci.* **1999**, *19*, 1959–1964. [CrossRef] [PubMed]
66. Otero-Garcia, M.; Mahajani, S.U. Molecular Signatures Underlying Neurofibrillary Tangle Susceptibility in Alzheimer's Disease. *Neuron* **2022**, *110*, 2929–2948.e8. [CrossRef]
67. Rummel, N.G.; Butterfield, D.A. Altered Metabolism in Alzheimer Disease Brain: Role of Oxidative Stress. *Antioxid. Redox Signal.* **2022**, *36*, 1289–1305. [CrossRef]
68. Barone, E.; Di Domenico, F. Biliverdin Reductase—A Protein Levels and Activity in the Brains of Subjects with Alzheimer Disease and Mild Cognitive Impairment. *Biochim. Biophys. Acta* **2011**, *1812*, 480–487. [CrossRef] [PubMed]
69. Triani, F.; Tramutola, A. Biliverdin Reductase-A Impairment Links Brain Insulin Resistance with Increased Aβ Production in an Animal Model of Aging: Implications for Alzheimer Disease. *Biochim. Biophys. Acta (BBA) Mol. Basis Dis.* **2018**, *1864*, 3181–3194. [CrossRef]
70. Barone, E.; Mancuso, C. Biliverdin Reductase-A: A Novel Drug Target for Atorvastatin in a Dog Pre-Clinical Model of Alzheimer Disease. *J. Neurochem.* **2012**, *120*, 135–146. [CrossRef] [PubMed]
71. Liu, J.; Dong, H. Bilirubin Increases Insulin Sensitivity by Regulating Cholesterol Metabolism, Adipokines and PPARγ Levels. *Sci. Rep.* **2015**, *5*, 9886. [CrossRef]

72. Jayanti, S.; Moretti, R. Bilirubin and Inflammation in Neurodegenerative and Other Neurological Diseases. *Neuroimmunol. Neuroinflamm.* **2020**, *7*, 92–108. [CrossRef]
73. Di Domenico, F.; Barone, E. HO-1/BVR-a System Analysis in Plasma from Probable Alzheimer's Disease and Mild Cognitive Impairment Subjects: A Potential Biochemical Marker for the Prediction of the Disease. *J. Alzheimer's Dis.* **2012**, *32*, 277–289. [CrossRef]
74. Feigin, V.L.; Abajobir, A.A. Global, Regional, and National Burden of Neurological Disorders during 1990–2015: A Systematic Analysis for the Global Burden of Disease Study 2015. *Lancet Neurol.* **2017**, *16*, 877–897. [CrossRef]
75. Mao, Q.; Qin, W. Recent Advances in Dopaminergic Strategies for the Treatment of Parkinson's Disease. *Acta Pharmacol. Sin.* **2020**, *41*, 471–482. [CrossRef] [PubMed]
76. Jenner, P. Oxidative Stress in Parkinson's Disease. *Ann. Neurol.* **2003**, *53*, S26–S38. [CrossRef]
77. Wei, Z.; Li, X. Oxidative Stress in Parkinson's Disease: A Systematic Review and Meta-Analysis. *Front. Mol. Neurosci.* **2018**, *11*, 236.
78. Tanner, C.M.; Kamel, F. Rotenone, Paraquat, and Parkinson's Disease. *Environ. Health Perspect.* **2011**, *119*, 866–872. [CrossRef] [PubMed]
79. Schapira, A.H.; Cooper, J.M. Mitochondrial Complex I Deficiency in Parkinson's Disease. *Lancet* **1989**, *1*, 1269. [CrossRef]
80. Jayanti, S.; Moretti, R. Bilirubin: A Promising Therapy for Parkinson's Disease. *Int. J. Mol. Sci.* **2021**, *22*, 6223. [CrossRef]
81. Yoo, M.S.; Chun, H.S. Oxidative Stress Regulated Genes in Nigral Dopaminergic Neuronal Cells: Correlation with the Known Pathology in Parkinson's Disease. *Mol. Brain Res.* **2003**, *110*, 76–84. [CrossRef]
82. Li, J.; Zhao, L. Association of Serum Indirect Bilirubin Concentrations with Motor Subtypes of Parkinson's Disease. *Neurodegener. Dis.* **2019**, *19*, 155–162. [CrossRef]
83. Hatano, T.; Saiki, S. Identification of Novel Biomarkers for Parkinson's Disease by Metabolomic Technologies. *J. Neurol. Neurosurg. Psychiatry* **2016**, *87*, 295–301. [CrossRef] [PubMed]
84. Scigliano, G.; Girotti, F. Increased Plasma Bilirubin in Parkinson Patients on L-Dopa: Evidence against the Free Radical Hypothesis? *Ital. J. Neurol. Sci.* **1997**, *18*, 69–72. [CrossRef] [PubMed]
85. Kataura, T.; Saiki, S. BRUP-1, an Intracellular Bilirubin Modulator, Exerts Neuroprotective Activity in a Cellular Parkinson's Disease Model. *J. Neurochem.* **2020**, *155*, 81–97. [CrossRef] [PubMed]
86. Jayanti, S.; Moretti, R. Bilirubin Prevents the TH^+ Dopaminergic Neuron Loss in a Parkinson's Disease Model by Acting on TNF-α. *Int. J. Mol. Sci.* **2022**, *23*, 14276. [CrossRef]
87. Gao, H.-M.; Zhou, H. Oxidative Stress, Neuroinflammation, and Neurodegeneration. In *Neuroinflammation and Neurodegeneration*; Peterson, P.K., Toborek, M., Eds.; Springer: New York, NY, USA, 2014; pp. 81–104. [CrossRef]
88. Schipper, H.M.; Song, W. Heme Oxygenase-1 and Neurodegeneration: Expanding Frontiers of Engagement. *J. Neurochem.* **2009**, *110*, 469–485. [CrossRef]
89. Schipper, H.M. Brain Iron Deposition and the Free Radical-Mitochondrial Theory of Ageing. *Ageing Res. Rev.* **2004**, *3*, 265–301. [CrossRef]
90. Schipper, H.M. Heme Oxygenase-1: Role in Brain Aging and Neurodegeneration. *Exp. Gerontol.* **2000**, *35*, 821–830. [CrossRef]
91. Compston, A.; Coles, A. Multiple Sclerosis. *Lancet* **2008**, *372*, 1502–1517. [CrossRef]
92. Reich, D.S.; Lucchinetti, C.F. Multiple Sclerosis. *N. Engl. J. Med.* **2018**, *378*, 169–180. [CrossRef]
93. Pegoretti, V.; Swanson, K.A. Inflammation and Oxidative Stress in Multiple Sclerosis: Consequences for Therapy Development. *Oxidative Med. Cell. Longev.* **2020**, *2020*, e7191080. [CrossRef]
94. van Horssen, J.; Schreibelt, G. Severe Oxidative Damage in Multiple Sclerosis Lesions Coincides with Enhanced Antioxidant Enzyme Expression. *Free Radic. Biol. Med.* **2008**, *45*, 1729–1737. [CrossRef]
95. Haider, L.; Fischer, M.T. Oxidative Damage in Multiple Sclerosis Lesions. *Brain* **2011**, *134*, 1914–1924. [CrossRef] [PubMed]
96. Mendiola, A.S.; Ryu, J.K. Transcriptional Profiling and Therapeutic Targeting of Oxidative Stress in Neuroinflammation. *Nat. Immunol.* **2020**, *21*, 513–524. [CrossRef]
97. Liu, Y.; Zhu, B. Heme Oxygenase-1 Plays an Important Protective Role in Experimental Autoimmune Encephalomyelitis. *Neuroreport* **2001**, *12*, 1841–1845. [CrossRef]
98. Liu, Y.; Liu, J. Biliverdin Reductase, a Major Physiologic Cytoprotectant, Suppresses Experimental Autoimmune Encephalomyelitis. *Free Radic. Biol. Med.* **2006**, *40*, 960–967. [CrossRef]
99. Liu, Y.; Zhu, B. Bilirubin as a Potent Antioxidant Suppresses Experimental Autoimmune Encephalomyelitis: Implications for the Role of Oxidative Stress in the Development of Multiple Sclerosis. *J. Neuroimmunol.* **2003**, *139*, 27–35. [CrossRef] [PubMed]
100. Armon-Omer, A.; Waldman, C. New Insights on the Nutrition Status and Antioxidant Capacity in Multiple Sclerosis Patients. *Nutrients* **2019**, *11*, 427. [CrossRef] [PubMed]
101. Ljubisavljevic, S.; Stojanovic, I. Association of Serum Bilirubin and Uric Acid Levels Changes during Neuroinflammation in Patients with Initial and Relapsed Demyelination Attacks. *Metab. Brain Dis.* **2013**, *28*, 629–638. [CrossRef]
102. van Es, M.A.; Hardiman, O. Amyotrophic Lateral Sclerosis. *Lancet* **2017**, *390*, 2084–2098. [CrossRef]
103. Feldman, E.L.; Goutman, S.A. Amyotrophic Lateral Sclerosis. *Lancet* **2022**, *400*, 1363–1380. [CrossRef]
104. Goutman, S.A.; Hardiman, O. Recent Advances in the Diagnosis and Prognosis of Amyotrophic Lateral Sclerosis. *Lancet Neurol.* **2022**, *21*, 480–493. [CrossRef] [PubMed]

105. Motataianu, A.; Serban, G. Oxidative Stress in Amyotrophic Lateral Sclerosis: Synergy of Genetic and Environmental Factors. *Int. J. Mol. Sci.* **2022**, *23*, 9339. [CrossRef] [PubMed]
106. Calingasan, N.Y.; Chen, J. β-Amyloid 42 Accumulation in the Lumbar Spinal Cord Motor Neurons of Amyotrophic Lateral Sclerosis Patients. *Neurobiol. Dis.* **2005**, *19*, 340–347. [CrossRef] [PubMed]
107. Ferrante, R.J.; Browne, S.E. Evidence of Increased Oxidative Damage in Both Sporadic and Familial Amyotrophic Lateral Sclerosis. *J. Neurochem.* **1997**, *69*, 2064–2074. [CrossRef]
108. Smith, R.G.; Henry, Y.K. Presence of 4-Hydroxynonenal in Cerebrospinal Fluid of Patients with Sporadic Amyotrophic Lateral Sclerosis. *Ann. Neurol.* **1998**, *44*, 696–699. [CrossRef]
109. Ihara, Y.; Nobukuni, K. Oxidative Stress and Metal Content in Blood and Cerebrospinal Fluid of Amyotrophic Lateral Sclerosis Patients with and without a Cu, Zn-Superoxide Dismutase Mutation. *Neurol. Res.* **2005**, *27*, 105–108. [CrossRef]
110. Mitsumoto, H.; Santella, R.M. Oxidative Stress Biomarkers in Sporadic ALS. *Amyotroph. Lateral Scler.* **2008**, *9*, 177–183. [CrossRef]
111. Zuo, X.; Zhou, J. TDP-43 Aggregation Induced by Oxidative Stress Causes Global Mitochondrial Imbalance in ALS. *Nat. Struct. Mol. Biol.* **2021**, *28*, 132–142. [CrossRef]
112. Hoang, T.T.; Johnson, D.A. Angiogenin Activates the Astrocytic Nrf2/Antioxidant-Response Element Pathway and Thereby Protects Murine Neurons from Oxidative Stress. *J. Biol. Chem.* **2019**, *294*, 15095–15103. [CrossRef]
113. Sheng, J.; Xu, Z. Three Decades of Research on Angiogenin: A Review and Perspective. *Acta Biochim. Biophys. Sin.* **2016**, *48*, 399–410. [CrossRef] [PubMed]
114. Ward, C.L.; Boggio, K.J. A Loss of FUS/TLS Function Leads to Impaired Cellular Proliferation. *Cell Death Dis.* **2014**, *5*, e1572. [CrossRef] [PubMed]
115. Wang, H.; Guo, W. Mutant FUS Causes DNA Ligation Defects to Inhibit Oxidative Damage Repair in Amyotrophic Lateral Sclerosis. *Nat. Commun.* **2018**, *9*, 3683. [CrossRef] [PubMed]
116. Jiménez-Villegas, J.; Kirby, J. Dipeptide Repeat Pathology in C9orf72-ALS Is Associated with Redox, Mitochondrial and NRF2 Pathway Imbalance. *Antioxidants* **2022**, *11*, 1897. [CrossRef] [PubMed]
117. Kraft, A.D.; Resch, J.M. Activation of the Nrf2–ARE Pathway in Muscle and Spinal Cord during ALS-like Pathology in Mice Expressing Mutant SOD1. *Exp. Neurol.* **2007**, *207*, 107–117. [CrossRef]
118. Velde, C.V.; McDonald, K.K. Misfolded SOD1 Associated with Motor Neuron Mitochondria Alters Mitochondrial Shape and Distribution Prior to Clinical Onset. *PLoS ONE* **2011**, *6*, e22031. [CrossRef]
119. Bergström, P.; von Otter, M. Association of NFE2L2 and KEAP1 Haplotypes with Amyotrophic Lateral Sclerosis. *Amyotroph. Lateral Scler. Front. Degener.* **2014**, *15*, 130–137. [CrossRef]
120. Iłżecka, J.; Stelmasiak, Z. Serum Bilirubin Concentration in Patients with Amyotrophic Lateral Sclerosis. *Clin. Neurol. Neurosurg.* **2003**, *105*, 237–240. [CrossRef]
121. Lastres-Becker, I.; de Lago, E. New Statement about NRF2 in Amyotrophic Lateral Sclerosis and Frontotemporal Dementia. *Biomolecules* **2022**, *12*, 1200. [CrossRef]
122. Dwyer, B.E.; Lu, S.-Y. Heme Oxygenase in the Experimental ALS Mouse. *Exp. Neurol.* **1998**, *150*, 206–212. [CrossRef]
123. Minj, E.; Upadhayay, S. Nrf2/HO-1 Signaling Activator Acetyl-11-Keto-Beta Boswellic Acid (AKBA)-Mediated Neuroprotection in Methyl Mercury-Induced Experimental Model of ALS. *Neurochem. Res.* **2021**, *46*, 2867–2884. [CrossRef] [PubMed]
124. Wyant, K.J.; Ridder, A.J. Huntington's Disease—Update on Treatments. *Curr. Neurol. Neurosci. Rep.* **2017**, *17*, 33. [CrossRef] [PubMed]
125. Kim, A.; Lalonde, K. New Avenues for the Treatment of Huntington's Disease. *Int. J. Mol. Sci.* **2021**, *22*, 8363. [CrossRef] [PubMed]
126. Jamwal, S.; Kumar, P. Antidepressants for Neuroprotection in Huntington's Disease: A Review. *Eur. J. Pharmacol.* **2015**, *769*, 33–42. [CrossRef]
127. Maiuri, T.; Suart, C.E. DNA Damage Repair in Huntington's Disease and Other Neurodegenerative Diseases. *Neurotherapeutics* **2019**, *16*, 948–956. [CrossRef]
128. Park, H.; Kam, T.-I. Poly (ADP-Ribose) (PAR)-Dependent Cell Death in Neurodegenerative Diseases. *Int. Rev. Cell Mol. Biol.* **2020**, *353*, 1–29. [CrossRef] [PubMed]
129. Dickey, A.S.; Pineda, V.V. PPAR-δ Is Repressed in Huntington's Disease, Is Required for Normal Neuronal Function and Can Be Targeted Therapeutically. *Nat. Med.* **2016**, *22*, 37–45. [CrossRef]
130. Jin, J.; Albertz, J. Neuroprotective Effects of PPAR-γ Agonist Rosiglitazone in N171-82Q Mouse Model of Huntington's Disease. *J. Neurochem.* **2013**, *125*, 410–419. [CrossRef]
131. Corona, J.C.; Duchen, M.R. PPARγ as a Therapeutic Target to Rescue Mitochondrial Function in Neurological Disease. *Free Radic. Biol. Med.* **2016**, *100*, 153–163. [CrossRef]
132. Kiaei, M. Peroxisome Proliferator-Activated Receptor-gamma in Amyotrophic Lateral Sclerosis and Huntington's Disease. *PPAR Res.* **2008**, *2008*, e418765. [CrossRef]
133. Huang, H.-T.; Liao, C.-K. Ligands of Peroxisome Proliferator-Activated Receptor-Alpha Promote Glutamate Transporter-1 Endocytosis in Astrocytes. *Int. J. Biochem. Cell Biol.* **2017**, *86*, 42–53. [CrossRef]
134. Wójtowicz, S.; Strosznajder, A.K. The Novel Role of PPAR Alpha in the Brain: Promising Target in Therapy of Alzheimer's Disease and Other Neurodegenerative Disorders. *Neurochem. Res.* **2020**, *45*, 972–988. [CrossRef]
135. Gordon, D.M.; Neifer, K.L. Bilirubin Remodels Murine White Adipose Tissue by Reshaping Mitochondrial Activity and the Coregulator Profile of Peroxisome Proliferator-Activated Receptor α. *J. Biol. Chem.* **2020**, *295*, 9804–9822. [CrossRef]

136. Vítek, L. Bilirubin as a Signaling Molecule. *Med. Res. Rev.* **2020**, *40*, 1335–1351. [CrossRef]
137. Khan, A.; Jamwal, S. Neuroprotective Effect of Hemeoxygenase-1/Glycogen Synthase Kinase-3β Modulators in 3-Nitropropionic Acid-Induced Neurotoxicity in Rats. *Neuroscience* **2015**, *287*, 66–77. [CrossRef]
138. Chin, K.S.; Teodorczuk, A. Dementia with Lewy Bodies: Challenges in the Diagnosis and Management. *Aust. N. Z. J. Psychiatry* **2019**, *53*, 291–303. [CrossRef]
139. Mukaetova-Ladinska, E.B.; Monteith, R. Cerebrospinal Fluid Biomarkers for Dementia with Lewy Bodies. *Int. J. Alzheimer's Dis.* **2010**, *2010*, 536538. [CrossRef]
140. McKeith, I.G.; Burn, D.J. Dementia with Lewy Bodies. *Semin. Clin. Neuropsychiatry* **2003**, *8*, 46–57. [CrossRef] [PubMed]
141. Lyras, L.; Perry, R.H. Oxidative Damage to Proteins, Lipids, and DNA in Cortical Brain Regions from Patients with Dementia with Lewy Bodies. *J. Neurochem.* **1998**, *71*, 302–312. [CrossRef] [PubMed]
142. Dalfó, E.; Portero-Otín, M. Evidence of Oxidative Stress in the Neocortex in Incidental Lewy Body Disease. *J. Neuropathol. Exp. Neurol.* **2005**, *64*, 816–830. [CrossRef] [PubMed]
143. Navarro, A.; Boveris, A. Human Brain Cortex: Mitochondrial Oxidative Damage and Adaptive Response in Parkinson Disease and in Dementia with Lewy Bodies. *Free Radic. Biol. Med.* **2009**, *46*, 1574–1580. [CrossRef] [PubMed]
144. Zhong, X.; Liao, Y. Abnormal Serum Bilirubin/Albumin Concentrations in Dementia Patients With Aβ Deposition and the Benefit of Intravenous Albumin Infusion for Alzheimer's Disease Treatment. *Front. Neurosci.* **2020**, *14*, 859. [CrossRef] [PubMed]
145. Kalousová, M.; Novotny, L. Decreased Levels of Advanced Glycation End-Products in Patients with Gilbert Syndrome. *Cell. Mol. Biol.* **2005**, *51*, 387–392. [PubMed]
146. Grinberg, L.T.; Heinsen, H. Toward a Pathological Definition of Vascular Dementia. *J. Neurol. Sci.* **2010**, *299*, 136–138. [CrossRef] [PubMed]
147. O'Brien, J.T.; Thomas, A. Vascular Dementia. *Lancet* **2015**, *386*, 1698–1706. [CrossRef] [PubMed]
148. Shabir, O.; Berwick, J. Neurovascular Dysfunction in Vascular Dementia, Alzheimer's and Atherosclerosis. *BMC Neurosci.* **2018**, *19*, 62. [CrossRef]
149. Casado, Á.; López-Fernández, M.E. Lipid Peroxidation and Antioxidant Enzyme Activities in Vascular and Alzheimer Dementias. *Neurochem. Res.* **2008**, *33*, 450–458. [CrossRef]
150. Gackowski, D.; Rozalski, R. Oxidative Stress and Oxidative DNA Damage Is Characteristic for Mixed Alzheimer Disease/Vascular Dementia. *J. Neurol. Sci.* **2008**, *266*, 57–62. [CrossRef]
151. Gustavsson, A.-M.; van Westen, D. Midlife Atherosclerosis and Development of Alzheimer or Vascular Dementia. *Ann. Neurol.* **2020**, *87*, 52–62. [CrossRef]
152. Vítek, L.; Jirsa, M. Gilbert Syndrome and Ischemic Heart Disease: A Protective Effect of Elevated Bilirubin Levels. *Atherosclerosis* **2002**, *160*, 449–456. [CrossRef]
153. Boon, A.-C.; Hawkins, C.L. Reduced Circulating Oxidized LDL Is Associated with Hypocholesterolemia and Enhanced Thiol Status in Gilbert Syndrome. *Free Radic. Biol. Med.* **2012**, *52*, 2120–2127. [CrossRef] [PubMed]
154. Kim, J.B.; Pjanic, M. TCF21 and the Environmental Sensor Aryl-Hydrocarbon Receptor Cooperate to Activate a pro-Inflammatory Gene Expression Program in Coronary Artery Smooth Muscle Cells. *PLoS Genet.* **2017**, *13*, e1006750. [CrossRef]
155. Zhu, K.; Meng, Q. Aryl Hydrocarbon Receptor Pathway: Role, Regulation and Intervention in Atherosclerosis Therapy (Review). *Mol. Med. Rep.* **2019**, *20*, 4763–4773. [CrossRef] [PubMed]
156. Phelan, D.; Winter, G.M. Activation of the Ah Receptor Signal Transduction Pathway by Bilirubin and Biliverdin. *Arch. Biochem. Biophys.* **1998**, *357*, 155–163. [CrossRef]
157. Gutiérrez-Vázquez, C.; Quintana, F.J. Regulation of the Immune Response by the Aryl Hydrocarbon Receptor. *Immunity* **2018**, *48*, 19–33. [CrossRef]
158. Longhi, M.S.; Vuerich, M. Bilirubin Suppresses Th17 Immunity in Colitis by Upregulating CD39. *JCI Insight* **2017**, *2*, e92791. [CrossRef]
159. Charlson, F.J.; Ferrari, A.J. Global Epidemiology and Burden of Schizophrenia: Findings From the Global Burden of Disease Study 2016. *Schizophr. Bull.* **2018**, *44*, 1195–1203. [CrossRef]
160. Garrison, J.R.; Fernandez-Egea, E. Reality Monitoring Impairment in Schizophrenia Reflects Specific Prefrontal Cortex Dysfunction. *Neuroimage Clin.* **2017**, *14*, 260–268. [CrossRef]
161. Krishnan, R.R.; Kraus, M.S. Comprehensive Model of How Reality Distortion and Symptoms Occur in Schizophrenia: Could Impairment in Learning-Dependent Predictive Perception Account for the Manifestations of Schizophrenia? *Psychiatry Clin. Neurosci.* **2011**, *65*, 305–317. [CrossRef]
162. Lin, C.-H.; Huang, C.-L. Clinical Symptoms, Mainly Negative Symptoms, Mediate the Influence of Neurocognition and Social Cognition on Functional Outcome of Schizophrenia. *Schizophr. Res.* **2013**, *146*, 231–237. [CrossRef]
163. Li, S.-B.; Liu, C. Revisiting the Latent Structure of Negative Symptoms in Schizophrenia: Evidence from Two Second-Generation Clinical Assessments. *Schizophr. Res.* **2022**, *248*, 131–139. [CrossRef] [PubMed]
164. Murray, A.J.; Rogers, J.C. Oxidative Stress and the Pathophysiology and Symptom Profile of Schizophrenia Spectrum Disorders. *Front. Psychiatry* **2021**, *12*, 703452.
165. Ermakov, E.A.; Dmitrieva, E.M. Oxidative Stress-Related Mechanisms in Schizophrenia Pathogenesis and New Treatment Perspectives. *Oxid. Med. Cell. Longev.* **2021**, *2021*, 8881770. [CrossRef] [PubMed]

166. Maas, D.A.; Vallès, A. Oxidative Stress, Prefrontal Cortex Hypomyelination and Cognitive Symptoms in Schizophrenia. *Transl. Psychiatry* **2017**, *7*, e1171. [CrossRef] [PubMed]
167. Okusaga, O.O. Accelerated Aging in Schizophrenia Patients: The Potential Role of Oxidative Stress. *Aging Dis.* **2014**, *5*, 256–262. [CrossRef]
168. Bitanihirwe, B.K.Y.; Woo, T.-U.W. Oxidative Stress in Schizophrenia: An Integrated Approach. *Neurosci. Biobehav. Rev.* **2011**, *35*, 878–893. [CrossRef] [PubMed]
169. Flatow, J.; Buckley, P. Meta-Analysis of Oxidative Stress in Schizophrenia. *Biol. Psychiatry* **2013**, *74*, 400–409. [CrossRef]
170. Więdłocha, M.; Zborowska, N. Oxidative Stress Biomarkers among Schizophrenia Inpatients. *Brain Sci.* **2023**, *13*, 490. [CrossRef]
171. Bošković, M.; Vovk, T. Oxidative Stress in Schizophrenia. *Curr. Neuropharmacol.* **2011**, *9*, 301–312. [CrossRef]
172. O'Donnell, P. Cortical Interneurons, Immune Factors and Oxidative Stress as Early Targets for Schizophrenia. *Eur. J. Neurosci.* **2012**, *35*, 1866–1870. [CrossRef]
173. Dornelles, E.P.; Marques, J.G. Unconjugated Bilirubin and Schizophrenia: A Systematic Review. *CNS Spectr.* **2019**, *24*, 577–588. [CrossRef]
174. Becklén, M.; Orhan, F. Plasma Bilirubin Levels Are Reduced in First-Episode Psychosis Patients and Associates to Working Memory and Duration of Untreated Psychosis. *Sci. Rep.* **2021**, *11*, 7527. [CrossRef] [PubMed]
175. Gama Marques, J.; Ouakinin, S. Clinical Profile in Schizophrenia and Schizoaffective Spectrum: Relation with Unconjugated Bilirubin in a Prospective and Controlled Study with Psychopathological and Psychosocial Variables. *CNS Spectr.* **2020**, *25*, 782–789. [CrossRef] [PubMed]
176. Miyaoka, T.; Seno, H. Schizophrenia-Associated Idiopathic Unconjugated Hyperbilirubinemia (Gilbert's Syndrome). *J. Clin. Psychiatry* **2000**, *61*, 868–871. [CrossRef] [PubMed]
177. Vítek, L.; Novotná, M. Serum Bilirubin Levels and UGT1A1 Promoter Variations in Patients with Schizophrenia. *Psychiatry Res.* **2010**, *178*, 449–450. [CrossRef]
178. Rodrigues, C.M.P.; Solá, S. Perturbation of Membrane Dynamics in Nerve Cells as an Early Event during Bilirubin-Induced Apoptosis. *J. Lipid Res.* **2002**, *43*, 885–894. [CrossRef]
179. Brito, M.A.; Brites, D. A Link between Hyperbilirubinemia, Oxidative Stress and Injury to Neocortical Synaptosomes. *Brain Res.* **2004**, *1026*, 33–43. [CrossRef]
180. Rodrigues, C.M.P.; Solá, S. Bilirubin Directly Disrupts Membrane Lipid Polarity and Fluidity, Protein Order, and Redox Status in Rat Mitochondria. *J. Hepatol.* **2002**, *36*, 335–341. [CrossRef]
181. Ercan, I.; Cilaker Micili, S. Bilirubin Induces Microglial NLRP3 Inflammasome Activation in Vitro and in Vivo. *Mol. Cell. Neurosci.* **2023**, *125*, 103850. [CrossRef]
182. Li, Y.; Huang, B. Physiological Concentrations of Bilirubin Control Inflammatory Response by Inhibiting NF-KB and Inflammasome Activation. *Int. Immunopharmacol.* **2020**, *84*, 106520. [CrossRef]
183. Bora, E.; Murray, R.M. Meta-Analysis of Cognitive Deficits in Ultra-High Risk to Psychosis and First-Episode Psychosis: Do the Cognitive Deficits Progress over, or after, the Onset of Psychosis? *Schizophr. Bull.* **2014**, *40*, 744–755. [CrossRef] [PubMed]
184. Rapoport, J.L.; Giedd, J.N. Neurodevelopmental Model of Schizophrenia: Update 2012. *Mol. Psychiatry* **2012**, *17*, 1228–1238. [CrossRef] [PubMed]
185. Maimburg, R.D.; Væth, M. Neonatal Jaundice: A Risk Factor for Infantile Autism? *Paediatr. Perinat. Epidemiol.* **2008**, *22*, 562–568. [CrossRef] [PubMed]
186. Hokkanen, L.; Launes, J. Adult Neurobehavioral Outcome of Hyperbilirubinemia in Full Term Neonates—A 30 Year Prospective Follow-up Study. *PeerJ* **2014**, *2*, e294. [CrossRef]
187. Nilsen, S.T.; Finne, P.H. Males with Neonatal Hyperbilirubinemia Examined at 18 Years of Age. *Acta Paediatr.* **1984**, *73*, 176–180. [CrossRef]
188. Ozmert, E.; Erdem, G. Long-Term Follow-up of Indirect Hyperbilirubinemia in Full-Term Turkish Infants. *Acta Paediatr.* **1996**, *85*, 1440–1444. [CrossRef]
189. Amin, S.B.; Smith, T. Developmental Influence of Unconjugated Hyperbilirubinemia and Neurobehavioral Disorders. *Pediatr. Res.* **2019**, *85*, 191–197. [CrossRef]
190. Gunn, C.H. HEREDITARY ACHOLURIC JAUNDICE in a New Mutant Strain of Rats. *J. Hered.* **1938**, *29*, 137–139. [CrossRef]
191. Hayashida, M.; Miyaoka, T. Hyperbilirubinemia-Related Behavioral and Neuropathological Changes in Rats: A Possible Schizophrenia Animal Model. *Prog. Neuropsychopharmacol. Biol. Psychiatry* **2009**, *33*, 581–588. [CrossRef]
192. Liaury, K.; Miyaoka, T. Morphological Features of Microglial Cells in the Hippocampal Dentate Gyrus of Gunn Rat: A Possible Schizophrenia Animal Model. *J. Neuroinflamm.* **2012**, *9*, 56. [CrossRef]
193. Llido, J.P.; Fioriti, E. Bilirubin-Induced Transcriptomic Imprinting in Neonatal Hyperbilirubinemia. *Biology* **2023**, *12*, 834. [CrossRef] [PubMed]
194. Reddy-Thootkur, M.; Kraguljac, N.V. The Role of Glutamate and GABA in Cognitive Dysfunction in Schizophrenia and Mood Disorders—A Systematic Review of Magnetic Resonance Spectroscopy Studies. *Schizophr. Res.* **2022**, *249*, 74–84. [CrossRef] [PubMed]
195. Roberts, R.C.; McCollum, L.A. Ultrastructural Evidence for Glutamatergic Dysregulation in Schizophrenia. *Schizophr. Res.* **2022**, *249*, 4–15. [CrossRef] [PubMed]

196. McDonald, J.W.; Shapiro, S.M. Role of Glutamate Receptor-Mediated Excitotoxicity in Bilirubin-Induced Brain Injury in the Gunn Rat Model. *Exp. Neurol.* **1998**, *150*, 21–29. [CrossRef]
197. Cayabyab, R.; Ramanathan, R. High Unbound Bilirubin for Age: A Neurotoxin with Major Effects on the Developing Brain. *Pediatr. Res.* **2019**, *85*, 183–190. [CrossRef]
198. Verma, M.; Lizama, B.N. Excitotoxicity, Calcium and Mitochondria: A Triad in Synaptic Neurodegeneration. *Transl. Neurodegener.* **2022**, *11*, 3. [CrossRef]
199. Ashizawa, T.; Xia, G. Ataxia. *Continuum* **2016**, *22*, 1208–1226. [CrossRef]
200. de Silva, R.N.; Vallortigara, J. Diagnosis and Management of Progressive Ataxia in Adults. *Pract. Neurol.* **2019**, *19*, 196–207. [CrossRef]
201. Kinoshita, C.; Kubota, N. Glutathione Depletion and MicroRNA Dysregulation in Multiple System Atrophy: A Review. *Int. J. Mol. Sci.* **2022**, *23*, 15076. [CrossRef]
202. Zhou, L.; Jiang, Y. Oxidative Stress and Environmental Exposures Are Associated with Multiple System Atrophy in Chinese Patients. *Can. J. Neurol. Sci.* **2016**, *43*, 703–709. [CrossRef]
203. Parsons, D.W.; Jones, S. An Integrated Genomic Analysis of Human Glioblastoma Multiforme. *Science* **2008**, *321*, 1807–1812. [CrossRef]
204. McLendon, R.; Friedman, A. Comprehensive Genomic Characterization Defines Human Glioblastoma Genes and Core Pathways. *Nature* **2008**, *455*, 1061–1068. [CrossRef]
205. Qi, X.; Jha, S.K. Antioxidants in Brain Tumors: Current Therapeutic Significance and Future Prospects. *Mol. Cancer* **2022**, *21*, 204. [CrossRef] [PubMed]
206. Vilar, J.B.; Christmann, M. Alterations in Molecular Profiles Affecting Glioblastoma Resistance to Radiochemotherapy: Where Does the Good Go? *Cancers* **2022**, *14*, 2416. [CrossRef] [PubMed]
207. Ramírez-Expósito, M.J.; Martínez-Martos, J.M. The Delicate Equilibrium between Oxidants and Antioxidants in Brain Glioma. *Curr. Neuropharmacol.* **2019**, *17*, 342–351. [CrossRef]
208. Conti, A.; Gulì, C. Role of Inflammation and Oxidative Stress Mediators in Gliomas. *Cancers* **2010**, *2*, 693–712. [CrossRef]
209. Alghamri, M.S.; McClellan, B.L. Targeting Neuroinflammation in Brain Cancer: Uncovering Mechanisms, Pharmacological Targets, and Neuropharmaceutical Developments. *Front. Pharmacol.* **2021**, *12*, 680021.
210. Atukeren, P.; Oner, S. Oxidant and Anti-Oxidant Status in Common Brain Tumors: Correlation to TP53 and Human Biliverdin Reductase. *Clin. Neurol. Neurosurg.* **2017**, *158*, 72–76. [CrossRef]
211. Kim, S.S.; Seong, S. Biliverdin Reductase Plays a Crucial Role in Hypoxia-Induced Chemoresistance in Human Glioblastoma. *Biochem. Biophys. Res. Commun.* **2013**, *440*, 658–663. [CrossRef]
212. Salaroglio, I.C.; Abate, C. Validation of Thiosemicarbazone Compounds as P-Glycoprotein Inhibitors in Human Primary Brain–Blood Barrier and Glioblastoma Stem Cells. *Mol. Pharm.* **2019**, *16*, 3361–3373. [CrossRef]
213. Alves, A.L.V.; Gomes, I.N.F. Role of Glioblastoma Stem Cells in Cancer Therapeutic Resistance: A Perspective on Antineoplastic Agents from Natural Sources and Chemical Derivatives. *Stem Cell Res. Ther.* **2021**, *12*, 206. [CrossRef]
214. Gazzin, S.; Berengeno, A.L. Modulation of Mrp1 (ABCc1) and Pgp (ABCb1) by Bilirubin at the Blood-CSF and Blood-Brain Barriers in the Gunn Rat. *PLoS ONE* **2011**, *6*, e16165. [CrossRef] [PubMed]
215. Xu, P.; Ling, Z. Unconjugated Bilirubin Elevation Impairs the Function and Expression of Breast Cancer Resistance Protein (BCRP) at the Blood-Brain Barrier in Bile Duct-Ligated Rats. *Acta Pharmacol. Sin.* **2016**, *37*, 1129–1140. [CrossRef] [PubMed]
216. Gao, X.; Yu, X. Telomeres and Mitochondrial Metabolism: Implications for Cellular Senescence and Age-Related Diseases. *Stem Cell Rev. Rep.* **2022**, *18*, 2315–2327. [CrossRef] [PubMed]
217. Rossiello, F.; Jurk, D. Telomere Dysfunction in Ageing and Age-Related Diseases. *Nat. Cell Biol.* **2022**, *24*, 135–147. [CrossRef] [PubMed]
218. Hao, L.; Chen, Q. Association of Serum Total Bilirubin Concentration with Telomere Length: The National Health and Nutrition Examination Survey. *Oxid. Med. Cell. Longev.* **2021**, *2021*, 4688900. [CrossRef]
219. Tosevska, A.; Moelzer, C. Longer Telomeres in Chronic, Moderate, Unconjugated Hyperbilirubinaemia: Insights from a Human Study on Gilbert's Syndrome. *Sci. Rep.* **2016**, *6*, 22300. [CrossRef]
220. Wallner, M.; Blassnigg, S.M. Effects of Unconjugated Bilirubin on Chromosomal Damage in Individuals with Gilbert's Syndrome Measured with the Micronucleus Cytome Assay. *Mutagenesis* **2012**, *27*, 731–735. [CrossRef]
221. Croft, K.D.; Zhang, D. Structural Requirements of Flavonoids to Induce Heme Oxygenase-1 Expression. *Free Radic. Biol. Med.* **2017**, *113*, 165–175. [CrossRef]
222. Smith, A.; Alam, J. Regulation of Heme Oxygenase and Metallothionein Gene Expression by the Heme Analogs, Cobalt-, and Tin-Protoporphyrin. *J. Biol. Chem.* **1993**, *268*, 7365–7371. [CrossRef]
223. Mancuso, C.; Barone, E. The Heme Oxygenase/Biliverdin Reductase Pathway in Drug Research and Development. *Curr. Drug Metab.* **2009**, *10*, 579–594. Available online: https://www.eurekaselect.com/70167/article (accessed on 27 July 2020). [CrossRef]
224. Kim, J.S.; Yoon, T.-J. Toxicity and Tissue Distribution of Magnetic Nanoparticles in Mice. *Toxicol. Sci.* **2006**, *89*, 338–347. [CrossRef] [PubMed]
225. Petters, C.; Irrsack, E. Uptake and Metabolism of Iron Oxide Nanoparticles in Brain Cells. *Neurochem. Res.* **2014**, *39*, 1648–1660. [CrossRef] [PubMed]

226. Sim, T.M.; Tarini, D. Nanoparticle-Based Technology Approaches to the Management of Neurological Disorders. *Int. J. Mol. Sci.* **2020**, *21*, 6070. [CrossRef] [PubMed]
227. Kim, M.J.; Lee, Y. PEGylated Bilirubin Nanoparticle as an Anti-Oxidative and Anti-Inflammatory Demulcent in Pancreatic Islet Xenotransplantation. *Biomaterials* **2017**, *133*, 242–252. [CrossRef]
228. Thomsen, L.B.; Thomsen, M.S. Targeted Drug Delivery to the Brain Using Magnetic Nanoparticles. *Ther. Deliv.* **2015**, *6*, 1145–1155. [CrossRef]
229. Ficiarà, E.; Ansari, S.A. Beyond Oncological Hyperthermia: Physically Drivable Magnetic Nanobubbles as Novel Multipurpose Theranostic Carriers in the Central Nervous System. *Molecules* **2020**, *25*, 2104. [CrossRef]

antioxidants

MDPI

Review

A Preclinical Model for Parkinson's Disease Based on Transcriptional Gene Activation via KEAP1/NRF2 to Develop New Antioxidant Therapies

Juan Segura-Aguilar [1,*] and Bengt Mannervik [2,3]

[1] Molecular & Clinical Pharmacology, ICBM, Faculty of Medicine, University of Chile, Independencia, Santiago 8380000, Chile
[2] Department of Biochemistry and Biophysics, Arrhenius Laboratories, Stockholm University, SE-10691 Stockholm, Sweden
[3] Department of Chemistry, Scripps Research, La Jolla, CA 92037, USA
* Correspondence: jsegura@med.uchile.cl; Tel.: +56-229786057

Abstract: Investigations of the effect of antioxidants on idiopathic Parkinson's disease have been unsuccessful because the preclinical models used to propose these clinical studies do not accurately represent the neurodegenerative process of the disease. Treatment with certain exogenous neurotoxins induces massive and extremely rapid degeneration; for example, MPTP causes severe Parkinsonism in just three days, while the degenerative process of idiopathic Parkinson´s disease proceeds over many years. The endogenous neurotoxin aminochrome seems to be a good alternative target since it is formed in the nigrostriatal system neurons where the degenerative process occurs. Aminochrome induces all the mechanisms reported to be involved in the degenerative processes of idiopathic Parkinson's disease. The presence of neuromelanin-containing dopaminergic neurons in the postmortem brain of healthy elderly people suggests that neuromelanin synthesis is a normal and harmless process despite the fact that it requires oxidation of dopamine to three ortho-quinones that are potentially toxic, especially aminochrome. The apparent contradiction that neuromelanin synthesis is harmless, despite its formation via neurotoxic ortho-quinones, can be explained by the protective roles of DT-diaphorase and glutathione transferase GSTM2-2 as well as the neuroprotective role of astrocytes secreting exosomes loaded with GSTM2-2. Increasing the expression of DT-diaphorase and GSTM2-2 may be a therapeutic goal to prevent the degeneration of new neuromelanin-containing dopaminergic neurons. Several phytochemicals that induce DT-diaphorase have been discovered and, therefore, an interesting question is whether these phytochemical KEAP1/NRF2 activators can inhibit or decrease aminochrome-induced neurotoxicity.

Keywords: dopamine; Parkinson's disease; neuromelanin; antioxidants; aminochrome; glutathione transferase M2-2; DT-diaphorase; ferroptosis; KEAP1/NRF2; dopaminergic neurons

Citation: Segura-Aguilar, J.; Mannervik, B. A Preclinical Model for Parkinson's Disease Based on Transcriptional Gene Activation via KEAP1/NRF2 to Develop New Antioxidant Therapies. *Antioxidants* **2023**, *12*, 673. https://doi.org/10.3390/antiox12030673

Academic Editors: Ana-Maria Buga and Carmen Nicoleta Oancea

Received: 16 February 2023
Revised: 1 March 2023
Accepted: 4 March 2023
Published: 9 March 2023

1. Mechanisms Involved in Neurodegeneration in Parkinson's Disease

Although 65 years have passed since the discovery that the motor symptoms of idiopathic Parkinson's disease are related to the massive loss of neuromelanin-containing neurons in the nigrostriatal system, it is still unclear what triggers the degenerative process of this neuronal system [1,2]. The first widely studied mechanism was the role of oxidative stress in this disease, then mitochondrial dysfunction, and, in the early 1990s, the existence of a mutation in the alpha-synuclein gene was discovered in some families with genetic Parkinson's. This discovery was a major boost in basic research as it was the first gene with mutations that induced familial or genetic Parkinson's [3]. Subsequently, more genes related to familial Parkinson's disease were identified, such as the parkin gene, PINK-1, LRRK2, VPS35, DJ1, ATP13A2, etc. [4]. Although the origin of neurodegeneration in the nigrostriatal system is unclear, there is a general consensus that certain mechanisms

are involved in the loss of neuromelanin-containing dopaminergic neurons. They are related to the appearance of motor symptoms and involve oxidative stress, mitochondrial dysfunction, aggregation of alpha-synuclein to neurotoxic oligomers, dysfunction of both lysosomal and proteasomal protein degradation systems, endoplasmic reticulum stress, and neuroinflammation [5–8].

2. Clinical Studies to Develop Antioxidant Therapies

The recognition of oxidative stress in the degenerative process of the nigrostriatal system has been a focus for several decades. The discovery that the motor movements of Parkinson's disease are related to the loss of the neuromelanin-containing dopaminergic neuron of the nigrostriatal system that generates a significant drop in the release of dopamine has implied that preclinical models based on exogenous neurotoxins such as 6-hydroxydopamine have played an important role in the investigation of this degenerative process and the development of potential therapies. There are two sources of oxidative stress generation in dopaminergic neurons, one being the oxidative deamination of dopamine catalyzed by the enzyme monoamine oxidase that generates ammonia and hydrogen peroxide [9], which in the presence of reduced iron generates hydroxyl radicals and therefore profuse oxidative stress within dopaminergic neurons. Another specific source of oxidative stress within dopaminergic neurons arises during the synthesis of neuromelanin which requires the oxidation of dopamine to three ortho-quinones (dopamine ortho-quinone, aminochrome, and 5,6-indolequinone). Aminochrome reduction with one electron generates leukoaminochrome *o*-semiquinone radical that is extremely reactive with oxygen [10] generating oxidative stress in neuromelanin-containing dopaminergic neurons of the nigrostriatal system [11]. Another source of permanent oxidative stress, although not specific for dopaminergic neurons, is the leakage of electrons from the mitochondrial electron transport chain during the generating of ATP through the oxidative phosphorylation of ADP [12].

Toxicity due to oxidative stress has prompted major efforts to developing antioxidant therapies using successful results in preclinical models with exogenous neurotoxins. Coenzyme Q10 works as a scavenger of reactive species during oxidative stress [13] and has also been shown to reduce the degenerative effects of MPTP in mice, supporting the idea of conducting clinical studies in patients with Parkinson's [14]. Coenzyme Q10 also protects against 6-hydroxydopamine neurotoxicity [15]. Preclinical studies and a clinical study phase with coenzyme Q suggested clinical benefits for Parkinson's patients. However, a randomized phase III clinical study was performed with 600 participants administered placebo, 1200 mg/d of CoQ10, or 2400 mg/d of CoQ10, and in addition all participants received 1200 IU/d of vitamin E. This study concluded that this treatment has no benefits for patients with Parkinson's disease [16]. Another study in 2015, involving reduced coenzyme Q10, was carried out with 10 Parkinson's patients and showed positive effects [17]. However, we must take into account the chemical characteristics of reduced coenzyme Q10 that after being administered to the patient will be oxidized again inside the neuron. A coenzyme Q10 analogue (MitoQ10) obtained by binding coenzyme Q10 with triphenylphosphonium cation has been shown to have protective effects in preclinical models of MPTP [18] and 6-hydroxydopamine [19,20]. However, a double-blind study with 120 patients with newly diagnosed Parkinson's disease without treatment did not demonstrate clinical benefits [21].

Urate is another antioxidant that has been used in clinical studies with Parkinson's patients. Urate is a product of purine metabolism and, in preclinical studies with 1-methyl-4-phenyl-1,2,5,6-tetrahydropyridine (MPTP)-induced oxidative stress, urate showed an antioxidant effect. Urate is also neuroprotective in a 6-hydroxydopamine-lesioned rat model linked to the Akt/GSK3β signaling pathway [22]. Protective effects were also shown in preclinical models involving MPTP; urate increases the expression of γ-glutamate-cysteine ligase catalytic subunit, heme oxygenase-1, and DT-diaphorase via NFR2 [23,24]. However, a phase 3 study with 298 pharmacologically untouched Parkinson's patients

treated with the urate precursor inosine for up to 2 years to increase urate levels showed no clinical benefit [25].

3. Neurotoxins in Preclinical Models for Parkinson's Disease

The lessons that we can draw from these preclinical models, based on exogenous neurotoxins causing a massive and extremely rapid degeneration, are that: (i) A preclinical model must resemble the extremely slow degenerative process in idiopathic Parkinson's has to be different. The triggering of all the mechanisms that have been observed to be involved in this degenerative process occurs at different time scales. For this reason, the neurotoxin for a preclinical model to study the mechanisms and be able to test new drugs for idiopathic Parkinson's must have other properties, presumably of endogenous origin. (ii) The neuronal death induced by this endogenous neurotoxin cannot be expansive or massive but must be focused on individual dopaminergic neurons containing neuromelanin. Only such a model would mimic the extremely slow degenerative process and progression of the disease that takes many years.

3.1. Exogenous Neurotoxins in Preclinical Models for Parkinson's Disease

Most of the preclinical studies that have contributed to new clinical trials in the search for new pharmacological treatments for modifying or halting the progress of Parkinson's disease have used 6-hydroxydopamine and subsequently MPTP. 6-hydroxydopamine has high affinity to transporters of dopamine and noradrenaline, inducing neurotoxicity in both dopaminergic and noradrenergic neurons, and its use in animals for Parkinson's experimental models requires the presence of an inhibitor of the noradrenaline transporter to obtain specificity for dopaminergic neurons [26,27]. A major characteristic of 6-hydroxydopamine is that it is unstable in the presence of oxygen, which implies that its injection into the striatum, substantia nigra, or the axonal bundle requires the use of ascorbic acid to prevent its autoxidation before being transported to dopaminergic neurons. 6-hydroxydopamine in the cytosol of dopaminergic neurons is autoxidized, generating a semiquinone radical that is also extremely reactive with oxygen, generating oxidative stress [28,29]. This relationship of oxidative stress with the massive degeneration of neuromelanin-containing dopaminergic neurons of the nigrostriatal system motivated the development of clinical studies with antioxidants. 6-hydroxydopamine is the source of oxidative stress in this preclinical model, but this molecule does not exist in the human brain. The difference between 6-hydroxydopamine and MPTP is that the latter has been shown to generate Parkinsonism in humans when drug addicts have used illegal drugs contaminated with MPTP. However, these two exogenous neurotoxins have in common that they cause extremely rapid and massive degeneration of the nigrostriatal system. MPTP induced severe Parkinsonism to drug addicts in just 3 days [30], which is in contrast to the extremely slow progression of idiopathic Parkinson's disease. The latter takes years to develop motor symptoms, which emerge when 60% of the neuromelanin-containing neurons of the nigrostriatal system have disappeared. After the onset of motor symptoms, at least 15 years may pass before death. The question is whether investigations with exogenous neurotoxins can serve as a preclinical model to study the mechanisms of the disease and also test possible drugs for a treatment that can modify the course of the disease. The number of dopaminergic neurons of the nigrostriatal system has been estimated to be between 800,000 to 1,000,000, counting both sides of the brain [31]. If we consider that the motor symptoms appear when 60% of the neuromelanin-containing dopaminergic neurons have degenerated, these patients have between 360,000 to 400,000 surviving neurons. This implies that if a patient survives for around 15 years, between 58 and 73 dopaminergic neurons that contain neuromelanin die each day. By contrast, a subchronic animal model with one daily injection of MPTP for 5 days induces a 50% loss of dopaminergic neurons in only 28 days [32]. It is difficult to apply the results of such an extremely rapid cell death as a preclinical model compared with the extremely slow progression of nigrostriatal degeneration in idiopathic Parkinson's disease. In a clinical study that, for example, uses coenzyme Q10, if it inhibited 100% oxidative

stress and the death of dopaminergic neurons, this antioxidant would prevent the death of 0.0073% of these neurons per day or 1.3% in 6 months. The question is, can this result be significant for delaying or halting the progression of idiopathic Parkinson's disease? It is doubtful whether successful results would be obtained in clinical studies using exogenous neurotoxins that induce an extremely rapid and massive degenerative process that is the complete opposite of what occurs in the development of idiopathic Parkinson's disease.

3.2. Endogenous Neurotoxins as Preclinical Model for Parkinson's Disease

The question is: what endogenous neurotoxins, formed in neuromelanin-containing dopaminergic neurons, might serve in preclinical models for idiopathic Parkinson's disease? There are three endogenous neurotoxins that can be involved in the degeneration of dopaminergic neurons containing neuromelanin:

3.2.1. Neurotoxic Oligomers of Alpha-Synuclein

Alpha-synuclein is a protein that exists in a monomeric form and, under certain conditions, can aggregate to form fibrils, which are deposited in Lewy bodies seen in postmortem tissue [33]. However, the formation of these neurotoxic oligomers requires the existence of a mutation in familial Parkinson's disease and, in the case of idiopathic Parkinson's, requires the existence of products of the oxidation of dopamine to neuromelanin, such as aminochrome [34]. Another argument against alpha-synuclein as the neurotoxin that triggers all the degenerative mechanisms reported in idiopathic Parkinson's is that the expression of alpha-synuclein is not limited to the nigrostriatal system, since alpha-synuclein is also expressed in other regions such as the cerebellum and the cortex [35]. It has been postulated that the aggregation of alpha-synucleins to fibrils and their accumulation in Lewy bodies could be responsible for the progression of the disease from one region to another region of the brain. The neurons that form these Lewy bodies secrete them through exosomes that penetrate neighboring neurons. This dissemination of Lewy bodies containing alpha-synuclein fibrils would allow spreading from one region to another region [33]. This hypothesis is controversial, because, if Lewy bodies were to participate in the spread of the disease, why are these observed in postmortem tissues? When a neuron dies, it is phagocytosed by the microglia, eliminating all traces of Lewy bodies formed through years of degeneration [36]. Therefore, the postmortem tissue represents the neurons surviving the degenerative process that has existed for years. This rather suggests that the formation of Lewy bodies is a neuroprotective mechanism to prevent alpha-synuclein from aggregating to neurotoxic oligomers [37]. An additional argument against the hypothesis of the spread of idiopathic Parkinson's disease through Lewy bodies migrating from one neuron to neighboring neurons and subsequently from one region to another region of the brain is the propagative process that not only affects a single neighboring neuron but hundreds of neurons existing around the neuron that secretes exosomes containing Lewy bodies.

3.2.2. 3,4-Dihydroxyphenylacetaldehyde

3,4-Dihydroxyphenylacetaldehyde also known as DOPAL, is a product of the oxidative deamination of dopamine catalyzed by the enzyme monoamine oxidase that generates hydrogen peroxide and ammonium [38]. The enzyme aldehyde dehydrogenase-1 participates in the further degradation of dopamine, which converts DOPAL into 3,4-dihydroxyphenylacetic acid. In a study of protein expression in postmortem material, it was observed that the levels of aldehyde dehydrogenase-1 were lower in Parkinson's patients than in controls [39]. DOPAL accumulation could be neurotoxic because DOPAL induces oxidative stress and alpha-synuclein aggregation [38]. The problem is that the postmortem tissue is the tissue surviving the degenerative process during many years of Parkinson's disease and, if there is a low expression of aldehyde dehydrogenase-1 in these tissues surviving years of a degenerative process, DOPAL cannot play a neurotoxic role in dopaminergic neurons that contain neuromelanin.

3.2.3. Aminochrome

Aminochrome is an endogenous neurotoxin formed in the synthesis of neuromelanin in dopaminergic neurons that contain neuromelanin, which are precisely the neurons that disappear in Parkinson's disease. To synthesize neuromelanin, dopamine needs to be oxidized sequentially to three transient ortho-quinones (dopamine ortho-quinone, aminochrome, and 5,6-indolequinone), among which the latter is finally polymerized to form the pigment neuromelanin. Neuromelanin is a dark pigment contained in membrane vesicles called neuromelanin-containing organelles with a diameter of 200–600 nm that, besides neuromelanin, contain lipids and metals such as S, Fe, and Cu in healthy subjects [40]. A study carried out with infrared spectroscopy in different regions of the human brain revealed that the neuromelanin of the regions that degenerate in Parkinson's disease, substantia nigra and locus coeruleus, have a similar structure but different from those regions not affected by the disease [41]. The synthesis of neuromelanin is a normal and harmless process that also has a neuroprotective role by preventing the neurotoxic effects of reactive metals. However, neuromelanin released from dead dopaminergic neurons is able to activate microglia, generating proinflammatory molecules and reactive oxygen and nitrogen species [42]. Neuromelanin injected into the substantia nigra of rats induces microglia activation and loss of tyrosine hydroxylase-positive neurons [43]. All three ortho-quinones derived from dopamine are neurotoxic, but the most neurotoxic and most long-lived is aminochrome. Aminochrome induces oxidative stress, neuroinflammation, mitochondrial dysfunction, alpha-synuclein aggregation to neurotoxic oligomers, dysfunction of both lysosomal and proteasomal protein degradation systems, and plasma reticulum stress [11,34,44–51]. Due to the chemical characteristics of aminochrome, it does not induce expansive neurotoxic effects such as alpha-synuclein fibrils. Aminochrome has been shown to be stable for up to 40 min before its conversion to 5,6-indolequinone begins [52].

4. Preclinical Model for Idiopathic Parkinson's Disease

The preclinical model for idiopathic Parkinson's disease should use (i) an endogenous neurotoxin that is formed within the neuromelanin-containing dopaminergic neurons of the nigrostriatal system; (ii) a neurotoxin that induces a focal (non-expansive) degeneration; (iii) it should trigger all the mechanisms involved in the degenerative process, such as oxidative stress, mitochondrial dysfunction, alpha-synuclein aggregation to neurotoxic oligomers, protein degradation dysfunction (lysosomal and proteasomal system), endoplasmic reticulum stress, and neuroinflammation. As we have seen previously, the only one of the endogenous neurotoxins that we have previously described that meets these requirements is aminochrome.

Aminochrome is neurotoxic by being one-electron reduced to leukoaminochrome *o*-semiquinone radical by most flavoenzymes with the exception of DT-diaphorase (NADP(H): quinone oxidoreductase), which is the unique flavoenzyme that reduces quinones with two electrons [53]. In studies performed with electron spin resonance (ESR), NADPH cytochrome P450 reductase was found to reduce both dopamine ortho-quinone and aminochrome to the free radicals dopamine *o*-semiquinone and leukoaminochrome *o*-semiquinone, respectively. The ESR spectrum of dopamine *o*-semiquinone and of leukoaminochrome *o*-semiquinone radical was detected at 1 min. However, at 2 min only the dopamine *o*-semiquinone radical spectrum was detectable by ESR due to the high reactivity of leukoaminochrome *o*-semiquinone radical with oxygen [10]. Aminochrome one-electron reduction to the leukoaminochrome *o*-semiquinone radical induces oxidative stress due to the extremely rapid reaction with oxygen, which causes re-oxidation to aminochrome. This generates a redox cycling between aminochrome and leukoaminochrome *o*-semiquinone radical that functions until cellular dioxygen and/or NAD(P)H are depleted. This redox cycling generates oxidative stress and the depletion of cytosolic NADH for its use to generate ATP in the mitochondrial electron transport chain (Figure 1).

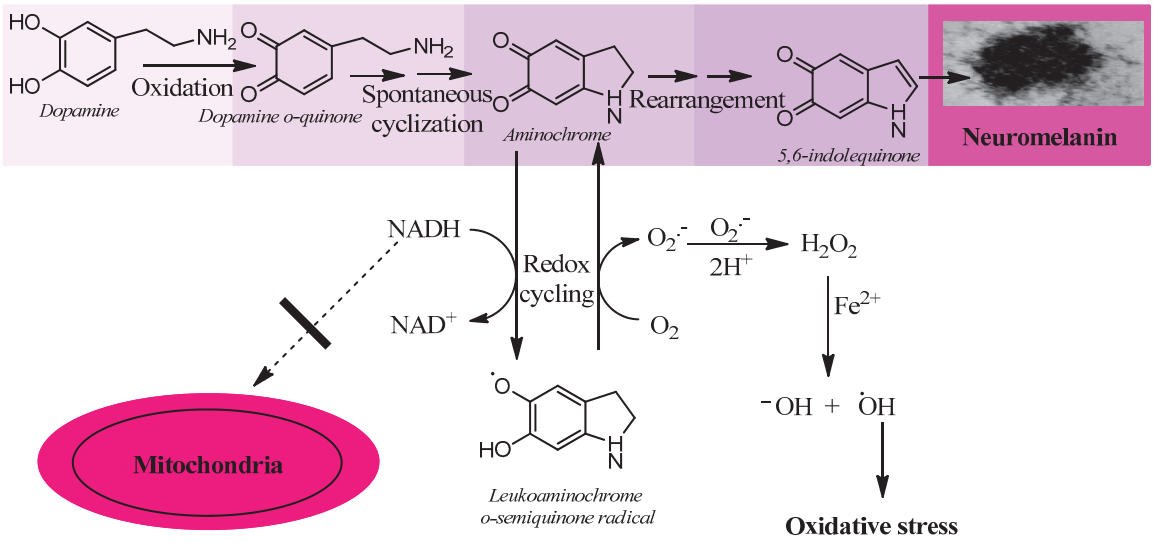

Figure 1. Aminochrome induces oxidative stress. Aminochrome can be reduced with one electron to produce the leukoaminochrome *o*-semiquinone radical by flavoenzymes using the cytosolic NADH generated to be used in the mitochondria to generate ATP through the transport chain coupled to oxidative phosphorylation from ADP to ATP. The leukoaminochrome *o*-semiquinone radical is extremely unstable in the presence of dioxygen and autoxidizes to regenerate aminochrome, which is reduced again, creating a redox cycle between aminochrome and leukoaminochrome *o*-semiquinone radical. This redox cycling is very fast and depletes as much oxygen as NADH with the concomitant production of oxidative stress.

Aminochrome is also neurotoxic by forming covalent complexes with proteins such as alpha-synuclein that induce the formation of neurotoxic oligomers [34]. Aminochrome forms adducts also with actin and α- and β-tubulin disrupting the cytoskeleton architecture [54], which plays an important role in microtubule formation [55]. Aminochrome inhibits complex I of the mitochondrial respiratory chain, resulting in the inhibition of ATP production and mitochondrial dysfunction [45,46]. Aminochrome induces protein degradation dysfunction by inhibiting lysosomal and proteasomal systems [48–50]. Aminochrome induces lysosomal dysfunction by inhibiting the vacuolar-type H^+-ATPase that plays an essential role in maintaining an acidic pH by pumping protons into lysosomes [56]. Aminochrome also induces endoplasmic reticulum stress and neuroinflammation [44,47,48].

Aminochrome in vivo induces neuronal dysfunction as a consequence of a significant decrease in dopamine release with concomitant enhanced GABA release [57]. Aminochrome induces mitochondrial dysfunction with a significant decrease in ATP production, affecting axonal transport of monoaminergic vesicles for neurotransmission to the terminals that explain the significant decrease in the number of these vesicles in the terminals compared with saline as control. Aminochrome induces a progressive degeneration of dopaminergic neurons while the striatal dopaminergic fibers are intact, accompanied by a dramatic change of tyrosine positive neuron morphology, a phenomenon known as cell shrinkage [57].

The ideal model for idiopathic Parkinson's disease should consider that the neurotoxin that triggers the degenerative process is generated within the same neuromelanin-containing dopaminergic neuron and induces a degenerative process focused on a single neuron. This last requirement is practically impossible to achieve, since the injection of aminochrome into the striatum or substantia nigra will affect all the neurons that are in contact with aminochrome solution. However, if aminochrome is the neurotoxin that triggers neurodegeneration in idiopathic Parkinson's, this model could be a good target to

search for possible pharmacological compounds that prevent, inhibit, or slow down this degenerative process in idiopathic Parkinson's.

There is a study in which the human enzyme tyrosinase was overexpressed in the substantia nigra of rats, exacerbating the production of neuromelanin in this region of the brain in all types of neurons and glial cells, inducing nigrostriatal neurodegeneration, hypokinesia, and Lewy body-like formation [58]. The problem with this model is that (i) this overexpression affects the majority of dopaminergic neurons, generating a massive effect on the degenerative process; (ii) the oxidative effect of tyrosinase is not specific for dopaminergic neurons since this overexpression affects all neurons and glial cells. Tyrosinase catalyzes the oxidation of monophenols or diphenols in the presence of dioxygen without the need for a cofactor; however, its catalytic activity with diphenols is higher than with monophenols [59]. Therefore, indiscriminate overexpression in all types of neurons and glial cells reduces the specificity of the model, since tyrosinase can oxidize monophenols in other types of neurons or glial cells with unknown effects. In the case of overexpression of tyrosinase in astrocytes, this enzyme can also oxidize dopamine, since this type of glial cell can take up dopamine released during neurotransmission; (iii) the triggering agent of the neurodegenerative process in this preclinical model is not a neurotoxin that can be the target of new pharmacological drugs attempting to stop the degenerative process, but rather it is tyrosinase, which is not expressed in the human substantia nigra. However, there are some reports that suggest its expression in this tissue [60], but if it were true that tyrosinase is normally expressed in neuromelanin-containing dopaminergic neurons, the presence of the pigment would be observed from an early age in children. Several studies have indeed shown that tyrosinase is not present in the human substantia nigra, even using highly specific and sensitive mass spectroscopy [61,62] (Zucca et al., 2018; Tribl et al., 2007). It has been proposed that animals that produce more neuromelanin and more closely resemble the human brain such as sheep and goats are more appropriate as a preclinical animal model for Parkinson's disease [63] (Capucciati et al., 2021).

5. Transcriptional Gene Activation via KEAP1/NRF2

Transcriptional activation of genes encoding a battery of cellular defense enzymes that provide protection against oxidative and electrophilic stress is affected by the transcription factor NRF2 (nuclear factor (erythroid-derived 2)-like 2) binding to an antioxidant responsive element or an electrophile responsive element (ARE/EpRE). Among the various cytoprotective proteins are γ-glutamylcysteine ligase, GSTs, and DT-diaphorase [18,64]. NFR2 is bound to KEAP1 (Kelch-like ECH-associated protein 1) in the cytosol, where it is directed to rapid proteasomal degradation. KEAP1 senses reactions of its sulfhydryl groups with electrophiles and oxidants and, as a consequence, NRF2 is released and targets ARE/ErRE elements of DNA in the nucleus. KEAP1/NRF2 is recognized as the most prominent protective system against electrophilic and oxidative insults; the upregulation of key enzymes in the defense against toxicants implicated in Parkinson's disease and other neurodegenerative conditions is noteworthy. For obvious reasons, the KEAP1/NFR2 system has been considered for pharmacological interventions in Parkinson's disease [19,65], Figure 2.

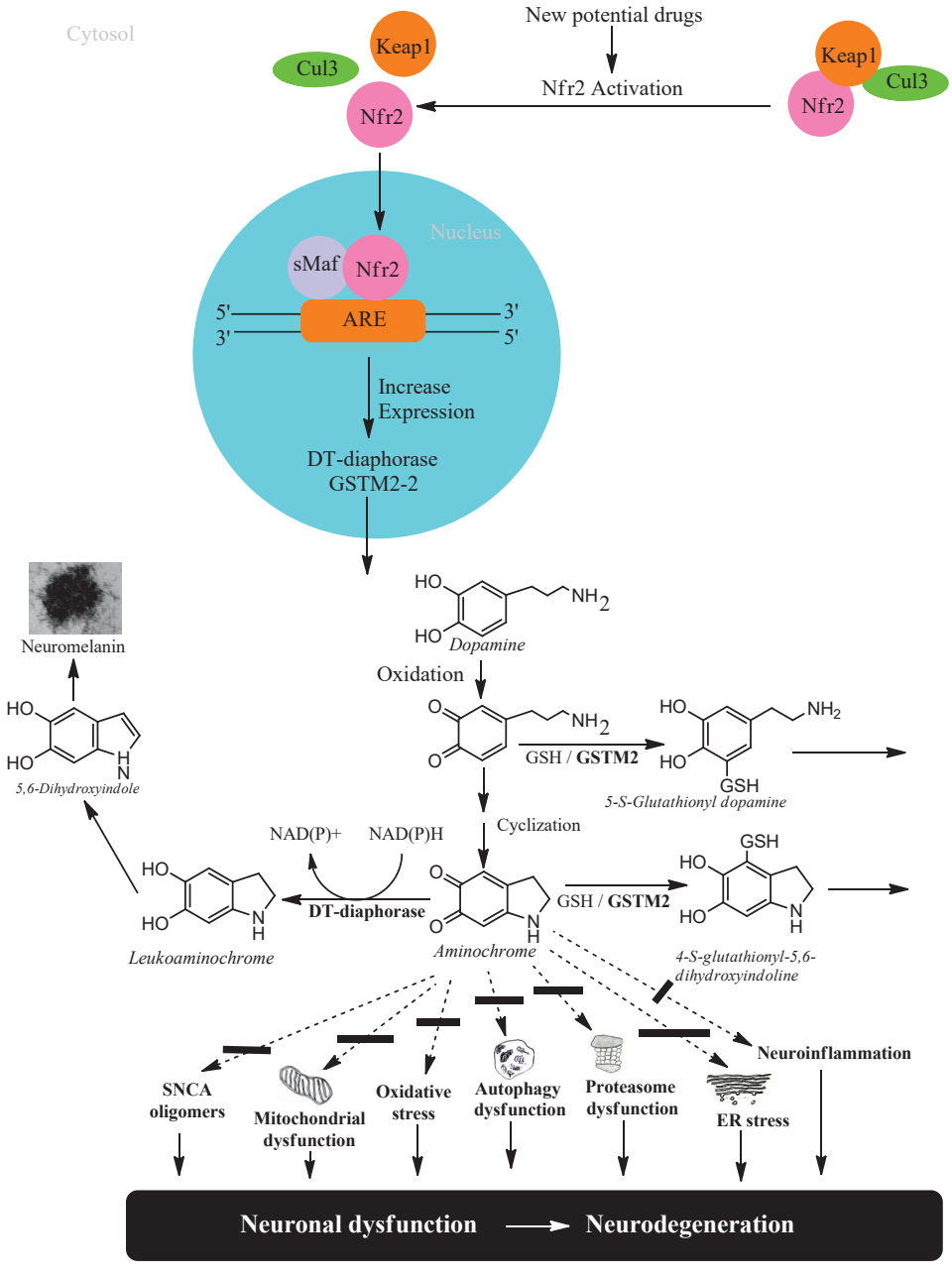

Figure 2. NFR2 activation to protect dopaminergic neurons from aminochrome neurotoxicity.

6. Neuroprotection against Neurodegeneration of Nigrostriatal System in Parkinson's Disease

Studies carried out with postmortem material from healthy elderly people show intact neuromelanin-containing dopaminergic neurons, suggesting that neuromelanin synthesis is a natural and harmless process. Neuromelanin has been observed to increase

over the years in the human brain [66]. However, there is an apparent contradiction, since the synthesis of neuromelanin requires the oxidation of dopamine to three ortho-quinones that can be neurotoxic. Among these aminochrome is the most toxic that induces oxidative stress, the formation of neurotoxic alpha-synuclein oligomers, dysfunction of both lysosomal and proteasomal protein breakdown systems, plasma reticulum stress, mitochondrial dysfunction, and neuroinflammation. The reason why the elderly have their neuromelanin-containing dopaminergic neurons intact at the time of death is because there are two enzymes that prevent the neurotoxic effects of aminochrome DT-diaphorase and glutathione transferase M2-2.

6.1. DT-Diaphorase

DT-diaphorase (NAD(P)H: quinone oxidoreductase, NQO1) is a flavoenzyme with FAD as a prosthetic group that transfers two electrons from either NADH or NADPH to quinones, thereby reducing them to hydroquinones [53,61,67]. This enzyme is 90% located in the cytosol and 5% associated with the endoplasmic reticulum and mitochondria. It is widely expressed in different organs; in the brain it is expressed in the substantia nigra, striatum, cortex, hypothalamus, and hippocampus. In rat substantia nigra, DT-diaphorase is responsible for 97% of the total quinone reductase activity. DT-diaphorase is expressed in tyrosine hydroxylase positive neurons and in astrocytes. DT-diaphorase reduces aminochrome to leukoaminochrome, preventing its neurotoxic effects in a catecholaminergic cell line [68], but DT-diaphorase also prevents aminochrome induced-toxicity in a human astrocyte cell line [69]. DT-diaphorase prevents aminochrome-induced oxidative stress, mitochondrial dysfunction, formation of neurotoxic alpha-synuclein oligomers, proteasome dysfunction, autophagy dysfunction, and lysosome dysfunction [11,26,34,40,47–49,51,54,56,62,64].

6.2. Glutathione Transferase M2-2

Electrophilic compounds such as epoxides, alkenals, and quinones can react with GSH and thereby become inactivated and form glutathione conjugates suitable for export from the cytosol [12,70]. The reactions are catalyzed by 20-odd enzymes, which are differentially distributed in cells and tissues. In humans and other mammals, the GSTs have been grouped into membrane-bound (microsomal) and soluble (cytosolic) proteins [13,71]. The former are members of the MAPEG (membrane-associated proteins in eicosanoid and glutathione metabolism) family [14,72]. The soluble GSTs are dimeric proteins occurring in eight classes of homologous sequences, which are catalytically active as homodimers as well as heterodimers [15,73]. The dimers are thus denoted according to their subunit composition, for example, as GST M1-1, GST M1-2, and GST M2-2 encoded by the GSTM1 and GSTM2 genes of the Mu class. With respect to the large variety of compounds identified as substrates for the various GSTs, it is noteworthy that only GST M2-2 has been found to catalyze with high efficiency the conjugation of ortho-quinones derived from dopamine [17,74,75]. The most active glutathione transferase catalyzing aminochrome conjugation is glutathione transferase M2-2, which gives rise to 4-S-glutathionyl-5,6-dihydroxyindoline. Interestingly, 4-S-glutathionyl-5,6-dihydroxyindoline is not oxidized by physiologically occurring oxidants such as dioxygen, hydrogen peroxide, and superoxide. Glutathione transferase M2-2 also catalyzes glutathione conjugation of the aminochrome precursor dopamine ortho-quinone to 5-glutathionyl dopamine that is degraded to 5-cysteinyl dopamine, which has been detected in human cerebrospinal fluid and neuromelanin [16,17,72–78] (Figure 3).

However, whether 5-cysteinyl is an end product is controversial as it has been reported by in vitro experiments that 5-cysteinyldopamine may be neurotoxic by being oxidized to 5-cysteinyldopamine o-quinone, which is converted to a bicyclic o-quinone imine [76,79]. If this mechanism is correct, it remains to explain the presence of 5-cysteinyldopamine in human cerebrospinal fluid and neuromelanin [77,78], since 5-cysteinyldopamine is converted to bicyclic o-quinone imine [79].

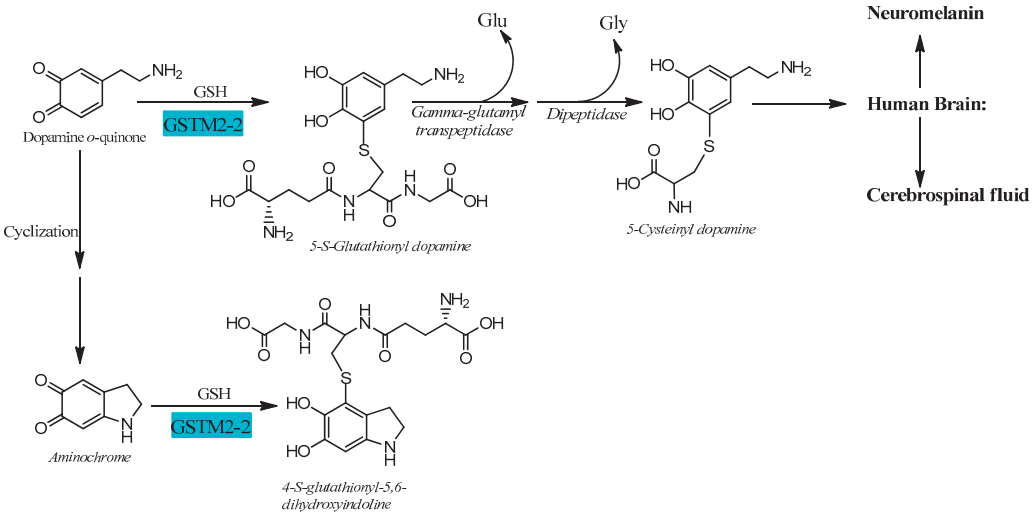

Figure 3. Glutathione transferase M2-2 catalyzes glutathione conjugation of ortho-quinones.

6.3. Astrocytes Protect Dopaminergic Neurons against Aminochrome Neurotoxicity

The brain is responsible for more than 20% of the energy consumption in the human body. The organism derives ATP via oxidation of carbohydrates, fats, and proteins and by coupling electron transport with phosphorylation of ADP to ATP. Neurons require ATP to transport proteins and neurotransmission vesicles to neuronal terminals, and neurotransmission itself is completely dependent on ATP. In other words, neuronal function is absolutely dependent on the presence of ATP, which, to a large extent, is generated in the mitochondria. Electrons in the transport chain from NADH flowing through complex I or complex II are further transmitted to ubiquinone Q10 (also known as coenzyme Q10), which in turn transfers the electrons to complex III. In this transfer of electrons, ubiquinone Q10 is reduced with one electron to the free radical ubiquinone Q10 semiquinone. The latter is subsequently reduced to ubiquinone Q10 hydroquinone, which transfers the electrons to complex III. However, the radical ubiquinone Q10 semiquinone is able to reduce dioxygen to superoxide, generating electron transport leakage and oxidative stress. Superoxide enzymatically or spontaneously can generate hydrogen peroxide, which, in the presence of reduced iron, forms hydroxyl radicals. This leakage of electrons from the mitochondrial electron transport chain permanently exposes neurons to conditions of oxidative stress. Astrocytes play an important role in protecting neurons against oxidative stress since astrocytes secrete precursors of glutathione, which is an important antioxidant [77,80,81]. Neuromelanin-containing dopaminergic neurons are also exposed to the neurotoxic effects of aminochrome, leading to oxidative stress, mitochondrial dysfunction, formation of neurotoxic alpha-synuclein oligomers, dysfunction of both lysosomal and proteasomal protein degradation systems, neuroinflammation, and endoplasmic reticulum stress [44–49,62,63]. However, astrocytes also play a neuroprotective role for neuromelanin-containing dopaminergic neurons by secreting exosomes loaded with the enzyme glutathione transferase M2-2 that penetrate dopaminergic neurons to, in concert with DT-diaphorase, prevent the neurotoxic effects of aminochrome [73,77,78,80–82] (Figure 4).

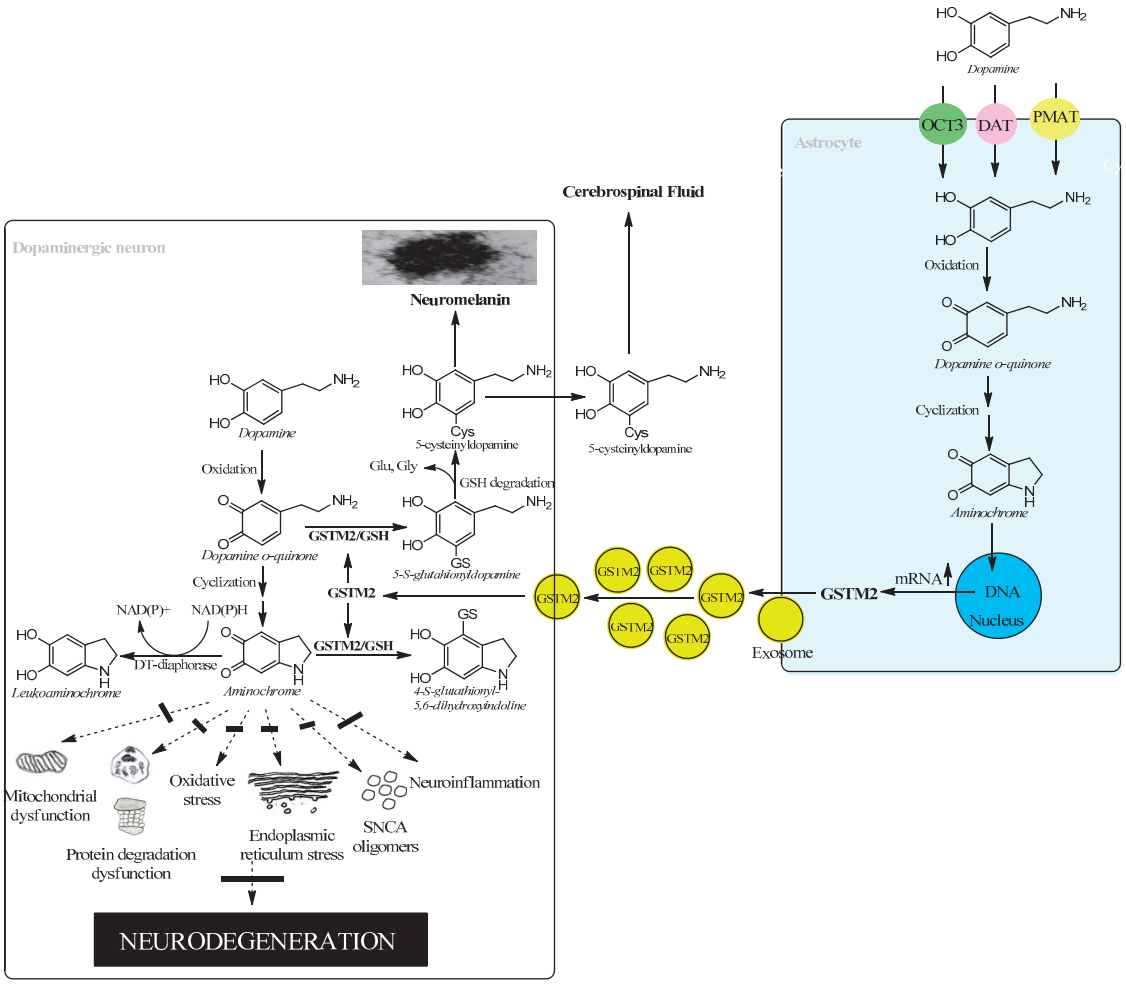

Figure 4. Astrocytes protect dopaminergic neurons against aminochrome neurotoxicity.

6.4. Glutathione and Oxidative Stress

Glutathione (GSH) is a fundamental endogenous constituent of the molecular defense that provides protection against electrophilic agents and oxidative stress [1,83]. GSH, L-γ-glutamyl-L-cysteinylglycine, is formed by the sequential actions of γ-glutamylcysteine ligase and glutathione synthetase, of which reactions the first is rate-limiting in GSH biosynthesis [2,84]. It has been demonstrated that GSH is ubiquitously present in the brain and that substantia nigra in Parkinson's patients is selectively depleted in GSH content compared with healthy individuals [3,4,85,86]. Whether the loss of GSH is a cause or an effect of the disease remains unknown but attempts to raise the GSH concentration by pharmacological intervention have been made under the premise that an elevated GSH level would provide a therapeutic consequence [5,87]. In general, GSH cannot cross cell membranes or penetrate the blood–brain barrier and oral administration has been ruled out. Nasal spray delivery of GSH has been attempted, but the efficacy is unclear [6,88]. The amino acid limiting the biosynthesis of GSH is cysteine, which is normally transported into cells as the disulfide cystine via the system xc-cystine/glutamate antiporter [7,89]. Thus, intravenous administration of the precursor N-acetylcysteine has been reported

to increase the GSH concentration in the brain [8,90]. The characteristic pathological features of substantia nigra in Parkinson's patients comprise enhanced iron deposition and lipid peroxidation, as wells as defects in the transport system xc-. These attributes are congruent with the hallmarks of ferroptosis, which is currently receiving attention in various diseases [9,91]. Preventing the progressive loss of dopaminergic neurons by interfering with ferroptosis is a new approach to treatment [6,10,88,92]. GSH can serve as an antioxidant and five selenium-dependent peroxidases (GPXs) catalyze the reduction of hydrogen peroxide and various lipid hydroperoxides [11,93]. The enzymes play a prominent role in the protection against reactive oxygen species (ROS). GPX4 is particularly active with phospholipid hydroperoxides and appears to play an essential function in preventing ferroptosis [9,91].

7. Conclusions and Future Directions

It is clear that oxidative stress plays a role in the degenerative process of the nigrostriatal system in idiopathic Parkinson's disease. In our opinion, the failure of clinical studies with antioxidants is due to the fact that the preclinical models used to propose these clinical studies are based on exogenous neurotoxins (MPTP and 6-hydroxydopamine) that do not represent what happens in the neurodegenerative process of idiopathic Parkinson's disease. These neurotoxins induce massive and extremely rapid degeneration; for example, MPTP induces severe Parkinsonism in just three days, while the degenerative process takes many years. How to test a possible new drug for idiopathic Parkinson's disease if the preclinical model does not include what triggers the degenerative process? The drug examined for potential use in the disease cannot inhibit the degenerative process, since these exogenous neurotoxins do not exist in the human nigrostriatal system. Aminochrome seems to be a good alternative, since it is formed in the nigrostriatal neurons where the degenerative process occurs and induces all the mechanisms that have been reported to be involved in the degenerative process of idiopathic Parkinson's disease, such as oxidative stress, dysfunction mitochondrial, formation of neurotoxic alpha-synuclein oligomers, endoplasmic reticulum stress, neuroinflammation, and dysfunction of both lysosomal and proteasomal protein degradation systems. Unfortunately, aminochrome must be injected into the striatum or substantia nigra and a neuron-in-neuron focal degeneration such as occurs in the disease cannot be reproduced. However, although the injection of aminochrome affects many neurons immediately, it produces a progressive neuronal dysfunction that progresses slowly. In addition, if aminochrome is what triggers the degeneration of neuromelanin-containing dopaminergic neurons in idiopathic Parkinson's disease, this preclinical model could serve to detect potential new drugs that change the progress of the disease or stop the neurodegenerative process.

The presence of neuromelanin-containing dopaminergic neurons in the postmortem brain of healthy elderly people suggests that neuromelanin synthesis is a normal and harmless process, despite the fact that it requires the oxidation of dopamine to three ortho-quinones that are potentially toxic, especially aminochrome. This apparent contradiction that neuromelanin synthesis is harmless despite the formation of neurotoxic ortho-quinones can be explained by the neuroprotective role of DT-diaphorase and GSTM2-2 and the neuroprotective role of astrocytes secreting exosomes loaded with GSTM2-2. However, the neuroprotective capacity of DT-diaphorase and GSTM2-2 is not infinite but depends on their Km with respect to aminochrome. Excess aminochrome formation that exceeds the neuroprotective capacity of these enzymes may explain the degenerative process in idiopathic Parkinson's disease. Aminochrome is neurotoxic by inducing the formation of neurotoxic alpha-synuclein oligomers, mitochondrial dysfunction, oxidative stress, dysfunction of both lysosomal and proteasomal protein degradation systems, endoplasmic reticulum stress, and neuroinflammation. Therefore, increasing the expression of DT-diaphorase and GSTM2-2 may be a therapeutic modality to prevent the degeneration of new neuromelanin-containing dopaminergic neurons. The activation of NFR2 induces the expression phase 2 enzymes, including both DT-diaphorase and GST [79,92], and therefore its activation may be the

target of potential new drugs that slow down the neurogenerative process in idiopathic Parkinson's disease. Several phytochemicals in natural products that have different biological actions have been shown to be activators of NFR2. Sesamol is a component of sesame oil having an anti-inflammatory and antioxidant effect that has been proposed as a cardioprotector [80,93]. A component of Rhododendron l. is farrerol that has been shown to have an anti-inflammatory, antioxidant, and neuroprotective effect [81,94]. Oxyphylla A is a component of Alpinia oxyphylla that is used in traditional Chinese medicine to treat memory loss and has been shown to decrease cognitive deficits and improve muscle strength [82,95]. Sargahydorquinoic acid, isolated from the marine alga Sargassum serratifolium, has been shown to be a potent antioxidant [83,96]. Ginsenoside Re has been isolated from the stem, berry, leaf, flower bud, and root of Panax ginseng and has exhibited a long list of pharmacological effects including neuroprotective effects [84,85,97,98]. Sulforaphane, found in cruciferous vegetables such as broccoli, Brussels sprouts, cabbage, and cauliflower, has anti-apoptotic, antioxidant, and anti-inflammatory properties [86,99]. Protopanaxatriol, present in Panax ginseng Mayer, protects against oxidative stress [87,100]. The flavonoids naringin and naringenin, present in tomatoes, bergamots, and various citrus, have anti-inflammatory, antioxidant, and neuroprotective properties [88,101–105]. Several phytochemicals inducing DT-diaphorase have been reported that include farrerol, sesamol, oxyphylla A, sargassum serratifolium, ginsenoside Re, sulforaphane, protopanaxatriol, and naringin [80–95,99]. Therefore, an interesting question is whether these phytochemical NFR2 activators can inhibit or decrease aminochrome-induced neurotoxicity.

Author Contributions: Conceptualization, J.S.-A.; writing—original draft preparation, J.S.-A.; writing—review and editing, J.S.-A. and B.M.; All authors have read and agreed to the published version of the manuscript.

Funding: Swedish Cancer Society and the Swedish Research Council (grant 2015-04222; B.M.)

Institutional Review Board Statement: Not applicable.

Informed Consent Statement: Not applicable.

Data Availability Statement: Not applicable.

Conflicts of Interest: The authors declare no conflict of interest.

References

1. Balestrino, R.; Schapira, A.H.V. Parkinson disease. *Eur. J. Neurol.* **2020**, *27*, 27–42. [CrossRef] [PubMed]
2. Simon, D.K.; Tanner, C.M.; Brundin, P. Parkinson Disease Epidemiology; Pathology, Genetics, a50nd Pathophysiology. *Clin. Geriatr. Med.* **2020**, *36*, 1–12. [CrossRef]
3. Yoo, J.M.; Lin, Y.; Heo, Y.; Lee, Y.H. Polymorphism in alpha-synuclein oligomers and its implications in toxicity under disease conditions. *Front. Mol. Biosci.* **2022**, *9*, 959425. [CrossRef]
4. Day, J.O.; Mullin, S. The Genetics of Parkinson's Disease and Implications for Clinical Practice. *Genes* **2021**, *12*, 1006. [CrossRef] [PubMed]
5. Mercado, G.; Castillo, V.; Soto, P.; Sidhu, A. ER stress and Parkinson disease: Pathological inputs that converge into the secretory pathway. *Brain Res.* **2016**, *16*, 30260–30268.
6. Moors, T.; Paciotti, S.; Chiasserini, D.; Calabresi, P.; Parnetti, L.; Beccari, T.; van de Berg, W.D. Lysosomal Dysfunction and α-Synuclein Aggregation in Parkinson's Disease. *Diagnostic. Links Mov. Disord.* **2016**, *6*, 791–801. [CrossRef]
7. Rocha, E.M.; De Miranda, B.; Sanders, L.H. Alpha-synuclein: Pathology, mitochondrial dysfunction and neuroinflammation in Parkinson's disease. *Neurobiol. Dis.* **2018**, *109 Pt B*, 249–257. [CrossRef]
8. Jankovic, J.; Tan, E.K. Parkinson's disease: Etiopathogenesis and treatment. *J. Neurol. Neurosurg. Psychiatry* **2020**, *91*, 795–808. [CrossRef]
9. Segura-Aguilar, J. Parkinson´s disease. In *Clinical Studies and Therapies in Parkinson's Disease: Translations from Preclinical Models*; Segura-Aguilar, J., Ed.; Elsevier: Cambridge, MA, USA, 2021; pp. 1–175.
10. Segura-Aguilar, J.; Metodiewa, D.; Welch, C.J. Metabolic activation of dopamine o-quinones to *o*-semiquinones by NADPH cytochrome P450 reductase may play an important role in oxidative stress and apoptotic effects. *Biochim. Biophys. Acta* **1998**, *1381*, 1–6. [CrossRef]

11. Arriagada, C.; Paris, I.; Sanchez de las Matas, M.J.; Martinez-Alvarado, P.; Cardenas, S.; Castañeda, P.; Graumann, R.; Perez-Pastene, C.; Olea-Azar, C.; Couve, E.; et al. On the neurotoxicity mechanism of leukoaminochrome *o*-semiquinone radical derived from dopamine oxidation: Mitochondria damage, necrosis, and hydroxyl radical formation. *Neurobiol. Dis.* **2004**, *16*, 468–477. [CrossRef]
12. Musatov, A.; Robinson, N.C. Susceptibility of mitochondrial electron-transport complexes to oxidative damage. Focus on cytochrome c oxidase. *Free Radic. Res.* **2012**, *46*, 1313–1326. [CrossRef]
13. Jing, L.; He, M.T.; Chang, Y.; Mehta, S.L.; He, Q.P.; Zhang, J.Z.; Li, P.A. Coenzyme Q10 protects astrocytes from ROS-induced damage through inhibition of mitochondria-mediated cell death pathway. *Int. J. Biol. Sci.* **2015**, *11*, 59–66. [CrossRef] [PubMed]
14. Beal, M.F. Coenzyme Q10 administration and its potential for treatment of neurodegenerative diseases. *Biofactors* **1999**, *9*, 261–266. [CrossRef] [PubMed]
15. Park, H.W.; Park, C.G.; Park, M.; Lee, S.H.; Park, H.R.; Lim, J.; Paek, S.H.; Choy, Y.B. Intrastriatal administration of coenzyme Q10 enhances neuroprotection in a Parkinson's disease rat model. *Sci. Rep.* **2020**, *10*, 9572. [CrossRef] [PubMed]
16. Beal, M.F.; Oakes, D.; Shoulson, I.; Henchcliffe, C.; Galpern, W.R.; Haas, R.; Juncos, J.L.; John, G.N.; Tiffini Smith, V.; Bernard, R.; et al. A randomized clinical trial of high-dosage coenzyme Q10 in early Parkinson disease: No evidence of benefit. *JAMA Neurol.* **2014**, *71*, 543–552.
17. Yoritaka, A.; Kawajiri, S.; Yamamoto, Y.; Nakahara, T.; Ando, M.; Hashimoto, K.; Nagase, M.; Saito, Y.; Hattori, N. Randomized, double-blind, placebo-controlled pilot trial of reduced coenzyme Q10 for Parkinson's disease. *Parkinsonism. Relat. Disord.* **2015**, *21*, 911–916. [CrossRef]
18. Ghosh, A.; Chandran, K.; Kalivendi, S.V.; Joseph, J.; Antholine, W.E.; Hillard, C.J.; Kanthasamy, A.; Kanthasamy, A.; Kalyanaraman, B. Neuroprotection by a mitochondria-targeted drug in a Parkinson's disease model. *Free Radic. Biol. Med.* **2010**, *49*, 1674–1684. [CrossRef]
19. Xi, Y.; Feng, D.; Tao, K.; Wang, R.; Shi, Y.; Qin, H.; Murphy, M.P.; Yang, Q.; Zhao, G. MitoQ protects dopaminergic neurons in a 6-OHDA induced PD model by enhancing Mfn2-dependent mitochondrial fusion via activation of PGC-1α. *Biochim. Biophys. Acta Mol. Basis Dis.* **2018**, *1864*, 2859–2870. [CrossRef]
20. Solesio, M.E.; Prime, T.A.; Logan, A.; Murphy, M.P.; Del Mar Arroyo-Jimenez, M.; Jordán, J.; Galindo, M.F. The mitochondria-targeted anti-oxidant MitoQ reduces aspects of mitochondrial fission in the 6-OHDA cell model of Parkinson's disease. *Biochim. Biophys. Acta* **2013**, *1832*, 174–182. [CrossRef]
21. Snow, B.J.; Rolfe, F.L.; Lockhart, M.M.; Frampton, C.M.; O'Sullivan, J.D.; Fung, V.; Smith, R.A.; Murphy, M.P.; Taylor, K.M.; Protect Study Group. A double-blind, placebo-controlled study to assess the mitochondria-targeted antioxidant MitoQ as a disease-modifying therapy in Parkinson's disease. *Mov. Disord.* **2010**, *25*, 1670–1674. [CrossRef]
22. Gong, L.; Zhang, Q.L.; Zhang, N.; Hua, W.Y.; Huang, Y.X.; Di, P.W.; Huang, T.; Xu, X.S.; Liu, C.F.; Hu, L.F.; et al. Neuroprotection by urate on 6-OHDA-lesioned rat model of Parkinson's disease: Linking to Akt/GSK3β signaling pathway. *J. Neurochem.* **2012**, *123*, 876–885. [CrossRef]
23. Huang, T.T.; Hao, D.L.; Wu, B.N.; Mao, L.L.; Zhang, J. Uric acid demonstrates neuroprotective effect on Parkinson's disease mice through Nrf2-ARE signaling pathway. *Biochem. Biophys. Res. Commun.* **2017**, *493*, 1443–1449. [CrossRef]
24. Crotty, G.F.; Ascherio, A.; Schwarzschild, M.A. Targeting urate to reduce oxidative stress in Parkinson disease. *Exp. Neurol.* **2017**, *298*, 210–224. [CrossRef]
25. Schwarzschild, M.A.; Ascherio, A.; Casaceli, C.; Curhan, G.C.; Fitzgerald, R.; Kamp, C.; Lungu, C.; Macklin, E.A.; Marek, K.; Mozaffarian, D.; et al. Effect of Urate-Elevating Inosine on Early Parkinson Disease Progression: The SURE-PD3 Randomized Clinical Trial. *JAMA* **2021**, *326*, 926–939. [PubMed]
26. Kostrzewa, R.M.; Jacobowitz, D.M. Pharmacological actions of 6-hydroxydopamine. *Pharmacol. Rev.* **1974**, *26*, 199–288.
27. Simola, N.; Morelli, M.; Carta, A.R. The 6-hydroxydopamine model of Parkinson's disease. *Neurotox. Res.* **2007**, *11*, 151–167. [CrossRef]
28. Varešlija, D.; Tipton, K.F.; Davey, G.P.; McDonald, A.G. 6-Hydroxydopamine: A far from simple neurotoxin. *J. Neural. Transm.* **2020**, *127*, 213–230. [CrossRef]
29. Martí, M.J.; Saura, J.; Burke, R.E.; Jackson-Lewis, V.; Jiménez, A.; Bonastre, M.; Tolosa, E. Striatal 6-hydroxydopamine induces apoptosis of nigral neurons in the adult rat. *Brain Res.* **2002**, *20*, 185–191. [CrossRef]
30. Williams, A. MPTP parkinsonism. *Br. Med. J.* **1984**, *289*, 1401–1402. [CrossRef]
31. Ni, A.; Ernst, C. Evidence That Substantia Nigra Pars Compacta Dopaminergic Neurons Are Selectively Vulnerable to Oxidative Stress Because They Are Highly Metabolically Active. *Front. Cell. Neurosci.* **2022**, *16*, 826193. [CrossRef]
32. Sikorska, M.; Lanthier, P.; Miller, H.; Beyers, M.; Sodja, C.; Zurakowski, B.; Gangaraju, S.; Pandey, S.; Sandhu, J.K. Nanomicellar formulation of coenzyme Q10 (Ubisol-Q10) effectively blocks ongoing neurodegeneration in the mouse 1-methyl-4-phenyl-1,2,3,6-tetrahydropyridine model: Potential use as an adjuvant treatment in Parkinson's disease. *Neurobiol. Aging* **2014**, *35*, 2329–2346. [CrossRef] [PubMed]
33. Braak, H.; Del Tredici, K.; Rüb, U.; de Vos, R.A.; Jansen Steur, E.N.; Braak, E. Staging of brain pathology related to sporadic Parkinson's disease. *Neurobiol. Aging* **2003**, *24*, 197–211. [CrossRef]
34. Muñoz, P.; Cardenas, S.; Huenchuguala, S.; Briceño, A.; Couve, E.; Paris, I.; Segura-Aguilar, J. DT-Diaphorase Prevents Aminochrome-Induced Alpha-Synuclein Oligomer Formation and Neurotoxicity. *Toxicol. Sci.* **2015**, *145*, 37–47. [CrossRef] [PubMed]

35. Yang, J.L.; Gao, J.H.; Du, T.F.; Yi, H.K.; Ma, K.L. Distribution of the Alpha-Synuclein in the Brain and the Primary Organs of the Rhesus Monkey. *Appl. Biochem. Biotechnol.* **2021**, *193*, 3187–3201. [CrossRef]
36. Segura-Aguilar, J. Can we conclude a potential therapeutic action for Parkinson's disease by using postmortem tissue and a preclinical model based on an exogenous neurotoxin? *Cell Death Dis.* **2018**, *9*, 748. [CrossRef] [PubMed]
37. Wakabayashi, K.; Tanji, K.; Odagiri, S.; Miki, Y.; Mori, F.; Takahashi, H. The Lewy body in Parkinson's disease and related neurodegenerative disorders. *Mol. Neurobiol.* **2013**, *47*, 495–508. [CrossRef]
38. Goldstein, D.S. The Catecholaldehyde Hypothesis for the Pathogenesis of Catecholaminergic Neurodegeneration: What We Know and What We Do Not Know. *Int. J. Mol. Sci.* **2021**, *22*, 5999. [CrossRef]
39. Grünblatt, E.; Ruder, J.; Monoranu, C.M.; Riederer, P.; Youdim, M.B.; Mandel, S.A. Differential Alterations in Metabolism and Proteolysis-Related Proteins in Human Parkinson's Disease Substantia Nigra. *Neurotox. Res.* **2018**, *33*, 560–568. [CrossRef]
40. Biesemeier, A.; Eibl, O.; Eswara, S.; Audinot, J.N.; Wirtz, T.; Pezzoli, G.; Zucca, F.A.; Zecca, L.; Schraermeyer, U. Elemental mapping of Neuromelanin organelles of human Substantia Nigra: Correlative ultrastructural and chemical analysis by analytical transmission electron microscopy and nano-secondary ion mass spectrometry. *J. Neurochem.* **2016**, *138*, 339–353. [CrossRef]
41. Engelen, M.; Vanna, R.; Bellei, C.; Zucca, F.A.; Wakamatsu, K.; Monzani, E.; Ito, S.; Casella, L.; Zecca, L. Neuromelanins of human brain have soluble and insoluble components with dolichols attached to the melanic structure. *PLoS ONE* **2012**, *7*, e48490. [CrossRef]
42. Zucca, F.A.; Capucciati, A.; Bellei, C.; Sarna, M.; Sarna, T.; Monzani, E.; Casella, L.; Zecca, L. Neuromelanins in brain aging and Parkinson's disease: Synthesis, structure, neuroinflammatory, and neurodegenerative role. *IUBMB Life* **2023**, *75*, 55–65. [CrossRef]
43. Zhang, W.; Phillips, K.; Wielgus, A.R.; Liu, J.; Albertini, A.; Zucca, F.A.; Faust, R.; Qian, S.Y.; Miller, D.S.; Chignell, C.F.; et al. Neuromelanin activates microglia and induces degeneration of dopaminergic neurons: Implications for progression of Parkinson's disease. *Neurotox. Res.* **2011**, *19*, 63–72. [CrossRef] [PubMed]
44. Santos, C.C.; Araújo, F.M.; Ferreira, R.S.; Silva, V.B.; Silva, J.H.C.; Grangeiro, M.S.; Soares, É.N.; Pereira, É.P.L.; Souza, C.S.; Costa, S.L.; et al. Aminochrome induces microglia and astrocyte activation. *Toxicol. In Vitro* **2017**, *42*, 54–60. [CrossRef]
45. Aguirre, P.; Urrutia, P.; Tapia, V.; Villa, M.; Paris, I.; Segura-Aguilar, J.; Núñez, M.T. The dopamine metabolite aminochrome inhibits mitochondrial complex I and modifies the expression of iron transporters DMT1 and FPN1. *Biometals* **2012**, *25*, 795–803. [CrossRef]
46. Paris, I.; Muñoz, P.; Huenchuguala, S.; Couve, E.; Sanders, L.H.; Greenamyre, J.T.; Caviedes, P.; Segura-Aguilar, J. Autophagy protects against aminochrome-induced cell death in substantia nigra-derived cell line. *Toxicol. Sci.* **2011**, *121*, 376–388. [CrossRef] [PubMed]
47. Xiong, R.; Siegel, D.; Ross, D. Quinone-induced protein handling changes: Implications for major protein handling systems in quinone-mediated toxicity. *Toxicol. Appl. Pharmacol.* **2014**, *280*, 285–295. [CrossRef]
48. Zafar, K.S.; Inayat-Hussain, S.H.; Siegel, D.; Bao, A.; Shieh, B.; Ross, D. Overexpression of NQO1 protects human SK-N-MC neuroblastoma cells against dopamine-induced cell death. *Toxicol. Lett.* **2006**, *166*, 261–267. [CrossRef] [PubMed]
49. Huenchuguala, S.; Muñoz, P.; Zavala, P.; Villa, M.; Cuevas, C.; Ahumada, U.; Graumann, R.; Nore, B.; Couve, E.; Mannervik, B.; et al. Glutathione transferase mu 2 protects glioblastoma cells against aminochrome toxicity by preventing autophagy and lysosome dysfunction. *Autophagy* **2014**, *10*, 618–630. [CrossRef]
50. Muñoz, P.; Huenchuguala, S.; Paris, I.; Segura-Aguilar, J. Dopamine oxidation and autophagy. *Parkinsons. Dis.* **2012**, *2012*, 920953. [CrossRef]
51. Segura-Aguilar, J. Dopamine oxidation to neuromelanin and neurotoxic metabolites. In *Clinical Studies and Therapies in Parkinson's Disease: Translations from Preclinical Models*; Segura-Aguilar, J., Ed.; Elsevier: Cambridge, MA, USA, 2021; pp. 213–227.
52. Bisaglia, M.; Mammi, S.; Bubacco, L. Kinetic and structural analysis of the early oxidation products of dopamine: Analysis of the interactions with alpha-synuclein. *J. Biol. Chem.* **2007**, *282*, 1559715-605. [CrossRef]
53. Segura-Aguilar, J. Neuroprotective mechanisms against dopamine oxidation-dependent neurotoxicity. In *Clinical Studies and Therapies in Parkinson's Disease: Translations from Preclinical Models*; Segura-Aguilar, J., Ed.; Elsevier: Cambridge, MA, USA, 2021; pp. 229–240.
54. Paris, I.; Perez-Pastene, C.; Cardenas, S.; Iturriaga-Vasquez, P.; Muñoz, P.; Couve, E.; Caviedes, P.; Segura-Aguilar, J. Aminochrome induces disruption of actin, alpha-, and beta-tubulin cytoskeleton networks in substantia-nigra-derived cell line. *Neurotox. Res.* **2010**, *18*, 82–92. [CrossRef]
55. Briceño, A.; Muñoz, P.; Brito, P.; Huenchuguala, S.; Segura-Aguilar, J.; Paris, I.B. Aminochrome Toxicity is Mediated by Inhibition of Microtubules Polymerization Through the Formation of Adducts with Tubulin. *Neurotox. Res.* **2016**, *29*, 381–393. [CrossRef]
56. Meléndez, C.; Muñoz, P.; Segura-Aguilar, J. DT-Diaphorase Prevents Aminochrome-Induced Lysosome Dysfunction in SH-SY5Y Cells. *Neurotox. Res.* **2019**, *35*, 255–259. [CrossRef] [PubMed]
57. Herrera, A.; Muñoz, P.; Paris, I.; Díaz-Veliz, G.; Mora, S.; Inzunza, J.; Hultenby, K.; Cardenas, C.; Jaña, F.; Raisman-Vozari, R.; et al. Aminochrome induces dopaminergic neuronal dysfunction: A new animal model for Parkinson's disease. *Cell. Mol. Life Sci.* **2016**, *73*, 3583–3597. [CrossRef] [PubMed]
58. Carballo-Carbajal, I.; Laguna, A.; Romero-Giménez, J.; Cuadros, T.; Bové, J.; Martinez-Vicente, M.; Parent, A.; Gonzalez-Sepulveda, M.; Peñuelas, N.; Torra, A.; et al. Brain tyrosinase overexpression implicates age-dependent neuromelanin production in Parkinson's disease pathogenesis. *Nat. Commun.* **2019**, *10*, 973. [CrossRef]

59. Do, H.; Kang, E.; Yang, B.; Cha, H.J.; Choi, Y.S. A tyrosinase, mTyr-CNK, that is functionally available as a monophenol monooxygenase. *Sci. Rep.* **2017**, *7*, 17267. [CrossRef]
60. Yamamuro, Y.; Ogura, S. Regional expression of tyrosinase in central catecholaminergic systems of colored mice. *Exp. Anim.* **2019**, *68*, 49–56. [CrossRef]
61. Tribl, F.; Arzberger, T.; Riederer, P.; Gerlach, M. Tyrosinase is not detected in human catecholaminergic neurons by immunohistochemistry and Western blot analysis. *J. Neural. Transm. Suppl.* **2007**, *72*, 51–55. [CrossRef]
62. Zucca, F.A.; Vanna, R.; Cupaioli, F.A.; Bellei, C.; De Palma, A.; Di Silvestre, D.; Mauri, P.; Grassi, S.; Prinetti, A.; Casella, L.; et al. Neuromelanin organelles are specialized autolysosomes that accumulate undegraded proteins and lipids in aging human brain and are likely involved in Parkinson's disease. *NPJ Parkinsons. Dis.* **2018**, *4*, 7. [CrossRef]
63. Capucciati, A.; Zucca, F.A.; Monzani, E.; Zecca, L.; Casella, L.; Hofer, T. Interaction of Neuromelanin with Xenobiotics and Consequences for Neurodegeneration; Promising Experimental Models. *Antioxidants* **2021**, *10*, 824. [CrossRef]
64. Yamamoto, M.; Kensler, T.W.; Motohashi, H. The KEAP1-NRF2 System: A Thiol-Based Sensor-Effector Apparatus for Maintaining Redox Homeostasis. *Physiol. Rev.* **2018**, *98*, 1169–1203. [CrossRef]
65. Yang, X.X.; Yang, R.; Zhang, F. Role of Nrf2 in Parkinson's Disease: Toward New Perspectives. *Front. Pharmacol.* **2022**, *13*, 919233. [CrossRef] [PubMed]
66. Zecca, L.; Fariello, R.; Riederer, P.; Sulzer, D.; Gatti, A.; Tampellini, D. The absolute concentration of nigral neuromelanin, assayed by a new sensitive method, increases throughout the life and is dramatically decreased in Parkinson's disease. *FEBS Lett.* **2002**, *510*, 216–220. [CrossRef] [PubMed]
67. Segura-Aguilar, J.; Muñoz, P.; Inzunza, J.; Varshney, M.; Nalvarte, I.; Mannervik, B. Neuroprotection against Aminochrome Neurotoxicity: Glutathione Transferase M2-2 and DT-Diaphorase. *Antioxidants* **2022**, *11*, 296. [CrossRef]
68. Lozano, J.; Muñoz, P.; Nore, B.F.; Ledoux, S.; Segura-Aguilar, J. Stable expression of short interfering RNA for DT-diaphorase induces neurotoxicity. *Chem. Res. Toxicol.* **2010**, *23*, 1492–1496. [CrossRef] [PubMed]
69. Huenchuguala, S.; Muñoz, P.; Graumann, R.; Paris, I.; Segura-Aguilar, J. DT-diaphorase protects astrocytes from aminochrome-induced toxicity. *Neurotoxicology* **2016**, *55*, 10–12. [CrossRef]
70. Mannervik, B. Evolution of glutathione transferases and related enzymes for the protection of cells against electrophiles. *Biochem. Soc. Trans.* **1996**, *24*, 878–880. [CrossRef]
71. Mannervik, B.; Board, P.G.; Hayes, J.D.; Listowsky, I.; Pearson, W.R. Nomenclature for mammalian soluble glutathione transferases. *Methods Enzymol.* **2005**, *401*, 1–8.
72. Jakobsson, P.J.; Morgenstern, R.; Mancini, J.; Ford-Hutchinson, A.; Persson, B. Common structural features of MAPEG—A widespread superfamily of membrane associated proteins with highly divergent functions in eicosanoid and glutathione metabolism. *Protein Sci.* **1999**, *8*, 689–692. [CrossRef]
73. Mannervik, B.; Jensson, H. Binary combinations of four protein subunits with different catalytic specificities explain the relationship between six basic glutathione S-transferases in rat liver cytosol. *J. Biol. Chem.* **1982**, *257*, 9909–9912. [CrossRef]
74. Segura-Aguilar, J.; Baez, S.; Widersten, M.; Welch, C.J.; Mannervik, B. Human class Mu glutathione transferases, in particular isoenzyme M2-2, catalyze detoxication of the dopamine metabolite aminochrome. *J. Biol. Chem.* **1997**, *272*, 5727–5731. [CrossRef] [PubMed]
75. Baez, S.; Segura-Aguilar, J.; Widersten, M.; Johansson, A.S.; Mannervik, B. Glutathione transferases catalyse the detoxication of oxidized metabolites (o-quinones) of catecholamines and may serve as an antioxidant system preventing degenerative cellular processes. *Biochem. J.* **1997**, *324*, 25–28. [CrossRef]
76. Dagnino-Subiabre, A.; Cassels, B.K.; Baez, S.; Johansson, A.S.; Mannervik, B.; Segura-Aguilar, J. Glutathione transferase M2-2 catalyzes conjugation of dopamine and dopa o-quinones. *Biochem. Biophys. Res. Commun.* **2000**, *274*, 32–36. [CrossRef] [PubMed]
77. Cheng, F.C.; Kuo, J.S.; Chia, L.G.; Dryhurst, G. Elevated 5-S-cysteinyldopamine/homovanillic acid ratio and reduced homovanillic acid in cerebrospinal fluid: Possible markers for and potential insights into the pathoetiology of Parkinson's disease. *J. Neural. Transm.* **1996**, *103*, 433–446. [CrossRef] [PubMed]
78. Rosengren, E.; Linder-Eliasson, E.; Carlsson, A. Detection of 5-S-cysteinyldopamine in human brain. *J. Neural. Transm.* **1985**, *63*, 247–253. [CrossRef]
79. Mosca, L.; Lendaro, E.; d'Erme, M.; Marcellini, S.; Moretti, S.; Rosei, M.A. 5-S-Cysteinyl-dopamine effect on the human dopaminergic neuroblastoma cell line SH-SY5Y. *Neurochem. Int.* **2006**, *49*, 262–269. [CrossRef]
80. Cuevas, C.; Huenchuguala, S.; Muñoz, P.; Villa, M.; Paris, I.; Mannervik, B.; Segura-Aguilar, J. Glutathione transferase-M2-2 secreted from glioblastoma cell protects SH-SY5Y cells from aminochrome neurotoxicity. *Neurotox. Res.* **2015**, *27*, 217–228. [CrossRef]
81. Valdes, R.; Armijo, A.; Muñoz, P.; Hultenby, K.; Hagg, A.; Inzunza, J.; Nalvarte, I.; Varshney, M.; Mannervik, B.; Segura-Aguilar, J. Cellular Trafficking of Glutathione Transferase M2-2 Between U373MG and SHSY-S7 Cells is Mediated by Exosomes. *Neurotox Res.* **2021**, *39*, 182–190. [CrossRef]
82. Segura-Aguilar, J.; Mannervik, B.; Inzunza, J.; Varshney, M.; Nalvarte, I.; Muñoz, P. Astrocytes protect dopaminergic neurons against aminochrome neurotoxicity. *Neural. Regen. Res.* **2022**, *17*, 1861–1866. [CrossRef]
83. Labarrere, C.A.; Kassab, G.S. Glutathione: A Samsonian life-sustaining small molecule that protects against oxidative stress, ageing and damaging inflammation. *Front. Nutr.* **2022**, *9*, 1007816. [CrossRef]
84. Meister, A.; Anderson, M.E. Glutathione. *Annu. Rev. Biochem.* **1983**, *52*, 711–760. [CrossRef]

85. Jenner, P. Oxidative damage in neurodegenerative disease. *Lancet* **1994**, *344*, 796–798. [CrossRef] [PubMed]
86. Sian, J.; Dexter, D.T.; Lees, A.J.; Daniel, S.; Agid, Y.; Javoy-Agid, F.; Jenner, P.; Marsden, C.D. Alterations in glutathione levels in Parkinson's disease and other neurodegenerative disorders affecting basal ganglia. *Ann. Neurol.* **1994**, *36*, 348–355. [CrossRef]
87. Aoyama, K. Glutathione in the Brain. *Int. J. Mol. Sci.* **2021**, *22*, 5010. [CrossRef]
88. Lin, K.J.; Chen, S.D.; Lin, K.L.; Liou, C.-W.; Lan, M.-Y.; Chuang, Y.-C.; Wang, P.-W.; Lee, J.-J.; Wang, F.-S.; Lin, H.-Y.; et al. Iron Brain Menace: The Involvement of Ferroptosis in Parkinson Disease. *Cells* **2022**, *11*, 3829. [CrossRef]
89. Bridges, R.J.; Natale, N.R.; Patel, S.A. System xc^- cystine/glutamate antiporter: An update on molecular pharmacology and roles within the CNS. *Br. J. Pharmacol.* **2012**, *165*, 20–34. [CrossRef]
90. Holmay, M.J.; Terpstra, M.; Coles, L.D.; Mishra, U.; Ahlskog, M.; Öz, G.; Cloyd, J.C.; Tuite, P.J. N-Acetylcysteine boosts brain and blood glutathione in Gaucher and Parkinson diseases. *Clin. Neuropharmacol.* **2013**, *36*, 103–106. [CrossRef]
91. Stockwell, B.R.; Jiang, X.; Gu, W. Emerging Mechanisms and Disease Relevance of Ferroptosis. *Trends Cell. Biol.* **2020**, *30*, 478–490. [CrossRef] [PubMed]
92. Wang, Z.L.; Yuan, L.; Li, W.; Li, J.Y. Ferroptosis in Parkinson's disease: Glia-neuron crosstalk. *Trends Mol. Med.* **2022**, *28*, 258–269. [CrossRef] [PubMed]
93. Brigelius-Flohé, R.; Flohé, L. Regulatory Phenomena in the Glutathione Peroxidase Superfamily. *Antioxid. Redox. Signal* **2020**, *33*, 498–516. [CrossRef]
94. Zhang, M.; An, C.; Gao, Y.; Leak, R.K.; Chen, J.; Zhang, F. Emerging roles of Nrf2 and phase II antioxidant enzymes in neuroprotection. *Prog. Neurobiol.* **2013**, *100*, 30–47. [CrossRef] [PubMed]
95. Jayaraj, P.; Narasimhulu, C.A.; Rajagopalan, S.; Parthasarathy, S.; Desikan, R. Sesamol: A powerful functional food ingredient from sesame oil for cardioprotection. *Food Funct.* **2020**, *11*, 1198–1210. [CrossRef]
96. Lai, Y.; Zeng, H.; He, M.; Qian, H.; Wu, Z.; Luo, Z.; Xue, Y.; Yao, G.; Zhang, Y. 6,8-Di-C-methyl-flavonoids with neuroprotective activities from Rhododendron fortunei. *Fitoterapia* **2016**, *112*, 237–243. [CrossRef] [PubMed]
97. Ying, L.; Wang, D.; Du, G. Analysis of Bioactive Components in the Fruit, Roots, and Leaves of Alpinia oxyphylla by UPLC-MS/MS. *Evid. Based Complement. Alternat. Med.* **2021**, *2021*, 5592518. [CrossRef] [PubMed]
98. Seong Choi, K.; Shin, T.S.; Chun, J.; Ahn, G.; Jeong Han, E.; Kim, M.J.; Kim, J.B.; Kim, S.H.; Kho, K.H.; Heon Kim, D.; et al. Sargahydroquinoic acid isolated from Sargassum serratifolium as inhibitor of cellular basophils activation and passive cutaneous anaphylaxis in mice. *Int. Immunopharmacol.* **2022**, *105*, 108567. [CrossRef] [PubMed]
99. Qiao, J.; Zhao, Y.; Liu, Y.; Zhang, S.; Zhao, W.; Liu, S.; Liu, M. Neuroprotective effect of Ginsenoside Re against neurotoxin-induced Parkinson's disease models via induction of Nrf2. *Mol. Med. Rep.* **2022**, *25*, 215. [CrossRef] [PubMed]
100. Gao, X.Y.; Liu, G.C.; Zhang, J.X.; Wang, L.H.; Xu, C.; Yan, Z.A.; Wang, A.; Su, Y.F.; Lee, J.J.; Piao, G.C.; et al. Pharmacological Properties of Ginsenoside Re. *Front. Pharmacol.* **2022**, *13*, 754191. [CrossRef]
101. Schepici, G.; Bramanti, P.; Mazzon, E. Efficacy of Sulforaphane in Neurodegenerative Diseases. *Int. J. Mol. Sci.* **2020**, *21*, 8637. [CrossRef]
102. Gao, Y.; Chu, S.F.; Li, J.P.; Zhang, Z.; Yan, J.Q.; Wen, Z.L.; Xia, C.Y.; Mou, Z.; Wang, Z.Z.; He, W.B.; et al. Protopanaxtriol protects against 3-nitropropionic acid-induced oxidative stress in a rat model of Huntington's disease. *Acta Pharmacol. Sin.* **2015**, *36*, 311–322. [CrossRef]
103. Emran, T.B.; Islam, F.; Nath, N.; Sutradhar, H.; Das, R.; Mitra, S.; Alshahrani, M.M.; Alhasaniah, A.H.; Sharma, R. Naringin and Naringenin Polyphenols in Neurological Diseases: Understandings from a Therapeutic Viewpoint. *Life* **2022**, *13*, 99. [CrossRef]
104. Ren, B.; Yuan, T.; Diao, Z.; Zhang, C.; Liu, Z.; Liu, X. Protective effects of sesamol on systemic oxidative stress-induced cognitive impairments via regulation of Nrf2/Keap1 pathway. *Food Funct.* **2018**, *9*, 5912–5924. [CrossRef] [PubMed]
105. Bian, Y.; Chen, Y.; Wang, X.; Cui, G.; Ung, C.O.L.; Lu, J.H.; Cong, W.; Tang, B.; Lee, S.M. Oxyphylla A ameliorates cognitive deficits and alleviates neuropathology via the Akt-GSK3β and Nrf2-Keap1-HO-1 pathways in vitro and in vivo murine models of Alzheimer's disease. *J. Adv. Res.* **2021**, *34*, 1–12. [CrossRef] [PubMed]

antioxidants

MDPI

Review

New Directions to Approach Oxidative Stress Related to Physical Activity and Nutraceuticals in Normal Aging and Neurodegenerative Aging

Manuela Violeta Bacanoiu [1], Mircea Danoiu [1], Ligia Rusu [1,*] and Mihnea Ion Marin [2]

[1] Sport Medicine and Physical Therapy Department, Faculty of Physical Education and Sport, University of Craiova, 200585 Craiova, Romania; manuela.bacanoiu@edu.ucv.ro (M.V.B.); mircea.danoiu@edu.ucv.ro (M.D.)
[2] Faculty of Mechanics, University of Craiova, 200585 Craiova, Romania; mihnea.marin@edu.ucv.ro
* Correspondence: ligiarusul@hotmail.com or ligia.rusu@edu.ucv.ro; Tel.: +40-723-867-738

Abstract: Oxidative stress (OS) plays, perhaps, the most important role in the advanced aging process, cognitive impairment and pathogenesis of neurodegenerative disorders. The process generates tissue damage via specific mechanisms on proteins, lipids and nucleic acids of the cells. An imbalance between the excessive production of oxygen- and nitrogen-reactive species and antioxidants leads to a progressive decline in physiological, biological and cognitive functions. Accordingly, we need to design and develop favourable strategies for stopping the early aging process as well as the development of neurodegenerative diseases. Exercise training and natural or artificial nutraceutical intake are considered therapeutic interventions that reduce the inflammatory process, increase antioxidant capacities and promote healthy aging by decreasing the amount of reactive oxygen species (ROS). The aim of our review is to present research results in the field of oxidative stress related to physical activity and nutraceutical administration for the improvement of the aging process, but also related to reducing the neurodegeneration process based on analysing the beneficial effects of several antioxidants, such as physical activity, artificial and natural nutraceuticals, as well as the tools by which they are evaluated. In this paper, we assess the recent findings in the field of oxidative stress by analysing intervention antioxidants, anti-inflammatory markers and physical activity in healthy older adults and the elderly population with dementia and Parkinson's disease. By searching for studies from the last few years, we observed new trends for approaching the reduction in redox potential using different tools that evaluate regular physical activity, as well as antioxidant and anti-inflammatory markers preventing premature aging and the progress of disabilities in neurodegenerative diseases. The results of our review show that regular physical activity, supplemented with vitamins and oligomolecules, results in a decrease in IL-6 and an increase in IL-10, and has an influence on the oxidative metabolism capacity. In conclusion, physical activity provides an antioxidant-protective effect by decreasing free radicals and proinflammatory markers.

Keywords: oxidative stress; older adults; normal aging; physical activity; neurodegenerative pathology aging; redox potential

Citation: Bacanoiu, M.V.; Danoiu, M.; Rusu, L.; Marin, M.I. New Directions to Approach Oxidative Stress Related to Physical Activity and Nutraceuticals in Normal Aging and Neurodegenerative Aging. *Antioxidants* **2023**, *12*, 1008. https://doi.org/10.3390/antiox12051008

Academic Editor: Jackob Moskovitz

Received: 23 March 2023
Revised: 14 April 2023
Accepted: 18 April 2023
Published: 26 April 2023

1. Introduction

Concern for a healthy lifestyle in older adults and delaying the evolution of deficiencies in neurodegenerative diseases represent two of the most important problems in healthy people. The decline that accompanies normal aging and pathological aging involves socioeconomic and psychosocial determinants that must be limited. Elderly people's quality of life deteriorates owing to the lowering of motor functions and mental health, problems that require solutions. Improving these functions not only requires financial interventions both in specialised medical units and at home, but also the active involvement of health policies with governmental participation. From this point of view, the independence of elderly people in apparent good health or with neurodegenerative disabilities must be

stimulated, personal identity needs to be strengthened and confidence in participating in independent daily activities must be increased. In the last decade, premature aging was one of the most important concerns because this phenomenon is accompanied by a decline in physical functions and increased cognitive impairment. At the same time, quality of life and wellbeing are affected, and the recovery and treatment procedures require rehabilitation, institutionalisation and hospitalisation, with large financial implications. Thus, the advancement in age with the related decline has prompted massive research due to a need for new strategies that allow as much delay as possible in the alteration of elderly adults' state of health. Age-related morphological and functional changes induce changes in mobility, balance and joint flexibility, and increase the risk of falls, as well as functional cognitive decline. Therefore, aging is a biological and irreversible process that is often accompanied by multiple comorbidities, especially neurodegenerative diseases, examples being dementia and Alzheimer's disease. Accordingly, the impairment of physical and intellectual capacities leads to an alteration in daily activities in terms of wellbeing and quality of life and decreases independent living capability. The hallmarks of aging include reduced physical capacities, altered cognitive status and, at the infrastructure level, disrupted balance in homeostasis, genomic stability and mitochondrial functionality. Since 1956, aging has been associated with oxidative stress, which is defined as an alteration balance between oxidant and antioxidant biomolecules [1]. There are several factors that contribute to the aging process, such as a sedentary lifestyle, poor diet, loss of intellectual activity and an induced altered redox status. Continuous functional fitness activities and low-, moderate- or high-intensity physical exercises improve the gait pattern, strength and resistance of muscles, balance, flexibility of joints and the mobility in movements. In this regard, physical interventions represent a preventive strategy for avoiding chronic oxidative stress [2]. On the other hand, changes in variables such as lifestyle, behavioural habits, intake of natural and artificial nutraceuticals and anti-inflammatory compounds succeed in lowering oxidant agents and bio-inflammatory markers in healthy older adults or seniors with neurodegenerative disorders.

2. Methods of the Literature Review

In order to create a narrative review, we browsed the PubMed database with the keywords: "oxidative stress", "older adults", "normal aging", "physical activity", "aging and neurodegenerative disorders" and "nutraceuticals". Our research includes original articles, review articles and case reports from the last five to six years. All original articles and clinical trials, regarding physical training, functional fitness or supplementation with natural and artificial antioxidants, demonstrated a decrease in oxygen- or nitrogen-reactive species and inflammatory markers in elderly people. By applying these strategies, the importance of physical training and positive nutraceutical intervention was proven to delay premature aging as well as the progress of neurodegenerative diseases, thereby influencing quality of life or wellbeing. Finally, only the most relevant studies, written in English, were selected from the reference list. Our review proposes to present information about the following important topics: oxidative stress and aging pathophysiology, the impact of physical activity and nutraceutical compounds on oxidative stress for healthy aging, the impact of physical activity and oxidative stress for older adults and the impact of recovery methods using physical activity and nutraceutical compounds on oxidative stress for neurodegenerative diseases.

3. Oxidative Stress and Aging Process Pathophysiology

Oxidative stress is the result of an imbalance between excessive production of reactive oxygen species and reactive nitrogen species (ROS/RNS) and an antioxidant defence that cannot neutralise them. Free radicals are markers of oxidative stress and are atoms or molecules with one or more than one unpaired electron in an external shell. They are formed from the interaction between oxygen and certain molecules [3].

Reactive oxygen species (ROS) and reactive nitrogen species (RNS) are two species of reactive oxygen, both produced by aerobic cells and associated with the aging process, as well as age-related diseases [4].

RONS (reactive oxygen and nitrogen species) have endogenous sources, including nicotinamide adenine dinucleotide phosphate (NADPH) oxidase, myeloperoxidase (MPO), lipoxygenase and angiotensin II, as well as exogenous sources such as air and water pollution, tobacco, alcohol, heavy or transition metals, drugs, industrial solvents, cooking and radiation, all of which result in metabolization into free radicals inside the body [5].

Methods for the assessment of oxidative stress are focused on the direct measurement of reactive oxygen species—responsible for the deleterious effects of oxidative stress—using fluorogenic probes [6]. The indirect measurement of ROS is also a method based on the analysis of the oxidative damage these radicals cause to lipids (lipid peroxidation, malondialdehyde and oxidised levels of low-density lipoproteins), proteins (protein carbonyl and the detection of advanced oxidation protein products) and cell nucleic acids (8-hydroxy-2′-deoxyguanosine, and thymidine glycol, which is a specific marker for oxidative DNA damage) [7].

Regarding the treatment of oxidative stress, the administration of antioxidant molecules, including nutritional supplements such as vitamin A (which modifies the effect of apolipoproteins on the risk of myocardial infarction), is the recommended treatment [8]. Vitamin C can control endothelial cell proliferation and apoptosis and smooth muscle-mediated vasodilation. Novel omega-3-based antioxidants and novel therapeutic strategies using miRNA and nanomedicine are also being developed [9].

Oxidative stress alters macromolecules in the body, such as lipids, proteins and nucleic acids. Finally, ROS and RNS can lead to chronic inflammation and to the activation of pathological metabolic pathways that cause illness. Redox stress/oxidative stress is a complex process. Its impact on the body depends on the type of oxidant, the place and intensity of its production, the composition, the activities of various enzymatic or nonenzymatic antioxidants and the capacity of self-repair systems. The oxidative stress theory is currently the most accepted explanation for aging, stipulating that excess ROS leads to genetic, molecular, cell, tissue and systemic changes—the level of reactive oxygen species (ROS) increases and is associated with an increased risk of tissue damage. This increase in oxidative activity generates impairments in nucleic acids (DNA/RNA), lipids and proteins, and affects metabolic and biochemical pathways, modifying cell homeostasis, signal transduction and gene expression. Therefore, in the process of cell respiration in the mitochondria, organic peroxides, reactive aldehydes such as malondialdehyde (MDA) and nitric oxide—which generates pathological modifications in proteins, lipids and DNA/RNA and increases the chance of genetic mutations—are produced [2]. Endogenous antioxidants include superoxide dismutase (SOD), catalase (CAT), glutathione reductase (GSR) and glutathione peroxidase (GPX) as a defence system. They cannot counteract the oxidizing action of free radicals responsible for the appearance of heat-shock proteins (HSPs), inflammatory markers that ultimately lead to cell apoptosis [10]. Oxidised proteins produce protein carbonyl (CP) via lipid peroxidation related to isoprostanes (8-iso-PGF2α) or produce glycated compounds that lead to neuron degeneration, damage synaptic networks, increase neuroinflammation and result in subsequent memory loss with the onset and progression of neurodegenerative diseases [11]. Oxidative stress can activate a variety of proinflammatory factors, such as the tumour necrosis factor alpha (TNF-α), interleukins IL-6 and IL-8, thiobarbituric acid-reactive substances (TBARS) and homocysteine (Hcy), all of which are associated with a brain-level neuroinflammation response [12,13]. Oxidative stress in the brain is mostly due to the production of the factor insoluble amyloid plaques (Aβ42), oligomers that stimulate hyperphosphorylation of tau proteins (p-tau). Neuroinflammation is a key player in Alzheimer's disease (AD), with the active participation of proinflammatory cytokines such as IL-1β and TNF-α, which promote neuronal and synaptic disorders [14]. For healthy aging and delaying the evolution of the pathological neurodegenerative process in elderly people, mechanisms must be promoted to adjust the imbalance between the excessive

production of ROS and the decrease in the defensive enzyme system and, implicitly, the attenuation of proinflammatory capacity. In this regard, the first favourable interventions would be the promotion of constant physical activity accompanied by the addition of some natural or artificial factors to dietary intake. Aging is an irreversible process that makes alterations to physical capacity, current and autonomous activities and resistance to stress, and promotes a decrease in physical and cognitive abilities with the onset of pathological aging, especially neurodegenerative disabilities. Thus, by promoting regular physical activity, one can maintain the elderly's ability to carry out daily activities, to have an independent, safe life, and thus ensure their wellbeing and quality of life. The functional fitness approach represented a very good achievement for improving muscle strength and power, flexibility and mobilisation of lower and upper limb joints, balance, endurance and agility, decreasing the risk of falling and improving the performance of functional movements. In a previous study, reducing training intensity and frequency led to the alteration of functional fitness parameters and negatively modified antioxidant biomarkers [15]. Cognitive aging represents one of the most common manifestations in the elderly, and increasing oxidative stress, as demonstrated by high reactive oxygen metabolites (ROM) levels, remains the biggest problem to be addressed. Furthermore, decreasing antioxidant capacity plays an important role in the pathophysiology of neurodegenerative disorders such as AD, Parkinson's disease (PD), multiple sclerosis, mild cognitive impairment, etc. [16]. Nutraceutical intervention using natural and artificial compounds represents a new success in healthy aging or delaying the progress of neurodegenerative impairment. Certain foods, rich in flavonoids, proteins, polyphenols or vitamins, have demonstrated beneficial effects in terms of ameliorating blood oxidative stress and inflammation biomarkers [17,18].

3.1. Instruments/Tools—Determinants of Oxidative Stress, Inflammation Status, Nutraceutical Compounds and Scales of Assessment of Motor and Cognitive Functions on Normal Aging and Aging Pathology

Age-related changes and the correlation with oxidative stress must be approached in the context of the relationship between oxidative stress and inflammatory capacity. From this point of view, there is a need to discuss the most relevant tools for limiting disorders at both the macroscopic and the infrastructural levels. Therefore, the variables required to evaluate and mitigate the impact of oxidative stress and, implicitly, inflammatory capacity, need to be present. Knowledge of pathophysiological mechanisms such as oxidative stress—which influences the installation and progression of motor and cognitive changes for older adults—has led to finding means to limit them. Thus, the most relevant tools in this area are: (1) oxidative stress biomarkers, (2) inflammatory markers, (3) nutraceutical compounds and (4) motor and cognitive scales. All these indicators are used for both normal aging and pathological aging and are presented below in Table 1.

Table 1. Oxidative stress, inflammatory markers, nutraceuticals and motor/cognitive scales/tools/instruments.

Oxidative Stress Tools	Inflammatory Tools	Nutraceutical Compounds Tools	Motor and Cognitive Scales
SOD	Lipid profile	AX/AX + Sesamin	IPAQ
TBARS	IL1/IL1b/IL6 /IL-8/IL-10 IL-12	Beetroot juice (Nitrate dietary) NO^{3-}	MET
FRAP	I CAM-3	Vitamin C	HOMA-IR
ROS/iNOS ROM	E/P-selectin Adhesion molecules		VAS/NPRS
TOS/TOC TAS/TAC/TACV	Thrombomodulin Endothelin-1	Capsinoids	1RM

Table 1. *Cont.*

Oxidative Stress Tools	Inflammatory Tools	Nutraceutical Compounds Tools	Motor and Cognitive Scales
3-NT	TUBB	Isoflavone	POMS2/TMD
CP	CRP	Cryotherapy	GDS/S-GDS
MDA	TNFα	N3 PUFA	BDHQ
GPx SOD/GPx ratio	HCY	European/Spanish/ Majorcan/ dietary intake	PASE
PCOOH	BNDF	Vitamins A/C/D Tocopherol	PHQ-8
CAT	8-iso PGF2α	Beta-carotene	PSQI/OSA-MA
GSR	IL-12/IL-10 ratio /IL-12-p70/ IL-8/IL-10 ratio	Acrylamide	MMSE/ MoCA
HSPs	Ferritin	Cocoa beverage powder	DS/DSF /DSB
H_2O_2	Fibrinogen	L-glutamine	TMT/ATMT/CDT
BAP		Ozone	SF-36-HRQOL
TRX		Vitamin E/Zn/Se	RAPA/GPAQ
GRd		Protein intake	EQ-5D
AOPP		Niacin	COWAT
GSH/GSSG		FST	UPDRS/H&Y /PDQ
NO		PM-EE	LOTCA
8-OHdG		Melatonin	D-KEFS–CWI
		H_2/Photo-modulation	RAVLT/ CVLT/AVLT /LMT/SDMT
		Benfotiamine	IADL/ADL
		Vitamin B	WHODAS/DHQ/FFQ Er-Med
		NAC	FFQ
		Ladostigil	BDI/BAI
		Polyphenols/ Mind foods	BBS
		Kefir Probiotics	EDSS /SEP-59/MSQOL/
		LF	ADAS–cog/ ADCS–ADL/DAD/ CERAD-K/CDR
		CC	NPI/RBANS/NTB

Oxidative stress markers: SOD—superoxide dismutase enzyme; TBARS—thiobarbituric acid-reactive substances; TOC—total oxidative capacity; TAC—total antioxidant capacity; TACV—total antioxidative capacity; FRAP—plasma ferric reduction capacity; 3-NT—3 nitro-tyrosine; iNOS—nitric oxide synthase; CP—protein carbonyls; MDA—malondialdehyde; GPx—glutathione peroxidase; SOD/GPx ratio—stress score; PCOOH—plasma phosphatidylcholine hydroperoxide; CAT—catalase; GSR—glutathione reductase; HSPs—heat-shock proteins; H_2O_2—hydrogen peroxide; BAP—biological antioxidant potential; TRX—thioredoxin reductase; GRd—glutathione reductase; AOPP—advanced oxidative protein products; GSH/GSSG—reduced/oxidised glutathione; NO—nitric oxide; 8-OH-dG—8-hydroxy-deoxyguanosine. Inflammatory markers: lipid profile—total cholesterol; HDL-cholesterol—high-density lipoprotein cholesterol; LDL-cholesterol—low-density lipoprotein cholesterol; triglycerides; IL-1/IL-1b/IL-6/IL-8/IL-10/IL-12—interleukin 1, 1b, 6, 8, 10, 12; ICAM-3—intercellular adhesion molecule;

TUBB—tubulin beta class I; CRP—C-reactive protein; TNF—tumour necrosis factor α; HCY—homocysteine; BNDF—brain-derived neurotrophic factor; 8-isoPGF2α—8-isoprostaglandin F2α. Nutraceutical compounds: AX/AX + Sesamin—astaxanthin/astaxanthin + sesamin; n3-PUFA—omega-3-polyunsaturated fatty acids; FST—Laminaria japonica; PM-EE—PhytoMeal ethanol extract; NAC—N-acetyl cysteine; LF—lactoferrin; CC—Cosmos caudatus. Motor and cognitive scales: IPAQ—International Physical Activity Questionnaire; MET—physical activity score; HOMA-IR—homeostatic model for the assessment of insulin resistance; VAS/NPRS—visual analogue scale/numeric pain rating scale; 1RM—test–retest reliability of one repetition, maximum assessment of the strength capacity of individuals; POMS2/TMD—profile of mood status/total mood disturbance; GDS/S-GDS—geriatric depressive scale/short geriatric depressive scale; BDHQ—brief-type dietary history questionnaire; PASE—Physical Activity Scale for the Elderly; PHQ-8/PSQ—Patient Health Questionnaire 8, which evaluates depression status; PSQI—Pittsburgh Sleep Quality Index/Ogri–Shirakawa–Azumi Sleep Inventory; MMSE/MoCA—Mini Mental State Examination test/Montreal Cognitive Assessment; DS/DSF/DSB—digit span/digit span forwards/digit span backwards; TMT/ATMT/CDT—Trail-Making Test/Advanced Trail-Making Test/Clock-Drawing Test using visuospatial memory; SF36-HRQ—short-form health-related quality of life questionnaire with 36 items; RAPA/GPAQ—Rapid Assessment of Physical Activity Questionnaire/Global Physical Activity Questionnaire; EQ-5D—Euro quality of life, which includes five dimensions: self-care, usual activities, mobility, depression/anxiety, pain/discomfort; COWAT—Controlled Oral Word Association Test; UPDRS/H&Y/PDQ—Unified Parkinson's Disease Rating Scale/Hoehn and Yahr/Parkinson's Disease Questionnaire (39 items); LOTCA—Loewenstein Occupational Therapy Cognitive Assessment; D-KEFS–CWI—Delis Kaplan executive function system–colour and word interference; RAVLT/CVLT/AVLT (IR, SR, LR)—Rey Auditory–Verbal Learning Test/California Verbal Learning Test/Auditory Verbal Learning Test (immediate recall, short recall, long recall); LMT/SMDT—Logical Memory Test/Symbol Digit Modalities Test; IADL/ADL—instrumental activities of daily learning/activities of daily living; WHODAS/DHQ/FFQ/Er-Med—WHO disability assessment schedule-related dietary intake (protein, fibre, fruits, vitamins)/dietary history questionnaire/food frequency questionnaires/17-item questionnaire for Mediterranean foods; BDI/BAI—Beck Depression Inventory (score ranges 0–63, with 21 items)/Beck Anxiety Inventory; BBS—Berg Balance Scale; EDSS/SEP-59/MSQOL—expanded disability status score/59-item multiple sclerosis quality of life questionnaire; ADAS–cog/ADCS–ADL/DAD/CERAD-K/CDR—Alzheimer's disease assessment scale–cognitive subscale/Alzheimer's disease cooperative study–activities of daily living/disability assessment in dementia/consortium to establish a registry for Alzheimer's disease/clinical dementia rating; NPI/RBANS/NTB—neuropsychiatric inventory/repeatable battery for the assessment of neuropsychological status/neuropsychological test battery.

3.1.1. Oxidative Stress Biomarkers/Tools

It is well-known that aging-related oxidative stress and free radicals can cause protein, lipid and DNA molecule oxidation. The process is accelerated by the increase in protein carbonyl molecules through protein oxidation, and large amounts of malondialdehyde and isoprostanes are formed from lipid peroxidation. Thus, increased ROS and NOS concentrations are generated, exceeding the body's compensatory defence system [2,12]. Nitro-oxidative stress plays an important role in endothelial cell disorders and is implicit in the inflammatory process [14,16]. Oxidative stress is determined by an imbalance between the antioxidant enzyme defence system—represented by SOD, CAT, GPx, GRd—and free radical monitoring through increasing MDA, CP and isoprostanes [2,19,20]. MDA represents lipid peroxidation and oxygen reactive species (ROS) indicators, which are generated in excess when oxidative stress increases [19,21,22]. The increase in oxidative stress reduces mitochondrial activity coupled with oxidative phosphorylation, and implicitly disrupts the balance of redox homeostasis [23]. Cellular aging is the consequence of oxidative stress, which later causes significant tissue damage. The enzymatic antioxidant system (SOD, CAT, GSH, GPx, GR) acts against the oxidative reactive system. The enzymatic complex superoxide dismutase represents the SOD family, which annihilates free radicals, such as superoxide anions. Glutathione is one of the most powerful antioxidants found in all body cells. When it is in small amounts in the body and peroxides increase, pathological mechanisms that induce the inflammatory process are activated. ROS result from molecular oxygen following the processes carried out at the cellular level. The most important endoge-

nous oxidising agents are hydroxyl radicals, hydrogen peroxide and superoxide anions [24]. Therefore, the balances between TOS/TOC and TAS/TAC must be estimated to monitor cellular stress [25]. The 3-NT represents a reactive nitrogen species marker that correlates with the increase in oxidative status [14,21,26]. The accentuation of oxidative stress is correlated with the increase in lipid peroxidation, and the relevant markers in this regard are TBARS and MDA [2,13,22,27]. Protein oxidation represents one of the biggest causes of damage from oxidative stress and can be monitored by determining AOPPs (advanced oxidation protein products), which are an indirect biomarker of accentuated oxidative status [28]. Alzheimer's disease is one of the most common neurodegenerations and causes progressive dementia, especially on older adults. From a pathophysiological point of view, AD compromises inter-neuronal transmission at the synapse level through amyloid deposit accumulation, intracellular neurofibrillary tangles and pathological synthesis protein generation [15]. Another OS biomarker is phosphatidylcholine hydroperoxide (PCOOH), whose concentration increases by intensifying lipid peroxidation, which disintegrates cell membranes and initiates cell apoptosis [29].

3.1.2. Inflammatory Markers/Tools

Oxidative stress triggers an inflammatory response directly involved in the pathogenesis of diseases. With increasing age, the lipid profile becomes unfavourable and increases the inflammatory capacity, accentuating the imbalance between the antioxidant defence system and prooxidative factors [1,2,13,21,23]. Therefore, the excess production of reactive oxygen species induces mitochondrial dysfunction and maintains a proinflammatory status that becomes chronic through the oxidation of lipids, proteins or DNA. Thus, triggering a cascade of events that initiates cytokine production, such as IL-1, IL-1b, IL-6 and IL-8, which maintains the chronic inflammatory process [10,13–15,18,21,30]. Heightened redox potential stimulates the tissue macrophages that produce and release TNF-α into the circulation and upregulates inflammatory mediators, such as intercellular adhesion molecule-3 and BDNF, leading to neuron degeneration [10,21,26]. Their release into the circulation activates blood platelets that cause acute-phase reactants such as CRP and prothrombotic vascular factors (homocysteine, fibrinogen, thrombomodulin, endothelin-1, E/P selectin) [10,14,21,25,26,31].

3.1.3. Nutraceutical Compounds/Tools

The human body has several options for countering the effects of free radicals and oxidative stress based on enzymatic antioxidant molecules, such as SOD, CAT, GPx and GSH, but also nonenzymatic molecules (coenzyme Q10, L arginine) that are endogenous products. Apart from these, there are exogenous antioxidant compounds of animal or plant origin that can be introduced into the body using diet or nutritional supplementation. Next, we discuss the most relevant nutraceutical antioxidants and their protective actions for human health. Astaxanthin and sesamin are carotenoids found in seafoods and fish that have a strong antioxidant effect, preventing muscle fatigue and improving aerobic capacity [23,29]. Dietary nitrate supplementation, such as with beetroot juice, can enhance NO bioavailability, which has favourable effects on peripheral and central haemodynamic responses and metabolic health [26]. Vitamin C supplementation related to iron metabolism change balances pro/antioxidative activity by decreasing proinflammatory cytokine gene expression [2,22,25]. The anti-inflammatory and antioxidant effects of dietary supplementation with capsinoides, along with their improvement to metabolism and decrease in body fat mass, is worth mentioning [32]. The activity of antioxidant enzymes in menopausal women is improved by the addition of phytoestrogen-type flavonoids to the diet. They reduce MDA activity, reactive species and the inflammatory effect of cytokines [13]. Regular cocoa powder that enriches flavonoid consumption has positive effects regarding cardiovascular risk, neurodegeneration and quality of life in older adults [33]. It is also beneficial in neuroprotection; for example, when mitigating mood status and cognitive functions, Cosmos caudatus (CC) turned out to be the high flavonoid integrated in the

power supply [34]. Repeated exposure to low temperatures reduces nitro-oxidative stress by improving NO bioavailability and decreasing the activity of inflammatory markers [14]. Diets supplemented with n3-PUFA managed to reduce inflammatory phenomena by reducing the triglycerides concentration and decreasing oxidative stress. Beneficial effects were observed regarding function, muscle mass and anabolic responses. These external antioxidants had positive results for redox homeostasis amelioration [35,36]. Vitamin deficiencies can affect human health, especially cognitive and emotional status, behaviour and personality, causing functional and mental disorders. Apart from the fact that they intervene in numerous metabolic reactions as coenzymes, they play essential roles in maintaining the antioxidant capacity/prooxidative capacity balance by actively participating as supplements in European, Majorcan and Spanish dietary intakes. Vitamin C decreases the inflammatory status by lowering free iron and ferritin levels and decreasing cytokine mRNA expression [25]. Decreasing vitamin D levels can cause muscle impairments such as weakness, pain and diminished adipogenesis [31]. Along with omegA-3, a reduced mitochondrial DNA copy number (mtDNAcn) is considered an oxidative stress biomarker and may improve muscle strength. Omega-3 intake enhances synaptic transmission at the end plate, and it also modulates the contractility of the striated muscle fibre and strength muscle [37,38]. The vitamin B group (vitamin B6, vitamin B12, folate) is associated with a decline in mental disorders and dementia by decreasing HCY trans-sulphuration or re-methylation. Consequently, hyper-homocysteinemia causes DNA metabolism alteration and promotes cognitive impairment and dementia [31,39]. Diet intake supplemented with niacin mitigates the cognitive frailty of dementia [40]. The vitamin E group comprises lipophilic molecules synthesised by vegetal organisms, and the most representative of them is α-tocopherol. Vitamin E inhibits monocyte invasion's implicit inflammation and depresses oxidative stress by preventing LDL-cholesterol oxidation [41]. Nutritional intake supplemented with vitamin A, vitamin D and beta-carotene mitigates the formation of reactive oxygen species through antioxidant and anti-inflammatory effects [2,25]. Neuroprotective effects associated with aging and with antioxidant potential were signalled by supplementing diets with Laminaria japonica (FST) and desalted Salicornia europaea (PM-EE). Bioactive molecules of FST such as GABA (gamma amino butyric acid) demonstrated an improvement in antioxidant capacity with a protective effect against progressive neurodegeneration. Using PhytoMeal ethanol extract would be safe for seniors with dementia for improving cognitive performance [42,43]. Melatonin is a bioactive molecule with neuroprotective and antioxidant properties. It regulates mitochondrial respiratory complex 1 activity and reduces reactive oxygen species [20]. Molecular hydrogen induced using photo-biomodulation can mitigate cellular oxidative stress and improve mitochondrial functionality, making it a potent and possibly therapeutic antioxidant with neuroprotective effects for Parkinson's disease [44]. Administration of N acetylcysteine (NAC)—known as a glutathione precursor and an antioxidant agent—is associated with protective effects on brain oxidative stress [45]. Diet intake with benfotiamine, a synthetic precursor of thiamine, can directly participle in multiple metabolic pathways related to oxidative stress or inflammation. Benfotiamine is an antioxidant involved in glucose metabolism, and finally, it decreases advanced glycation end products responsible for the enhancement of reactive oxygen species. Moreover, it increases anti-inflammatory factors in microglia, having an important role in delaying the decline of AD [46]. Ladostigil administration is correlated with delayed dementia progression due to its decreasing effect on microglial activation and reactive oxygen species production. Cerebral atrophy reduction, especially at the medial temporal lobe level, was also mentioned [47]. Polyphenols represent a class of biomolecules that can be natural or biosynthesised compounds. They have acquired strong antioxidant roles and integration into the most diverse food sources due to their ability to reduce free radical oxidation and chelate metal ions, such as iron and copper [10,34]. Symbiotic supplementation such as with kefir improves cognitive decline by alleviating oxidative stress, systemic inflammation and blood cell damage [28]. Lactoferrin, or lactotransferrin (LF), is an iron-building glycoprotein with anti-inflammatory and antioxidative effects.

Its presence in the brain is related to aging and neurological disorders. Its participation in protein kinase modulation and tensin homolog pathways justifies the identification of antioxidant and anti-neuroinflammation characteristics [15].

We also address nutraceuticals due to their important role in restabilizing digestion and absorption of minerals and vitamins to prevent their deficiency, detoxify cells, inhibit harmful biochemical reactions, facilitate the growth of beneficial microbiota and excrete waste.

The mechanism involving nutraceutical antioxidant effects is based on help from endogenous enzymes when the antioxidant role is less than normal, i.e., the action mechanism used to cure a particular ailment [48] of the human body possesses several antioxidant compounds and enzymes, and their role is to maintain the reactive species' level of function. Nutraceuticals contain vitamin C, zinc, selenium, vitamin E and enzymes such as glutathione peroxidases and catalases, whose primary job is to scavenge reactive species. This is possible due to nuclear factor erythroid-derived 2-related factor 2 (Nrf2) transcription factor pathway activation. Other action mechanisms from these compounds that have neuroprotective effects are signal transduction cascade modulation and gene expression effects.

3.1.4. Motor and Cognitive Scales/Tools

The assessment of motor and cognitive functions for healthy elderly people and seniors with neurodegenerative disorders is performed using various scales or tools. The investigation of motor skills is conducted using the following instruments: IPAQ, RAPA and GPAQ, which evaluate physical activity based on questionnaires [17,26,27,49,50]. The physical training score and confidence in balancing activities were evaluated using MET and PASE [18,26,40]. Monitoring posture and balance, both static and dynamic, were quantified using BBS [51]. ADL and IADL are tasks linked to personal care. They refer to activities such as bed mobility, eating, toileting or transfer [40,52]. Power and muscle strength were measured in physical training with weights using 1RM [13]. Apart from the presence of difficulties in physical autonomy, aging speed and pathology are accompanied by cognitive changes influenced by several variables. Instruments used to appreciate degrees of mood, depression or sleep disorders are POMS2, TMD, GDS, S-GDS, PHQ-8, PSQ and PSQI [18,29,30,32,37,50,53]. Disturbances in emotional status have been observed with BDI or BAI scales [51]. For the assessment of mental disorders or cognitive impairments, the following tools have been utilised: MoCA, MMSE and LOTCA [17,28,34,36,39,42,43,46,47,49,49,53]. Neuropsychological profile evaluation has been investigated using NPI, RBANS and NTB [13,14,34]. Instruments used to evaluate quality of life related to independent living, mobility, pain, difficulties, self-care and dietary intake are SF-36-HRQOL, EQ-5D, VAS, NPRS, BDHQ, WHODAS, DHQ, FFQ and Er-Med [16,18,32–34,39,40,49,51]. Regarding neurodegenerative disorders such as PD, AD and SM, the tools used for assessing their progression are UPDRS, H&Y, EDSS, SEP-59, MSQOL, ADAS–cog, ADCS–ADL, DAD, CERAD-K and CDR. All these variables evaluate motor and cognitive disabilities as well as the progress of these diseases [15,42,44–47,54,55]. In addition to those that are specific to the respective neurodegenerative diseases, instruments that evaluate motor status disorders, speech, hearing, vision or logic have been used, such as DS, DSF, DSB, TMT, ATMT, CDT, COWAT, D-FEFS-CWI, RAVLT, CVLT, AVLT, LMT and SDMT diseases [36,39,40,42,47,49,53].

3.2. The Impact of Interventions through Physical Activity and Nutraceutical Compounds on Oxidative Stress for Healthy Aging

Concern for the development of autonomous physical activities, motor capacity and muscular abilities in premature aging required finding new intervention strategies to maintain them. Functional autonomy is defined as the capacity to promote daily living activities both at home and in the ambient environment, but also the maintenance of sensory and mental capacities, implicitly promoting quality of life. In order to achieve these desires, it is

necessary to find methods of action that mitigate the pathophysiological mechanisms developed in the muscle tissue and in the brain. Aging is often accompanied by disturbances in skeletal muscle contraction and morphology. The characteristic infrastructural signs for the establishment of dysfunction at the skeletal muscle level are protein synthesis alteration, significant mitochondrial-level changes or genomic instability. All these muscular- or nervous-level disturbances are the consequences of the imbalance between the reactive oxygen species production and the body's defence system in the sense of decreasing antioxidant capacity. Physical activity, regardless of the intensity, frequency, endurance, volume or type, is considered a therapeutic instrument for decreasing oxidative stress [11]. Therefore, one of the strategies for addressing premature aging is the promotion of physical exercise in its most varied forms, starting with daily routine activities and reaching sustained, regular physical training necessary to maintain posture, balance, strength and muscle resistance. In addition to exercise, supplementing the diet with natural or artificial antioxidant exogenous animal or vegetal biomolecules plays a significant role in improving the redox potential and delaying premature aging. Nutraceutical antioxidants, such as vitamins B, C, D, E, polyphenols, omega-3, proteins, flavonoids, oxygen or hydrogen therapy, showed beneficial effects in the health of older adults.

Below, we present Table 2, showing previous studies describing aspects of physical activity and nutraceuticals and oxidative stress according to different types of physical activity and dietary intake.

Analysis of the references provided demonstrates the effects of endurance training performed on the treadmill for 12 weeks, with 3 sessions/week, or physical tasks for 4 h/day with a cycle ergometer for 4 weeks. In addition, near-physical and mental tasks were applied for 4 h/day in sets of 30 min, using an advanced trail-making test. In both cases, a nutraceutical antioxidant diet with astaxanthin (AX) was administrated, represented by red, powerful, oceanic carotenoids found in algae, shellfish and fish, or AX with sesamin, i.e., the oleaginous seed found in sesame. After the two interventions in both sexes, through sustained physical activity and a supplemented diet, beneficial effects regarding the lipid profile through increased fat oxidation, decreased carbohydrate oxidation and an anti-fatigue effect through lowered plasma phosphatidylcholine hydroperoxide were observed during physical and mental tasks. By applying the trail-making test for 4 weeks, improvements were observed in the emotional status and quality of sleep in older adults [23,29]. Moreover, some other authors have shown the effect of the physical intervention, quantified by cycling 10 M with a pedalling cadence of 50 rpm with moderate or intense effort. As a supplemented diet, 70 mL × 2/day of beetroot juice (dietary nitrate NO_3^-) was used for 7 days. The results did not show a favourable influence on haemodynamic and cardiac parameters, but changes in inflammatory and oxidative markers such as E/P selectin, thrombomodulin and ICAM-3 were observed. IL-6, 3-NT and glycaemic levels were quantified in a positive sense using HOMA-IR [26]. In other writings, the authors evaluated the results obtained after applying physical training and dietary intake vitamins of type A, C, E, tocopherol and beta-carotene, or trace elements such as Zn and Se. Physical exercises were carried out for 6 weeks, 3 times/week for 60 min, either using cycle ergometer sessions or gyrokinesis, Nordic walking and stabilisation training. Other options were physical fitness or intermediate and active exercise training. Vitamin therapy was administrated using tablets (1000 mg/day, 6 weeks) or nutraceutical food with vitamins. The studies showed that anthropometric index, muscle mass, fat mass and cardiorespiratory parameters underwent favourable changes, such as a decreased BMI and increased muscle mass. Beneficial effects were observed in oxidative stress and inflammatory marker levels. Improved antioxidative/prooxidative balance and anti-inflammatory/proinflammatory capacity were monitored using SOD, CAT, GRx, GRd, 3-NT, MDA, TBARS, protein carbonyls or isoprostanes, and IL-1, Il-6, IL-10, CRP, tubulin beta class 1 and CCL2 (chemokine ligand 2). In conclusion, a decrease of about 10% in oxidative stress and enhanced antioxidant defence, changes in lipid profile and glycaemic level, decreased IL-6, increased Il-1 and increased oxidative metabolism capacity after regular physical activity and supplementa-

tion with vitamins and oligomolecules were noticed [2,22,25]. Physical activity of various degrees, from low to moderate or vigorous, monitored using an activity meter together with the consumption of 9 mg/day of capsinoids (CH-19 sweet) for 12 weeks, was determined in terms of body composition, decreased waist circumference, visceral fat index and body fat percentage through lipid oxidation, augmenting the physiological consequences of ingestion of capsinoids. The tools that quantified the effects were FAS, METs and parameters of mood status such as POMS2 and TMD. Other effects of interventions were increased energy expenditure in sedentary participants, homeostatic capacity regulation, with a lowered occurrence of chilly sensation in older adults, and enhanced oxidative phosphorylation in striated muscles. Capsinoid consumption stimulated physical activity in the sedentary elderly of the CP group [32]. Another nutraceutical option alongside resistance and aerobic training was supplementation with 100 mg/day of isoflavone for 10 weeks. This study evaluated the effect of an isoflavone diet mixed with physical exercises and investigated the lipid profile, oxidative stress and inflammatory markers in postmenopausal women. The physical training comprised mixed aerobic (carried out with a treadmill) and resistance activity over 30 sessions for 50 min/session, 3 times/week, mediated using the 1RM test with eccentric and concentric phases. Beneficial results were registered, with increased IL-8 levels being an important angiogenic agent, and lowered total cholesterol, which is associated with the anti-inflammatory status [13]. By applying whole-body cryotherapy, over 24 exposures for 3 min, 7 times/week for 7 days, and endurance training (long-distance runners), another author demonstrated no change in the 3 nitro-tyrosine level and no change in nitro-oxidative stress in male seniors. The increasing iNOS concentration and implicit enhancing bioavailability of nitric oxide demonstrated that WBC has a beneficial effect on vascular vasodilatation and important antioxidant and anti-inflammatory results, such as stimulating lipid oxidation through the metabolic effect of IL-6 and decreasing IL-6 levels in the RUN (long-distance runners) group. Nitro-oxidative stress and inflammation markers did not change after exposure to WBC [14]. Aging is accompanied by progressive loss of function and mass skeletal muscle-related frailty. Sarcopenia can cause mobility disorders, risk of falls, lack of independence and alteration to metabolic health in the elderly through mitochondrial disturbances, insulin resistance and oxidative stress. Another study demonstrated that the association between acute or resistance training with n3-PUFA supplementation for six months determined a modest increase in skeletal muscle strength by decreasing inflammatory effects and reducing oxidative stress at the mitochondrial level. Improving the contraction energy level after n3-PUFA during exercise training and decreasing the rate of protein synthesis attenuated functional disorders, sarcopenia and chronic inflammation in skeletal muscle. The addition of omega-3 to diets improves muscle strength in elderly adults with normal glycaemia [35,38]. Another paper, namely the PHYSMED project, observed an association between physical fitness of different degrees and blood biomarker levels associated with inflammatory status or oxidative stress. Therefore, the lower physical fitness group obtained decreasing triglyceride and vitamin B12 concentrations and increased values outside the normal range for homocysteine, creatinine and the lipid profile. In the vast majority of elderly Spanish people, vitamin D(OH) values were low. In the three groups, low-, medium- and high-fitness dietary intake was seen in European, Spanish or Majorcan food. Regular physical activity and a diet associated with a healthy lifestyle and delayed premature aging were found for the high-fitness group [31]. A study carried out based on the association between increased acrylamide consumption and physical activity showed a poor capacity for effort and even negative effects regarding muscle mass quality, implicitly accentuating sarcopenia and obesity in the elderly. Monitoring was performed using walking training, chair stands repeated five times, FFQ and PASE [18]. A higher dietary intake of flavonoids (cocoa beverage powder, once/day, 12 weeks) showed positive effects in muscle strength and resistance, increasing exercise capacity, and reducing anti-inflammatory effects and oxidative stress. Physical performance, cognitive profile and quality of life reflected through SMI and EQ-5 were improved in older adults [33]. Nutraceutical dietary supplementation with L-glutamine (Gln) for 30 days, demonstrated

in another study, increased the physical capacity regarding knee muscle strength/power in elderly women using endurance and strength training, 60–70 min/session, 3 times/week, monitored using an isokinetic test. Glycaemic-level regulation using lower insulin concentrations and oxidative stress amelioration with increased oxidised glutathione (GSH, GSSG) and lowered thiobarbituric acid-reactive substances were also mentioned [27]. In a large study with 391 elderly participants (non-Hispanic white, Black and Hispanic populations) and with habits such as cigarette smoking and alcohol consumption, physical activity testing was carried out, graded in effort intensities. The diet was supplemented with vitamin D and omega-3 (VITAL-DEP program). The mitochondrial DNA copy number is a biomarker associated with premature aging, oxidative stress and behavioural habits. The monitoring of the effect of low, intermediate and vigorous physical activity and the supplemented diet was carried out using METs, PHQ-8 and mtDNAcn. A lowered mtDNA copy number for smoking participants was registered as a negative impact for elderly Black people [37]. It is known that exposure to ozone causes endothelial and cardiovascular effects and is correlated with inflammation and an increase in reactive oxygen species due to the absence of the glutathione S-transferase Mu1 (GSMT1) gene. However, controlled exposures to ozone with concentrations increasing from 0 ppb (parts per billion) to 120 ppb, together with moderate exercise training in elderly adults, did not determine obvious inflammatory effects, but increases in CRP 8-isoprostane and Il-6 and endothelin-1 were recorded in another study. A decrease in 3-NT and nitrosative stress levels was reported as a positive effect [21]. It is not clearly stipulated that dietary intake supplemented with protein can improve muscle injuries and fatigue induced by prolonged walking exercises in elderly adults. The study carried out on the target and placebo groups after walking training for three consecutive days showed comparable increases in creatine kinase following intense muscular effort, and protein supplementation in the study group did not demonstrate faster elimination of muscle pain or fatigue compared to the control group. Inflammatory markers such as CRP, IL-6 and Il-10 had comparable values in both groups because the muscle protein synthesis response to anabolic stimuli was diminished [30].

Endurance training performed on a treadmill for 12 weeks with 3 sessions/week or physical tasks for 4 h/day with a cycle ergometer for 4 weeks is recommended. Mental tasks for 4 h/day with sets of 30 min, using an advanced trail-making test, have also been applied. The administration of a nutraceutical antioxidant diet with astaxanthin (AX), represented by powerful, red oceanic carotenoids found in algae, shellfish and fish, or AX with sesamin, i.e., oleaginous seed found in sesame, is also recommended.

3.3. The Influence of Physical Activity on Oxidative Stress for Healthy Older Adults

Aging is traditionally accompanied by functional autonomy restriction, skeletal muscles' capacity decline, frailty, risk of falls and, often, cognitive disorders. Low muscle strength found in older adults, legitimised by evidence of a slowed-down skeletal muscle response to anabolic agents, accentuates motor disabilities and the risk of mortality. Therefore, the intervention of strategies that address both the maintenance and recovery of functional deficiencies as well as the slowing down of cognitive decline is required. The concern for promoting a healthy lifestyle and maintaining quality of life must be made a priority in order to prevent or delay premature aging. Physical activity (PA) in its various forms, such as physical exercises, resistance or endurance training, or both, represents an essential direction in promoting healthy aging at the motor level and in the cognitive domain. One aspect of age progression is damage caused to the balance between the antioxidant defence system and reactive oxygen species. Oxidative stress initiates proinflammatory factors, which causes muscle frailty and motor function decline and affects mental health. The main results regarding different PA program recommendations that could influence the oxidative stress are presented in Table 3.

Table 2. Beneficial effects through physical activity and nutraceutical dietary intake on measurement outcomes.

Authors	Design	Dietary Intake	Age/ Gender	Physical Activity	Primary Outcomes	Secondary Outcomes	Tools/ Instruments	Conclusions
Liu S.Z. et al. (2021) [23]	42 subjects: 23 females 17 males	Nutraceutical dietary (AX) AX group PL (placebo) group	65–82 years	12 weeks endurance training for 3 sessions/week	FATox (g/min) CHO (g/min) RER Exercise efficiency (%) = work (kcal/min)/energy expenditure (kcal/min) × 10	GXT, TA, blood chemistry test: lipid profile (total cholesterol, HDL, LDL, triglycerides insulin level)	Treadmill, custom-built exercise device	Improved exercise efficiency for males, enhanced FA tox for both sexes and groups, increased fat oxidation under the same exercise intensity, improved exercise efficiency, decreased carbohydrate oxidation during lower-intensity training in older males.
Oggioni C. et al. (2018) [26]	20 participants 10 females 10 males	Nitrate dietary (NO_3^-) beetroot juice: 70 mL × 2/day for seven days	60–70 years	Cycling with 10-M, pedalling cadence of 50 rpm, vigorous/moderate-intensity activity, walking, sitting	IPAQ, MET, haemodynamic parameters: BP, CO, CI, SV, HR, AIx	Glucose, insulin, HOMA-IR, IL-6, cGMP, E-selectin, P-selectin, thrombomodulin ICAM-3, 3-NT	Bicycle ergometer, micromanometer	The nitrate nutraceutical diet did not favourably influence the haemodynamic and cardiac parameters at rest or during physical activity of various degrees, nor the oxidative stress.
Żychowska M. et al. (2021) [17]	24 women SUP (supported group), CON (control) group	1000 mg vitamin C/day for 6 weeks	≥65 years	6-week training program three times/week 60 min, either session, gyrokinesis–Nordic walking, stabilisation training	VO_2 max, muscle mass, fat mass, BMI, TOS/TOC, TAS/TAC vitamin C prooxidative/ antioxidative ratio	TUBB, IL-1, IL-6, IL-10, CCL2, CRP	Cyclo-ergometer Ergoline (60 rpm cadence)	Decreased BMI and increasing muscle mass after regular exercise training-related CON group, insignificant changes for both groups after 6 weeks of exercise training supported/not supported with vitamin C, non-influencing oxidative/antioxidative balance after support using vitamin C and health training, decreased IL-6 and increasing IL-10 mRNA in supported group, small increase in IL-1 after aerobic training and nutraceutical vitamin C supplementation.
Yokoyama K. et al. (2020) [32]	69 subjects 52 females 17 males CP group PL group	9 mg capsinoids (*Capsicum anuum* L., CH-19 Sweet) daily for 12 weeks	52–87 years	VPA (≥6 METs), LMPA (1.5–5.9 METs), physical strength test, 10 m walking time	FAS METs, energy expenditure (Kcal/day = METs × time × body weight (kg) × 1.05	Mood profile: POMS2, TMD, LBM, BMI, % body fat, visceral fat index, muscle mass %, FFM (kg), VAS	Accelerometer with 3 axes, stadiometer, Scala Yamato with weight, activity meter	In terms of body composition, ingestion of capsinoids decreased waist circumference, body fat percentage and visceral fat index, increasing energy expenditure in sedentary participants. Homeostatic capacity regulation with decreased chilly sensation in adults 80 years or older. Enhanced energy expenditure, oxidative phosphorylation in muscles, insulin resistance and lipids' use under conditions of increased amount and time devoted to LMPA.

Table 2. *Cont.*

Authors	Design	Dietary Intake	Age/ Gender	Physical Activity	Primary Outcomes	Secondary Outcomes	Tools/ Instruments	Conclusions
Jéssica S. Giolo et al. (2018) [13]	32 females ISO group = 17 PL group = 15	100 mg/day isoflavone nutraceutical for 10 weeks intervention	50–70 years	Aerobic training, resistance training (7 exercises, 30 sessions, 10 weeks 50 min/session)	BMI, VE/O_2 ratio, VE/CO_2 ratio, 1RM	Total cholesterol, triglycerides, HDL, LDL, uric acid, HBA1c, IL-8, IL-1β, TNF, IL-10, SOD, TBARS, FRAP	Stadiometer Sanny, treadmill (5.5 km/hour)	Lipid profile and markers of oxidative stress were not influenced by isoflavone nutraceuticals and the association with aerobic or resistance exercise, enhanced IL-8 levels and reduced total cholesterol from aerobic and resistance training promotion.
Wiecek M. et al. (2021) [14]	RUN = 10 UTR = 10	WBC—24 exposures to −130° for 3 min in cryochamber (whole-body cryotherapy), 3 times/week, 7 days	53–56 years	3–5 times/week, 55–150 km at 2 marathons/year 10/6 METs—very hard/hard PA for RUN, 4 METs—moderate-intensity exercise for UTR	BMI, Height, Fat mass, % body fat, Haemoglobin (g/dL), Haematocrit (%), ESR (mm/h), Leucocytes ($10^3/\mu L$), Platelets ($10^3/\mu L$), Fasting glucose, HBA1c, Total cholesterol, Triglycerides, HDL, LDL, Total protein, Fibrinogen (g/L), AIP	iNOS, ADMA, 3-NTR, CRP, IL-6, IL-1β, IL-10, HCY	Bamet KN-1 cryogenic chamber, Stopwatch	Increased i-NOS levels in older adults after 24 WBC treatments, no change in the level of 3-NTR, which is an indicator of nitro-oxidative stress, stimulated lipid oxidation using IL-6 metabolic effect, decreased IL-6 levels in RUN group compared with UTR group.
Kunz H.E. et al. (2022) [35]	63 elderly n3-PUFA = 30, PL = 33 Male = 29 Female = 34	n3-PUFA diet for 6 months	71.5 ± 4.8 years	Free-living physical activity (MVPA), cardiorespiratory fitness (VO_2 max), 1RM, leg endurance test	BMI, SMI, body fat (%) RBC-EPA RBC-DHA CRP, ESR, lean mass (kg), leg lean mass (kg)	ROS, jO2, jATP, ACR, Phe, Tyr, FSR	Waist-worn accelerometer, treadmill	Enhanced anabolic response after supplementation with n3-PUFA related to acute and resistance physical activity, physical mobility maintenance and strengthened skeletal muscles, increased resistance training and strength gain, improved ATP level (contraction energy) after n3-PUFA during physical training with decreased protein synthesis rate, involving anti-inflammatory status after n3-PUFA addition.

Table 2. *Cont.*

Authors	Design	Dietary Intake	Age/ Gender	Physical Activity	Primary Outcomes	Secondary Outcomes	Tools/ Instruments	Conclusions
Aparicio-Ugarriza R. et al. (2018) [31]	429 older adults Females = 57% Males = 43%	Low fitness group (low PF), Medium fitness group (medium PF), High fitness group (high PF), PHYSMED project, dietary intake (European, Spanish or Majorcan food)	55–85 years	Chair stand test, aerobic endurance, dynamic balance test (8-foot up-and-go), 6-minute walk test, handgrip strength	BMI, TDW, FFM,	25(OH)D, total cholesterol, vitamin B12, folate, triglycerides, HDL-c/LDL-c, HCY, creatinine, urea, uric acid, glucose, total protein albumin, haemoglobin, haematocrit, RBC folate, Fe/FER	Handgrip dynamometer	Decreased vitamin B12 and triglycerides in blood concentration and increased HCY, TC, HDL, LDL and creatinine levels, especially in the low PF group.
Kawamura T. et al. (2021) [2]	873 participants Females—296 Males—577	Dietary intake with vitamin A, C, tocopherol, beta-carotene, WASEDA'S health study	50–65 years	PF: leg extension power, CRF (mL/kg/min)	BDHQ, BMI, LBM, body fat %, HR, blood pressure, VO_2 max	Fasting glucose, HBA1c, TC, HDL-c, LDL-c, TG, TBARS, PC, F2-IsoP, vitamin A, vitamin C α-tocopherol, β-carotene	-	Decrease in oxidative stress by about 10% after physical fitness and nutraceutical intake (with vitamin A, C, tocopherol and beta-carotene) for elderly females and males.
Veronese N. et al. (2021) [18]	4436 participants Females—2578 Males—1858	Dietary acrylamide intake	61.3 years	20 m repeated 2 times, 400 m walking, chair stands repeated 5 times	FFQ, BMI	PASE	-	Poor physical performance was associated with higher acrylamide dietary intake.
Munguia L. et al. (2019) [33]	60 subjects, Flavonoid (F) group, nonflavonoid (NF) group but highly alkalinised, placebo group	Cocoa beverage powder once/day	55–70 years	12 weeks 6 min walking test, 30 min/day training	TUG, sit-up test, 2 min step-in-place test, glycaemia, TG, HDL-c, LDL-c, TG/HDL index	SMI, EQ-5D	Handgrip strength	Reduced oxidative stress through dietary intake intervention, improved functional and cognitive profile with physical activity and nutraceuticals from the flavonoid group.

Table 2. *Cont.*

Authors	Design	Dietary Intake	Age/ Gender	Physical Activity	Primary Outcomes	Secondary Outcomes	Tools/ Instruments	Conclusions
Amirato G.R. et al. (2021) [27]	44 participants, exercising group (PE)—21, non-exercising group (NPE)—23	L-glutamine (Gln) nutraceutical (maltodextrin) 30 days	60–80 years	Endurance training, strength training, 60–75 min/session 3 times/week	FFT, TUG, 5XST, IPAQ, BMI	D-fructoso amine, insulin, GSH, GSSG, iron, uric acid, TBARs, average power of extensor and flexor knee muscles	Cycle ergometer	Gln administration stimulated gluconeogenesis and controlled glycaemia levels for older adults, increasing redox potential and metabolic immunological, cardiovascular, respiratory and neuromotor adaptations using endurance and strength training for elderly women.
Vyas C.M. et al. (2020) [37]	391 participants, non-Hispanic white—183, Black—110, Hispanic—98	Behavioural factors (cigarette smoking, alcohol consumption, depression) Nutraceutical dietary supplement with vitamin D and omega-3	Mean 67 years	Low, intermediate and vigorous physical activity (LMVPA) training (<5.5–29.9 > 30 MET hours/week)	METs PHQ-8, BMI	mtDNAcn	Bicycle	Lowered mtDNA copy number for smoking participants and negative impact, especially on Black population, not related to other lifestyle and behavioural factors for lower mtDNA copy.
Balmes J.R. et al. (2019) [21]	87 participants 65%–females 35%–males	Ozone-controlled chambers with different concentrations (0 ppb, 70 ppb, 120 ppb)	55–70 years	Moderate exercise training	BMI, CT, LDL-c, CRP, IL-6, 8-isoprostane, P-selectin, monocyte-platelets conjugated	Endothelin-1, 3-NT, GSTM1, fibrinogen	-	Decreased 3-NT levels and increased CRP, 8-isoprostane, ET-1 and IL-6 proinflammatory markers after ozone exposure to elderly. However, changes in serum levels of proinflammatory factors had no significant effect.
Busquets-Cortés C. et al. (2018) [22]	127 participants Female—66 Male—61 Inactive group—40 Intermediate group—41 Active group—46	European food, Spanish food, dietary intake with vitamin C, vitamin E, Zn, Se	55–80 years	Intermediate and active exercise training	BMI, body fat %	CAT, SOD, GRd, GPx, MDA, 3-NT, TrxR1, PBMCs	-	Increased antioxidative activity and attenuated inflammatory status-related aging due to an active lifestyle and regular physical activity promotion, improved oxidative metabolism capacity in PBMCs and enhanced antioxidant defences.
Ten Haaf D.S.M, et al. (2020) [30]	104 subjects 81%—male 19%—female protein group—50 placebo group—54	Protein dietary intake for 12 weeks with 2 nutraceutical proteins/day	67–73 years	30/40/50 km/day walking training (endurance exercises), 3 days, consecutive	BMI, NPRS	CK, CRP, IL-6, IL-10	-	Protein nutraceutical administered to healthy older adults did not affect muscle damage, soreness and fatigue after prolonged moderate-intensity walking training.

Table 2. *Cont.*

Authors	Design	Dietary Intake	Age/ Gender	Physical Activity	Primary Outcomes	Secondary Outcomes	Tools/ Instruments	Conclusions
Batista R.A.B. et al. (2022) [38]	950 subjects 474—females 476—males	Glycohaemoglobin group (<5.7%), glycohaemoglobin group (>5.7%), dietary intake with omega-3 (2–4 weeks)	50–85 years	Moderate or vigorous physical activity, strength training	BMI	Fasting glucose, HBA1c %, plasma omega-3, ALA, EPA, DHA	Handgrip strength-isokinetic dynamometer	Increased plasma omega-3 level improved muscle strength in elderly people with normal glycaemia, decreased inflammation and oxidative stress related to physical activity training of different degrees.

AX: astaxanthin; PL: placebo; FA tox: fat oxidation; CHO: carbohydrate oxidation; RER: respiratory exchange ratio = VCO_2/VO_2; GXT: graded exercise test; TA: tibial anterior endurance test; IPAQ: international physical activity questionnaire; FFQ: food frequency questionnaire (energy intake kcal/day); BP: blood pressure; CO: cardiac output; CI: cardiac index; AIx: augmentation index related to % pulse pressure; SV: stroke volume; HR: heart rate; HOMA-IR: homeostatic model for the assessment of insulin resistance; IL-6,1,10: interleukin-6,1,10; cGMP: guanosine monophosphate; ICAM-3: intercellular adhesion molecule; 3-NT: nitro-tyrosine; TOS: total oxidative status; TOC: total oxidative capacity; TAC: total antioxidant capacity; TACV: total antioxidative capacity; BMI: body mass index; TUBB: tubulin beta class I; CRP: C-reactive protein; LMPA: light to moderate physical activity; FFM: fat-free mass; VAS: visual analogue scale; VPA: vigorous physical activity; FAS: fitness age score; METs: metabolic equivalents; POMS2: profile of mood status; TMD: total mood disturbance; LBM: lean body mass; VE/O_2 ratio: ventilatory equivalents for oxygen; VE/CO_2 ratio: ventilatory equivalents for dioxide; 1RM: test–retest reliability of one repetition maximum assessing the strength capacity of individuals; HDL: high-density lipoprotein; LDL: low-density lipoprotein; HBA1c: glycated haemoglobin; TNF: tumour necrosis factor; SOD: superoxide dismutase enzyme; TBARS: thiobarbituric acid-reactive substances; FRAP: plasma ferric reduction capacity; RUN: long-distance runners; UTR: untrained men; WBC: whole-body cryotherapy; iNOS: inducible nitric oxide synthase; ADMA: asymmetric dimethylarginine; 3-NTR: 3 nitro-tyrosine; HCY: homocysteine; ESR: erythrocyte sedimentation rate; AIP: atherogenic; n3-PUFA: omega-3 polyunsaturated fatty acids; MVPA: moderate to vigorous physical activity; SMI: skeletal muscle index; RBC: red blood cell; ROS: reactive oxygen species; jO2: oxygen flux; ATP: adenosine triphosphate flux; Phe: phenylalanine; Tyr: tyrosine; FSR: fractional synthesis rate; 25(OH)D: vitamin D; TG: total cholesterol; TDW: total body water; Fe: iron; FER: ferritin; RBC: red blood cell; PTPA: leisure-time physical activity; LOPCA: Loewenstein occupational therapy cognitive assessment; GDS: geriatric depression scale; BDHQ: brief-type dietary history questionnaire; CRF: cardiorespiratory fitness; PC: protein carbonyl; F2-IsoP: F2-isoprostane; PASE: Physical Activity Scale for the Elderly; TSDG: Taekwondo self-defence training course group; CG: control group; MDA: malondialdehyde; GPx: glutathione peroxidase; HST: handgrip strength test; CSST: chair sit-to-stand test; BST: back stretch test; V-SRT: sit and reach test; TUG: timed up-and-go test; 6-MWT: six min walk test; AS: astaxanthin and sesamin; CFQ: Chalder Fatigue Questionnaire; PCOOH: plasma phosphatidylcholine hydroperoxide; ATMT: Advanced Trail-Making Test; OSA-MA: Ogri–Shirakawa–Azumi Sleep Inventory; 5XST: five-time sit-to-stand test; RT: resistance training; CAT: catalase; GSR: glutathione reductase; TMPT: Trail-Making Peg Test; PHQ-8: Patient Health Questionnaire 8; mtDNA cn: mitochondrial DNA copy number; GSTM1: glutathione S-transferase Mu 1; TrxR1: thioredoxin reductase; UCP3: uncoupling protein 3; PBMCs: peripheral blood monocellular cells; LTPA: moderate leisure time physical activity; NPRS: numeric pain rating scale (0–10); EPA: eicosapentaenoic acid; DHA: docosahexaenoic acid; ALA: alpha linolenic acid.

Table 3. Physical activity and oxidative stress outcomes.

Authors	Participants	Characteristics	Age/Gender	Physical Exercises	Primary Outcomes	Secondary Outcomes	Tools	Conclusions
Daimiel L. et al. (2020) [49]	6874 participants 48.5% females, 51.5% males	PREDIMED-plus trial PF—physical fitness (PF quartiles) Chair stand test PA—physical activity (PA levels) Rapid assessment physical activity questionnaires	60–70 years	Chair stand test (30 s), light physical activities, moderate physical activities (≤150 min/week), vigorous physical activities (≤75 min/week), high PA (>150 min/week)	BMI, Er-Med diet, MMSE, COWAT, DS, TMT, CDT	SF36-HRQL, RAPA, MET/min/week	Chair stand, Stopwatch	Enhanced scores for verbal and phonemic verbal fluency related to PF, decreased TMT time in PF, improved neurocognitive parameters related to PF, increased cognitive function and quality of life in activities correlated with PF and PA.
Alghadir A.H. et al. (2021) [17]	106 individuals 44 females 62 males	Sedentary group (n = 29), moderately active group (n = 37), highly active group (n = 40)	56–81 years	Active exercises LTPA	VO_2 max, RER, HCY, Vitamin E, NO, TAC	GPAQ, METs, LOTCA, MMSE	Treadmill, Accelerometer	Decreased glycosylated haemoglobin and homocysteine levels related to moderate and high physical activity, lowered vitamin E levels related to degrees of cognitive capacity damage, increased serum levels of oxidative stress markers and α- and γ-tocopherol at higher-intensity physical activity, and better cognition capacity.
Netz Y. et al. (2021) [50]	122 subjects	Younger elderly female (<74 years) elderly female (≥75 years) Males (n = 36) PA, PF	65–82 years	PA: habitual physical activity, low-, moderate- or high-level exercises, PF	BMI, IPAQ-SF, MMSE, METs, PSQI, GDS	FI, VO_2 max, H_2O_2	Treadmill	The correlation of FI with oxidative stress markers, BMI, physical and fitness activities and sleep disorders suggested an improvement in motor function, mental and emotional status and sleep quality in elderly men and younger elderly women.
Ku B.J. et al. (2021) [19]	16 women TSDG—8 Control G—8	Postmenopausal status	>45 years	12-week Taekwondo training course, 4 times/week, session—60 min	BMI, fat mass (kg), percent fat (%), LBM	MDA, SOD, IL-6, α-TNF	Wear M430 device	Decreased MDA and increased SOD after Taekwondo training course, reduced oxidative stress after physical activity, decreased IL-6 and TNF blood levels, improved agility and motor functions for menopausal women after intervention of Taekwondo training course.
Morucci G. et al. (2022) [16]	18 participants 14—female 4—men	Functional fitness, reactive oxygen metabolites, biological antioxidant potential	62–86 years	24-week multimodal exercise program, 1 h/session, twice/week	BMI, body fat % FFIs (HST, CSST, BST, V-SRT, TUG, 6-MWT)	Salivary cortisol levels, ROM, EuroQol-5 dimension-3 level	Chairs, Elastic bands, Sticks, Electronic hand dynamometer	Increased flexibility for upper and lower limbs after multimodal exercise training application, fitness capacity maintenance from daily living activities, decreased body fat percentage improved muscle strength, aerobic endurance, dynamic balance and biomechanical and physiological parameters, cognitive function amelioration due to intense physical activity, which stabilised anti- and pro-oxidative balance status.

Table 3. *Cont.*

Authors	Participants	Characteristics	Age/Gender	Physical Exercises	Primary Outcomes	Secondary Outcomes	Tools	Conclusions
Takahashi M. et al. (2019) [52]	38 participants	Active group (PA)—19 Control group—19	70.2 ± 3.9 years	8 weeks MVPA, ADL	BMI, METs systolic blood pressure, diastolic blood pressure	GDS, step count (steps/day) BDNF, serotonin, ROMs, HEL, BAP, TRX	Uniaxial accelerometer	Increased step count, BDNF, serotonin levels after MVPA, depression prevention associated with decreased serotonin concentrations in older women due to PA, decreased oxidative stress, which promotes depression in older adults, using PA.
Mesquita P. et al. (2019) [11]	13 Participants (males)	Muscle biopsies, HSPs	64 ± 9 years	6 weeks RT twice/week, 3 sets with 10–12 repetitions	mRNA analysis, FFM	CAT, GDS, SOD, GAPDH	Isokinetic dynamometer	Benefit effect promotion in redox status, especially for CAT and GDS in skeletal muscles after RT training.
Yoon J. et al. (2020) [56]	24 participants, Synap group—15 Control group—9	Synapsology (SYNAP), Dual-task exercise using traditional games	65–77 years	8 weeks, 2 times/week, 60 min/session	BMI, TUG, 5XST, 5 m habitual test,	TMPT, ROMs, BNDF,	Game-like dual-task	Improved motor and cognitive abilities for older adults who participated in intervention games such as dual-tasks.
Valado A. et al. (2022) [24]	37 participants, experimental group—27, control group—10	Therapeutic pool with aquatic exercise training	60–89 years	hydrotherapy exercises, 15 sessions, 30 min/session	SOD	GPx, GR	-	Decreased bone damage risk due to aquatic exercise protocol application, increased enzyme-related antioxidant effects, hydrotherapy stimulated antioxidant defence for older adults.
Sánchez-Rodríguez M.A. et al. (2021) [1]	177 subjects (women)	Mexican community-dwelling women, behavioural factors	46–69 years	PA (walking, aerobics exercises, swimming, yoga, running) > 30 min/day	BMI, glucose, cholesterol, triglycerides, HDL-c	MDA, GPx, SOD, uric acid, SOD/GPx ratios, SS (stress score)	-	Increased oxidative stress index associated with sedentary lifestyle, smoking and coffee and alcoholic beverage consumption.
Kozakiewicz M. et al. (2019) [12]	327 participants Younger elderly inactive (YN)—112, younger elderly active (YA)—112, older inactive (ON)—128, older active (OA)—41	Younger elderly—65–74 years, Older—90–99 years	65–99 years	LTPA	BMI, METs, SDPAR, TC	MDA, SOD, CAT, GPx GR, SOD/GPx ratios, CP, isoprostanes	-	Increased GPx and CAT activity in both younger elderly and the oldest groups related to moderate physical activity, enhanced SOD/GPx ratios in younger elderly men compared with inactive older men of all groups, promoting moderate physical exercises caused decreased oxidative stress and had a beneficial effect on both younger elderly and the oldest groups.

Er-Med diet: 17-item questionnaire for Mediterranean foods; MMSE: Mini Mental State Examination test; COWAT: Controlled Oral Word Association Test; DS: digit span test; TMT: Trail-Making Test; CDT: Clock-Drawing Test using visuospatial memory; SF36-HRQL; Short-form health-related quality of life questionnaire with 36 items; RAPA: Rapid Assessment of Physical Activity Questionnaire; HBA1c: glycated haemoglobin; EPA: eicosapentaenoic acid; DHA: docosahexaenoic acid; ALA: alpha linolenic acid; GPAQ: Global Physical Activity Questionnaire; LTPA: leisure-time physical activity; FI: frailty index; PSQI: Pittsburgh Sleep Quality Index; GDS: Geriatric Depression Scale; H_2O_2: hydrogen peroxide; MDA: malondialdehyde; GPx: glutathione peroxidase; FFTs: senior functional fitness tests; TUG: timed up-and-go test; 6-MWT: six min walk test; 5XST: five-time sit-to-stand test; BDNF: brain-derived neurotrophic factor; HEL: hexanoyl lysine; BAP: biological antioxidant potential; TRX: thioredoxin; CAT: catalase; GSR: glutathione reductase; RT: resistance training; GAPDH: glyceraldehyde 3-phosphate dehydrogenase; GRd: glutathione reductase; TMTP: Trail-Making Peg Test; SDPAR: seven-day physical activity recall; CP: protein carbonyls.

Two references discussed the association between physical activity of different degrees of intensity (low, moderate and vigorous) and physical fitness (PF) associated with muscular and cardiorespiratory endurance, muscular strength, flexibility and body composition. Within the wide PREDIMED program with 6874 participants, the results of the interventions were monitored using MMSE and TMT, showing an improvement in neurocognitive parameters linked to physical fitness. Enhanced scores for verbal and phonemic verbal fluency were quantified using COWAT, CDT and DS, and increased quality of life using SF36-HRQOL. Physical fitness was associated with better cognitive activity [49]. The frailty index decreased and motor function, mental and emotional status and sleep quality improved, as measured using IPAQ-SF, PSQOI and MMSE. PF levels together with PA favourably contribute to motor and nonmotor skills and functions [50]. Moderate- or high-level PA demonstrated a greater increase in plasma α- and γ-tocopherol and a decrease in oxidative stress and homocysteine levels than in senior individuals who performed low-intensity physical activities. Exercise training is associated with cognitive function; thus, markers such as vitamin E, homocysteine level and free radical species can be used as predictive factors for assessing mental health in elderly adults. Monitoring was evaluated using GPAQ, LOTCA, METs and MMSE [17]. Regular low- or moderate-intensity physical activity stimulates antioxidant and anti-inflammatory capacities, as evidenced by increased SOD or GPx and decreased MDA, Il-6 and TNF-α levels. Moreover, 12 weeks of Taekwondo martial art training for 60 min, 4 times/week, showed an improvement in motor function and agility motions, and ameliorated depression, anxiety and sleep disorders in terms of antioxidative and anti-inflammatory responses in postmenopausal women [19]. Multimodal exercise training (back-scratch, chair sit-to-stand or grip strength), such as functional fitness for 24 weeks, 1 hour/session, twice per week, improved flexibility motions, muscle strength, dynamic balance and other biomechanical parameters. Regarding blood biomarker levels, the study measured decreased reactive oxygen metabolites, prooxidant activity and hormone stress concentrations (cortisol). Functional fitness by performing daily tasks increased upper and lower limb flexibility, muscle strength, cognitive function amelioration, and decreased body fat percentage and prooxidative status. Increased quality of life and mental health was observed using EuroQol-5 [16]. Another study assessed the involvement of daily physical activity from moderate-to-vigorous levels for 8 weeks on postmenopausal women using an axial accelerometer. After exercise training, the observed findings were an increased step count, brain-derived neurotrophic factor and serotonin levels. These results demonstrated decreased oxidative stress quantified using biological antioxidant potential (BAP) and prevented depression, measured using GDS [52]. Advancing age is associated with suffering of the striated muscle mass and function regarding oxidative damage biomarkers. In another study, the author demonstrated the influence of resistance training for 6 weeks, twice/week, using 3 sets with 10–12 repetitions, on skeletal muscle redox potential. Oxidative stress markers such as 4-hydroxynonenal, heat-shock proteins (HSP60) and protein carbonyls (PC), using CAT, SOD, GDS and GAPDH, were investigated. After resistance training carried out on many levels, positive results were identified from muscle biopsies, mRNA and various endogenous antioxidants [11]. The risk of cognitive disorders in elderly adults is a serious mental health problem. Another reference discussed the contribution of a game-like dual-task exercise, named "synapsology" (SYNAP), which improved physical and cognitive responses in older adults. Physical activity and cognitive profiling were carried out over 8 weeks, 60 min/session, twice a week, and investigated using timed up-and-go (TUG), the five-time sit-to-stand movement test (5XST), the Trail-Making Peg Test (TMPT), reactive oxidative metabolites and brain-derived neurotrophic factor (BNDF). Beneficial results have been observed after using the SYNAP program to assess cognitive status, daily functional abilities and healthy life [54]. A hydrotherapy program performed over 15 sessions stimulated the antioxidant profile by upregulating glutathione reductase, peroxidase activity and superoxide dismutase enzymes, and decreasing reactive oxygen species in the body. Thus, regular exercise training prevents disorders caused by premature aging [24]. A sedentary lifestyle and behavioural factors such as

smoking and coffee and alcoholic beverage consumption on older women is associated with oxidative stress, and progressed aging was demonstrated in another study. OS was measured using MDA, SOD, GPx and the SOD/GPx ratio. A stress score ranging from 0 to 7 was associated with marker modification. A stress score of ≤4 and physical activity of <30 min/day in sedentary Mexican women were associated with increased oxidative stress [1]. In the same sense, another author discussed the importance of moderate physical activity associated with oxidative defence capacity on free radicals and progressed aging. Increased SOD/GPx ratio, SOD, CAT and GPx levels in blood compared with decreased MDA, carbonyl protein and isoprostane concentrations were noted in older adults who participated in moderate exercise programs versus the sedentary elderly. In conclusion, it was demonstrated that physical activity provides an antioxidant-protective effect by decreasing free radicals and proinflammatory markers [12].

3.4. The Impact of Recovery Using Physical Activity and Nutraceutical Compounds on Oxidative Stress for Neurodegenerative Diseases

Neurodegeneration is the result of cerebral metabolism disorders, glial system-level changes, as well as neurotransmitter communication alterations in synaptic networks and abnormalities at the blood–brain barrier, such as endothelial cell lesions. Oxidative stress occurs in neurodegeneration disorders such as Alzheimer's disease (AD), Parkinson's disease (PD), amyotrophic lateral sclerosis (ALS) and multiple sclerosis (MS). In AD, the neuropathological mechanism is described as an amyloid protein accumulation outside the cell and the presence of neurofibrillary tangles composed of hyper-phosphorylated "tau proteins". Thus, synaptic connection loss occurs in selective brain regions. Along with OS, mitochondrial function is also affected by an increase in free radicals that leads to nerve cell apoptosis. PD is defined as a loss of melanin-pigmented nigral neurons with dopamine depletion in the basal ganglia and the presence of Lewy bodies. By increasing oxidative stress, it accentuates the destruction of the substantia nigra and the acceleration of cell death. In ALS, increased accumulations of carbonyl protein, nitro-tyrosine and superoxide radicals lead to certain irreversible cellular alterations. In SM, intensive lipid peroxidation is activated, which leads to demyelination, which causes severe neural destruction. Decreasing SOD levels and enhancing TBARS and nitrite concentrations contribute to the amplification of oxidative stress, proinflammatory capacity and damage to nervous cells. Therefore, the need to improve morphological and functional neuron decline and delaying pathophysiological neurodegeneration mechanisms has prompted the intervention of neurorehabilitation strategies and methods of prolonging the evolution of neurodegenerative diseases. Thus, the combined promotion of physical activity in various forms and intensities and nutraceutical compound diet participation has demonstrated favourable effects in limiting the oxidative stress and inflammatory phenomena developed in neurodegenerative impairments. In Table 4, we present the relationship between different types of PA, dietary intake and oxidative stress.

Usual and enhanced physical activity, such as aerobic exercise training using a treadmill for 26 weeks, 150 min/week, in 3 sessions/week, and dietary intake with phospholipids and PUFAs, were performed on 23 older adults with familial and genetic risks of AD. Blood systemic biomarker levels involved in cognitive function (memory, learning), such as myokine cathepsin B (CTSB), BDNF, lipid profile and klotho, were adjusted after physical training, which showed positive mental wellbeing and brain function effects [36]. In another study, the influence of physical fitness, ADL and IADL with a handgrip and additional low-niacin dietary intake on mental health, depression or emotional disorders was assessed. A total of 815 participants with frailty and pre-frailty cognitive status took part in a LRGS-TUA study. They were monitored using nonmotor scales such as GDS, MMSE, MoCA, RAVLT, digit span, WHODAS, DHQ and SOD, MDA, BDNF and DNA damage. The telomerase level results demonstrated beneficial effects on oxidative stress amelioration and cognitive frailty identification in elderly people with mild impairments or dementia [40]. Aerobic training with low intensity carried out in an aquatic environment

for 12 weeks, 2 times/week, 45 min/session, was credited with decreasing depression and anxiety scores, functionally independently, and the implicit decrease in reactive oxygen species. The quantification was carried out using the Borg scale, BAI, BDI, TUG, GSH, SOD NO and protein carbonyl levels [51]. Dietary intake of a functional food such as Laminaria japonica (FST) from seaweed—which has a six-week antioxidant effect—together with physical fitness training provided protective action against progressive neurodegeneration caused by free radicals. The results measured after the interventions were improved physical autonomy, cognitive functions and antioxidant activity, indicated by increased SOD, GSR and GPx levels, and the capping of oxidative stress markers such as TBARS, 8-oxoDG and BDNF. Mental health evaluation monitoring was used, including the MMSE, the numerical memory test, Raven's test, Flanker test and the iconic memory test, with positive results [43]. High-intensity interval training performed using a cycle ergometer, weights, a dynamometer and elastic bands for 12 weeks, with 1 session/week, demonstrated a reduction in fatigue and spasticity, and an improvement in muscle strengthening, resistance and aerobic performance, implicitly increasing the quality of life. The results obtained using QOL, SEP-59 and MSQOL-54 demonstrated the possibility of carrying out autonomous activities and improving living conditions [55]. AD dementia is associated with both autonomous functional decline and that of cognitive status. Daily regularly exercise in combination with desalted *Salicornia europaea* L. (SE), a species of halophytic plant, was shown to improve frontal executive functions, such as oxidative stress amelioration, proinflammatory biomolecule decrease and neuroprotective pathway stimulation. The program was carried out for 12 weeks by administering PhytoMeal (SE) ethanol extract, 600 mg/day, with physical training. Notable performances were observed in cognitive tasks assessing perception, attention, working memory and language using ADAS–cog, CERAD-K, K-CWST and S-GDS. Beneficial results were registered regarding quality of life in older adults with AD, such as an increased ability to perform daily living activities.

3.5. The Effects of Recovery Using Nutraceutical (Antioxidant) Biomolecules on Oxidative Stress for Neurodegenerative Diseases

Neurodegenerative disorders are associated with oxidative stress and mitochondrial dysfunction via protein aggregates, which compromises the activity of mitochondrial enzyme complex I, thus stimulating free radical production. Therefore, the use of natural or artificial agents with antioxidant action capable of limiting and delaying motor and cognitive disorders within the neurodegenerative process is required. Daily supplementation with 50 mg of melatonin for 3 months decreased reactive oxygen species through increasing mitochondrial complex I and the respiratory ratio, catalase and superoxide dismutase, and lowering glutathione, malondialdehyde and carbonyl protein levels in older adults with Parkinson's disease. The beneficial effects of melatonin refer to the reduction in mitochondrial dysfunctions from oxidative stress and the proinflammatory effects [20]. The relationships between antioxidants and oxidative stress in neurodegenerative diseases are presented in Table 5.

Table 4. Relationship between dietary supplementation, physical activity and oxidative stress.

Authors	Participants	Characteristics	Age/Gender	Physical Exercises	Primary Outcomes	Secondary Outcomes	Tools	Conclusions
Gaitán J.M. et al. (2021) [36]	23 subjects: 50% female	Dietary nutraceuticals, UPA group, EPA group	60–69 years	26 weeks, aerobic exercise training, 150 min/week UPA, EPA, 3 sessions/week	VO_2 peak CTSB, BDNF, Klotho protein, MMSE, CVLT	TC, TG, HDL-c, LDL-c, Non-HDL-c, lipid metabolites, nonlipid metabolism	Treadmill, accelerometer,	Increased CTSB associated with EPA, ameliorated cognitive function associated with aerobic training, decreased BDNF during physical activity, cardiorespiratory fitness associated with Klotho, enhanced phospholipids and PUFAs in the EPA group.
Malek Rivan N.F. et al. (2019) [40]	815 participants: cognitively pre-frail group (37.4%), cognitively frail group (2.2%),	LRGS-TUA study, questionnaire–interview low niacin intake	60 years	ADL, IADL, physical fitness,	BMI, MMSE, GDS, PASE, digit span, RAVLT, MoCA, MOS-SS, WHODAS, DHQ	SOD, MDA, DNA damage, vitamin D, BDNF, telomerase	Handgrip, chair	Decreased ADL associated with cognitive impairments and physical frailty, lowered niacin intake associated with enhanced risk of cognitive frailty in dementia, oxidative stress markers such as MDA and telomerase levels being suggestive of cognitive frailty in older adults.
Silva L.A.D. et al. (2019) [51]	Depression group—16 subjects, Non-depression group—14 subjects	Pool with depth of 1.20 m, 25 m × 12.5 m, water with temperature about 26 °C, dietary intake protein	63.5 ± 8.8 years	12 weeks of aquatic training, 2 times/week, 45 min/session	BMI, HR, Borg scale, BDI, BAI, TUG, BBS	GSH, SOD, nitric oxide, protein carbonylation	Stopwatch, ruler, chair	Aquatic training program contributed to decreasing anxiety, depression and other cognitive impairments, improved physical functions and SOD/GSH levels in the non-depression group, lowered oxidative stress after undergoing aquatic training.
Reid S.N.S. et al. (2019) [43]	60 participants: FST group—32, control group—28	Nutraceutical dietary intake with fermented Laminaria japonica (FST) 1.5 g/day for 6 weeks.	67–81 years	Physical fitness	MMSE, numerical memory test, Raven's test, Flanker test, iconic memory test, TMT, 6-MW, TUG	SOD, GSR, GPx, TBARS, 8-oxoDG, BDNF	Stopwatch, armchair	Increased cognitive functions after supplementation with FST, enhanced antioxidant activity for enzymes such as: SOD, GSR, GPx, decreased oxidative stress markers' (TBARS and 8-oxoDG) levels after FST administration for 6 weeks, increased BDNF levels associated with neuromuscular integrity and physical functions after FST nutraceuticals.

Table 4. *Cont.*

Authors	Participants	Characteristics Age/Gender		Physical Exercises	Primary Outcomes	Secondary Outcomes	Tools	Conclusions
Zaenker P. et al. (2018) [55]	26 participants: female—19, male—7	EDSS 0–5 Dietary intake	about 54 years	12 weeks, high-intensity training—one session/week, resistance training—one session/week.	VO_2 peak, HR, MTP	LET, QOL, SEP-59, MSQOL-54	Cycle ergometer, dynamometer, weights, elastic bands	Improved functional capacity for resistance and endurance training in multiple sclerosis, enhanced quality of life, especially for men with multiple sclerosis.
Lee W.J. et al. (2020) [42]	53 participants: PM-EE group—26, placebo group—27	Nutraceutical with PM-EE times 12 weeks, 600 mg/day	50–85 years	Regular exercises 2–3–4 times or every day	MMSE CERAD-K, K-CWST, S-GDS	ADAS–cog, memory, language, executive function	-	Improvement in K-CWST, ADAS–cog scales, enhanced cognitive task scores such as attention, perception, spoken language, working memory increased ADL abilities in AD patients.

CTSB: myokine cathepsin B; BDNF: brain-derived neurotrophic factor; UPA: usual physical activity; EPA: enhanced physical activity; VO_2: cardiorespiratory fitness; CVLT: California Verbal Learning Test; D-KEFS–CWI: Delis Kaplan executive function system–colour and word interference; PUFA: polyunsaturated fatty acids; LRGS-TUA: LRGS towards useful aging (TUA); PASE: Physical Activity Scale for the Elderly; RAVLT: Rey Auditory–Verbal Learning Test; MoCA: Montreal Cognitive Assessment; ADL: activities of daily living, IADL: instrumental activities of daily living; MOS-SS: medical outcomes study social support survey; WHODAS: WHO disability assessment schedule-related dietary intake (protein, fibre, fruits, vitamins); DHQ: dietary history questionnaire; BDI: Beck Depression Inventory (score ranges 0–63, with 21 items); BAI: Beck Anxiety Inventory; BBS: Berg Balance Scale; EDSS: expanded disability status score; MTP: maxim tolerated power; LET: lactates at the end of training; SEP-59: 59-item multiple sclerosis and quality of life questionnaire; MSQOL-54: multiple sclerosis and quality of life 54-item questionnaire; SE: Salicornia europaea; PM-EE: PhytoMeal ethanol extract; CERAD-K: consortium to establish a registry for Alzheimer's disease; K-CWST: Korean version of the colour–word Stroop test; S-GDS: short-form geriatric depression scale.

Table 5. Relationships between antioxidants and oxidative stress in neurodegenerative disease.

Authors	Participants	Characteristics	Age/Gender	Primary Outcomes	Secondary Outcomes	Tools	Conclusions
Jiménez-Delgado A. et al. (2021) [20]	26 participants with PD	Nutraceutical dietary melatonin—25 mg for 3 months, melatonin–placebo group, placebo–melatonin group	60–69 years	Lipoperoxides, nitric oxide metabolites, carbonyl groups, CAT	Mitochondrial complex I activity, mitochondrial respiratory control ratio		Decreased oxidative stress markers after supplementation with melatonin, increased complex I activity, catalase and respiratory control ratio.

Table 5. *Cont.*

Authors	Participants	Characteristics	Age/Gender	Primary Outcomes	Secondary Outcomes	Tools	Conclusions
Hong C.T. et al. (2021) [44]	18 patients with PD	Combination of molecular hydrogen (H_2) and Photo-biomodulation therapy for 2 weeks	50–80 years	UPDRS part I, II and III H&Y (II/III)	Bun, creatinine, GOT, GPT, WBC, Hb, PLT	Light-emitting diode array	Decreased reactive oxidative species using H_2 water intervention, stimulated mitochondrial functions, which increased ATP levels, alleviated cognitive function deterioration.
Coles L.D. et al. (2018) [41]	5 participants (3 female, 2 male) with PD	Nutraceutical with NAC 6000 mg/day for 28 days	54–73 years	UPDRS (I-III), H&Y,	NAC, Cys, GSH, GSH/GSSG, CAT, MDA, 4-HNE	MRS-Siemens Magnetom	Decreased oxidative stress markers after NAC administration, increased cysteine levels and implicit antioxidant capacity, such as GSH/GSSG and catalase.
Yoritaka A. et al. (2021) [54]	15 patients PD	Molecular hydrogen (H_2) inhalation, 2 L/min, 2 times/day, 1 hour, for 16 weeks.	50–70 years	MDS-UPDRS, PDQ-39	N1, N8-dyacetylspermidin, 8-hydroxy-2-deoxiguanosine	MHG-2000α-H_2 producing machine	H_2 gas supplementation is sure and safe but did not beneficially influence PD patients.
Gibson G.E. et al. (2020) [46]	70 patients with AD, benfotiamine group—34, placebo group—36	Nutraceutical with oral benfotiamine for 12 months, 300 mg, twice/day	60 years	ADAS–cog, MMSE, METS, SRT, NPI, ADCS–ADL	CDR, FDG, thiamine (Th), AGE	PET (brain positron emission tomography)	Ameliorated cognitive and functional status in AD patients after administration of nutraceuticals with benfotiamine.
An Y. et al. (2019) [39]	MCI group—102, control group—68	Dietary nutraceutical intake with vitamin B, EMCOA study	50–70 years	MMSE, MoCA, SDMT, AVLT (IR, SR, LR) LMT, DSF, DSB, FFQ (33 items)	Vitamin B_6, folate, vitamin B_{12}, Hcy, ROS, MDA, 8-OHdG, 8-isoPGF2α	MALDI-TOF mass spectrometry	Decreased cognitive decline associated with vitamin B_{12} intake deficiency, adequate diet with folate and vitamin B_6 was associated with better cognitive reserves, enhanced Hcy levels and oxidative stress markers in MCI patients with vitamin B deficiency.

Table 5. *Cont.*

Authors	Participants	Characteristics	Age/Gender	Primary Outcomes	Secondary Outcomes	Tools	Conclusions
You Y.X. et al. (2021) [53]	48 participants	Supplemented nutraceutical with CC 250 mg twice daily for 12 weeks	60–70 years	MMSE, digit span, RAVLT, VR, POMS	BNDF, COX-2, GSH, MDA, iNOS, SOD		Improved global cognitive function after CC supplementation for 12 weeks, ameliorated mood status after CC, decreased lipid peroxidation and implicit oxidative stress markers.
Schneider L.S. et al. (2019) [47]	210 participants, ladostigil group—103, placebo group—107	Addition ladostigil 10 mg/day for 3 years	55–85 years	CDR (score-0.5), MMSE (>24), WMS-RC (≤18),	NTB, DAD, RAVLT, GDS (>5), medial temporal lobe atrophy scale (>1)		Ameliorated neurodegeneration with ladostigil in mild cognitive impairments after administration at a low dose.
Clark D.O. et al. (2019) [34]	180 participants, MINDspeed study	MindFoods dietary intake (high-polyphenol food) and speed training (playing control games) for 12 weeks	60–69 years	FFQ, MMSE, Trail-Making Test, GDS, RBANS	Proinflammatory cytokines, anti-inflammatory cytokines, TBARS, mRNA	iPad, BrainHQ program	Decreased proinflammatory cytokines and oxidative stress markers after intervention with dietary intake of MindFoods and MINDspeed (cognitive training), enhanced anti-inflammatory cytokine levels after administration of nutraceuticals for patients with AD.
Ton A.M.M. et al. (2020) [28]	13 participants: women—11 men—2	Probiotic kefir nutraceutical dietary intake (2 mL/kg/day) for 90 days	78 ± 7 years	MMSE, immediate memory test, delayed memory test, Cookie Theft Picture Test, similarity test, Boston Naming Test, TMT-A, Clock-Drawing Test	IL-6, IL-1b, TNF-α, IL-8, IL12p70, IL-10, IL-8/IL-10 ratio, IL-12/IL-10 ratio, ROS, AOPP, NO, PARP-1	Recall board, picture	Improved cognitive functions, such as memory, visual–spatial function, language abstraction and conceptualisation skills, decreased oxidative stress markers associated with ROS, Increased NO levels and implicit mitochondrial activity enhancement due to lowered membrane potential and improved antioxidant capacity.

Table 5. *Cont.*

Authors	Participants	Characteristics	Age/Gender	Primary Outcomes	Secondary Outcomes	Tools	Conclusions
Mohamed W.A. et al. (2019) [15]	50 participants: female—22, male—28, LF group, placebo group	Supplemented with lactoferrin (LF) 250 mg/day for 3 months	60–85 years	MMSE, CDR, ADAS–cog 11	PI3K, p-Akt, Ach, 5-HT, MDA, NO, GSH, TAC, IL-6, IL-10, p-tau, Aβ42, caspase-3, HSPs, cholesterol		Decreased A beta 42, cholesterol, proinflammatory and oxidative stress markers after LF supplementation for 3 months, lowered heat-shock protein, caspase-3, and p-tau upon intake, ameliorated cognitive functions for patients with AD due to decreased inflammation and oxidative status.

PD: Parkinson's disease; RCR: mitochondrial respiratory control ratio; UPDRS: Unified Parkinson's Disease Rating Scale; H&Y; Hoehn and Yahr; ATP: adenosine triphosphate acid; NAC: N-acetylcysteine; Cys: cysteine; 4-HNE: 4 hydroxynonenal; MRS: magnetic resonance spectroscopy; MDS: Movement Disorder Society; PDQ: Parkinson's disease questionnaire (39 items); DiAcSpd: N1, N8-dyacetylspermidine; ADAS–cog: Alzheimer's disease assessment scale–cognitive subscale; CDR: clinical dementia rating; FDG: fluorodeoxyglucose; AGE: advanced glycation end products; METS: memory evaluation treatment service; SRT: the Buschke selective reminding test; NPI: neuropsychiatric inventory; ADCS–ADL: Alzheimer's disease cooperative study–activities of daily living; MCI: mild cognitive time of light impairment; EMCOA: effects and mechanism investigation of cholesterol and oxycholesterol on AD; SDMT: symbol digit modalities test; AVLT (IR, SR, LR): Auditory–Verbal Learning Test (immediate recall, short recall, long recall); LMT: logical memory test; DSF: digit span forwards; DSB: digit span backwards; WMS-RC: Wechsler memory scale revised, Chinese version; 8-isoPGF2α: 8-iso prostaglandin F2α; MALDI-TOF: matrix-assisted laser desorption ionisation time of flight; CC: Cosmos caudatus; VR: visual reproduction; POMS: profile of mood state; COX-2: cyclooxygenase-2; iNOS: inducible nitric oxide synthase; NTB: neuropsychological test battery; DAD: disability assessment in dementia; RBANS: repeatable battery for the assessment of neuropsychological status; AOPP: advanced oxidative protein products; PARP-1: Poly ADP-ribose polymerase 1; PI3k: phosphatidylinositole-4,5 biphosphate 3-kinase; p-Akt: protein kinase; ACh: acetylcholine; 5-HT: serotonin; Aβ42: amyloid β; HSP: heat-shock protein.

A strong antioxidant effect on pathophysiology neurodegeneration has been mentioned for molecular hydrogen (H_2). Molecular hydrogen intake was carried out through the daily ingestion of H_2—water associated with photo-biomodulation (PBM)—for 2 weeks, or inhalation of 6.5 vol% H_2 gas in 2 L/min for 16 weeks, twice/day, and mixed air was obtained using electrolysis in patients with PD. The effects of molecular hydrogen administration were decreased reactive oxygen species, stimulated mitochondrial activity with enhanced ATP levels and mitigated cognitive function deterioration [44,54]. Another author discussed the intravenous administration of N-acetylcysteine (NAC), a powerful antioxidant that stimulates brain glutathione levels, 6000 mg/day for 28 days, in elderly people with PD. Oxidative stress indicators such as MDA or 4-hydroxynonenal (4-HNE) remained unchanged, while antioxidant biomarkers of the same type reduced the oxidised ratio (GSH/GSSG), and catalase increased in the concentrations [45]. Another antioxidant used as a supplement was benfotiamine, a synthetic thiamine derivative (pharmacokinetic marker belonging to the vitamin B group) administered orally for 12 months, 300 mg twice/day. Spectacular results were obtained in terms of cognitive and functional status, demonstrated using ADAS–cog, CDR, MMSE, NPI and ADCS–ADL scales. Therefore, ADAS–cog and CDR scores decreased by 43% and 77%, respectively, after benfotiamine administration with amelioration of cognitive abilities, such as memory, praxis, language, attention, orientation, judgement and verbal memory. In this sense, improvements were observed in daily activities carried out independently and the ability to make one's own decisions and judgments. Decreased oxidative stress and proinflammatory activity were demonstrated by lowered blood biomarkers such as advanced glycation end-product levels [46]. Dietary intake of vitamins from group B, especially vitamin B12 and folate, was used in an EMCOA study, showing decreased cognitive decline, especially with better cognitive reserves and MDA, HCY, 8-OHdG and 8-isoPG2α oxidative stress marker types. The results were monitored using mitigated MMSE, MoCA, AVLT, DSF, DSB and SDMT scores [39]. Mild cognitive disorders represent a heterogeneous syndrome defined by a decline in memory performance, with this being a transitional line between normal aging and dementia in terms of neurodegenerative diseases. The addition of Cosmos caudatus, a vegetable of the Cosmos-type annual plant, turned out to have beneficial effects on mood status amelioration and global cognitive status improvement after 12 weeks with 250 mg twice daily. Lowered lipid peroxidation reduced oxidative stress, proven by assessing MDA, BNDF, SOD, iNOS, GSH and COX-2 levels. The scales used for measuring mild cognitive impairment were MMSE, digit span, RAVLT and POMS [53]. Another author discussed alleviating neurodegeneration, especially in medial temporal lobe atrophy after low-dose ladostigil administration at about 10 mg/day for three years. The quantification of favourable responses was performed using MMSE, WMS-RC CDR, DAD, RAVLT and GDS scales [47]. Dietary intake with polyphenols combined with the MindFoods (cognitive training) program was proven to decrease reactive oxygen species and proinflammatory cytokines after supplementation for 12 weeks in older adults with AD. Improved neurobiological health and enhanced anti-inflammatory cytokine levels were demonstrated using MMSE, TMT, GDS and RBANS scores, and TBARS and mRNA markers [34]. The antioxidant effects of probiotics such as kefir using nutraceutical supplementation for 90 days at 2 mL/kg/day were proposed in another study that measured systemic oxidative stress, proinflammatory and anti-inflammatory cytokines, NO bioavailability and cognitive function or capping metabolic disorder improvements. The assessment was performed using MMSE, immediate memory delay, TMT-A, the clock-drawing test, the delayed memory test and the Boston test, whose scores improved in terms of visual–spatial function, language abstraction, memory and conceptualisation skills. Oxidative stress (ROS, AOPP, PARP-1), systemic inflammation (IL-8/IL-10 ratio, IL-12/Il-10 ratio, Il-6, TNF-α, IL-1b) and metabolic cellular damage were modulated using the probiotic antioxidant intervention [28]. Another study proved the antioxidant and anti-inflammatory role of lactoferrin, a multifunctional glycoprotein iron fastener, after administration for 3 months at 250 mg/day. The favourable intervention of lactoferrin using the modulation protein kinase B/phosphatase and tensin

homolog (PTEN) pathway and acetylcholine (Ach) and serotonin (5-HT) serum levels was demonstrated. Decreased MDA, IL-6, heat-shock proteins, cholesterol and tau proteins, and increased SOD, GSH and IL-10 levels validated the antioxidative and anti-inflammatory effects of lactoferrin. The positive cognitive function results were monitored using MMSE, ADAS–cog 11 and CDR. Thus, lactoferrin administration seems to be a protective intervention, modulating oxidant and proinflammatory pathological cascades and cognitive decline [15].

4. Discussion

Biological aging is characterised by decreasing functional and cognitive abilities, being much more pronounced in elderly adults' motor impairments and cognitive decline. Thus, functional autonomy loss as well as a decrease in mental and behavioural progress accelerate the onset of motor decline and dementia. Hence, these aspects cause great concern for the health and care systems. Although these disorders have multiple causes, the most publicised hypothesis in this regard is that related to oxidative stress. Disturbing the balance between the body's antioxidant defence power and the production of free radicals leads to mitochondrial dysfunctions and cellular metabolism damage. Reactive oxygen species and proinflammatory cytokines are thus generated, which promote lipid peroxidation, hyperphosphorylation or oxidised proteins, and DNA damage. Synthesis of the relationship between oxidative stress markers and normal aging, physical activity, pathological aging and nutraceutical compounds is presented in Figure 1.

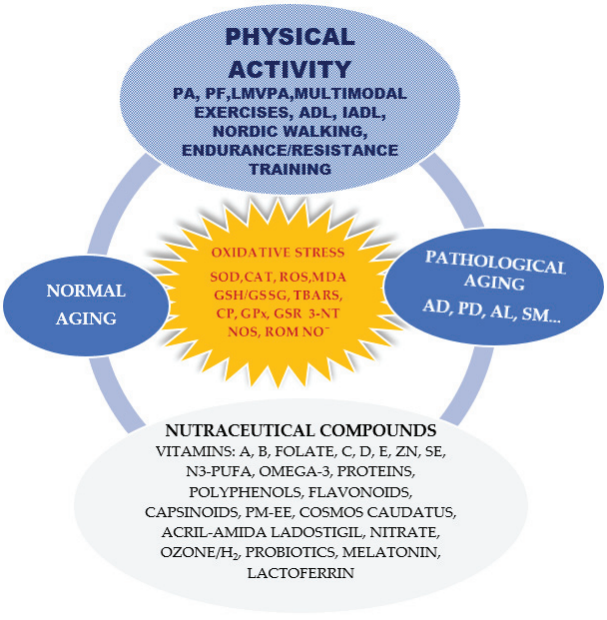

Figure 1. Relationship between oxidative stress, physical activity and nutraceutical compounds in the aging process. Legend: PA—physical activity; PF—physical fitness; ADL—activities of daily living; IADL—instrumental activities of daily living; SOD—superoxide dismutase; CAT—catalase; ROS—reactive oxygen species; MDA—malondialdehyde; GSH/GSSG—reduced/oxidised glutathione; TBARS—thiobarbituric acid-reactive substances; CP—protein carbonyl; GPx—glutathione peroxidase; GSR—glutathione reductase; 3-NT—3 nitro-tyrosine; NOS—nitric oxide synthase; ROM—range of motion; AD—Alzheimer's diseases; PD—Parkinson's disease; ALS—amyotrophic lateral sclerosis; MS—multiple sclerosis; N3-PUFA—omega-3-polyunsaturated fatty acids; PM-EE—PhytoMeal ethanol extract.

These processes create abnormal amyloid beta–peptide aggregations and intracellular neurofibrillary tangles, disturbing synaptic networks with changes in acetylcholine, dopamine and serotonin levels, which generates neuroinflammation and neurodegeneration. In our study, we performed a review of the research findings in the literature regarding how different types of physical activity and supplementation with natural and artificial nutraceutical compounds could delay the aging process and the development of neurodegenerative disorders. Physical activity, starting from ADL and IADL, and continuing with walking training, resistance or endurance exercises, physical fitness, multimodal exercises or physical tasks, managed to maintain and improve functional autonomy and delay cognitive decline. Applying moderate-intensity training for six or twelve weeks, such as habitual activities, Nordic walking, gyrokinesis, 400 m walking or chair stands repeated five times, showed significant improvements in VO_2 max, systolic and diastolic blood pressure, BMI, muscle mass or fat mass, physical frailty, mental health, emotional status and sleep disorders. MMSE, IPAQ-SF, PSQOI, PASE, MoCA WHODAS and GDS scores demonstrated beneficial results in healthy elderly adults and seniors with neurodegeneration for both genders [1,18,25,33,40,50,52]. Promoting low, moderate or vigorous physical activity (LMVPA) contributed to improving the gait pattern, strength, gait, physical mobility, skeletal muscle strengthening, body fat percentage, BMI and the visceral fat index, including oxidised stress parameters.

In the lipidic modulation profile, decreased HCY, 3-NT, MDA, IL-6, CRP and mtDNA copy number, or increased SOD, CAT, GRd and GPx, resulted after the physical training intervention at different intensities applied for 6–8 weeks for 75 min/week, 150 min/week or 5.5–30 MET hours/week. Increased functional autonomy, quality of life and enhanced cognitive capacities, including neurocognitive parameters, were monitored using MMSE, COWAT, DS, CDT, TMT, METS, LOTCA and GPAQ scores [12,14,17,21,22,32,35,37,38,49]. Endurance or resistance training were another form of physical activity, using devices such as a treadmill, cycle ergometer or handgrip dynamometer, being applied 6–12 weeks for 60 min/session, 3 times/week. Improved antioxidant or anti-inflammatory status, cardiovascular, respiratory and immunological parameters, and implicitly increased motor and cognitive functions, both for normal and pathological aging, were measured. The tools that evidenced beneficial effects for both healthy older adults and seniors with neurodegenerative impairments were MMSE, FFT, TUG, 5xST, POMS2, COWAT, DS, TMT, CDT, LOTCA, PSQOI and GDS, with influence on motor functions, neurocognitive capacity and quality of life [10,13,19,23,24,26,27,30,31,36,50–52,55]. Physical fitness is another way to evaluate oxidative stress reduction and improved cognitive abilities by measuring the ameliorating effects on neuromuscular integrity, sleep disorders, emotional and mental motor status and cognitive scales, such as a lowered risk of frailty index. Positive results were demonstrated for both genders and for healthy or neuropathological elderly adults using BDHQ, MMSE, IPAQ-SF, PSQOI, PASE, RAVLT, DS, MOS-SS, GDS, numerical, the iconic memory test, TMT or Raven's test [2,40,43,50]. Multimodal exercises determined enhanced flexibility in upper and lower limbs, and improvements in dynamic balance, endurance and muscle strength, evidenced by alleviated oxidative stress and proinflammatory capacity [16]. A special approach was the implementation of physical tasks using a visual display, a game-like dual-task or ergometer task, with significant improvements in attention, working memory, spoken language and motor functions [29,42,56]. Another direction for promoting normal aging without unfavourable events and mitigating neurodegenerative disorders in older adults is the promotion of nutraceutical dietary supplements with natural and artificial antioxidants administered using diet or medication. The antioxidant power of vitamins A, C, D, E, complex B, folate and their derivatives were recognised. Using these interventions allowed to obtain increased antioxidant agents, demonstrated by the activation of potential redox enzymes such as SOD, CAT, GSH, GRd, GPx and TOS/TOC and TAS/TAC, which attenuated cellular and mitochondrial disruptions, and showed anti-inflammatory effects. The beneficial action of vitamins is expressed by the modulation of pathophysiological biomolecule synthesis pathways that act in free radicals and proinflammatory markers (IL-6,

Il-8, IL-1, CRP, TNFα, BDNF). Antioxidant and anti-inflammatory effects improve functional capacity and mental health in elderly adults of both genders [2,22,25]. Along with vitamins D and E, other nutrients intervene in the same sense, such as omega-3 and n3-PUFA, which strengthen the antioxidant effect, modulate lipid and carbohydrate profiles, increase phospholipids and intracellular and mitochondrial ATP levels, and decrease concentrations of inflammatory substances, such as BDNF and Klotho proteins. Enhanced motor and cognitive function were demonstrated using these interventions in healthy older adults and elderly patients with neurodegenerative diseases [35–38]. Other nutraceuticals were supplemented using dietary proteins and N-acetyl cysteine. The results showed favourable effects on antioxidant/oxidant agent balance by using CAT, GSH/GSSG, SOD/GSH, MDA, 4-HNE, protein carbonylation and scores of scales such as IPAQ, NPRS, UPDRS, H&Y, BDI, BAI and BBS. They improved physical or neuromotor functions for normal aging and ameliorated depression, anxiety and sleep disorders in seniors of both sexes with neurodegeneration impairments [27,30,45,51]. European, Spanish or Majorcan foods have made significant contributions to functional capacity and reactive oxygen species' decrease. The results were demonstrated using TDW, FFM, LET, QoL SEP-59 and MSQOL [14,31,55]. Supplementation with polyphenols, flavonoids, capsinoids, Laminaria japonica, Cosmos caudatus or acrylamide showed the same aspects regarding oxidative stress and favourable results regarding motor abilities and mental functions. PASE, SMI, EQ-5D, FFQ, VAS, TMD, POMS2, LBM, MMSE, CERAD-K, K-CWST and GDS demonstrated progress in terms of motor and cognitive autonomy effects [13,18,32,33,42,53]. Nitrate dietary supplementation had no favourable influences on neither cardiac and haemodynamic parameters, nor oxidative stress. After taking small doses of ladostigil, neurodegeneration due to dementia was mitigated. Quantification was carried out using MMSE, CDR, WMS-RC, NTB, DAD, RAVLT and GDS, which estimated medial temporal lobe atrophy and showed favourable evolution in mild cognitive impairment [47]. The proposal for supplementation with ozone or molecular hydrogen did not provide effective results regarding oxidative stress, but the administration of molecular hydrogen together with photo-biomodulation stimulated mitochondrial activity with increased ATP levels, associated with alleviating cognitive disorders [21,44,54]. The presence of probiotics such as kefir demonstrated memory improvement, language abstraction and conceptualisation skills and decreased reactive oxygen species and proinflammatory biomarkers. A beneficial antioxidant effect was proven in the progress reflected using cognitive scales such as MMSE, immediate and delayed memory tests, TMT-A and the clock-drawing test [28]. The addition of melatonin for three months at 25 mg/day proved beneficial in reducing oxidative stress biomarkers when analysing CAT, mitochondrial complex I activity and the mitochondrial respiratory control ratio [20]. Decreased free radicals and proinflammatory agents demonstrated by assessing afferent blood biomarker levels and cognitive scales such as MMSE, CDR and ADAS–cog 11, showed mental function alleviation in elderly patients with AD dementia.

5. Conclusions

The aging process reduces physical capacities, alters the cognitive status and is related to oxidative stress, which is defined as an alteration in the balance between oxidant and antioxidant biomolecules. This is because ROS leads to genetic, molecular, cellular, tissue and systemic changes.

In the search for healthy aging and a delayed pathological neurodegenerative evolution process in elderly people, mechanisms must be promoted to adjust the imbalance between the excessive production of ROS and the decrease in the defensive enzyme system and, implicitly, proinflammatory capacity attenuation. Therefore, the promotion of constant physical activity accompanied by the addition of natural or artificial factors to dietary intake is the first favourable intervention in this regard.

Protein oxidation represents one of the biggest damages caused by oxidative stress and can be monitored by determining AOPPs (advanced oxidation protein products), being an indirect biomarker for an accentuated oxidative status.

Regular physical activity and supplementation with vitamins and oligomolecules elicit decreased IL-6 and increased IL-1 oxidative metabolism capacity. In conclusion, this study demonstrated that physical activity provides an antioxidant-protective effect by decreasing free radicals and proinflammatory markers.

Author Contributions: M.V.B., conceptualisation, methodology, resources, writing—original draft preparation; M.D., methodology, formal analysis, visualisation; L.R., methodology, supervision, formal analysis; M.I.M., formal analysis, review and editing. All authors have read and agreed to the published version of the manuscript.

Funding: This research received no external funding.

Institutional Review Board Statement: Not applicable.

Informed Consent Statement: Not applicable.

Data Availability Statement: Not applicable.

Conflicts of Interest: The authors declare no conflict of interest.

References

1. Sánchez-Rodríguez, M.A.; Zacarías-Flores, M.; Correa-Muñoz, E.; Arronte-Rosales, A.; Mendoza-Núñez, V.M. Oxidative stress risk is increased with a sedentary lifestyle during aging in Mexican women. *Oxid. Med. Cell. Longev.* **2021**, *2021*, 9971765. [CrossRef] [PubMed]
2. Kawamura, T.; Tanisawa, K.; Kawakami, R.; Usui, C.; Ito, T.; Tabata, H.; Nakamura, N.; Kurosawa, S.; Choi, W.; Ma, S.; et al. Determinants of Resting Oxidative Stress in Middle-Aged and Elderly Men and Women: WASEDA'S Health Study. *Oxid. Med. Cell. Longev.* **2021**, *2021*, 5566880. [CrossRef] [PubMed]
3. Chandrasekaran, A.; Idelchik, M.D.P.S.; Melendez, J.A. Redox control of senescence and age-related disease. *Redox Biol.* **2017**, *11*, 91–102. [CrossRef]
4. Sies, H.; Jones, D.P. Reactive oxygen species (ROS) as pleiotropic physiological signalling agents. *Nat. Rev. Mol. Cell Biol.* **2020**, *21*, 363–383. [CrossRef]
5. To, T.; Terebessy, E.; Zhu, J.; Zhang, K.; Lakey, P.S.; Shiraiwa, M.; Hatzopoulou, M.; Minet, L.; Weichenthal, S.; Dell, S.; et al. Does early life exposure to exogenous sources of reactive oxygen species (ROS) increase the risk of respiratory and allergic diseases in children? A longitudinal cohort study. *Environ. Health* **2022**, *21*, 90. [CrossRef]
6. Katerji, M.; Filippova, M.; Duerksen-Hughes, P. Approaches and Methods to Measure Oxidative Stress in Clinical Samples: Research Applications in the Cancer Field. *Oxid. Med. Cell. Longev.* **2019**, *2019*, 1279250. [CrossRef] [PubMed]
7. Murphy, M.P.; Bayir, H.; Belousov, V.; Chang, C.J.; Davies, K.J.; Davies, M.J.; Dick, T.P.; Finkel, T.; Forman, H.J.; Janssen-Heininger, Y.; et al. Guidelines for measuring reactive oxygen species and oxidative damage in cells and in vivo. *Nat. Metab.* **2022**, *4*, 651–662. [CrossRef]
8. Visioli, F.; Artaria, C. Astaxanthin in cardiovascular health and disease: Mechanisms of action, therapeutic merits, and knowledge gaps. *Food Funct.* **2017**, *8*, 39–63. [CrossRef]
9. Cuadrado, A.; Manda, G.; Hassan, A.; Alcaraz, M.J.; Barbas, C.; Daiber, A.; Ghezzi, P.; León, R.; López, M.G.; Oliva, B.; et al. Transcription Factor NRF2 as a Therapeutic Target for Chronic Diseases: A Systems Medicine Approach. *Pharmacol. Rev.* **2018**, *70*, 348–383. [CrossRef]
10. Hussain, T.; Tan, B.; Yin, Y.; Blachier, F.; Tossou, M.C.; Rahu, N. Oxidative stress and inflammation: What polyphenols can do for us? *Oxid. Med. Cell. Longev.* **2016**, *2016*, 7432797. [CrossRef]
11. Mesquita, P.H.C.; Lamb, D.A.; Godwin, J.S.; Osburn, S.C.; Ruple, B.A.; Moore, J.H.; Vann, C.G.; Huggins, K.W.; Fruge, A.D.; Young, K.C.; et al. Effects of resistance training on the redox status of skeletal muscle in older adults. *Antioxidants* **2021**, *10*, 350. [CrossRef] [PubMed]
12. Kozakiewicz, M.; Rowiński, R.; Kornatowski, M.; Dąbrowski, A.; Kędziora-Kornatowska, K.; Strachecka, A. Relation of moderate physical activity to blood markers of oxidative stress and antioxidant defense in the elderly. *Oxid. Med. Cell. Longev.* **2019**, *2019*, 5123628. [CrossRef]
13. Giolo, J.S.; Costa, J.G.; da Cunha-Junior, J.P.; Pajuaba, A.C.; Taketomi, E.A.; de Souza, A.V.; Caixeta, D.C.; Peixoto, L.G.; de Oliveira, E.P.; Everman, S.; et al. The effect of isoflavone supplementation plus combined exercise on lipids levels and inflammatory and oxidative stress markers in postmenopausal women. *Nutrients* **2018**, *10*, 424. [CrossRef] [PubMed]
14. Wiecek, M.; Szygula, Z.; Gradek, J.; Kusmierczyk, J.; Szymura, J. Whole body cryotherapy increases the activity of nitric oxide synthase in older men. *Biomolecules* **2021**, *11*, 1041. [CrossRef] [PubMed]
15. Mohamed, W.A.; Salama, R.M.; Schaalan, M.F. A pilot study on the effect of lactoferrin on Alzheimer'disease pathological sequelae: Impact of the p-Akt/PTEN pathway. *Biomed. Pharmacother.* **2019**, *111*, 714–723. [CrossRef]
16. Morucci, G.; Ryskalin, L.; Pratesi, S.; Branca, J.J.V.; Modesti, A.; Modesti, P.A.; Gulisano, M.; Gesi, M. Effects of a 24-week exercise program on functional fitness, oxidative stress, and salivary cortisol levels in elderly subjects. *Medicina* **2022**, *58*, 1341. [CrossRef]

17. Alghadir, A.H.; Gabr, S.A.; Answer, S.; Li, H. Associations between vitamin E, oxidative stress markers, total homocysteine levels, and physical activity or cognitive capacity in older adult. *Sci. Rep.* **2021**, *11*, 12867. [CrossRef]
18. Veronese, N.; Dominguez, L.J.; Ragusa, S.; Solimando, L.; Smith, L.; Bolzetta, F.; Maggi, S.; Barbagallo, M. Dietary acrylamide and physical performance tests: A cross-sectional analysis. *PLoS ONE* **2021**, *16*, e025932. [CrossRef]
19. Ku, B.J.; Ko, K.; Shin, K.O.; Bae, J.Y. Effect of regular Taekwondo self-defense training on oxidative stress and inflammation markers in postmenopausal women. *Healthcare* **2021**, *9*, 985. [CrossRef]
20. Jiménez-Delgado, A.; Ortiz, G.G.; Delgado-Lara, D.L.; González-Usigli, H.A.; González-Ortiz, L.J.; Cid-Hernández, M.; Cruz-Serrano, J.A.; Pacheco-Moisés, F.P. Effect of melatonin administration on mitochondrial activity and oxidative stress markers in patients with Parkinson's disease. *Oxid. Med. Cell. Longev.* **2021**, *2021*, 5577541. [CrossRef]
21. Balmes, J.R.; Arjomandi, M.; Bromberg, P.A.; Costantini, M.G.; Dagincourt, N.; Hazucha, M.J.; Hollenbeck-Pringle, D.; Rich, D.Q.; Stark, P.; Frampton, M.W. Ozone effects on blood markers of systemic inflammation, oxidative stress, endothelial function, and thrombosis: The multicenter ozone study in older subjects. *PLoS ONE* **2019**, *14*, e0222601. [CrossRef] [PubMed]
22. Busquets-Cortés, C.; Capó, X.; Bibiloni, M.D.M.; Martorell, M.; Ferrer, M.D.; Argelich, E.; Bouzas, C.; Carreres, S.; Tur, J.A.; Pons, A.; et al. Peripheral blood mononuclear cells antioxidant adaptations to regular physical activity in elderly people. *Nutrients* **2018**, *10*, 1555. [CrossRef]
23. Liu, S.Z.; Valencia, A.P.; VanDoren, M.P.; Shankland, E.G.; Roshanravan, B.; Conley, K.E.; Marcinek, D. Astaxanthin supplementation enhances metabolic adaptation with aerobic training in the elderly. *J. Physiol. Rep.* **2021**, *9*, e14887. [CrossRef] [PubMed]
24. Valado, A.; Fortes, S.; Morais, M.; Barreira, R.; Figueiredo, J.P.; Caseiro, A. Impact of hydrotherapy an antioxidant enzyme activity in an elderly population. *Geriatrics* **2022**, *7*, 64. [CrossRef]
25. Żychowska, M.; Grzybkowska, A.; Zasada, M.; Piotrowska, A.; Dworakowska, D.; Czerwińska-Ledwig, O.; Pilch, W.; Antosiewicz, J. Effect of six weeks 1000 mg/day vitamin C supplementation and healthy training in elderly women on genes expression associated with the immune response-a randomized controlled trial. *J. Int. Soc. Sports Nutr.* **2021**, *18*, 19. [CrossRef] [PubMed]
26. Oggioni, C.; Jakovljevic, D.G.; Klonizakis, M.; Ashor, A.W.; Ruddock, A.; Ranchordas, M.; Williams, E.; Siervo, M. Dietary nitrate does not modify blood pressure and cardiac output at rest during exercise in older adults: A randomized cross-over study. *Int. J. Food Sci. Nutr.* **2018**, *69*, 74–83. [CrossRef] [PubMed]
27. Amirato, G.R.; Borges, J.O.; Marques, D.L.; Santos, J.M.B.; Santos, C.A.F.; Andrade, M.S.; Furtado, G.E.; Rossi, M.; Luis, L.N.; Zambonatto, R.F.; et al. L-glutamine supplementation enhances strength and power of knee muscles and improves glycemia control and plasma redox balance in exercising elderly women. *Nutrients* **2021**, *13*, 1025. [CrossRef]
28. Ton, A.M.M.; Campagnaro, B.P.; Alves, G.A.; Aires, R.; Côco, L.Z.; Arpini, C.M.; Guerra, E.; Oliveira, T.; Campos-Toimil, M.; Meyrelles, S.S.; et al. Oxidative stress and dementia in Alzheimer's patients: Effects of symbiotic supplementation. *Oxid. Med. Cell. Longev.* **2020**, *2020*, 2638703. [CrossRef] [PubMed]
29. Imai, A.; Oda, Y.; Ito, N.; Seki, S.; Nakagawa, K.; Miyazawa, T.; Ueda, F. Effects of dietary supplementation of asthaxanthin and sesamin on daily fatigue: A randomized, double-blind, placebo-controlled, two-way crossover study. *Nutrients* **2018**, *10*, 281. [CrossRef]
30. Ten Haaf, D.S.M.; Bongers, C.C.W.G.; Hulshof, H.G.; Eijsvogels, T.M.H.; Hopman, M.T.E. The impact of protein supplementation on exercise-induced muscle damage, soreness and fatigue following prolonged walking exercise in vital older adults: A randomized double-blind placebo-controlled trial. *Nutrients* **2020**, *12*, 1806. [CrossRef]
31. Aparicio-Ugarriza, R.; Díaz, Á.E.; Palacios, G.; Bibiloni, M.D.M.; Julibert, A.; Tur, J.A.; González-Gross, M. Association between blood marker analyses regarding physical fitness levels in Spanish older adults: A cross-sectional study from the PHYSMED project. *PLoS ONE* **2018**, *13*, e0206307. [CrossRef]
32. Yokoyama, K.; Yamada, Y.; Akamatsu, Y.; Yoshinaka, Y.; Yamamoto, A.; Koizumi, T.; Ohyama, K.; Suzuki, K.; Hashimoto, M.; Sato, H.; et al. Effects of capsinoids on daily physical activity, body composition and cold hypersensitivity in middle-age and older adults: A randomized study. *Nutrients* **2020**, *12*, 212. [CrossRef] [PubMed]
33. Munguia, L.; Rubio-Gayosso, I.; Ramirez-Sanchez, I.; Ortiz, A.; Hidalgo, I.; Gonzalez, C.; Meaney, E.; Villarreal, F.; Najera, N.; Ceballos, G. High flavonoid cocoa supplement ameliorates plasma oxidative stress and inflammation levels while improving mobility and quality of life in older subjects: A double-blind randomized clinical trial. *J. Gerontol. A Biol. Sci. Med. Sci.* **2019**, *74*, 1620–1627. [CrossRef] [PubMed]
34. Clark, D.O.; Xu, H.; Moser, L.; Adeoye, P.; Lin, A.W.; Tangney, C.C.; Risacher, S.L.; Saykin, A.J.; Considine, R.V.; Unverzagt, F.W. Mind food and speed of processing training in older adults with low education, the MINDSpeed Alzheimer's disease prevention pilor trial. *Contemp. Clin. Trials* **2019**, *84*, 105814. [CrossRef] [PubMed]
35. Kunz, H.E.; Michie, K.L.; Gries, K.J.; Zhang, X.; Ryan, Z.C.; Lanza, I.R. A randomized trial of the effects of dietary n3-PUFAs on skeletal muscle function and acute exercise response in healthy older adults. *Nutrients* **2022**, *14*, 3537. [CrossRef]
36. Gaitán, J.M.; Moon, H.Y.; Stremlau, M.; Dubal, D.B.; Cook, D.B.; Okonkwo, O.C.; van Praag, H. Effects of aerobic exercise training on systemic biomarkers and cognition in late middle-age adults at risk for Alzheimer's disease. *Front. Endocrinol.* **2021**, *12*, 660181. [CrossRef]
37. Vyas, C.M.; Ogata, S.; Reynolds, C.F., 3rd; Mischoulon, D.; Chang, G.; Cook, N.R.; Manson, J.E.; Crous-Bou, M.; De Vivo, I.; Okereke, O.I. Lifestyle and behavioral factors and mithocondrial DNA copy number in a diverse cohort of mid-life and older adults. *PLoS ONE* **2020**, *15*, e0237235. [CrossRef]

38. Batista, R.A.B.; de Branco, F.M.S.; Nehme, R.; de Oliveira, E.P.; Pena, G.D.G. Association between Plasma Omega-3 and Handgrip Strength According to Glycohemoglobin Levels in Older Adults: Results from NHANES 2011–2012. *Nutrients* **2022**, *14*, 4060. [CrossRef]
39. An, Y.; Feng, L.; Zhang, X.; Wang, Y.; Wang, Y.; Tao, L.; Qin, Z.; Xiao, R. Dietary intakes and biomarker patterns of folate, vitamin B_6 and vitamin B_{12} can be associated with cognitive impairment by hypermethylation of redox-related genes NUDT15 and TXNRD1. *Clin. Epigenetics* **2019**, *11*, 139. [CrossRef]
40. Malek Rivan, N.F.; Shahar, S.; Rajab, N.F.; Singh, D.K.A.; Din, N.C.; Hazlina, M.; Hamid, T.A. Cognitive frailty among Malaysian older adults: Baseline findings from the LRGS TUA cohort study. *Clin. Interv. Aging* **2019**, *14*, 1343–1352. [CrossRef]
41. Pizzino, G.; Irrera, N.; Cucinotta, M.; Pallio, G.; Mannino, F.; Arcoraci, V.; Squadrito, F.; Altavilla, D.; Bitto, A. Oxidative stress: Harms and benefits for human health. *Oxid. Med. Cell. Longev.* **2017**, *2017*, 8416763. [CrossRef]
42. Lee, W.J.; Shin, Y.W.; Kim, D.E.; Kweon, M.H.; Kim, M. Effect of desalted Salicornia europaeaL. Ethanol extract (PM-EE) on the subjects complaining memory dysfunction without dementia: A 12 week, randomized, double-blind, placebo-controlled clinical trial. *Sci. Rep.* **2020**, *10*, 19914. [CrossRef] [PubMed]
43. Reid, S.N.S.; Ryu, J.K.; Kim, Y.; Jeon, B.H. The effects of fermented Laminaria japonica on short-term working memory and physical fitness in the elderly. *Evid. Based Complement. Alternat Med.* **2018**, *2018*, 8109621.
44. Hong, C.T.; Hu, C.J.; Lin, H.Y.; Wu, D. Effects of concomitant use of hydrogen water and photo biomodulation on Parkinson disease. *Medicine* **2021**, *100*, e24191. [CrossRef] [PubMed]
45. Coles, L.D.; Tuite, P.J.; Öz, G.; Mishra, U.R.; Kartha, R.V.; Sullivan, K.M.; Cloyd, J.C.; Terpstra, M. Repeated-dose oral N-acetylcysteine in Parkinson disease: Pharmacokinetics and effect on brain glutathione and oxidative stress. *J. Clin. Pharmacol.* **2018**, *58*, 158–167. [CrossRef]
46. Gibson, G.E.; Luchsinger, J.A.; Cirio, R.; Chen, H.; Franchino-Elder, J.; Hirsch, J.A.; Bettendorff, L.; Chen, Z.; Flowers, S.A.; Gerber, L.M.; et al. Benfotiamine and cognitive decline in Alzheimer's disease: Results of a randomized placebo-controlled phase IIa clinical trial. *J. Alzheimers. Dis.* **2020**, *78*, 989–1010. [CrossRef] [PubMed]
47. Schneider, L.S.; Geffen, Y.; Rabinowitz, J.; Thomas, R.G.; Schmidt, R.; Ropele, S.; Weinstock, M. Low-dose ladostigil for mild cognitive impairment. Ladostigil Study Group. *Neurology* **2019**, *93*, 1474–1484. [CrossRef]
48. Al Ali, M.; Alqubaisy, M.; Aljaafari, M.N.; Al Ali, A.O.; Baqais, L.; Molouki, A.; Abushelaibi, A.; Lai, K.S.; Lim, S.H.E. Nutraceuticals: Transformation of conventional foods into health promoters/disease preventers and safety considerations. *Molecules* **2021**, *26*, 2540. [CrossRef]
49. Daimiel, L.; Martínez-González, M.A.; Corella, D.; Salas-Salvadó, J.; Schröder, H.; Vioque, J.; Romaguera, D.; Martínez, J.A.; Wärnberg, J.; Lopez-Miranda, J.; et al. Physical fitness and physical activity association with cognitive function and quality of life: Baseline cross-sectional analysis of the PREDIMED-Plus trial. *Sci. Rep.* **2020**, *10*, 3472. [CrossRef]
50. Netz, Y.; Ben-Zaken, S.; Zeev, A.; Dunsky, A. Correlates of Early-Stage Frailty-Sleep, Fitness, Oxidative Stress, and BMI. *Front. Med.* **2021**, *7*, 594710. [CrossRef]
51. Silva, L.A.D.; Tortelli, L.; Motta, J.; Menguer, L.; Mariano, S.; Tasca, G.; Silveira, G.B.; Pinho, R.A.; Silveira, P.C.L. Effects of aquatic exercise on mental health, functional autonomy and oxidative stress in depressed elderly individuals: A randomized clinical trial. *Clinics* **2019**, *74*, e322. [CrossRef] [PubMed]
52. Takahashi, M.; Lim, P.J.; Tsubosaka, M.; Kim, H.K.; Miyashita, M.; Suzuki, K.; Tan, E.L.; Shibata, S. Effects of increased daily physical activity on mental health biomarkers in postmenopausal women. *J. Phys. Ther. Sci.* **2019**, *31*, 408–413. [CrossRef]
53. You, Y.X.; Shahar, S.; Rajab, N.F.; Haron, H.; Yahya, H.M.; Mohamad, M.; Din, N.C.; Maskat, M.Y. Effects of 12 weeks Cosmos caudatus supplement among older adults mild cognitive impairment: A randomized double-blind and placebo-controlled trial. *Nutrients* **2021**, *13*, 434. [CrossRef]
54. Yoritaka, A.; Kobayashi, Y.; Hayashi, T.; Saiki, S.; Hattori, N. Randomized double-blind placebo-controlled trial of hydrogen in halation for Parkinson's disease: A pilot study. *Neurol. Sci.* **2021**, *42*, 4767–4770. [CrossRef]
55. Zaenker, P.; Favret, F.; Lonsdorfer, E.; Muff, G.; de Seze, J.; Isner-Horobeti, M.E. High-intensity interval training combined with resistance training improves physiological capacities, strength and quality of life in multiple sclerosis patients: A pilot study. *Eur. J. Phys. Rehabil. Med.* **2018**, *54*, 58–67. [CrossRef] [PubMed]
56. Yoon, J.; Isoda, H.; Okura, T. Evaluation of beneficial effect of a dual-task exercise based on Japanese traditional games in older adults: A pilot study. *Aging* **2020**, *12*, 18957–18969. [CrossRef] [PubMed]

antioxidants

MDPI

Review

Green Tea Catechins as Therapeutic Antioxidants for Glaucoma Treatment

Tsz Kin Ng [1,2,†], Kai On Chu [2,3,†], Chi Chiu Wang [3] and Chi Pui Pang [1,2,*]

[1] Joint Shantou International Eye Center of Shantou University and The Chinese University of Hong Kong, Shantou 515041, China; micntk@hotmail.com
[2] Department of Ophthalmology and Visual Sciences, The Chinese University of Hong Kong, Hong Kong
[3] Department of Obstetrics and Gynaecology, The Chinese University of Hong Kong, Hong Kong
* Correspondence: cppang@cuhk.edu.hk; Tel./Fax: +86-0754-88393560
† These authors contributed equally to this work.

Abstract: Glaucoma is the leading cause of irreversible blindness and visual impairment, affecting more than 80 million individuals worldwide. Oxidative stress and inflammation-induced neurodegenerative insults to retinal ganglion cells are the main pathogenesis of glaucoma. Retinal ganglion cells, the retinal neurons transmitting the visual signals to the visual cortex in the brain, have very limited regeneration or recovery capacity after damages. Apart from intraocular pressure-lowering treatments, there is still no clinically effective treatment to rescue the degeneration of retinal ganglion cells in glaucoma. Dietary antioxidants are easily accessible and can be applied as supplements assisting in the clinical treatments. Catechins, a chemical family of flavonoids, are the phenolic compounds found in many plants, especially in green tea. The anti-oxidative and anti-inflammatory properties of green tea catechins in vitro and in vivo have been well proven. They could be a potential treatment ameliorating retinal ganglion cell degeneration in glaucoma. In this review, the chemistry, pharmacokinetics, and therapeutic properties of green tea catechins were summarized. Research updates on the biological effects of green tea catechins in cellular and animal experimental glaucoma models were reviewed. In addition, clinical potentials of green tea catechins for glaucoma treatment were also highlighted.

Keywords: green tea; EGCG; glaucoma; retinal ganglion cells; anti-oxidation; anti-inflammation

Citation: Ng, T.K.; Chu, K.O.; Wang, C.C.; Pang, C.P. Green Tea Catechins as Therapeutic Antioxidants for Glaucoma Treatment. *Antioxidants* **2023**, *12*, 1320. https://doi.org/10.3390/antiox12071320

Academic Editor: Wonkyu Ju

Received: 5 May 2023
Revised: 2 June 2023
Accepted: 9 June 2023
Published: 21 June 2023

1. Green Tea Catechins: Chemistry and Pharmacokinetics

1.1. Chemistry of Green Tea Constituents

Tea is the most commonly consumed beverage worldwide. It comes from the leaves of the tea plant, *Camellia sinensis*. Different harvesting, manufacturing, and fermentation processes result in different types of tea, such as white, black, green, or oolong tea. Green tea is obtained by steaming and roasting fresh tea leaves under strictly controlled conditions so as to preserve the polyphenols from oxidation by polyphenol oxidase. Many constituents are present in the green tea infusion, including polyphenol polymers, amino acids, polysaccharides, saponins, alkaloids, and polyphenols (Figure 1). The compositions depend on the *Camellia* species, harvesting process, storage conditions, and processing methods. Polyphenol polymers, including theaflavins, thearubigins, and proanthocyanidin polymers, are oxidized and polymerized products of catechins monomers. Their anti-inflammatory and hepato-protective properties have been reported in experimental rodent models [1,2]. The concentrations of polyphenol polymers, theaflavins, and thearubigins are about 3–6% in green tea, 12–18% in black tea, and 8 to 20% of catechins in oolong tea, respectively. Amongst the tea amino acids, L-theanine is known to possess relaxation and cognitive improvement properties for humans [3]. Polysaccharides of glucose, galactose, rhamnose, and arabinose in tea are conjugated with different chemical groups resulting in diversified biological activities, including anti-oxidative and anti-diabetic activities [4,5].

Tea saponins, the natural non-ionic surfactants extracted from the aqueous layer, have displayed anticancer, antimicrobial, and cardiovascular protective properties in animal studies [6]. Benefits to human have also been shown [7]. Tea alkaloids, including caffeine, theobromine, and theophylline could improve cognition with antioxidative, anti-diabetic, and anti-obesity effects according to animal studies [8,9]. Polyphenols in tea have been the most extensively studied among the tea constituents due to their strong biological activity and high abundance [10]. Polyphenols in green tea are mainly flavonoids. Based on their nuclear structures, green tea flavonoids can be classified into flavanones, isoflavanones, flavones, flavonols, flavan-3-ols (catechins), and hydroxycinnamic acid. Amongst the polyphenols, catechins (flavan-3-ols) possess the most beneficial biomedical properties for human health [11]. The main catechins in green tea are as follows: (+)-catechin (C), (−)-epicatechin (EC), (−)-gallocatechin (GC), (−)-epigallocatechin (EGC), and their gallate derivatives, (−)-catechin-3-gallate (CG), (−)-epicatechin-3-gallate (ECG), gallocatechin-3-gallate (GCG), and (−)-epigallocatechin-3-gallate (EGCG), respectively (Figure 1). The flavan-3-ol concentration is about 50% in green tea and 10% in black tea, respectively.

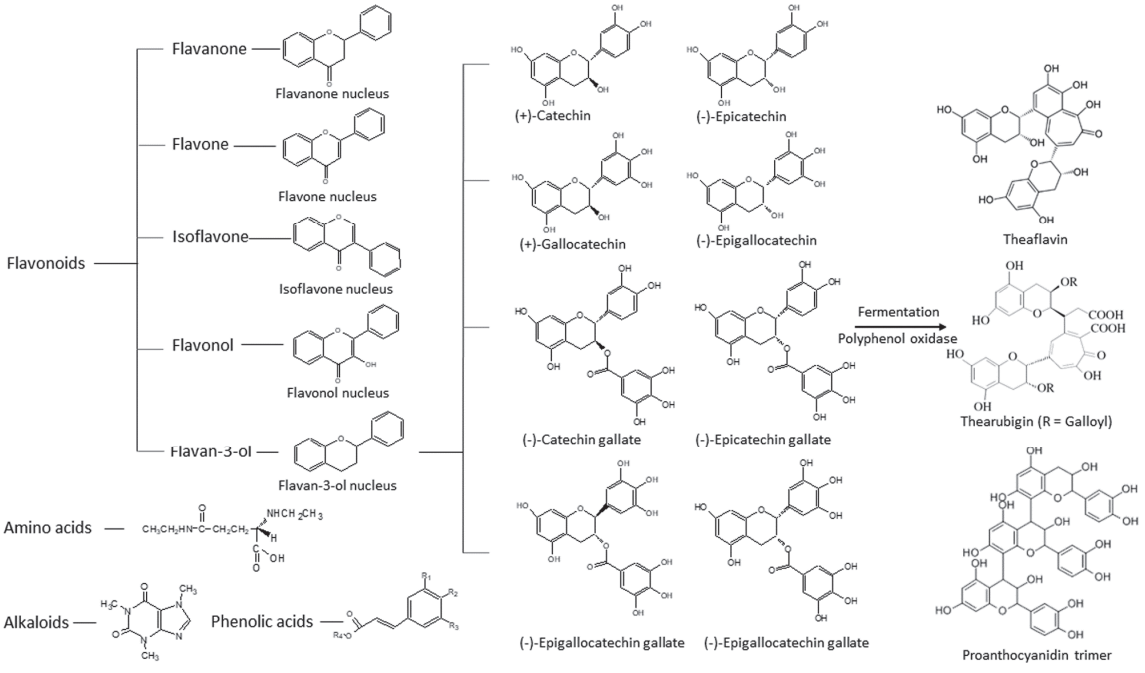

Figure 1. Structures of polyphenols, amino acids, and alkaloids that are present in green tea.

EGCG is the most abundant and biologically active catechin with proven health-promoting properties [12,13]. Its biochemical activities are attributed to its structural moiety and hydroxyl groups [14]. EGCG has eight hydroxyl groups that contribute hydrogen radicals to reactive oxygen species and form stable resonance structures (Figure 2). Unlike the other flavonoids of green tea polyphenols, the pro-oxidant activity of catechins is relatively low as they do not have any double bonds in C2–C3, nor any ketone groups in C4 to form further resonance structures in the C ring [15]. Therefore, catechins can cross-link with each other to form stable polymers, such as thearubin [16]. Consequently, catechins are lower in toxicity compared toother tea polyphenols.

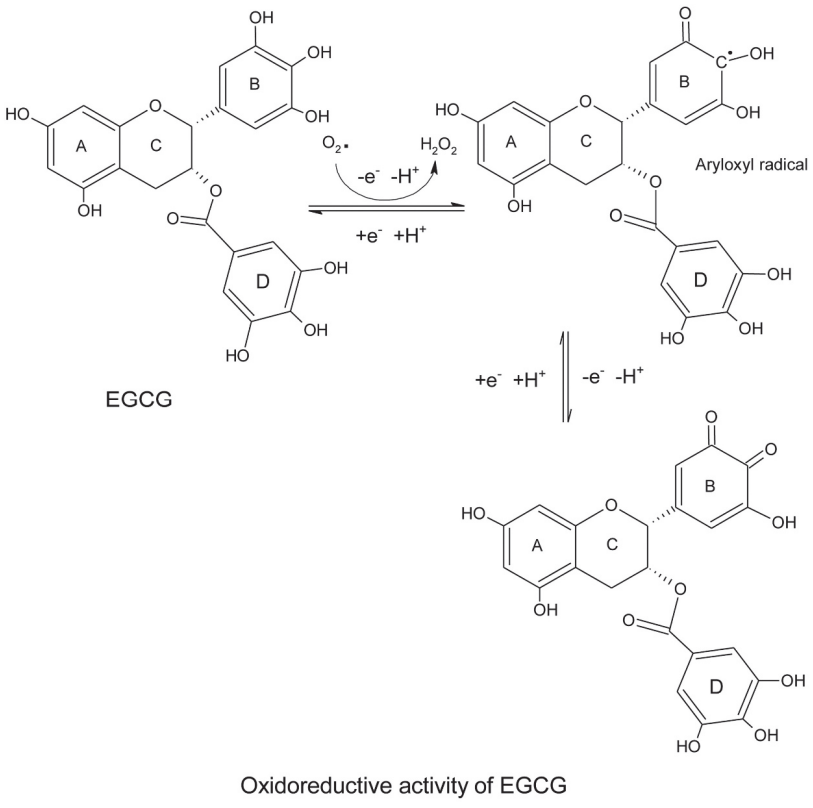

Figure 2. Resonance structures of epigallocatechin-3-gallate after reaction with reactive oxygen species.

The standard reduction potential (E°) is correlated to the cellular antioxidant activity (CAA). Green tea catechins all have a lower reduction potential than the endogenous antioxidant glutathione (GSH), thereby being indicative of a higher antioxidant activity. GSH (0.310 V) < C (0.281 V) = EGC (0.287 V) < EC (0.277 V) < EGCG (0.104 V) < ECG (0.098 V) [17].

Besides its intrinsic antioxidative properties, the anti-inflammatory and antioxidative activities of EGCG have been attributed to its interaction with the cellular membrane protein receptor (Figure 3). It binds to 67 kDa laminin receptors (67 LR) to upregulate the Toll-interacting protein (Tollip). Increased Tollip expression induces negative effects of inflammatory associated Toll-like receptor (TLR) signaling, leading to the deactivation of the NF-kB and MAPK pathways, which act on anti-oxidant response elements (AREs) in the nucleus for both anti-inflammatory and anti-oxidant responses [18]. The subsequent lowering of inflammatory mediators, such as inducible nitric oxide synthetase (iNOS) decreases the production of reactive oxidative species. As the EGCG molecule possesses multiple hydroxyl groups, it is potent in binding through hydrogen bonding with amino acid residues including serine and tyrosine on the active sites of the membrane receptor to change the structural conformation and exert various signaling and biological activities. It interacts with the serine residue at the N-terminal domain of tumor suppressor p53, which is a sensor of oxidative stress, to change the structural conformation and inhibit the ubiquitination of p53 by murine double minute 2 (MDM2). The stabilized p53 can thus be retained for anti-tumor activities [19]. The pleiotropic effects of EGCG have also been attributed to its multiple binding properties. It can moderate the redox, inflammation, and cell cycle status through its multiple receptor affinities. It activates the epidermal growth factor (EGF) receptor in the absence of EGF but inhibits EGF-induced EGF receptor

activation by affecting the topology of the EGF receptor transmembrane domain [20]. EGCG can also inhibit the activation of the wild-type and some mutants of the EGF receptor in non-small cell lung cancer cell lines [21].

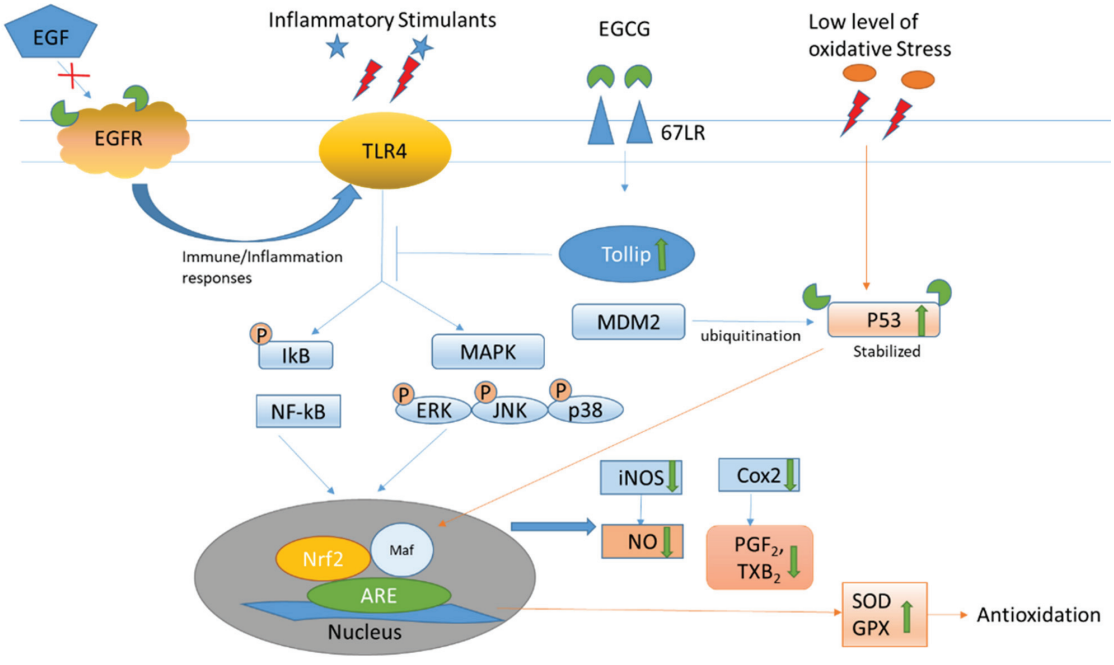

Figure 3. Epigallocatechin-3-gallate interacts with various receptor/mediators to relieve inflammation and oxidation. The green arrow indicates the effects of EGCG on the oxidative stress.

Apart from binding to specific receptors, such as to 67LR for anti-inflammation, pro-oxidation of catechins generate reactive oxygen species (ROS) to act as secondary messengers to stimulate various signaling pathways, which may be mediated by receptors from the cell surface to the nucleus. For example, EGCG can bind to the active sites of thioredoxin (Trx) to inhibit the Trx/Trx receptor, which facilitates anti-oxidation to increase the ROS level [22]. ROS in turn can serve as an anti-bacterial agent [23]. EGCG activates calcium/calmodulin-dependent protein kinase β (CaMKKβ) to increase energy metabolism and elevate cytosolic calcium levels, thereby contributing to increase NO production [24]. It increases cyclic adenosine 5′ monophosphate (cAMP) in endothelial cells and platelets to promote the phosphorylation of eNOS and vasodilator=stimulated phosphoprotein [25] to cause vaso-relaxation [26]. Furthermore, it activates adenosine 5′ monophosphate-activated protein kinase (AMPK), which reduces endothelin-1 expression [27,28] to improve vasodilation [29] (Table 1).

Table 1. Summary of the biological properties of green tea catechins.

Biological Properties	Mechanisms	References
(1) Pro-oxidation	Electron resonance within the phenolic moiety following abstraction of proton by ROS.	[15,16]
(2) Antioxidation/-reduction	High reduction potential of catechins compared to endogenous antioxidants; reducing and recycling the oxidized endogenous molecules.	[17]
(3) Anti-inflammation	Binding to 67LR to increase Tollip expression, which negatively regulates TLR signaling to suppress inflammatory mediators.	[18]
(4) Anti-tumor, antioxidation, and anti-inflammation	Binding to the active sites of p53 and changing the structural conformation to prevent ubiquitination by MDM2; retaining the biological level and activities of p53. Inhibiting the activation of the wild-type and some mutant EGF receptors in non-small cell lung cancer cell lines.	[19,21]
(5) Moderate redox, inflammation, and cell cycle	Binding to the EGF receptor to change the topology and block EGF to activate the receptor for subsequent inflammation activities.	[20]
(6) Generation of secondary messengers for vasodilation	Inhibiting anti-oxidative molecules, including the Trx/Trx receptor to increase ROS, which acts as a secondary messenger for various pathways Activating CaMKKβ to increase energy metabolism; elevating cytosolic calcium to increase nitric oxide production. Increasing cAMP to promote the phosphorylation of eNOS and vasodilator-stimulated phosphoprotein to cause vaso-relaxation. Activating AMPK to reduce endothelin-1 expression for vasodilation.	[22,24–29]

67 LR: 67 kDa laminin receptors; AMPK: adenosine 5′ monophosphate-activated protein kinase; cAMP: cyclic adenosine 5′ monophosphate; CaMKKβ: calcium/calmodulin-dependent protein kinase beta; EGF: epidermal growth factor; eNOS: endothelial nitric oxide synthetase; MDM2: murine double minute 2; ROS: reactive oxygen species; TLR: Toll-like receptor; Tollip: Toll-interacting protein; and Trx: thioredoxin.

1.2. Pharmacokinetics of Catechins in the Eye

Following oral administration, tea catechins are first absorbed by the small intestine, where they are conjugated with glucuronic acid, sulfate, or O-methylation before passing to the liver tissue cells for metabolism. Excess catechins are either secreted with the bile into the small intestine for the enterohepatic recirculation or pass into the colon for degradation by the resident microorganisms. The catabolites are either reabsorbed into plasma and excreted into the urine or passed out through the feces. The catechins, conjugates, and catabolites are distributed to various organs and tissues to exert various biological activities. As the bioavailability of catechins depends on its absorption and metabolism, the extensive metabolic processes render the levels of catechins to be very low, which is a limitation for antioxidative treatment.

The absorption efficiency of the catechins depends on the physicochemical properties, including molecular size, steric configuration, solubility, hydrophilicity, pKa, the presence of galloylated derivatives, and the presence of food matrix [30]. As the absorption involves efflux transporters, such as multidrug resistance-associated protein 2 (MRP2) in the small intestine [31], this results in a low bioavailability [32,33] and variability of the absorption rate. Co-administration of food and drugs can interact with the absorption of catechins [34]. The maximum plasma levels of free EGCG and EGC can increase more than 3.5-fold in the fasting condition [35]. When food is co-administrated with catechins, the time of maximum concentration (T_{max}) of catechins would be prolonged for two times due to the gastric emptying rate slowing down. This rendered the maximum concentration (C_{max}) of catechins to decrease by 3.5 times with breakfast. However, when catechins were co-

administrated with carbohydrates, the oral bioavailability (AUC) of flavanol was found to have increased by 140% [36], which was deemed to be possible by suppressing the intestinal efflux and stabilizing the catechins in the lumen.

Catechin absorption is sterically and structurally dependent [37]. The levels of epi-isomers are higher than its enantiomers, EGC > GC, EC > C, and EGCG > GCG, respectively in the plasma of SD rats after oral administration. The plasma levels of non-gallated catechins, including EGC, GC, EC, and C, are higher than the gallated catechins, EGCG, GCG, and ECG. However, when green tea extract (GTE), with a higher proportion of EGCG is administered, the relative AUC of C was higher than that of EC, suggesting an unknown interaction between C and EGCG during absorption [38]. Although EGCG is a dominant component of green tea extract, its relative AUC level is low, indicating that the absorption ability of EGCG is poor.

After a single dose administration of 550 mg/kg GTE into the SD rats, the ingested catechins are distributed across various ocular tissues, including aqueous humor, vitreous humor, choroid–sclera, retina, lens, and the cornea (Figure 4) [37]. The C_{max} of GC and ECG can reach a hundred micromolar levels in the choroid–sclera and retina, but only 1.5 μM in the lens, respectively (Table 2). These were the effective doses used in many in vitro studies. GTE can exert antioxidative, anti-inflammatory, and anti-apoptotic effects on the ocular tissues, especially for the retina [37–39]. Steric selectivity of distribution was also found in different ocular compartments. Vitreous humor was selective to non-epimer catechins but did not show a preference to the non-gallate derivatives preference as the plasma. Other ocular tissues did not show any steric and structural specificity except for the finding that GC was dominated. Catechins could also pass into various fetal tissues, including the eye [40]. However, the C_{max} levels of catechins were at the nanomolar level which may not be biologically effective. On the other hand, the C_{max} of EGCG in the fetal eye could reach to 0.83 μM which may therefore affect or benefit various tissue developments.

Catechins are mainly eliminated through urine and biliary excretion. More water-soluble non-gallated catechin derivatives, such as parent and conjugated compounds are mainly excreted in the urine, while major gallated catechins, which are less water-soluble, are excreted through the bile to the colon. A few epi- or gallocatechin-O-sulfate conjugates, but not the gallated catechin conjugates from ECG and EGCG, have been found in the urine [41]. This suggests that the gallated derivatives that undergo phase II metabolism are minimal. The levels of flavan-3-ol metabolites, mainly from (−)-epigallocatechin and (+)-gallocatechin, excreted into urine was calculated to be about 8.1–28.5% of the intake [42]. EGCG was excreted through the bile and eliminated through the feces but not through the kidneys [43], possibly due to the hydrophobic gallated catechins bound to plasma protein that limited renal excretion as a result [44,45].

The elimination rates of catechins in the ocular tissues were found to be higher than in the humors and plasma of SD rats [38]. The elimination rate of GC was from 0.2 h^{-1} to 2.4 h^{-1} in the retina, whereas the elimination rate of ECG in the vitreous humor was 0.04 to 0.2, respectively. On the other hand, the EGCG level can affect the elimination rates of other catechins in the ocular tissues (Table 2). Doubling the level of EGCG present can lower the elimination rates of other catechins, particularly in the retina, and aqueous and vitreous humors (Figure 4) [39]. Some active elimination or metabolic mechanisms, which can be affected by EGCG, could also arise in the ocular tissues. This mechanism could be associated with aqueous and vitreous humor elimination.

The elimination rates of catechins in the maternal plasma were faster than the fetal tissue. The elimination rates of GC and EC were 0.26 and 0.3 h^{-1} for the maternal plasma and 0.08 and 0.1 h^{-1} for the fetal kidney, respectively [41]. The fetal organs were not well developed for the elimination process. Similarly, the levels of GC and EGCG in the fetal eye were sustained at relative high levels (about 50 ρmol/g) without an apparent elimination during the studying period, while the elimination rate of EC was very slow ($0.06 \pm 0.06\ h^{-1}$). It has been suggested that catechins can perfuse into the fetal eye and remain there for a long time.

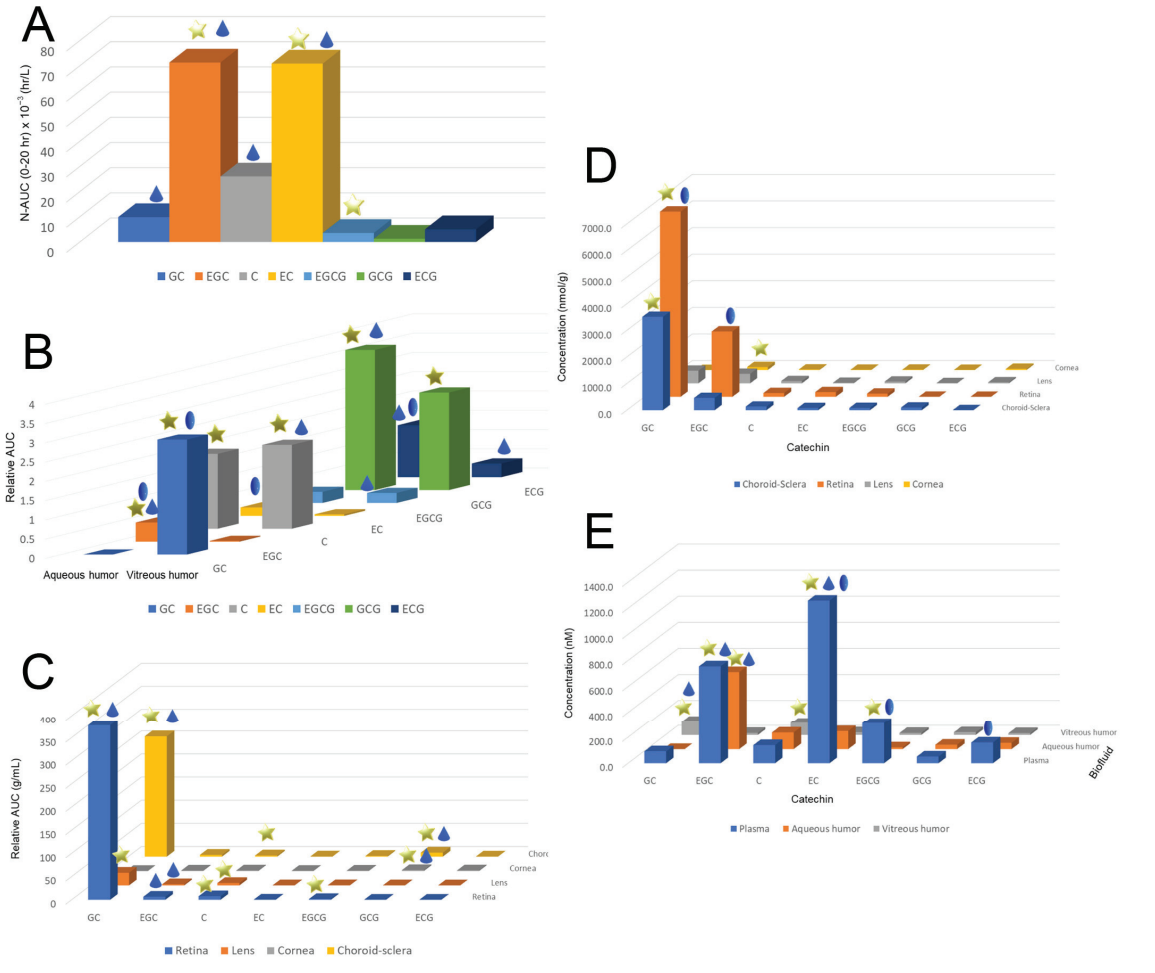

Figure 4. The exposure level, maximum concentration, and elimination of total catechins in the plasma, ocular fluid, and tissues of Sprague–Dawley rats. (**A**) Relative area under the curve (AUC) levels of different catechins in the plasma after normalization by the corresponding input catechin dose in the GTE. Non-gallated levels were higher than of the gallated derivatives while epimers were higher than the non-epimers. (**B**) Relative AUC levels of catechins in vitreous and aqueous humor. Vitreous humor was selective to non-epimer but showed no selectivity on gallated and non-gallated catechins. No particular trend of catechin selectivity appeared in the aqueous humor. (**C**) Relative AUC levels of catechins in the retina, lens, cornea, and choroid–sclera. (**D**) Maximum concentration of catechins in the plasma, aqueous and vitreous humors, and (**E**) eye tissues after a single dose of 550 mg/kg of Sunphenon DCF-1 green tea extract administrated orally to rats. Star: the level of an epimer was significantly higher than the corresponding non-epimer or vice versa in the same ocular compartment ($p < 0.05$); Droplet: the level of a catechin was higher than the corresponding gallate derivative or vice versa in the same compartment; Oval: the level of one of the catechins was significantly higher in one compartment than the other compartment ($p < 0.05$). GC: (−)-gallocatechin; EGC: (−)-epigallocatechin; C: (+)-catechin; EC: (−)-epicatechin; EGCG: (−)-epigallocatechin-3-gallate; GCG: gallocatechin-3-gallate; and ECG: (−)-epicatechin-3-gallate.

Table 2. Pharmacokinetics of the catechins of different green tea extracts in different ocular compartments.

Maximum Concentration	GTE	GC	EGC	C	EC	EGCG	GCG	ECG
C_{max} (nM)								
Plasma	Sunphenon DCF-1	91.5 ± 57.4	754.9 ± 235.8	139.0 ± 57.0	1258.4 ± 294.0	310.4 ± 59.9	50.8 ± 10.4	159.1 ± 33.9
	Theaphenon® E	530.8 ± 200.2	13718.0 ± 4948.0	2990.0 ± 1990.0	9143.0 ± 1912.0	6687.0 ± 4437.0	131.3 ± 91.7	443.8 ± 352.3
Aqueous humor	Sunphenon DCF-1	-	602.9 ± 116.7	127.4 ± 62.8	138.9 ± 58.5	13.2 ± 5.1	33.5 ± 20.4	47.8 ± 8.1
	Theaphenon® E	246.9 ± 34.9	911.3 ± 250.5	98.3 ± 19.2	708.1 ± 127.8	284.4 ± 58.4	0.57 ± 0.98	26.5 ± 10.3
Vitreous humor	Sunphenon DCF-1	110.6 ± 22.1	15.9 ± 7.0	96.5 ± 23.3	20.5 ± 10.6	15.4 ± 2.7	20.9 ± 9.9	14.0 ± 5.1
	Theaphenon® E	4492.0 ± 443.5	404.1 ± 102.5	321.7 ± 69.5	436.8 ± 102.5	2224.4 ± 805.4	33.9 ± 31.0	369.6 ± 74.0
C_{max} (ρmol/g)								
Choroid–sclera	Sunphenon DCF-1	11461.8 ± 5168.7	1506.3 ± 941.1	477.6 ± 346.9	283.5 ± 66.5	184.4 ± 39.0	220.5 ± 69.7	10.7 ± 4.3
	Theaphenon® E	188.28 ± 111.3	542.2 ± 335.1	294.7 ± 32.8	1818.0 ± 563.0	1183.0 ± 611.0	59.0 ± 54.8	518.0 ± 292.0
Retina	Sunphenon DCF-1	22729.4 ± 4229.4	8020.8 ± 1658.5	492.7 ± 235.2	608.0 ± 112.0	259.1 ± 67.2	3.2 ± 1.9	-
	Theaphenon® E	61.0 ± 43.5	118.2 ± 55.6	35.7 ± 15.0	174.5 ± 45.8	784.4 ± 195.9	59.0 ± 54.8	64.0 ± 16.0
Lens	Sunphenon DCF-1	1558.1 ± 318.4	1172.3 ± 207.8	300.0 ± 151.5	72.3 ± 19.1	149.1 ± 26.5	18.0 ± 6.6	90.3 ± 45.8
	Theaphenon® E	1.9 ± 3.0	10.9 ± 8.9	4.1 ± 4.8	4.6 ± 6.9	43.9 ± 25.8	0.4 ± 0.6	1.0 ± 3.0
Cornea	Sunphenon DCF-1	-	359.4 ± 66.8	58.5 ± 15.4	30.6 ± 5.7	25.2 ± 15.5	10.7 ± 3.9	91.1 ± 18.7
	Theaphenon® E	10.8 ± 16.7	59.5 ± 26.7	61.7 ± 17.5	536.4 ± 61.1	634.6 ± 122.9	18.8 ± 24.2	101.8 ± 43.1
Elimination	**GTE**	**GC**	**EGC**	**C**	**EC**	**EGCG**	**GCG**	**ECG**
λz (h^{-1})								
Plasma	Sunphenon DCF-1	0.107 ± 0.010	0.213 ± 0.015	0.104 ± 0.038	0.371 ± 0.000	0.236 ± 0.007	0.171 ± 0.013	0.211 ± 0.010
	Theaphenon® E	0.270 ± 0.030	0.390 ± 0.040	0.370 ± 0.080	0.400 ± 0.050	0.230 ± 0.020	1.250 ± 0.380	0.210 ± 0.040
Aqueous humor	Sunphenon DCF-1	-	0.045 ± 0.001	0.209 ± 0.012	0.093 ± 0.062	0.304 ± 0.012	0.111 ± 0.033	0.124 ± 0.043
	Theaphenon® E	0.110 ± 0.020	0.240 ± 0.020	0.130 ± 0.030	0.210 ± 0.040	0.090 ± 0.020	-	0.130 ± 0.120

Table 2. *Cont.*

Vitreous humor	Sunphenon DCF-1	0.166 ± 0.010	0.041 ± 0.001	0.106 ± 0.030	0.067 ± 0.004	0.058 ± 0.012	0.042 ± 0.006	0.224 ± 0.035
	Theaphenon® E	0.020 ± 0.010	0.110 ± 0.090	0.110 ± 0.060	0.100 ± 0.030	0.080 ± 0.020	-	-
Choroid–sclera	Sunphenon DCF-1	0.057 ± 0.001	0.461 ± 0.015	0.220 ± 0.014	0.488 ± 0.007	0.267 ± 0.019	0.929 ± 0.049	-
	Theaphenon® E	-	0.250 ± 0.090	0.220 ± 0.090	0.370 ± 0.060	0.080 ± 0.040	-	0.150 ± 0.070
Retina	Sunphenon DCF-1	0.188 ± 0.045	0.203 ± 0.050	0.245 ± 0.010	2.432 ± 0.154	0.413 ± 0.040	-	-
	Theaphenon® E	-	0.040 ± 0.030	0.040 ± 0.010	0.060 ± 0.020	0.040 ± 0.020	-	0.090 ± 0.030
Lens	Sunphenon DCF-1	0.302 ± 0.049	0.084 ± 0.020	0.234 ± 0.032	0.049 ± 0.004	0.269 ± 0.011	3.160 ± 0.130	-
	Theaphenon® E	-	-	-	-	0.130 ± 0.060	-	-
Cornea	Sunphenon DCF-1	-	0.170 ± 0.031	0.116 ± 0.007	0.043 ± 0.012	0.125 ± 0.001	0.372 ± 0.006	0.477 ± 0.021
	Theaphenon® E	-	-	0.220 ± 0.100	0.220 ± 0.100	0.090 ± 0.020	-	0.100 ± 0.090

GTE: green tea extract; GC: (−)-gallocatechin; EGC: (−)-epigallocatechin; C: (+)-catechin; EC: (−)-epicatechin; EGCG: (−)-epigallocatechin-3-gallate; GCG: gallocatechin-3-gallate; and ECG: (−)-epicatechin-3-gallate.

Steric structures of catechins also affect the metabolism [46]. Equal quantities of (−)-EC, (−)-C, (+)-EC, and (+)-C fed to human males resulted in different bioavailabilities. Different levels of stereoisomers, including (−)-EC > (+)-EC > (+)-C > (−)-C, non-methylated conjugations, and 3′- and 4′-*O*-methylation of epimers were found in the plasma and urine. Also, the conjugation of gallate derivatives, including ECG and EGCG, were not found in the plasma and urine [47], which was deemed to probably be due to the inhibition of phase II enzymes by the gallated moiety of the catechins. The extensive metabolism and enzymatic resistance of some conjugates, including sulphates during sample processing can lead to large variations in pharmacokinetics [37].

2. Therapeutic Properties of Green Tea Catechins: Antioxidation and Anti-Inflammation in the Eye

Polyphenols, especially catechins, are known for their beneficial effects for health maintenance, along with their therapeutic effects [48]. These effects have been attributed to the powerful anti-oxidative and inhibition of lipid peroxidation through the chelation of metal ions to prevent oxidation reactions [49], and the hydroxyl groups for free radical scavenging. Therefore, the scavenging power of galloylated catechins, such as (−)-EGC, are stronger than non-galloylated catechins such as (+)-C [50]. The gallate derivative, (−)-EGCG, has the strongest radical scavenging capacity amongst the catechins [51]. Moreover, owing to the possession of a vicinal diol in the B-ring galloyl moiety, and an ortho-hydroxyl group in the A-ring, catechins can chelate the catalytic metal ions to generate free radicals. Since the hydroxyl groups in the catechins are essential for antioxidation, methylation can subsequently reduce the anti-oxidation power.

In addition to the radical scavenging process, catechins and their conjugates can cover or even incorporate themselves into the lipid membrane bilayer externally and internally to block the access of free radicals and stabilize the membrane through decreased lipid fluidity [52]. EGCG interacts with both the hydrophobic and hydrophilic regions of the lipid bilayers to protect the membrane from attack by the hydrophilic and hydrophobic oxidants [53]. Meanwhile, polyphenols can also induce various endogenous molecular pathways to activate the expression of antioxidant enzymes and suppress the pro-oxidative pathways. Catechins can activate glutathione S-transferase and deactivate xanthine oxidase and nitric oxide synthase, respectively [54]. More recently, the oral administration of EGCG to rats has been shown to increase ascorbic acid levels and oxygen radical absorbance capacity in the plasma [55].

Whilst the anti-oxidative effects of catechins have been attributed as beneficial health effects, the pro-oxidative effects and the subsequent stimulation of the relevant signaling pathways may account for the in vivo protection mechanisms. EGCG can be oxidized to produce hydrogen peroxide in cell culture medium, but these cellular actions can be abolished by SOD and catalase [56]. The anti-tumor activity caused by hydrogen peroxide generated from the pyrogallol moiety can reduce Fe (III) to Fe (II), triggering ROS production [57,58]. In an in vivo study, GTE, EGCG, EGC, and gallic acid showed pro-oxidative effects in that they significantly reduced GSH from 33.3–43.3% and increased GSSG, methemoglobin, and plasma hemoglobin in GPD-deficient erythrocytes, which are vulnerable to oxidative stress [59]. However, pro-oxidation has usually been demonstrated under experimental conditions and non-physiologically high concentrations under in vitro studies [58]. The concentration of EGCG and metabolites present in vivo (1–2 μM) can produce low levels of intracellular ROS to promote signal transduction pathways [27,60]. Moreover, GTE containing a high concentration of EGCG could increase oxidative stress in the plasma, aqueous humor, vitreous humor, cornea, and retina in SD rats even under lower physiological levels (<1 μM in plasma); yet, the 8-isoprostane level was lower than half of the EGCG level. GTE with a high EGCG content was found to induce superoxide dismutase 1 and glutathione peroxidase-3 expression, but also suppressed catalase in the retina. These pro-oxidation effects can occur at physiological level and is influenced by

both chemical and biological activities of GTE, indicating that an optimal EGCG level is needed if GTE is used for health remedies [38].

The inhibition of inflammation was accompanied with the elevation of oxidative stress [61]. The increased ROS activates NF-κB and NF-E2-related factor 2 (Nrf2) to express the antioxidative factors HO-1 and glutathione [62]. In many antioxidative and anti-inflammatory studies, EGCG pre-treatment was required to protect against oxidative insult and inflammation induction [63]. We have proposed that the protective actions against oxidative stress and inflammation may be secondary to the induction of endogenous antioxidant proteins, as influenced by the pre-conditioned, pro-oxidative effects under physiological conditions [64].

Since EGCG can activate antioxidative nuclear translocation elements in the Nrf2/HO-1 pathway for both the antioxidative and anti-inflammatory responses, the antioxidation and anti-inflammation effects of catechins are always simultaneous as a result. In the retina of a rat model, GTE suppressed the activation of microglial cells, astrocytes, and Müller glia in a dose-dependent manner following lipopolysaccharide (LPS) induction. It also reduced the expression of the pro-inflammatory cytokines IL-1β, TNF-α, and IL-6 in the retina and vitreous humor through the suppression of the phosphorylation of STAT3 and NF-κB, and the binding of 67LR on the neurons and glia [65]. We also found similar ocular anti-inflammatory effects in the anterior chamber of the eye following LPS induction [39]. It ameliorated the expression of tumor necrosis factor-alpha (TNF-α), interleukin-6 (IL-6), and monocyte chemoattractant protein-1 (MCP-1) by CD43-positive leucocytes and CD68-positive macrophages and reduced the infiltration of leucocytes and macrophages into the iris and ciliary body. Our recent metabolomic analysis has shown that the ocular anti-inflammation caused by GTE was indirect through induced systemic phosphorylcholine lipids to suppress the inflammatory responses and alleviate the hepatic damage and mitochondrial stress [66]. Furthermore, GTE was able to attenuate uveitis on a murine model of experimental autoimmune uveoretinitis (EAU). It partially alleviated uveitis phenotypes and recovered visual function. GTE and EGCG are also able to down-regulate Th-17-associated pro-inflammatory genes, such as interleukin 1 beta (IL-1β), IL-6, IL-17A, and tumor necrosis factor-alpha (TNF-α) [67]. These findings provide evidence for the ocular anti-inflammatory effects of GTE and EGCG.

However, the bioavailability of EGCG is low, thereby limiting its capability for antioxidation and anti-inflammation treatments, especially for neural tissues and retina that are separated by various barriers. Nanotechnology may overcome such a limitation by a flavonoid-containing nanoparticle formulation [68]. EGCG-loaded liposomes enveloped with phosphatidylcholine or phosphatidylserine could improve the bioavailability. These liposomes attenuated LPS-induced pro-inflammatory cytokines and restored motor impairment in a Parkinsonian syndrome rat model, which was deemed to be possible through the inhibition of murine BV-2 microglial cells [69]. Meanwhile, EGCG has been per-acetylated as pro-EGCG to increase its tissue level and protect EGCG from oxidation before entering the cell [70]. Pro-EGCG is a potent anti-angiogenesis agent that acts against angiogenesis-dependent diseases, such as endometriosis [71]. In addition, the drug-delivery systems, such as encapsulation, can also be used to improve the stability and bioavailability of green tea catechins [72,73].

3. Pathophysiological Conditions in Glaucoma: Oxidative Stress and Inflammation

Glaucoma is a common and serious form of irreversible optic neuropathy, with abnormalities and dysfunction of the optic nerve estimated to affect over 100 million people by the year 2040 [74]. Glaucoma is characterized by the progressive loss of retinal ganglion cells (RGCs) and their axon, thinning of the retinal nerve fiber layer, cupping of the disc, and visual field defects [75]. The two major forms of glaucoma, primary open angle glaucoma (POAG) and primary angle closure glaucoma (PACG), are complex and multi-factorial in etiology involving genetic and environmental factors [76]. Risk factors for POAG include older age, elevated intraocular pressure (IOP), sub-Saharan African

ethnic origin, positive family history, and high myopia. PACG is affected by older age, hyperopia, and east Asian ethnic origin [77]. Treatments based on topical eye drops, laser therapy, and surgical intervention to lower IOP is a clinically proven approach to prevent glaucoma progression [78]. RGC loss could arise happen in some patients who present with a good control of IOP [79]. RGCs are responsible for transmitting image-forming and non-image forming visual information from the retina to the brain. After optic nerve injury, activation of apoptosis, autolysis, pyroptosis, and ferroptosis, together with the early downregulation of autophagy and phagocytosis, are the major modes of cell death involved in RGC death [80]. Besides the modes of cell death, oxidative stress and inflammation are the major pathophysiological conditions that are implicated in the pathogenesis of glaucoma [81,82].

Dysregulation in the ocular blood flow is another major pathological factor in glaucoma. Unstable ocular blood flow causes chronic and repeated mild reperfusion, which induces the peroxynitrite and superoxide production in the astrocytes and the mitochondria of the RGCs [83]. Signs of chronic oxidative stress have been reported in the retinas from glaucomatous donors with increased levels of oxidative by-products compared to the control donors [81]. Increases in the superoxide dismutase (SOD) and glutathione peroxidase (GPX) activities were found in the aqueous humor of POAG and PACG patients compared to the cataract patients, while the levels of vitamin C and vitamin E were found to be significantly lower in the aqueous humor of POAG and PACG [84]. Moreover, lower levels of reduced and total glutathione were also found in POAG patients as compared to the control subjects adjusted for age and sex [85]. A lower redox index was found in the POAG patients than the age-matched controls [86]. Additionally, the immunostaining for hypoxia-inducible factor-1α (HIF1A), which is tightly regulated by the cellular oxygen concentration, was found to be increased in the retina and optic nerve head of glaucomatous donor eyes compared to the control eyes. The retinal location of the increased immunostaining for HIF1A was closely concordant with the location of the visual field defects recorded in some of the glaucomatous eyes [87].

Retinal microglia, the resident yolk sac-derived macrophage cells in the retina, act as the first and key active immune defense in the central nervous system, constantly scavenging for plaques, damaged or unnecessary neurons and synapses, and infectious agents [88]. Microglia are extremely sensitive to pathological changes to prevent pathological damage, including glaucoma-related stress. Their intricate interactions affect the diverse outcomes of the microglia–RGC relationship as either being neurosupportive or neurodestructive in nature [89]. Histological studies on human specimens indicated the proliferation of microglia in the optic nerve head from human donors with advanced glaucoma, including the lamina cribrosa, along with the upregulation of immunomodulating (transforming growth factor (TGF)-β2 and prostaglandin E2) and pro-inflammatory mediators (tumor necrosis factor (TNF)-α and inducible nitric oxide synthase) [90]. Moreover, increased levels of pro-inflammatory cytokines (TNF-α, interleukin (IL)-1β, IL-6, IL-8, and interferon (IFN)-γ) [91] as well as inflammasome components (NOD-like receptor pyrin (NLRP)-3 and caspase-1) [92] were reported in human glaucomatous eyes/retinas. Our previous animal experiments also demonstrated that acute IOP elevation upregulates inflammation protein marker (IL-1β, TLR-4, and TNF-α) expression in the rat retina [93].

There is thus abundant evidence supporting oxidative stress and inflammation in glaucomatous retina (Figure 5). Accordingly, oxidative stress and inflammation in the retina should be targeted for treatments in order to ameliorate RGC death in glaucoma.

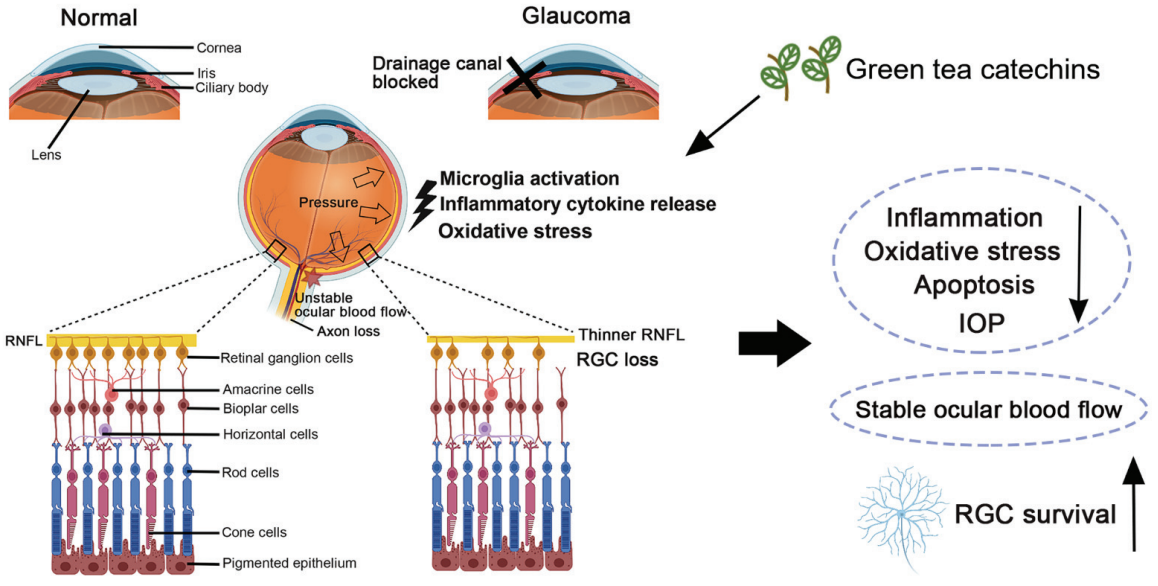

Figure 5. Pathophysiological conditions in glaucoma and the retinal ganglion cell protective effect of green tea catechins in glaucoma. RGC: retinal ganglion cell; and IOP: intraocular pressure.

4. Green Tea Catechins in Experimental Cellular Models of Glaucoma

Catechins attenuating oxidative stress and the inflammatory response could, in part, account for their neuroprotective capabilities [94]. To investigate the in vitro effect of green tea catechins, the primary culture of isolated RGCs [95], human stem cell-derived RGCs [96,97], and the retinal explant culture [98] have been used as glaucoma-related platforms on RGCs. However, these platforms have not been adopted to study the in vitro effects of green tea catechins on RGCs. Instead, a transformed mouse cell line, RGC-5 [99], was adopted in cellular studies, although this cell line later was characterized as the mouse SV-40 T antigen-transformed photoreceptor cell line, 661 W [100]. Earlier studies have demonstrated that 50 μM EGCG significantly reduces the apoptosis and ROS production in RGC-5 cells caused by 400 μM hydrogen peroxide [101]. Consistently, EGCG (2.5–10 μg/mL) was found to be able to improve the survival of RGC-5 cells upon hydrogen peroxide and ultraviolet radiation insults [102]. Moreover, EGCG (IC_{50}: 0.8 μM) was found to be able to attenuate the formation of thiobarbituric acid reactive substance formation, a measure of lipid peroxidation, as induced by 20 μM sodium nitroprusside in rat brain homogenates [103]. Similarly, an one-hour pretreatment of EGCG (50 μM) and epicatechin (EC; 50 μM) was able to attenuate rotenone-induced toxicity in RGC-5 cells and inhibit sodium nitroprusside-induced lipid peroxidation (EGCG IC_{50}: 2.5 μM; EC IC_{50}: 1.5 μM) [103]. EGCG at concentrations greater than 10 μg/mL has been proven to inhibit RGC-5 cell growth [102]. This is consistent with our previous study on green tea extract (Theaphenon E; ≥16.25 μg/mL) and EGCG (≥25 μM) attenuating cell proliferation and migration [104,105]. For immunomodulation, EGCG treatment can cause immunosuppressive alterations on human monocyte-derived dendritic cells by inducing cell apoptosis and suppressing cell surface molecules and antigen presentation [106]. Administration of EGCG can also increase IL-10 levels in cell culture supernatants [107].

5. Green Tea Catechins in Experimental Animal Models of Glaucoma

Green tea catechins are able to cross the blood-brain barrier [108]. Tea polyphenols can reduce oxidative stress and IOP and stabilize ocular blood flow [109]. Glaucoma and RGC-injury animal models have been applied to evaluate the treatment effects of

green tea extract and EGCG on RGC survival after injury (Figure 5). In the study of N-methyl-D-aspartate (NMDA)-induced excitotoxicity, NMDA-treated rats received two-day prophylactic treatments of intraperitoneal EGCG injections (25 mg/kg) showed a higher cell density in the ganglion cell layer and thickness of Thy-1 immunoreactivity than those received intraperitoneal saline injections [110]. For the optic nerve axotomy model, intraperitoneal injections of 50 mg/kg EGCG at 30 min before axotomy, and at Day 2 and 4 after axotomy were able to attenuate RGC loss by 12% in rat retina along with reducing the upregulation of neuronal nitric oxide synthase and Bax protein expression, and further enhancing ERK 1/2 and Akt activation after axotomy [111]. Inhibition of the ERK and Akt pathways could attenuate the protection effects of EGCG on RGCs against axotomy injury. In the optic nerve crush model, optic nerve-injured rats treated with EGCG showed a significantly higher density of RGCs at Day 7, 14, and 28 post-optic nerve crush, respectively, compared to those treated with the vehicle. Furthermore, there was a significantly higher expression of the neurofilament triplet L protein observed in the optic nerve-injured rats treated with EGCG than those treated with the vehicle [112]. Similarly, our recent study demonstrated that rats with pre- or post-operative treatment of 275 mg/kg green tea extract (Theaphenon E) showed a higher RGC survival and axonal regeneration and improved pupillary light reflex post-optic nerve injury with the activation of Akt, Erk p42/44, and Stat3, as well as the downregulation of inflammation, apoptosis, and microglia activation genes, compared to the saline-treated rats [113]. Pre-treatment of 275 or 550 mg/kg green tea extract was also able to reduce the activation of microglia in rats with an optic nerve injury.

In the chronic IOP elevation model induced by microbead injection into the anterior chamber, the IOP-elevated mice fed with EGCG-supplemented drinking water showed a higher RGC density than those fed with normal drinking water at Day 15 and 27 post-injury [114]. Notably, in the acute IOP elevation model, intraperitoneal injections of 50 mg/kg EGCG at 30 min before ischemia injury (raising the IOP to 150 mm Hg for 60 min) was able to reduce RGC death by 10%. There were also improvements in the TUNEL-positive cells observed in the inner retina, and neuronal NOS and nicotinamide adenine dinucleotide phosphate diaphorase-positive cells in the rat retina at Day 3 post-injury with the downregulation of ischemia injury-induced glial fibrillary acidic protein and lipid peroxidation [115]. Similarly, the ischemia-injured (raising the IOP to 120 mm Hg for 45 min) rats that received the EGCG treatment were determined to be able to attenuate the reduction in the a-wave and b-wave amplitudes of the electroretinograms, decrease Thy1 and neurofilament-L expression, increase retinal caspase-3 and caspase-8 expression, and blunt the changes in the localization of the retinal Thy-1 and ChAT immunoreactivities [101]. EGCG present in the drinking water (0.5%, 200 mL/day for 3 days before ischemia injury and 5 days after ischemia injury) was also able to ameliorate the ischemia injury (120 mm Hg for 45 min)-induced thinning of Thy-1 and choline acetyltransferase immunoreactivities, reduce a-wave and b-wave amplitudes of the electroretinograms, and Thy1 and neurofilament-L expression in the rat retina [116]. Similarly, our previous study on an experimental acute IOP elevation rat model (110 mm Hg for 2 h) demonstrated the anti-oxidative and anti-inflammatory properties of the green tea extract on ischemia-injured RGCs such that the oral administration of green tea extract (Theaphenon E; 275 mg/kg, 4 times within the first 2 days after the injury) ameliorated ischemic injury-induced RGC apoptosis and promoted RGC survival by reducing caspase-3 and caspase-8 expression, p38 phosphorylation, and inflammation marker (Il1β, Tlr4, and Tnfa) expression, as well as enhancing Jak phosphorylation in the retina [116].

In addition to the studies conducted with rodents, a single intravenous injection dose of 15 mg/kg EGCG in saline was found to reduce the TUNEL-positive and high-mobility group box-1-positive cells in the retinal sections of the ischemia-injured (raising the IOP to 100 mm Hg for 60 min) New Zealand male rabbits with the nuclear translocation of Nrf2 and increase in HO-1 expression at 6 h after treatment [117]. Moreover, EGCG can act directly on RGC axons in *Xenopus* embryos to increase the number of growth cone filopodia

that responded to extrinsic signals in a Sema3a-independent manner and led to a dramatic defect in the guided growth of RGC axons, whilst EGCG itself had no influence on RGC axon behavior in *Xenopus* embryos [118].

6. Clinical Applications of Green Tea Catechins for Glaucoma Treatments

Antioxidants, including green tea components, have been proposed as biotherapies for glaucoma prevention [119]. In young males with CrossFit training, green tea extract supplementation (two capsules once daily for six weeks; 250 mg green tea extract per capsule, containing 245 mg polyphenols (200 mg catechins, among which 137 mg EGCG, <4 mg caffeine, microcrystalline cellulose, and magnesium stearate) doubled the total antioxidant capacity in the venous blood test while also lowering the plasma concentration of lipid peroxidation products [120]. Regular consumption of moderate quantities of green tea could effectively modulate the antioxidant capacity in people subjected to oxidative stress, along with lowering the glucose, lipid, and uric acid levels [121]. A combined analysis from the Nurses' Health Study and the Health Professionals Follow-up Study in the United States reported that higher intakes of flavonols and monomeric flavanols were nominally associated with a lower POAG risk, and consuming ~2 cups of tea per day was associated with an 18% lower POAG risk [122]. Consistently, the United States 2005–2006 National Health and Nutrition Examination Survey reported that the participants who consumed at least one cup of hot tea daily showed a 74% decreased odds of having glaucoma compared with those who did not consume hot tea [123]. However, the Korea National Health and Nutrition Examination Survey 2010 to 2011 reported no significant associations between the frequency of tea consumption during the past 12 months and the risk of POAG with adjusting for multiple covariates [124]. The Rotterdam Study in the Netherlands also found no significant associations between flavonoid intake and the risk of POAG [125].

There were 122 studies on EGCG and 890 studies on green tea in the registry of ClinicalTrials.gov at the time of writing this manuscript. There was one study on EGCG and five studies on green tea extract related to ocular health/disease (Table 3). A randomized, placebo-controlled, double-blind, cross-over design clinical trial on EGCG in Italy (clinicaltrials.gov identifier: NCT00476138) reported that POAG patients who received oral EGCG treatment (200 mg/day) for 3 months in addition to standard IOP-lowering therapy showed increases in the amplitude of pattern-evoked electroretinograms as compared to the baseline values or to the patients who received the placebo treatment [126]. The magnitude of the pattern-evoked electroretinogram amplitude increments after EGCG treatment was inversely related to the corresponding baseline amplitudes. However, standard automated perimetry did not show significant changes after EGCG treatment. In addition, a recent clinical study from Lithuania reported that young volunteers receiving 400 mg green tea extract or EGCG capsules showed significant reductions in IOP after 2 h in the green tea extract group and after 1 h in the EGCG group as compared to the baseline [127].

Table 3. Registered clinical trials of green tea extract or EGCG application for eye diseases.

Identifier.	Country	Status	Phase	Enrollment	Targeted Eye Diseases or Conditions	Intervention	Dosage	Duration
NCT00476138	Italy	Unknown	Phase I/II	40	Primary open angle glaucoma Ocular hypertension	Oral EGCG treatment	200 mg/day	3 months
NCT00718653	United States	Completed	Not Applicable	40	Eye health	Lutein plus green tea extract	Lutein (12 mg/day) Green tea extract (200 mg/day)	Unknown
NCT01646047	United States	Completed [118]	Not Applicable	70	Diabetes Mellitus—Type 1 Diabetes Mellitus—Type 2 Non-proliferative diabetic retinopathy	Multi-component nutritional supplement capsules (vitamin C, mixed tocopherols/tocotrienols, vitamin D, fish oil, lutein, zeaxanthin, pine bark extract, benfotiamine, curcumin, and green tea extract)	2 capsules/day	6 months
NCT02984813	United States	Terminated	Phase I	21	Open-angle glaucoma Diabetic retinopathy	Nutritional supplements capsules (alpha lipoic acid, citicoline, Co-enzyme Q10, Ginkgo biloba extract, grape seed extract, N-acetyl-cysteine, curcumin, and green tea extract)	2 capsules/day	3 months
NCT03866005	United States	Unknown	Not Applicable	150	Center-involved diabetic macular edema	Multi-component nutritional supplement capsules (macular carotenoids lutein, zeaxanthin, vitamins B1, B12, C, D, E, lipoic acid, coenzyme Q10, resveratrol, patented extract of French maritime pine bark grape seed, curcumin, and green tea extract)	2 or 4 capsules/day	Study duration
NCT04117022	United States	Recruiting	Not Applicable	45	Diabetes Diabetic Retinopathy	Multi-component nutritional supplement capsules (vitamins C, D3 and E (d-α tocopherol), zinc oxide, eicosapentaenoic acid, docosahexaenoic acid, α-lipoic acid, coenzyme Q10, mixed tocotrienols/tocopherols, zeaxanthin, lutein, benfotiamine, N-acetyl cysteine, grape seed extract, resveratrol, turmeric root extract, Pycnogeno, and green tea leaf)	2 capsules/day	6 months

Information obtained from http://clinicaltrials.gov/ (accessed on 27 June 2022). EGCG: (−)-epigallocatechin-3-gallate.

A 6 month randomized, placebo-controlled clinical trial study in Washington (clinicaltrials.gov identifier: NCT01646047) aimed to evaluate the effects of a multi-component dietary supplement (containing vitamin C, mixed tocopherols/tocotrienols, vitamin D, fish oil, lutein, zeaxanthin, pine bark extract, benfotiamine, green tea extract, and curcumin; two capsules per day) on the visual function and retinal structure of the patients with type 1 or type 2 diabetes without retinopathy, or with mild-to-moderate non-proliferative retinopathy [123]. The study reported that study subjects on active supplement had a significantly better visual function and displayed significant improvements in most serum lipids, high-sensitivity C-reactive protein, and diabetic peripheral neuropathy compared to those who received the placebo. However, no significant changes in retinal thickness, hemoglobin A1c, total cholesterol, and TNF-α were found. A follow-up double-blinded, randomized, placebo-controlled clinical trial study in Washington (clinicaltrials.gov identifier: NCT03866005) aimed to evaluate the effects of "Diabetes Visual Function Study" softgels (containing lutein, zeaxanthin, vitamins B1, B12, C, D, and E, lipoic acid, coenzyme Q10, resveratrol, EPA/DHA, Pycnogenol™, grape seed extract, green tea extract, and curcumin; two or four capsules per day) to standard anti-vascular endothelial growth factor therapy for the subjects with diabetic macular edema. Another follow-up open-label, single-arm clinical trial study in California and Oklahoma (clinicaltrials.gov identifier: NCT04117022), which was estimated to be completed at the end of 2022, aimed to evaluate the ability of the chromatic electroretinogram and the full-field flicker electroretinogram in detecting the changes in global retinal function in diabetic retinopathy patients with dietary supplement treatments (DVS formula, consisting of vitamins C, D3, and E, zinc oxide, eicosapentaenoic acid, docosahexaenoic acid, α-lipoic acid, coenzyme Q10, mixed tocotrienols/tocopherols, zeaxanthin, lutein, benfotiamine, N-acetyl cysteine, grape seed extract, resveratrol, turmeric root extract, green tea leaf, and Pycnogenol; 2 softgels per day for 6 months). In addition, a randomized double-blinded clinical trial study conducted in Massachusetts (clinicaltrials.gov identifier: NCT00718653) aimed to measure the macular pigments and plasma lutein concentrations in subjects with lutein (12 mg per day) plus green tea extract (200 mg per day) treatment. Although this study was stated as completed, no results from this study have been reported as of yet.

7. Summary, Challenges, and Future Prospects

The pathophysiological mechanisms for RGC degeneration in glaucoma are complex. Although oxidation and inflammation are the major insults to RGCs, multiple modes of cell death are involved in RGC loss after optic nerve injury [80]. Targeting oxidation and inflammation alone do not adequately rescue RGCs from glaucomatous degeneration. The combined treatment of neurotrophic factors with antioxidative and anti-inflammatory agents should generate pronounced therapeutic effects against RGC degeneration [128,129]. Our study on sodium iodate-induced retinal degeneration model demonstrated that green tea extract (Theaphenon E) showed better treatment effects than EGCG alone or custom-made catechin mixture with EGCG [130], indicating that other constituents in green tea extract also possessed neuroprotective effects on RGCs. Furthermore, EGCG has a poor bioavailability, which could therefore affect its therapeutic effects on disease treatment. To enhance the stability and bioavailability of EGCG, the prodrug of EGCG (pro-EGCG, EGCG octaacetate) could be useful [71,131]. Further research is needed to delineate the stability, bioavailability, and neuroprotective effects of each catechin and their constituents in green tea extract as well as their metabolites. Currently, there has only been one double-blinded randomized placebo-controlled clinical trial for EGCG on eye disease, and none for the sole green tea extract treatment. Whether green tea extract and catechins could be a therapeutic treatment prescribed for glaucoma patients still requires additional clinical trials to confirm its clinical applications in glaucoma and different eye diseases. It has been reported that an herbal product made of a dry aqueous extract of green tea containing 90% of EGCG (one tablet per day) was prescribed by an ophthalmologist to treat a glaucoma patient. However, green tea-related hepatotoxicity was suspected [132]. Therefore, the dosage and

safety of green tea extract or EGCG treatment for glaucoma patients should be seriously studied. Nevertheless, as multiple pre-clinical studies have proven the efficacy of green tea extract and EGCG on ameliorating RGC degeneration, green tea catechins could be a potential co-adjuvant counteracting the oxidation and inflammation in RGCs for glaucoma management in addition to the IOP-lowering therapies.

Author Contributions: Conceptualization, T.K.N., C.C.W. and C.P.P.; data curation, T.K.N. and K.O.C.; writing—original draft preparation, T.K.N. and K.O.C.; writing—review and editing, C.C.W. and C.P.P.; funding acquisition, T.K.N. All authors have read and agreed to the published version of the manuscript.

Funding: This research was funded by the Natural Science Foundation of Guangdong Province (grant number: 2023A1515010195 to T.K.N.), China.

Acknowledgments: We are grateful to Yao Yao and Xin Bin from the Joint Shantou International Eye Center of Shantou University and The Chinese University of Hong Kong for assisting in assembly of figures and tables and reference organization.

Conflicts of Interest: The authors declare no potential conflict of interest.

References

1. Ramadan, G.; El-Beih, N.M.; Talaat, R.M.; Abd El-Ghffar, E.A. Anti-inflammatory activity of green versus black tea aqueous extract in a rat model of human rheumatoid arthritis. *Int. J. Rheum. Dis.* **2017**, *20*, 203–213. [CrossRef] [PubMed]
2. Santamarina, A.B.; Carvalho-Silva, M.; Gomes, L.M.; Okuda, M.H.; Santana, A.A.; Streck, E.L.; Seelaender, M.; Do Nascimento, C.; Ribeiro, E.B.; Lira, F.S.; et al. Decaffeinated green tea extract rich in epigallocatechin-3-gallate prevents fatty liver disease by increased activities of mitochondrial respiratory chain complexes in diet-induced obesity mice. *J. Nutr. Biochem.* **2015**, *26*, 1348–1356. [CrossRef]
3. Turkozu, D.; Sanlier, N. L-theanine, unique amino acid of tea and its metabolism, health effects, and safety. *Crit. Rev. Food Sci. Nutr.* **2017**, *57*, 1681–1687. [CrossRef] [PubMed]
4. Yang, X.H.; Huang, M.J.; Qin, C.Q.; Lv, B.Y.; Mao, Q.L.; Liu, Z.H. Structural characterization and evaluation of the antioxidant activities of polysaccharides extracted from Qingzhuan brick tea. *Int. J. Biol. Macromol.* **2017**, *101*, 768–775. [CrossRef] [PubMed]
5. Wang, H.J.; Shi, S.S.; Bao, B.; Li, X.J.; Wang, S.C. Structure characterization of an arabinogalactan from green tea and its anti-diabetic effect. *Carbohyd. Polym.* **2015**, *124*, 98–108. [CrossRef]
6. Song, C.W.; Yu, Q.S.; Li, X.H.; Jin, S.N.; Li, S.; Zhang, Y.; Jia, S.L.; Chen, C.; Xiang, Y.; Jiang, H.L. The hypolipidemic effect of total saponins from kuding tea in high-fat diet-induced hyperlipidemic mice and its composition characterized by UPLC-QTOF-MS/MS. *J. Food Sci.* **2016**, *81*, H1313–H1319. [CrossRef]
7. Xu, D.P.; Li, Y.; Meng, X.; Zhou, T.; Zhou, Y.; Zheng, J.; Zhang, J.J.; Li, H.B. Natural antioxidants in foods and medicinal plants: Extraction, assessment and resources. *Int. J. Mol. Sci.* **2017**, *18*, 96. [CrossRef]
8. Luca, V.S.; Stan, A.M.; Trifan, A.; Miron, A.; Aprotosoaie, A.C. Catechins profile, caffeine content and antioxidant activity of *Camellia sinensis* teas commercialized in romania. *Med. Sur. J. Revista Med.-Chirurgicala* **2016**, *120*, 457–463.
9. Xu, Y.; Zhang, M.; Wu, T.; Dai, S.D.; Xu, J.L.; Zhou, Z.K. The anti-obesity effect of green tea polysaccharides, polyphenols and caffeine in rats fed with a high-fat diet. *Food Funct.* **2015**, *6*, 297–304. [CrossRef]
10. Tang, G.Y.; Zhao, C.N.; Xu, X.Y.; Gan, R.Y.; Cao, S.Y.; Liu, Q.; Shang, A.; Mao, Q.Q.; Li, H.B. Phytochemical composition and antioxidant capacity of 30 Chinese teas. *Antioxidants* **2019**, *8*, 180. [CrossRef]
11. Yang, H.; Xue, X.J.; Li, H.; Apandi, S.N.; Tay-Chan, S.C.; Ong, S.P.; Tian, E.F. The relative antioxidant activity and steric structure of green tea catechins—A kinetic approach. *Food Chem.* **2018**, *257*, 399–405. [CrossRef]
12. Pastore, R.L.; Fratellone, P. Potential health benefits of green tea (*Camellia sinensis*): A narrative review. *Explore* **2006**, *2*, 531–539. [CrossRef]
13. Yang, C.S.; Lambert, J.D.; Ju, J.; Lu, G.; Sang, S. Tea and cancer prevention: Molecular mechanisms and human relevance. *Toxicol. Appl. Pharmacol.* **2007**, *224*, 265–273. [CrossRef]
14. Du, G.J.; Zhang, Z.; Wen, X.D.; Yu, C.; Calway, T.; Yuan, C.S.; Wang, C.Z. Epigallocatechin Gallate (EGCG) is the most effective cancer chemopreventive polyphenol in green tea. *Nutrients* **2012**, *4*, 1679–1691. [CrossRef]
15. Metodiewa, D.; Jaiswal, A.K.; Genas, N.; Dickancaite, E.; Segora-Aguilar, J. Quercetin may act as a cytotoxic prooxidant after its metabolic activation to semiquinone and quinoidal product. *Free Radic. Biol. Med.* **1999**, *26*, 107–116. [CrossRef] [PubMed]
16. Yamamoto, T.; Juneja, L.R.; Chu, D.C.; Kim, M. *Chemistry and Application of Green Tea*; CRC Press: Boca Raton, FL, USA; Taylor & Francis Group: Abingdon, UK, 1997; pp. 1–5.
17. Baranowska, M.; Suliborska, K.; Chrzanowski, W.; Kusznierewicz, B.; Namieśnik, J.; Bartoszek, A. The relationship between standard reduction potentials of catechins and biological activities involved in redox control. *Redox Biol.* **2018**, *17*, 355–366. [CrossRef] [PubMed]

18. Byun, E.B.; Kim, W.S.; Sung, N.Y.; Byun, E.H. Epigallocatechin-3-Gallate Regulates Anti-Inflammatory Action Through 67-kDa Laminin Receptor-Mediated Tollip Signaling Induction in Lipopolysaccharide-Stimulated Human Intestinal Epithelial Cells. *Cell. Physiol. Biochem.* **2018**, *46*, 2072–2081. [CrossRef] [PubMed]
19. Zhao, J.; Blayney, A.; Liu, X.R.; Gandy, L.; Jin, W.H.; Yan, L.F.; Ha, J.H.; Canning, A.J.; Connelly, M.; Yang, C.; et al. EGCG binds intrinsically disordered N-terminal domain of p53 and disrupts p53-MDM2 interaction. *Nat. Commun.* **2021**, *12*, 986. [CrossRef] [PubMed]
20. Ye, F.; Yang, C.S.; Kim, J.Y.; MacNevin, C.J.; Hahn, K.M.; Park, D.; Ginsberg, M.H.; Kim, C.H. Epigallocatechin gallate has pleiotropic effects on transmembrane signaling by altering the embedding of transmembrane domains. *J. Biol. Chem.* **2017**, *292*, 9858–9864. [CrossRef] [PubMed]
21. Minnelli, C.; Cianfruglia, L.; Laudadio, E.; Mobbili, G.; Galeazzi, R.; Armeni, T. Effect of Epigallocatechin-3-Gallate on EGFR Signaling and Migration in Non-Small Cell Lung Cancer. *Int. J. Mol. Sci.* **2021**, *22*, 11833. [CrossRef]
22. Zhang, H.H.; Cao, D.; Cui, W.; Ji, M.J.; Qian, X.H.; Zhong, L.W. Molecular bases of thioredoxin and thioredoxin reductase-mediated prooxidant actions of (−)-epigallocatechin-3-gallate. *Free Radic. Biol. Med.* **2010**, *49*, 2010–2018. [CrossRef] [PubMed]
23. Aribisala, J.O.; Sabiu, S. Redox Impact on Bacterial Macromolecule: A Promising Avenue for Discovery and Development of Novel Antibacterials. *Biomolecules* **2022**, *12*, 1545. [CrossRef] [PubMed]
24. O'Neill, L.A.; Hardie, D.G. Metabolism of inflammation limited by AMPK and pseudo-starvation. *Nature* **2013**, *493*, 346–355. [CrossRef] [PubMed]
25. Lorenz, M.; Wessler, S.; Follmann, E.; Michaelis, W.; Dusterhoft, T.; Baumann, G.; Stangl, K.; Stangl, V. A constituent of green tea, epigallocatechin-3-gallate, activates endothelial nitric oxide synthase by a phosphatidylinositol-3-OH-kinase-, cAMP-dependent protein kinase-, and Akt-dependent pathway and leads to endothelial-dependent vasorelaxation. *J. Biol. Chem.* **2004**, *279*, 6190–6195. [CrossRef] [PubMed]
26. Alvarez, E.; Campos-Toimil, M.; Justiniano-Basaran, H.; Lugnier, C.; Orallo, F. Study of the mechanisms involved in the vasorelaxation induced by (−)-epigallocatechin-3-gallate in rat aorta. *Br. J. Pharmacol.* **2006**, *147*, 269–280. [CrossRef]
27. Collins, Q.F.; Liu, H.Y.; Pi, J.; Liu, Z.; Quon, M.J.; Cao, W. Epigallocatechin-3-gallate (EGCG), a green tea polyphenol, suppresses hepatic gluconeogenesis through 5′-AMP-activated protein kinase. *J. Biol. Chem.* **2007**, *282*, 30143–30149. [CrossRef]
28. Reiter, C.E.; Kim, J.A.; Quon, M.J. Green tea polyphenol epigallocatechin gallate reduces endothelin-1 expression and secretion in vascular endothelial cells: Roles for AMP-activated protein kinase, Akt, and FOXO1. *Endocrinology* **2010**, *151*, 103–114. [CrossRef]
29. Jang, H.J.; Ridgeway, S.D.; Kim, J.A. Effects of the green tea polyphenol, epigallocatechin-3-gallate (EGCG), on high fat diet-induced insulin resistance and endothelial dysfunction. *Am. J. Physiol. Endocrinol. Metab.* **2013**, *305*, E1444–E1451. [CrossRef]
30. Lee, M.J.; Wang, Z.Y.; Li, H.; Chen, L.; Sun, Y.; Gobbo, S.; Balentine, D.A.; Yang, C.S. Analysis of plasma and urinary tea polyphenols in human subjects. *Cancer Epidemiol. Biomark. Prev.* **1995**, *4*, 393–399.
31. Hong, J.; Lambert, J.D.; Lee, S.H.; Sinko, P.J.; Yang, C.S. Involvement of multidrug resistance-associated proteins in regulating cellular levels of (−)-epigallocatechin-3-gallate and its methyl metabolites. *Biochem. Biophys. Res. Commun.* **2003**, *310*, 222–227. [CrossRef] [PubMed]
32. Chen, L.; Lee, M.J.; Li, H.; Yang, C.S. Absorption, distribution, elimination of tea polyphenols in rats. *Drug. Metab. Dispos.* **1997**, *25*, 1045–1050. [PubMed]
33. Lambert, J.D.; Lee, M.J.; Lu, H.; Meng, X.; Hong, J.J.; Seril, D.N.; Sturgill, M.G.; Yang, C.S. Epigallocatechin-3-gallate is absorbed but extensively glucuronidated following oral administration to mice. *J. Nutr.* **2003**, *133*, 4172–4177. [CrossRef] [PubMed]
34. Jodoin, J.; Demeule, M.; Beliveau, R. Inhibition of the multidrug resistance P-glycoprotein activity by green tea polyphenols. *Biochim. Biophys. Acta.* **2002**, *1542*, 149–159. [CrossRef] [PubMed]
35. Chow, H.H.; Hakim, I.A.; Vining, D.R.; Crowell, J.A.; Ranger-Moore, J.; Chew, W.M.; Celaya, C.A.; Rodney, S.R.; Hara, Y.; Alberts, D.S. Effects of dosing condition on the oral bioavailability of green tea catechins after single-dose administration of Polyphenon E in healthy individuals. *Clin. Cancer Res.* **2005**, *11*, 4627–4633. [CrossRef] [PubMed]
36. Schramm, D.D.; Karim, M.; Schrader, H.R.; Holt, R.R.; Kirkpatrick, N.J.; Polagruto, J.A.; Ensunsa, J.L.; Schmitz, H.H.; Keen, C.L. Food effects on the absorption and pharmacokinetics of cocoa flavanols. *Life Sci.* **2003**, *73*, 857–869. [CrossRef]
37. Chu, K.O.; Chan, K.P.; Wang, C.C.; Chu, C.Y.; Li, W.Y.; Choy, K.W.; Rogers, M.S.; Pang, C.P. Green tea catechins and their oxidative protection in the rat eye. *J. Agric. Food Chem.* **2010**, *58*, 1523–1534. [CrossRef]
38. Chu, K.O.; Chan, K.P.; Yang, Y.; Qin, Y.J.; Li, W.Y.; Chan, S.O.; Wang, C.C.; Pang, C.P. Effects of EGCG content in green tea extract on pharmacokinetics, oxidative status and expression of inflammatory and apoptotic genes in the rat ocular tissues. *J. Nutr. Biochem.* **2015**, *26*, 1357–1367. [CrossRef]
39. Qin, Y.J.; Chu, K.O.; Yip, Y.W.; Li, W.Y.; Yang, Y.P.; Chan, K.P.; Ren, J.L.; Chan, S.O.; Pang, C.P. Green tea extract treatment alleviates ocular inflammation in a rat model of endotoxin-induced uveitis. *PLoS ONE* **2014**, *9*, e103995. [CrossRef]
40. Chu, K.O.; Wang, C.C.; Chu, C.Y.; Choy, K.W.; Pang, C.P.; Rogers, M.S. Uptake and distribution of catechins in fetal organs following in utero exposure in rats. *Hum. Reprod.* **2007**, *22*, 280–287. [CrossRef]
41. Fung, S.T.; Ho, C.K.; Choi, S.W.; Chung, W.Y.; Benzie, I.F.F. Comparison of catechin profiles in human plasma and urine after single dosing and regular intake of green tea (*Camellia sinensis*). *Br. J. Nutr.* **2013**, *109*, 2199–2207. [CrossRef]
42. Manach, C.; Williamson, G.; Morand, C.; Scalbert, A.; Rémésy, C. Bioavailability and bioefficacy of polyphenols in humans. I. Review of 97 bioavailability studies. *Am. J. Clin. Nutr.* **2005**, *81*, 230S–242S. [CrossRef]

43. Auger, C.; Hara, Y.; Crozier, A. Bioavailability of polyphenon E flavan-3-ols in humans with an ileostomy. *J. Nutr.* **2008**, *138*, 1535S–1542S. [CrossRef] [PubMed]
44. Ishii, T.; Ichikawa, T.; Minoda, K.; Kusaka, K.; Ito, S.; Suzuki, Y.; Akagawa, M.; Mochizuki, K.; Goda, T.; Nakayama, T. Human serum albumin as an antioxidant in the oxidation of (−)-epigallocatechin gallate: Participation of reversible covalent binding for interaction and stabilization. *Biosci. Biotechnol. Biochem.* **2011**, *75*, 100–106. [CrossRef]
45. Ishii, T.; Minoda, K.; Bae, M.J.; Mori, T.; Uekusa, Y.; Ichikawa, T.; Aihara, Y.; Furuta, T.; Wakimoto, T.; Kan, T.; et al. Binding affinity of tea catechins for HSA: Characterization by high-performance affinity chromatography with immobilized albumin column. *Mol. Nutr. Food Res.* **2010**, *54*, 816–822. [CrossRef] [PubMed]
46. Donovan, J.L.; Crespy, V.; Oliveira, M.; Cooper, K.A.; Gibson, B.B.; Williamson, G. (+)-Catechin is more bioavailable then (−)-catechin: Relevance to the bioavailability of catechin from cocoa. *Free Radic. Res.* **2006**, *40*, 1029–1034. [CrossRef]
47. Stalmach, A.; Troufflard, S.; Serafini, M.; Crozier, A. Absorption, metabolism and excretion of Choladi green tea flavan-3-ols by humans. *Mol. Nutr. Food Res.* **2009**, *53* (Suppl. S1), S44–S53. [CrossRef]
48. Lambert, J.D.; Elias, R.J. The antioxidant and pro-oxidant activities of green tea polyphenols: A role in cancer prevention. *Arch. Biochem. Biophys.* **2010**, *501*, 65–72. [CrossRef] [PubMed]
49. Treml, J.; Šmejkal, K. Flavonoids as potent scavengers of hydroxyl radicals. *Compr. Rev. Food Sci. Food Saf.* **2016**, *15*, 720–738. [CrossRef]
50. Nanjo, F.; Goto, K.; Seto, R.; Suzuki, M.; Sakai, M.; Hara, Y. Scavenging effects of tea catechins and their derivatives on 1,1-diphenyl-2-picrylhydrazyl radical. *Free Radic. Biol. Med.* **1996**, *21*, 895–902. [CrossRef]
51. Lee, L.S.; Kim, S.H.; Kim, Y.B.; Kim, Y.C. Quantitative analysis of major constituents in green tea with different plucking periods and their antioxidant activity. *Molecules* **2014**, *19*, 9173–9186. [CrossRef]
52. Martínez, V.; Ugartondo, V.; Vinardell, M.P.; Torres, J.L.; Mitjans, M. Grape epicatechin conjugates prevent erythrocyte membrane protein oxidation. *J. Agric. Food Chem.* **2012**, *60*, 4090–4095. [CrossRef] [PubMed]
53. Oteiza, P.I.; Erlejman, A.G.; Verstraeten, S.V.; Keen, C.L.; Fraga, C.G. Flavonoid-membrane interactions: A protective role of flavonoids at the membrane surface? *Clin. Dev. Immunol.* **2005**, *12*, 19–25. [CrossRef] [PubMed]
54. Butt, M.S.; Imran, A.; Sharif, M.K.; Ahmad, R.S.; Xiao, H.; Imran, M.; Rsool, H.A. Black tea polyphenols: A mechanistic treatise. *Crit. Rev. Food Sci. Nutr.* **2014**, *54*, 1002–1011. [CrossRef] [PubMed]
55. Yokotani, K.; Umegaki, K. Evaluation of plasma antioxidant activity in rats given excess EGCg with reference to endogenous antioxidants concentrations and assay methods. *Free Radic. Res.* **2017**, *51*, 193–199. [CrossRef] [PubMed]
56. Li, G.X.; Chen, Y.K.; Hou, Z.; Xiao, H.; Jin, H.; Lu, G.; Lee, M.J.; Liu, B.; Guan, F.; Yang, Z.; et al. Pro-oxidative activities and dose-response relationship of (−)-epigallocatechin-3-gallate in the inhibition of lung cancer cell growth: A comparative study in vivo and in vitro. *Carcinogenesis* **2010**, *31*, 902–910. [CrossRef]
57. Nakagawa, H.; Hasumi, K.; Woo, J.T.; Nagai, K.; Wachi, M. Generation of hydrogen peroxide primarily contributes to the induction of Fe (II)-dependent apoptosis in Jurkat cells by (−)-epigallocatechin gallate. *Carcinogenesis* **2004**, *25*, 1567–1574. [CrossRef]
58. Nakagawa, H.; Wachi, M.; Woo, J.T.; Kato, M.; Kasai, S.; Takahashi, F.; Lee, I.S.; Nagai, K. Fenton reaction is primarily involved in a mechanism of (−)-epigallocatechin-3-gallate to induce osteoclastic cell death. *Biochem. Biophys. Res. Commun.* **2002**, *292*, 94–101. [CrossRef]
59. Ko, C.H.; Li, K.; Ng, P.C.; Fung, K.P.; Li, C.L.; Wong, R.P.O.; Chui, K.M.; Gu, G.J.S.; Yung, E.; Wang, C.C.; et al. Pro-oxidative effects of tea and polyphenols, epigallocatechin-3-gallate and epigallocatechin, on G6PD-deficient erythrocytes in vitro. *Int. J. Mol. Med.* **2006**, *18*, 987–994. [CrossRef]
60. Elbling, L.; Herbacek, I.; Weiss, R.M.; Jantschitsch, C.; Micksche, M.; Gerner, C.; Pangratz, H.; Grusch, M.; Knasmuller, S.; Berger, W. Hydrogen peroxide mediates EGCG-induced antioxidant protection in human keratinocytes. *Free Radic. Biol. Med.* **2010**, *49*, 1444–1452. [CrossRef]
61. Bae, Y.S.; Lee, J.H.; Choi, S.H.; Kim, S.; Almazan, F.; Witztum, J.L.; Miller, Y.I. Macrophages generate reactive oxygen species in response to minimally oxidized low-density lipoprotein: Toll-like receptor 4- and spleen tyrosine kinase-dependent activation of NADPH oxidase 2. *Circ. Res.* **2009**, *104*, 210–218. [CrossRef]
62. Pullikotil, P.; Chen, H.; Muniyappa, R.; Greenberg, C.C.; Yang, S.; Reiter, C.E.; Lee, J.W.; Chung, J.H.; Quon, M.J. Epigallocatechin gallate induces expression of heme oxygenase-1 in endothelial cells via p38 MAPK and Nrf-2 that suppresses proinflammatory actions of TNF-alpha. *J. Nutr. Biochem.* **2012**, *23*, 1134–1145. [CrossRef]
63. Wu, C.C.; Hsu, M.C.; Hsieh, C.W.; Lin, J.B.; Lai, P.H.; Wung, B.S. Upregulation of heme oxygenase-1 by Epigallocatechin-3-gallate via the phosphatidylinositol 3-kinase/Akt and ERK pathways. *Life Sci.* **2006**, *78*, 2889–2897. [CrossRef]
64. Chu, K.O.; Chan, S.O.; Pang, C.P.; Wang, C.C. Pro-oxidative and antioxidative controls and signaling modification of polyphenolic phytochemicals: Contribution to health promotion and disease prevention? *J. Agric. Food Chem.* **2014**, *62*, 4026–4038. [CrossRef] [PubMed]
65. Ren, J.L.; Yu, Q.X.; Liang, W.C.; Leung, P.Y.; Ng, T.K.; Chu, W.K.; Pang, C.P.; Chan, S.O. Green tea extract attenuates LPS-induced retinal inflammation in rats. *Sci. Rep.* **2018**, *8*, 429. [CrossRef]
66. Chu, K.O.; Chan, K.P.; Yip, Y.W.Y.; Chu, W.K.; Wang, C.C.; Pang, C.P. Systemic and Ocular Anti-Inflammatory Mechanisms of Green Tea Extract on Endotoxin-Induced Ocular Inflammation. *Front. Endocrinol.* **2022**, *13*, 899271. [CrossRef] [PubMed]

67. Li, J.; Yip, Y.W.Y.; Ren, J.L.; Hui, W.K.; He, J.N.; Yu, Q.X.; Chu, K.O.; Ng, T.K.; Chan, S.O.; Pang, C.P.; et al. Green tea catechins alleviate autoimmune symptoms and visual impairment in a murine model for human chronic intraocular inflammation by inhibiting Th17-associated pro-inflammatory gene expression. *Sci. Rep.* **2019**, *9*, 2301. [CrossRef] [PubMed]
68. Maity, S.; Mukhopadhyay, P.; Kundu, P.P.; Chakraborti, A.S. Alginate coated chitosan core-shell nanoparticles for efficient oral delivery of naringenin in diabetic animals-An in vitro and in vivo approach. *Carbohydr. Polym.* **2017**, *170*, 124–132. [CrossRef] [PubMed]
69. Cheng, C.Y.; Barro, L.; Tsai, S.T.; Feng, T.W.; Wu, X.Y.; Chao, C.W.; Yu, R.S.; Chin, T.Y.; Hsieh, M.F. Epigallocatechin-3-Gallate-Loaded Liposomes Favor Anti-Inflammation of Microglia Cells and Promote Neuroprotection. *Int. J. Mol. Sci.* **2021**, *22*, 3037. [CrossRef] [PubMed]
70. Chu, K.O.; Man, G.C.W.; Chan, K.P.; Chu, C.Y.; Chan, T.H.; Pang, C.P.; Wang, C.C. Determination of exogenous epigallocatechin gallate peracetate in mouse plasma using liquid chromatography with quadrupole time-of-flight mass spectrometry. *J. Sep. Sci.* **2014**, *37*, 3473–3480. [CrossRef]
71. Wang, C.C.; Xu, H.; Man, G.C.W.; Zhang, T.; Chu, K.O.; Chu, C.Y.; Cheng, J.T.Y.; Li, G.; He, Y.X.; Qin, L.; et al. Prodrug of green tea epigallocatechin-3-gallate (Pro-EGCG) as a potent anti-angiogenesis agent for endometriosis in mice. *Angiogenesis* **2013**, *16*, 59–69. [CrossRef]
72. Rodrigues, C.F.; Ascenção, K.; Silva, F.A.; Sarmento, B.; Oliveira, M.B.; Andrade, J.C. Drug-delivery systems of green tea catechins for improved stability and bioavailability. *Curr. Med. Chem.* **2013**, *20*, 4744–4757. [CrossRef]
73. Yin, Z.Y.; Zheng, T.; Ho, C.T.; Huang, Q.R.; Wu, Q.L.; Zhang, M. Improving the stability and bioavailability of tea polyphenols by encapsulations: A review. *Food Sci. Hum. Wellness* **2022**, *11*, 537–556. [CrossRef]
74. Tham, Y.C.; Li, X.; Wong, T.Y.; Quigley, H.A.; Aung, T.; Cheng, C.Y. Global prevalence of glaucoma and projections of glaucoma burden through 2040: A systematic review and meta-analysis. *Ophthalmology* **2014**, *121*, 2081–2090. [CrossRef]
75. Jonas, J.B.; Aung, T.; Bourne, R.R.; Bron, A.M.; Ritch, R.; Panda-Jonas, S. Glaucoma. *Lancet* **2017**, *390*, 2183–2193. [CrossRef]
76. Gharahkhani, P.; Jorgenson, E.; Hysi, P.; Khawaja, A.P.; Pendergrass, S.; Han, X.; Ong, J.S.; Hewitt, A.W.; Segrè, A.V.; Rouhana, J.M.; et al. Genome-wide meta-analysis identifies 127 open-angle glaucoma loci with consistent effect across ancestries. *Nat. Commun.* **2021**, *12*, 1258. [CrossRef]
77. Weinreb, R.N.; Aung, T.; Medeiros, F.A. The pathophysiology and treatment of glaucoma: A review. *JAMA* **2014**, *311*, 1901–1911. [CrossRef] [PubMed]
78. Gazzard, G.; Konstantakopoulou, E.; Garway-Heath, D.; Garg, A.; Vickerstaff, V.; Hunter, R.; Ambler, G.; Bunce, C.; Wormald, R.; Nathwani, N.; et al. Selective laser trabeculoplasty versus eye drops for first-line treatment of ocular hypertension and glaucoma (LiGHT): A multicentre andomized controlled trial. *Lancet* **2019**, *393*, 1505–1516. [CrossRef] [PubMed]
79. Davis, B.M.; Crawley, L.; Pahlitzsch, M.; Javaid, F.; Cordeiro, M.F. Glaucoma: The retina and beyond. Acta. *Neuropathologica* **2016**, *132*, 807–826. [CrossRef] [PubMed]
80. Yao, Y.; Xu, Y.; Liang, J.J.; Zhuang, X.; Ng, T.K. Longitudinal and simultaneous profiling of 11 modes of cell death in mouse retina post-optic nerve injury. *Exp. Eye Res.* **2022**, *222*, 109159. [CrossRef]
81. Tezel, G. Oxidative stress in glaucomatous neurodegeneration: Mechanisms and consequences. *Prog. Retin. Eye Res.* **2006**, *25*, 490–513. [CrossRef]
82. Baudouin, C.; Kolko, M.; Melik-Parsadaniantz, S.; Messmer, E.M. Inflammation in Glaucoma: From the back to the front of the eye, and beyond. *Prog. Retin. Eye Res.* **2021**, *83*, 100916. [CrossRef]
83. Mozaffarieh, M.; Grieshaber, M.C.; Flammer, J. Oxygen and blood flow: Players in the pathogenesis of glaucoma. *Mol. Vis.* **2008**, *14*, 224–233. [PubMed]
84. Goyal, A.; Srivastava, A.; Sihota, R.; Kaur, J. Evaluation of oxidative stress markers in aqueous humor of primary open angle glaucoma and primary angle closure glaucoma patients. *Curr. Eye Res.* **2014**, *39*, 823–829. [CrossRef] [PubMed]
85. Gherghel, D.; Griffiths, H.R.; Hilton, E.J.; Cunliffe, I.A.; Hosking, S.L. Systemic reduction in glutathione levels occurs in patients with primary open-angle glaucoma. *Investig. Ophthalmol. Vis. Sci.* **2005**, *46*, 877–883. [CrossRef] [PubMed]
86. Gherghel, D.; Mroczkowska, S.; Qin, L. Reduction in blood glutathione levels occurs similarly in patients with primary-open angle or normal tension glaucoma. *Investig. Ophthalmol. Vis. Sci.* **2013**, *54*, 3333–3339. [CrossRef]
87. Tezel, G.; Wax, M.B. Hypoxia-inducible factor 1alpha in the glaucomatous retina and optic nerve head. *Arch. Ophthalmol.* **2004**, *122*, 1348–1356. [CrossRef]
88. Fan, W.; Huang, W.; Chen, J.; Li, N.; Mao, L.; Hou, S. Retinal microglia: Functions and diseases. *Immunology* **2022**, *166*, 268–286. [CrossRef]
89. Tezel, G. Molecular regulation of neuroinflammation in glaucoma: Current knowledge and the ongoing search for new treatment targets. *Prog. Retin. Eye Res.* **2022**, *87*, 100998. [CrossRef]
90. Yuan, L.; Neufeld, A.H. Activated microglia in the human glaucomatous optic nerve head. *J. Neurosci. Res.* **2001**, *64*, 523–532. [CrossRef]
91. Gramlich, O.W.; Beck, S.; von Thun Und Hohenstein-Blaul, N.; Boehm, N.; Ziegler, A.; Vetter, J.M.; Pfeiffer, N.; Grus, F.H. Enhanced insight into the autoimmune component of glaucoma: IgG autoantibody accumulation and pro-inflammatory conditions in human glaucomatous retina. *PLoS ONE* **2013**, *8*, e57557. [CrossRef]

92. Yang, X.; Luo, C.; Cai, J.; Powell, D.W.; Yu, D.; Kuehn, M.H.; Tezel, G. Neurodegenerative and inflammatory pathway components linked to TNF-α/TNFR1 signaling in the glaucomatous human retina. *Investig. Ophthalmol. Vis. Sci.* **2011**, *52*, 8442–8454. [CrossRef] [PubMed]
93. Yang, Y.; Xu, C.; Chen, Y.; Liang, J.J.; Xu, Y.; Chen, S.L.; Huang, S.; Yang, Q.; Cen, L.P.; Pang, C.P.; et al. Green Tea Extract Ameliorates Ischemia-Induced Retinal Ganglion Cell Degeneration in Rats. *Oxid. Med. Cell. Longev.* **2019**, *2019*, 8407206. [CrossRef] [PubMed]
94. Sutherland, B.A.; Rahman, R.M.; Appleton, I. Mechanisms of action of green tea catechins, with a focus on ischemia-induced neurodegeneration. *J. Nutr. Biochem.* **2006**, *17*, 291–306. [CrossRef] [PubMed]
95. Mak, H.K.; Yung, J.S.Y.; Weinreb, R.N.; Ng, S.H.; Cao, X.; Ho, T.Y.C.; Ng, T.K.; Chu, W.K.; Yung, W.H.; Choy, K.W.; et al. MicroRNA-19a-PTEN Axis Is Involved in the Developmental Decline of Axon Regenerative Capacity in Retinal Ganglion Cells. *Mol. Ther. Nucleic Acids* **2020**, *21*, 251–263. [CrossRef]
96. Ng, T.K.; Yung, J.S.; Choy, K.W.; Cao, D.; Leung, C.K.; Cheung, H.S.; Pang, C.P. Transdifferentiation of periodontal ligament-derived stem cells into retinal ganglion-like cells and its microRNA signature. *Sci. Rep.* **2015**, *5*, 16429. [CrossRef] [PubMed]
97. Suen, H.C.; Qian, Y.; Liao, J.; Luk, C.S.; Lee, W.T.; Ng, J.K.W.; Chan, T.T.H.; Hou, H.W.; Li, I.; Li, K.; et al. Transplantation of Retinal Ganglion Cells Derived from Male Germline Stem Cell as a Potential Treatment to Glaucoma. *Stem Cells Dev.* **2019**, *28*, 1365–1375. [CrossRef]
98. Cen, L.P.; Ng, T.K.; Liang, J.J.; Zhuang, X.; Yao, X.; Yam, G.H.; Chen, H.; Cheung, H.S.; Zhang, M.; Pang, C.P. Human Periodontal Ligament-Derived Stem Cells Promote Retinal Ganglion Cell Survival and Axon Regeneration After Optic Nerve Injury. *Stem Cells* **2018**, *36*, 844–855. [CrossRef]
99. Maher, P.; Hanneken, A. The molecular basis of oxidative stress-induced cell death in an immortalized retinal ganglion cell line. *Investig. Ophthalmol. Vis. Sci.* **2005**, *46*, 749–757. [CrossRef]
100. Krishnamoorthy, R.R.; Clark, A.F.; Daudt, D.; Vishwanatha, J.K.; Yorio, T. A forensic path to RGC-5 cell line identification: Lessons learned. *Investig. Ophthalmol. Vis. Sci.* **2013**, *54*, 5712–5719. [CrossRef]
101. Zhang, B.; Safa, R.; Rusciano, D.; Osborne, N.N. Epigallocatechin gallate, an active ingredient from green tea, attenuates damaging influences to the retina caused by ischemia/reperfusion. *Brain Res.* **2007**, *1159*, 40–53. [CrossRef]
102. Jin, J.; Ying, H.; Huang, M.; Du, Q. Bioactive compounds in green tea leaves attenuate the injury of retinal ganglion RGC-5 cells induced by H_2O_2 and ultraviolet radiation. *Pak. J. Pharm. Sci.* **2015**, *28*, 2267–2272.
103. Zhang, B.; Osborne, N.N. Oxidative-induced retinal degeneration is attenuated by epigallocatechin gallate. *Brain Res.* **2006**, Stem Cells*1124*, 176–187. [CrossRef]
104. Yang, Y.; Chen, S.L.; Xu, Y.; Yao, Y.; Liang, J.J.; Wang, L.; Jhanji, V.; Sun, X.; Ma, D.; Ng, T.K. Green Tea Catechins Attenuate Human Primary Pterygium Cell Survival and Migration Via Modulation of ERK p42/p44 and p38 Pathways. *J. Agric. Food Chem.* **2021**, Stem Cells*69*, 12209–12218. [CrossRef]
105. Cao, L.; Liu, H.; Lam, D.S.; Yam, G.H.; Pang, C.P. In vitro screening for angiostatic potential of herbal chemicals. *Investig. Ophthalmol. Vis. Sci.* **2010**, *51*, 6658–6664. [CrossRef]
106. Yoneyama, S.; Kawai, K.; Tsuno, N.H.; Okaji, Y.; Asakage, M.; Tsuchiya, T.; Yamada, J.; Sunami, E.; Osada, T.; Kitayama, J.; et al. Epigallocatechin gallate affects human dendritic cell differentiation and maturation. *J. Allergy Clin. Immunol.* **2008**, *121*, 209–214. [CrossRef]
107. Yang, N.; Shang, Y.X. Epigallocatechin gallate ameliorates airway inflammation by regulating Treg/Th17 imbalance in an asthmatic mouse model. *Int. Immunopharmacol.* **2019**, *72*, 422–428. [CrossRef] [PubMed]
108. Mandel, S.; Amit, T.; Reznichenko, L.; Weinreb, O.; Youdim, M.B. Green tea catechins as brain-permeable, natural iron chelators-antioxidants for the treatment of neurodegenerative disorders. *Mol. Nutr. Food Res.* **2006**, *50*, 229–234. [CrossRef] [PubMed]
109. Mozaffarieh, M.; Grieshaber, M.C.; Orgül, S.; Flammer, J. The potential value of natural antioxidative treatment in glaucoma. *Surv. Ophthalmol.* **2008**, *53*, 479–505. [CrossRef] [PubMed]
110. Chen, F.; Jiang, L.; Shen, C.; Wan, H.; Xu, L.; Wang, N.; Jonas, J.B. Neuroprotective effect of epigallocatechin-3-gallate against N-methyl-D-aspartate-induced excitotoxicity in the adult rat retina. *Acta Ophthalmol.* **2012**, *90*, e609–e615. [CrossRef]
111. Peng, P.H.; Chiou, L.F.; Chao, H.M.; Lin, S.; Chen, C.F.; Liu, J.H.; Ko, M.L. Effects of epigallocatechin-3-gallate on rat retinal ganglion cells after optic nerve axotomy. *Exp. Eye Res.* **2010**, *90*, 528–534. [CrossRef]
112. Xie, J.; Jiang, L.; Zhang, T.; Jin, Y.; Yang, D.; Chen, F. Neuroprotective effects of Epigallocatechin-3-gallate (EGCG) in optic nerve crush model in rats. *Neurosci. Lett.* **2010**, *479*, 26–30. [CrossRef]
113. Yuan, X.L.; Chen, S.L.; Xu, Y.Y.; Yao, Y.; Liang, J.J.; Zhuang, X.; Hald, E.S.; Ng, T.K. Green tea extract enhances retinal ganglion cell survival and axonal regeneration in rats with optic nerve injury. *J. Nutr. Biochem.* **2023**, *117*, 109333. [CrossRef]
114. Shen, C.; Chen, L.; Jiang, L.; Lai, T.Y. Neuroprotective effect of epigallocatechin-3-gallate in a mouse model of chronic glaucoma. *Neurosci. Lett.* **2015**, *600*, 132–136. [CrossRef]
115. Peng, P.H.; Ko, M.L.; Chen, C.F. Epigallocatechin-3-gallate reduces retinal ischemia/reperfusion injury by attenuating neuronal nitric oxide synthase expression and activity. *Exp. Eye Res.* **2008**, *86*, 637–646. [CrossRef] [PubMed]
116. Zhang, B.; Rusciano, D.; Osborne, N.N. Orally administered epigallocatechin gallate attenuates retinal neuronal death in vivo and light-induced apoptosis in vitro. *Brain Res.* **2008**, *1198*, 141–152. [CrossRef] [PubMed]

117. Rivera-Pérez, J.; Martínez-Rosas, M.; Conde-Castañón, C.A.; Toscano-Garibay, J.D.; Ruiz-Pérez, N.J.; Flores, P.L.; Mera Jiménez, E.; Flores-Estrada, J. Epigallocatechin 3-Gallate Has a Neuroprotective Effect in Retinas of Rabbits with Ischemia/Reperfusion through the Activation of Nrf2/HO-1. *Int. J. Mol. Sci.* **2020**, *21*, 3716. [CrossRef]
118. Atkinson-Leadbeater, K.; Hehr, C.L.; Johnston, J.; Bertolesi, G.; McFarlane, S. EGCG stabilizes growth cone filopodia and impairs retinal ganglion cell axon guidance. *Dev. Dyn.* **2016**, *245*, 667–677. [CrossRef] [PubMed]
119. Pinazo-Duran, M.D.; Shoaie-Nia, K.; Zanon-Moreno, V.; Sanz-Gonzalez, S.M.; Del Castillo, J.B.; Garcia-Medina, J.J. Strategies to Reduce Oxidative Stress in Glaucoma Patients. *Curr. Neuropharmacol.* **2018**, *16*, 903–918. [CrossRef]
120. Sadowska-Krępa, E.; Domaszewski, P.; Pokora, I.; Żebrowska, A.; Gdańska, A.; Podgórski, T. Effects of medium-term green tea extract supplementation combined with CrossFit workout on blood antioxidant status and serum brain-derived neurotrophic factor in young men: A pilot study. *J. Int. Soc. Sport Nutr.* **2019**, *16*, 13. [CrossRef]
121. Peluso, I.; Serafini, M. Antioxidants from black and green tea: From dietary modulation of oxidative stress to pharmacological mechanisms. *Br. J. Pharmacol.* **2017**, *174*, 1195–1208. [CrossRef]
122. Kang, J.H.; Ivey, K.L.; Boumenna, T.; Rosner, B.; Wiggs, J.L.; Pasquale, L.R. Prospective study of flavonoid intake and risk of primary open-angle glaucoma. *Acta Ophthalmol.* **2018**, *96*, e692–e700. [CrossRef]
123. Chous, A.P.; Richer, S.P.; Gerson, J.D.; Kowluru, R.A. The Diabetes Visual Function Supplement Study (DiVFuSS). *Br. J. Ophthalmol.* **2016**, *100*, 227–234. [CrossRef]
124. Bae, J.H.; Kim, J.M.; Lee, J.M.; Song, J.E.; Lee, M.Y.; Chung, P.W.; Park, K.H. Effects of consumption of coffee, tea, or soft drinks on open-angle glaucoma: Korea National Health and Nutrition Examination Survey 2010 to 2011. *PLoS ONE* **2020**, *15*, e0236152. [CrossRef]
125. Ramdas, W.D.; Wolfs, R.C.; Kiefte-de Jong, J.C.; Hofman, A.; de Jong, P.T.; Vingerling, J.R.; Jansonius, N.M. Nutrient intake and risk of open-angle glaucoma: The Rotterdam Study. *Eur. J. Epidemiol.* **2012**, *27*, 385–393. [CrossRef]
126. Falsini, B.; Marangoni, D.; Salgarello, T.; Stifano, G.; Montrone, L.; Di Landro, S.; Guccione, L.; Balestrazzi, E.; Colotto, A. Effect of epigallocatechin-gallate on inner retinal function in ocular hypertension and glaucoma: A short-term study by pattern electroretinogram. *Graefes Arch. Clin. Exp. Ophthalmol.* **2009**, *247*, 1223–1233. [CrossRef]
127. Gasiunas, K.; Galgauskas, S. Green tea—A new perspective of glaucoma prevention. *Int. J. Ophthalmol.* **2022**, *15*, 747–752. [CrossRef] [PubMed]
128. Renno, W.M.; Khan, K.M.; Benov, L. Is there a role for neurotrophic factors and their receptors in augmenting the neuroprotective effect of (−)-epigallocatechin-3-gallate treatment of sciatic nerve crush injury? *Neuropharmacology* **2016**, *102*, 1–20. [CrossRef] [PubMed]
129. Li, M.; Xu, J.; Shi, T.; Yu, H.; Bi, J.; Chen, G. Epigallocatechin-3-gallate augments therapeutic effects of mesenchymal stem cells in skin wound healing. *Clin. Exp. Pharmacol. Physiol.* **2016**, *43*, 1115–1124. [CrossRef] [PubMed]
130. Yang, Y.; Qin, Y.J.; Yip, Y.W.; Chan, K.P.; Chu, K.O.; Chu, W.K.; Ng, T.K.; Pang, C.P.; Chan, S.O. Green tea catechins are potent anti-oxidants that ameliorate sodium iodate-induced retinal degeneration in rats. *Sci. Rep.* **2016**, *6*, 29546. [CrossRef]
131. Wang, J.; Man, G.C.W.; Chan, T.H.; Kwong, J.; Wang, C.C. A prodrug of green tea polyphenol (−)-epigallocatechin-3-gallate (Pro-EGCG) serves as a novel angiogenesis inhibitor in endometrial cancer. *Cancer Lett.* **2018**, *412*, 10–20. [CrossRef]
132. Mazzanti, G.; Menniti-Ippolito, F.; Moro, P.A.; Cassetti, F.; Raschetti, R.; Santuccio, C.; Mastrangelo, S. Hepatotoxicity from green tea: A review of the literature and two unpublished cases. *Eur. J. Clin. Pharmacol.* **2009**, *65*, 331–341. [CrossRef] [PubMed]

MDPI AG
Grosspeteranlage 5
4052 Basel
Switzerland
Tel.: +41 61 683 77 34

Antioxidants Editorial Office
E-mail: antioxidants@mdpi.com
www.mdpi.com/journal/antioxidants

Academic Open
Access Publishing

mdpi.com

ISBN 978-3-7258-2226-3